

1994

THE TECHNIQUE OF DETERMINATION OF STRUCTURAL PARAMETERS FROM FORCED VIBRATION TESTING

TSANG, WAI FAN

<http://hdl.handle.net/10026.1/2820>

<http://dx.doi.org/10.24382/3439>

University of Plymouth

All content in PEARL is protected by copyright law. Author manuscripts are made available in accordance with publisher policies. Please cite only the published version using the details provided on the item record or document. In the absence of an open licence (e.g. Creative Commons), permissions for further reuse of content should be sought from the publisher or author.

**THE TECHNIQUE OF DETERMINATION
OF STRUCTURAL PARAMETERS
FROM FORCED VIBRATION TESTING**

BY

WAI FAN TSANG B.Sc. (Hons.)

A thesis submitted to the University of Plymouth
in partial fulfilment for the degree of

DOCTOR OF PHILOSOPHY

SCHOOL OF CIVIL AND STRUCTURAL ENGINEERING

November 1994

UNIVERSITY OF PLYMOUTH LIBRARY SERVICES	
Item No.	900 222906 0
Class No.	T 620.32 TSA
Contl. No.	X703031855

90 0222906 0



REFERENCE ONLY

THE TECHNIQUE OF DETERMINATION OF STRUCTURAL PARAMETERS FROM FORCED VIBRATION TESTING

Wai Fan Tsang

ABSTRACT

This thesis details the results of an investigation into a technique for determination of "useful" structural parameters from forced vibration testing. The implementation of this technique to full scale civil engineering structures was achieved by several developments in the experimental and computational fronts: a vibration generator and a computer-aided-testing system for the former and two computational algorithms for the latter.

The experimental developments are instrumental to exciting large structures and acquisition of large quantities of useful data in digital format. These data serve as inputs to the computational algorithms whose outputs are structural parameters. These parameters are in either modal or spatial forms which cannot be measured directly but have to be extracted from the raw data.

The modal-parameter-extraction method is based on direct Least-Square fitting technique and is simple to implement. The technique can yield good accuracy if the residual effects from out-of-range modes are removed from the raw data before fitting. The spatial-parameter-extraction method distinguishes itself from other conventional methods in the way that the *orthogonality* property is not explicitly used. This method is applicable to situations where conventional methods are not; i.e. in cases if modal matrices are not square. Some success was achieved in cases in which computer synthesized or good quality laboratory test data were used.

Full scale field tests of a tall office block and a slender tower were carried out and their modal models obtained. Attempts to obtain spatial models of these structures were not carried out, however, as this task can be a separate research topic in its own right. Further research in such application is still required.

CONTENTS

	Page
Copyright Statement	i
Title page	ii
Abstract	iii
List of Contents	iv
List of figures	ix
List of tables	xvi
Nomenclature	xix
Acknowledgement	xxviii
Author's declaration	xxix
1 Introduction	
1.0 Aims of this research	1
1.1 Background to this research	1
1.2 An overview of the process of modelling	3
1.3 Strategies and methodologies	4
1.4 The scope of this research	6
2 Forced vibration tests on civil engineering structures	
2.0 Introduction	9
2.1 Review of previous works	9
2.1.1 Test methods	10
2.1.1.1 Ambient excitation technique	10
2.1.1.1.1 Wind	11
2.1.1.1.2 Earthquake	11
2.1.1.2 Artificially induced excitation	12
2.1.1.2.1 Eccentric rotating mass (ERM) exciter	12
2.1.1.2.2 Rectilinear motion exciter	14
2.1.2 Historical Account	15
2.1.2.1 The pioneers in full scale testing	15
2.1.2.2 The Earthquake Engineering Research Laboratory (USA)	16
2.1.2.3 The Building Research Establishment (UK)	17
2.1.2.4 Other investigations	19

2.2	Contribution of previous works	21
2.2.1	Information feed back	21
2.2.2	Justification of the use of simple models	21
2.2.3	Empirical relationships	22
2.3	Limitation of previous works	23
2.3.1	Quantity of measurements	23
2.3.2	Quality of measurements	24
2.3.3	Test methods	24
2.4	Conclusions	25
3	Theory	
3.0	Introduction	26
3.1	Concepts and approaches	27
3.1.1	Mathematical modelling	28
3.1.2	Structural modelling	28
3.2	Theoretical approaches of modelling	30
3.2.1	Continuous systems	30
3.2.1.1	Formulation of problems	31
3.2.1.2	Methods of solution	34
3.2.2	Discrete or Lumped systems	35
3.2.2.1	Formulation of problems	35
3.2.2.2	Solutions using Finite Element Method	37
3.2.2.2.1	Construction of structural matrices	38
3.2.2.2.2	Eigenvalue solutions	46
3.2.2.2.3	Modes of Vibration	49
3.2.2.2.4	Orthogonality of modes	50
3.2.2.2.5	Application of Modal Analysis to non-proportionally damped system	53
3.3	Experimental approaches of modelling	
3.3.1	System identification	59
3.3.1.1	Black box approach	60
3.3.1.2	Grey box approach	61
3.3.2	Implementation	61
3.3.2.1	Experimentation	62
3.3.2.2	Frequency response function measurements	62

	3.3.2.3	Data analysis	65
	3.3.2.3.1	Modal methods	65
	3.3.2.3.2	Non-modal methods	66
	3.4	Conclusions	68
4		Instrumentation	
	4.0	Introduction	70
	4.1	The instrumentation system	70
	4.2	The new excitation mechanism	72
	4.2.1	Brief descriptions	73
	4.2.2	Technical developments	75
	4.2.3	Performance tests	77
	4.2.4	Calibrations	80
	4.3	Sensors and transducers	80
	4.3.1	Stroke measurement	80
	4.3.2	Accelerometers	81
	4.3.2.1	Descriptions	81
	4.3.2.2	Calibrations	81
	4.4	Signal conditioning and processing	82
	4.4.1	General signal conditioning	82
	4.4.2	Signal recording	83
	4.4.2.1	Analogue tape recording	83
	4.4.2.2	Digital data recording	83
	4.4.3	Excitation signal generation	83
	4.4.3.1	Sinusoidal signals	83
	4.4.3.2	Periodic random signals	84
	4.4.4	Spectral analysis	84
	4.5	Computer-Aided-Testing (CAT)	85
	4.5.1	The hardware configuration	86
	4.5.2	Control programs	87
	4.6	Summary	88
5		Extraction of modal structural parameters from forced vibration data	
	5.0	Introduction	89
	5.1	Conventional methods	91
	5.1.1	SDOF-FIT methods	94
	5.1.1.1	Circle-fit method	95

	5.1.1.2	Straight-line-fit method	97
	5.1.2	MDOF-FIT methods	99
	5.1.2.1	Partial fraction methods	100
	5.1.2.2	Gleeson's methods	101
	5.1.2.3	Rational fraction Polynomial methods	101
	5.1.2.4	Maia-Ewins's method	102
	5.1.2.5	State space method	102
	5.1.2.6	Frequency domain poly-reference method	103
	5.1.3	Summary	104
	5.2	The method used in this investigation	105
	5.2.1	Background	105
	5.2.2	Development of the algorithm	106
	5.3	Implementation and Verification	114
	5.4	Comparisons of the proposed with some conventional methods	125
	5.5	Conclusions	128
6		Extraction of spatial structural parameters from forced vibration data	
	6.0	Introduction	129
	6.1	Conventional modal methods	131
	6.1.1	An overview of the Historical development	131
	6.1.2	Methods requiring priori assumptions	133
	6.1.3	Methods using orthogonality properties	134
	6.1.4	Methods using Optimization techniques	135
	6.1.5	Summary of modal methods	136
	6.2	The proposed non-modal method	137
	6.2.1	Background	137
	6.2.2	Development of the algorithm	139
	6.2.3	Implementation and Verification of the algorithm	150
	6.2.3.1	Computer simulations	150
	6.2.3.2	Quality-of-fit factor	153
	6.2.3.3	Results	155
	6.2.4	Practical applications	160
	6.3	Discussions	175
	6.4	Conclusions	177
7		Full scale forced vibration tests on the British Rail (BR) building	
	7.0	Introduction	178

7.1	Description of the structure	179
7.2	The test programme	181
7.2.1	Test environment	181
7.2.2	Test techniques	181
7.2.2.1	Ambient vibration tests	187
7.2.2.2	Steady state step-sine tests	188
7.2.2.3	Periodic random tests	190
7.3	Data recording and reductions	191
7.4	Test results	191
7.5	Analytical model of the BR building	206
7.6	Comparisons of experimental and analytical results	211
7.7	Summary	212
8	Full scale forced vibration tests on a fire drill tower	
8.1	Introduction	213
8.2	Description of the structure	213
8.3	Test arrangements and procedures	214
8.4	Test results	216
8.5	Discussion of results	246
8.6	Summary	247
9	Conclusions and Recommendations	253
	Appendices	
	Appendix 4.5.2	Listing of the CONTROL program
	Appendix 5.3	Listing of the modal parameter extraction program
	Appendix 5.4	Comparison of errors in the modal parameters determined by the three methods
	Appendix 6.3	Listing of the spatial parameter extraction program
	Appendix 8.3	A schedule of test identifications

References

LIST OF FIGURES

	PAGE NUMBER
Figure 2.1.1.2-1	14
A photograph featuring the BRE's ERM exciter in the field	
Figure 3.2.2.2-1	38
A simple bending beam subjected to shear and bending.	
Figure 3.3.2.3.2-1	67
A schematic drawing showing the design, analysis, testing and redesign cycle	
Figure 4.1-1	72
Schematic presentation of the configuration of the instrumentation system	
Figure 4.2.1-1	74
A photograph showing the dismantled DARTEC hydraulic power system	
Figure 4.2.2-1	75
A schematic drawing showing the hardware configuration of the excitation system.	
Figure 4.2.2-2	76
A photograph showing the excitation system.	
Figure 4.2.3-1	78
Acceleration responses of the loaded ram of the actuator over a range of input voltages and frequencies.	
Figure 4.2.3-2	78
Stroke responses of the loaded ram of the actuator over a range of input voltages and frequencies.	
Figure 4.2.3-3	79
Load generation capability of the exciter over a range of input voltages and frequencies.	
Figure 4.4.3.2-1	84
The Hewlett Packard HP 3582A spectrum analyzer	
Figure 5.1.1.1-1	96
A modal circle traced by consecutive FRF data points	
Figure 5.3-1	121
Marking of resonant peaks with vertical lines on the modulus and imaginary Inertance FRF plots	
Figure 5.3-2	121
Overlaid plots of original and regenerated Inertance FRF for the fictitious system with frequency resolution of 0.1 Hz and damping factor of 0.1 % of critical damping	
Figure 5.3-3	122
Overlaid plots of original and regenerated Inertance FRF for the fictitious system with frequency resolution of 0.1 Hz and damping factor of 1 % of critical damping	
Figure 5.3-4	122
Overlaid plots of original and regenerated Inertance FRF for the fictitious system with frequency resolution of 1 Hz and damping factor of 0.001 % of critical damping	

Figure 5.3-5	Overlaid plots of original and regenerated Inertance FRF for the fictitious system with frequency resolution of 1 Hz and damping factor of 0.01 % of critical damping	123
Figure 5.3-6	Overlaid plots of original and regenerated Inertance FRF for the fictitious system with frequency resolution of 1 Hz and damping factor of 0.1 % of critical damping	123
Figure 5.3-7	Overlaid plots of original and regenerated Inertance FRF for the fictitious system with frequency resolution of 2.5 Hz and damping factor of 0.001 % of critical damping	124
Figure 5.3-8	Overlaid plots of original and regenerated Inertance FRF for the fictitious system with frequency resolution of 2.5 Hz and damping factor of 10 % of critical damping	124
Figure 6.2-1	A schematic showing how the proposed method bypasses the conventional modal procedures to obtain the spatial matrices	138
Figure 6.2.3.3-1	Receptance spectrum for the 3 DOF fictitious system at spatial point No. 1	156
Figure 6.2.3.3-2	Receptance spectrum for the 3 DOF fictitious system at spatial point No. 2	156
Figure 6.2.3.3-3	Receptance spectrum for the 3 DOF fictitious system at spatial point No. 3	157
Figure 6.2.3.3-4	Overlaid plots of original and regenerated Receptance spectra for spatial point 1 from a reduced model of order 6	158
Figure 6.2.3.3-5	Overlaid plots of original and regenerated Receptance spectra for spatial point 2 from a reduced model of order 6	159
Figure 6.2.3.3-6	Overlaid plots of original and regenerated Receptance spectra for spatial point 3 from a reduced model of order 6	159
Figure 6.2.3.3-7	Overlaid plots of original and regenerated Receptance spectra for spatial point 4 from a reduced model of order 6	160
Figure 6.2.4-1	A schematic drawing showing the test set up and equipment used	161

Figure 6.2.4-2	A schematic drawing of the four-mass torsional system	162
Figure 6.2.4-3	Correlation between the measured and the regenerated FRF curves for the mass m_1	162
Figure 6.2.4-4	Correlation between the measured and the regenerated FRF curves for the mass m_2	163
Figure 6.2.4-5	A schematic drawing showing the beam test arrangement	165
Figure 6.2.4-6a to 6.2.4-6f	Overlaid plots of original and regenerated Receptance FRF at all 6 spatial points on the beam (model A)	171
Figure 6.2.4-7a to 6.2.4-7f	Overlaid plots of original and regenerated Receptance FRF at all 6 spatial points on the beam (model B)	172
Figure 6.2.4-8a to 6.2.4-8f	Overlaid plots of original and regenerated Receptance FRF at all 6 spatial points on the beam (model C)	173
Figure 6.2.4-9a to 6.2.4-9f	Overlaid plots of original and regenerated Receptance FRF at all 6 spatial points on the beam (model D)	174
Figure 7.1-1	A photographic view of the BR Building.	179
Figure 7.1-2	A typical floor plan of the BR Building.	180
Figure 7.2.2-2	A time response record of the structure's amplitude response	183
Figure 7.2.2-3	Locations of the travelling and the reference accelerometers in the BR building.	184
Figure 7.2.2-4	Locations of the exciter in the BR building.	185
Figure 7.2.2-5a	A photograph featuring the setting up of equipment in the field	186
Figure 7.2.2-5b	A photograph featuring the fully assembled hydraulic power supply unit in the field	187
Figure 7.2.2.2-1	A sample of typical time response recorded	189
Figure 7.2.2.2-2	A typical load spectrum when excitation frequency was set at 1 Hz.	190
Figure 7.2.2.2-3	The resulting acceleration response spectrum.	190

Figure 7.4-1a	The autospectrum obtained in the ambient vibration tests from accelerometer A	192
Figure 7.4-1b	Another autospectrum obtained in the ambient vibration tests from accelerometer B	192
Figure 7.4-2	A Coherence spectrum obtained from ambient tests.	194
Figure 7.4-3	A Phase spectra from ambient tests.	194
Figure 7.4-4	The Inertance FRF spectrum from SS tests with the exciter aligned in the NS direction.	195
Figure 7.4-5	The Inertance FRF spectrum from SS tests with the exciter aligned in the EW direction.	196
Figure 7.4-6	A typical time history record of the PRBS excitation force (load) and the resulting responses from the two accelerometers	197
Figure 7.4-7	The NS1 mode shape determined from the SS and PRBS tests.	199
Figure 7.4-8	An overlaid plot of the NS1 mode shapes of the BR building.	200
Figure 7.4-9	The EW1 mode shape of the BR building.	201
Figure 7.4-10	An overlaid plot of the EW1 mode shapes of the BR building	202
Figure 7.4-11	The T1 mode shape of the BR building.	203
Figure 7.4-12	The NS2 mode shape of the BR building.	204
Figure 7.4-13	The EW2 mode shape of the BR building.	205
Figure 7.5-1	The finite element wire-framed model of the BR building.	207
Figure 7.5-2a	A 3 dimensional perspective view of the EW1 mode shape from the finite element model of the BR building	208
Figure 7.5-2b	A side view of the EW1 mode shape from the finite element model of the BR building.	209
Figure 7.5-3a	A 3 dimensional perspective view of the T1 mode shape from the finite element model of the BR building	209
Figure 7.5-3b	A side view of the T1 mode shape from the finite element model of the BR building.	210
Figure 7.5-4	The EW2 mode shape from the finite element model of the BR building.	210

Figure 8.2-1	A photographic view of the Camel's Head fire drill tower.	214
Figure 8.3.-1	Locations of the exciter and designation of the grid points	215
Figure 8.4.-1	Modulus inertance FRF spectrum using SS tests	217
Figure 8.4.-2a	Change of acceleration and inertance of the mode at 2.34 Hz with increase magnitude of force using SS excitation	218
Figure 8.4.-2b	Change of acceleration and inertance of the mode at 2.48 Hz with increase magnitude of force using SS excitation	218
Figure 8.4.-3a	Modulus and phase inertance FRF plot using SS excitation. Measurement was made at 5A1 with exciter acting in the EW direction and force amplitudes of 0.05 KN (r.m.s.)	219
Figure 8.4.-3b	Modulus and phase inertance FRF plot using SS excitation. Measurement was made at 5A1 with exciter acting in the EW direction and force amplitudes of 0.1 KN (r.m.s.)	219
Figure 8.4.-3c	Modulus and phase inertance FRF plot using SS excitation. Measurement was made at 5A1 with exciter acting in the EW direction and force amplitudes of 0.15 KN (r.m.s.)	220
Figure 8.4.-4	Modulus inertance FRF plot using SS excitation Measurement was made at 5A1 with exciter acting in the EW direction.	221
Figure 8.4.-5	Modulus inertance FRF plot using SS excitation Measurement was made at 5A1 with exciter acting in the NS direction.	221
Figure 8.4.-6a	Inertance FRF spectra from PRBS excitation (EW) test (R2304007) zooming in at 2 Hz	223
Figure 8.4.-6b	Inertance FRF spectra from PRBS excitation (EW) test (R2304006) zooming in at 5 Hz	223
Figure 8.4.-6c	Inertance FRF spectra from PRBS excitation (EW) test (R2304003) zooming in at 10 Hz	223

Figure 8.4.-7a	Inertance FRF spectra from PRBS excitation (NS) test (R2504001) zooming in at 2 Hz	225
Figure 8.4.-7b	Inertance FRF spectra from PRBS excitation (NS) test (R2504002) zooming in at 5 Hz	225
Figure 8.4.-7c	Inertance FRF spectra from PRBS excitation (NS) test (R2504003) zooming in at 10 Hz	226
Figure 8.4.-7d	Inertance FRF spectra from PRBS excitation (NS) test (R2504004) zooming in at 17 Hz	226
Figure 8.4.-7e	Inertance FRF spectra from PRBS excitation (NS) test (R2504003) zooming in at 25 Hz	226
Figure 8.4.-8a	The modulus spectra obtained from the grid point at 5A1 whilst the shaker was aligned along the EW direction	228
Figure 8.4.-8b	The phase spectra obtained from the grid point at 5A1 whilst the shaker was aligned along the EW direction	228
Figure 8.4.-9	Marking resonant mode positions at the peaks in the modulus or imaginary Inertance spectra	229
Figure 8.4.-10	Inertance FRF spectra from PRBS test (R25X021X)	230
Figure 8.4.-11	Inertance FRF spectra from PRBS test (R25Y021Y)	230
Figure 8.4.-12	Inertance FRF spectra from PRBS test (R25Y021X)	231
Figure 8.4.-13	Inertance FRF spectra from PRBS test (R25Y017Y)	231
Figure 8.4.-14	Inertance FRF spectra from PRBS test (R25Y001Z)	232
Figure 8.4.-15a	A view of the swaying EW1 mode	234
Figure 8.4.-15b	Another view of the swaying EW1 mode	234
Figure 8.4.-16a	A view of the torsional T1 mode	235
Figure 8.4.-16b	Another view of the torsional T1 mode	235
Figure 8.4.-17	A view of the swaying EW2 mode	236
Figure 8.4.-18a	A view of the mode with natural frequency around 17 Hz	236
Figure 8.4.-18b	Another view of the torsional T2 mode	237
Figure 8.4.-18c	The mode with natural frequency around 18 Hz	238
Figure 8.4.-19	The mode with natural frequency around 24 Hz	238
Figure 8.4.-20	The swaying NS1 mode	239
Figure 8.4.-21	The torsional T1 mode	240

Figure 8.4.-22	The NS2 mode	240
Figure 8.4.-23	The mode with natural frequency around 16 Hz	241
Figure 8.4.-24	The mode with natural frequency around 18 Hz	241
Figure 8.4.-25	The mode with natural frequency around 25 Hz	242
Figure 8.4.-26a to 8.4-26d	The operating mode shapes at frequency 2.36, 10.2, 11.4 and 16.7 Hz with the exciter acting along the EW direction	244
Figure 8.4.-27a to 8.4-27d	The operating mode shapes at frequency 2.36, 5.3, 10.2, 11.4 and 16.7 Hz with the exciter acting along the NS direction	245

LIST OF TABLES

	PAGE
Table 4.3.2.2-1	82
Comparison of the experimental and the manufacturer's calibration of the accelerometers	
Table 5.3-1	115
Table illustrating the mechanics of the calculation using the proposed algorithm	
Table 5.3-2	117
Assumed modal parameters for a four-modes fictitious system	
Table 5.3-3	119
Results of modal parameters determined using iterative mode subtraction for the four-modes fictitious system	
Table 5.3-4	120
Effects on QF Factors by using various mode combinations	
Table 5.4-1	127
Percentage errors in the modal parameters determined using author's method	
Table 6.2.3.1-1	151
Specified spatial parameters of the 3 DOF system used in the computer simulation studies	
Table 6.2.3.1-2	152
The specified mass matrix of the 10 DOF system used in the computer simulation studies	
Table 6.2.3.1-3	153
The specified stiffness matrix of the 10 DOF system used in the computer simulation studies	
Table 6.2.3.3-1	157
The reduced order 6 x 6 mass matrix of the 10 DOF fictitious system determined by the algorithm	
Table 6.2.3.3-2	158
The reduced order 6 x 6 stiffness matrix of the 10 DOF fictitious system determined by the algorithm	
Table 6.2.4-1	163
The derived spatial matrices of the torsional system (undamped model)	
Table 6.2.4-2	164
The derived spatial matrices of the torsional system (damped model)	
Table 6.2.4-3	166
Details of analysis conditions to derive the spatial model of the beam	
Table 6.2.4-4	167
The spatial matrices of order 6 derived for the beam (undamped model) with selected data points covering all six modes (model A)	

Table 6.2.4-5	The spatial matrices of order 6 derived for the beam (undamped model) with selected data points covering only four modes (model B)	168
Table 6.2.4-6	The spatial matrices of order 6 derived for the beam (undamped model) with selected data points covering only three modes (model C)	169
Table 6.2.4-7	The spatial matrices of order 6 derived for the beam (undamped model) with selected data points covering only two modes (model D)	170
Table 6.3-1	The derived spatial matrices of the torsional system (undamped model) using conventional modal approach.	175
Table 7.4-1	The table of exemplary values of the resonance frequencies of the various modes of the BR Building	198
Table 7.6-1	The table of comparison of the values of the resonance frequencies of the various modes from experiments and the undamped natural frequencies from the finite element model	211
Table 8.4-1	Zoom analysis with a resolution of 0.04 Hz (EW excitation)	224
Table 8.4-2	Zoom analysis with a resolution of 0.04 Hz (NS excitation)	227
Table 8.4-3	Modal parameters set determined from test data 220487001R (from 25 Hz PRBS tests with exciter acting EW and measurements made at grid point 5A1 in the EW direction)	248
Table 8.4-4	Modal parameters set determined from test data 230487009R (from 25 Hz PRBS tests with exciter acting NS and measurements made at grid point 5A1 in the NS direction)	248
Table 8.4-5	Modal parameters set determined from test data 250487017R (from 25 Hz PRBS tests with exciter acting NS and measurements made at grid point 5B2 in the NS direction)	249
Table 8.4-6	Modal parameters set determined from test data	249

	260487008R (from 25 Hz PRBS tests with exciter acting NS and measurements made at grid point 4A2 in the NS direction)	
Table 8.4-7	Modal parameters set determined from test data R25X021X (from 25 Hz PRBS tests with exciter acting EW and measurements made at grid point 5A2 in the EW direction)	250
Table 8.4-8	Modal parameters set determined from test data R25Y023Y (from 25 Hz PRBS tests with exciter acting NS and measurements made at grid point 5B2 in the NS direction)	250
Table 8.4-9	Modal parameters set determined from test data R 25Y021X (from 25 Hz PRBS tests with exciter acting NS and measurements made at grid point 5A2 in the EW direction)	251
Table 8.4-10	Modal parameters set determined from test data R 25Y017Y (from 25 Hz PRBS tests with exciter acting NS and measurements made at grid point 4A1 in the NS direction)	251
Table 8.4-11	Modal parameters set determined from test data R 25Y001Z (from 25 Hz PRBS tests with exciter acting NS and measurements made at grid point 0A1 in the Vertical direction)	252

NOMENCLATURE

DEFINITION OF TERMS AND ABBREVIATIONS

Chapter 1

CAT	Computer-Aided-Testing
FEM	Finite Element Modelling
BEM	Boundary Element Modelling
EMA	Experimental Modal Analysis
FRF	Frequency Response Function
Modal parameters	A set of parameters (natural frequencies, modal damping factors and modal constants) which characterise the modes of vibration of a physical structure
Spatial parameters	A set of parameters (mass, damping and stiffness) which characterise the inertial, energy dissipation and elastic properties of a physical structure
IRF	Impulse Response Functions
RMHI	Rectilinear motion hydraulic inertial exciter
ERM	Eccentric rotating mass exciter
SS	Step-sine excitation
PRBS	Pseudo-Random-Binary-Sequence technique to generate random wave

Chapter 2

EERL	Earthquake Engineering Research Laboratory in USA
CIT	California Institute of Technology, USA.
BRE	Building Research Establishment in UK
EERC	Earthquake Engineering Research Centre in USA
CEGB	Central Electricity Generating Board
3D	three dimensional

FE	Finite Element
r	wall ratio (the total length of all walls divided by the sum of the floor areas of all floors).
f_{nat}	the natural frequency of vibration (in Hz)
T	natural period of vibration (in seconds)
N	number of storey of a building
H	height of a building
B	width of a building
ESDU	Engineering Science Data Unit
DOF	Degree of freedom

Chapter 3

$[\epsilon_{ij}]$ and $[\sigma_{ij}]$	Strain and stress tensors respectively in indicial notation
$\{u_i\}$	spatial displacement vector in rectangular Cartesian coordinates
F_i	the internal body forces
P	the surface traction
\mathcal{L}	a function of differential operators
c_{ijkl}	a fourth order elastic constants tensor
E and G	the Young's modulus and Shear modulus respectively
λ and μ	the two Lamé constants
ρ	mass density of material
Δ	dilatation
∇^2	Laplacian operator
FEM	Finite Element Methods
BEM	Boundary Element Methods
u_0	a true solution of displacement u
Ω	a symbol denoting the domain
$G(u_0)=g$	an expression denoting the essential boundary conditions
$S(u_0)=g$	an expression denoting the natural boundary conditions
Γ_1 and Γ_2	denoting the total boundary
$Y_k(x)$	a set of linear independent functions to approximate u_0

α_i	a set of undetermined parameters used to approximate u_0
ε	<i>residual error</i>
Ψ_i and w	a set of weighting functions
u_y or $u_y(x)$	displacement in the y-direction along the length of the beam x
a_i	arbitrary constants used to specify the deformation field of a beam
[POLY]	a polynomial matrix as a function of x used to specify the deformation field of a beam
u_e	nodal displacements
S.E	strain energy
K.E.	kinetic energy
E	Young's Modulus of a material
I	moment of inertia of a beam section
$U_x(x)$ and $q(x)$	axial and torsional displacement respectively
ρ	mass density of materials
ω	angular frequency of vibration
V	Volume
L	length of a beam
[M]	mass matrix
[K]	stiffness matrix
[C]	damping matrix
$\{x\}, \{\dot{x}\}, \{\ddot{x}\}$	displacement, velocity, acceleration vectors respectively in arbitrary Cartesian coordinates
$\{\eta\}, \{\dot{\eta}\}, \{\ddot{\eta}\}$	displacement, velocity, acceleration vectors respectively in natural coordinates
$[\Phi]$	the modal matrix and is a matrix whose columns are eigenvectors
$[\Phi]^T$	is the transpose of modal matrix
$[M^*], [K^*], [C^*]$	are the diagonal Generalised mass, stiffness and damping matrices respectively
K^*_{rs} and M^*_{rs}	are the r^{th} row s^{th} column elements of the matrices $[K^*]$ and $[M^*]$ respectively
α and β	are the two proportional parameters used in the Rayleigh's damping model

$\{f\}$	the forcing vector
$[\xi]$	is a diagonal matrix of modal damping factors
$[\omega_r^2]$ or $[\omega^2]$	is the spectral matrix and is a diagonal matrix of the eigenvalues ω_r^2
ω_r	is the undamped natural frequency
subscript r	denotes the r^{th} mode when used in conjunction with modal parameters
ξ_r	modal damping factor
ϕ_r or $\{\phi_r\}$	is eigenvectors (or natural mode shape) of the r^{th} mode
$[\xi]$	is the diagonal matrix of modal damping factors
c_r, φ_r	are the amplitude and phase angle respectively used in defining the manifestation of a mode shape
$\{\varphi_r\}$	is a vector of phase angles φ_r
Δ_{cd}	the <i>characteristic determinant</i>
ω_{rD}	equals $\omega_r(1 - \xi_r^2)^{0.5}$ and is the <i>damped natural frequency</i>
$[C_{nd}]$	a damping matrix where the subscript nd denotes non-diagonal
$[C_{rc}]$	a damping matrix where the subscript rc denotes it is a reconstruction
$[C_d]$	a diagonal damping matrix which is obtained by retaining only the diagonal terms of the matrix $[C_{nd}]$
$[2\xi_r \omega_r]$	is a diagonal matrix constructed from known modal damping factors ξ_r and undamped natural frequencies ω_r
a	a proportional constant independent of frequency of harmonic oscillation used in describing energy dissipated by hysteretic damping
X_0	is the amplitude of displacement oscillation
Ω	is the frequency of harmonic oscillation
c	is the viscous damping coefficient
γ_{ij}	the coefficients of structural damping
$[\gamma k]$ or $[H]$	hysteretic damping matrix
$(1 + j\gamma) [K]$	complex stiffness
\otimes	a superscript denotes complex quantities
$\{\phi_i^*\}$	are complex eigenvectors
$[\Phi^*]$	a complex modal matrix

$\{\}^*$	denotes a complex conjugate of a vector
SISO	Single-Input-Single-Output
SIMO	Single-Input-Multiple-Output
MISO	Multiple-Input-Single-Output
MIMO	Multiple-Input -Multiple-Output
FRF or $H(\omega)$	Frequency Response Function
α_{ij}	receptance defined as a ratio of the spectral displacement response at coordinate i and the force applied at another coordinate j of a structure
TF	Transfer Function
DFT	Discrete Fourier Transformation
$\mathcal{F}(\)$	denotes the Fourier Transform operator
PSD	Power Spectral Density function
$G(\omega)$	a complex valued PSD function
$G_{xf}(\omega)$	the Cross PSD functions of response x and force f
$G_{ff}(\omega), G_{xx}(\omega)$	the Auto PSD functions of force f and response x respectively
$\text{COH}_{xf}(\omega)$	a coherence spectral function
$H_{xf}(\omega)$ or α_{ij}	receptance defined as a ratio of the spectral displacement response at coordinate i and the force applied at another coordinate j of a structure
$H_{vf}(\omega)$	mobility defined as a ratio of the spectral velocity response at coordinate i and the force applied at another coordinate j of a structure
$H_{af}(\omega)$	accelerance or inertance defined as a ratio of the spectral acceleration response at coordinate i and the force applied at another coordinate j of a structure

Chapter 4

DARTEC	Manufacturer of the hydraulic actuator
INSTRON	Manufacturer of the load cell used in calibration
SCHAEVITZ	Manufacturer of the accelerometers
DC	Signal with constant amplitude and zero frequency
FM	Frequency Modulation
DFT	Discrete Fourier Transform
FFT	Fast Fourier Transform
ADC	Analogue-to-digital converter

Chapter 5

TD	Time Domain methods
FD	Frequency Domain methods
γ_i	is a hysteretic damping loss factor
subscript i	denotes the i^{th} mode of vibration when used in conjunction with modal parameters
[H]	hysteretic damping matrix
ω_i	is the undamped natural frequency
$G_{sr\ i}$, $G^*_{sr\ i}$	are the real and complex modal constants respectively
$ G^*_{sr\ i} $	magnitude of the complex modal constant
N	is the total number of degree of freedom (or modes) of the system
subscript sr	denotes response at coordinate s and force at coordinate r
j	is the imaginary unit $\sqrt{-1}$
SDOF	single-degree-of-freedom
MDOF	multi-degree-of-freedom
θ_1 , ω_1 , θ_2 and ω_2	are quantities corresponding to any two neighbouring points (one on each side of the data point corresponds to ω_i) on a modal circle as shown in Figure 5.1.1.1-1.

$D_{sr\ i}$	is the diameter of a modal circle
a_k and b_k	unknown parameters used in the rational fraction polynomial method
$H(\omega)$	receptance FRF and is a function of angular frequency ω
p_k and p_k^*	k^{th} pole and its conjugate
r_k and r_k^*	residue of the k^{th} pole and its conjugate
ω_k	damped natural frequencies (the imaginary part of a complex eigenvalue)
σ_k	damping coefficients (the real part of a complex eigenvalue)
ω	angular frequency
$\{X\}$ and $\{F\}$	are respectively the Fourier Transforms of displacement $\{x(t)\}$ and force vectors $\{f(t)\}$ and are functions of angular frequency ω .
$[\Phi]$	undamped modal matrix
η	natural (or modal) coordinates
$[M^*]$	is the diagonal modal or generalised mass matrix.
$[K^*]$	is the diagonal modal or generalised stiffness matrix.
$[C^*]$	is the diagonal modal or generalised damping matrix.
ϕ_{si}	the element of the s^{th} row, i^{th} column of the undamped modal matrix
M'_i	effective mass
K'_i	effective stiffness
C'_i	effective damping
α or $\alpha(\omega)$	is receptance (a complex quantity) and is a function of angular frequency ω
$1/\alpha$	reciprocal of receptance (or dynamic stiffness)
\Re and \Im	the real and imaginary part of receptance respectively
$\gamma_{rs}(\omega)$	accelerance or inertance and is a function of angular frequency ω
$A_{sr}(\omega)$ and $B_{sr}(\omega)$	are the real and imaginary part of dynamic stiffness respectively
$A'_{sr}(\omega)$ and $B'_{sr}(\omega)$	are the real and imaginary parts of the inverse of accelerance respectively
ξ_i	the modal damping factor of the i^{th} mode

$M(r,s)$	an indicial notation devised and defined to illustrated the mode subtraction operations where r is the mode number s is the number of iterative cycles performed
QF	quality-of-fit factor which quantifies the degree of correlation between two sets of data

Chapter 6

DSPED	Deriving Spatial Parameters from Experimental Data
NASA	US National Astronautical and Space Administration
$\mathcal{L}(\)$	Laplace Transformation operator
s	Laplace Transformation variable
[T]	Transfer Matrix
$\{X_R(\omega)\}$	the real part of the vector $\{X(\omega)\}$
$\{X_I(\omega)\}$	the imaginary part of the vector $\{X(\omega)\}$
$\{F_R(\omega)\}$	the real part of the vector $\{F(\omega)\}$
$\{F_I(\omega)\}$	the imaginary part of the vector $\{F(\omega)\}$
$R\alpha(\omega)$	the real part of $\alpha(\omega)$
$I\alpha(\omega)$	the imaginary part of $\alpha(\omega)$

Chapter 7

BR	the British Rail building
EW	East West direction
NS	North South direction
RMS	Root-Mean-Square
PAFEC	Name of a commercially available finite element analysis software
PRIME	Name of a powerful network computer manufactured by IBM
1D	one-dimensional

Chapter 8

r.m.s.	root-mean-square
TI	Test Identification used to encode different tests carried out
%C	attenuator dial reading
MT	Motion Transmissibility
GINO	Name of a generally available graphics plotting software

ACKNOWLEDGEMENT

The author would like to thank the University of Plymouth (formerly Plymouth Polytechnic) for providing financial support and the Science and Engineering Research Council for a grant (Grant No. GR/D/02119) which was instrumental in the purchase of the actuator. My next thanks go to my supervisors Dr. Clive Williams and Mr Peter Hewson (both Principal Lecturers of the University) for their foresight in the inception of the project.

I thank my past colleagues in the Polytechnic in general, those in the Department of Civil and Structural Engineering in particular. Special thanks go to Dr. Mike Foulkes (Lecturer) and Gregory Reagan (Research Assistant) who have helped in many ways.

Thanks also go to the teams in the University of Bristol and the Building Research Establishment for their invitation to join in as an observer when they carried out tests on the Humber Bridge and the Hume Point tower block in London.

Thanks are also due to the British Rail and the Devon Fire Brigade for granting permission for me to carry out tests on the Plymouth British Rail Building and the Camel's Head Fire Station Tower respectively.

Thanks go to the Royal Naval Engineering College for allowing me to use college facilities during off-working hours for finalizing this work. Thanks are due to past and present colleagues in the Department of Mechanics and Power with whom I have worked.

I would also like to thank my wife and my children for bearing a lot of the emotional aggravation and long periods of desertion which are, inevitably, part-and-parcel of research work.

Space limitation does not allow me to name each individual who helped in various ways, as I am sure the list would run to several pages.

AUTHOR'S DECLARATION

At no time during the registration for the degree of Doctor of Philosophy has the author been registered for any other University award.

This study was financed with the aid of a position of research assistant from the former Plymouth Polytechnic and a grant from the Science and Engineering Research Council towards the equipment.

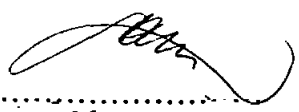
During this research, the author attended a course on Fundamentals of Structural Dynamics run by the Institute of Computational Mechanics, Southampton.

International Conferences and Seminars on Experimental Modal Analysis, Structural Dynamics, Identification and Smart Structures were attended at which work was often presented. Visits to laboratories of other institutions were made and discussions with other researchers undertaken.

Publications :

1. C Williams and W F Tsang. "Dynamic characteristics of reinforced concrete structures". Paper presented and published in the Proceedings of the Research Seminar on The Behaviour of Concrete Structures, Cement and Concrete Association, Fulmer Grange, 30 June - 2 July, 1986.
2. C Williams and W F Tsang. "Determination of structural parameters from full scale vibration tests". Paper presented and published in the Proceedings of the Conference On Civil Engineering Dynamics, University of Bristol, 24-25 March 1988.
3. W F Tsang, C Williams. "Application of Experimental Modal Analysis to full scale civil engineering structures". Paper presented and published in the Proceedings of the 3rd International Conference On Recent Advances In Structural Dynamics, July 1988, University of Southampton, Paper 88.

4. W F Tsang and E Rider. "Modelling of structures using experimental forced vibration data with a particular application in force prediction". Paper presented at the 4th SAS-World Conference FEMCAD-88, Paris 17-19 October, 1988 and published in RNEC research report RNEC-RP-88023, Royal Naval Engineering College, Plymouth.
5. W F Tsang and E Rider. "The technique of extraction of structural parameters from experimental forced vibration data". Paper presented and published in the Proceedings of the 7th International Modal Analysis Conference, Las Vegas, 30 Jan- 2 Feb 1989.
6. W F Tsang , E Rider and P George. "Application of acceleration and strain measurements in forced vibration testing". Paper presented and published in the Proceedings of the Conference of Modern Practice In Stress And Vibration Analysis, University of Liverpool, 3-5 April 1989.
7. W F Tsang. "Use of dynamic strain measurements for the modelling of structures". Paper presented and published in the Proceedings of the 8th International Modal Analysis Conference, Orlando, Florida, 29 Jan- 1 Feb 1990.
8. W F Tsang, C Williams. "A comparison of some methods of modal parameters extraction". Paper presented and published in the Proceedings of the 8th International Modal Analysis Conference, Orlando, Florida, 29 Jan- 1 Feb 1990.
9. W F Tsang, R J Randal. "Identification of Rheological models of elasto-visco-plastic Electro-rheological Fluids". Paper presented and published in the Proceeding of the International Symposium On Identification of Nonlinear Mechanical Systems from Dynamic Tests - EUROMECH 280. Ecully, France, 29-31 October 1991.
10. W F Tsang, R J Randal. "Use of Electro-rheological Fluids for Adaptive Vibration Isolation". Paper published in the Proceeding of the First European Conference On Smart Structures and Materials. Glasgow, UK, 12-14 May, 1992.

Signed.....
Date.....30th Jan 1995.....

CHAPTER 1

INTRODUCTION

1.0 AIMS OF THIS RESEARCH

The main aim of this research is to investigate the transfer of technology, developed in the so-called Experimental Modal Analysis field, to civil engineering applications: in particular, the technology of performing forced vibration testing to obtain useful structural parameters of full-scale civil engineering structures. The second aim is to improve or devise alternative testing methodology to the existing full-scale forced vibration testing methods adopted in civil engineering in the UK, by making use of an alternative excitation mechanism, a computer-aided-testing (CAT) system and computational algorithms to obtain the structural parameters.

1.1 BACKGROUND TO THIS RESEARCH

This research project was initiated in late 1984 as an extension of the work conducted by Williams^[1.1] in the mid 1970s. The objective of his work was to determine the real dynamic performance of some full scale civil engineering structures through in-situ vibration measurements. The initiative then, as it is now, was driven by the need for an experimental tool which could provide some information feed back for engineers to evaluate how a structure really behaved as a contrast to what was intended in the design.

Vibration can be a nuisance if it is not intended but can be very useful if it is skilfully induced to a structure. To most people, vibration is often perceived as something undesirable or as an early tell-tale sign of trouble in machinery. Perhaps this psychological effect can partly explain why most people show a negative feeling about vibration and very little tolerance to it in certain circumstances.

Excessive vibration not only causes physiological and psychological distress to the

inhabitants of a vibrating structure, it also causes structural 'distress' such as fatigue and failure of the materials of the structure itself. Hence, most engineers are taught how to avoid or eliminate vibration during their education. Very little emphasis is placed on the advantages of vibration.

Structural dynamicists have for many years, used controlled vibration as an interrogation tool in the same way as stethoscopes are used by doctors. This technology is branched into several subsidiaries. One branch is called *dynamic testing* which is widely used in the aircraft and automobile industries. As vibration tests can often be carried out non-intrusively and non-destructively, it is a very useful structural diagnostic tool.

Another branch is called *condition monitoring* which utilizes the detection of undue vibration as an indication of the 'health condition' or otherwise of machineries. Condition monitoring is widely practised in the field of power generation and propulsion industries involving high speed rotational machinery. Knowing the true state of health of machines means a saving of expenditure on unnecessary re-fits and early detection of faults can prevent an expensive repair bill because further and more serious damage can be avoided. Without this technique, actions taken are either too prudent or too complacent but both actions produce the same expensive outcome.

Traditionally, civil/structural engineers have little training on vibration. Unlike structural statics which is taught in all civil/structural engineering courses, structural dynamics is often reserved only for the specialists. Given this background, it is not difficult to imagine that a dynamic problem is often transformed to a quasi-static problem for design and analysis. In Britain, wind loading design is covered by the **British Standard Code of Practice CP3** ^[1,2].

Early civil engineering structures, especially those constructed in Telford's and Brunel's times, were less prone to ambient induced vibration. Structures built today are, however, increasingly lighter in weight, more slender in shape and more flexible as a result of the use of lighter but stronger construction materials. Such structures are more vulnerable to vibration from natural causes such as wind and/or seismic activities.

Misunderstanding of the effects of vibration can sometimes be fatal. The static behaviour of a structure cannot and must not be used to extrapolate to the dynamic

regime. A structure which is adequately designed for static loadings may not be adequate for dynamic loadings. The collapse of the Tacoma bridge was a typical example of such a tragedy. Critics often point their fingers at engineers for badly designed structures as the major promoter of misadventure. So a better understanding of the dynamics of structures is vital for the advancement of design and construction methods.

The following Sections introduce the theory and concept of forced vibration testing and explain how this technique can be applied.

1.2 AN OVERVIEW OF THE PROCESS OF MODELLING

Most investigative techniques, be they analytical or experimental in nature, can often be collectively described as *modelling*. *Physical modelling* which, often first springs to mind, is another modelling technique but is not of concern here. What is concerned here is *mathematical modelling*. Mathematical modelling is a prevalent task mutual to almost all analysis techniques. This exercise results in the realization of a complex system to a simplified conceptual model amenable to mathematical analysis.

Currently there are two main approaches available in the field of structural dynamic modelling. One is theoretical, based on Finite Element Modelling (FEM) or Boundary Element Modelling (BEM) and the other is experimental, based on Experimental Modal Analysis (EMA). FEM and BEM are instrumental in the modern practice of theoretical engineering analysis. However, recent advancement in instrumentation and signal processing technology is set to correct this imbalance. The dominance of analytical over experimental techniques is beginning to change.

FEM and BEM theories are based on a set of assumptions and idealizations upon which the feasibility and credibility of these methods depend entirely. The results of this analysis should never be accepted at their face values without the proper exercise of scrutiny. Otherwise, it is merely reduced to an unproductive "number crunching" exercise. Theoretical analysis alone cannot provide the sole solution to the need of a reliable engineering analysis tool. Other methods have to be sought to complement but not to substitute these theoretical techniques.

Experimental Modal Analysis which has been developing rapidly in another discipline,

is a very promising technique. The experimental technique advocated in this research is based partly on EMA (*modal* approach) and partly on another alternative called *spatial* approach. Modal approach relies on the determination of the modal parameters (undamped natural frequencies, modal damping factors and modal constants for each of the modes of vibration of a structure) to construct a modal model. Whereas spatial approach determines the spatial parameters (mass, damping and stiffness matrices) to construct a spatial model. The two approaches share some similarities in methodology but differ in the ways that data analysis or parameter extraction is carried out. Further explanation of these two methods will be given in chapters 3, 5 and 6 accordingly.

1.3 STRATEGIES AND METHODOLOGIES

The basic underlying methodology is called *system identification* and *parameter estimation* which originates from Control Engineering. In essence, system identification is a process of determining a mathematical relationship between the input and output of a system. Since its inception, its application to other disciplines such as Robotics, Aerospace and Mechanical Engineering has become increasingly popular. However, so far, Civil/Structural engineering is slow to exploit this technique.

In structural dynamics, characterization of a structural system is based on a set of simultaneous 'cause-effect' type measurements regarding the imposed forces (*inputs*) and the resulting responses (*outputs*) of a tested structure. This input-output relationship can be obtained in various forms such as Impulse Response Functions (IRF) or Frequency Response Functions (FRF). These two functions constitute a time-domain and a frequency-domain descriptions of a system respectively .

IRF and FRF are regarded as *secondary* characteristics as they themselves are dependent on other more fundamental ones, called *primary* characteristics. Theory shows that the dynamics of a structural system can be characterised in terms of either a modal or a spatial model. In a modal model, the primary characteristics refer to the modal parameters (as defined earlier). Modal theory stipulates that a structure's dynamics can be approximated by a scaled superposition of a sufficient number of vibration modes which are influential within the frequency band of analysis. Whereas in a spatial model, the primary characteristics refer to the spatial parameters (also defined earlier) which depict the inertial, elastic and energy dissipating properties of a system.

However, most of these parameters are 'latent' properties, usually not directly measurable quantities, and a computational algorithm is required to extract these parameters from the raw experimental FRF or IRF data. This extraction process is called parameter estimation. It enables a system's behaviour to be characterized based on only a handful of these parameters.

Having established a valid mathematical model, it enables either the imparted forces or the responses to be determined if the other one is known. *Force determination* or *response prediction* are typical applications using this methodology.

Results and findings of a particular tested structure are more-or-less pertinent to that structure only and generalisation to other structures may not be allowed unless they are similar or identical in many respects. However civil engineering structures are rarely identical. Incurring research and development costs on a one-off product, rather than spreading them over millions of identical products such as cars, is often considered as uneconomical. A concerted and structured strategy is needed so that the individual test results can benefit the understanding of different forms of structures at large.

A so-called *building block* approach is fruitful to this end. Most structures are often built with simple and repetitive structural elements as building blocks. The understanding of the dynamics of these building blocks will help one to understand those of the structure as a whole.

The lack of understanding of some integral components of a structure has close bearing to some lapses in design philosophy and practice. Current practice often chooses to ignore the structural actions of the so-called non-structural elements believing that discounting their added strength is a prudent measure. With the cost of these elements often occupying a good proportion of the total construction costs, it make economic sense to find out if these discounted in-situ structural properties can be utilised in order to achieve optimum structural efficiency. In buildings, the structural actions of partition walls and exterior cladding have, for a long time, attracted strong interests. A number of investigations into the behaviour of cladding in tall buildings were undertaken by Oppenheim ^[1.3], Palsson ^[1.4] and Freeman ^[1.5]. But so far, the findings from these investigations are not comprehensive enough to warrant change in design practice.

Similar efforts were reported by a number of earlier investigators such as **Honda** ^[1.6], **Blume and Binder** ^[1.7] in the early 1960s. They studied the changes in stiffness of a number of structures by measuring the corresponding changes in the global modal characteristics following different construction stages. This approach is obviously limited by the impracticality of performing tests within a hectic construction schedule. It is also difficult to obtain good quality data when disturbance of the sort expected to be found in a construction site is so prominent.

Computational methods were also undertaken such as an investigation carried out by **Mirtaheri**. ^[1.8] This investigation was based primarily on numerical parametric studies. By performing numerous iterative computations, he attempted to construct some feasible analytical models which could be reconciled with measured modal characteristics. This approach, inevitably by its very nature, is largely a 'hit-and-miss' exercise and it does not always guarantee success. Again, alternative strategies and methods are still required.

1.4 THE SCOPE OF THIS RESEARCH

The scope of this research covers both experimental and theoretical work. The task was tackled by research and development in a number of key areas. These key areas covered vibration generation, measurement and analysis which were all considered to be essential to achieve the following stated objectives :

- a. to develop an exciter which can excite large structures with random, sinusoidal or periodic forcing
- b. to incorporate computer control in full-scale tests in the field
- c. to develop algorithms which can extract useful information from forced vibration test data
- d. to use the developed system/technique to determine the real characteristics and performance of a full scale structure

A special rectilinear motion hydraulic inertial (RMHI) exciter was developed for exciting large structure. This exciter was capable of generating excitation which conventional eccentric rotating mass (ERM) exciters could not do. According to the literature surveyed, the application of such an exciter to excite large structure was not well

documented. This research used this exciter on two civil engineering structures using both periodic random as well as step-sine (SS) excitation methods. The periodic random control signal is based on Pseudo-Random-Binary-Sequence (PRBS) technique. The two structures tested cover different types of building and structural systems: an eleven-storey reinforced concrete (RC) frame-shear-wall office building, and a slender RC frame tower used for fire fighting training.

In accordance with the stated objectives, a so-called computer-aided-testing (CAT) system was also developed. This system was formed by integrating a number of experimental facilities with a desk top computer which provided centralised automatic control of equipment and fast digital data processing and recording. With this system, the required test sequences could be pre-programmed and the correct setting of various testing instruments be 'switched' remotely and precisely by the computer under the control of a program. This system not only reduced testing time tremendously but also allowed better quality data to be obtained because the error-prone task of manual operation was alleviated. The CAT system was an essential and indispensable part of this research since the requirement of a large amount of useful data could not be satisfied without it.

Two computational algorithms were developed by the author during the course of this research. The first algorithm carried out the task of extracting modal parameters from measured forced vibration data. The method is similar to the dynamic stiffness method but is in direct least-square formulation. Although it is based on a single-mode assumption, with proper pre-treatment of data, this algorithm can yield good accuracy. A comparison of the algorithm and two conventional methods was also undertaken for comparison purpose.

The second algorithm extracts the spatial parameters which are a set of spatial matrices (mass, damping and stiffness matrices) which characterize an equivalent or 'reduced' structural model of a structure. The procedure is a "direct" approach which distinguishes itself in some ways from other conventional modal methods. The procedure was validated using computer synthesized as well as experimentally collected data. Promising results were obtained in most cases as the determined spatial matrices do provide a good model description of the tested structures especially simple ones.

By following much the same principle, this research found that similar matrices can be derived using Strain Frequency Response data instead of Motion Frequency Response data. These matrices were also shown to be capable of providing a good model at least for the simple beam specimen tested. However, only the works using the "Motion" data are presented.

This investigation was intended to lay the ground work by solving much of the fundamental hardware and software requirements for full scale forced vibration tests. It was intended that the system developed could be used as a 'work-horse' for further investigations in the future. Results of the tests on the two structures are presented as test cases for the advocate technique.

CHAPTER 2

FORCED VIBRATIONS TESTS

ON CIVIL ENGINEERING STRUCTURES

2.0 INTRODUCTION

This chapter is a review of some of the more notable works on forced vibration testing of full scale civil engineering structures. In general, these structures are usually so massive and complex that special considerations on excitation and measurement methods are required. Therefore methods applicable to tests in conventional laboratories are usually quite different from those used in the field on full scale ones. Although this review concerns civil engineering structures in general, buildings are emphasized more because a great number of tests were carried out on them.

This review begins with a summary of the test methods with a particular reference to the means of generating excitation. This is followed by a brief description of the fundamentals of the ambient and artificial means of excitation and a few examples of their applications. A more detailed historical account of the pioneering works on artificial forced vibration tests is also given. Finally, the various contributions and limitations of these works are discussed and conclusions drawn.

2.1 REVIEW OF PREVIOUS WORKS

This review is not intended as an exhaustive account of all previous efforts but is only a highlight of those orthodox test techniques and procedures practised. In fact, a majority of these procedures is still being used today.

The literature study reveals that while forced vibration tests to other engineering structures

are reported quite extensively, only a few studies are concerned with full scale tests on civil engineering ones. The major impetus to the latter was attributed to only a few organisations notably : the Earthquake Engineering Research Laboratory (EERL) in the USA during the 50s and 60s, the Building Research Establishment (BRE) in the UK during the 70s and 80s and others in countries such as Japan and New Zealand.. Because of the strong influence from these organisations, the historical account of this development as detailed in Section 2.1.2 are naturally divided under these headings.

2.1.1 TEST METHODS

Before the invention of mechanical exciters, massive civil engineering structures could only be excited by natural means e.g. by winds and earthquakes. These means were by their very nature, not amenable to human control as regards to when and where they would occur. As a result, strictly limited information could only be obtained. Many artificial excitation methods were tried. From the one extreme where novelty methods such as explosives, gas turbine aero-engines and propulsion rockets to the other extreme where very primitive means were used. An interesting example could be found from a simple means of excitation using synchronized human body motion suggested by **Hudson et al** ^[2.1, 1964] back in 1964. It was primitive but nevertheless useful. So simple was this technique that its use was reported in other investigations. (**Czarnecki** ^[2.2, 1974] and **Williams** ^[1.1, 1979]) Whatever the forms these various excitation methods might have taken, they served the same purpose i.e. to impart force/energy to a structure and set it into vibratory motion.

2.1.1.1 AMBIENT EXCITATION TECHNIQUE

Ambient excitation sources are those disturbances originated from the environment of a structure. For civil engineering structures, these disturbances are usually due to the ground, the hydro- and atmosphere: i.e. earthquake, wave and wind. Because these sources were uncontrollable, the quality of measurements obtained from these means was inferior to those from controlled excitation. However these methods offered a viable alternative in situations where expensive artificial excitation system were not available.

2.1.1.1.1 WIND

Wind was and still is one of the most commonly used technique in the field of civil engineering for exciting large scale building and bridge structures. The physics of wind is a complex subject and is beyond the scope of this short review to give a full description. In brief, wind is a result of the movement of atmospheric air due to difference in atmospheric pressure. The characteristics of wind is governed by the so-called short-term or long-term meteorological events. Apart from mean wind speed, another important physical characteristics is the temporal variation of wind speed called gust. The latter is particularly important for dynamic consideration and the former for quasi-static one.

In 1966, **Ward and Crawford** ^[2.4, 1966] used this technique on a number of buildings. With some relatively simple equipment they demonstrated the feasibility of determining the dynamic characteristics of these buildings in this way. Since then, the interests in this technique grew and numerous researchers reported similar trials on a variety of structures : **Trifunac** ^[2.5, 1970], **Lam and Lam** ^[2.6, 1973], **Dagliesh and Rainer** ^[2.7, 1978].

2.1.1.1.2 EARTHQUAKE

Earthquake is a natural phenomenon which occurs as a result of the internal magmatic activities of the earth. However, small scale man-made earthquake can also be created for instance by underground nuclear explosion. Natural earthquake can occur with low to extremely high intensity which can produce catastrophic effects and cause damages and even destruction to structures.

As early as 1950s, **Hudson** ^[2.9, 1952] and **Housner** ^[2.10, 1959] reported the use of explosives to generate ground motions. During 1960s, **URS/ John A. Blume & Associates Engineers** conducted an extensive structural response research programme which was sponsored by the **US Energy Research And Development Administration**. This programme lasted for more than 10 years during which behaviours of a number of tall buildings resulting from nuclear underground explosions at the Nevada Test Site were monitored. In 1968, **Jennings** ^[2.11, 1963; 2.12, 1968] also reported a study on the response of yielding structures to earthquake excitation. His work improved the understanding of the failure and collapse modes of those structures due to strong ground motion.

In Japan, where seismic activity is fairly active, similar investigations were also undertaken. One such work was reported by **Hiroyoshi and Kobayashi** ^[2.13, 1960] in 1960. However, very few publications were published in English and the extent of the works in this country cannot be ascertained.

2.1.1.2 ARTIFICIALLY INDUCED EXCITATION

Artificial excitation offers many desirable benefits over ambient ones. Indeed, the invention of artificial exciters added a new dimension to the ways vibration tests were carried out. With purpose-built, sophisticated exciters, controllable forces with sufficient magnitudes can be imparted to very big structures. The spectral characteristics of these forces can be tailored to the most meticulous requirements using modern electronics and signal processing techniques. Artificial exciters have facilitated the development of many more powerful testing techniques. They came about in various shapes and forms: mechanical, hydraulic or electromagnetic etc. However, only works using the following two particular types of exciters are focused and discussed.

2.1.1.2.1 ECCENTRIC ROTATING MASS (ERM) EXCITER

The force generation mechanism in this type of exciter was based on utilizing the reactionary force due to the inertia from masses rotating at certain speeds. These masses were bolted to carriers at some eccentricity from the axis of rotation. Hence by varying masses and rotating speeds, forces of different amplitudes and frequencies were generated. With suitable arrangements of a number of these exciters, uni-directional harmonic forces or torques were produced. Such exciters are believed to have been first designed and built by **Blume** in 1934. These exciters were capable of producing 1.5 tonnes of force at about 1 Hz.

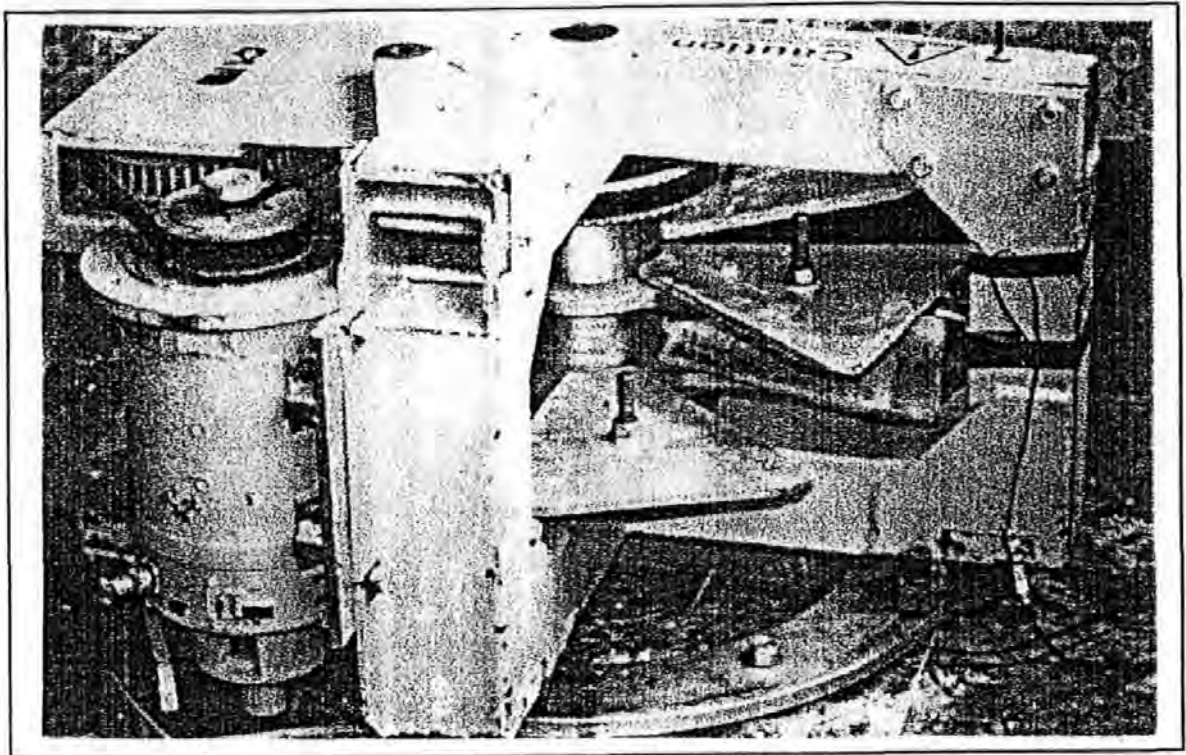
Later in 1961, **Hudson** ^[2.14, 1961] developed another one which, in many ways, was similar to the one built by Blume but was different in the novel use of synchronization. Synchronization of as many as four exciters was attempted. This system was able to generate a maximum force of 3.56 KN at 1 Hz.

Around the same period, another exciter was reported to have been developed in Japan by **Takeuchi** ^[2.15, 1960]. This was a 3-wheeled eccentric rotating mass exciter and was

capable of rotating at a maximum speed of 7 revolutions per second and generating 2.4 tonnes forces. Each wheel carried a mass of 20 Kg and a total mass of 60 Kg was required to produce this force.

Unfortunately, the attempts of synchronisation of a number of ERM exciters were unsuccessful because of the formidable problems in upholding the accuracy in speed control. Very accurate and stable speeds were required to provide a fine frequency resolution. It was not until significant improvements were achieved, by using modern electronics and control techniques, that the problem of accurate synchronization was solved. The improvements required were later adopted in the design of BRE's ERM exciters: a work undertaken by the University of Bristol. The prototype system was completed in December 1977 and the full system was operational by August 1978. A brief description of the few important characteristics of this system is given below.

The whole system comprised four separate exciters. Each one was driven by its own 'slave' control which were, in turn, under an overall control of a 'master' unit. This control was servo-driven which permitted a precision as fine as 0.001 Hz. Using crystal oscillator, the frequency of the control signals was maintained accurately to a precision of one part in 10 million. The maximum usable frequency of this exciter was about 20 Hz. The system produced harmonic forces, which were precise to within 3% of a maximum amplitude of around 1 tonne (at 1 Hz peak-to-peak). It also allowed each unit to be run either at 0 or 180 degree relative phase difference which was accurate to 0.01 radians. The exciters were mounted on heavy steel rings and designed as turnable to any desired orientation in the horizontal plane. Figures 2.1.1.2.1-1 shows one such exciter mounted in the field.



Figures 2.1.1.2.1-1 A photograph featuring the BRE's ERM exciter mounted in the field.

2.1.1.2.2 RECTILINEAR MOTION EXCITER

As a distinct contrast to ERM exciters, a rectilinear motion exciter operates in reciprocal and rectilinear motions. Hence it is able to generate a unidirectional force with just one unit. There is no need for delicate balancing as required in the case of ERM exciters. Most rectilinear motion exciters belong to the electromagnetic, magnetostrictive or piezoelectric types. However the drawbacks common to these exciters are very small force and stroke capacities and therefore are not applicable to massive structures.

Another type of rectilinear motion exciters is hydraulically operated and is branded as rectilinear motion hydraulic inertial (RMHI) exciters. As far as the author is aware, there is only a handful of literature reporting any attempt in the design, construction and application of such exciters. According to the literature surveyed, one of the first of these attempts was reported to have been undertaken by **Burrough et al** ^[2.16, 1970] of the Central Electricity Generating Board, UK in 1970. This exciter was reported as capable of generating a maximum of 11 tonnes force when operating at 0.46 Hz. This development marked a significant departure in the means of generating excitation force at low frequencies. Another attempt was reported by **Stephen, Hollings and Bouwkamp** ^[2.17, 1973] in 1973 but the outcome of this development was not reported. In

1979, **Galambos and Mayes** ^[2.18, 1979] also reported using this type of exciter on an apartment block due to be demolished. However further details about this work was unable to be obtained.

2.1.2 A HISTORICAL ACCOUNT

A brief historical account of the developments in the early days in USA, UK, Japan and other places is given.

2.1.2.1 THE PIONEERS

The subject of resonance of a complete structure was first noted by **Omori** ^[2.19, 1901] in 1901. Later in the 1930s, a programme to investigate buildings' dynamic response was commissioned by the **U S Coast And Geodetic Survey** ^[2.20, 1936] after a string of disastrous earthquakes in California which caused a lot of damage to buildings and people. As a consequence of this programme, In 1934 **Blume** designed and built the first ERM exciter and used it to characterize the periods of vibration of some 212 buildings.

Later in 1958, **Hudson**, ^[2.21, 1961] of EERL, developed this type of exciter further to produce a new system capable of synchronizing several exciters. Around the same time, there was a similar development in Japan. Between 1960 and 1965, **Takeuchi** ^[2.15, 1960] and **Karapetian** ^[2.22, 1965] tried out their own designed ERM exciters on a large number of buildings in Japan. One of their major achievements was the successful compilation of the experimental results to produce a set of very useful empirical formulae describing the relationships between certain building characteristics in relation to their natural frequencies. These empirical formulae are widely adopted in various building design codes in a number of countries. They are valued as a very simple but useful guide for the initial stages of building design. (further details on these formulae can be found in Section 2.2.3)

Literature on the subject during these periods are in general very patchy. However it is reasonable to believe that these people are the pioneers in the practice of artificially induced forced vibration tests on civil engineering structures. **Hudson** ^[2.23, 1964] and more recently **Jeary** ^[2.24, 1981] have summarized these early developments.

2.1.2.2 THE EARTHQUAKE ENGINEERING RESEARCH LABORATORY (USA)

Research at EERL was started as early as 1950s by a number of eminent and internationally renowned academics in the field of earthquake engineering : Hudson, Housner, Keightley and Caughey etc. EERL was based at the Dynamic laboratory, Disasters Research Centre, California Institute of Technology in USA. In addition to the role as a leading research establishment in this field, EERL also served as an information centre administering the publication and distribution of research reports and earthquake accelerograms to the earthquake engineering communities.

A programme of research was initiated at EERL under the sponsorship of the California State Division of Architecture and Construction. This research was marked by the development of **Hudson's** ERM exciters in 1958. This work started a 'chain-of-reaction' later and as a result, a series of research programmes on buildings were carried out by various EERL researchers: **Hudson**^[2.25, 1964] **Keightley et al**,^[2.26, 1961] **Keightley**,^[2.27, 1963] **Nielsen**,^[2.28, 1964] **Bouwkamp and Blohm**,^[2.29, 1966] **Kuroiwa**^[2.30, 1967] and **Jennings**^[2.31, 1971].

Nielsen used Hudson's exciters on two multi-storey buildings. Among his various achievements was the formulation of a series of equations from which the stiffness and damping matrices could be determined using known information about the mass matrix and the experimentally determined modal properties of a tested structure. These equations were developed specifically for buildings which fitted the 'shear building' models and had infinitely rigid floors. He noted that because these equations were ill-conditioned, large errors often occurred in obtaining these matrices.

Jennings and Kuroiwa^[2.32, 1968] used the EERL's exciters on a library building with an objective to study the damping characteristics of this building. From the field measurements taken from this building, he discovered that the energy dissipation characteristics (measured as damping factors) of this structure tended to vary markedly with the amplitude of vibration and its loading history. The damping factors were found to vary somewhere between 0.006 and 0.02 during small and large amplitude vibrations. Larger amplitude vibrations were indicative of the energy dissipation levels to be expected in really strong earthquake conditions. They undertook another research project on another building with an objective of characterizing the interactions of the motion of the structure with its surrounding soil. During the course of this study, they discovered that the

building acted as a 'force amplifier' (i.e. a force transmissibility larger than unity). This capability of amplifying the forces produced by a small excitation equipment to bigger forces imparting on the surrounding soil was perceived as a novelty at the time. It was regarded as such because without this technique, equipments of much larger scale would be required to produce such magnitudes of force on the soil directly.

Over a period of forty years, their works covered tests on a range of structures : dams, buildings and bridges etc. Further details on their works can be found in the cited publications by the EERL or the Earthquake Engineering Research Centre (EERC). The latter was a new organisation set up jointly by EERL and the University of California, USA. The EERC now performs much of the previous roles of the EERL. Their recent research activities include forced vibration tests on a number of concrete dams as reported by : **Clough and Chang** ^[2.33, 1984] of EERC and **Hall and Duron** ^[2.34]

2.1.2.3 THE BUILDING RESEARCH ESTABLISHMENT (UK)

In the UK, a long-term research programme was also initiated in the 1970's by the Building Research Establishment. The BRE is a government owned research establishment under the auspice of the Department of Environment, and is responsible for promoting research on subjects appropriate to the building and construction industries. The programme of work during this period was conducted in collaboration with a number of other organisations. The thrust behind these developments was the needs to provide real information regarding the dynamics of civil engineering structures, especially tall buildings. As a result of these works, the BRE has carried out one of the most extensive full scale dynamic test programme on civil engineering structures in this country. The structures investigated ranged from tall buildings, bridges, chimneys off-shore platforms to dams. Both wind and artificial forced vibration test techniques were used. A short extract from this wide spectrum of works are briefly described below.

Tests on several large multi-flue chimneys were carried out by **Jeary and Winney** ^[2.35, 1972] and **Jeary** ^[2.36, 1974] in the early 1970s using wind excitation technique. This work was a collaboration between the BRE and the CEGB. The results from field measurements reinforced a view that dissipation of most of the vibrational energy in these structures was due to the fundamental bending mode and that the damping values for this mode were

within the range from 0.03 to 0.05. These results justified the usual assumption of a value of 0.06 for damping in the design of these structures. This is a good example to show how experimental findings interact with design practices.

A rockfill dam and a buttress dam were also tested by **Severn et al** ^[2.37, 1979; 2.38, 1980] in late 1970s using the BRE exciters. This work was a collaboration between BRE and the University of Bristol. Amongst other things, this work discovered that the resonance frequencies of these dams had reduced as water level rose and that the experimental results were in good agreement with those from the corresponding three dimensional (3D) Finite Element (FE) models. This is yet another example illustrating the value of testing for validating analytical models. The results also demonstrated that forced vibration tests using artificial excitation on massive structures such as dams was plausible. Such application was considered unthinkable before.

Later, more research on more buildings continued covering a wide variety of building types and heights. They ranged from a 177 m high concrete communication tower to a 21m high office block. The programme of works during this period was marked by the collaborative efforts between the BRE and other organisations and by the proliferation of this technology to a wider sphere. The various organizations which had a formal involvement in this work included the Centre Experimental de Recherches et d'Etudes du Batiment et des Trauvau Publics (France), Plymouth Polytechnic (now University of Plymouth) (UK) and University of Sheffield (UK). The results concerning the dynamic swaying characteristics of these buildings were reported by **Jeary and Sparks** ^[2.39, 1977].

A short extract of these findings are reproduced below :

- a. Buildings which possessed shear walls and cores on the whole were found to have better sway resistance than those of similar dimensions that did not.
- b. Cladding and partitions added additional stiffness against swaying : a structural action not quantifiable in design but measurable from experiment.
- c. Torsional movements in buildings were a significant component of building's response to wind in addition to swaying.
- d. Asymmetry in the distribution of mass and stiffening elements could lead to severe coupling between modes and produced complicated mode shapes.
- e. A well designed building possessing reasonable amounts of shear and

bending resistance would normally have a fundamental mode shape of a straight line. Any deficiency in shear resistance would have made a building to take up a shear deformation mode which, for a given mass distribution, would have a higher associated modal mass than a straight line mode.

- f. The modal damping factors for reinforced concrete buildings were found to be less than 0.015 in the normal circumstances. By implication, those buildings possessing damping factors in excess of this level could be suspect of suffering damages or considered as inadequately designed.

Their more recent research efforts include testing the Humber suspension Bridge in Humberside and Hume Point (the sister block of the infamous Ronan Point tower block) in London. Full details of their works are obtainable from the BRE publications. In summary, the contributions by BRE and others during the early periods were instrumental in consolidating the state-of-the-art of full scale forced vibration tests on tall buildings. The ERM exciter provided a good 'work horse' and established the position of artificial forced vibration testing as a useful structural diagnostic tool.

2.1.2.4 OTHER INVESTIGATIONS

This section samples and summarises research efforts by other individuals not already described above. Significant contributions were due to those in Japan : **Kawasumi et al** [2.40, 1956], **Hisada et al** [2.41, 1956] and **Takeuchi** [2.15, 1960] whose works mirrored closely those of the EERL during the 1950s. As their works have already been described in other sections of this report, it is not to be repeated here.

Englekirk and Matthiesen [2.42, 1967] reported tests on an eight storey reinforced concrete building using mechanical exciters to determine both translational and torsional responses of this building. They used two ERM exciters to generate excitation torques by running the two exciters at 180 degree out of phase. By doing so, they could excite large torsional response allowing a more accurate measurement of the centre of torsion of this building. This work is noted as one of the earliest attempts to excite a structure with a torque .

Much concern in the earlier days was focused on the interaction between cladding and

the main frame structure and recognized that full scale dynamic testing could provide an answer. A number of attempts tried to determine the effects on stiffness of structures from these non-structural elements. Some of these attempts were based on a methodology of detecting changes in modal characteristics at different stages of construction. **Blume and Binder** ^[2.43, 1969] used this method on a 15 storey high steel frame building. **Honda** ^[2.44, 1976] followed a similar line of thinking and his tests on three buildings revealed that reduction of some 60 to 70% of the periods of vibration could result from the addition of partitions.

More recent efforts along this line were also noted. **Palsson** ^[2.45, 1982] reported an investigation on the influence of heavily contoured precast concrete cladding panels on the overall dynamic behaviour of a 25 storey building. The building was symmetrical in the two principal directions and was of shear core construction. This study was both experimental and analytical. **Huang** ^[2.46] reported tests on two buildings to determine the changes in behaviour at different levels of excitation. His investigation showed that floor slabs did not behave as rigid diaphragms as normally assumed and that base movements were found to be too significant to be ignored. Such an assumption are still widely taken in the usual analysis of this type of structures.

Oppenheim ^[2.47, 1978] carried out similar studies on several buildings including a 20 storey reinforced masonry apartment block. His work led to the discovery of a behaviour mechanism between lintels and reinforced masonry walls which most analysis did not anticipate.

In summary, all the investigations reviewed here provide useful but fragmented information on the real behaviours of a range of civil engineering structures. Very few of these discoveries or findings have filtered through to be incorporated accordingly in design practice. The method of carrying out tests at different stages of construction was not entirely feasible both on technical or practical grounds. All these lead to a common conclusion i.e. much research effort is still needed to circumvent difficulties in the practice of full scale forced vibration tests on civil engineering structures.

2.2 CONTRIBUTIONS OF PREVIOUS WORKS

2.2.1 INFORMATION FEED BACK

To date, a wealth of knowledge about the real dynamic behaviours of tall building structures has been obtained. These findings help to substantiate certain facts which cannot have otherwise been found. Such information is invaluable in providing feed back to civil/structural designers to appraise their design i.e. to evaluate the assumptions and suggestions provided in design literature rather than accepting them without question.

Various subject areas necessary for further research are also highlighted after these works. They include :

- the behaviour of tall buildings at various amplitudes of vibration i.e. non-linearity,
- the interactions of structures and soils,
- the interactions of structural and non-structural elements and finally,
- the significance and effects of torsional responses of building structures.

These continue to be subjects of great interest in civil /structural engineering.

2.2.2 JUSTIFICATION OF THE USE OF SIMPLE MODELS

For tall building structures of slight structural and geometrical complexities, simple lumped mass model are deemed acceptable in providing a first approximations of the natural periods of these structures. A multistorey building structure, of the sway-frame or central-core type construction, can be modelled as a 'shear building'. In formulating such a model, the masses of each floor level are lumped together at the floor level and the inter-storey lateral stiffness lumped together as a shear beam between the floors. Such idealization is found to be appropriate and more economical than formulating a full FE model. This modelling approach is adopted in a British design guide published by the Engineering Science Data Unit (ESDU a commercial establishment which provides authoritative and validated design methods and data for design). Recommendations are provided in the forms of design data sheets or computer software programs (see ESDU [2.48, 2.49, 2.50]).

2.2.3 EMPIRICAL RELATIONSHIPS

The results of these full-scale tests on building structures are compiled to obtain a set of empirical formulae using statistical analysis techniques. These empirical relationships provide a means of estimating the natural frequencies f_{nat} (or natural periods, T which are the inverse of natural frequencies) and the levels of damping of a building structure by simply considering a building's architectural characteristics such as the type, height H , number of storeys N , width B .

Taniguchi ^[2.51] proposed the formula to calculate the fundamental natural period T of translational vibration of a building:

$$T = N * (0.07 \text{ to } 0.09)$$

Takeuchi ^[2.15] derived similar formulae based on the tests results of some 60 buildings carried out in the 1960s. His formulae modified Taniguchi's formula by the inclusion of a new parameter r : the *wall ratio* of a building (the total length of all walls divided by the sum of the floor areas of all floors). It is noted that other characteristics of the walls such as thickness and the positions of the walls were not considered. His results indicated that most experimental data on T were bounded by the values calculated by the following two equations :

$$T = \frac{ \{ 4 + H * (1 - 4 r) \} }{50}$$

and

$$T = \frac{ \{ 4 + H * (1 - 4 r) \} }{80}$$

Other empirical relationships were also derived to determine the natural period of higher modes, such as :

$$(T_{\text{of the 2nd mode}}) = 3 * (T_{\text{of fundamental mode}})$$

More recently, **Ellis** ^[2.52] has also derived similar empirical formulae based on the field test results of a total of 163 buildings. Again these formulae utilize the overall dimensional characteristics of buildings as inputs parameters. The formulae are expressed as:

the natural frequency of the lowest translational mode:

$$f_{nat} = \frac{46}{H}$$

the natural frequency of the next lowest orthogonal translational mode:

$$f_{nat} = \frac{58}{H}$$

the natural frequency of the lowest torsional mode:

$$f_{nat} = \frac{72}{H}$$

Most of these formulae are accepted in various British, Japanese and American Building Design Regulations and Codes of Practice [2.53, 2.54, 2.55]. Although large errors are likely to occur in using these formulae, the simplicity of calculation is still an invaluable asset. These formulae are particularly useful because they permit an early estimation of the fundamental natural frequencies of a building long before any structural details are known. Any potential problem in terms of structural vibration can be spotted as earlier as when the overall architectural or dimensional details are finalised.

Like natural frequencies, damping factors of a building structure can also be estimated using similar empirical relationships. For instance, ESDU [2.56] compiled the results of damping measurements from full-scale tests on a range of concrete and steel buildings to produce a series of design monographs. Except for some unusual structures, the estimates are generally acceptable.

2.3 LIMITATIONS OF PREVIOUS WORKS

Due to the lack of sophisticated instrumentation and computer equipment in the past, the results obtained are still somewhat scant and inconclusive.

2.3.1 QUANTITY OF MEASUREMENTS

Most civil engineering structures are complex in terms of sizes and structural complexities. For these structures, a large number of Degrees of freedom (DOFs) (hence the quantities

of measurement) are necessary to produce better models. Most pieces of equipment used in these studies were bulky and slow to operate. For instance, a modest computer was a bulky cabinet in those days rather than a small lap-top of today. To bring a computer to the field was unimaginable. As a result, only a very limited amount of data could be obtained within a short time. To gain any benefit from modern system identification methods, more measurements are required.

2.3.2 QUALITY OF MEASUREMENTS

The primitive testing equipment and inefficient procedures produced inferior results as judged by today's technology standard. Most equipments used in those days were not only laborious to use but also very troublesome to calibrate and to set up. Often, measurement records were analog and not digital in form. As a result, data retrieval and transfer were difficult and inaccurate. The quality of these measurements was also generally undermined because the tested structures were situated in their natural and uncontrollable environment. Extraneous sources of disturbance due to wind, traffic and human activities could not be eliminated. Noisy, spurious and incoherent measurements caused formidable problems to these investigations and limited their potentials..

2.3.3 TEST METHODS

Ambient excitation techniques lack the sophistication and controllability that artificial excitation techniques have. Furthermore, they do not allow the direct measurement of the excitation forces. Hence the causality relationship, in terms of both amplitudes and phases, between the excitations and the responses cannot be determined. Consequently, these shortcomings render the aforementioned methods inappropriate and incomplete within the context of system identification.

ERM exciters offer some improvements but because they can only generate harmonic forces of a fixed frequency at any one time, they are both laborious and very time intensive to use. In fact, man-power and time are often the most precious resources in any field test programme. Therefore wide band random test techniques can have greater potentials in this respect.

2.4 CONCLUSIONS

In conclusion, this literature study has highlighted the difficulties and shortcomings of the traditional methods used and suggested certain areas in need of improvement. Learning from these experiences, the priority in this research must be to device new test and data analysis methods to circumvent some or all these difficulties.

CHAPTER 3

THEORY

3.0 INTRODUCTION

Although this project is civil engineering oriented, much of the theories are not normally found in civil engineering. So instead of going straight into the theories on experimental modal analysis (introduced in Section 1.2), for the benefits of the readers from the civil engineering background, this chapter is presented under the main theme of mathematical modelling. Under this theme, this research is identified as an experimental modelling approach as a contrast to a theoretical modelling approach such as finite element method which most civil engineers are familiar with. The bulk of the theories concerning experimental modal or spatial analysis are saved for deliberation in much greater depth later in chapters 5 and 6.

Much of the background theories underpinning this research come mainly from vibration and control engineering. The two disciplines share a lot of common ground. In fact, the mathematical foundations governing systems in control and structural vibration are strikingly similar. Nevertheless, formulation of equations and terminology differs a great deal. This chapter is not meant to be an exhaustive account of these theories but only an introduction to the ideas described in the following chapters.

There is no shortage of literature which deals with these theories in great depth. Some literature deal with very fundamental mathematical concepts such as *existence* and *uniqueness* of solutions to a formulated vibration problem. Others deal with highly complicated theoretical issues such as *non-linearity* etc. However, few practical engineers would find these theories interesting to read. A simplified approach is therefore presented here.

The concept of mathematical modelling in a wider context is introduced first. The more specific application of modelling to structural dynamics is then explained. It is considered convenient and conceptually important to describe the conventional theoretical methods under the two categories: continuous (Section 3.2.1) and discrete approaches (Section 3.2.2) applicable to distributive and lumped systems respectively.

The steps leading to the derivation of the governing system equations are described: partial differential equations in the case of a continuous system or a set of linear ordinary differential equations in the case of a lumped system. The methods of solution of these equations are also briefly discussed.

In particular, Eigenvalue solution (Section 3.2.2.2.2), interpretation of Modes of Vibration (Section 3.2.2.2.3) and Orthogonality properties between different modes of vibration (Section 3.2.2.2.4) are introduced in this Chapter. Because these are important theoretical issues which need to be explained and are necessary pre-requisites before deliberating further theories in Chapter 5 and 6. The coverage in these Sections is intended to explain the concept of modal decomposition which forms the whole basis of theoretical and experimental modal analysis. The theories dealing with real modes (associated with undamped or proportionally damped systems) and complex modes (associated with generally or nonproportionally damped systems) are explained in much greater depth in Section 3.2.2.2.5.

The theoretical basis of the experimental approach of modelling, upon which this project is based, is reviewed in Section 3.3. The concept of system identification is introduced in Section 3.3.1 followed by the implementation of this methodology as given in Section 3.3.2. Data measurement and analysis methods are briefly explained in Section 3.3.2.3. Modal methods which derive models in terms of a system's modal parameters are briefly explained in Section 3.3.2.3.1. Non-modal (or spatial) methods which derive models in terms of a system's spatial parameters are also briefly explained in Section 3.3.2.3.2.

3.1 CONCEPTS AND APPROACHES

In essence, the basis of the approach of this investigation can be summarised as an exercise of *mathematical modelling*. The term *mathematical* is important here because it distinguishes itself from *physical modelling* which is the one usually perceived. Physical

modelling is a technique based on the Law of Similitude. By studying a reduced scale replica of the original structure, results are then extrapolated to those of the full scale structure. However the latter is not a subject of concern within the scope of this investigation.

3.1.1 MATHEMATICAL MODELLING

Mathematical modelling is a process in which a complex physical system is conceptualized and simplified so that it can be expressed in mathematical terms i.e. a series of so called *Governing Equations*. These equations are equivalent statements of some Laws of Physics, such as the Law of Conservation of Energy and the Newtonian Laws of Motion etc to name a few which are commonly used in the field of mechanics. Having formulated the governing equations in an appropriate form, a *closed-form* analytical solution can often be sought in the case of a simple model or an approximated solution in the case of a complex model, using available analytical or numerical methods.

The derived mathematical representation is called a *model* whose major function is to characterize and predict the behaviour of the system studied. A useful model should be one which can make correct prediction in some if not in all situations. Most physical systems in the 'real world' are often too complex for any one model to take into account every single conceivable aspect affecting the system. Important factors have to be correctly chosen and less significant ones be discarded. This process is called *conceptual idealization*. The well established fundamental Laws of Physics which most models are built upon are themselves products of conceptual idealization of nature.

Because idealized assumptions are introduced, the subsequent established model can only be treated as an approximation rather than an exact representation. Mathematical modelling is an art which requires both skill and good judgement rather than sheer manipulations of arithmetic. In most situations, this is carried out iteratively until arriving at an optimal model. This is particularly true for unfamiliar systems whose behaviour is not well understood.

3.1.2 STRUCTURAL MODELLING

Within the scope of structural mechanics, mathematical modelling is an essential and an

integral process in analysing structural/mechanical systems: from modelling of behaviours of structural materials, of simple structural elements such as beams and plates to those of complex integral structures in various shapes and forms.

In structural dynamics, structural resonance phenomena can be modelled quite successfully using Eigenvalue theories. Briefly speaking, the natural frequencies and mode shapes of a structure are analogous to the eigenvalues and eigenvectors of the corresponding *system equations* formulated for the structure (Sections 3.2.2.2 will give more details on this). Because mathematical modelling can provide a far-reaching insight into the dynamic characteristics of a structure, even before the structure is built, it is a very useful design and analysis tool.

In essence, the formulated *governing equations* furnish a relationship between the state of the system (or *state variables*) and the *system parameters*. In fluid mechanics, these variables are kinematic quantities such as flow velocity; thermodynamic quantities such as pressure, temperature, enthalpy or entropy. In structural dynamics, the state variables are force (or stress), displacement and its derivatives (or strain/deformation) at a spatial point (or coordinate) of a structure.

The system parameters refer to those quantities, usually constants in the temporal (time) domain, which depend on the geometric, configurational and the constitutive properties of materials of a system. At the microscopic (or material) level, these parameters refer to the Young's modulus, Shear modulus or Lamé constants in the case of homogeneous and isotropic structural materials. Whereas at the macroscopic (or structural) level, these parameters are the inertial, stiffness and damping characteristics of an integral structure. It is the method of determining structural parameters (at the structural level) which is the principal concern of this investigation.

Structural models can have varying degrees of sophistication. In many cases, simple methods are more preferential to use (especially for initial design purposes) than sophisticated ones as the latter often require considerable computational efforts. With the advances of computer technology and methods, models derived from finite elements or boundary elements theories are becoming increasingly popular and sophisticated.

Apart from theoretical means, the advances of computer and instrumentation technology

also allow structural modelling to be pursued by experimental means as well.

3.2 THEORETICAL APPROACHES OF MODELLING

The various approaches are explained according to the logical division of continuous and lumped systems. It can be shown that the equations of motion for both systems can be derived using the same set of principles. Among these principles, the Principle of Virtual Work (for static equilibrium cases) can be applied. This principle states: If a system of forces is in equilibrium, the work done by the externally applied forces through virtual displacements (compatible with the constraints of the system) is zero. For dynamic cases, the Virtual Work Principle can be extended to cover *dynamic equilibrium* using D'Alembert's principle which states that the resultant force must be in equilibrium with the inertia force in a system. Using Variational principle such as the Hamilton's principle, which reduces the problems of dynamics to the investigation of a scalar integral that does not depend on the coordinates system used. The Equations of Motions are obtained from the condition rendering the value of the integral stationary and this is the basis of the Lagrange's Equation.

3.2.1 CONTINUOUS SYSTEMS

A continuous system (or a continuum) is an assemblage of an infinite number of infinitesimally sized particles. All structures, apart from molecular or atomic structures, are continua by nature. By applying the Principles of Equilibrium for each individual particle, the differential equations of motion can be obtained. Alternatively, by integrating these equations within the boundary and domain of a continuum, the integral equations of motion can be obtained. The solution of these differential and integral equations in turn describes the distribution and the gross effects of the state of a system respectively.

A complete theory can be obtained from the mathematical theory of elasticity of solid bodies in general, and elastodynamics in particular. These theories deal with the determination of the state of infinitesimal strain within a solid body which is being subjected to the actions of an equilibrating system of forces. The restriction of infinitesimal strain is important to ensure the validity of linearization of the governing equations to be given below. Nonlinear equations are known to be notorious for presenting

difficulties in numerical treatment. Once the equations are linearized, complete solutions can be obtained by superposition of simpler solutions. Other simplified theories based on elementary theory of engineering mechanics are, in fact, derivatives or special cases of these theories. An excellent historical account of the development of the theories of structural modelling is given by Love ^[3.1].

3.2.1.1 FORMULATION OF PROBLEMS

In 1827, Navier derived a set of general governing equations of vibration of elastic bodies based on infinitesimal strain (geometrical compatibility) and stress (force equilibrium) analyses. These equations are now widely known as the **Navier Equations** which are fundamental to almost all continuum mechanics analysis. Full coverage of this theory is prohibitively long, therefore readers should find the missing details in other standard text books on this subject such as the one written by Love ^[3.1].

The state of strain and stress in the body of a material is usually represented by tensors ϵ_{ij} and σ_{ij} respectively (using indicial notation) as given below :

$$[\epsilon_{ij}] = \begin{bmatrix} \epsilon_{11} & \epsilon_{12} & \epsilon_{13} \\ \epsilon_{21} & \epsilon_{22} & \epsilon_{23} \\ \epsilon_{31} & \epsilon_{32} & \epsilon_{33} \end{bmatrix} \quad 3.2.1.1-a$$

$$[\sigma_{ij}] = \begin{bmatrix} \sigma_{11} & \sigma_{12} & \sigma_{13} \\ \sigma_{21} & \sigma_{22} & \sigma_{23} \\ \sigma_{31} & \sigma_{32} & \sigma_{33} \end{bmatrix} \quad 3.2.1.1-b$$

The spatial displacement of each particle of the continuum is represented by a vector $\{u\}$ (or u_i for $i = 1, 2, 3$ according to the convention of indicial notation which denotes x_i

, x_2 , x_3 or x, y, z in the rectangular Cartesian coordinates) and the various strain components can be determined by pure consideration of geometry of small deformation.

$$\epsilon_{ij} = \frac{1}{2} * (u_{i,j} + u_{j,i}) \quad (3.2.1.1-2a)$$

$$\text{where } u_{i,j} \equiv \frac{\partial u_i}{\partial x_j} \quad (3.2.1.1-2b)$$

The stress and strain tensors are both symmetric,

$$\text{i.e. } \sigma_{ij} = \sigma_{ji} \text{ and } \epsilon_{ij} = \epsilon_{ji} \quad (3.2.1.1-3)$$

There are six independent stress and strain components which occupy the upper triangles of the respective tensors. The condition of the equilibrium of forces in an infinitesimal particle allows the derivation of the *equilibrium equations*.

$$\sigma_{ij,j} + F_i = P * u \quad (3.2.1.1-4a)$$

where F_i is the internal body forces

P is the *surface traction*

or these differential equations can be written in symbolic form as :

$$\mathcal{L}(\sigma_{ij}) - P = 0 \quad (3.2.1.1-4b)$$

Where \mathcal{L} is a function of differential operators.

The equations depicted above hold generally regardless of the materials involved. However, the relationship between stress and strain is a function of the properties of a material known as the *constitutive relations*. In mathematical terms, this means that the stress and strain tensors are linked together by fourth order elastic constants tensor c_{ijkl} .

$$\sigma_{ij} = c_{ijkl} * \epsilon_{kl} \quad (3.2.1.1-5)$$

Each coefficient c_{ijkl} of this tensor is an elastic constant. For isotropic and homogenous materials, these coefficients are functions of only two independent material constants called the Lamé constants. It can also be shown that the usual material constants: the *Young's modulus* E and *Shear modulus* G , can be expressed in terms of the two *Lamé constants* λ and μ . Using indicial notation, this relationship can be written as :

$$\sigma_{ij} = \lambda * \delta_{ij} * \epsilon_{kk} + 2 * \mu * \epsilon_{ij} \quad (3.2.1.1-6)$$

In the absence of internal body forces F_i , the following Navier's equations can be obtained:

$$\rho \frac{\partial^2 u_i}{\partial t^2} = (\lambda + \mu) \frac{\partial \Delta}{\partial x_i} + \mu \nabla^2 u_i \quad (3.2.1.1-7)$$

where ρ is mass density of material

and Δ , ∇^2 are given in *extenso*:

$$\Delta = \frac{\partial u_1}{\partial x_1} + \frac{\partial u_2}{\partial x_2} + \frac{\partial u_3}{\partial x_3} = \epsilon_{11} + \epsilon_{22} + \epsilon_{33} \quad \text{called the dilatation}$$

$$\nabla^2 = \frac{\partial^2}{\partial x_1^2} + \frac{\partial^2}{\partial x_2^2} + \frac{\partial^2}{\partial x_3^2} \quad \text{called the Laplacian Operator}$$

After some manipulations, these equations can be reduced to the well known *Wave Equations* which describe the propagation of dilatational and shear waves in solids or the vibratory motions in an elastic continuum. Detail discussions on this subject are given by Clark ^[33].

A closed-form solution can only be obtained if the compatibility (or integrability) requirements are also satisfied in addition to the equilibrium and constitutive requirements. This is because the condition of a stress distribution in equilibrium with the given imposed

loads does not necessarily imply a compatible strain field and vice versa. The compatibility equations are given below:

$$\frac{\partial^2 \epsilon_{11}}{\partial x_2 \partial x_3} = \frac{\partial}{\partial x_1} \left(-\frac{\partial \epsilon_{23}}{\partial x_1} + \frac{\partial \epsilon_{31}}{\partial x_2} + \frac{\partial \epsilon_{12}}{\partial x_3} \right) \quad (3.2.1.1-8a)$$

$$\frac{\partial^2 \epsilon_{22}}{\partial x_3 \partial x_1} = \frac{\partial}{\partial x_2} \left(-\frac{\partial \epsilon_{31}}{\partial x_2} + \frac{\partial \epsilon_{12}}{\partial x_3} + \frac{\partial \epsilon_{23}}{\partial x_1} \right) \quad (3.2.1.1-8b)$$

$$\frac{\partial^2 \epsilon_{33}}{\partial x_3 \partial x_1} = \frac{\partial}{\partial x_3} \left(-\frac{\partial \epsilon_{12}}{\partial x_3} + \frac{\partial \epsilon_{23}}{\partial x_1} + \frac{\partial \epsilon_{31}}{\partial x_2} \right) \quad (3.2.1.1-8c)$$

$$2 \frac{\partial^2 \epsilon_{12}}{\partial x_1 \partial x_2} = \frac{\partial^2 \epsilon_{11}}{\partial x_2^2} + \frac{\partial^2 \epsilon_{22}}{\partial x_1^2} \quad (3.2.1.1-8d)$$

$$2 \frac{\partial^2 \epsilon_{23}}{\partial x_2 \partial x_3} = \frac{\partial^2 \epsilon_{22}}{\partial x_3^2} + \frac{\partial^2 \epsilon_{33}}{\partial x_2^2} \quad (3.2.1.1-8e)$$

$$2 \frac{\partial^2 \epsilon_{31}}{\partial x_3 \partial x_1} = \frac{\partial^2 \epsilon_{33}}{\partial x_1^2} + \frac{\partial^2 \epsilon_{11}}{\partial x_3^2} \quad (3.2.1.1-8f)$$

Equation (3.2.1.1-7) formulates the problem entirely in terms of displacements u_i . The true solution would also require u_i to satisfy the prescribed boundary displacement condition as well. However since the problem is posed entirely in terms of displacements, compatibility Equation (3.2.1.1-8) will be satisfied automatically.

3.2.1.2 METHODS OF SOLUTION

Having derived the partial differential governing equations, it remains to find a solution when traction and displacements on the boundary of a continuum are prescribed.

Under suitable conditions, a unique closed-form solution depicting the stress and strain state of each particle can be determined.

There are a variety of methods available to solve these equations: series, singularities, difference, collocation and variational methods to name a few. However it is beyond the scope of this thesis to fully explain these methods. Further details can be found in **Love** ^[3.1] and **Richards** ^[3.4].

3.2.2 DISCRETE OR LUMPED SYSTEMS

A closed-form solution to the governing differential equations shown in Section 3.2.1 can be very difficult to obtain except for simple cases only. An alternative approach can be applied using approximations. This approach performs a conceptual subdivision of the continuous domain into discrete elements of simpler forms. This process is often known as *discretization*. There are two different techniques available in this respect i.e. a *domain* discretization method typified by Finite Element Methods (FEM) and a *boundary* discretization method typified by Boundary Element Methods (BEM). In domain methods, the governing equations of the problem are approximated over the region by functions which fully, or partially, satisfy the boundary conditions. However in boundary methods, approximating functions are used which satisfy the domain but not the boundary conditions. Though BEM are claimed to have certain advantages over FEM in some ways, such as :

- a. a smaller problem size in term of data storage and computation,
- b. more efficient in handling problems with an infinite domain or small surface to volume ratio and
- c. quicker to converge to a solution etc,

FEM are more popular with many commercial software available such as PAFEC, NASTRAN and ANSYS etc. In contrast, very few commercial BEM software are available.

3.2.2.1 FORMULATION OF PROBLEM

FEM and BEM can be derived from the Weighted Residual, Variational or Functional principles. Furthermore, it can be shown that the Weighted-Residue theory can provide

a unified description of both methods (see **Brebbia** ^[3.51]). The Weighted-Residual methods are numerical procedures for approximating the true solution u_0 of a set of differential equations of the form :

$$\mathcal{L}(u_0) = P \quad \text{in } \Omega$$

3.2.2.1-1

where Ω is the domain

when subjected to the following boundary conditions:

$$\begin{aligned} &\text{essential boundary conditions } G(u_0) = g \text{ (on } \Gamma_1) \\ &\text{and natural boundary conditions } S(u_0) = q \text{ (on } \Gamma_2) \end{aligned}$$

3.2.2.1-2

where Γ_1 and Γ_2 is the total boundary

The approximate solution u of the true solution u_0 is approximated by a set of functions $Y_k(x)$ such as:

$$u = \sum_{k=1}^N \alpha_k Y_k(x)$$

3.2.2.1-3

*where $Y_1(x), Y_2(x) \dots Y_k(x) \dots Y_N(x)$ are a set of linear independent functions
and $\alpha_1, \alpha_2 \dots \alpha_k \dots \alpha_N$ are a set of undetermined parameters*

The *residual error* is defined as the error function ε as depicted in the following equation

$$\varepsilon = \mathcal{L}(u) - P \neq 0$$

3.2.2.1-4

This *residual error* is generally non-zero except in the case of an exact solution. However this can be forced to zero in an average sense by a weighted integral of the

following form:

$$\int \epsilon \Psi_i dx = 0 \quad \text{for } i = 1, 2, \dots, N \quad 3.2.2.1-5$$

where Ψ_i is a set of weighting functions

Convergence towards the exact solution is achieved as the number of terms increase. A variety of methods are available: the Galerkin's and the Rayleigh-Ritz methods to mention a few. However, a unified description of these methods can be obtained using the ideas of weighting functions w . In its simplest description, the governing equation 3.2.2.1-1 can be re-written by the introduction of weighting functions :

$$\int (\mathcal{L}(u) - P) * w * d\Omega = 0 \quad 3.2.2.1-6$$

where w is the weighting functions.

It can be shown that methods such as Galerkin's, Rayleigh's and Virtual Work only differ in the ways in which the weighting functions are chosen. In the case of Galerkin's method, the weighting functions are chosen in the same way as the trial functions.

$$\int (\mathcal{L} (\sum_{k=1}^N \alpha_k \Upsilon_k(x)) - P) * \Upsilon_i * d\Omega = 0 \quad 3.2.2.1-7$$

where $i = 1, 2, 3, \dots, N$

$$\int \alpha_k (\mathcal{L} (\Upsilon_k(x))) * \Upsilon_i * d\Omega = \int P \Upsilon_k(x) d\Omega \quad 3.2.2.1-8$$

where $k=1, 2, 3, \dots, N$ and $i = 1, 2, 3, \dots, N$

Equation 3.2.2.1-8 produce a system of equations from which the unknown parameters α_k can be solved.

3.2.2.2 SOLUTION USING FINITE ELEMENT METHODS

In essence, the analysis of an integral structure is conceptually broken down into one of an assemblage of a large number of elements (called finite elements) which are of various shapes and sizes. Most structures can be idealized as an assemblage of beams, membranes, plates etc. The results of discretization are manifold. Firstly, a structure is replaced conceptually by elements forming a mesh: the lines occur where element boundaries come together and the nodes where the element corners meet. Secondly, the governing equations of the continuum are replaced by a set of simultaneous algebraic linear equations. Further theories on FEM can be found in some authoritative text books such as those written by **Robinson** ^[3,6] and **Zienkiewicz** ^[3,7].

3.2.2.2.1 CONSTRUCTION OF STRUCTURAL MATRICES

The construction of the mass and stiffness matrices of an integral structure is no different to assembling these matrices of the individual finite elements. As an illustration, the construction of the structural matrices of a simple beam element is shown. Figure 3.2.2.2.1-1 shows a beam bending in one of its principal planes. Subjected to the usual assumptions as adopted in simple beam bending theories, the displacement in the y-direction u_y along the length of the beam x is given by the following polynomial as a first approximation.

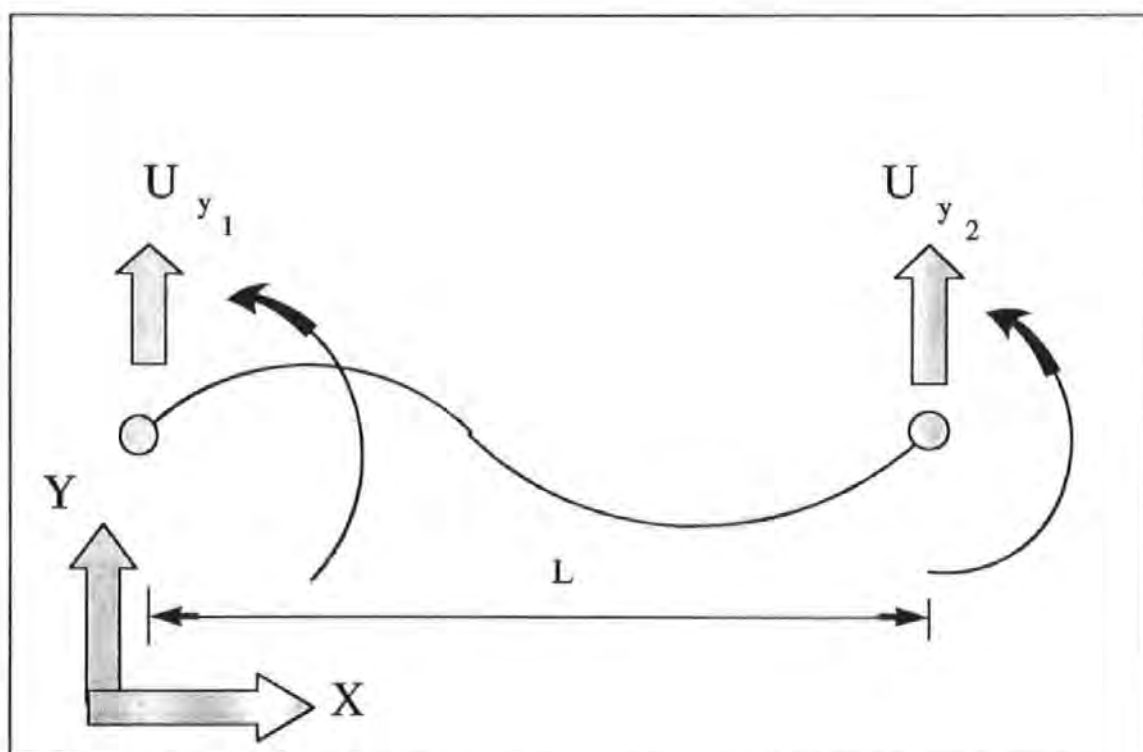


Figure 3.2.2.2.1-1 A simple bending beam with shear and bending moment at each node.

$$u_y = a_1 + a_2 x + a_3 x^2 + a_4 x^3 \quad 3.2.2.2.1-1$$

where the a 's are arbitrary constants. If expressed in matrix notation:

$$\{ u_y \} = [POLY] * \{ a \} \quad 3.2.2.2.1-2$$

where $\{a\}$ is a vector of the constants a 's and $[POLY]$ is a polynomial matrix :

$$[POLY] = \begin{bmatrix} 1 & x & x^2 & x^3 \end{bmatrix} \quad 3.2.2.2.1-3$$

The constants a 's can be solved if the nodal displacement boundary conditions are known. The choice of a 3rd order polynomial now becomes apparent since the four pieces of information on the nodal displacement enable the constants a_1 , a_2 , a_3 and a_4 to be solved. This relationship can be expressed in matrix form :

$$\{ u_e \} = [A] * \{ a \} \quad 3.2.2.2.1-4$$

where

$$[A] = \begin{bmatrix} 1 & 0 & 0 & 0 \\ 0 & 1 & 0 & 0 \\ 1 & L & L & L \\ 0 & 1 & 2L & 3L \end{bmatrix} \quad 3.2.2.2.1-5$$

Therefore the displacement of any intermediate point between the nodal points can be interpolated using :

$$\{ u_y \} = [POLY] * [A]^{-1} \{ u_e \} \quad 3.2.2.2.1-6$$

when expanded:

$$[POLY] [A]^{-1} = \left[\left(1 - \frac{3x^2}{L^2} + \frac{2x^3}{L^3} \right) \left(x - \frac{2x^2}{L} + \frac{x^3}{L^3} \right) \left(\frac{3x^2}{L^2} - \frac{2x^3}{L^3} \right) \left(-\frac{x^2}{L} + \frac{x^3}{L^3} \right) \right]$$

3.2.2.2.1-7

The strain energy S.E. associated with such beam deformation is given by :

$$S.E. = \int_0^L \frac{1}{2} * E * I * \left(\frac{\partial^2 u_y}{\partial x^2} \right)^2 dx \quad 3.2.2.2.1-8$$

$$\text{where } \frac{\partial^2 u_y}{\partial x^2} \text{ is the curvature of the beam} \quad 3.2.2.2.1-9$$

As by definition, the S.E. can also be expressed as:

$$S.E. = \frac{1}{2} * \{ u_e \}^T * [K] * \{ u_e \} \quad 3.2.2.2.1-10$$

therefore

$$S.E. = \frac{1}{2} E I \{ u_e \}^T [A]^{-T} \left(\int_0^L \left(\frac{\partial^2 POLY}{\partial x^2} \right)^T * \left(\frac{\partial^2 POLY}{\partial x^2} \right) dx \right) [A]^{-1} \{ u_e \} \quad 3.2.2.2.1-11$$

$$[K] = E I [A]^{-T} \left(\int_0^L \left(\frac{\partial^2 POLY}{\partial x^2} \right)^T * \left(\frac{\partial^2 POLY}{\partial x^2} \right) dx \right) [A]^{-1} \quad 3.2.2.2.1-12$$

In 3D analysis, a beam can be subjected to twist and axial deformations when under the action of couples and axial forces. As these deformations do not affect those due to flexure, the effects are combined together using superposition. The axial and torsional displacements of any one point between the nodal points can be approximated by including the axial $u_x(x)$ and torsional $q(x)$ displacement fields :

$$\begin{aligned}u_x(x) &= a_5 + a_6 x \\q(x) &= a_7 + a_8 x\end{aligned}$$

Then the steps described previously can be repeated to determine the full stiffness matrix taking into account axial, bending, shear and torsion. This matrix is too large to be presented here and only the stiffness matrix due to shear and bending of a beam is given here:

$$[K] = \begin{bmatrix} \frac{12 EI}{L^3} & \frac{6 EI}{L^2} & \frac{-12 EI}{L^3} & \frac{6 EI}{L^2} \\ \frac{6 EI}{L^2} & \frac{4 EI}{L} & \frac{-6 EI}{L^2} & \frac{2 EI}{L} \\ \frac{-12 EI}{L^3} & \frac{-6 EI}{L^2} & \frac{12 EI}{L^3} & \frac{-6 EI}{L^2} \\ \frac{6 EI}{L^2} & \frac{2 EI}{L} & \frac{-6 EI}{L^2} & \frac{4 EI}{L} \end{bmatrix} \quad 3.2.2.2.1-13$$

Similarly, the mass matrix derived is based on Kinetic Energy considerations. The kinetic energy K.E. of a beam with the aforementioned deformations is given by :

$$K.E. = \frac{1}{2} \int_{\text{volume}} \rho \omega^2 (u_x^2 + u_y^2 + u_z^2) dV \quad 3.2.2.2.1-14$$

where ω is the angular frequency of oscillation

Also by definition, the K.E. can also be expressed as :

$$K.E. = \frac{1}{2} \{ \dot{u}_e \}^T * [M] * \{ \dot{u}_e \} \quad 3.2.2.2.1-16$$

Therefore the mass matrix can be obtained by using :

$$[M] = \rho[A][A]^{-T} \left(\int_0^L [POLY]^T [POLY] dx \right) [A]^{-1} \quad 3.2.2.2.1-17$$

Although the derivation process of a relatively simple beam element is shown, other elements such as membrane and plate bending elements etc. can also be obtained by

following these procedures:

- a. To make an assumption of the displacement fields which are appropriate to the element's geometry and proposed structural actions. These displacement fields are expressed in the form of polynomials and in terms of some arbitrary constants.
- b. To write the expression of the strain energy in terms of displacements by making use of interpolation to determine the displacements of any point within the element from the nodal displacements.

Having obtained the elemental structural matrices of each individual element, the global structural matrices can be obtained by *assembling* the individual elemental matrix. The end product of these operations is a set of linear algebraic equations ready for solution. So far, the theoretical development covers a free undamped system and these equations are usually stated as:

$$[M] * \{ \ddot{x} \} + [K] * \{ x \} = \{ 0 \} \quad 3.2.2.2.1-18$$

where $\{x\}$ is a vector of nodal displacement

According to the coordinate system, the scheme of numbering of elements and nodes used, $[M]$ and $[K]$ are not usually diagonal matrices ($[M]$ may be diagonal if lumped mass model is assumed). In this case, the system of equations are *coupled*. *Decoupling* of the equations is achieved (to be proved later in Section 3.2.2.2.4) through linear transformation of the arbitrary coordinate system $\{x\}$ to natural coordinates $\{\eta\}$ using the classical *undamped modal matrix* $[\Phi]$ (as illustrated in Equation 3.2.2.2.1-19):

$$\{ x \} = [\Phi] * \{ \eta \} \quad 3.2.2.2.1-19$$

Note that the coordinate transformation does not change the character of the system, it simply facilitates solution. Pre-multiplying Equation 3.2.2.2.1-18 by $[\Phi]^T$ and with the substitution of Equation 3.2.2.2.1-19, Equation 3.2.2.2.1-20 is obtained:

$$[\Phi]^T[M][\Phi] * \{ \ddot{\eta} \} + [\Phi]^T[K]\Phi * \{ \eta \} = \{ 0 \} \quad 3.2.2.2.1-20$$

Denoting:

$$[\Phi]^T [M] [\Phi] = [M^*] \quad 3.2.2.2.1-21a$$

$$[\Phi]^T [K] [\Phi] = [K^*] \quad 3.2.2.2.1-21b$$

where $[M^*]$ and $[K^*]$ will be shown later in Section 3.2.2.2.3 that they are diagonal matrices and are usually called the *Generalised mass and stiffness matrices* respectively

then a set of decoupled equations is obtained:

$$[M^*] * \{ \ddot{\eta} \} + [K^*] * \{ \eta \} = \{ 0 \} \quad 3.2.2.2.1-22$$

This technique of decoupling the system of equations forms the whole basis of *modal analysis*. The undamped modal matrix is obtained from the solution of an Eigenvalue problem which will be discussed in Section 3.2.2.2.2. The properties depicted in Equations 3.2.2.2.1-21a and 3.2.2.2.1-21b are termed *orthogonality* which is to be further explained in Section 3.2.2.2.3.

The assumption of an undamped system is a mathematical convenience rather than a physical reality. Hence, the inclusion of damping in analysis is necessary. The analytical derivation of a damping matrix $[C]$ is less trivial than those of $[M]$ and $[K]$ because, so far, there is still a lack of understanding of the mechanism and the means of modelling damping. In fact, the subject of damping is a complicated subject in its own right. It is not the intention of this research to be indulged in the philosophical argument of what type of damping is really appropriate for the structures studied.

By definition, damping is a measure of the energy dissipating property of a material under cyclic loading conditions. This energy is usually dissipated as heat or is absorbed by internal structural changes. The latter results in raising the energy level of a material or system. The three most popular damping mechanisms used are: viscous, hysteretic and Coulomb damping. The different forms of damping all exhibit one feature in common: i.e. the cyclic load-deformation (or stress-strain) curve is not a single valued function but forms a hysteretic loop. The area enclosed by the loop represents the damping energy dissipated.

Linear viscous damping property is characterised by a *dashpot*. Viscous damping force acts in a direction opposite to the direction of and with amplitude proportional to the amplitude of velocity of a coordinate. Viscous damping force is also frequency dependent. Hysteretic damping is associated with internal energy loss due to material hysteresis. Hysteretic damping force acts in a direction opposite to the velocity of and with amplitude proportional to the amplitude of displacement of a coordinate. Coulomb damping is attributed from the energy loss by friction at an interface or joint between mating members where relative mechanical motion occurs. Coulomb damping force acts in a direction opposite to the velocity of a coordinate and with constant amplitude. It is independent of amplitude of displacement and velocity of a coordinate. Both hysteretic and coulomb damping forces are frequency independent.

The choice of a suitable damping model is not usually an exact science and is often a matter of preference or convenience. Viscous damping is widely used especially in the civil engineering community. However, some people show special preference to hysteretic damping because of the expedience it can offer in simplifying some complicated mathematical expressions.

In general, the decoupling technique using undamped modal matrix transformation does not work with any except a few very specialised forms of damping such as *proportional damping*:

$$[C] = \alpha * [M] + \beta * [K] \quad 3.2.2.2.1-23$$

Here, the damping matrix $[C]$ is expressed as a linear combination of the mass $[M]$ and stiffness $[K]$ utilising two proportional parameters α and β .

This is often referred to as the Rayleigh's damping model. From Equation 3.2.2.2.1-23, it can be observed that the damping matrix is also orthogonal with respect to the undamped modal matrix $[\Phi]$ since $[M]$ and $[K]$ both are and so as the scaled linear combination of them. A simple proof is now given. If Equation 3.2.2.2.1-23 is pre-multiplied and post-multiplied by $[\Phi]^T$ and $[\Phi]$ respectively, one can obtain:

$$[\Phi]^T [C] [\Phi] = \alpha * [\Phi]^T [M] [\Phi] + \beta * [\Phi]^T [K] [\Phi] \quad 3.2.2.2.1-24$$

After some appropriate substitutions, one can obtain:

$$[\Phi]^T [C] [\Phi] = \alpha [M^*] + \beta [K^*] = [C^*] \quad 3.2.2.2.1-25$$

where $[C^*]$ is a diagonal matrix similar to $[M^*]$ and $[K^*]$, and is called the *Generalised Damping matrix*.

Hence the proof is completed. From Equation 3.2.2.2.1-26, one can obtain a relationship which enables the two Rayleigh's constants α and β to be determined if values of modal damping factor ξ_r and undamped natural frequency ω_r are known.

$$\xi_r = \frac{\alpha}{2 \omega_r} + \frac{\omega_r \beta}{2} \quad 3.2.2.2.1-26$$

If experimental data on the modal damping factors is available, the damping matrix $[C]$ can be constructed using $[\xi]$ (which is a diagonal matrix of the modal damping factors of the various modes of vibration), the analytically determined spectral matrix and the undamped modal matrix (i.e. they are obtained after solving an eigenvalue problem associated with the corresponding undamped system):

$$[C] = 2 [\Phi]^{-T} [\xi] [\omega^2]^{-\frac{1}{2}} [\Phi]^T \quad 3.2.2.2.1-27$$

where $[\Phi]$ is the undamped modal matrix
 $[\xi]$ is the diagonal matrix of modal damping factors
 $[\omega^2]$ is the diagonal spectral matrix

So with the inclusion of damping, the fully assembled equation of motion for a damped system under forced vibration is:

$$[M] * \{ \ddot{x} \} + [C] * \{ \dot{x} \} + [K] * \{ x \} = \{ f \} \quad 3.2.2.2.1-28$$

where $\{f\}$ is the forcing vector

The sizes of the structural matrices $[M]$, $[C]$ and $[K]$ depend on the number of degrees

of freedom required to specify the deformation field. They can be very large even for a structure of modest size and complexity. Hence a process known as *condensation* (static or dynamic condensation) is often applied to reduce the size of these matrices before carrying out a computer solution. In essence, the original matrices are condensed by only retaining the *master degrees of freedom* and eliminating all the unwanted *slave degrees of freedom* in the equations. It can be shown that in the case of static or dynamic condensation, the *condensed stiffness matrix* is exact, but the *condensed mass matrix* is not but an approximation only.

A complete solution of the eigenvalue problem of large matrix size can involve very intensive computation. However, if only a small number of the lower natural frequencies and mode shapes of a system is required, there are a few computational schemes available which do not require a complete solution.

3.2.2.2.2 EIGENVALUE SOLUTIONS

Eigenvalue problems are found in many disciplines of science: buckling load analysis, principal stress-strain analysis etc to name a few in the field of structural mechanics. So eigenvalues are not merely a set of mathematical quantities but are important physical characteristics of a system. The Eigenvalue problem as found in structural dynamics are now deliberated. Supposing a possible solution of the governing equations of a free undamped system (Equation 3.2.2.2.1-18) is of the form which is separable in time t and space:

$$\{x\} = \{\phi_r\} * \eta_r(t) \quad 3.2.2.2.2-1$$

Here $\{\phi_r\}$ is a shape function independent of time (it can be shown that this is actually a modal vector and subscript r denotes the r^{th} mode of vibration of a system) and $\eta_r(t)$ is a time function. By substituting Equation 3.2.2.2.2-1 to Equation 3.2.2.2.1-18:

$$[M] \{\phi_r\} \ddot{\eta}_r(t) + [K] \{\phi_r\} \eta_r(t) = \{0\} \quad 3.2.2.2.2-2$$

which is a set of N (the total number of degrees of freedom of a system) equations each of the type:

$$\sum_{j=1}^N m_{ij} \phi_{jr} \ddot{\eta}_r(t) + \sum_{j=1}^N k_{ij} \phi_{jr} \eta_r(t) = 0 \text{ for } i=1,2,3,\dots,N \quad 3.2.2.2.2-3$$

Using the method of separation of variables,

$$\frac{-\ddot{\eta}_r(t)}{\eta_r(t)} = \frac{\sum_{j=1}^N k_{ij} \phi_{jr}}{\sum_{j=1}^N m_{ij} \phi_{jr}} = \text{constant (say } +\omega_r^2) \quad i=1,2,3,\dots,N \quad 3.2.2.2.2-4$$

The positive sign is chosen for a conservative system. Hence two sets of equations are obtained:

$$\ddot{\eta}_r(t) + \omega_r^2 \eta_r(t) = 0 \quad 3.2.2.2.2-5$$

$$\sum_{j=1}^N (k_{ij} - \omega_r^2 m_{ij}) \phi_{jr} = 0 \text{ for } i=1,2,3,\dots,N \quad 3.2.2.2.2-6$$

The solution to Equation 3.2.2.2.2-5 is of the form:

$$\eta_r = c_r \cos(\omega_r t + \varphi_r) \quad 3.2.2.2.2-7$$

where the amplitude c_r and phase angle φ_r are determined by the initial conditions. This solution stipulates that all the coordinates perform a harmonic motion with identical frequency ω_r and identical phase angle φ_r . The values of these frequency ω_r are governed by the Equation 3.2.2.2.2-6 which can be recast in matrix form as:

$$[K] * \{ \phi_r \} = \omega_r^2 * [M] * \{ \phi_r \} \quad (3.2.2.2.2-8a)$$

$$\text{or } [M]^{-1}[K] * \{ \phi_r \} = \omega_r^2 * \{ \phi_r \} \quad (3.2.2.2.2-8b)$$

which is the standard formulation for a special mathematical problem called *Eigenvalue* problem. A trivial solution to Equation 3.2.2.2.2-8 is $\{\phi_r\}$ which is equal to a zero vector. Such a solution represents the static equilibrium case. Non-trivial solutions exist if the *characteristic equation* (Equation 3.2.2.2.2-9) is satisfied.

$$\Delta_{cd} = \left| [K] - \omega_r^2 [M] \right| = 0$$

where Δ_{cd} is called the *characteristic determinant*.

The solutions consist of a set of ω_r^2 's (called *eigenvalues*) and a corresponding set of $\{\phi_r\}$'s (called *eigenvectors*). Equation 3.2.2.2.2-8 is often expressed in full matrix representation as:

$$[K] * [\Phi] = [\omega_r^2] * [M] * [\Phi] \quad (3.2.2.2.2-10)$$

where $[\omega_r^2]$ is called the *spectral matrix* and is a diagonal matrix of the eigenvalues ω_r^2

ω_r is the *undamped natural frequency*

and $[\Phi]$ is the *real undamped modal matrix* and is a matrix whose columns are eigenvectors (or *natural mode shapes*) of the undamped system's natural mode of vibration.

Since the $[M]$ and $[K]$ matrices are both *symmetric and positive definite*, all the eigenvalues ω_r^2 will be real, positive numbers. Moreover, the eigenvectors of a symmetric matrix are independent and the modal matrix $[\Phi]$ is non-singular. Usually, all the eigenvalues are distinct but repeating values are possible for some systems. When two eigenvalues are equal, the associated eigenvectors are orthogonal to all the other eigenvectors but not orthogonal to each other: a characteristics known as *degenerate*. However they can be taken in any linear combination to form orthogonal eigenvectors. The eigenvectors represent a unique *shape* but arbitrary *amplitude* (i.e. values within any one eigenvector are relative and not absolute). These values can be fixed according to a process called *normalisation*. Hence the eigenvectors are called *normal mode shapes*. There are a number of Eigenvalue solvers available: Jacobi, Householder, Cholesky and QR methods to mention a few.

The theoretical development so far considers only an undamped system for which the eigenvalues ω_r^2 and eigenvectors $\{\phi_r\}$ are real. However, for damped system with general forms of damping, the eigenvalues and eigenvectors will be complex quantities (i.e. complex modes). Later in Section 3.2.2.2.5, an entire Section will be devoted to cover the theoretical issues concerning generally damped systems.

3.2.2.2.3 MODES OF VIBRATION

Each pair of eigenvalue and eigenvector is associated with a natural mode of vibration. The shape an undamped structure manifests when it is resonating in the r^{th} mode with frequency ω_r is of the form:

$$\{x\} = c_r \{\phi_r\} \cos(\omega_r t + \{\varphi_r\}) \quad 3.2.2.2.3-1$$

where c_r is a proportional constant and $\{\varphi_r\}$ is a vector of phase angles φ_r .

As mentioned earlier, the eigenvalues ω_r^2 and the eigenvectors $\{\phi\}$ are real numbers for an undamped system. Hence the system possesses real normal modes. For a real mode, every coordinate of the system will oscillate synchronously and harmonically at a frequency which is the undamped natural frequency of that mode. In other words, all coordinates reach their extreme displaced positions at the same time and the nodal (stationary) points remain the same over every cycle of oscillation. The phase angles between coordinates (i.e. φ_r) are either 0 or 180 degrees. The real modes are influenced by the system's mass and stiffness properties only.

For a damped system, the deformation shape is of the form:

$$\{x\} = c_r e^{-\xi_r \omega_r t} \{\phi_r\} \cos(\omega_{rD} t + \{\varphi_r\}) \quad 3.2.2.2.3-2$$

where ω_{rD} which equals $\omega_r(1 - \xi_r^2)^{0.5}$ is the *damped natural frequency* of the r^{th} mode

ξ_r is the modal damping factor of the r^{th} mode

For a proportionally damped system, ξ_r is non-zero, but the phase angles φ_r between coordinates are still either 0 or 180 degrees. Hence, the system is oscillating with decaying magnitudes (due to the exponential decay term), but the mode shapes are still real.

For a generally or unproportionally damped system, eigenvalues and eigenvectors are complex numbers, hence the system possesses complex modes. A complex mode shape

exhibits a so-called '*galloping effect*' i.e. some coordinates will reach their extreme displaced positions some times after other coordinates reach theirs. This phenomenon is due to the difference in phase angles between them which are neither 0 nor 180 but somewhere between these two values.

3.2.2.2.4 ORTHOGONALITY OF MODES

In this Section, the mathematical basis of the important orthogonality property which exists between the different modes of vibration is given. The proof is conducted by considering any two modes of vibration: say modes r and s . As for mode r , the natural frequency and the modal vector for mode s should also satisfy Equation 3.2.2.2.2-8 :

$$[K] * \{ \phi_s \} = \omega_s^2 * [M] * \{ \phi_s \} \quad 3.2.2.2.4-1$$

By pre-multiplying Equation 3.2.2.2.2-8 and Equation 3.2.2.2.4-1 by $\{\phi_s\}^T$ and $\{\phi_r\}^T$ respectively to produce:

$$\{ \phi_s \}^T [K] \{ \phi_r \} = \omega_r^2 \{ \phi_s \}^T [M] \{ \phi_r \} \quad 3.2.2.2.4-2$$

$$\{ \phi_r \}^T [K] \{ \phi_s \} = \omega_s^2 \{ \phi_r \}^T [M] \{ \phi_s \} \quad 3.2.2.2.4-3$$

By transposing Equation 3.2.2.2.4-3:

$$\left(\{ \phi_r \}^T [K] \{ \phi_s \} \right)^T = \left(\omega_s^2 \{ \phi_r \}^T [M] \{ \phi_s \} \right)^T \quad 3.2.2.2.4-4$$

Since both $[M]$ and $[K]$ are symmetric matrices, then Equation 3.2.2.2.4-4 becomes :

$$\{ \phi_s \}^T [K] \{ \phi_r \} = \omega_s^2 \{ \phi_s \}^T [M] \{ \phi_r \} \quad 3.2.2.2.4-5$$

So subtracting Equation 3.2.2.2.4-2 by Equation 3.2.2.2.4-5:

$$(\omega_r^2 - \omega_s^2) \{ \phi_s \}^T [M] \{ \phi_r \} = 0 \quad 3.2.2.2.4-6$$

Now let M_{sr}^* and K_{rs}^* denotes the matrix triple products as depicted in Equations 3.2.2.2.4-7 and 3.2.2.2.4-8 (note the order of the matrix products is denoted by the subscripts: sr and rs respectively).

In general, all the natural frequencies of a structure are distinct i.e. $\omega_r \neq \omega_s$ then

$$M_{sr}^* = \{ \phi_s \}^T [M] \{ \phi_r \} = 0 \quad 3.2.2.2.4-7$$

By following much of the above procedures once more, Equation 3.2.2.2.4-8 is also obtained:

$$K_{rs}^* = \{ \phi_r \}^T [K] \{ \phi_s \} = 0 \quad 3.2.2.2.4-8$$

If $\omega_r = \omega_s$ (i.e. for the same mode), then the matrix triple products are:

$$M_{rr}^* = \{ \phi_r \}^T [M] \{ \phi_r \} \neq 0 \quad 3.2.2.2.4-9$$

$$K_{rr}^* = \{ \phi_r \}^T [K] \{ \phi_r \} \neq 0 \quad 3.2.2.2.4-10$$

Hence K_{rs}^* and M_{rs}^* are zero if r is not equal to s and are not zero if r is equal to s . In fact, K_{rs}^* and M_{rs}^* are the r^{th} row s^{th} column elements of the matrices $[K^*]$ and $[M^*]$ (the *Generalised stiffness and mass matrices* as introduced earlier) respectively. Hence $[K^*]$ and $[M^*]$ are diagonal matrices. The last four equations stipulate a property known as *orthogonality* (note that this statement is true only if $[M]$ and $[K]$ are symmetric matrices which are valid for most systems except nonlinear systems). The full matrix representation of the orthogonality properties involving all the modes are given as:

$$[\Phi]^T [M] [\Phi] = [M^*] \quad 3.2.2.2.4-11$$

$$[\Phi]^T [K] [\Phi] = [K^*] \quad 3.2.2.2.4-12$$

If the eigenvectors are *normalised* in such a way as to make $[M^*]$ an identity matrix, then the eigenvectors are called *normal vectors or normal modes* and matrix $[K^*]$ becomes a diagonal matrix known as *spectral matrix*, $[\omega_r^2]$ (or $[\omega_r^2]$ as denoted earlier; subscript r is used instead of rr as the diagonality of the matrix is understood).

$$[\Phi]^T [M] [\Phi] = [I] \quad 3.2.2.2.4-13a$$

$$[\Phi]^T[K][\Phi] = [\omega_{rr}^2] \quad 3.2.2.2.4-13b$$

Recalling Equation 3.2.2.2.1-20:

$$[\Phi]^T[M][\Phi] * \{\ddot{\eta}\} + [\Phi]^T[K][\Phi] * \{\eta\} = \{0\} \quad 3.2.2.2.1-20$$

Using the orthogonality properties, it can be simplified as:

$$\{\ddot{\eta}\} + [\omega_{rr}^2] * \{\eta\} = \{0\} \quad 3.2.2.2.4-14$$

Equation 3.2.2.2.4-14 represents a set of uncoupled second order differential equations which are typical of the form (Note: the decoupling of equation of motions in the case of a damped system will be dealt with separately in Section 3.2.2.2.5.) :

$$\ddot{\eta}_r + \omega_r^2 * \eta_r = 0 \quad 3.2.2.2.4-15$$

The solution to this equation is already given in Equation 3.2.2.2.2-7. So any displacement $\{x\}$ can be obtained by a weighted superposition of the harmonic motions (of all the N modes) with frequencies equal to the natural frequencies ω_r , amplitudes c_r and phase angles ϕ_r as stipulated by the equation:

$$\{x\} = [\Phi] \{\eta\} = \sum_{r=1}^N c_r [\phi_r] \cos(\omega_r t + \phi_r) \quad 3.2.2.2.4-16$$

The philosophical importance of the property of orthogonality is that these orthogonal eigenvectors form a *basis* of the deformation space i.e. any deformation vector can be generated by a linear combination of these linearly independent eigenvectors. This statement is known as the *expansion theorem* which allows modal analysis to be used to obtain the response of a system from the knowledge of the system's modal properties.

Orthogonality of modes are often used to check for the consistency of the experimentally measured modal vectors. These modal vectors should, in theory, be orthogonal to each other when weighted with respect to the mass, stiffness or certain limited form of damping matrices. And as a common practice, the mass matrix is chosen in preference to the other two in testing the orthogonal condition because of the relative ease in determining masses

from design drawings.

In general, the modal vectors obtained from experiments rarely satisfy Equation 3.2.2.2.4-7. This may be due to errors in measurement, in modal parameter extraction or in the assumed mass matrix. In practice, no alarm should be raised if Equation 3.2.2.2.4-7 (using *normal* modal vectors) yields a value of not more than 0.1 (with normalisation, the modal mass of each mode has a value of unity).

3.2.2.2.5 APPLICATION OF MODAL ANALYSIS TO NON-PROPORTIONALLY DAMPED SYSTEM

So far, the modal analysis technique (i.e. the technique of decoupling the coupled equations of motion using undamped modal matrix transformation) as applied to undamped systems and systems with a specialised form of damping i.e. proportional damping, has been discussed but not systems with the more general forms of damping. Proportional damping assumes that damping is a distributive property like mass and stiffness. Such an assumption is not always justifiable especially in situations where heavy localised damping devices such as joint dampers, shock absorbers etc are applied to the system. For nonproportionally damped systems, the damping matrix $[C]$ cannot be reduced to a diagonal form by means of undamped modal matrix transformation:

$$\text{i.e.} \quad [\Phi]^T * [C] * [\Phi] \text{ is not a diagonal matrix}$$

3.2.2.2.5-1

In these circumstances, there are a number of approximation schemes which, in essence, try to retain all the niceties associated with the proportionally damped cases. One such scheme is applied in the following ways:

$$\text{let } [C_{nd}] = [\Phi]^T [C] [\Phi] \quad 3.2.2.2.5-2$$

i.e. the original system damping matrix is pre- and post-multiplied by $[\Phi]^T$ and $[\Phi]$ to obtain a matrix $[C_{nd}]$ where the subscript nd denotes non-diagonal. Then a new system damping matrix $[C_{rc}]$ (where the subscript rc denotes reconstruction) is reconstructed by:

$$[C_{rc}] = [\Phi]^{-T} [C_{nd}] [\Phi]^{-1} \quad 3.2.2.2.5-3$$

The matrix $[C_d]$ is a diagonal matrix which is obtained by retaining only the diagonal terms

of the matrix $[C_{nd}]$. Another scheme works very much the same way. The matrix $[C_{nd}]$ is reconstructed based on Equation 3.2.2.2.5-4:

$$[C_{rc}] = [\Phi]^{-T} [2\xi_r \omega_r] [\Phi]^{-1} \quad 3.2.2.2.5-4$$

where $[2\xi_r \omega_r]$ is a diagonal matrix constructed from known modal damping factors ξ_r and undamped natural frequencies ω_r .

Once $[C_{rc}]$ is obtained, it will be used instead of the original system damping matrix $[C]$ and the whole cycle of analysis will be repeated once more. The rationale behind these schemes is that coupling can be considered as secondary effects and dropping of the off-diagonal terms do not introduce serious errors. These techniques can be used in situations where damping level is light.

For systems with hysteretic damping, the analysis procedures are now explained. Recalling that the energy loss per cycle of cyclic stress-strain variation is a measure of damped or dissipated energy. For hysteretic damping materials, this energy is found to satisfy the equation:

$$\Delta E_{cycle} = a X_0^2 \quad 3.2.2.2.5-5$$

where a is a proportional constant independent of frequency of harmonic oscillation
 X_0 is the displacement amplitude of oscillation

Similarly, the energy loss for viscous damping materials is found to be:

$$\Delta E_{cycle} = c \pi \Omega X^2 \quad 3.2.2.2.5-6$$

where Ω is the frequency of harmonic oscillation
 c is the viscous damping coefficient

Hence, for the harmonic excitation case, a structurally damped system may be treated as a viscously damped system with an equivalent viscous damping coefficient which is inversely proportional to the frequency of oscillation. Recalling the equation of motion for a viscously damped system:

$$[M] * \{\ddot{x}\} + [C] * \{\dot{x}\} + [K] * \{x\} = \{f\} \quad 3.2.2.2.5-7$$

If excitation $\{f\}$ is harmonic (i.e. $\{f\} = \{F_0\}e^{j\Omega t}$) then the response $\{x\}$ is also harmonic (i.e. $\{x\} = \{X_0\}e^{j\Omega t}$) provided the system is linear. Now for every hysteretic damping coefficient a_{ij} , it is transformed to an equivalent viscous damping coefficient c_{ij} :

$$c_{ij} = \frac{1}{\pi \Omega} a_{ij} \quad 3.2.2.2.5-8$$

or in matrix formulation:

$$[C] = \frac{1}{\pi \Omega} [a] \quad 3.2.2.2.5-9$$

For harmonic oscillation:

$$\{\dot{x}\} = j \Omega \{x\} \quad 3.2.2.2.5-10a$$

$$\{\ddot{x}\} = (j \Omega)^2 \{x\} = - \Omega^2 \{x\} \quad 3.2.2.2.5-10b$$

Equation 3.2.2.2.5-7 then becomes:

$$- \Omega^2 [M] * \{ X_0 \} + \frac{j \Omega}{\pi \Omega} [a] * \{ X_0 \} + [K] * \{ X_0 \} = \{ F_0 \} \quad 3.2.2.2.5-11$$

By introducing the coefficients of structural damping γ_{ij} :

$$\gamma_{ij} = \frac{a_{ij}}{\pi k_{ij}} \quad 3.2.2.2.5-12$$

Then Equation 3.2.2.2.5-11 becomes:

$$- \Omega^2 [M] * \{ X_0 \} + j [\gamma k] * \{ X_0 \} + [K] * \{ X_0 \} = \{ F_0 \} \quad 3.2.2.2.5-13$$

In the general hysteretic damping cases, Equation 3.2.2.2.5-13 cannot be decoupled via the linear transformation using the undamped modal matrix. However, if the hysteretic damping matrix $[\gamma k]$ (often denoted as $[H]$) is further assumed as proportional to the stiffness matrix, then all γ_{ij} have the same value i.e. $\gamma_{ij} = \gamma$.

$$3.2.2.2.5-14$$

$$- \Omega^2 [M] * \{ X_0 \} + (j \gamma + 1) [K] * \{ X_0 \} = \{ F_0 \}$$

Equation 3.2.2.2.5-14 can be decoupled by the linear transformation using the undamped modal matrix (i.e. $\{X_0\} = [\Phi] \{\eta_0\}$ and $\{\eta\} = \{\eta_0\}e^{j\Omega t}$ is also harmonic):

$$- \Omega^2 [\Phi]^T [M] [\Phi] * \{ \eta_0 \} + (j \gamma + 1) [\Phi]^T [K] [\Phi] * \{ \eta_0 \} = [\Phi]^T \{ F_0 \}$$

3.2.2.2.5-15

Hence based on the orthogonality properties, a set of uncoupled equations are obtained:

$$- \Omega^2 [I] * \{ \eta_0 \} + (j \gamma + 1) [\omega_r^2] * \{ \eta_0 \} = [\Phi]^T \{ F_0 \}$$

3.2.2.2.5-16a

$$\left[- \Omega^2 + (j \gamma + 1) \omega_r^2 \right] * \{ \eta_0 \} = [\Phi]^T \{ F_0 \}$$

3.2.2.2.5-16b

Equation 3.2.2.2.5-16 can be treated as a set of decoupled equations of motion for a system whose stiffness $[K]$ term is replaced by a *complex stiffness* term $(1 + j \gamma) [K]$. Such analytical expedience has lent itself more popularity amongst some sections of the modal analysis community.

For generally or non-proportionally damped system, then the decoupling technique using the real-valued undamped modal matrix, as discussed so far, cannot be applied. This is because in general, orthogonality of eigenvectors can only diagonalise two matrices at a time (such as $[M]$ and $[K]$ in an undamped case). This diagonalisation technique do not work for more than two matrices unless the other matrices (such as $[C]$ or $[H]$) are linearly proportional to the two matrices $[M]$ and $[K]$.

In the case of a non-proportionally damped system, the solution of the eigenvalue problem is pursued by transforming the second order differential equations (of size N) to one of first order differential equations but having twice the matrix size (i.e. $2N$).

$$- \begin{bmatrix} M & 0 \\ 0 & -K \end{bmatrix} \begin{bmatrix} \dot{x} \\ x \end{bmatrix} + \begin{bmatrix} 0 & M \\ M & C \end{bmatrix} \begin{bmatrix} \ddot{x} \\ \dot{x} \end{bmatrix} = \begin{bmatrix} 0 \\ f(t) \end{bmatrix} \quad 3.2.2.2.5-17a$$

$$\text{or } -[A] \{Y\} + [B] \{\dot{Y}\} = \{F(t)\} \quad 3.2.2.2.5-17b$$

$$\text{where } \{Y\} = \begin{pmatrix} \dot{x} \\ x \end{pmatrix}, [A] = \begin{bmatrix} M & 0 \\ 0 & -K \end{bmatrix}, [B] = \begin{bmatrix} 0 & M \\ M & C \end{bmatrix} \text{ and } \{F\} = \begin{bmatrix} 0 \\ f(t) \end{bmatrix}$$

$$3.2.2.2.5-18$$

Equations 3.2.2.2.5-17 are obtained by adding a set of auxiliary equations, Equation 3.2.2.2.5-19, to the system of equations 3.2.2.2.5-7:

$$[M]\{\ddot{X}\} - [M]\{\dot{X}\} = \{0\} \quad 3.2.2.2.5-19$$

The homogeneous solution (corresponding to the free vibration case i.e. $\{F(t)\} = \{0\}$) is a formulation for an eigenvalue problem:

$$[B] \{\dot{Y}\} = [A] \{Y\} \text{ or } [A]^{-1} [B] \{Y\} = \frac{1}{\lambda} \{Y\} \quad 3.2.2.2.5-20$$

$$\text{where } [A]^{-1}[B] = \begin{bmatrix} 0 & I \\ -K^{-1}M & -K^{-1}C \end{bmatrix} \quad 3.2.2.2.5-21$$

Because the inverse of $[A]$ is easier to obtain than that of $[B]$, so the *dynamical matrix* is expressed as $[A]^{-1} [B]$ and not $[B]^{-1} [A]$. The eigenvalues are determined by solving the following *characteristic equation*:

$$\Delta = \left| \begin{bmatrix} 0 & I \\ -K^{-1}M & -K^{-1}C \end{bmatrix} - \frac{1}{\lambda} [I] \right| = 0 \quad 3.2.2.2.5-22a$$

This eigenvalue problem formulation has a few similarities to that of an undamped case:

- $[M]$ and $[K]$ are now replaced by $[B]$ and $[A]$ respectively.
- The *dynamical matrix* $[K]^{-1} [M]$ is now replaced by $[A]^{-1} [B]$.

- c. The *characteristic equation* of an undamped case is a set of algebraic equations of order N (the total number of degree of freedom of a system) in ω^2 . The N roots ω_i^2 ($i = 1, 2, \dots, N$) are real and positive (because $[M]$ and $[K]$ are real, symmetric and positive definite). Whereas in the generally damped case, the characteristic equation is a set of algebraic equations of order $2N$ in λ . The $2N$ roots λ_i ($i = 1, 2, \dots, 2N$) are generally complex and the corresponding set of $2N$ eigenvectors $\{\phi_i^*$ are also complex. The complex damped modal matrix is denoted as $[\Phi^*]$ (here the superscript $*$ denotes complex quantities). These eigenvalues must appear as pairs of complex conjugates with negative real parts as depicted in Equation 3.2.2.2.5-22b:

$$\text{eigenvalues } \lambda_r = -\xi_r \omega_r \pm j \omega_r \sqrt{(1 - \xi_r^2)} \quad 3.2.2.2.5-22b$$

Here $\omega_r(1 - \xi_r^2)^{0.5}$ is often called the *damped natural frequency* ω_{dr} . The corresponding eigenvectors $\{\phi^*\}$ must coexist and form pairs with their complex conjugates $\{\phi^*\}^*$ (here $\{\}^*$ denotes a complex conjugate of a vector)

- d. Orthogonality, in the case of undamped modal matrix, ensures that the matrix triple products: $[\Phi]^T[M][\Phi]$ and $[\Phi]^T[K][\Phi]$ (all matrices are of size $N \times N$) are all diagonal matrices. Orthogonality, in the case of complex damped modal matrix, also ensures that the matrix triple products: $[\Phi^*]^T[B][\Phi^*]$ (denoted as $[B^*]$) and $[\Phi^*]^T[A][\Phi^*]$ (denoted as $[A^*]$) are all diagonal matrices. These matrices are of the size $2N$ by $2N$. So the diagonalisation technique using $[\Phi^*]$ can decouple Equations 3.2.2.2.5-17 via the transformation:

$$\{Y(t)\} = [\Phi^*] \{\eta(t)\} \quad 3.2.2.2.5-23$$

Equation 3.2.2.2.5-17b then becomes:

$$- [A^*] \{\eta\} + [B^*] \{\dot{\eta}\} = [\Phi^*]^T \{F(t)\} \quad 3.2.2.2.5-24$$

which is a set of decoupled system of equations. Once the solution in terms of the modal coordinates $\{\eta\}$ is complete, then the solution of $\{Y\}$ (hence $\{x\}$) can be pursued using the expansion theorem as in the undamped case.

$$\{Y(t)\} = \sum_{i=1}^{2N} \{\phi_i^*\} \eta_i \quad (\text{for } i = 1, 2, \dots, 2N) \quad 3.2.2.2.5-25$$

3.3 EXPERIMENTAL APPROACHES OF MODELLING

3.3.1 SYSTEM IDENTIFICATION

System identification as in conventional control engineering deals with electro-mechanical systems whose input-output characteristics (transfer functions) are described in :

- a rational fraction polynomial form or
- Poles and zeros form where the former and the latter are roots of the numerator and denominator polynomial respectively or
- sampled input-output time sequence form with governing parameters such as the orders, delays of the system or
- Z transform model.

System identification is therefore a process of determining the parameters in these various formulations (a process similar to that of the identification of modal and spatial parameters for structural systems as described in Chapters 5 and 6). Because the mathematical model representation in control is quite different from those used in structural engineering, so are the methods of solution. However, this distinction has become increasingly blurred as bilateral transfer between the two technological fields increases.

The introduction of system identification to the field of mechanical structures is briefly reviewed. In 1970, **Bekey** ^[3.9] presented a paper on an introduction and a survey of a number of methods for the identification of general dynamic systems, be they electrical or mechanical. He categorized the two different approaches in the tackling of most typical engineering problems known as the *direct* and the *inverse* approaches. According to his definition, system identification is an inverse approach in which the parameters in the governing equations are the subjects of determination from the known inputs and the outputs of a system.

Young and On ^[3.10] gave substantial coverage of the general methodology of mathematical modelling of structural systems utilizing experimental vibration data. They detailed the advantages and the disadvantages of a number of identification schemes. In particular to their work, they differentiated two different models which can be derived from experimental data: so-called *complete* and *incomplete* models. According to their definition, a complete model is a model which has the same number of degrees of freedom as the number of modes and an incomplete model is otherwise. Further contributions in this particular area are also due to **Berman and Flannelly** ^[3.11]. They presented a method of deriving incomplete models of mechanical structures. Further coverage on their work will be dealt with in chapter 6.

The dynamics of most engineering systems can be treated as linear, second order and time-invariant, at least as a first approximation. In fact, these assumptions are necessary for system identification to work. In essence, the technique requires a system (a structure) to be subjected to known input excitations (forces) and the responses (movements at different coordinates of a structure) to be measured. The excitations can be any suitable forms: be they periodic, harmonic (sinusoidal), transient (due to impact) or random.

System identification can be categorized as: *stochastic/deterministic*, *parametric/non-parametric*, *black box* or *grey box* approach and so on. It is beyond the scope of this report to provide a complete coverage on these methods. However, the last two categories are further explained below because of their philosophical importance.

3.3.1.1 THE BLACK BOX APPROACH

A *black box* approach describes an identification process in which no specific knowledge of the nature of a system is required. However this classification is only conceptually possible. In practice the *black box* approach can rarely be applied to real-life other than academic types of problems. Most engineering problems do rely on some prior knowledge of the engineering system: be they the form and the order of the governing equations or the values of some of the system parameters etc. Their prior knowledge is often desirable or sometimes even mandatory to obtain a physically realizable solution rather than an imaginary or a mathematical one. This modified approach is called the *grey box* approach.

3.3.1.2 THE GREY BOX APPROACH

The mathematical models derived using this approach are often called *priori models* (see Bekey^[3.9]). This may seem, at first sight, contradictory to the original requirement of system identification which is called upon because of the lack of full understanding of a system in the first place. It is due to these seemingly conflicting conditions that such an approach is only to be carried out iteratively. The approach adopted in this investigation falls in this category. In particular:

- a. A structure is assumed as a linear, second order and time-invariant system.
- b. The order of the structural matrices is assumed so that the derivation of an acceptable spatially and modally truncated model can be effected.
- c. The structural matrices are assumed to be either full, banded, diagonal or symmetric.
- d. The mechanism of damping is assumed to be either as viscous, hysteretic or even undamped.

Further details will be discussed in chapters 5 and 6.

3.3.2 IMPLEMENTATION

The implementation of this experimental modelling technique entails two basic steps which are common to and quite independent of the types of analysis methods, be they modal or non-modal methods. The first step involves the experimental acquisition of the so-called *input-output* data. In this *testing phase*, responses (outputs) of some specific test points of a structure when subjected to a particular form of excitation (inputs), applied at some other test point, have to be measured. The second step involves data analysis which try to fit the previously acquired data to a postulated *priori* model. In this *analysis phase*, some forms of curve-fitting methods (in the form of a computing algorithm) are applied to the data to extract the system's parameter.

3.3.2.1 EXPERIMENTATION

Data acquisition is often used synonymously with experimentation or instrumentation. Recent advances in instrumentation and computer technologies have brought about great changes in the various aspects of experimentation when compared to those one or two decades ago. The specific details of the instrumentation requirements will be dealt with in Chapter 4.

The basics of the experimentation involves the application of some forms of excitation to and the measurement of the subsequent responses of a structure. The number of excitation inputs and the way they are applied can affect the subsequent analysis procedures. A variety of methods are available: from Single-Input-Single-Output (SISO), Single-Input-Multiple-Output (SIMO), Multiple-Input-Single-Output (MISO) to Multiple-Input -Multiple-Output (MIMO) methods etc. Normal mode testing is an example of the techniques using multiple exciters. The amplitudes and phases of the mono-frequency force vector, generated simultaneously by an array of exciters, are carefully adjusted (or apportioned) until a so-called mono-phased response vector is obtained. The adjustment is required to produce a force vector to balance out the damping force vector.

Multiple excitations are generally difficult to implement in field testings because of the high equipment costs of exciters and operational restrictions imposed in the field. Among the methods available, this study has adopted the SISO method which is, by far, the easiest to implement. This method requires only one single excitation input and only response at one test point of a structure needs measuring at any one time. The SISO test procedures are simply repeated to cover the rest of the structure.

3.3.2.2 FREQUENCY RESPONSE FUNCTION MEASUREMENTS

The experimental data acquired are in the form of Frequency Response Function (FRF) measurements. FRF, as traditionally used in electronic engineering, refers to the amplitude ratio and phase difference between the sinusoidal voltage output and sinusoidal voltage input to a circuit (system). In structural dynamics, this relationship is usually expressed as a ratio (denoted by α_{ij} which is defined later as receptance) of the response x_i at coordinate i to the force f_j applied at another coordinate j of a structure. This output/input relationship is a function of different angular frequency of excitation ω .

$$\alpha_{ij}(\omega) = \frac{x_i(\omega)}{f_j(\omega)}$$

3.3.2.2-1

$$\text{or } x_i(\omega) = \alpha_{ij}(\omega) * f_j(\omega)$$

Sometimes FRF is wrongly used as synonymous with Transfer Function (TF). In control or electronic engineering, TF is defined as the Laplace transform of the ratio of temporal output and input over a complex S-plane with real (damping) and imaginary (frequency) axes. The singularities of TF are called *Poles*. The S values which make TF zero are called *Zeros*. Whereas FRF is a special case of TF when evaluated along the frequency axis. FRF can be obtained directly using Fourier instead of Laplace Transform.

With modern Discrete Fourier Transformation (DFT) analyzers, a variety of excitation signals can now be used to obtain FRF of a structure. Instead of the traditional mono-harmonic sinusoidal excitation, impulse, random and fast swept-sine excitation etc can now be used as well. Impulse excitation is usually applied with an instrumented hammer and the others with electromagnetic/piezoelectric exciters. However, because the DFT is obtained from finite length data, the implication on resolution and variance of the spectral estimates has to be borne in mind.

FRF are complex quantities and can be presented in a number of ways to convey different information regarding the characteristics of a system, namely:

- a. Bode plots: The amplitudes and phases are plotted against frequencies or
- b. Co-quad plots: the real and imaginary parts are plotted against frequencies and
- c. Argand or Nyquist plots: the imaginary parts are plotted against the real parts.

As already mentioned, FRF (denoted as $H(\omega)$) is, by definition, a ratio of the Fourier Transform of response to that of excitation :

$$H(\omega) = \frac{\mathcal{F}(x(t))}{\mathcal{F}(f(t))}$$

3.3.2.2-2

where $\mathcal{F}(\)$ denotes the Fourier Transform operator.

It is now shown that there are a variety of ways to obtain $H(\omega)$ from measurements. Let $G(\omega)$ be defined as the complex valued *Power Spectral Density* (PSD) function, then $H(\omega)$ can be obtained by:

$$H_{xf}(\omega) = \frac{G(x(\omega), f(\omega))}{G(f(\omega), f(\omega))} = \frac{G_{xf}(\omega)}{G_{ff}(\omega)} = H_1(\omega) \quad 3.3.2.2-3$$

$$H_{xf}(\omega) = \frac{G(x(\omega), x(\omega))}{G(x(\omega), f(\omega))} = \frac{G_{xx}(\omega)}{G_{xf}(\omega)} = H_2(\omega) \quad 3.3.2.2-4$$

Or alternatively by,

where $G_{xf}(\omega)$ is known as the *Cross* PSD functions of excitation and response .
and $G_{ff}(\omega)$, $G_{xx}(\omega)$ are known as the *Auto* PSD functions.

The two measurements (H_1 and H_2 respectively) should give, in theory, identical results under ideal conditions. However with the presence of noise in either excitation or response or both, an appropriate estimator for $H(\omega)$ has to be chosen for the best results. Uncorrelated noise can be eliminated from the *cross-spectrum* by sufficient *averaging*. However, averaging cannot reject noise in the *auto-spectra*. In the case of low levels of response relative to that of excitation (as in the neighbourhood of anti-resonances), H_1 is a better estimator. Whereas in the case of high levels of response (as in the neighbourhood of resonance) H_2 is a better estimator. The ratio of H_1 over H_2 yields a *coherence spectral function* $COH_{xf}(\omega)$, with values lying between 0 and 1, which is a quantitative measure of the effects of noise. $COH_{xf}(\omega)$ is again a function of frequency and is defined as:

$$COH_{xf}(\omega) = \frac{|G_{xy}(\omega)|^2}{G_{ff}(\omega) * G_{xx}(\omega)} \quad 3.3.2.2-5$$

A coherence value of 1 at a particular frequency means that the response and force have a very strong causality relationship and free from contamination of noise at that frequency. Whereas to the other extreme, a zero coherence means that there is no causality relationship between them. Low coherence is not only an indication of noise contamination but also non-linearity.

For structural systems, the responses can be displacement x , velocity v , acceleration a , or other suitable quantities; whilst excitation is usually force f . By definition:

$H_{xf}(\omega)$ (or more commonly denoted as α_{ij}) is called receptance,

$H_{vf}(\omega)$ is called mobility, and

$H_{af}(\omega)$ is called accelerance or inertance.

Once the measurement of these FRF at an array of spatial points of a structure is complete, parameter extraction can be proceeded in the ways as described in Chapter 5 and 6.

3.3.2.3 DATA ANALYSIS

The data analysis methods can broadly be classified into modal (or EMA) and non-modal (or Spatial) methods as defined in Section 1.2. EMA methods are well established techniques but non-modal methods are still to be developed further.

3.3.2.3.1 MODAL METHODS

EMA characterizes the dynamics of a structure in terms of its modal parameter set (i.e. undamped natural frequencies, modal damping factors and modal constants for each of the mode of vibration). In contrast to theoretical modal analysis, EMA determines these parameter set by experimental means and from experimentally measured Frequency

Historically, EMA techniques have undergone a gradual evolutionary process: from the early *Sine Testing*, *Resonance Testing* (see **Raney** ^[3.12], **Bishop and Gladwell** ^[3.13]), *Mobility testing* (see **Ewins** ^[3.14]), *Normal Mode Testing* to *Experimental Modal Analysis* as it is called today.

The growing popularity of EMA is illustrated by the increase in the number of organised activities dedicated to this technology: notably the International Modal Analysis Conference ^[3.15] which has been held annually since 1982 and the International Seminar On Modal Analysis ^[3.16] which has been held biannually since 1975. During the last decade, this technique has been widely applied to tackle a whole spectrum of engineering problems for modelling, troubleshooting and structural modification applications. Two new journals are published regularly on these subjects: The International Journal of Analytical and Experimental Modal Analysis ^[3.17] and Mechanical Systems And Signal Processing. ^[3.18] These publications show that the proliferation of this technology to other disciplines and applications is ever increasing particularly when there is a need to validate results from theoretical modelling techniques. The founding theory of this approach will be dealt with later in chapter 5.

3.3.2.3.2 NON-MODAL METHODS

Non-modal (or spatial) method refer to one which does not use the idea of modes of vibration explicitly. Usually, the identification process involves neither modal parameters determination nor the utilization of orthogonality properties of modes. The postulated mathematical model to fit is formulated in spatial rather than modal domain and is in terms of mass, stiffness and damping matrices of a structure. As for EMA, spatial method determine these parameter set from experimentally measured Frequency Response Functions also. So the two approaches use the same data set. Spatial approach can be classified as *direct* parameter identification method. The founding theory of this approach will be dealt with later in chapter 6.

It can be seen from the theoretical development in Section 3.2.2.2.2 that one can obtain the set of modal parameter (a modal model) by solving an eigenvalue problem posed in terms of the spatial matrices $[M]$, $[C]$ and $[K]$ (a spatial model). A spatial model can also be

obtained from a modal model if certain criteria can be met. The details on how this can be done will be further reviewed in Section 6.1.3.

In summary, both modal and spatial methods are useful testing techniques because they bridge the gap between *analysis* and *test* and amalgamate them into a complete cycle as illustrated in Figure 3.3.2.3.2-1.

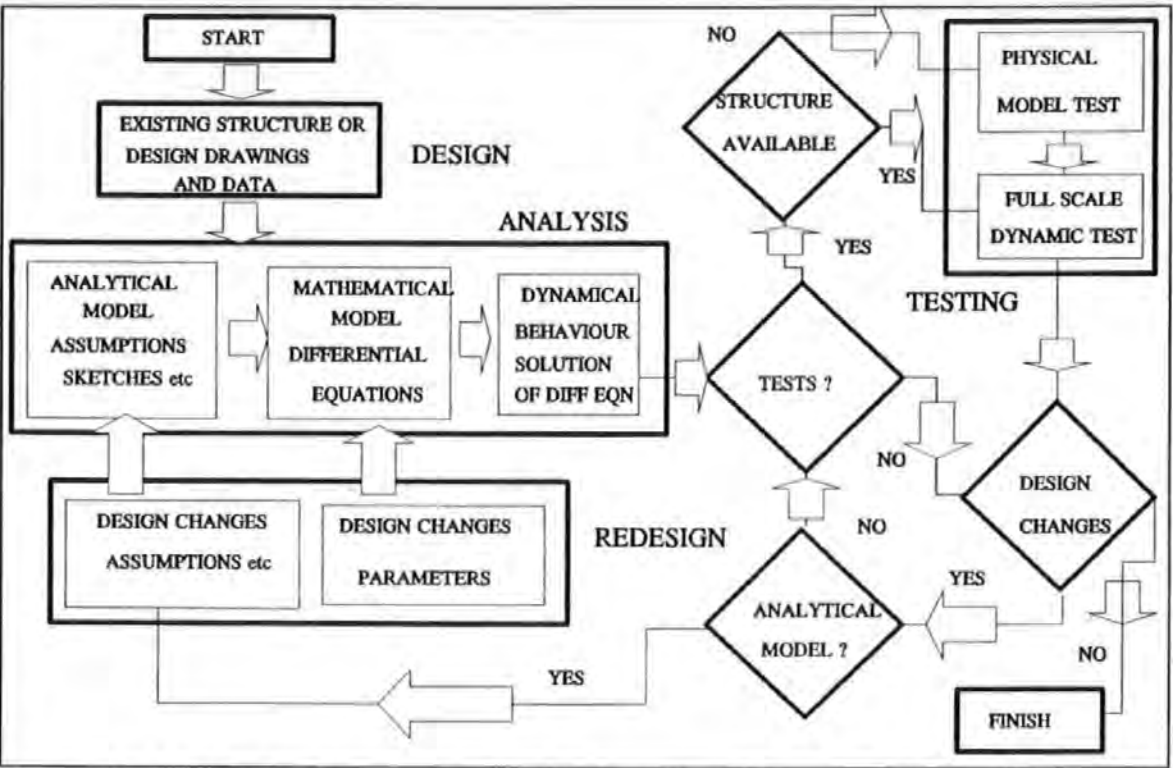


Figure 3.3.2.3.2-1 A schematic showing the interactions between design, analysis, testing and redesign cycle.

The completion of the links in this cycle has a very far reaching implication. It represent an evolutionary cycle within the context of better design and better construction of structures. Without the links provided by these experimental methods, designers or theoretical structural analysts would not have known whether the theoretical models derived truly describing the behaviour of the structure or meeting the design criteria.

3.4 CONCLUSIONS

Both theoretical and experimental methods can only be accurate if all the underlying assumptions are satisfied. Whilst this requirement can be met for simple structures, most engineering structures do not permit an accurate theoretical analysis.

Theoretical methods often produce spatial structural models of very large sizes. Damping assumed in these models is often not analytically derived but based on subjective assumptions. Theoretical modal models are obtained from theoretical spatial models via eigenvalue solutions and they too are of very large sizes. The technique of condensation of these large size matrices to smaller ones before carrying out a solution further introduce inaccuracies in these models.

Structural models obtained by the experimental methods introduced here, can either be in modal or spatial forms. The sizes of these models depend on the number of modes identified or number of coordinates measured and they are of much smaller sizes when compared with theoretical models. Both experimental modal and non-modal methods use the same experimental data set i.e. a set of frequency response functions measured at various coordinates of a structure. Therefore the same experimentation can be used for implementing the two techniques.

The basis of modal analysis is a linear transformation from an arbitrary coordinate space to normal coordinate space using the system's modal matrix and the utilisation of the orthogonality properties of the system's modes of vibration. In natural or normal coordinate space, modes are decoupled and this technique is called modal decoupling/decomposition. For undamped or proportionally damped systems, modal matrices are real. For generally damped or unproportionally damped systems, modal matrices are complex. Furthermore, orthogonality requires the system matrices to be symmetric which are generally true for most practical systems (with nonlinear systems as exceptions).

The validity of the experimental methods depends on the correct assumptions of a linear, second order and time-invariant system. Whilst few practical structures can perfectly fit all these assumptions, they should be borne in mind when applying these methods, especially when large discrepancies occur between the structures and their corresponding models.

Lastly, the experimental methods advocated here can be very useful supplements to though they may not be complete substitutes for theoretical methods.

CHAPTER 4

INSTRUMENTATION

4.0 INTRODUCTION

This chapter details the instrumentation system which was developed during the course of this investigation. As common to any experimental investigation, the instrumentation system is very important because good results can not have been obtained without good quality measurements and which, in turn, can not have been obtained without good instruments.

Section 4.1 provides an overview of the architecture of the system and the general requirements imposed on it. Sections 4.2 describes in greater details the technical development, performance and calibration of the new excitation mechanism. Sections 4.3 to 4.5 describe in turn each of the other key components of the system: transducers, signal generation and processing. Section 4.5 in particular depicts the hardware and software details of a computer-aided-test system which is instrumental for enhancing the efficiency and sophistication in experimentation.

4.1 THE INSTRUMENTATION SYSTEM

The conclusions drawn from the literature survey, as described in Chapter 2, highlight the inadequacy and limitations of the existing methods. This prompts the need for new methods to be developed. However, this could not be materialized without a concurrent development in instrumentations. The instrumentation system used in this investigation was the result of several stages of development which were geared to provide :

- a. a functional excitation system capable of generating periodic, pseudo random and harmonic forces of sufficiently large magnitude to excite large structure,
- b. a fast and efficient data collection and recording system which allows direct

digital processing and eliminates tedious, time-consuming analogue signal processing and

- c. a computer-controlled experimentation system offering programmability (i.e. customization of test procedures; fast and precise setting up of equipment for specific test requirements) and demanding minimum attention from an operator.

Before designing or building such a system, it was important to establish first what physical quantities should be measured and hence what instrument was to be used. In the field of structural dynamics, the influential physical quantities are excitation forces, kinematic or strain responses at some parts of a structure or, in some cases acoustic emission surrounding a vibrating structure. Force is usually measured with a piezoelectric force gauge or a resistive load cell. Kinematic response is measured with a linear voltage differential transformer (LVDT) for displacement, a seismometer for velocity, or an accelerometer for acceleration. Strain is conveniently measured with a strain gauge. And acoustic emission is measured with a microphone. It is a common practice of EMA to measure force and acceleration and hence these were chosen.

As common to the instrumentation used in most forced vibration tests, the system used included :

- an excitation mechanism
- movement response transducers
- a force transducer and
- signal conditioning, processing and recording equipment

In addition to these basic components, this research utilized a desk-top micro-computer which was linked to a digital signal synthesizer and a spectrum analyzer to form a powerful experimentation system. Figure 4.1-1 shows schematically the configuration of this system.

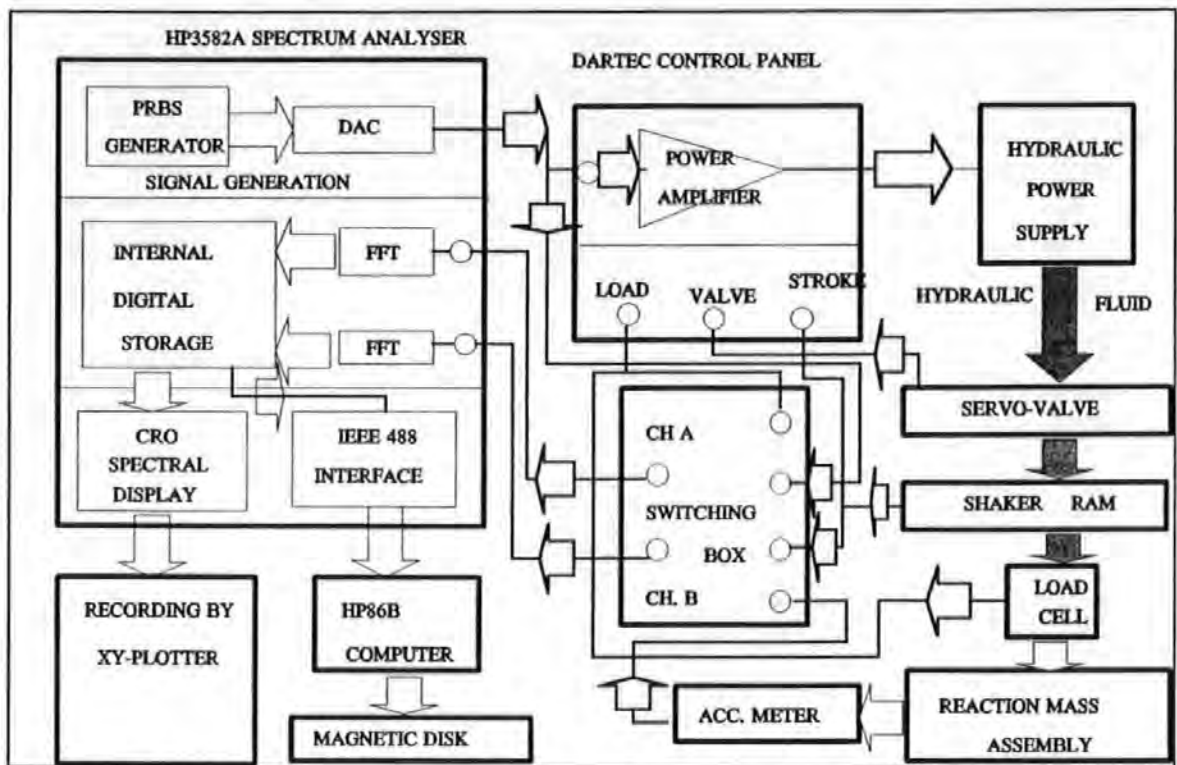


Figure 4.1-1 Schematic presentation of the configuration of the instrumentation system.

4.2 THE NEW EXCITATION MECHANISM

The new excitation mechanism (called shaker or exciter) was based on a hydraulic system funded by a Science and Engineering Research Council grant (Grant No. GR/D/02119). The exciter chosen has to fulfil the following functional and technical criteria :

- transportability
- force generation capability
- controllability and
- durability.

The reasons for the choice of a hydraulic system over others such as mechanical or electro-magnetic systems are manifold. First of all, the hydraulic actuation system offers large thrust and high precision in its operation. Unlike conventional eccentric rotating mass system which requires careful balancing of a multitude of units to produce a unidirectional force; the hydraulic system produces this force naturally with just a single unit. Secondly,

the hydraulic system can produce not only harmonic but also random forces. Thirdly, although an electro-magnetic actuation system can also be run rectilinearly and randomly, it has very small *stroke* capability. This is due to the limitation in the amount of movement of the moving armature allowed inside a fixed magnetized core. In contrast, the hydraulic system offers much larger stroke limits which are critical to producing forces of sufficiently large magnitudes at low frequencies.

4.2.1 BRIEF DESCRIPTIONS

The excitation mechanism was developed based on a proprietary hydraulic actuator manufactured and supplied by DARTEC (A schematic of the system is given in Figure 4.2.2.1). The excitation force is generated from the inertial reaction when the ram of the actuator propels and move a heavy 'dead mass'. A maximum stroke of 300 mm p.p. (peak-to-peak) is permitted by this system.

The movement of the ram is a result of pressurized oil thrusting a double acting piston which is housed inside a cylinder jacket. The jacket is completely sealed by two high pressure hydrostatic seals situated at both ends of the jacket. An electronic servo-valve controls the amount and the rate of oil flowing in-and-out of a manifold which is connected to a number of isolated chambers inside the cylinder. Apart from the sealing function, the two balanced hydrostatic seals also serve as bearings which eliminate any metal-to-metal contact between the moving parts, maintain centring of and provide lateral stiffness to the ram.

This actuator is powered by a 'portable' DARTEC hydraulic system which is consisted of the following units :

- a electrical power supply and control unit
- two powerful motor pumps unit
- a blast cooling fan unit
- an oil reservoir, high pressure hydraulic hoses and other ancillaries.

The system was specially adapted so that each unit could be dismantled into separate

smaller bits for ease of transportation (as shown in Figure 4.2.1-1). Re-assembling the units could also be done easily and quickly in the field.

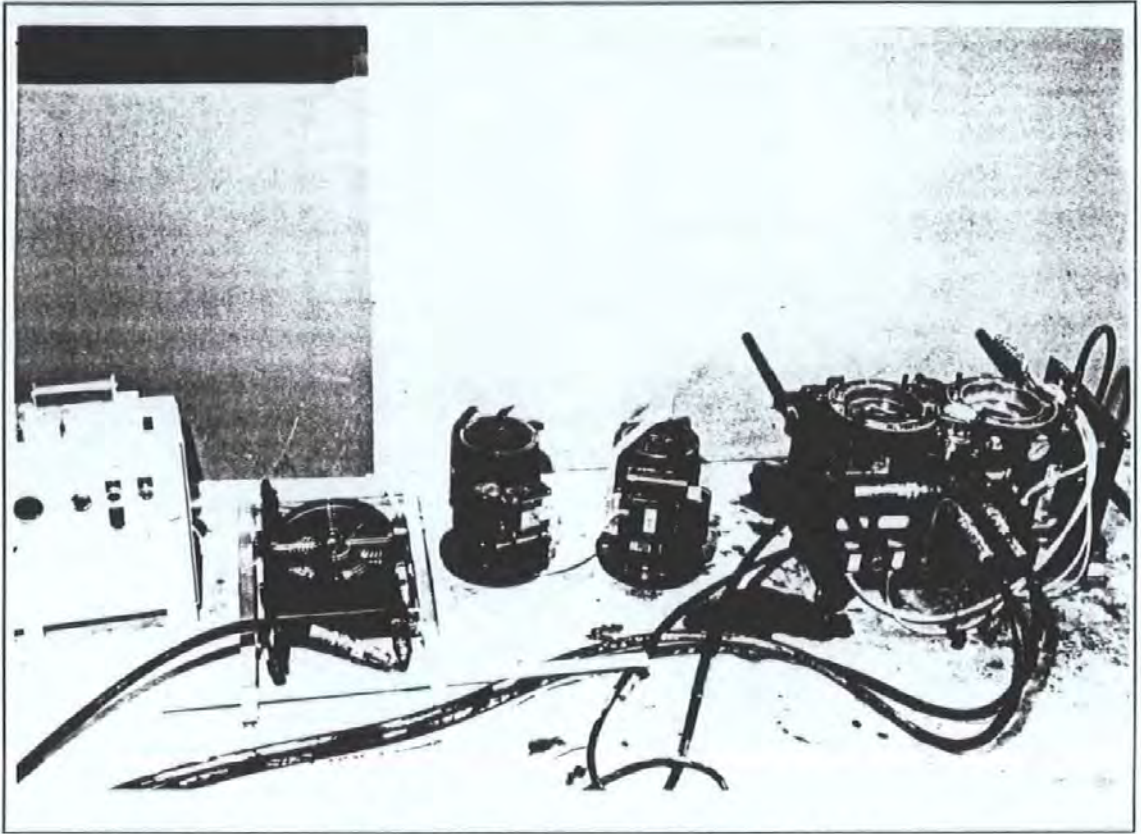


Figure 4.2.1-1 A photograph showing the dismantled DARTEC hydraulic power system.

The high pressure required for the operation of the actuator is delivered by two electric motor pumps which can be selected to run singly or jointly. The pressure is usually maintained at about 3000 psi during normal operation. The two pumps when working together can deliver a maximum oil flow rate of 9.6 litres per minute. This rate is considered small in comparison with those required by the normal sized actuators : usually in excess of 1000 litres per minute. The bore area of the ram is 0.4 square inches. These data are the important characteristics which governed the overall performance of the actuator in various ways such as :

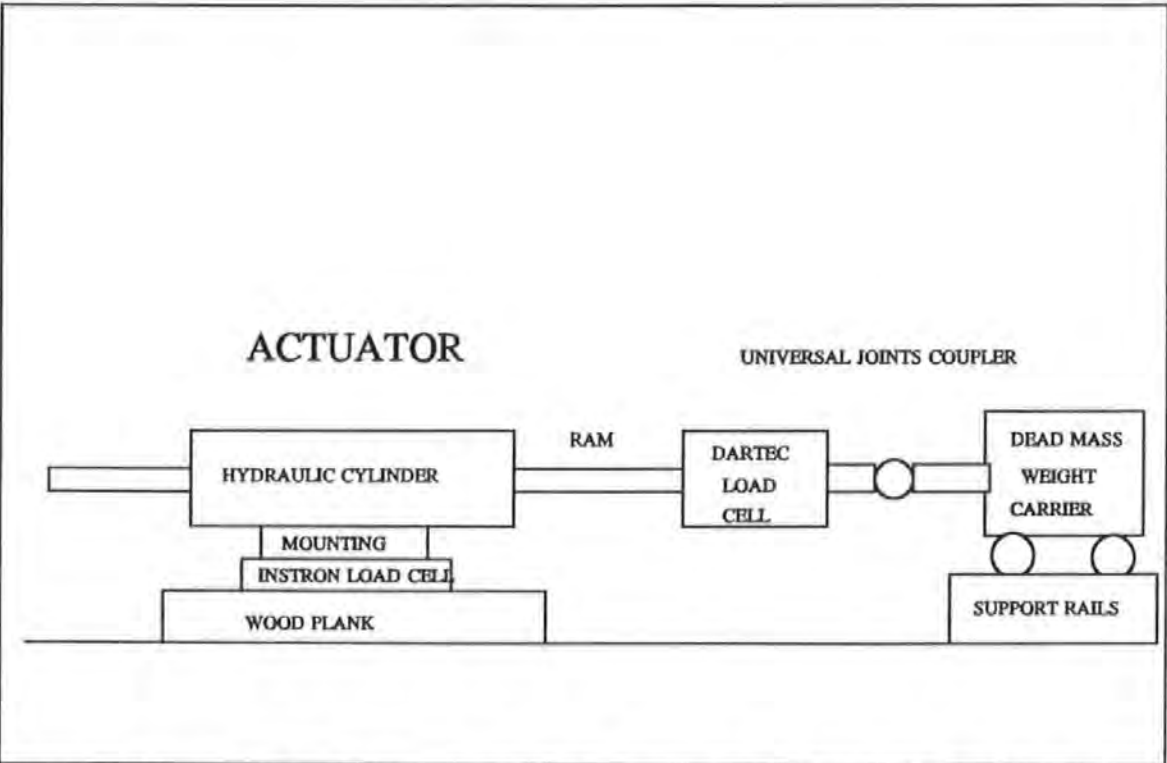
- the maximum allowable stroke at each frequency and
- the maximum allowable load carrying capacity.

The maximum static load capacity is rated at 5 KN. Generally speaking, the higher the frequencies, the smaller the stroke is allowed.

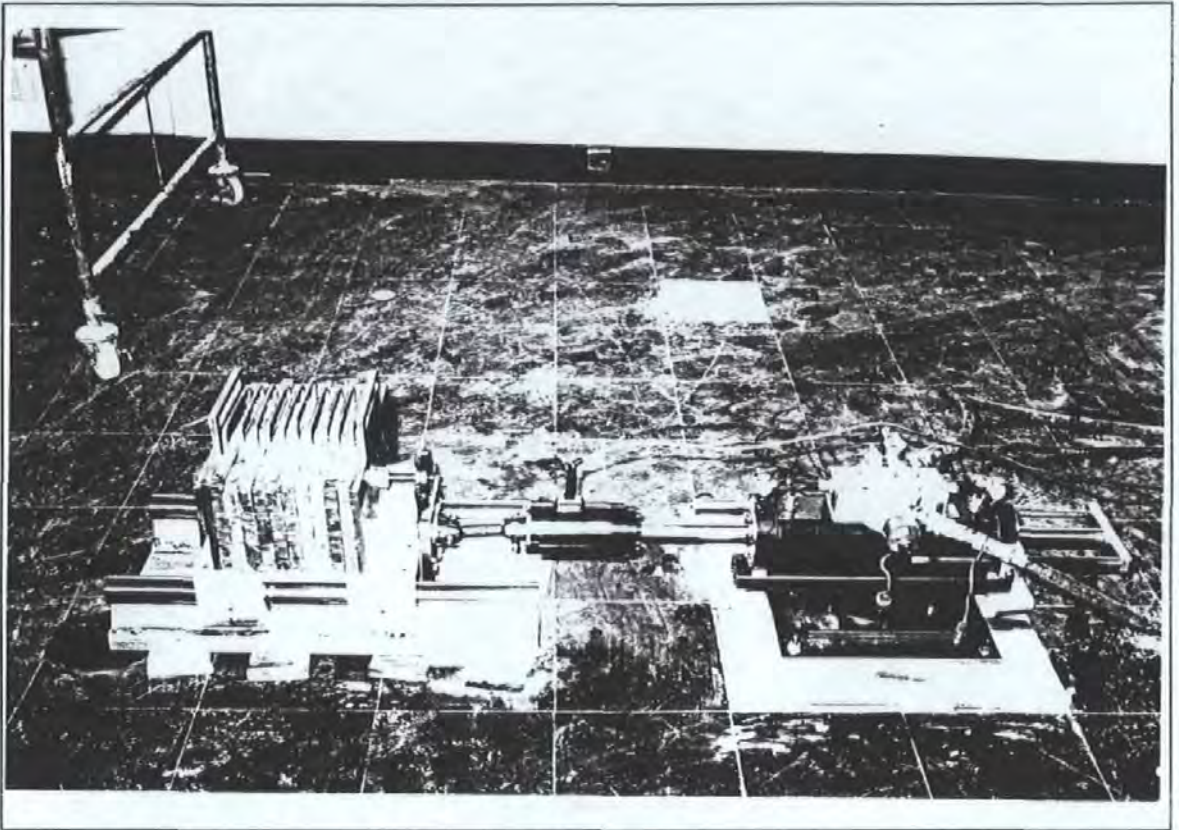
The stroke of the ram is monitored with an LVDT and the force measured with a resistive type load cell. Both transducers are powered electrically by the system's electronic control panel and their signals monitored with LED digital displays.

4.2.2 TECHNICAL DEVELOPMENTS

A schematic drawing and a photograph showing the hardware configuration of the excitation system are given in Figures 4.2.2-1 and 4.2.2-2 respectively.



Figures 4.2.2-1 A schematic drawing showing the hardware configuration of the excitation system.



Figures 4.2.2-2. A photograph showing the excitation system

Several items were added to the basic actuator to turn it into a functional exciter. The various 'add-on' components were :

- a mounting
- a reaction mass and its support and
- a coupler

A special mounting arrangement was designed and manufactured. This is a trunnion type mounting made from two square steel plates with one plate capable of sliding over the other and turning about a centre pivotal steel pin. The top plate has two semi-circular slots cut into it to allow bolts to go through and be secured onto the bottom plate. The bottom plate has holes at the four corners to receive the bolts from a wood plank which is glued to the floor of a tested structure. This arrangement allows the actuator to be turned to some other directions while in its secured position.

The final design of the reaction mass assembly was affected by a number of functional considerations. The dead masses were made from lead because of its high density. They

were cast as flat plates of approximately 15.5 Kg weight each. A steel handle and a slot was provided for each plate for easy loading and unloading from a weight carrier.

The weight carrier used for carrying these lead plates was a very sturdy unit made in the form of an open-box trolley with two steel plates welded at the two ends. A threaded screw rod was welded to the two end-plates. The lead plates were slotted one by one along the rod and through the slotting hole when loading. Two steel backing plates sandwiched the lead plates and were secured by two nuts at each end. Different numbers of plates, up to a maximum of 12, could be placed in the carrier to fulfil different force requirements.

The carrier was supported underneath by four linear ball bearings which ran on two rails with high quality surface finishes. These arrangements were instrumental in reducing nonlinear Coulomb friction.

A 'flexible' coupling joint was introduced between the carrier and the ram in order to eliminate any lateral load introduced to the ram which could damage the hydrostatic bearings. This coupler is a short 'push-rod' with universal ball-and-socket joints welded at both ends. An attachment freed from backlash is achieved by using two fine precision slotting pins. This coupling arrangement allows some vertical and horizontal misalignments between the ram and the carrier.

4.2.3 PERFORMANCE TESTS

Tests were carried out to determine the performance of the entire system in the low frequency range (i.e. 5 Hz or below) : not only the actuator system itself but also the other attachments to it. Performance in terms of the maximum force produced, the practical limits in stroke, acceleration etc of the ram in relation to driving frequencies was investigated. To eliminate other possible influential factors which might affect the performance of the actuator, simple sinusoidal instead of random or transient driving signals were used. Although the actuator allowed two modes of operation under either load or stroke control, only the latter was used. Details of this control can be found in the manufacturer's operation manual ^[4.1]. Some of the results from these tests are plotted in Figures 4.2.3-1 to 4.2.3-3.

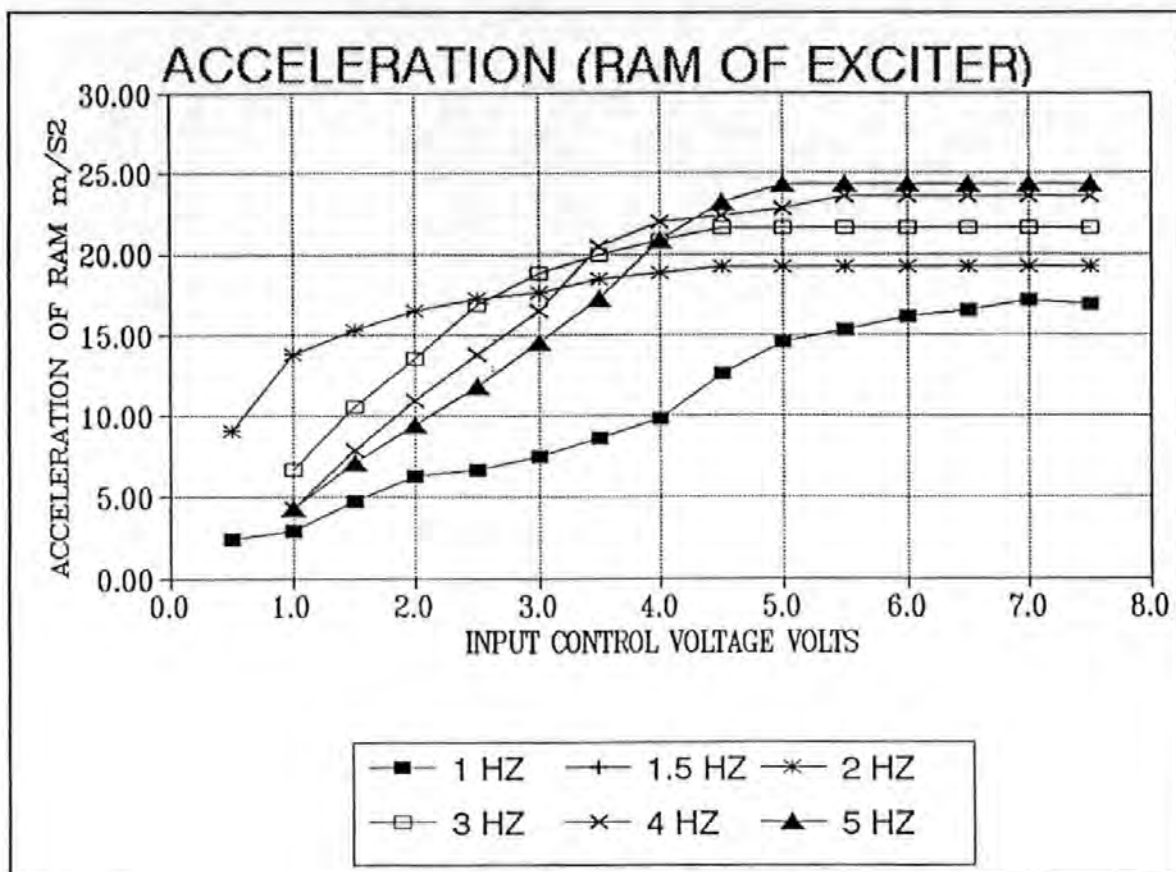


Figure 4.2.3-1 Acceleration responses of the loaded ram of the actuator over a range of input voltages and frequencies.

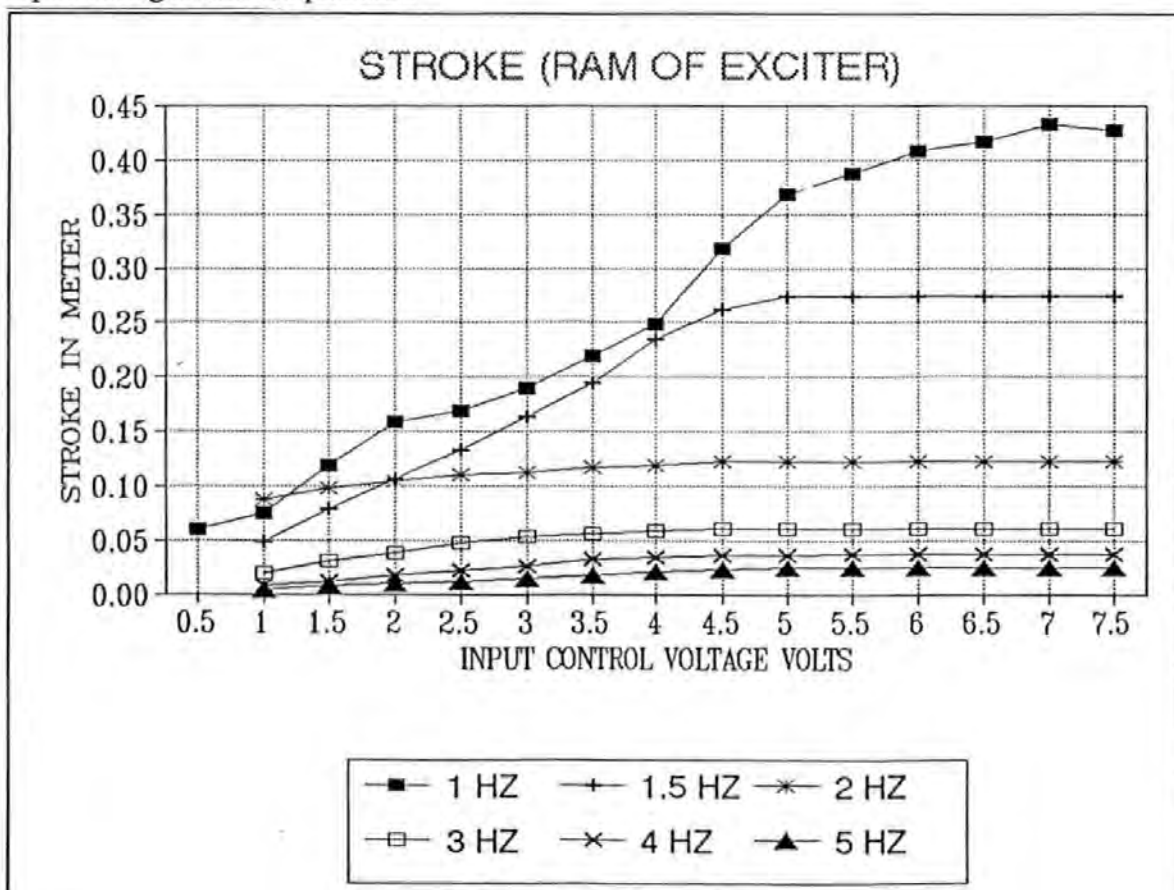


Figure 4.2.3-2 Stroke responses of the loaded ram of the actuator over a range of input voltages and frequencies.

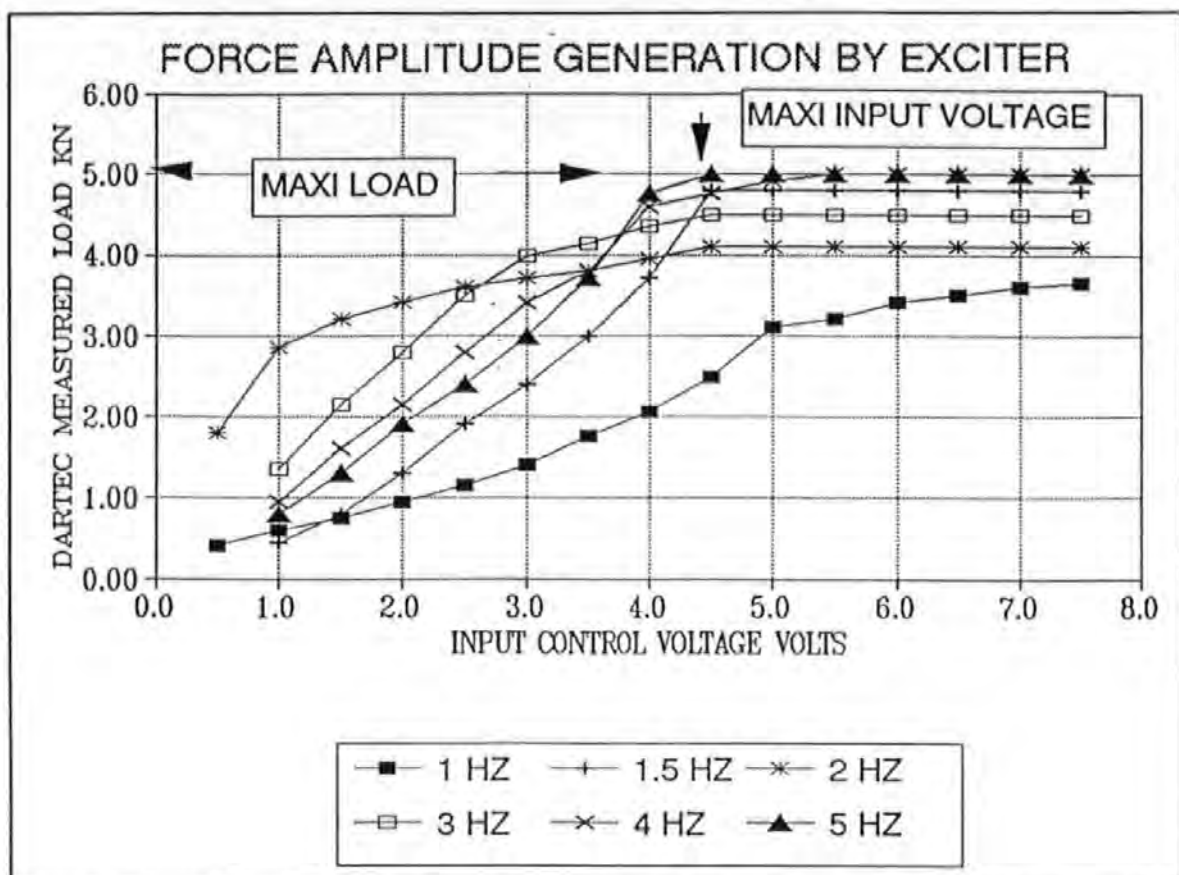


Figure 4.2.3-3 Load generation capability of the exciter over a range of input voltages and frequencies.

Figure 4.2.3-1 shows that the maximum accelerations allowed are 25 and 15 m/s^2 at 5 and 1 Hz respectively. These maxima stay the same for each of the frequencies even with further increase of the input voltages. Figure 4.2.3-2 show that the maximum strokes allowed are only 30 mm at 5 Hz which fall short of the 420 mm allowed at 1 Hz. The marginal decrease in the allowable maximum stroke is more subtle at lower frequencies. Figure 4.2.3-3 shows that the maximum force generated is 5 KN when driving at 5 Hz. No further increase in force is allowed when the input voltages exceed 4.5 Volts. These figures all show that if the control voltage is well below the maximum input voltage allowed (i.e. the capacity of the hydraulic system is not exceeded) then the performance of the exciter is essentially linear. All these maxima are governed mainly by the characteristics of the hydraulic actuator such as :

- the maximum supplied oil pressure
- the maximum oil flow rate and
- the effective bore area of the ram.

In these tests, the driving signal feeding the control panel was obtained from the Philips signal synthesizer. Whilst this signal might be regarded as a relatively pure sinusoid, the effects such as due to the nonlinear characteristics of the hydraulic exciter and its attachments which produced forces with the significant presence of harmonic components. These harmonics had frequencies of integer multiples of the forcing frequency. This was particularly so when the exciter was operating at conditions close to the limits imposed by the pumps, electronic valves etc.

4.2.4 CALIBRATIONS

A series of calibration tests were carried out to determine the relationships between the measured force from the DARTEC load cell and the actual shear force transmitted through the mounting and measured with the INSTRON load cell.

The ratios between the forces measured by the two transducers were determined using sinusoidal as well as PRBS (Pseudo-Random Binary Sequence) forces. The results show that these ratios (DARTEC reading over INSTRON reading) can vary from 1.04 to about 1.06 in sinusoidal tests, and from 1.05 to 1.06 in PRBS tests over a range of frequencies from 0 to 25 Hz and a combination of different loading conditions. Further information can be found in Reference ^[42]. So an average of 5 % error is expected if load is taken from the DARTEC instead of the INSTRON load cell.

4.3 SENSORS AND TRANSDUCERS

The sensors and transducers required were naturally fallen into two categories i.e. those concerning :

- a. the operation of the exciter and
- b. the responses of a structure.

4.3.1 STROKE MEASUREMENT

The proper operation of the exciter requires the stroke of the ram to be monitored at all times to ensure the satisfactory running of the actuator under the *stroke control*

mode. An LVDT (linear voltage differential transformer) was used for this purpose. The LVDT output signal is frequency modulated using a 5 KHz carrier. An LED digital display of the stroke is provided in the control panel.

4.3.2 ACCELEROMETERS

4.3.2.1 DESCRIPTIONS

The acceleration response of a structure was measured with servo-driven closed-loop torque balance **SCHAEVITZ** accelerometers. With the servo-control mechanism, these accelerometers are capable of working with DC signals which most piezoelectric types of accelerometers cannot. The transduction principle and details of the operations of these accelerometers can be found in Reference ^[4.3]. These accelerometers are externally powered so that they can be made very light and small. A special power pack and a junction box provide the required electrical power and cable connections. When used in the field, each accelerometer was screw-mounted on a heavy metal block for stability.

Each accelerometer has a sensitivity axis which is to be aligned along the intended response direction. Apart from the sensitivity direction, each accelerometer has also got a cross-axis sensitivity which is usually only a small value and no special considerations are required.

4.3.2.2 CALIBRATIONS

The accelerometers were calibrated both statically and dynamically. As these accelerometers are designed to work with DC, static gravimetric calibrations were performed using the Earth's gravitational field. These were carried out by placing the accelerometers on a *sine table* which could be tilted about a base to very precise angles. The corresponding voltage outputs from the accelerometers at various angles were used to calculate their sensitivities.

Dynamic calibrations were carried out by placing all the accelerometers side-by-side on the weight carrier. The ratios of the corresponding voltage outputs from each of the accelerometers and those from the LVDT were used to calculate their sensitivities. In taking these measurements the exciter's ram was set to wide band random motion.

The results of the calibration are summarized in Table 4.3.2.2-1.

TABLE 4.3.2.2-1 COMPARISON OF THE EXPERIMENTAL AND THE MANUFACTURER'S CALIBRATION OF THE ACCELEROMETERS.

Accelerometer serial number	Sensitivity volts/g	Linear regression coefficients	Manufacturer's calibration
1650	2.442	0.9981	NO RECORD
1652	2.454	0.9999	2.534
1653	2.490	0.9998	2.531
1654	2.450	0.9997	2.521
1658	2.396	0.9998	NO RECORD

The results show that the sensitivities of the accelerometers are ranging from 2.396 to about 2.490 (Volts/g) which are quite close to those specified by the manufacturer. The calibration had resulted a set of linear regression coefficients which were all very close to one. The linear regression coefficient is a measure of the linearity between voltage outputs and the corresponding sine of angles of tilt. This coefficient normally has a value ranging between 0 and 1. A coefficient of 1 indicates perfect linearity.

4.4 SIGNAL CONDITIONING AND PROCESSING

4.4.1 GENERAL SIGNAL CONDITIONING

Very often and especially in the field, the pick-up signals were weak and noisy. Signal conditioning was required before these signals could be read and recorded. Simple signal conditioning operations such as amplifying, DC off-setting and low-pass filtering were provided by an integrated electronic hardware.

Because of the inadvertent production of a small DC output when an accelerometer was not aligned properly on a horizontal plane, offsetting this DC output was required. Providing the magnitude of this DC signal was not too excessive, most modern signal processing equipments could cope with this situation because of the wide dynamic range

and high sensitivity they have. The HP 3582A spectrum analyzer has a 75 dB dynamic range to spare. So DC offset operation was often waived in return for a speedy measurement.

4.4.2 SIGNAL RECORDING

4.4.2.1 ANALOG TAPE RECORDING

The outputs from various transducers were analog voltage signals and were recorded using a RACAL instrumentation tape recorder. The recorder was a four channels FM tape recorder with a range of selectable recording speeds. A speed of 15/16 inches per second was chosen for most recordings. At this speed, the recorder has a useful bandwidth from DC to about 300 Hz. Details of the operation of the recorder can be found elsewhere^[4.4]. Tape recording was used for backup only.

4.4.2.2 DIGITAL DATA RECORDING

Handling and processing data recorded as analogue signals was very troublesome and inefficient. Digital data which are not only easy to transfer from one recording medium to another but also provide high *fidelity* of transfer. In Section 4.5, the details on the digital processing and recording of data utilizing a desk-top computer will be described.

4.4.3 EXCITATION SIGNAL GENERATION

4.4.3.1 SINUSOIDAL SIGNALS

The ram's motion is under the control of the input signal fed into the DARTEC control panel. These signals, and hence the ram's motion, could be sinusoidal or random. An internal sinusoidal signal generator is provided as an integral part of the control panel for this purpose. However an external signal source, a Philips PM 5190 programmable Low Frequency signal synthesizer, was used instead. Sinusoidal signal generation in the synthesizer is based on digital algorithms rather than crystal oscillations. This equipment can either be controlled from the front-panel or remotely via an IEC 625 interface. Signal frequencies are selectable from 1 MHz to 2 MHz, and AC voltage levels are also selectable from 0 to just below 20 Volts. It also allows an option of imposing an intended DC

bias voltage over the preset AC voltage levels. Details of the operation of the generator can be found elsewhere^[4,5].

4.4.3.2 PERIODIC RANDOM SIGNALS

A periodic random noise generator is provided by the Hewlett Packard spectrum analyzer which is shown in Figure 4.4.3.2-1. This noise source is functionally equivalent to a tracking generator with 256 parallel oscillators. The frequencies of these oscillators coincided with the 256 spectral lines provided by the analyzer. A carefully matched uniform pass-band filter is built in the analyzer. The signal generation is based on the use of a recursive Pseudo Random Binary Sequences (PRBS) shift registers and implemented in hard-wired chips. The exact details are outside the scope of this review and other references on signal generation techniques should be consulted.

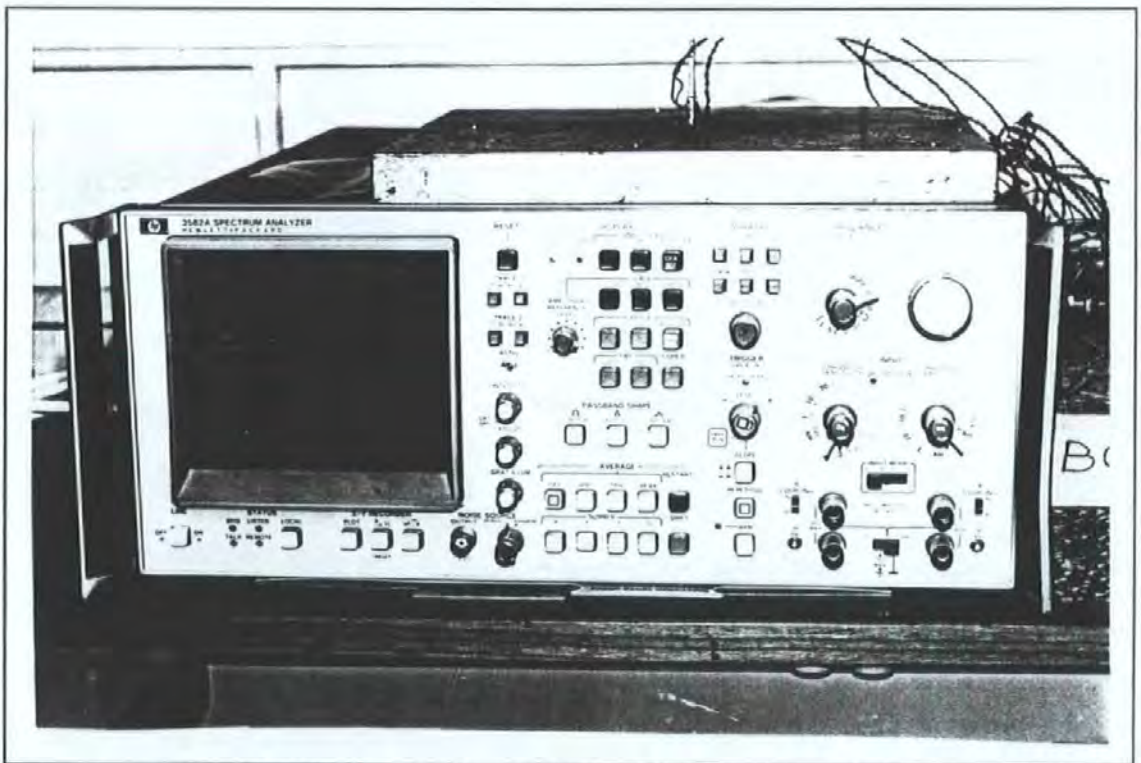


Figure 4.4.3.2-1 The Hewlett Packard HP 3582A spectrum analyzer.

4.4.4 SPECTRAL ANALYSIS

The power of modern signal processing techniques lies in the capability to perform Discrete Fourier Transform (DFT) on discrete, sampled time data of finite *block length*. DFT is an implementation of the Fast Fourier Transform (FFT) to extract spectral

information from sampled time data. Equipment with such capability is called a spectrum analyzer, or a Fourier analyzer. The analyzer used in this investigation was a Hewlett Packard HP 3582A dual channel real-time spectrum analyzer. A brief description of the signal processing performed in the analyzer is given below.

Incoming signals are first passed through an analogue 25 KHz low-pass filter. This filter eliminates any energy in the signals due to frequencies higher than the fastest sampling rate. Failure to do so produces *aliasing* (see Ewins ^[5,10] for a concise description). The filtered signals are then passed through an analogue-digital-converter (ADC) which has 12 bits precision of conversion.

Further digital filtering is performed by four Large Scale Integration chips which can be considered as a cascade of eight distinct filter stages as a close analogy. Each stage of the filter reduces the incoming signal bandwidth by a factor of 2 or 5. The ADC is set at a sampling rate of 102.4 KHz i.e. 102400 samples per second. The filtered time sequences are then stored in the time buffer until a full 1024 data points (data block length for single channel) or 512 (for dual channels) are recorded.

The time domain data are then 'windowed' which can be considered as a process of 'point-by-point' multiplication of the digitized time data and the stored weighting functions appropriate to the window selected. A suitable window has to be selected in relation to the types of signals encountered. Windowing suppresses a signal processing problem known as *leakage* (see Ewins ^[5,10] for a concise description).

The DFT computation is performed by a 16 bits built-in micro-processor inside the analyzer. The computed spectral data are then stored in the frequency buffers and can be called up for display on the analyzer screen. *Averaging* is also performed to improve the quality and accuracy of the measurements. A good selection of different averaging facilities are provided by the analyzer : such as time or root-mean-square RMS spectral averaging. Further information regarding the operation of the analyzer can be found elsewhere ^{[4.6], [4.7] and [4.8]}.

4.5 COMPUTER-AIDED-TESTING (CAT)

Labour and time intensive manual testing techniques are no longer adequate for the new

advanced methods. The advent of instrumentation technologies, and the successful miniaturization of computer hardware bring CAT from the laboratory to the field. Automation in data acquisition and recording can now be carried out in the field. Many more commercial systems are now available from well known manufacturers such as: Bruel & Kjaer, Solartron or Structural Dynamic Research Corporation etc. However this research had not have the opportunity of obtaining any one of these systems. Instead a system of very low cost was developed in-house.

4.5.1 THE HARDWARE CONFIGURATIONS

Basically, the CAT system was built upon the integration of several stand-alone instruments with a Hewlett Packard HP 86B micro-computer (a schematic of this system is shown in Figure 4.1-1). The resulting costs were low if the costs of software developments were discounted. The extra costs on the hardware required was small.

The physical integration was achieved by interfacing the computer, its peripherals and other remotely controlled ('remote control' is used here as a contrast to local 'front-panel' control) equipments via an IEEE 488 Interface, or otherwise known as the Hewlett Packard Interface Bus (HPIB). The IEEE 488 bus is one of the most popular universal interface standards which unify both the hardware and software interfacing requirements. This standard has been adopted by most instrument manufacturers in their products. Other standards such as the European IEC 625 or the RS 232 are also used.

Equipments with the same interface can simply be plugged together with suitable cables and connectors. Equipments complying with different standards can also be linked together provided suitable adaptors are used. These adaptors are more than just merely a device for mechanical compliance. A special adaptor was made to enable the interfacing of the PHILIPS signal synthesizer, which is based on the IEC 625 standard, to the IEEE 488 based bus.

On the HP 86 computer, this interface capability is supported by an input/output interface cartridge (an HP 82936A I/O ROM Drawer). In essence, this cartridge allows the computer :

- a. to address to each interfacing instrument,

- b. to perform controls and data input/output operations using high level programming languages rather than low level machine languages and
- c. to perform 'handshaking' according to the designated protocols during data transmission.

4.5.2 THE CONTROL PROGRAMS

The test sequences and the associated controls were coded as a computer program. This control program was written in extended HP BASIC and was designed and written in a modular structure so that future modifications and additions could be done easily. The running of the program was menu driven and an operator's intervention was kept to a minimum. This program was capable of the following tasks :

- a. Remote setting up of equipments (this was done by sending appropriate sequences of the GPIB interface commands from the computer to the various instruments via the IEEE 488 bus).
- b. Interrogation of the status of the measurement process, for instance to check if overloading had occurred (this was done by interrogating a particular bit in a special memory register chip inside the HP3582A analyzer)
- c. Recording digital data and spectral displays from the analyzer onto magnetic disks for storage (this was done by down-loading sequences of bits from the special memory registers inside the HP3582A analyzer which held the spectral and screen display data).

As a result, testing could be performed much more speedily than before and large quantities of useful data could be acquired with very little attention from the operator. Generally, this CAT system is beneficial to the experimentation process in a number of ways :

- a. It eliminates the tedious tasks of manual recording and switching.
- b. It increases the speed of data recording, retrieval and storage

- c. It makes immediate on-site processing possible for preliminary checking of data.
- d. It allows data transferability from one to another computing environments : between micros, PC or main-frame computers. The latter is particularly useful for very large scale data processing and calculation.

Details and listing of the control program are given in APPENDIX 4.5.2.

4.6 SUMMARY

A new excitation mechanism was developed and its performance checked. Generally, the exciter has to be operated well within the operating limits otherwise non-linear distortions will result. The sensors were all calibrated so that measured data can be converted to their real physical units. The force read by the Dartec load cell have a +5% error relative to the load transmitted to the mounting. A low cost but powerful CAT system was successfully developed and could be put to use in the field.

CHAPTER 5

EXTRACTION OF MODAL PARAMETERS FROM FORCED VIBRATION DATA

5.0 INTRODUCTION

This chapter is specifically concerned with the methods of extraction of modal parameters to obtain a modally truncated model of a real structure. A modally truncated model is defined as a modal model which is representative of the effects of a small number of identifiable modes within a limited frequency band only (instead of an infinite number of modes a continuous structure might have). The effects of the modes outside this frequency band is called the 'residual' effects. This will be explained more clearly when dealing with the receptance frequency response function in series expansion form in Section 5.1.1.

A brief review of some conventional methods will be given first and followed by the presentation of an alternative algorithm developed by the author. This algorithm is based on direct least-square fitting technique and shares some similarities to the dynamic stiffness method. An exercise to compare this algorithm with two commonly used methods was carried out and the results are reported. Modal parameter extraction is an essential process in the derivation of a modal model of a structure. The validity of this model depends very much on the capabilities and accuracies of the methods used in this process.

An assortment of methods is in existence nowadays. Broadly speaking, most of the popular methods used today can be categorised according to the types of data required for the operation. Those methods which work with time or frequency data are known as the time and frequency domain methods respectively.

In the early days when sophisticated instrumentation and digital computers were not available, the process of modal parameters determination could only be carried out by simple and rudimentary means. In those days, the data obtained were often in analogue form: such as magnetic signals on tape, strip charts or hand written readings and hence they were difficult to process.

Many early methods, such as the so called 'peak picking' method, were based on visual inspection and on simple arithmetic calculations to a large extent. The frequencies corresponding to the peaks in an FRF spectra (the resonance frequencies) give an estimate of the undamped natural frequencies. The modal damping factors were often determined using either the 'half-power' or the 'logarithmic decay' methods. All these methods did not require phase measurements and relatively simple instruments were adequate for their implementation. Much of the work carried out during the 1960's and the 1970's was based on these methods. In fact, many of these methods are still being used today.

With the introduction of better instruments, more sophisticated analysis methods have been employed. In particular, phase information allowed additional criteria to be used for modal parameters determination. For instance, the undamped natural frequency of a system with well separated modes (i.e. the assumptions of SDOF hold) can be located on the frequency axis corresponding to :

- a. the peak (or trough if negative) in the imaginary part of an FRF Bode plot,
- b. the maximum rate of frequency-swept-through-an-arc of a resonance circle in a Nyquist plot,
- c. zeros in a real component FRF Bode plot or
- d. 90 degree phase angle changes in phase FRF Bode plots

A string of methods were also available for the determination of other modal parameters using phase information. Schiff ^[5.4] had given an excellent account of the numerous methods of this category and further details can be found in this reference.

With the availability of even more powerful instruments, more sophisticated methods

have been applied. Most of these advance methods performed a process known as 'curve-fitting'. In essence, the object of this process is fitting measured data to a postulated mathematical model. Most of these methods apply least-square-fitting technique in one way or another.

Another broad categorization of the various methods can be made according to the number of modes assumed in this curve-fitting process. Methods which curve-fit a single mode at a time or a multitude of modes simultaneously are termed SDOF-fit and MDOF-fit methods respectively. Some methods, which perform this curve-fitting process by utilizing data from all measurement locations in a single run, are termed the *global* methods.

5.1 CONVENTIONAL METHODS

As already mentioned, most methods can be classified as Time Domain (TD) or Frequency Domain (FD) methods. In general, most TD methods require time data captured from the transient responses of a structure subsequent to an impulsive type excitation. Because these transient events (measured as a series of waveforms) usually happen only within a very short period of time, specialized equipments, such as a transient recorder capable of high sampling rates, are required. These waveforms have to be recorded at very closely spaced discrete instants of time in order to satisfy temporal and hence spectral resolution requirements. Furthermore, simultaneous recording of all the measurement locations of a structure are sometimes mandatory as in the case of multi-input methods. All these factors impose specific and often formidable requirements on data acquisition as well as analysis.

FD methods here refer to those methods which are often carried out with steady-state step-sine, slowly or rapidly swept-sine (also known as '*chirp*'), multi-sine, periodic or periodic-random type of excitation. Spectral frequency response data are then obtained from sampled time data via Discrete Fourier Transformation (DFT). The spectral resolution and accuracy of this transform depends on the various signal processing operations involved such as: selection of the rate of sampling, block length of time series, *windowing*, *anti-aliasing* filtering, *averaging* and so on appropriate to the test conditions. Because this study is mainly concentrated on FD methods, no further discussions of TD methods will be given here. Readers interested in the various TD methods such as: the Least Square Complex

Exponential ^[5.2], Z-Transform ^[5.3], Autoregressive Moving Average (ARMA)^[5.4], Poly-reference^[5.5] and Ibrahim TD methods ^[5.6] can consult the original papers cited in the references. In particular, two papers by Cooper ^[5.7] and Fullekrug ^[5.8] have given a general survey and comparison of these TD methods and are useful references.

The most frequently used model, using SISO (as introduced in Section 3.3.2.1), is the series representation of receptance of a multi-degree-of-freedom system:

$$\alpha_{sr} = \sum_{i=1}^N \frac{G_{sr,i}^*}{\omega_i^2 - \omega^2 + j \gamma_i \omega_i^2} \quad 5.1-1$$

where γ_i is the hysteretic damping loss factor
 ω_i is the undamped natural frequency
 $G_{sr,i}^*$ is the complex modal constant
 N is the total number of degrees of freedom (or modes) of the system
subscript i denotes the i^{th} mode of vibration
subscript sr denotes response at coordinate s and force at coordinate r
 j is the imaginary unit $\sqrt{-1}$

This equation is often considered as the keystone to the understanding of modal analysis which stipulates that receptance at any frequency is a summation (or superposition) of the contributions of all the system's modes at that frequency. As this is a rather important equation, a short derivation is given. The equation of motion with hysteretic damping matrix $[H]$ is often quoted as:

$$[M] * \{ \ddot{x} \} + j [H] * \{ \dot{x} \} + [K] * \{ x \} = \{ f \} \quad 5.1-2$$

The homogeneous solution to Equation 5.1-2 is again an eigen-value problem:

$$\omega_r^{*2} [M] \{ \phi^* \} = ([K] + j [H]) \{ \phi^* \} \quad 5.1-3$$

where ω_r^{*2} is a complex eigenvalue
 $\{ \phi^* \}$ is an associated complex eigenvector

Equation 5.1-3 has complex eigenvalues because the dynamical matrix $[M]^{-1} ([K] + j [H])$ is complex. It can be shown that orthogonality properties apply here as well. So the equation of motion can be diagonalized by the complex modal matrix $[\Phi^*]$ in the same way

as the undamped modal matrix $[\Phi]$ in the undamped case. Hence:

$$[\Phi^*]^T [M] [\Phi^*] = [M^*] \quad 5.1-4a$$

$$[\Phi^*]^T [K] [\Phi^*] = [K^*] \quad 5.1-4b$$

$$[\Phi^*]^T [H] [\Phi^*] = [H^*] \quad 5.1-4c$$

Where $[M^*]$, $[K^*]$ and $[H^*]$ are all diagonal matrices. In the forced vibration case, the frequency response function is obtained by applying Fourier Transform to Equation 5.1-2:

$$(-\omega^2 [M] + j [H] + [K]) \{X(\omega)\} = \{F(\omega)\} \quad 5.1-5$$

Pre-multiplying by $[\Phi^*]^T$ and applying the modal transformation to Equation 5.1-5 to obtain:

$$(-\omega^2 [M^*] + j [H^*] + [K^*]) \{\eta(\omega)\} = [\Phi^*]^T \{F(\omega)\} \quad 5.1-6$$

$$\{\eta(\omega)\} = (-\omega^2 [M^*] + j [H^*] + [K^*])^{-1} [\Phi^*]^T \{F(\omega)\} \quad 5.1-7$$

$$\{X(\omega)\} = [\Phi] (-\omega^2 [M^*] + j [H^*] + [K^*])^{-1} [\Phi^*]^T \{F(\omega)\} \quad 5.1-8$$

The inverse of diagonal matrices are obtained simply by inverting the diagonal elements of these matrices. The product of the matrices depicted in Equation 5.1-8 becomes a sum series. It can be shown that if there is only one force applied at coordinate r and the response X_s at coordinate s can be obtained:

$$X_s = \left(\sum_{i=1}^N \frac{\Phi_{si}^* \Phi_{ri}^*}{-\omega^2 m_i + j h_i + k_i} \right) F_r(\omega) \quad 5.1-9$$

$$\text{by denoting} \quad \frac{\Phi_{si}^* \Phi_{ri}^*}{m_i} = G_{sr,i}^* \quad \gamma_i \omega_i^2 = \frac{h_i}{m_i} \quad \omega_i^2 = \frac{k_i}{m_i}$$

$$X_s = \left(\sum_{i=1}^N \frac{\frac{\phi_{si}^* \phi_{ri}^*}{m_i}}{-\omega^2 + j \gamma_i \omega_i^2 + \omega_i^2} \right) F_r(\omega) \quad 5.1-10$$

The expression in bracket is in fact receptance α_{sr} as depicted in Equation 5.1-1.

5.1.1 SDOF-FIT METHODS

SDOF-fit methods are all based on the assumption that in the vicinity of the natural frequency of a mode on a frequency axis, the total response of a structure in this frequency band is dominated by the effects of that mode alone and those from the neighbouring modes are either negligible or their effects can be represented collectively by complex *residuals*. So considering frequencies close to the natural frequency of the i^{th} mode, receptance can be represented by (note that the summation sign is dropped):

$$\alpha_{sr} \text{ (for } \omega \text{ close to } \omega_i \text{)} = \frac{G_{sr,i}^*}{\omega_i^2 - \omega^2 + j \gamma_i \omega_i^2} + (a + b j)$$

5.1.1-1

The first term on the right hand side of the equation represents a circular loci in an Argand plot which will be explained further in Section 5.1.1.1. The second term $(a+bj)$ is the complex residual. This assumption works well for a structure with well-separated modes i.e. low modal density.

SDOF-fit methods are amongst the most widely used methods which can often be carried out by simple graphical techniques or elementary arithmetic manipulation of data. Some methods utilize certain geometrically realizable forms, such as straight lines and circles, exhibited by the data on special plots as the criteria for the determination of the modal parameters. They are usually referred as the Circle-Fit and Straight-Line-Fit methods respectively. Since these two methods had been used in the comparison exercise reported in Section 5.4, the theoretical basis of these two methods is to be expanded in

slightly greater details below.

5.1.1.1 CIRCLE-FIT METHOD

This is a method due to **Kennedy and Pancu** ^[5.9]. In this method, the real (coincident) part are plotted versus the imaginary (quadrature) part of the complex receptance or mobility data in an Argand plane. This plot is usually known as a Nyquist plot. By choosing the duality appropriately: i.e. a suitable damping model and the type of frequency data used (receptance α for hysteretic damping as given in Equation 5.1.1-1, or mobility β for viscous damping), the loci traced by the data points, which clustered around the regions of resonance, are in the form of a series of arcs of circles. A thorough explanation of the use of this method has been given by **Ewins** ^[5.10].

The accuracy which can be achieved by this method is found to be quite sensitive to two factors: i.e. the levels of noise in the data and frequency resolution between consecutive data points. Noisy data points will show up wandering irregularly, or randomly in the case of random noise, away from the true circle. Apart from random measurement noise, it is a known phenomenon that near resonance, the force amplitudes drop while the response amplitudes increase drastically. The large disparity between their magnitudes (or signals) causes measurement errors. Therefore the measured receptance can be highly 'contaminated' with noise in these circumstances. This problem is often reflected by showing a very low coherence between excitation and response near resonance.

The effects of frequency resolution will, in turn, depend on the levels of damping. At one extreme, low damping 'coupled' with insufficient frequency resolution will cause the data point to cluster together near the origin with sparsely distributed points or none at all to map out the rest of the circumference of a circle. At the other extreme, high damping 'coupled' with high frequency resolution will cause the data point to spread around closely along the loci of circles. When applying Circle-Fitting procedure to the first case i.e. poor mode resolution, the modal parameters determined will be erroneous.

The circle traced by the data points, based on the first term of Equation 5.1.1-1 alone but with real modal constant, is symmetrical about the imaginary axis and the circle passes the origin of the Argand plane as shown in Figure 5.1.1.1-1. In the case having a complex modal constant, the axis of symmetry will no longer be the imaginary axis but an axis

turned at an angle about the origin. Finally, the effects of the residual merely displace this circle by a vector $(a+bj)$ in the Argand plane.

To determine the undamped natural frequency of a mode of vibration, a particular criterion can be chosen which is based on the minimum rate of change of angular frequency squared (ω^2) per angle swept by the consecutive data points ($d\theta$ as shown in Figure 5.1.1.1-3).

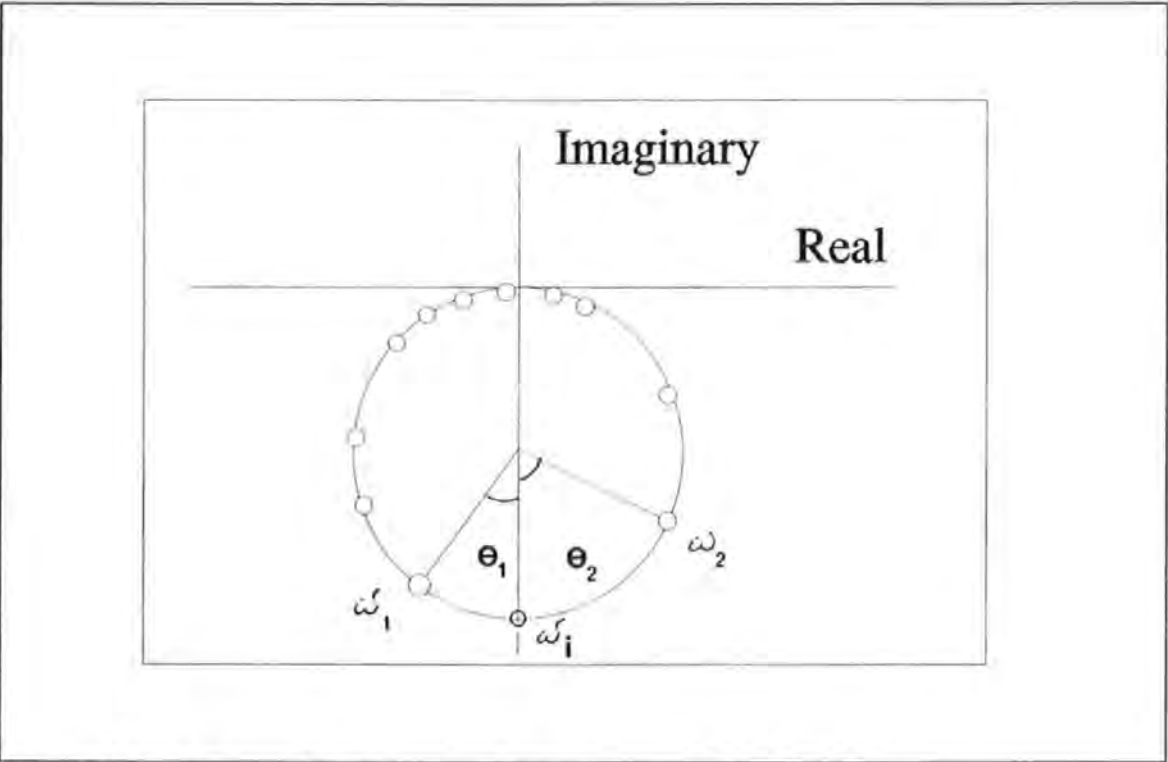


Figure 5.1.1.1-1 A modal circle traced by consecutive FRF data points.

The variation of these rates at different angular frequencies (ω) can be described by the equation :

$$\frac{d \omega^2}{d \theta} = \frac{\omega_i^2 \gamma_i}{2} \left[1 + \frac{1}{\gamma_i^2} \left(1 - \left(\frac{\omega}{\omega_i} \right)^2 \right)^2 \right] \quad (5.1.1.1-1)$$

It can be shown that the plot of $(d\omega^2/d\theta)$ against (ω^2) is theoretically a parabola. The undamped natural frequency ω_i is determined by the frequency at which $(d\omega^2/d\theta)$ is a minimum and can be interpolated from the fitted parabolic curve. The spacing of the

two neighbouring frequency points (corresponding to ω_1 and ω_2) on either side of the frequency point corresponding to ω_i on a modal circle can be used to determine the hysteretic damping loss factor γ_i by using the following equations :

$$\gamma_i = \frac{(\omega_2^2 - \omega_1^2)}{\omega_i^2} * \frac{1}{\text{TAN}(\frac{\theta_1}{2}) + \text{TAN}(\frac{\theta_2}{2})} \quad (5.1.1.1-2)$$

where θ_1 , ω_1 , θ_2 and ω_2 are shown in Figure 5.1.1.1-1. To determine the magnitude of the complex modal constant $|G_{s,r,i}^*|$, the following equation is used :

$$|G_{s,r,i}^*| = (D_{s,r,i} \text{ diameter of circle}) * \gamma_i * \omega_i^2 \quad (5.1.1.1-3)$$

The general problems associated with the circle-fit methods are:

- The data points around a resonance have different weighting in the effectiveness of defining the Nyquist circle of a mode. Data points further away from a resonance tend to cluster around the origin of the Argand plane rendering them less effective than those closer to the natural frequency of the mode. However, data measured near resonance is less accurate and more 'noisy' as explained earlier.
- Measurement of angles subtended by data points near resonance is very difficult to be accurate (for very much the same reasons as in a). Hence considerable errors result in estimating the hysteretic damping loss factor.
- The three modal parameters have to be determined in a prescribed order. So errors in determining one parameter can be accumulated in and propagated to the determination of the next parameter and so on.

5.1.1.2 STRAIGHT-LINE-FIT METHODS

It is generally known that plotting the real and imaginary parts of the inverse of receptance (called '*dynamic stiffness*') against the square of angular frequencies (ω^2) will produce

straight lines (see **Ewins** ^[5.13]). The theory is based on the formulation (by dropping the effects of residual and assuming proportional damping i.e. real modal constant):

$$\frac{1}{\alpha_{sr} \text{ (for } \omega \text{ close to } \omega_i \text{)}} = \frac{\omega_i^2 - \omega^2 + j \gamma_i \omega_i^2}{G_{sr,i}}$$

5.1.1.2-2

This straight-line technique using dynamic stiffness data has been proposed by a number of researchers: such as **Goyder** ^[5.11] and **Dobson** ^[5.12] (see further remarks given later in this Section). Full details of the specific application of this method can be found in the cited reference. Using dynamic stiffness method, the modal parameters of each mode can be determined from the geometry of these straight lines (i.e. the slopes and intercepts) corresponding to each of the respective modes of vibration. For instance, the undamped natural frequency ω_i can be identified as that at which the straight line in the real plot intercepts the ω^2 axis. The modal constant can then be determined using the equation:

$$G_{sr,i} = \frac{-1}{\left(\frac{\text{SLOPE OF THE STRAIGHT LINE IN THE REAL PLOT}}{\omega_i^2} \right)} \quad (5.1.1.2-3)$$

Because the plot of the imaginary part of dynamic stiffness against ω is also a straight line with zero slope and the intercept on the vertical axis can be used, in conjunction with the previously estimated modal constant and natural frequency, to determine the hysteretic damping coefficient γ_i using the following equation :

$$\gamma_i = G_{sr,i} * \left(\frac{\text{OFFSET OF THE STRAIGHT LINE IN THE IMAG PLOT}}{\omega_i^2} \right) * \frac{1}{\omega_i^2} \quad (5.1.1.2-4)$$

Notice that Equation 5.1.1.2-2 is only true when residual effects from the out of range modes are neglected. Hence raw data have to be pretreated before they can fit the straight-line model. The pretreatment necessary is that prior to inverting these data to obtain dynamic stiffness data, the residual term ($a + bj$) has to be determined first and then subtracted from the raw receptance data (as stipulated in Equation 5.1.1-1) before. One such

method is by determining the complex vector of displacement of the Nyquist circle in the Argand plane as explained in Section 5.1.1.1.

The method by **Dobson** ^[5.12] in particular, utilises the *difference equations* technique which has some advantages over the conventional dynamic stiffness method. This method can apply to a non-proportionally damped system (i.e. system with complex modal constants) whilst conventional methods assume a proportionally damped system. This method provides a direct determination of the complex residual as part of the fitting routine without the need to estimate the residual by separate means which is required as a pre-requisite with the conventional methods. (see **Dobson** ^[5.12] for full details)

5.1.2 MDOF-FIT METHODS

MDOF-FIT methods refer to those which perform a multi-modes-curve-fit in a single step which is in contrast to the iterative steps used in SDOF-FIT methods. Some MDOF methods are also called 'global' methods because these methods can perform curve-fitting to the global set of FRF data from all the measuring positions in a single run. Most methods stem from the assumption that the FRF of a linear second order dynamical system can be represented as a ratio of two polynomial functions with unknown parameters a_k and b_k (totalling $m+n+2$ in number, where $m=2N-1$, $n=2N$ and N =total degree-of-freedom of a system). As a convention, b_n is chosen as unity (a condition which can always be satisfied by appropriate factorization). Therefore only $(m+n+1)$ parameters need to be determined. As a rule, the value n is usually chosen as 2 times the number of modes present while the rule to fix the value of m is less certain.

$$H(\omega) = \frac{\sum_{k=0}^m a_k s^k}{\sum_{k=0}^n b_k s^k} \quad \text{where } s=j\omega \quad (5.1.2-1)$$

By convention, $H(\omega)$ is usually expressed as the sum of a rational fraction polynomial (i.e. $n>m$) and extra terms which account for the out-of-range modes's effect. A string of methods use different varieties of this formulation will be further explained below.

5.1.2.1 PARTIAL FRACTION METHODS

As a natural extension to the formulation in Equation 5.1.2-1, it can be rewritten in terms of partial fractions :

$$H(\omega) = \sum_{k=1}^{n/2} \left[\frac{r_k}{s-p_k} + \frac{r_k^*}{s-p_k^*} \right] \quad (5.1.2.1-1)$$

where

$$p_k = \sigma_k + j\omega_k = k^{th} \text{ pole} \quad 5.1.2.1-2$$

where σ_k and ω_k are damping coefficient and damped natural frequency respectively.

$$r_k = \text{residue of } k^{th} \text{ pole} \quad 5.1.2.1-3$$

$$p_k^* \text{ and } r_k^* = \text{conjugates of } p_k \text{ and } r_k \text{ respectively}$$

$$(5.1.2.1-4)$$

This approach again has a very strong origin from control engineering. It is evident from Equation 5.1.2.1-1 that this equation contains $2n+2$ unknown parameters: r_k, p_k, r_k^* and p_k^* for each of the n modes within the analyzed frequency band together with two residual parameters accounting for the residual effects of the out-of-range modes.

A number of approaches are available to solve the parameters from these equations. It is noticed that receptance FRF possess a linear relationship with the unknown constants r_k and r_k^* but a non-linear relationship with p_k and p_k^* (i.e. the damped natural frequencies ω_k and the damping coefficients σ_k). From these Equations, two strategies can be formulated:

- a. by a linear least-square solution of the $2n+2$ unknown parameters, using initial estimates as determined by some other methods; or

- b. by iterative nonlinear least-square solutions to all the unknown parameters.

Clearly the accuracy of these methods depend very much on the accuracy of the initial estimates. A poorly chosen estimate will often lead to divergence from the true solution. Further details of these methods have been documented by **Van Loon** ^[5,14].

5.1.2.2 GLEESON'S METHODS

For very lightly damped structures, **Gleeson** ^[5,15] had derived an algorithm which was methodically a special version of the **Van Loon's** approach but with a difference that a direct solution is pursued. In his approach, the modal damping coefficients σ_k are assumed zeros and the unknown modal constants are all real. Therefore the total number of unknown modal parameters has been reduced from $2n+2$ to n . Further details of this method can be consulted in the cited reference.

5.1.2.3 RATIONAL FRACTION POLYNOMIAL METHODS

An alternative method using Rational Fraction Polynomials formulation was also proposed by **Richardson and Formenti** ^[5,16, 5,17]. In this method, the FRF is expressed as rational fraction i.e. as a ratio of two orthogonal polynomials instead of partial fractions:

$$H(\omega) = \frac{\sum_{k=0}^m c_k \theta_{i,k}}{\sum_{k=0}^n d_k \theta_{i,k}} \quad \text{for } i=1, \dots, N \quad (5.1.2.3-1)$$

orthogonal polynomial $\theta_{i,k}$ must satisfy the orthogonality relation;

$$\sum_{i=1}^N \theta_{i,k} * \theta_{i,j} = \begin{pmatrix} 0 & , k \neq j \\ 0.5 & , k = j \end{pmatrix} \quad (5.1.2.3-2)$$

Orthogonal polynomials are used to avoid *ill-condition* of the matrices involved in the computational process. Therefore, the original problem of solving the unknown coefficients a_k and b_k in Equation 5.1.2-1 has been transformed to that of solving the c_k and d_k in Equation 5.1.2.3-1. Once the parameters c_k and d_k of the orthogonal polynomials are solved, the required modal parameters can then be determined.

5.1.2.4 MAIA-EWINS' METHOD

Maia and Ewins^[5,18] proposed an algorithm which is more suited to data from lightly damped structures i.e. structures with real modal constants. In this particular method, damping is first assumed as zero. Hence $H(\omega)$ is expressed in a rational fraction form as shown in Equation 5.1.2.4 -1:

$$H(\omega) = \frac{\sum_{k=0}^{N-1} a_k \omega^{2k}}{\prod_{r=1}^N (\omega_r^2 - \omega^2)} \quad (5.1.2.4-1)$$

Here the numerator is a polynomial in ω^2 whereas the denominator is expressed as the products of terms $(\omega_r^2 - \omega^2)$. As the system is assumed lightly damped, hence the resonant peaks are well visible. The frequencies correspond to the resonant peaks provide good estimates of the undamped natural frequencies ω_r and therefore the denominator terms are known. Once the unknowns a_k are determined, the modal constants are calculated from a_k using the method of partial fractions. The modal damping ratios are then determined from the correction factors which are required to compensate the differences in receptance values at each of the mode between the damped (actual measured values) and undamped cases (reconstructed from previously determined modal constants and undamped natural frequencies). Again, full details can be obtained from the cited reference.

5.1.2.5 STATE-SPACE METHOD

Another method which is derived from the polynomial fraction approach and adopts another so-called State-Space approach which is frequently used in control engineering as

well. In this method, the system equations are recast into a first order state-space formulation instead of the usual second order formulation (a technique which has already been reviewed in Section 3.2.2.2.5).

$$\begin{bmatrix} M & 0 \\ 0 & I \end{bmatrix} \begin{bmatrix} \ddot{x} \\ \dot{x} \end{bmatrix} + \begin{bmatrix} C & K \\ -I & 0 \end{bmatrix} \begin{bmatrix} \dot{x} \\ x \end{bmatrix} = \begin{bmatrix} f(t) \\ 0 \end{bmatrix} \quad 5.1.2.5-1$$

$$\text{or } \{ \dot{Y} \} = [D] \{ Y \} - [B]^{-1} \{ F(t) \} \quad 5.1.2.5-2$$

$$\text{where } \{ Y \} = \begin{pmatrix} \dot{x} \\ x \end{pmatrix}, [B] = \begin{bmatrix} M & 0 \\ 0 & I \end{bmatrix}, [A] = \begin{bmatrix} C & K \\ -I & 0 \end{bmatrix}, \{ F \} = \begin{bmatrix} f(t) \\ 0 \end{bmatrix}$$

$$\text{and } [D] = \begin{bmatrix} -M^{-1}C & -M^{-1}K \\ I & 0 \end{bmatrix} \quad 5.1.2.5-3$$

Equation 5.1.2.5-1 is obtained by adding a set of auxiliary Equations 5.1.2.5-4, instead of Equations 3.2.2.2.5-19 as used before:

$$[I] \{ \dot{X} \} - [I] \{ \dot{X} \} = \{ 0 \} \quad 5.1.2.5-4$$

The method works by determining the system matrix $[D]$ from the steady state frequency responses (using sinusoidal excitation). The complex Eigen-parameters of the system matrix $[D]$ are then determined using methods such as singular value decomposition and from these Eigen-parameters the modal parameters can be deduced. More details can be found in a paper by **Metwalli** ^[5,19].

5.1.2.6 FREQUENCY DOMAIN POLY-REFERENCE METHOD

A frequency domain version of the Poly-reference method (as a contrast to the time-domain one) was also developed by **Zhang et al.** ^[5,20]. As this method is quite involved in theory, readers are recommended to consult the cited references for more details.

5.1.3 SUMMARY

In summary, many of the methods described so far possess certain inherent strengths as well as weakness. The appropriateness of a method depends mainly on the particular situations encountered. Some methods work well in some situations but worse in others. Therefore no single method can be a panacea for all situations.

The brief review has highlighted the often conflicting requirements between the simple and the sophisticated methods, such as :

- a. the quantity and quality of data required,
- b. the accuracy achieved,
- c. the efficiency of use,
- d. the computational requirement etc.

Simple SDOF methods are intuitive to use but slow in operation and require a lot of interaction from an analyst. They are also less accurate unless remedial measures to account for the residual effects have been taken. In contrast, most MDOF methods can be programmed to run almost automatically once the initial estimates have been given to start the process. Because very little interaction is demanded from the analyst, these methods are extremely fast and efficient to analyzed a large set of data. Above all, the MDOF methods are capable of providing a consistent set of modal parameters for the complete set of data for all the test positions. Whereas this is difficult for SDOF methods to do. For the very same reason, these methods are also sensitive to discrepancy and inconsistency caused by measurement errors.

MDOF methods require computers with large memory capacity and high speed of computation for performing the large scale data processing involved. With the advent of computer technology, these requirements which a main frame barely meet a decade or two ago can now be fulfilled by a personal computer.

5.2 THE METHOD USED IN THIS INVESTIGATION

5.2.1 BACKGROUND

In general, experimental data obtained from field tests are of inferior quality than their laboratory counterparts. Field data are often noisy and have undesirable frequency resolution because of the severe time constraints in taking measurements. Global MDOF methods are thought to be unsuitable because the quality of the field data may not be good enough to be a consistent set.

The alternative algorithm developed during the course of this work is a direct least-square fitting method. The simplicity of the algorithm makes the curve-fitting process more apparent to the lay users and this is considered to be a distinct advantage. By performing the pre-treatment of data (as explained in Section 5.1.1.2) as a pre-requisite step, the algorithm can yield accuracy comparable with other accurate methods. However the algorithm is never meant to compete on these grounds. The algorithm has a few features common with the linear regression method which, to most people, is a very familiar mathematical technique. Hence, users can find it comfortable to use. In line with most SDOF methods in its class, this algorithm is also based on the usual single-mode assumption. The method has the following characteristics (some of these are common to other SDOF methods as well and are not necessarily unique to this method):

1. This algorithm does not rely on any geometrical forms: circles, straight lines or others, explicitly as a curve-fitting criterion.
2. This algorithm is computationally very simple, intuitive to use and can be easily implemented in a spread sheet or simple hand-held calculator application.
3. This algorithm does not require the manipulations of large matrices.
4. No initial estimate is required to start the calculation process.
5. The determination of damping parameters is totally independent of the other

modal parameters so errors in determining one parameter will not be accumulated in determining the next one.

5.2.2 DEVELOPMENT OF THE ALGORITHM

A stepwise development of the algorithm will be given in this section. It starts with the familiar equations of motion of a reduced order dynamic system under harmonic excitation:

$$(-\omega^2 [M] + j \omega [C] + [K]) \{X(\omega)\} = \{F(\omega)\} \quad (5.2.2-1)$$

where $\{X\}$ and $\{F\}$ are respectively the Fourier Transforms of displacement $\{x(t)\}$ and force vectors $\{f(t)\}$ and are functions of angular frequency ω .

which can be obtained by applying Fourier Transform to Equation 3.2.2.2.1-28. Using the linear transformation between spatial and natural (or modal) coordinates using the undamped modal matrix $[\Phi]$ (which is real):

$$\{X(\omega)\} = [\Phi] \{\eta(\omega)\} \quad (5.2.2-2)$$

Hence Equation. (5.2.2-1) becomes :

$$(-\omega^2 [M] [\Phi] + j \omega [C] [\Phi] + [K] [\Phi]) \{\eta(\omega)\} = \{F(\omega)\} \quad (5.2.2-3)$$

Pre-multiplying Equation. 5.2.2-3 by $[\Phi]^T$ to obtain :

$$(-\omega^2 [\Phi]^T [M] [\Phi] + j \omega [\Phi]^T [C] [\Phi] + [\Phi]^T [K] [\Phi]) \{\eta(\omega)\} = [\Phi]^T \{F(\omega)\} \quad (5.2.2-4)$$

From Section 3.2.2.2.4 concerning orthogonality, the matrix triple products depicted in Equation 5.2.2-5a and 5.2.2-5b are known to yield the diagonal modal (or sometimes known as Generalised) mass and stiffness matrices (which again are all real) :

$$[M^*] = [\Phi]^T [M] [\Phi] \quad (5.2.2-5a)$$

$$[K^*] = [\Phi]^T [K] [\Phi] \quad (5.2.2-5b)$$

If proportional damping is assumed, then $[C]$ can be diagonalised by the undamped modal matrix in the way as stipulated in Equation 5.2.2-5c :

$$[C^*] = [\Phi]^T [C] [\Phi] \quad (5.2.2-5c)$$

where $[C^*]$ is the diagonal modal or generalised damping matrix.

The modal force vector is given as :

$$\{F^*\} = [\Phi]^T \{F\} \quad (5.2.2-5d)$$

hence

$$(-\omega^2 [M^*] + j \omega [C^*] + [K^*]) \{\eta(\omega)\} = \{F^*(\omega)\} \quad (5.2.2-6)$$

In effect, Equation (5.2.2-6) represent a set of uncoupled equations of motion since the modal mass, stiffness and damping matrices are all diagonal matrices. The matrix Equation (5.2.2-6) can be re-written as a set of scalar equations for each mode :

$$(-\omega^2 M_i^* + j \omega C_i^* + K_i^*) \eta_i(\omega) = F_i^*(\omega) \quad (5.2.2-7)$$

where $i = 1, 2, 3, \dots$ so on and refers to the mode No.

since

$$X_s = \sum_{i=1}^N [\phi_{s i} \eta_i] \quad (5.2.2-8)$$

Within a narrow frequency band close to ω_i , if the response X_s at nodal point s is pre-dominantly contributed by the i^{th} mode, i.e. residual effect from out-of-range modes is

neglected, then:

$$X_s(\omega) \approx \phi_{si} * \eta_i(\omega) \quad (5.2.2-9)$$

hence

$$\eta_i(\omega) \approx \frac{X_s(\omega)}{\phi_{si}} \quad (5.2.2-10)$$

and if there is only one excitation force F_r being applied at point r , then

$$F_i^*(\omega) = \phi_{ir}^T * F_r(\omega) \quad (5.2.2-11a)$$

$$\text{and since } \phi_{ir}^T = \phi_{ri} \quad (5.2.2-11b)$$

hence Equation (5.2.2-7) becomes

$$(-\omega^2 M_i^* + j \omega C_i^* + K_i^*) X_s(\omega) = \phi_{si} \phi_{ri} F_r(\omega) \quad (5.2.2-11c)$$

if receptance α_{sr} is defined as :

$$\alpha_{sr}(\omega) = \frac{X_s(\omega)}{F_r(\omega)} \quad (5.2.2-12)$$

then

$$(-\omega^2 M_i' + j \omega C_i' + K_i') \alpha_{sr} = 1 \quad (5.2.2-13a)$$

$$\text{where } M_i' = \frac{M_i^*}{\phi_{si} \phi_{ri}} \quad 5.2.2-13b$$

K_i' and C_i' can be obtained similarly by dividing K_i^* and C_i^* with $\phi_{si} \phi_{ri}$ respectively. Notice that all M_i' , K_i' and C_i' (called effective mass, stiffness and damping) are assumed

real. Also since α is a complex quantity and so is its reciprocal (called dynamic stiffness):

$$\frac{1}{\alpha_{sr}(\omega)} = A_{sr}(\omega) + j B_{sr}(\omega) \quad (5.2.2-14)$$

where

$$A_{sr}(\omega) = \frac{\Re}{\Re^2 + \Im^2} \quad (5.2.2-15a)$$

$$B_{sr}(\omega) = \frac{-\Im}{\Re^2 + \Im^2} \quad (5.2.2-15b)$$

in which \Re and \Im stand for the real and imaginary parts of receptance respectively. A note of caution must be made here because of the assumption made in arriving at Equation 5.2.2-9 i.e. neglecting out-of-range residual effects. For an accurate analysis, the residual has to be subtracted from the raw receptance data before inverting them to obtain the dynamic stiffness data. Hence by equating the real and imaginary parts of Equation 5.2.2-13 :

$$\begin{aligned} (-\omega^2 M_i' + K_i') &= A_{sr}(\omega) \\ \omega C_i' &= B_{sr}(\omega) \end{aligned} \quad (5.2.2-16a \text{ and } b)$$

where $A_{sr}(\omega)$ and $B_{sr}(\omega)$ are the real and imaginary parts of dynamic stiffness respectively.

Or if re-written in matrix form :

$$\begin{bmatrix} -\omega^2 & 1 & 0 \\ 0 & 0 & \omega \end{bmatrix} * \begin{Bmatrix} M_i' \\ K_i' \\ C_i' \end{Bmatrix} = \begin{Bmatrix} A_{rs}(\omega) \\ \text{---} \\ B_{rs}(\omega) \end{Bmatrix} \quad (5.2.2-17)$$

for n different frequencies close to the i^{th} undamped natural frequency :

$$\omega = \omega_1, \omega_2, \omega_3, \dots, \omega_n$$

If the i^{th} mode is considered dominant within this range of frequencies, then each of these frequencies provide a set of equations, similar in form to Equation 5.2.2-17 :

$$\begin{bmatrix} -\omega_1^2 & 1 & 0 \\ -\omega_2^2 & 1 & 0 \\ \vdots & \vdots & \vdots \\ -\omega_n^2 & 1 & 0 \\ 0 & 0 & \omega_1 \\ 0 & 0 & \omega_2 \\ \vdots & \vdots & \vdots \\ 0 & 0 & \omega_n \end{bmatrix} * \begin{Bmatrix} M_i' \\ K_i' \\ C_i' \end{Bmatrix} = \begin{Bmatrix} A_{rs}(\omega_1) \\ A_{rs}(\omega_2) \\ \vdots \\ A_{rs}(\omega_n) \\ B_{rs}(\omega_1) \\ B_{rs}(\omega_2) \\ \vdots \\ B_{rs}(\omega_n) \end{Bmatrix} \quad (5.2.2-18)$$

which is of the standard form of most system of linear equations.

$$[A] \{x\} = \{b\} \quad (5.2.2-19)$$

The dimension of the coefficient matrix $[A]$ is $2n \times 3$. Since the number of unknowns in this case is only 3, hence a minimum of 3 equations is sufficient for a solution. The solution obtained by using more than this statutory minimum is called the pseudo-inverse solution which can be obtained by an application of the following equation

$$\{x\} = ([A]^T [A])^{-1} [A]^T \{b\} \quad (5.2.2-20)$$

Equation 5.2.2-20 provides an unbiased estimate of unknown vector $\{x\}$. So as the number of frequency points used in the curve-fitting process increase so does the size of $[A]$. However it can be shown that the following matrix multiplications can be reduced to very simple forms:

$$\text{first define } \sum \omega^p \equiv \sum_{t=1}^n \omega_t^p$$

$$\sum A_{sr} \equiv \sum_{t=1}^n A_{sr}(\omega_t) \text{ and } \sum B_{sr} \equiv \sum_{t=1}^n B_{sr}(\omega_t)$$

$$([A]^T [A]) = \begin{bmatrix} \sum \omega^4 & -\sum \omega^2 & 0 \\ -\sum \omega^2 & n & 0 \\ 0 & 0 & \sum \omega^2 \end{bmatrix} \quad 5.2.2-21$$

which is only a 3 X 3 matrix. Similarly, it can also be shown that :

$$[A]^T [b] = \begin{Bmatrix} -\sum \omega^2 A_{sr} \\ \text{-----} \\ \sum A_{sr} \\ \text{-----} \\ \sum \omega B_{sr} \end{Bmatrix} \quad 5.2.2-22$$

$$\begin{bmatrix} \sum \omega^4 & -\sum \omega^2 & 0 \\ -\sum \omega^2 & n & 0 \\ 0 & 0 & \sum \omega^2 \end{bmatrix} * \begin{Bmatrix} M'_i \\ K'_i \\ C'_i \end{Bmatrix} = \begin{Bmatrix} -\sum \omega^2 A_{sr} \\ \text{-----} \\ \sum A_{sr} \\ \text{-----} \\ \sum \omega B_{sr} \end{Bmatrix} \quad 5.2.2-23$$

If data were accelerance (or inertance), revised formulae would have to be used. The conversion from receptance to accelerance is quite straight forward :

$$\gamma_{rs}(\omega) = \alpha_{rs}(\omega) * (j\omega)^2 \quad 5.2.2-24$$

where accelerance $\gamma_{rs}(\omega)$ is similarly defined as receptance except that acceleration now replaces displacement. Similar to Equation 5.2.2-14, the reciprocal of accelerance is defined as:

$$\frac{1}{\gamma_{sr}(\omega)} = A'_{sr}(\omega) + j B'_{sr}(\omega) \quad 5.2.2-25$$

where A'_{sr} and B'_{sr} are similarly defined as their A_{sr} and B_{sr} counterparts as the real and imaginary parts of the inverse of accelerance. It can be shown that the following equations can be derived:

$$\begin{bmatrix} n & -\sum \frac{1}{\omega^2} & 0 \\ -\sum \frac{1}{\omega^2} & \sum \frac{1}{\omega^4} & 0 \\ 0 & 0 & \sum \frac{1}{\omega^2} \end{bmatrix} * \begin{Bmatrix} M'_i \\ K'_i \\ C'_i \end{Bmatrix} = \begin{Bmatrix} \sum A'_{sr} \\ -\sum \frac{A'_{sr}}{\omega^2} \\ \sum \frac{B'_{sr}}{\omega} \end{Bmatrix} \quad 5.2.2-26$$

The solution of the system of equations 5.2.2-23 (of order 3) provide explicit expressions for the three unknowns :

$$C'_i = \frac{\sum \omega B(\omega)}{\sum \omega^2} \quad 5.2.2-27a$$

$$M_i' = \frac{-n \sum (\omega^2 A_{sr}(\omega)) + (\sum \omega^2) (\sum A_{sr}(\omega))}{n(\sum \omega^4) - (\sum \omega^2)^2} \quad 5.2.2-27b$$

$$K_i' = \frac{(\sum A_{sr}(\omega)) (\sum \omega^4) - (\sum \omega^2) (\sum (\omega^2 A_{sr}(\omega)))}{n(\sum \omega^4) - (\sum \omega^2)^2} \quad 5.2.2-27c$$

To obtain the various modal parameters, the following formulae can be used :

$$\xi_i = \frac{C_i'}{2 \sqrt{M_i' K_i'}} = \frac{C_i^*}{2 \sqrt{M_i^* K_i^*}} \quad 5.2.2-28a$$

$$\omega_i^2 = \frac{K_i'}{M_i'} = \frac{K_i^*}{M_i^*} = \frac{(\sum A_{sr}(\omega)) (\sum \omega^4) - (\sum \omega^2) (\sum (\omega^2 A_{sr}(\omega)))}{-n \sum (\omega^2 A_{sr}(\omega)) + (\sum \omega^2) (\sum A_{sr}(\omega))} \quad 5.2.2-28b$$

$$G_{sr,i} = \frac{1}{M_i'} = \frac{\phi_{si} \phi_{ri}}{M_i^*} \quad 5.2.2-28c$$

where ω_i , ξ_i and $G_{sr,i}$ are respectively the undamped natural frequency, modal damping factor and modal constants of the i^{th} mode.

5.3 IMPLEMENTATION AND VERIFICATION

The algorithm was implemented in a number of computing environments and platforms :

- Hewlett Packard HP Basic® Version 4
- MATLAB ® routines and
- spread sheet application in QUATTRO PRO®.

The mechanics (not accuracy since values are rounded off to fit in the table) of the calculation at work can be illustrated by the following example (using the synthesized data of the four-mode fictitious system to be described below) :

TABLE 5.3-1 TABLE ILLUSTRATING THE MECHANICS OF THE CALCULATION
USING THE PROPOSED ALGORITHM

FREQ	REAL ACCEL	IMAG ACCEL	ω^2	A	B	$B\omega$	$A\omega^2$	ω^4
Hz	$\times 10^4$	$\times 10^4$		$\times 10^4$	$\times 10^4$	$\times 10^4$	$\times 10^4$	$\times 10^8$
23.39	3.60	0.48	21598	0.273	-0.036	-5.29	5896	4.66
23.88	4.86	0.98	22513	0.199	-0.040	-6.00	4480	5.07
24.38	7.58	2.86	23465	0.115	-0.044	-6.74	2698	5.51
24.88	8.41	16.50	24438	0.025	-0.048	-7.50	611	5.97
25.38	-8.79	6.17	25430	-0.076	-0.053	-8.45	-1932	6.47
25.87	-4.81	1.53	26421	-0.189	-0.060	-9.75	-4994	6.98
26.37	-3.03	0.66	27452	-0.315	-0.068	-11.27	-8647	7.54
Σ			171317	0.072		-55.00	-1888	42.20

Using Equations 5.2.2-27a to 5.2.2-27c in which only simple multiplications and divisions are involved, the modal parameters calculated are :

	ASSUMED VALUES	CALCULATED VALUES
undamped natural frequency (Hz)	25	25.18
damping factor	0.01	0.0076
modal constant (kg^{-1})	1.0	0.745

The discrepancy is due to rounding errors in the initial input data (accelerance values etc) and in performing the calculation. Also it is due to the fact that removal of residual effect from the data has not been performed.

Commercial spread sheet programs such as QUATTRO PRO[®] are best suited to perform these 'mechanical' row- and column-wise calculations. The program, which was written in Matlab[®] and run under Microsoft Window[®] 3.1, provided a very efficient interactive environment for performing the analysis reported here.

The computational procedure was verified based on computer simulations subjected to a number of scenarios. The data were synthesized from a fictitious 4-modes vibration system, with relatively well separated modes and known modal parameters. Hence the accuracies of this method can be quantified readily by comparing the results with their known values.

The various scenarios are intended to study the combined effects of the levels of damping and frequency resolutions on accuracy. The levels of damping assumed were ranged from .001% to 10% of critical damping values. These values covered from light to the heavily damped situations. The frequency resolutions of data were 0.1, 0.5, 1.0 and 2.5 Hz. The effects of random noise on sensitivity of the method have not been investigated because data deliberately polluted with artificial Gaussian type random noises may not be entirely representative of those encountered in practice.

The modal parameters assumed for the fictitious system are summarised and tabulated in Table 5.3-2.

TABLE 5.3-2 ASSUMED MODAL PARAMETERS FOR A FOUR-MODES FICTITIOUS SYSTEM

ASSUMED MODAL PARAMETERS FOR A FOUR-MODES FICTITIOUS SYSTEM		
UNDAMPED NATURAL FREQUENCY	MODAL CONSTANTS	RANGE OF DAMPING VALUES
Hz	kg ⁻¹	% OF CRITICAL DAMPING
25	1.0	.001 TO 10
50	2.0	.001 TO 10
65	2.0	.001 TO 10
80	0.5	.001 TO 10

In addition to comparing each of the individual assumed and determined modal parameters, a statistic called *quality-of-fit factor QF* is used to indicate quantitatively how good or bad the overall quality-of-fit or accuracy is. This QF factor has been defined in Section 6.2.3.2 and is subjected to the same limitations in its interpretation as stated there.

The effects of the selection of the frequency data points, in terms of their numbers and positions, have not been thoroughly investigated. However as a general rule, the use of a small number of points will yield good results. When choosing a large number of points for fitting, unless all the points are well within the resonant region, this action will be counter-productive and will yield bad results as the underlying assumptions are more likely to have been violated.

Although the analysis method is based on SDOF assumption, the effects of neighbouring modes (called *modal interference*) can be taken care of by subtracting the

effects of these modes from the analyzed mode. Hence accuracy can be further improved by repeating these subtraction procedures in an iterative fashion.

The case of 10 % of critical damping has been chosen as an illustration. Although the modal frequencies are relatively well spaced apart, the higher damping level causes considerable 'interference' in the FRF. Analysis conducted using mode subtraction on the first three modes has shown some improvements over those analysis without using mode subtraction.

For the sake of easy explanation, an indicial notation $M(r,s)$ was devised and defined to illustrate the mode subtraction operations carried out as follows :

where r is the mode number
 s is the number of iterative cycles performed

For instance, $M(3,2) = M(3,1) - M(2,1)$ means that the results for mode number 3 after two iterations is obtained by subtracting the effects of mode number 2 (from the first iteration) from those of mode number 3 (after the first iterations). Table 5.3-2 summarizes the results of analysis as follows :

TABLE 5.3-3 RESULTS OF MODAL PARAMETERS DETERMINATION USING
ITERATIVE MODE SUBTRACTION FOR THE FOUR-MODE
FICTITIOUS SYSTEM

RESULTS OF MODAL PARAMETERS DETERMINATION USING ITERATIVE MODE SUBTRACTION FOR THE FOUR-MODE FICTITIOUS SYSTEM							
MODE NO.	RESONANT FREQUENCY Hz		MODAL CONSTANT Kg^{-1}		DAMPING FACTORS		RESULT FROM
	ASSUMED	CALCULATE	ASSUMED	CALCULATE	ASSUMED	CALCULATE	
1	25	25.52	1.00	1.32	.1	.114	M(1,0)
2	50	50.87	2.00	2.92	.1	.125	M(2,0)
3	65	60.80	2.00	4.48	.1	.167	M(3,0)
M(3,1)	65	65.92	2.00	1.77	.1	.096	M(3,0)- M(2,0)
M(2,1)	50	49.68	2.00	2.27	.1	.110	M(2,0)- M(3,1)
M(1,1)	25	25.11	1.00	1.05	.1	.103	M(1,0)- M(2,1)
M(3,2)	65	65.03	2.00	2.19	.1	.108	M(3,0)- M(2,0)

TABLE 5.3-4 EFFECTS ON QF FACTORS BY USING VARIOUS MODE COMBINATIONS

EFFECTS ON QF FACTORS BY USING VARIOUS MODE COMBINATIONS		
MODE COMBINATIONS	QF FACTORS	IMPROVEMENT OVER PREVIOUS RUN
M(1,0) + M(2,0) + M(3,0)	.474	N/A
M(1,0) + M(2,0) + M(3,1)	.807	YES
M(1,0) + M(2,1) + M(3,1)	.854	YES
M(1,1) + M(2,1) + M(3,1)	.951	YES
M(1,1) + M(2,1) + M(3,2)	.937	NO

Table 5.3-4 shows the consistent improvement in QF values from .474 to .951 after a few iterations.

The running of the program in action and the graphical results obtained are briefly described below. Figure 5.3-1 shows a typical accelerance (or inertance) FRF of the fictitious system. The suspected resonant peaks in both the modulus and imaginary plots are first marked with vertical lines using a screen cursor.

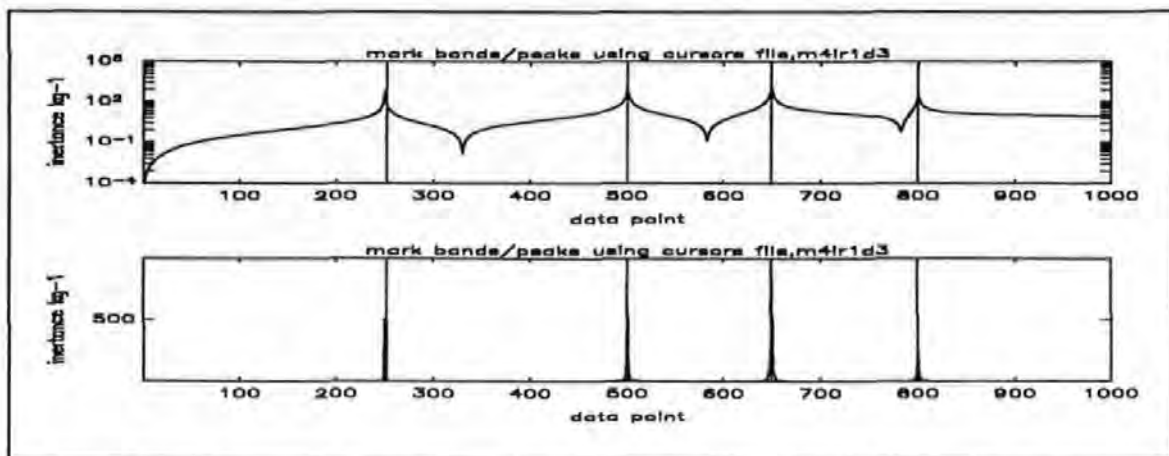


Figure 5.3-1 Marking of resonant peaks with vertical lines on the modulus and imaginary Inertance FRF plots.

After responding to a series of requested inputs by the program with regards to :

- the number of points neighbouring each of the marked peaks used for curve-fitting,
- whether or not mode subtraction is required,

computation then proceeds using the proposed algorithm. To appraise the results obtained, overlaid plots of the original and the so-called regenerated FRF curves are displayed for visual inspection by the analyst. The regenerated FRF curves are plotted based on the determined modal parameters determined (Note the full set of the modal parameters results determined in the simulation experiment are tabulated in Appendix 5.4). A selective sample of these results (plots) for the various conditions studied was shown in Figures 5.3-2 to 5.3-8.

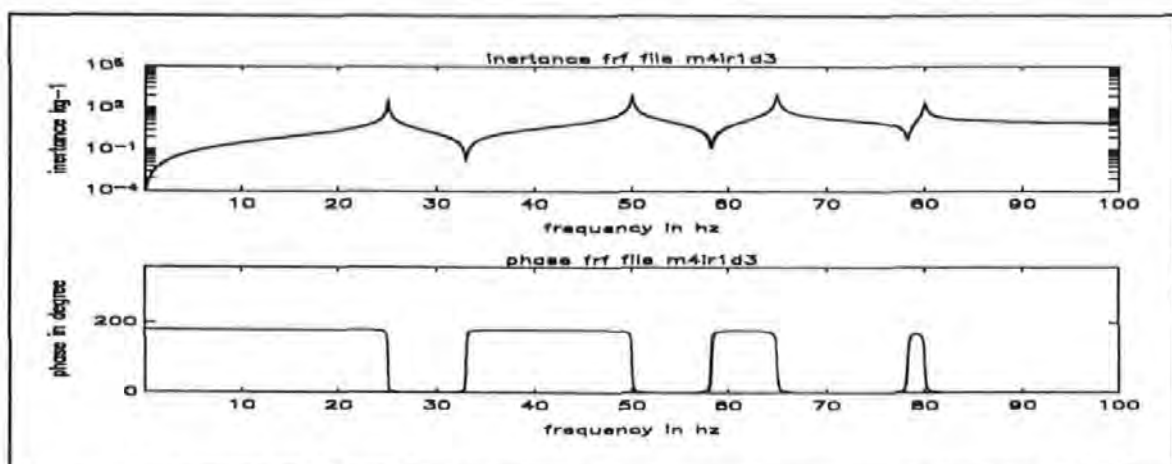


Figure 5.3-2 Overlaid plots of original and regenerated Inertance FRF for the fictitious system with frequency resolution of 0.1 Hz and damping factor 0.1 % of critical damping.

Figure 5.3-2 shows that for a frequency resolution of 0.1 Hz and light damping (0.1% of critical damping), the correlation between the two curves in both the modulus and phase plots are very good.

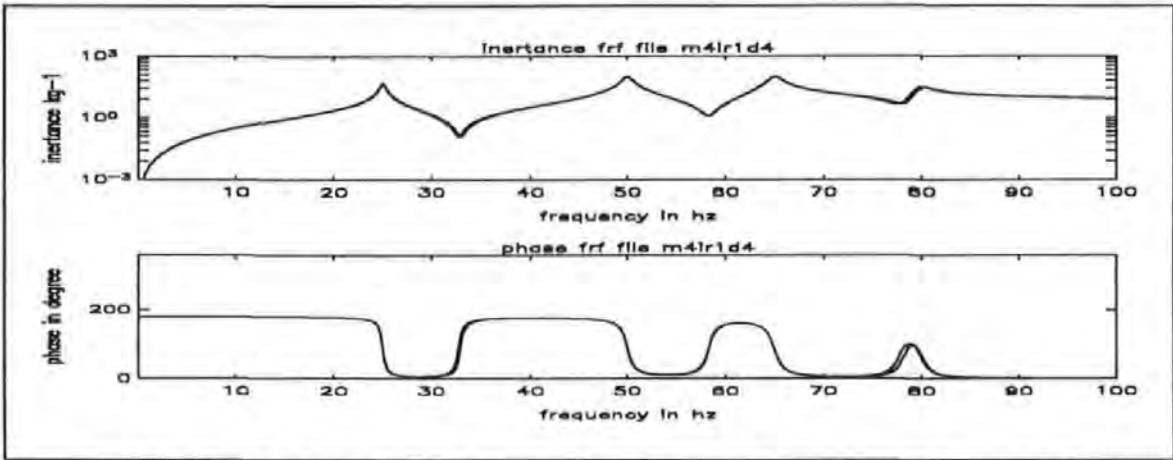


Figure 5.3-3 Overlaid plots of original and regenerated Inertance FRF for the fictitious system with frequency resolution of 0.1 Hz and damping factor 1 % of critical damping.

With 1% damping and the same resolution of 0.1 Hz, the correlation of the curves shown in Figure 5.3-3. is not as good as that shown by Figure 5.3-2.

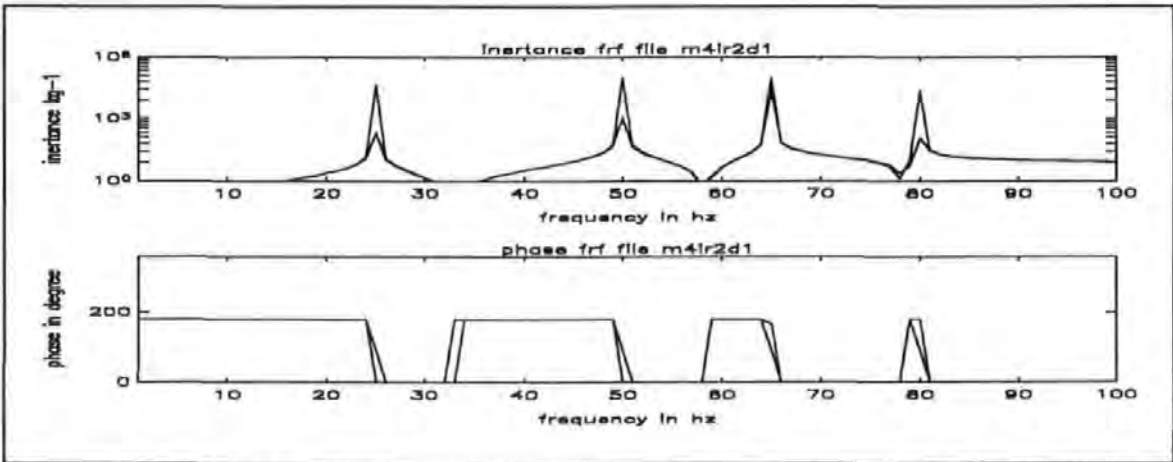


Figure 5.3-4 Overlaid plots of original and regenerated Inertance FRF for the fictitious system with frequency resolution of 1 Hz and damping factor 0.001 % of critical damping.

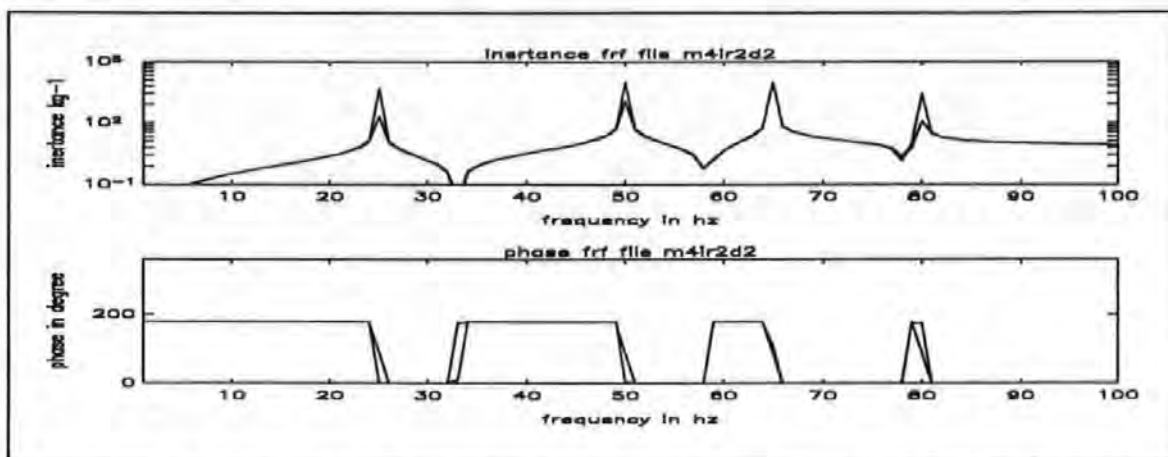


Figure 5.3-5 Overlaid plots of original and regenerated Inertance FRF for the fictitious system with frequency resolution of 1 Hz and damping factor .01 % of critical damping.

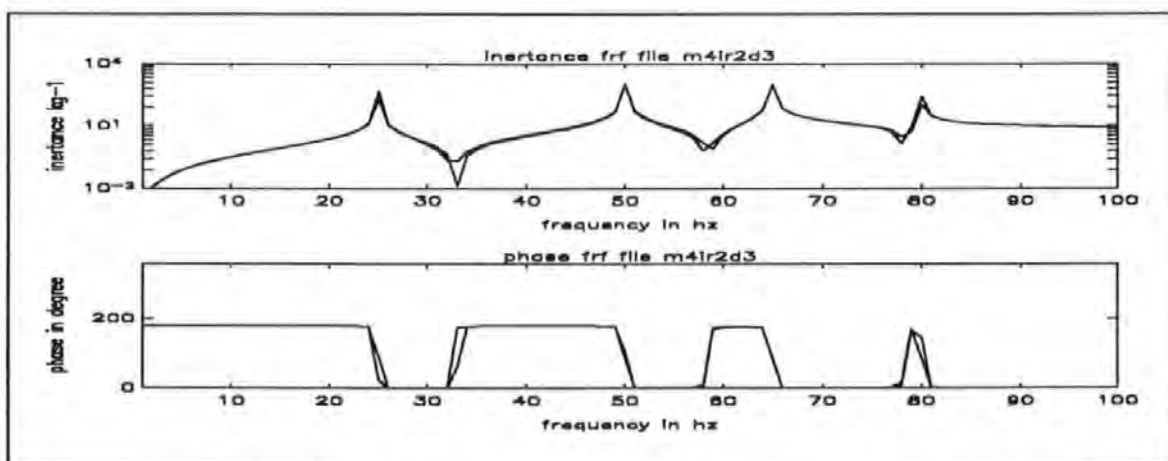


Figure 5.3-6 Overlaid plots of original and regenerated Inertance FRF for the fictitious system with frequency resolution of 1 Hz and damping factor 0.1 % of critical damping.

Figures 5.3-4 to 5.3-6 show that for a frequency resolution of 1 Hz and a range of damping (ranged between .001% to 0.1%), correlation is consistently worst at those regions near resonances and anti-resonances where phases change abruptly because of the lack of frequency resolution.

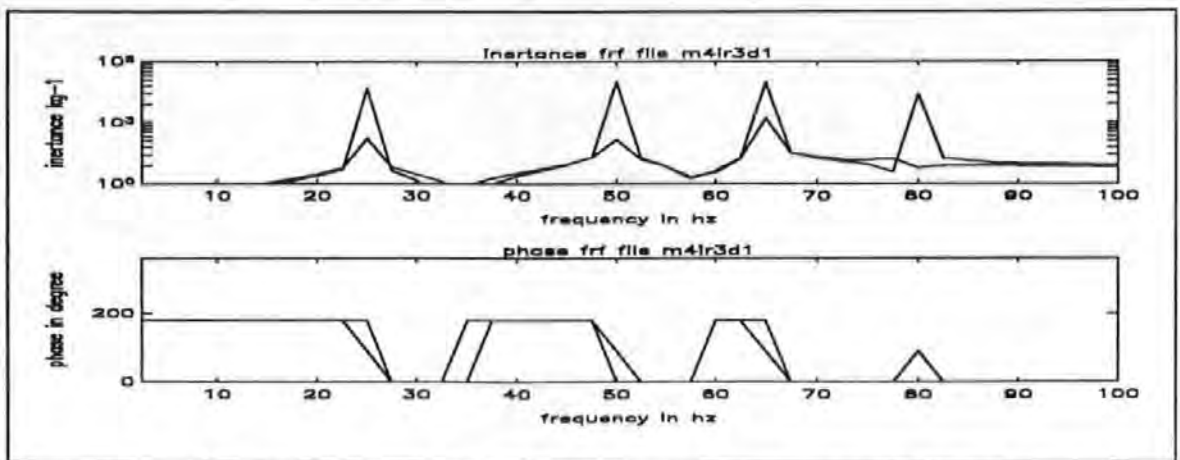


Figure 5.3-7 Overlaid plots of original and regenerated Inertance FRF fictitious system (with frequency resolution of 2.5 Hz and damping factor 0.001 % of critical damping).

With a even coarser resolution at 2.5 Hz, Figure 5.3-7 shows that even with the lightest damping, the correlation deteriorates badly. Results tabulated in Appendix 5.4 show that the errors on the modal parameters set determined are all significantly higher than that of the finer resolution cases given the same damping factors.

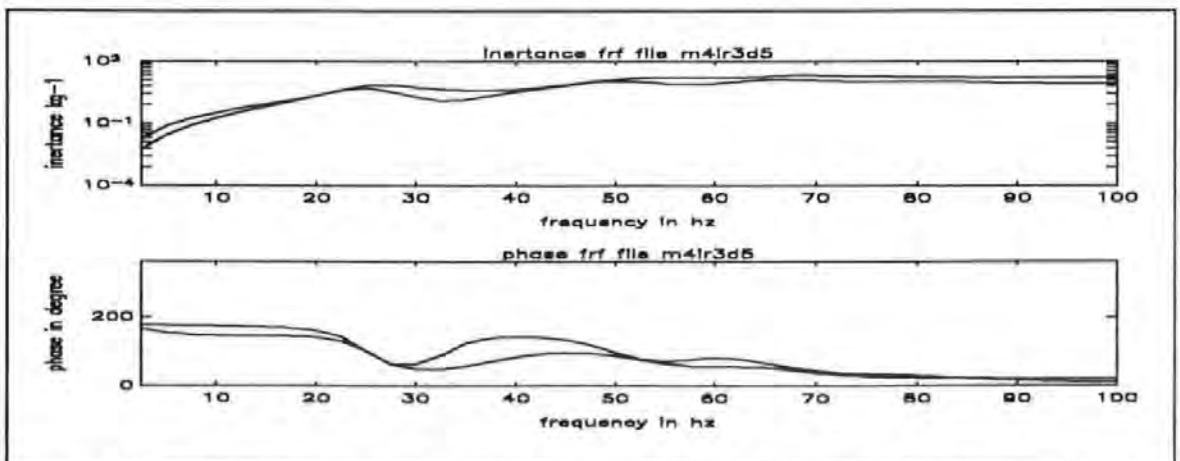


Figure 5.3-8 Overlaid plots of original and regenerated Inertance FRF for the fictitious system with frequency resolution of 2.5 Hz and damping factor 10 % of critical damping.

Figure 5.3-8 shows the worst scenario (i.e. heavy damping plus coarse resolution) amongst the conditions studied here. Results tabulated in Appendix 5.4 show that for mode 1 to 3, the errors can be as much as 50% or more in these circumstances.

5.4 COMPARISON OF THE PROPOSED WITH SOME CONVENTIONAL METHODS

There are a number of similarities between the proposed method and the dynamic stiffness method which are worthy of taking note. First of all, the proposed method requires the formulation of equation in the following ways:

$$(-\omega^2 M'_i + j \omega C'_i + K'_i) = \frac{1}{\alpha_{sr}} \quad (5.4-1)$$

Or in the case of hysteretic damping, the damping term in Equation 5.4-1 is adjusted accordingly:

$$(-\omega^2 M'_i + j \gamma_i K'_i + K'_i) = \frac{1}{\alpha_{sr}} \quad (5.4-2)$$

the usual formulation in dynamic stiffness method is of the form:

$$\frac{1}{\alpha_{sr}} = -\omega^2 \left(\frac{1}{G_{sr,i}} \right) + \omega_i^2 \left(\frac{1}{G_{sr,i}} \right) + j \gamma_i \omega_i^2 \left(\frac{1}{G_{sr,i}} \right)$$

5.4-3

Equations 5.4-1 and 5.4-2 are linear with unknown constants such as: M'_i , C'_i and K'_i . Using dynamic stiffness methodology, the plot of the real part of dynamic stiffness data against ω^2 will produce a straight line with a slope equals to $-M'_i$, and intercept on the vertical axis K'_i . Similarly, the plot of the imaginary part of dynamic stiffness data against ω will also be a straight line with a slope equals to C'_i . In the hysteretic damping case, the plot of the imaginary parts of dynamic stiffness against ω should also be a straight line with zero slope (i.e. it is independent of frequency ω) and the intercept on the vertical axis equals to a constant (equal to $\gamma_i K'_i$).

Whereas based on the Equation 5.4-3, the plot of the real part of dynamic stiffness against ω^2 will produce a straight line with a slope equals to $(-1/G_{sr,i})$ and the plot of the imaginary part of dynamic stiffness against ω will also be a straight line with zero slope and the intercept on the vertical axis equals $(\gamma_i \omega_i^2 / G_{sr,i})$.

Secondly, both the proposed method and the dynamic stiffness method require the removal of the residual effect of out-of-range modes from the raw data as a separate and a pre-requisite step for an accurate analysis. Thirdly, both the proposed method and the dynamic stiffness method assume real modes hence they all implicitly assume proportional damping.

However, despite these similarities, the two approaches do differ in the fundamental thinking. The proposed method here determine the spatial parameters M'_i , K'_i and C'_i (called effective mass, damping and stiffness) directly. This approach is in line with the philosophy as will be discussed in Chapter 6. From these spatial parameters, the modal parameters are then derived as 'by-products'. Whereas the dynamic stiffness method determines the modal parameters directly. Unlike modal parameters, these spatial parameters still retain some quantitative descriptions of mass, stiffness and damping of a system.

A comparison of the proposed algorithm with two other SDOF methods (i.e. the circle- and Dobson's improved straight-line-fit methods) was carried out. Again the same 4-modes fictitious system was used for this study. It was expected that the proposed method would achieve similar accuracy as the corresponding dynamic stiffness method would if the residual-removal step was carried out as a pre-requisite step before fitting,. The intention of this comparison study was to determine the accuracy of the proposed method in the event that the residual-removal step was not carried out. The areas of comparison were also concentrated on the effects of different levels of damping, frequency resolutions and fitting data points selections on accuracy. The results obtained from the three methods carried out are tabulated in Appendix 5.4 but some general observations are summarised below.

In general the circle-fit method is not suitable for very light damping cases and can produce large errors if frequency resolution is not fine enough. In the heavy damping situations, this method has yielded results with better accuracy.

The Dobson method has a good overall performance in many situations due to the elaborate procedures included in the program:

- a. to subtract or minimize the effects of modal 'interference' from neighbouring modes on the analyzed mode.

- b. to account for complex residual effects from out-of-range modes.

In the case of the author's method, it can still produce acceptable results with reasonable accuracy in the cases of good frequency resolution and low damping. For instance, in the cases of 1% critical damping and a frequency resolution of 0.1 Hz (these are similar to the situations encountered in the Fire Tower tests as described in Chapter 8), the author's method produces errors of no more than 5 % and in most cases less than 1 % in the case of modal constants. However in the cases of undamped natural frequencies and the damping factors, these are quite accurately determined as shown in Table 5.4-1 which is an extract from the more thoroughly reported results given in Appendix 5.4.

TABLE 5.4-1 PERCENTAGE ERRORS IN THE MODAL PARAMETERS DETERMINED USING AUTHOR'S METHOD

	WITHOUT MODE SUBTRACTION			WITH MODE SUBTRACTION		
	% ERRORS IN			% ERRORS IN		
	UNDAMPED NATURAL FREQUENCY	MODAL CONSTANT	DAMPING FACTOR	UNDAMPED NATURAL FREQUENCY	MODAL CONSTANT	DAMPING FACTOR
MODE 1	0	1.99	.02	0	1.7	.02
MODE 2	0	.33	.01	0	.01	.01
MODE 3	0	.27	.01	0	.002	.001
MODE 4	0	2.1	.3	0	4.42	.05

Hence a small sacrifice in accuracy may be a justifiable price to pay if simplicity and speed are desired. The column-wise operation as shown in Table 5.3-1 when implemented in spread sheet application is a very intuitive medium in which to see and learn the curve-fitting at work.

5.5 CONCLUSIONS

The proposed algorithm is an acceptable approximation tool for the determination of modal parameters. It works rather well if the modes are well separated, damping is light and frequency resolution is adequate. However, the built-in assumptions, such as: proportional damping and hence real modal constants etc, have to be borne in mind when applying the algorithm. For an accurate analysis, pre-treatment of raw receptance data is required to remove the residual effects before carrying out the curve-fitting.

CHAPTER 6

EXTRACTION OF SPATIAL PARAMETERS FROM FORCED VIBRATION DATA

6.0 INTRODUCTION

This chapter will first review a number of conventional (modal) methods in Section 6.1. An alternative non-modal (spatial) method developed by the author is presented in some details in Section 6.2. The background theory is covered in Section 6.2.1 and the steps in its derivation are described in Section 6.2.2. The computer simulation used to validate the method was reported in Section 6.2.3. The applications of this method to data obtained from a number of real structures are presented in Section 6.2.4. A general discussion of the method is presented in Section 6.3. Finally, the conclusions are stated in Section 6.4.

The exact origin of the use of the terms *spatial parameter* and *spatial model* is not known. It is believed, however, that it is probably attributed to the work published by Gleeson ^[6.1] in 1980 which was entitled 'Identification Of Spatial Models'. The spatial parameters here follow closely with Gleeson's definitions i.e. they refer to the mass, stiffness and damping matrices which, in physical terms, represent the inertial, elastic and energy dissipating properties of a structure.

The attempt to Derive Spatial Parameters from Experimental Data (DSPED) is not new. In fact, the history went back as far as the 1960's. Broadly speaking, these methods share a lot in common but also differ from each other in a number of respects such as:

- a. whether prior knowledge of or assumptions about some of the matrices are required,
- b. whether the approach is a direct one or is one based on iterative search or optimization methodology and
- c. whether the identification of modal parameters are required prior to the determination of the spatial matrices.

For the sake of brevity, some important concepts and terminologies which are frequently referred to in the text are first defined. A structural model is often classified as *low-order*, *high-order*, *complete* or *in-complete*. This classification is based on the relative magnitudes of the three non-negative integer quantities :

N : the total number of feasible DOF (or modes) of a structure,

n : measured DOF's in forced vibration tests and

r : the number of resonant modes within the frequency band of analysis.

Apart from fictitious ones, most real-life structures are continuous rather than discrete by nature. Therefore these structures should possess inherently infinite degrees of freedom or modes i.e. N is infinite. The natural frequencies corresponding to these modes are distributed over a wide frequency band. However some structures can often be classified as a SDOF or a MDOF (single- or multi- degree-of-freedom) system, where the degrees-of-freedom N is usually a small integer. Such a finite DOF system can exist because only a small number of possible DOF's is enough for defining its deformation field. This may be achieved by the ways the system is configured and constructed that the continuous system can be approximated as a finite DOF lumped system.

Closed-form analysis of complex continuous structures is seldom carried out because of the mathematical difficulty involved. This statement remains true with the exceptions of some of the simplest structures only i.e. a beam, a rod etc. Hence analysis are often pursued by approximation methods. Finite Elements (FE) and Boundary

Elements (BE) methods are the two most popular methods used by analysts. An FE or BE model of a structure usually incorporates a finite number, but still a very large number, of nodes and elements. The deformation field of each element is specified by the DOFs at all its nodes. Hence the total number of DOFs of all the active nodes and elements N is frequently very large. For this reason, an FE or a BE model is often classified as a high-order model.

By contrast, only a relatively small number of DOF can be measured from experiment. Therefore n is usually much smaller than N . For this reason, a model synthesized directly from measured data is often classified as a low-order, *condensed* or *spatially truncated* model.

Apart from spatial truncations, most practical models are also modally or spectrally truncated. This is because, in practice, only a small number of modes in a very narrow frequency band is determined experimentally. As a result, r is usually much smaller than n . The model so obtained is called an *incomplete model*. Otherwise, if r is equal to n then the model is called a *complete model*.

6.1 CONVENTIONAL MODAL METHODS

By definition, most of these methods require the determination of the relevant modal parameters as a pre-requisite step before the spatial matrices are determined.

6.1.1 AN OVERVIEW OF THE HISTORICAL DEVELOPMENT

The most notable contributions in this field can be traced back to the US National Aeronautical and Space Administration (NASA) research programme in the late 1960's and the early 1970's. This programme was commissioned to investigate the techniques of experimental determination of structural dynamic models for aerospace structures. The driving force behind this development was the need to obtain valid experimental models which could be used for response analysis, load prediction and validation of analytical models of existing or modified aerospace structures. This technique was seen as a soft option for the more expensive, time-consuming, hardware testing often done on a trial-and-error basis. A number of investigations conducted by Rodden^[62], Raney and

Hewlett ^[6.3], **Ross** ^[6.4], **Thoren** ^[6.5], **Young and On** ^[6.6], **Kozin** ^[6.7], **Berman and Wei** ^[6.8] were either a direct or an indirect result of this programme.

Historically, DSPED have undergone different phases of change and development. It was first perceived by **Rodden** ^[6.2] in 1967 as a process of determining the structural influencing coefficients using ground vibration tests. In 1968, **Kozin** ^[6.7] considered this as a parameter identification process. The identification procedure which he proposed was based upon statistical expectations and time averaging technique. The method was tested by a series of simulation studies and proven applicable to both linear and non-linear systems.

Later in 1969, DSPED was perceived by **Raney and Hewlett** ^[6.3] as a process of determining a set of coefficients of the governing equations of motions of a structure formulated at the tested coordinates. These coefficients were effectively the elements of the mass, stiffness and damping matrices. This approach relied solely on the use of experimental near-resonance response data of a structure. Detailed knowledge of neither the structural nor material properties of a structure was required.

Young and On ^[6.6] summarized the various efforts and activities in this field and systematically categorized the various methods into five practical schemes. His work consolidated much of the thoughts and concepts associated with this technology.

In 1971, **Ross** ^[6.4] proposed a method which he described as a kind of *synthesis* technique. Two basic approaches were proposed: i.e. one of synthesizing low-order complete or incomplete models and the other of improving or updating existing high-order models. In particular to his approach, he proposed a novel normalisation procedure for the measured eigenvectors based on preserving the kinetic and strain energies of the real system. In 1972, **Thoren** ^[6.5] reported similar efforts conducted in this area. He adopted a similar line of approach and applied his method to a real aerospace structural system. Some successes were claimed.

Since then, this activity was laid dormant for quite a while and relatively little literature on this subject was reported. However the recent up-surge of activities in experimental modal analysis has revived this activity again. Also because of the advance in computer software and hardware, the recently developed methods are increasingly geared

to large scale data processing associated with high order models.

6.1.2 METHODS REQUIRING PRIORI ASSUMPTIONS

These methods are all typical in the way that priori assumptions on some of the parameters have to be made before other interested parameters can be determined. Nielsen ^[6.8] is believed to be one of the first to have used this approach. He developed a number of procedures to calculate the elements in the stiffness and damping matrices from experimentally measured modal properties using classical normal mode theories.

In particular to his method, his procedures formulated the problem in such a way that the solution process was reduced to solving a system of simultaneous linear equations. The unknown vector in these equations contains the unknown elements of the stiffness and damping matrices. This method differs from the other methods based on optimization methodology in the way that the unknown parameters were determined directly rather than through iterative search schemes.

This procedure relied not only on a prior knowledge of the mass matrix but also on further restriction on the mass matrix for the procedures to work. In most cases, the mass matrix was assumed diagonal i.e. lumped mass rather than consistent mass model. With this method, the various requirements on the number of modes, hence the number of available equations, for a solution of a number of systems: known as *simply-coupled*, *far-coupled* and *close-coupled* systems, can be determined.

Sokal ^[6.9] proposed a similar approach which determined a stiffness matrix $[K]$ directly from an assumed mass matrix $[M]$ and an incomplete set of modal matrices. In particular to his approach, the algorithm proposed did not require the computation of the inverse of the modal matrix and was therefore applicable to incomplete models.

All these methods are based on the assumption that the mass of a structure can be estimated from design drawings with some degrees of certainty. However, in reality, the mass matrix $[M]$ of a structure is not easy to determine accurately. These methods were applied to relatively simple systems only and spatial matrices of the low order category only were obtained.

6.1.3 METHODS USING ORTHOGONALITY PROPERTIES

These methods require a prior determination of a complete set of modal parameters which can be used to construct three square matrices: i.e. a diagonal spectral matrix $[\omega_r^2]$ (or a matrix of eigenvalues or square of natural frequencies), a diagonal matrix $[2\xi_r \omega_r]$ (here proportional damping is assumed) and a square modal matrix $[\Phi]$ (or a matrix of eigenvectors or modal vectors). Then calculation proceeds by using the orthogonality property of the vibration modes (real modes in the case of proportionally damped cases and generally complex modes for non-proportionally damped cases). This property can be stated mathematically with the following equations :

$$\begin{aligned} [\Phi]^T * [M] * [\Phi] &= [I] \\ [\Phi]^T * [C] * [\Phi] &= [2\omega_r \xi_r] \\ [\Phi]^T * [K] * [\Phi] &= [\omega_r^2] \end{aligned} \quad 6.1.3-1$$

The matrices $[I]$ is an identity matrix (i.e. modal vectors are normalised). $[2\xi_r \omega_r]$ and $[\omega_r^2]$ have previously been defined in Chapter 5. If the inverses of $[\Phi]^{-1}$ and $[\Phi]^{-T}$ exist, then the spatial matrices can be obtained using Equations 6.1.3-2:

$$\begin{aligned} [M] &= [\Phi]^{-T} * [\Phi]^{-1} \\ [C] &= [\Phi]^{-T} * [2\omega_r \xi_r] * [\Phi]^{-1} \\ [K] &= [\Phi]^{-T} * [\omega_r^2] * [\Phi]^{-1} \end{aligned} \quad 6.1.3-2$$

Much of the works described previously in Section 6.1.1 have utilized this orthogonality property either implicitly or explicitly. These equations can be used whether a low order or a high order model is concerned.

Using *complex analysis*, different formulations can be obtained. **Potter and Richardson** ^[6.10] applied Laplace Transformation (denoted by the $\mathcal{L}()$ operator) to the governing equation of motion to obtain a *Transfer Matrix* $[T]$ which was defined as the inverse of the system matrix as defined in Equation 6.1.3-5:

$$\mathcal{L} ([M] * \{\ddot{x}(t)\} + [C] * \{\dot{x}(t)\} + [K] * \{x(t)\}) = \mathcal{L} (\{f(t)\})$$

6.1.3-3

$$\text{such that } \mathcal{L} (\{x(t)\}) = [T(s)] * \mathcal{L} (\{f(t)\}) \quad 6.1.3-4$$

$$\text{then } [T(s)] = (s^2 [M] + s [C] + [K])^{-1} \quad 6.1.3-5$$

where s is the complex Laplace domain variable.

Using this approach, expressions to obtain $[M]$, $[C]$ and $[K]$ were derived in terms of the poles and the complex modal vectors of a system. So far the methods described in Sections 6.1.1 to 6.1.3 concern mostly with the determination of low order spatial matrices. These matrices though provide a valid mathematical description of a structure, their physical interpretation is sometimes difficult to obtain. Because the order of these matrices were condensed or truncated both spatially and modally to such a small number, in relation to the complexity of a structure, that the elements in these spatial matrices had lost their precise physical interpretation. A term by term comparison of these matrices with those of a high order FEM model was impossible. This is often the very reason why these methods have lost their appeal despite all other benefits they can offer.

6.1.4 METHODS USING OPTIMIZATION TECHNIQUES

Because of the drawbacks associated with low-order models, various investigators such as O'Callahan et al^[6.11, 6.12], Baruch^[6.13] adopted another approach utilizing computational optimisation techniques i.e. by correcting existing inaccurate spatial matrices of an FE model rather than synthesizing new ones. The corrected spatial matrices were obtained by imposing orthogonality criteria in the optimisation process. In operation, these methods required a set of approximate spatial matrices, called *seeding matrices*, as a starter prior to executing the correction procedures. The success of these methods

often depended on how reasonably accurate the seeding matrices were in relation to their true counterparts. Otherwise, the iterative search might not converge to the true solution. So far, these methods have only been applied to analytical or academic type of problems. Successful applications to real systems are not reported.

6.1.5 SUMMARY OF MODAL METHODS

On the whole, all the methods discussed so far, are subjected to certain limitations in relation to their basic approach. In the case of synthesizing low-order models from a complete set of modes, the synthesis is a straight forward application of Equations 6.1.3-2. For the case of an incomplete set of modes, a direct use of these equations is impossible without proper pre-treatment. Because in practice, the number of measured DOFs p is usually much larger than the number of modes r , as a result the modal matrix is rectangular and neither $[\Phi]^{-1}$ and $[\Phi]^T$ is defined.

To overcome this problem, **Thoren** chose to artificially constraint the two numbers equal, i.e. $n = r$. In doing so, he selected n DOFs of a structure and r modes of vibration as to ensure that the modal matrix would be square. By adopting a rather different approach, **Ross** used a novel strategy by adding $(n-r)$ arbitrary linearly independent vectors to fill out the modal matrix to make it a square matrix.

Despite the drawbacks associated with low-order models, the advantages of having such models are readily apparent. First of all, the computational requirements and efforts are moderate compared with their high-order counterparts. Secondly, these models can predict and characterize the response of a structure quite accurately.

The utilization of measured data to correct a high-order analytical model is the next logical step which provides a direct link between FE modelling and experimental results. This approach is still being developed and will be very useful if much of the practical problems can be resolved.

6.2 THE PROPOSED NON-MODAL METHOD

6.2.1 BACKGROUND

The need for such a technique is based on the fact that modal parameters are very difficult to interpret. These parameters fail to convey useful structural information readily comprehensible to structural designers who usually do not have a background in structural dynamics. To civil engineers, structural information in the form of mass and stiffness are more readily understandable.

There were a small number of investigations directed to DSPED using a non-modal approach (however, the author was not aware of these publications at the time the algorithm was developed). Generally speaking, the literature on this subject was patchy and difficult to locate because partly of the differences in terminology used. For instance, **Mottershead et al** ^[6.19] called their proposed method a Recursive Frequency Domain Least-Square Filter. This method was based on an equation-error approach. This study concluded that the inclusion of any a priori information about a system would enhance convergency and produce better results. **Leuridan et al** ^[6.20] and **Ookuma et al** ^[6.18] have also reported works in this area. Their works will be further explained in Section 6.2.2.

The method being proposed here is categorized as a non-modal method which is in contrast to the conventional modal methods already described in Section 6.1. In essence, the basis of modal methods is the linear modal transformations: i.e a transformations of physical coordinates to modal coordinates, which results in decoupling the equations of motion. This transformation can also be visualised as a projection from the physical space to the modal space. The inverse projection from the modal space back to the physical space can only be accurate if all the modal information are preserved. However this is usually not the case. Basing on an incomplete or inaccurate set of modal parameters, the inverse projection can produce large errors, called *truncation errors*. It is the approximations and errors made at this level which present problems in the derivation of a system's spatial matrices using methods described in Section 6.1. Figure 6.2-1 shows how the proposed method has bypassed the conventional modal procedures to obtain the spatial matrices.

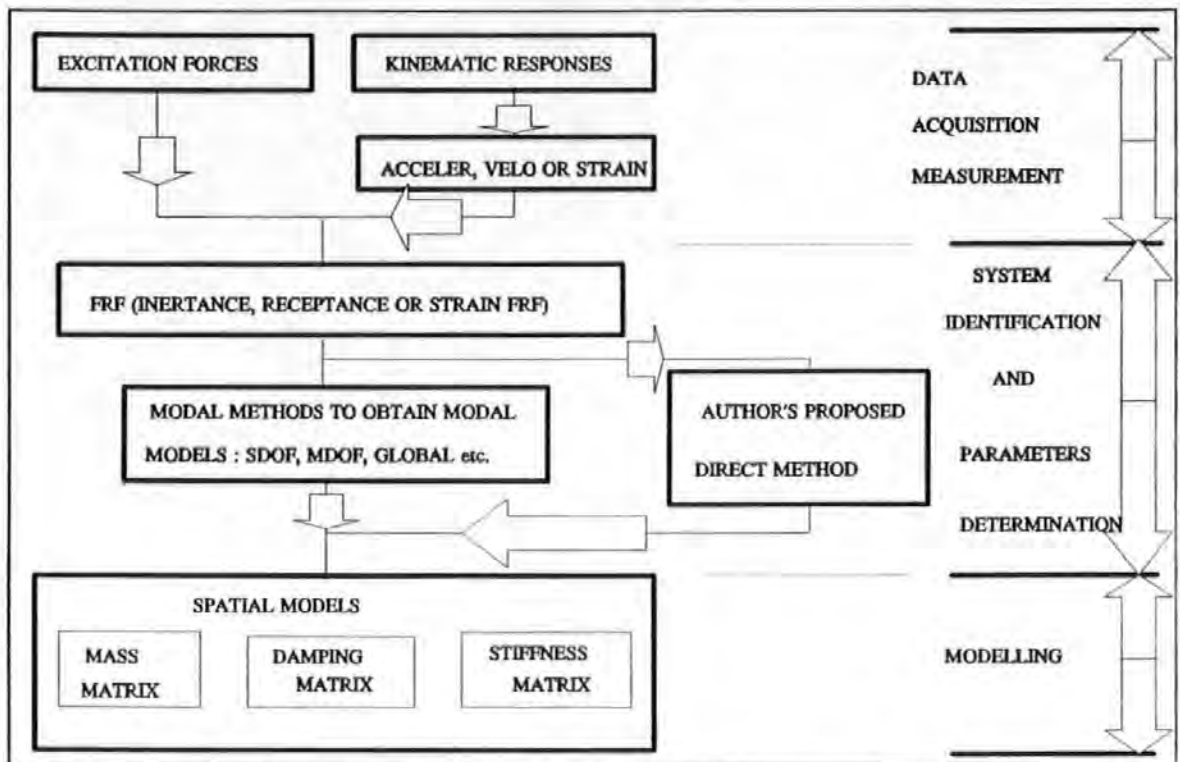


Figure 6.2-1 A schematic diagram showing how the proposed method bypasses the conventional modal procedures to obtain the spatial matrices.

The inspiration of this algorithm is accredited to **Nielsen's** ^[6,8] work and to the way he formulated the problem of determining $[M]$, $[C]$ and $[K]$ as the solution of simultaneous equations in which the elements of the spatial matrices are extracted to form the unknown vector. Hence there is some resemblance between the two algorithms in these respects.

As a summary, this algorithm has the following features:

1. No prior knowledge of the modal parameters is required.
2. No prior knowledge of the mass of structure is required.
3. No orthogonality is assumed.
4. A 'global' curve fitting technique is used i.e. instead of using only local data, spatial information from data at all other measurement locations are also used.
5. Consistent modal parameters are maintained for each individual

measurement.

6. The number of measured coordinates does not necessarily have to be equal to the number of measured modes as required in conventional methods.

With this method, less information on individual local test points is required as information can be subordinated by data from measurements at other spatial points of a structure. This *spatial reference* technique is very useful because more spatial measurements can be carried out at the expense of less detailed local measurements.

6.2.2 DEVELOPMENT OF THE ALGORITHM

The general equations of motion of an N degree of freedom system is given below :

$$[M] \{\ddot{x}(t)\} + [C] \{\dot{x}(t)\} + [K] \{x(t)\} = \{f(t)\} \quad 6.2.2-1$$

where

$[M]$ is the $n \times n$ system spatial mass matrix

$[C]$ is the $n \times n$ system spatial viscous damping matrix

$[K]$ is the $n \times n$ system spatial stiffness matrix

$\{\ddot{x}(t)\}, \{\dot{x}(t)\}, \{x(t)\}$ are the $n \times 1$ acceleration, velocity and displacement response vectors respectively

$\{f(t)\}$ is the $n \times 1$ excitation force vector

If the equations are re-written in the frequency domain by applying Fourier Transformation \mathcal{F} to (6.2.2-1), then :

$$-\omega^2 [M] \{X(\omega)\} + j \omega [C] \{X(\omega)\} + [K] \{X(\omega)\} = \{F(\omega)\}$$

6.2.2-2

where $\{X(\omega)\}$ is the vector of \mathcal{F} of displacement responses in ω

$\{F(\omega)\}$ is the vector of \mathcal{F} of external applied forces in ω

ω is the angular frequency

j is the imaginary unit

Also, the vectors $\{X(\omega)\}$ and $\{F(\omega)\}$ of (6.2.2-2) are in general complex quantities :

$$\begin{aligned}\{X(\omega)\} &= \{XR(\omega)\} + j \{XI(\omega)\} \\ \{F(\omega)\} &= \{FR(\omega)\} + j \{FI(\omega)\}\end{aligned}\tag{6.2.2-3}$$

Using these two equations and by equating the real and imaginary parts :

$$\{FI(\omega)\} = (-\omega^2 [M] + [K]) * \{XI(\omega)\} + \omega [C] * \{XR(\omega)\}\tag{6.2.2-5a}$$

$$\{FR(\omega)\} = (-\omega^2 [M] + [K]) * \{XR(\omega)\} - \omega [C] * \{XI(\omega)\}\tag{6.2.2-5b}$$

If these equations are re-arranged, transposed and separated into the real and imaginary parts as follows:

$$\begin{bmatrix} -\omega^2 \{XR(\omega)\}^T & -\omega \{XI(\omega)\}^T & \{XR(\omega)\}^T \end{bmatrix} \begin{bmatrix} [M] \\ [C] \\ [K] \end{bmatrix} = \{FR(\omega)\}^T\tag{6.2.2-6a}$$

$$[-\omega^2\{X I(\omega)\}^T \quad + \quad \omega\{XR(\omega)\}^T \quad \{X I(\omega)\}^T] \begin{bmatrix} [M] \\ [C] \\ [K] \end{bmatrix} = \{ FI(\omega) \}^T$$

(6.2.2-6b)

Then for a number of frequencies $\omega_1, \omega_2, \dots, \omega_s$, Two equations such as Equation (6.2.2-6) can be assembled for each frequency. The completely assembled matrix equations become :

$$\begin{bmatrix} -\omega_1^2\{X R(\omega_1)\}^T & -\omega_1\{X I(\omega_1)\}^T & \{X R(\omega_1)\}^T \\ \vdots & \vdots & \vdots \\ -\omega_s^2\{X R(\omega_s)\}^T & -\omega_s\{X I(\omega_s)\}^T & \{X R(\omega_s)\}^T \\ \hline -\omega_1^2\{X I(\omega_1)\}^T & \omega_1\{XR(\omega_1)\}^T & \{X I(\omega_1)\}^T \\ \vdots & \vdots & \vdots \\ -\omega_s^2\{X I(\omega_s)\}^T & \omega_s\{XR(\omega_s)\}^T & \{X I(\omega_s)\}^T \end{bmatrix} \begin{bmatrix} [M] \\ [C] \\ [K] \end{bmatrix} = \begin{bmatrix} \{FR(\omega_1)\}^T \\ \vdots \\ \{FR(\omega_s)\}^T \\ \hline \{FI(\omega_1)\}^T \\ \vdots \\ \{FI(\omega_s)\}^T \end{bmatrix}$$

(6.2.2-7)

If the number of measured frequency points s satisfy the following criteria :

$$2 s = 3 n$$

Then the coefficient matrix denoted by $[COEF(\omega)]$ in Equation 6.2.2-7 is square and its proper inverse $[COEF(\omega)]^{-1}$ exists. The unknown $[M]$, $[C]$ and $[K]$ matrices can be determined by Equation (6.2.2-7) in the normal way. However if

$$2s > 3n$$

then the coefficient matrix is rectangular, and $[\text{COEF}(\omega)]^{-1}$ does not exist. In this case a pseudo inverse $[\text{COEF}(\omega)]^*$ is used instead. Both **Leuridan et al** ^[6.20] and **Ookuma et al** ^[6.18] have reported using this type of formulation. A different formulation was developed by the author which offers some advantages over the formulation in Equation 6.2.2-7.

Now define the receptance frequency response function $\alpha_{ir}(\omega)$ as :

$$\alpha_{ir}(\omega) = \frac{X_i(\omega)}{F_r(\omega)} \quad 6.2.2-9$$

If one excitation force only is applied at point r such that

$$\{F(\omega)\} = \begin{Bmatrix} 0 \\ 0 \\ \vdots \\ \vdots \\ F_r(\omega) \\ \vdots \\ 0 \\ 0 \end{Bmatrix} \quad 6.2.2-10$$

then it is convenient to drop the subscript r and redefine (6.2.2-9) as

$$\alpha_i(\omega) = \alpha_{ir}(\omega) \quad (6.2.2-11)$$

Using this relationship , Equation (6.2.2-2) can be re-written as

$$(-\omega^2[M] + j\omega[C] + [K]) * \alpha_i(\omega) = \begin{bmatrix} 0 \\ 0 \\ \vdots \\ 1 \\ \vdots \\ 0 \\ 0 \end{bmatrix} \quad (6.2.2-12)$$

The receptance $\alpha_i(\omega)$ so defined in (6.1.2-11) is also a complex quantity having real $R\alpha_i(\omega)$ and imaginary $I\alpha_i(\omega)$ parts :

$$\alpha_i(\omega) = R\alpha_i(\omega) + j I\alpha_i(\omega) \quad 6.2.2-13$$

Hence by equating the real and imaginary parts of (6.2.2-11) :

$$(-\omega^2 [M] + [K]) * \{ R\alpha(\omega) \} - \omega [C] * \{ I\alpha(\omega) \} = \begin{Bmatrix} 0 \\ 0 \\ 0 \\ \vdots \\ \vdots \\ 1 \\ \vdots \\ 0 \\ 0 \end{Bmatrix} \quad (6.2.2-14a)$$

$$(-\omega^2 [M] + [K]) * \{ I\alpha(\omega) \} + \omega [C] * \{ R\alpha(\omega) \} = \begin{Bmatrix} 0 \\ 0 \\ 0 \\ \vdots \\ 0 \\ \vdots \\ 0 \\ 0 \end{Bmatrix}$$

(6.2.2-14b)

Initially, if the spatial matrices are assumed full matrices i.e.

$$[M] = \begin{bmatrix} m_{11} & m_{12} & \dots & m_{1n} \\ m_{21} & m_{22} & \dots & m_{2n} \\ \cdot & \cdot & \dots & \dots \\ \cdot & \cdot & \dots & \dots \\ m_{n1} & m_{n2} & \dots & m_{nn} \end{bmatrix}$$

(6.2.2-15a)

$$[C] = \begin{bmatrix} c_{11} & c_{12} & \dots & c_{1n} \\ c_{21} & c_{22} & \dots & c_{2n} \\ \cdot & \cdot & \dots & \dots \\ \cdot & \cdot & \dots & \dots \\ c_{n1} & c_{n2} & \dots & c_{nn} \end{bmatrix}$$

(6.2.2-15b)

$$[K] = \begin{bmatrix} k_{11} & k_{12} & \dots & k_{1n} \\ k_{21} & k_{22} & \dots & k_{2n} \\ \cdot & \cdot & \dots & \dots \\ \cdot & \cdot & \dots & \dots \\ k_{n1} & k_{n2} & \dots & k_{nn} \end{bmatrix}$$

(6.2.2-15c)

Then if each element in the matrices is extracted to form an unknown vector (a technique instigated by **Nielsen** ^[6.8] in deriving his algorithms as described Section 6.1.2):

$$\left\{ \begin{array}{c} Y \\ (3 \ n^2 \times 1) \end{array} \right\} = \left\{ \begin{array}{c} m_{11} \\ : \\ : \\ m_{nn} \\ c_{11} \\ : \\ : \\ c_{nn} \\ k_{11} \\ : \\ : \\ k_{nn} \end{array} \right\} \tag{6.2.2-16}$$

(Note that **Ookuma et al** ^[6.18] have reported using the same approach but the detailed formulation was not presented in their paper).

Equation (6.2.2-14) now takes the form:

$$\left[\begin{array}{ccc} [A_m] & [A_c] & [A_k] \end{array} \right] \left\{ \begin{array}{c} m_{11} \\ : \\ : \\ m_{nn} \\ c_{11} \\ : \\ : \\ c_{nn} \\ k_{11} \\ : \\ : \\ k_{nn} \end{array} \right\} = \left\{ \begin{array}{c} 0 \\ 0 \\ 0 \\ : \\ : \\ 1 \\ : \\ : \\ 0 \\ 0 \\ 0 \end{array} \right\} \tag{6.2.2-17}$$

where $[A_m]$, $[A_c]$ and $[A_k]$ are of the form

$$[A_m] = \left[\begin{array}{c} [-\omega^2 B(R\alpha(\omega))] \\ \hline [-\omega^2 B(I\alpha(\omega))] \end{array} \right] \quad (6.2.2-19a)$$

$$[A_c] = \left[\begin{array}{c} [-\omega B(I\alpha(\omega))] \\ \hline [\omega B(R\alpha(\omega))] \end{array} \right] \quad (6.2.2-19b)$$

$$[A_k] = \left[\begin{array}{c} [B(R\alpha(\omega))] \\ \hline [B(I\alpha(\omega))] \end{array} \right] \quad (6.2.2-19c)$$

where the matrix functions are defined as follows :

$$[B(R\alpha(\omega))] = \left[\begin{array}{c} (R\alpha_1 \dots R\alpha_n) \\ (R\alpha_1 \dots R\alpha_n) \\ \vdots \\ (R\alpha_1 \dots R\alpha_n) \end{array} \right]$$

(6.2.2-20a)

$$[B(I\alpha(\omega_1))] = \begin{bmatrix} (I\alpha_1 \dots I\alpha_n) & & & \\ & (I\alpha_1 \dots I\alpha_n) & & \\ & & \ddots & \\ & & & (I\alpha_1 \dots I\alpha_n) \end{bmatrix} \quad (6.2.2-20b)$$

It is evident that for each frequency ω , a total of $2n$ equations such as (6.2.2-17) can be formulated. If the frequency response data are available at s different frequencies i.e.

$$\omega_1, \omega_2, \omega_3, \dots, \omega_s$$

then the total number of equations available equals $2sn$. In order to solve the unknowns which now total $3n^2$, thence

$$2sn > 3n^2$$

and

$$s > 1.5n$$

The fully assembled matrix equation called *system equation* is too large to be shown here. The assembling process is similar to that of Equation 6.2.2-7. If the number of frequencies available to assemble equation (6.2.2-17) is more than the statutory minimum i.e. $1.5n$ then the system equations are over-specified and the pseudo-inverse method of solution may be employed. In such systems where the spatial matrices may be considered symmetric :

$$[M] = [M]^T, \quad [C] = [C]^T \text{ and } [K] = [K]^T$$

(6.2.2-21a)

(6.2.2-21b)

(6.2.2-21c)

Then the number of unknown parameters can be reduced and the upper triangular elements in these matrices only require solution. The number of unknowns in this case is now given by

$$\frac{3 * n * (n + 1)}{2}$$

The use of symmetry has the advantage of reducing the size of the matrices in the *system equation*. This in turn simplifies the mathematical operations. However, there are situations, such as non-linear systems, in which these matrices may not be symmetrical. If the assumption of symmetry is used, the sizes of the unknown vectors $\{m\}$, $\{c\}$ and $\{k\}$ are each reduced to:

$$\frac{n * (n + 1)}{2}$$

To enforce symmetry and other criteria in the computational process, two methods can be used. The first method is by appending a set of *constraint* equations to the *system equation*. These constraint equations impose the following constraints to the system.

$$M_{ij} - M_{ji} = 0 \quad \text{for all } i, j$$

$$C_{ij} - C_{ji} = 0 \quad \text{for all } i, j$$

$$K_{ij} - K_{ji} = 0 \quad \text{for all } i, j$$

One such typical constraint equation is given as follows :

$$\begin{bmatrix} & M_{ij} & & M_{ji} & & & & \\ 0 & 0 & 0 & . & -1 & . & . & 1 & 0 & 0 & 0 \\ & & & & & (1 \times 3n) & & & & & \end{bmatrix} [Y] = [0] \quad 6.2.2-23a$$

The positions for inserting 1 and -1 are corresponding to the positions of the terms M_{ij} and M_{ji} in the column vector $\{Y\}$. For those elements which are known to be zero, then constraint equations similar to Eq. 6.2.2-23a can be introduced as well. For instance if M_{ij} is zero, then one such typical constraint equation can be written as follows :

$$\begin{bmatrix} & M_{ij} & & & & & & \\ 0 & 0 & 0 & . & 1 & . & . & 0 & 0 & 0 \\ & & & & & (1 \times 3n) & & & & \end{bmatrix} [Y] = [0] \quad 6.2.2-23b$$

However this computational method is quite ineffective. A second method was therefore adopted. This method requires that all zero valued spatial parameters are eliminated from the $\{Y\}$ vector and the columns of the coefficient matrix in the *system equation* corresponding to these terms are deleted. This method also has an advantage of reducing the size of the matrices.

To enforced symmetry, reorganisation of the terms in the coefficient matrix is required. For instance, without symmetry, the terms in the coefficient corresponding to K_{ij} and K_{ji} are a and b respectively.

$$\begin{bmatrix} & K_{ij} & & K_{ji} & & & & \\ 0 & 0 & 0 & . & a & . & . & b & 0 & 0 & 0 \\ & & & & & (1 \times 3n) & & & & & \end{bmatrix} [Y] = [0] \quad 6.2.2-24$$

Now if K_{ij} equals K_{ji} then:

$$\begin{bmatrix} & K_{ij} & & & & & \\ 0 & 0 & 0 & . & a+b & . & . & . & 0 & 0 & 0 \\ & & & 1 \times (3n-1) & & & & & & & \end{bmatrix} [Y^*] = [0] \quad 6.2.2-25$$

where $\{Y\}$ is similar to $\{Y^*\}$ except that the element K_{ij} has been eliminated and its size decrease by 1. With symmetry, the total number of frequency points required should satisfy the following criteria.

$$2 s n > \frac{3 n (n + 1)}{2}$$

6.2.3 IMPLEMENTATION AND VERIFICATION OF THE ALGORITHM

The algorithm was coded as a computer program in Hewlett Packard Basic and verified using a series of computer simulations. The restraints on memory available on the HP 9816 desk-top computer had dictated much of the way the simulations were performed. The computation carried out involves very large matrices and the computer used can only cope with systems of a small number of degrees of freedom.

6.2.3.1 COMPUTER SIMULATIONS

The required FRF data used for the computer simulation were generated from two fictitious vibration systems with known spatial matrices but with no artificially added noise. By not introducing noise, error in the results of the computation can be localized to sources such as numerical sensitivity or instability associated which are known to be notorious in most *inverse* methods ('inverse' method was defined by **Bekey** ^[3.9] in Section 3.3.1).

In order to reduce computational memory requirements, two systems with only a small number of DOF were used.

SYSTEM 1. a 3 DOF damped system.

SYSTEM 2.

a 10 DOF undamped system.

The assumed spatial matrices of the two systems are summarized in Tables 6.2.3.1-1 to Tables 6.2.3.1-3.

TABLE 6.2.3.1-1 SPECIFIED SPATIAL PARAMETERS OF THE 3 DOF SYSTEM USED IN THE COMPUTER SIMULATION STUDIES.

SPATIAL MATRIX				UNIT
[M]	0.5	0	0	Kg
	0	1	0	
	0	0	1.5	
[C]	0.5	0	0	Ns/m
	0	1	0	
	0	0	1.5	
[K]	3000	-1000	-1000	N/m
	-1000	3000	-1000	
	-1000	-1000	3000	

TABLE 6.2.3.1-2 THE SPECIFIED MASS MATRIX OF THE 10 DOF SYSTEM
USED IN THE COMPUTER SIMULATION.

SPATIAL MATRIX											UNIT
[M]	1	0	0	0	0	0	0	0	0	0	Kg
	0	1	0	0	0	0	0	0	0	0	
	0	0	1	0	0	0	0	0	0	0	
	0	0	0	1	0	0	0	0	0	0	
	0	0	0	0	1	0	0	0	0	0	
	0	0	0	0	0	1	0	0	0	0	
	0	0	0	0	0	0	1	0	0	0	
	0	0	0	0	0	0	0	1	0	0	
	0	0	0	0	0	0	0	0	1	0	
	0	0	0	0	0	0	0	0	0	1	

TABLE 6.2.3.1-3 THE SPECIFIED STIFFNESS MATRIX OF THE 10 DOF SYSTEM USED IN THE COMPUTER SIMULATION.

SPATIAL MATRIX											UNIT
[K]	2	-1	0	0	0	0	0	0	0	0	x 10 ³ N/m
	-1	2	-1	0	0	0	0	0	0	0	
	0	-1	2	-1	0	0	0	0	0	0	
	0	0	-1	2	-1	0	0	0	0	0	
	0	0	0	-1	2	-1	0	0	0	0	
	0	0	0	0	-1	2	-1	0	0	0	
	0	0	0	0	0	-1	2	-1	0	0	
	0	0	0	0	0	0	-1	2	-1	0	
	0	0	0	0	0	0	0	-1	2	-1	
	0	0	0	0	0	0	0	0	-1	2	

A FRF data set was synthesized for each degree of freedom (or each spatial point). These data were effectively a set of receptance spectra which would have been obtained from experiment rather than synthesized in this way. For both SYSTEM 1 and 2, the receptance spectra were synthesized by assuming the single force input was applied at the spatial point No. 1.

6.2.3.2 QUALITY-OF-FIT FACTOR

the measure of the so called 'quality-of-fit' of a derived model is not a trivial task. Frequently, the readily available means is by visual inspection of the 'closeness' or correlation between the measured and the regenerated FRF curves. Because the

assumed spatial matrices used in the computer simulation are known then a direct comparison between the derived and the assumed matrices can be used to indicate how good or bad a model is. A quantifier or indicator QF_1 can be used and has been defined as follows:

$$QF_1 = \left[\frac{(\sum (m_{ass} * m_{derive}))^2 (\sum (c_{ass} * c_{derive}))^2 (\sum (k_{ass} * k_{derive}))^2}{(\sum m_{ass}^2) (\sum m_{derive}^2) (\sum c_{ass}^2) (\sum c_{derive}^2) (\sum k_{ass}^2) (\sum k_{derive}^2)} \right] \quad (6.2.3.2-1)$$

where the subscript ass refers to assumed values
the subscript derive refers to derived values

However this would not be the case for a real life situation where there is no advantage of knowing what these true parameters are. In this case, an indicator QF_2 can be used as the alternative and is defined as :

$$QF_2 = \left[\frac{(\sum (y_{regen} * y_{exp}))^2}{(\sum y_{exp}^2) (\sum y_{regen}^2)} \right] \quad (6.2.3.2-2)$$

where the subscript regen refers to regenerated FRF
the subscript exp refers to experimental FRF
y is the ordinate of modulus of a FRF curve at a particular frequency

These so-called QF Factors are dimensionless numbers normally lying between 0 and 1. A QF Factor of 1 indicates a perfect fit and otherwise if it is smaller than 1. However, this indicator is sometimes open to interpretation and sole reliance on it can be misleading. Supporting measures should always be taken e.g. by a visual correlation check on characteristics such as the locations of the resonant peaks and the general shapes of the FRF curves. In summary, a QF Factor close to 1 is a necessary indication for an

accurate model but not sufficient.

6.2.3.3 RESULTS

The simulation was performed to investigate the validity of the algorithm under a mixed combinations of the following different scenarios :

- | | |
|-------------|--|
| SCENARIO 1. | The selected data points were well distributed over the range of frequencies covering all the modes. |
| SCENARIO 2. | The selected data points were concentrated at a narrow range of frequencies covering fewer modes. |
| SCENARIO 3. | The full data set for all the spatial points was used. |
| SCENARIO 4. | A smaller data set chosen from some of the spatial points was used. |

In general, the accuracy of the derived spatial matrices was found to be affected in various ways by all four scenarios. Especially in SCENARIOS 1 and 3, exact spatial matrices (both the forms and values of the matrices) and QF Factors of 1 for both SYSTEM 1 and 2 were obtained if the following rules were followed:

- a. at least 2 data points on either side of each resonant peak were chosen
- b. the data points chosen did not cover more modes than the order of matrices to be derived.

The results for SYSTEM 1 are given in Figures 6.2.3.3-1 to 6.2.3.3-3. Good results are indicated by total eclipse of the original curves (plotted with solid dots) by the regenerated curves (plotted with asterisks).

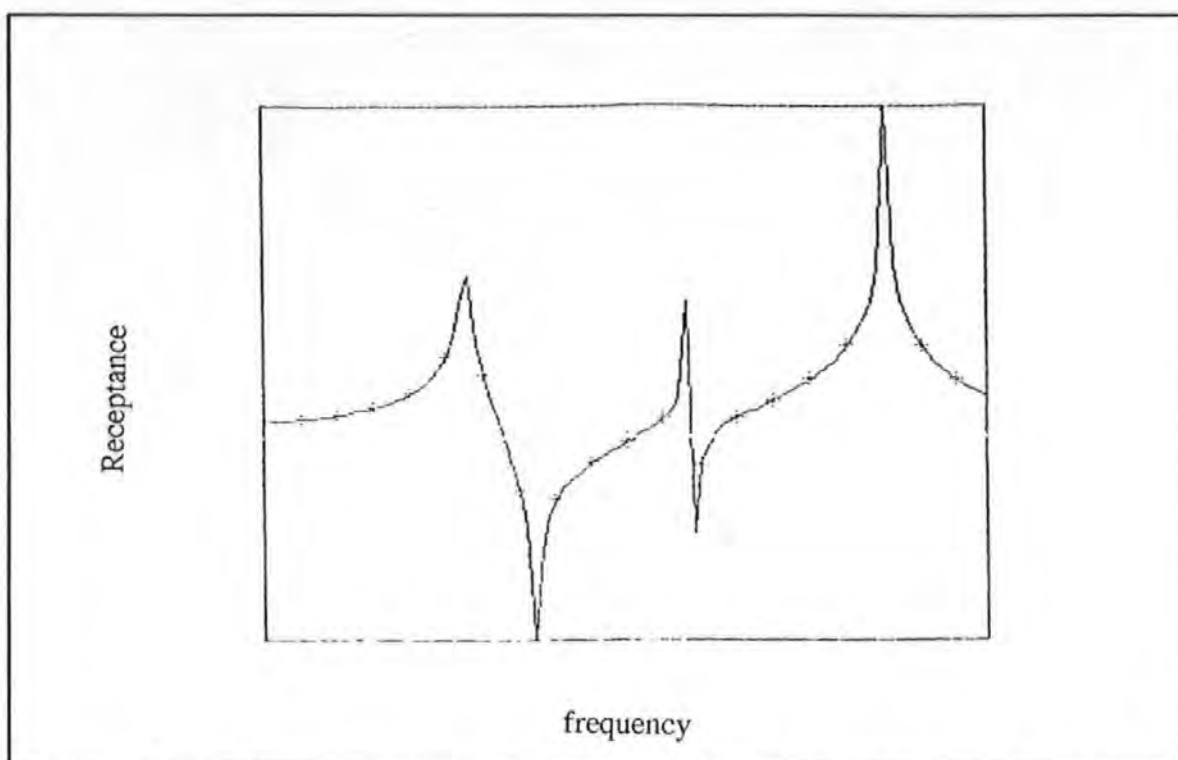


Figure 6.2.3.3-1 Receptance spectrum for the 3 DOF fictitious system at spatial point No.1.

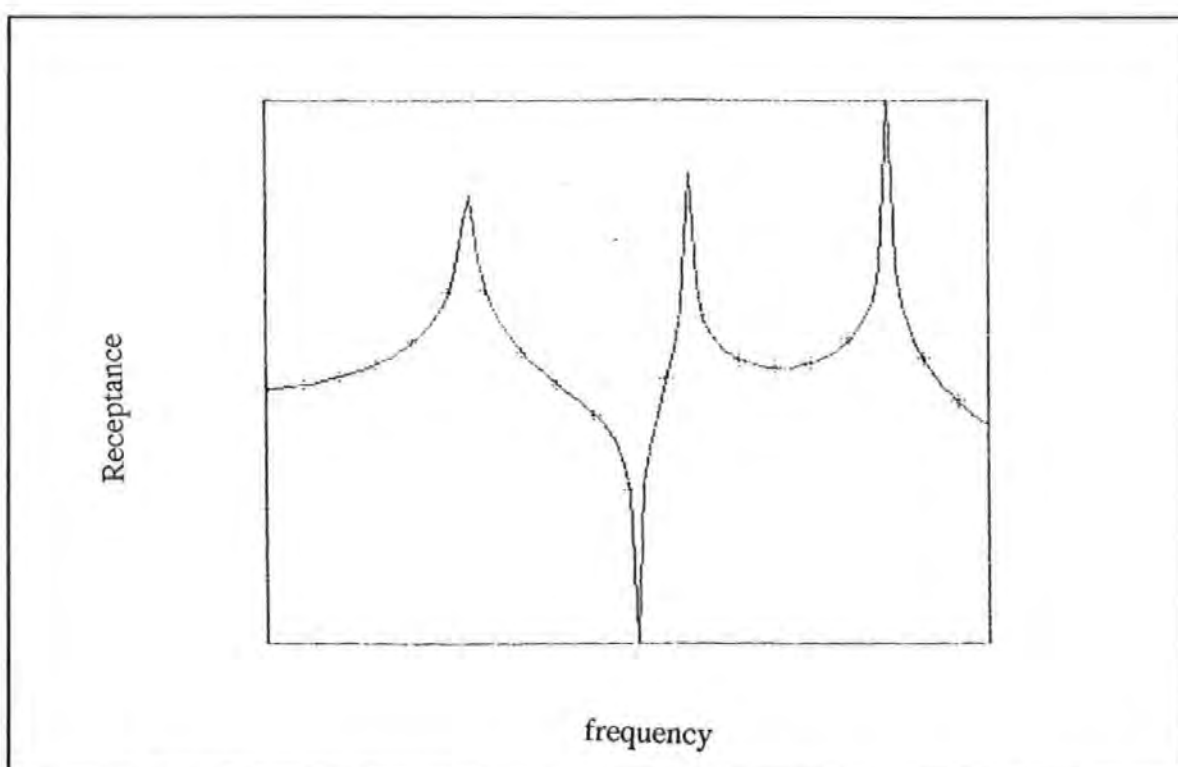


Figure 6.2.3.3-2 Receptance spectrum for the 3 DOF fictitious system at spatial point No.2.

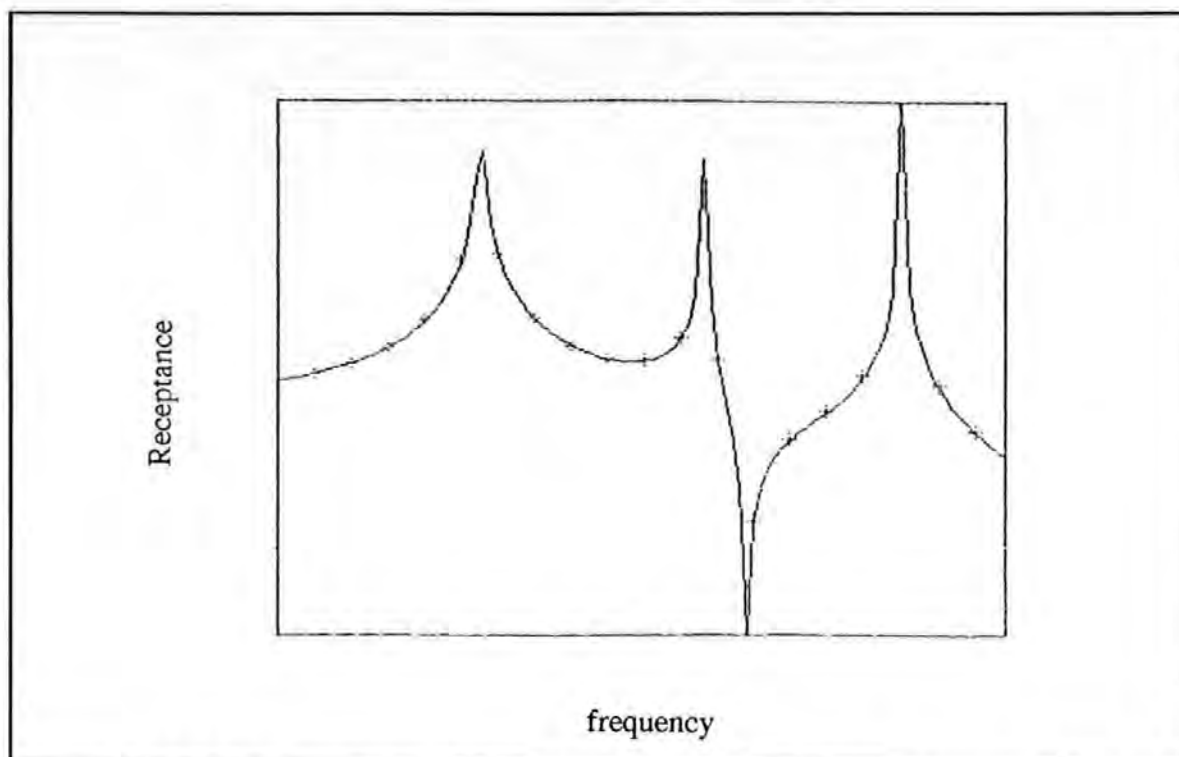


Figure 6.2.3.3-3 Receptance spectrum for the 3 DOF fictitious system at spatial point No.3.

However, more acute reduction in accuracy was found to occur in SCENARIOS 2 and 4. This is illustrated by the results obtained from SYSTEM 2 and given in Tables 6.2.3.3-1 and 6.2.3.3-2. In this simulation run, a reduced model of order 6 was derived using 6 out of the 10 FRF data set. The 6 frequency points chosen cover 3 out of the 10 modes presented.

TABLE 6.2.3.3-1 THE REDUCED ORDER 6X6 MASS MATRIX OF THE 10 DOF FICTITIOUS SYSTEM DETERMINED BY THE ALGORITHM.

[M]	-17.78	34.14	-97.88	112.11	-114.89	35.97
	34.14	-42.94	225.08	-297.33	355.45	-123.85
	-97.88	225.08	-568.66	603.75	-574.22	180.02
	112.11	-297.33	603.75	-535.87	421.25	114.19
	-114.19	355.45	-574.22	421.25	-189.00	18.38
	35.965	-123.85	180.02	-114.19	18.38	11.42

TABLE 6.2.3.3-2 THE REDUCED ORDER 6X6 STIFFNESS MATRIX OF THE 10 DOF FICTITIOUS SYSTEM DETERMINED BY THE ALGORITHM.

[K]	35781	-998441	126310	-74603	-6898	20432
	-99844	280510	-347720	193660	43607	-71450
	126310	-347720	437090	-259400	-51716	96194
	-74603	193660	-259400	200260	-8470	-50723
	-6898	43607	-51716	-8470	22580	-1498
	20432	-71450	96194	-50723	-1498	8136

The original and the regenerated curves are plotted in Figures 6.2.3.3-4 to 6.2.3.3-7 for 4 out of the 6 spatial points used.

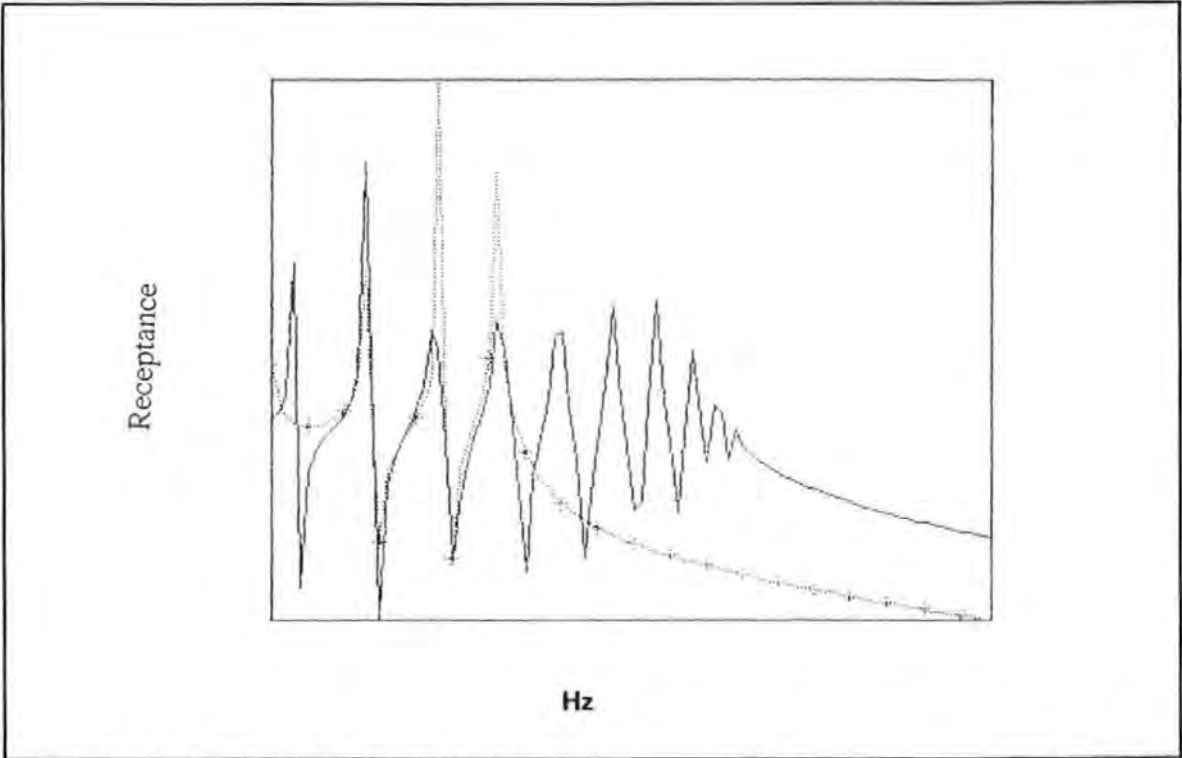


Figure 6.2.3.3-4 Overlaid plots of original and regenerated Receptance spectra for spatial point 1 from a reduced model of order 6

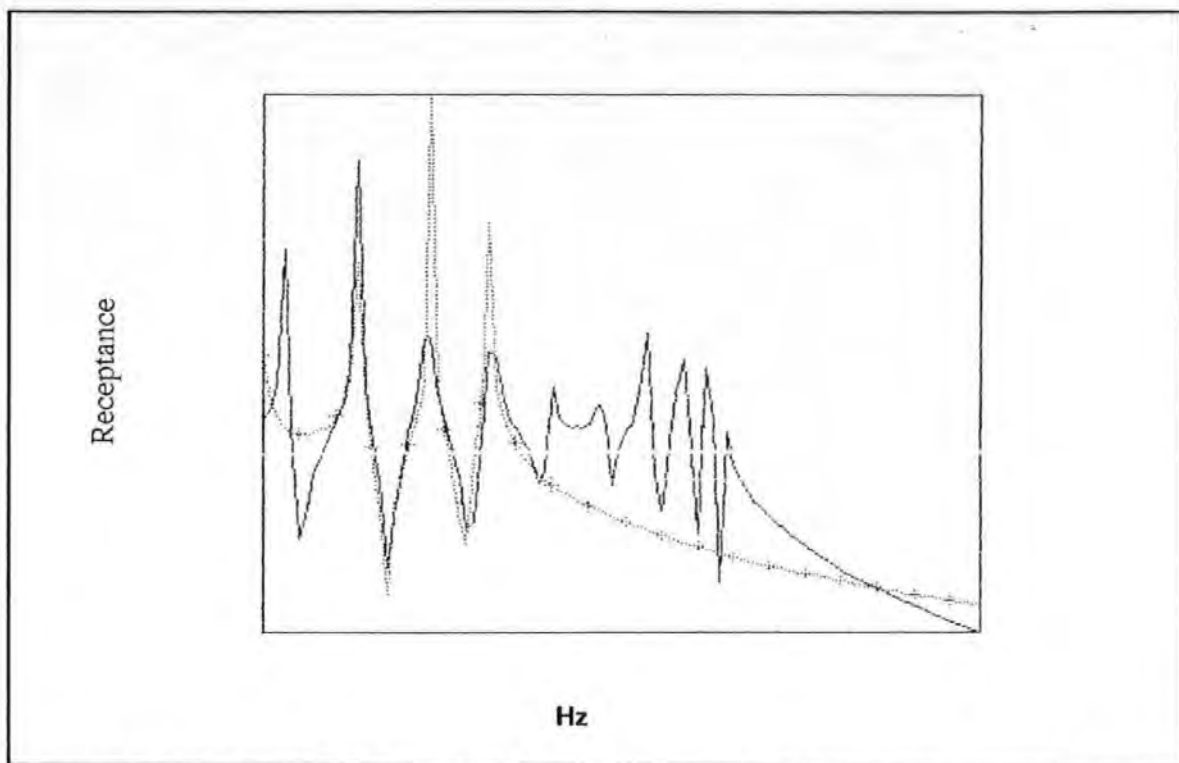


Figure 6.2.3.3-5 Overlaid plots of original and regenerated Receptance spectra for spatial point 2 from a reduced model of order 6.

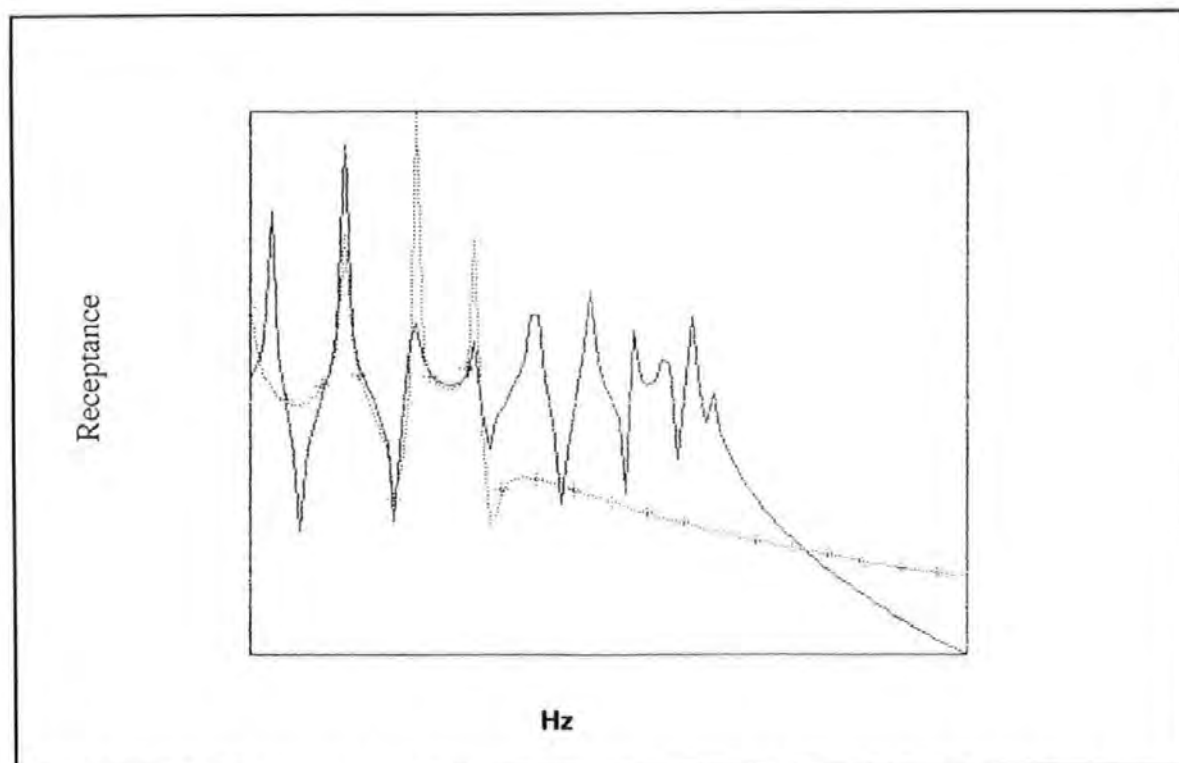


Figure 6.2.3.3-6 Overlaid plots of original and regenerated Receptance spectra for spatial point 3 from a reduced model of order 6 .

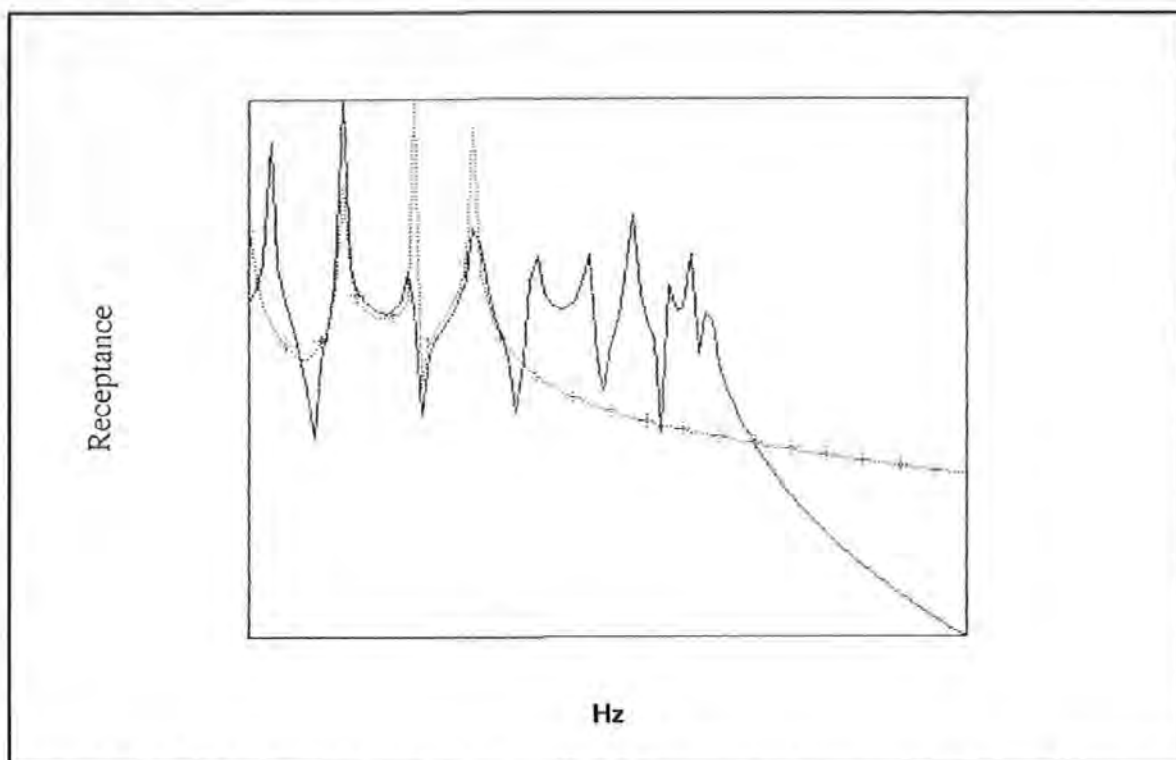


Figure 6.2.3.3-7 Overlaid plots of original and regenerated Receptance spectra for spatial point 4 from a reduced model of order 6 .

Although the original spatial matrices are known to be tri-diagonal, full matrices are used to account for the reduction of the order of the model from 10 to 6. The figures show that the regenerated curves only match the original curve in the narrow range covered by the 6 chosen data points.

6.2.4 PRACTICAL APPLICATIONS

Apart from fictitious systems, the algorithm was also applied to a variety of real systems using experimental data obtained mainly from laboratory tests. Two real systems: a 4-mass torsional system (discrete) and a cantilever beam (continuous) were used.

The tests were carried out at the Structural Dynamic Laboratory of the Royal Naval Engineering College Plymouth. The instrumentation used in these laboratory tests was quite separated from those used for full scale tests. As the data were of interest here, specific details on this experimentation are not to be discussed any further. Only a schematic diagram showing the test set-up and the list of equipment used are given in Figure 6.2.4-1.

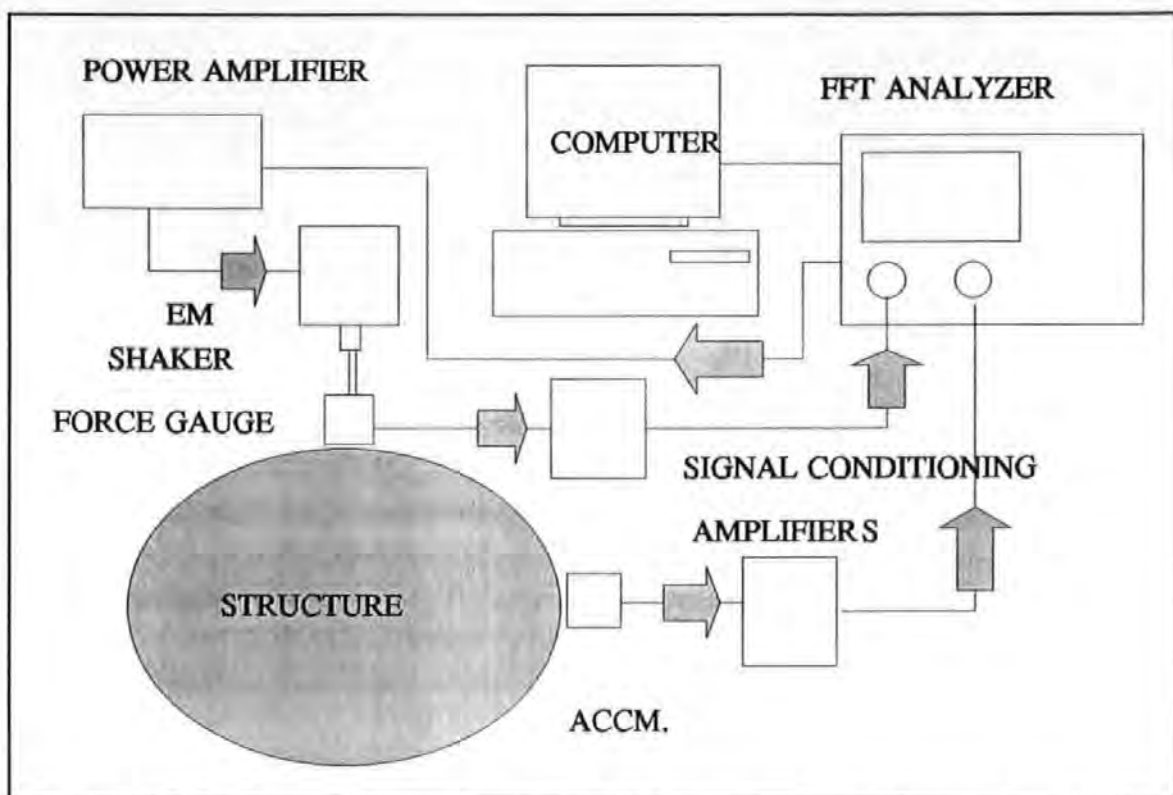


Figure 6.2.4-1 A schematic drawing showing the test set up and equipment used.

The torsional system was constructed by attaching four lumped masses along the length of a steel rod which was clamped rigidly at both ends as shown schematically in Figure 6.2.4-2. A series of roller bearings were spaced along the length of the rod. These bearings restrain lateral movement and allow only rotational (twisting) freedom. So the total number of vibrational modes was effectively confined to only 4. The system was excited by a miniature electromagnetic shaker through an attachment to the mass m_1 . All the modes of vibration involved were covered in the measurement. The spatial matrices obtained for this system are given in Table 6.2.4-1 for the undamped case and in Table 6.2.4-2 for the damped case. These matrices form a *complete model*. Correlation (for the undamped case) between the measured and the regenerated FRF curves for 2 of the masses measured are given in Figures 6.2.4-3 to 6.2.4-4.

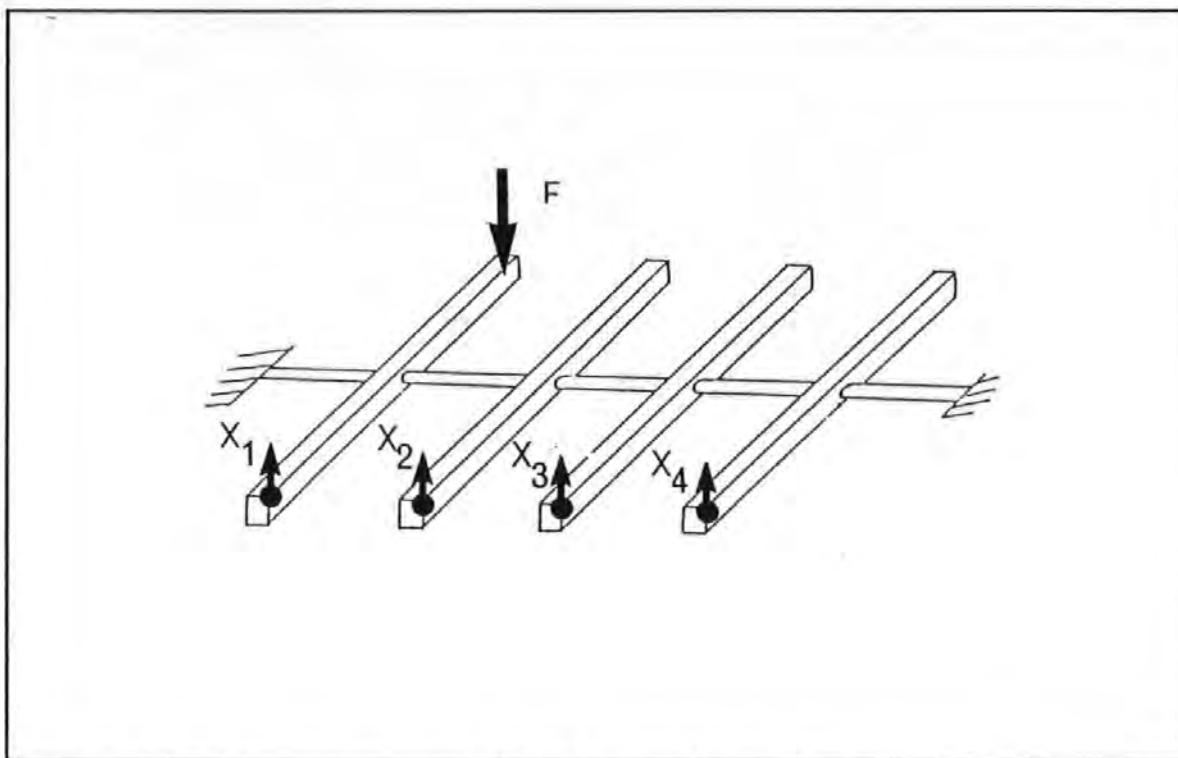


Figure 6.2.4-2 Schematic drawing of the 4 masses torsional vibration system.

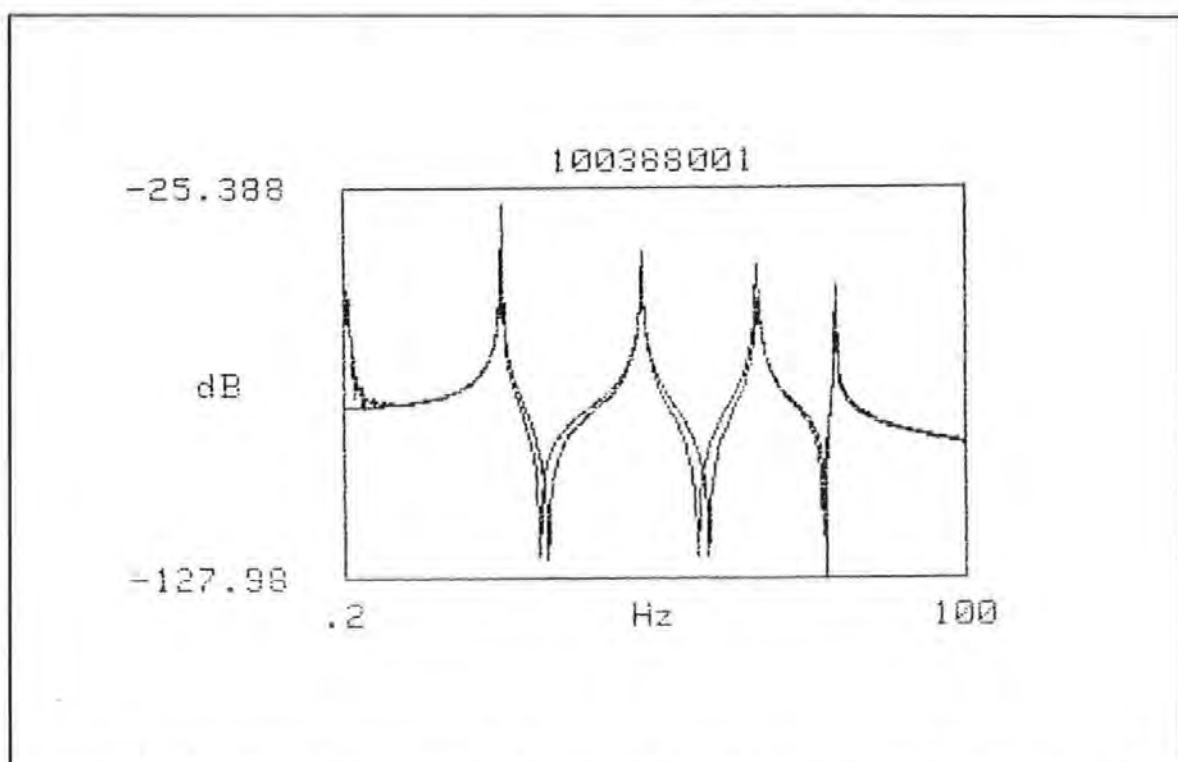


Figure 6.2.4-3 Correlation between the measured and the regenerated FRF curves for the mass m_1 .

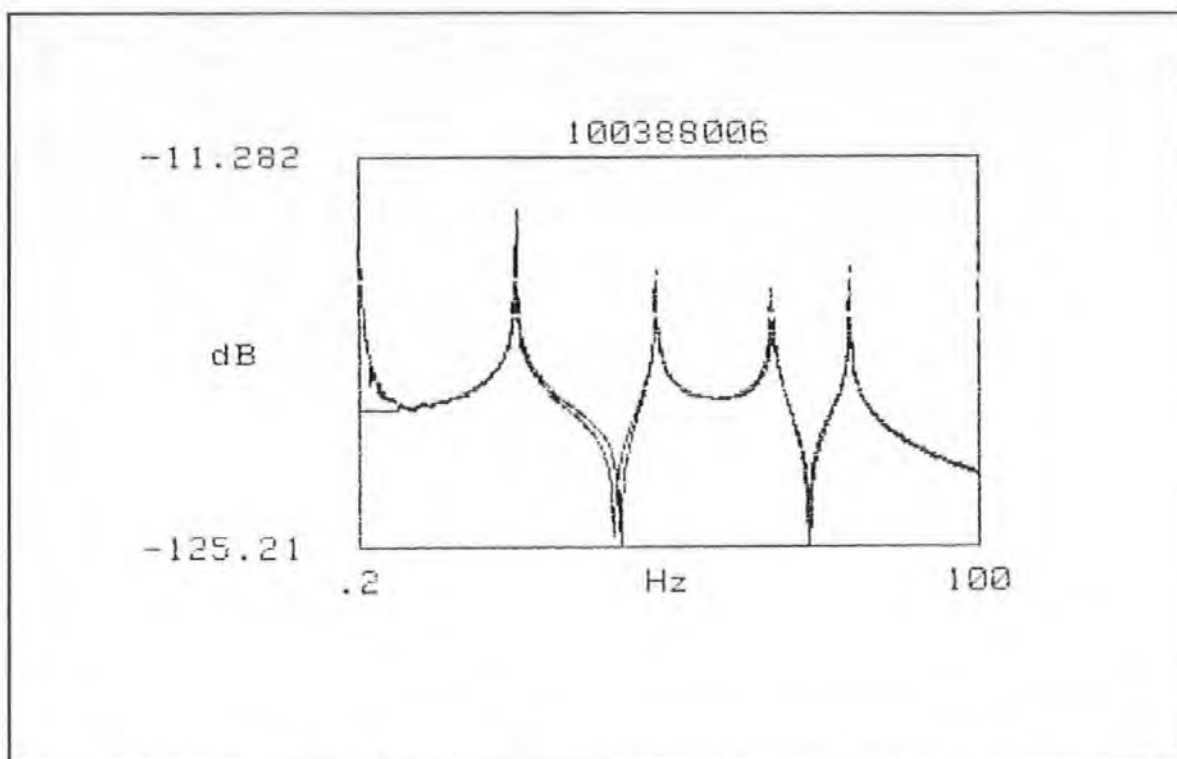


Figure 6.2.4-4 Correlation between the measured and the regenerated FRF curves for the mass m_2 .

TABLE 6.2.4-1 THE DERIVED SPATIAL MATRICES OF THE TORSIONAL SYSTEM (UNDAMPED MODEL).

[M]	0.1483	0	0	0
	0	0.161	0	0
	0	0	0.1847	0
	0	0	0	0.1109
[K]	19778	-10289	0	0
	-10289	22022	-12106	0
	0	-12106	26497	-9811
	0	0	-9811	14739

TABLE 6.2.4-2 THE DERIVED SPATIAL MATRICES OF THE TORSIONAL SYSTEM (DAMPED MODEL).

[M]	0.1505	0.0019	0.0057	0.0169
		0.1621	0.0045	0.0115
			0.1985	-0.0093
				0.0968
[C]	0.8124	0.5029	1.0149	-0.2337
		0.0877	-0.3326	-1.0964
			0.7422	0.2258
				0.7244
[K]	19924	-10353	-1018	1660
		22058	-12703	1685
			28526	-11147
				13310

Because the system is a torsional one, the corresponding equation of motion should all be in terms of moment of inertia instead of mass and similarly for the other quantities. The [M], [C], [K] are used here to denote inertia, damping and stiffness in the most general sense.

The second system tested was a beam (a continuous system) which possesses an infinite number of vibration modes. Any approximation based on a low-order, discretized and small DOF model are as usual subjected to truncation errors. These tests were intended to study precisely the severity of these errors caused by discretization and truncation of a real system.

Data were obtained from a steel beam with the following dimensions: 4.88 mm x 24.85 mm in cross section and 696 mm in length. The beam was clamped at one end and

lateral responses at six designated locations covering the length of the beam were measured using Bruel & Kjaer piezoelectric accelerometers and signal conditioning hardware. A single excitation force was applied at the spatial point No.1 near the support end using an electromagnetic shaker. Figure 6.2.4-5 show a schematic drawing of the beam test arrangement. FRF data covering a frequency band of 4 to 1200 Hz and 6 modes were obtained for analysis. Because these tests were carried out in a well controlled laboratory environment, very high quality data was able to be obtained.

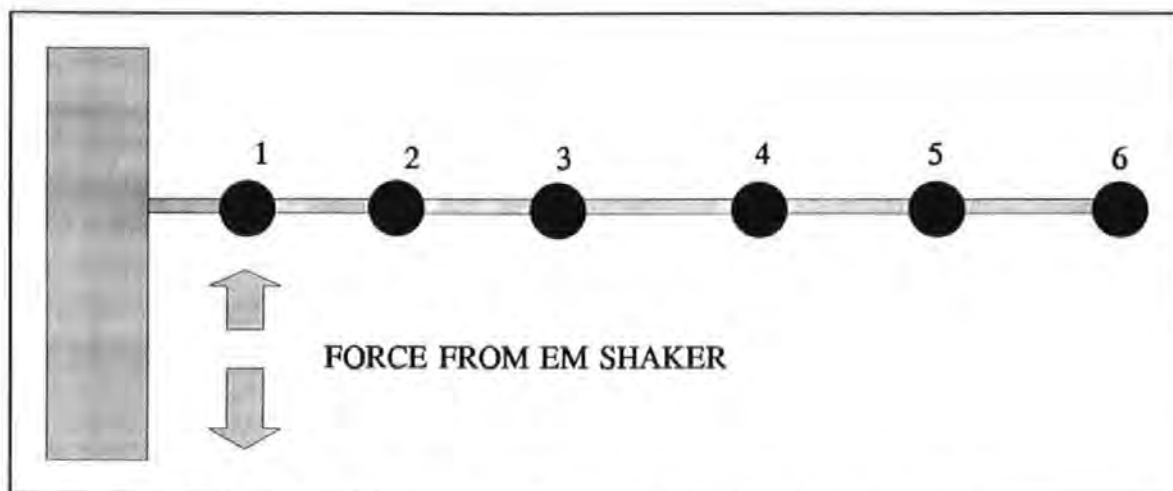


Figure 6.2.4-5 A schematic drawing showing the beam test arrangement.

Since the beam was very lightly-damped, the assumption of zero damping was thought to be justifiable. This assumption was also necessary, because the resulting computational problem would exceed computer memory limit if otherwise. Four models were obtained from the four conditions listed in Table 6.2.4-3.

TABLE 6.2.4-3. DETAILS OF THE ANALYSIS CONDITIONS TO DERIVE THE SPATIAL MODEL OF THE BEAM.

MODEL REFERENCES	NO OF MODES COVERED BY DATA POINTS CHOSEN	RANGE OF FREQUENCIES COVERED BY THE CHOSEN DATA POINTS
MODEL A	6	114 TO 888 Hz
MODEL B	4	54 TO 470 Hz
MODEL C	3	4 TO 208 Hz
MODEL D	2	42 TO 150 Hz

The results of the derived spatial matrices are summarized in Table 6.2.4-4 and 6.2.4-7. The measured receptance frequency response curves are plotted in Figures 6.2.4-6 to 6.2.4-9 with the regenerated curves overlaid onto the measured curves. (Note that the last digit in the title of each figure denotes the spatial point. For example: S3_12 denotes the spatial point 2 and so on)

TABLE 6.2.4-4 THE SPATIAL MATRICES OF ORDER 6 DERIVED FOR THE BEAM (UNDAMPED MODEL) WITH SELECTED DATA POINTS COVERING ALL SIX MODES (MODEL A).

[M]	0.0900	0.0015	0.0139	0.0087	0.0081	0.0140
		0.249	0.081	0.085	0.051	-0.063
			0.210	0.108	0.107	0.068
				0.199	0.264	0.325
					0.780	1.151
						2.422
[K]	911550	-1.0E6	170230	-2.6E5	259770	735930
		1.8E6	-6.6E5	519530	-1.7E5	-6.3E5
			1.0E6	20091	2.0E6	2.7E6
				866350	2.2E6	3.5E6
					1.1E7	1.6E7
						2.4E7

TABLE 6.2.4-5 THE SPATIAL MATRICES OF ORDER 6 DERIVED FOR THE BEAM (UNDAMPED MODEL) WITH SELECTED DATA POINTS COVERING ONLY FOUR MODES (MODEL B).

[M]	0.119	0.0354	0.0126	-0.021	-0.025	-0.016
		0.117	0.128	0.120	0.304	0.309
			0.297	0.051	0.169	0.177
				0.156	-0.025	-0.037
					-0.055	-0.049
						0.466
[K]	741290	-6.3E5	-2.4E5	-3.4E5	-9.2E5	-9.8E5
		1.1E5	-3.1E5	5.8E5	8.8E5	1.1E6
			9.8E5	-3.7E5	6.9E5	5.2E5
				5.0E5	31678	3.6E5
					1.5E6	1.3E6
						1.7E6

TABLE 6.2.4-6 THE SPATIAL MATRICES OF ORDER 6 DERIVED FOR THE BEAM(UNDAMPED MODEL) WITH SELECTED DATA POINTS COVERING ONLY THREE MODES (MODEL C).

[M]	2.178	-4.858	4.063	-2.402	0.631	-0.577
		13.061	-10.71	8.074	-1.070	2.629
			8.567	-6.662	0.570	-2.296
				5.764	0.167	2.653
					0.947	3.508
						2.248
[K]	287	3286	-3007	2653	386	248
		5.9E5	-4.6E5	17989	-6.1E4	2.3E5
			4.2E5	-9.2E4	1.1E5	2.1E5
				2.0E5	-2.0E5	3387
					2.5E5	-2.0E4
						1.4E5

TABLE 6.2.4-7 THE SPATIAL MATRICES OF ORDER 6 DERIVED FOR THE BEAM (UNDAMPED MODEL) WITH SELECTED DATA POINTS COVERING ONLY TWO MODES (MODEL D).

[M]	1.095	-0.971	0.114	0.650	-0.348	0.574
		1.343	0.024	-0.791	0.486	-0.753
			-0.324	0.191	-0.295	0.029
				0.592	-0.214	0.250
					-0.024	-0.311
						0.296
[K]	19826	33766	5629	-7849	10652	12849
		203340	27485	-2.6E5	1.6E5	-1.2E5
			-2.4E4	1667	-1.6E5	60043
				3.2E5	-2.4E5	1.1E5
					2.2E5	-1.2E5
						43848

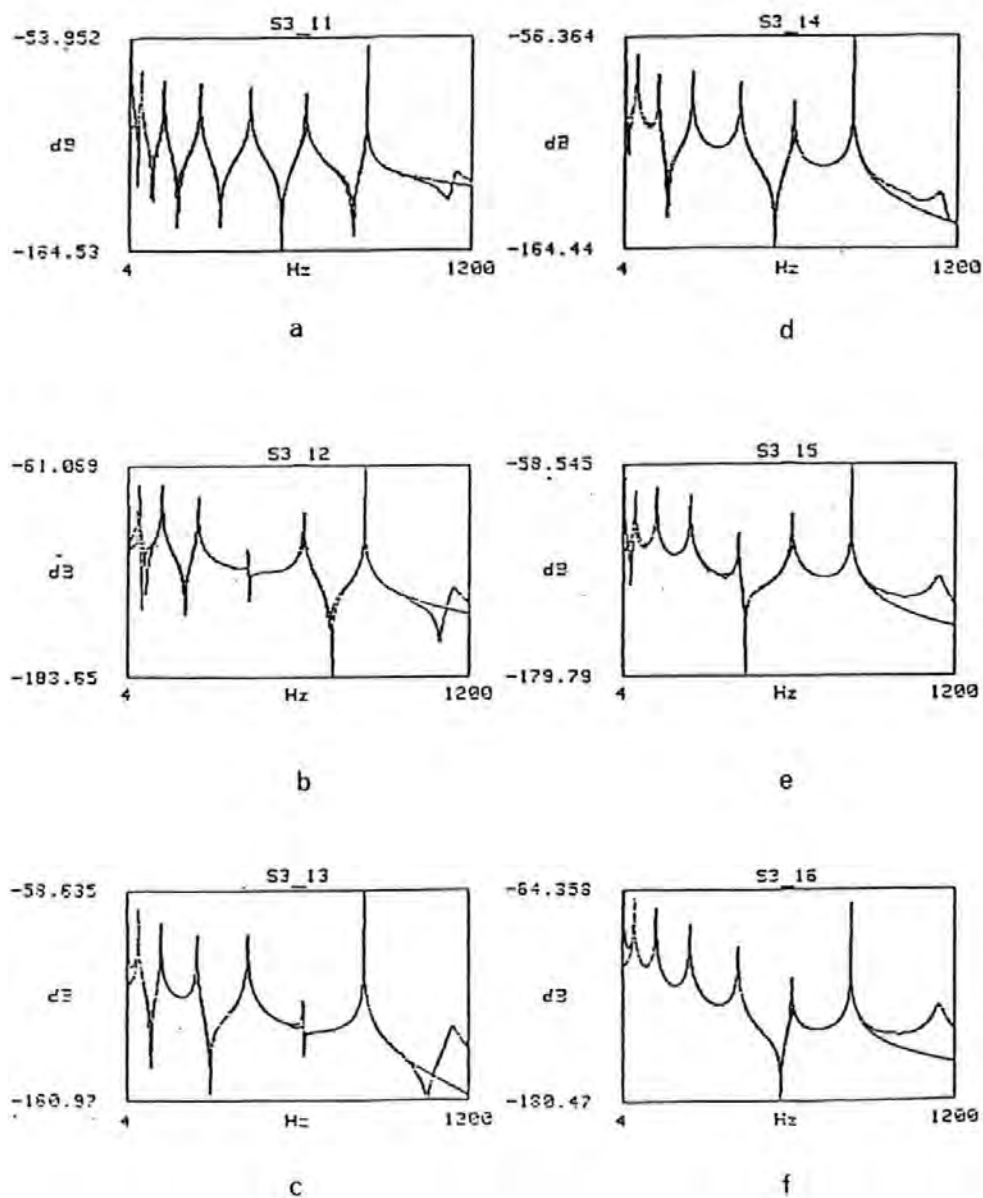


Figure 6.2.4-6a to 6.2.4-6f Overlaid plots of experimental and regenerated receptance FRF at all 6 spatial points on the beam. (Model A)

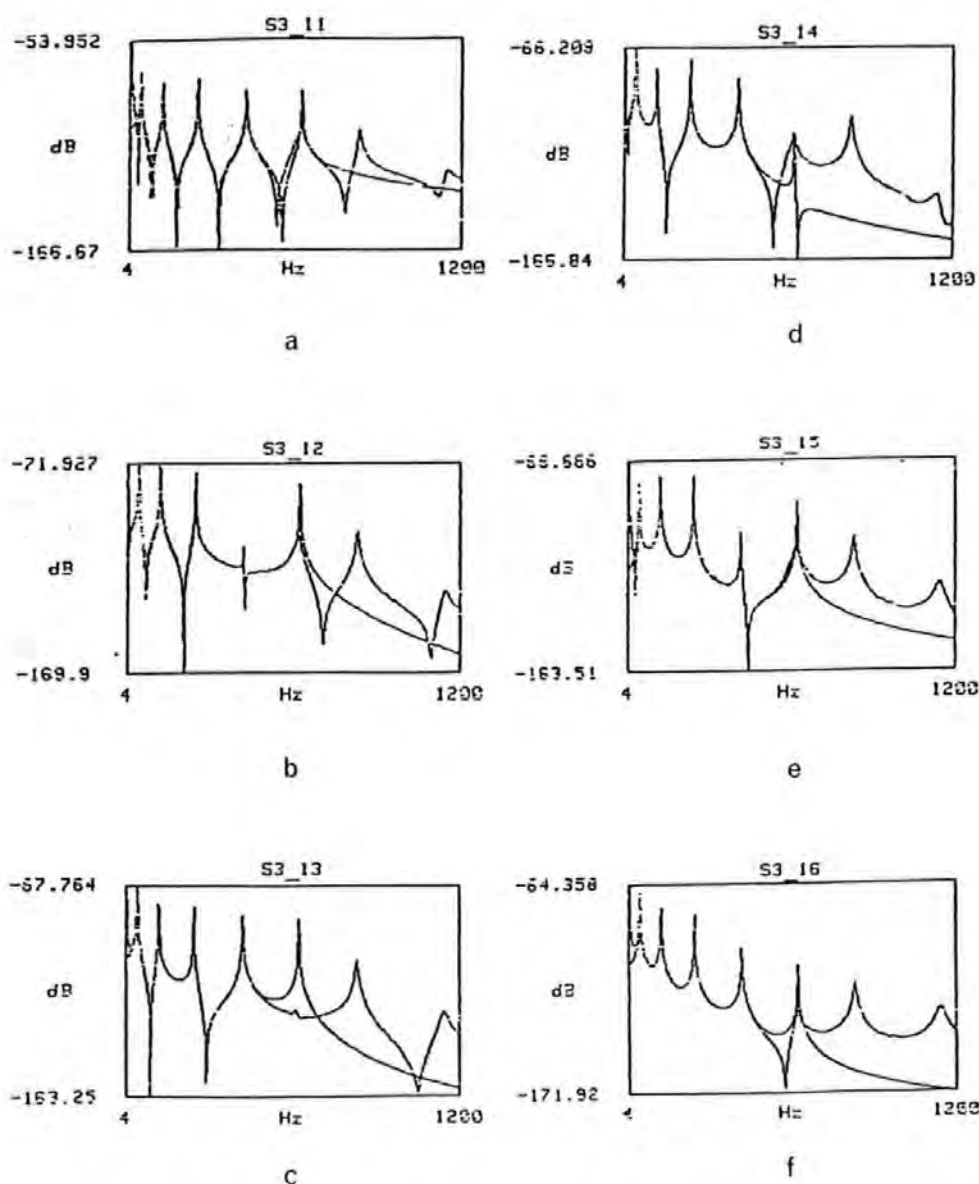
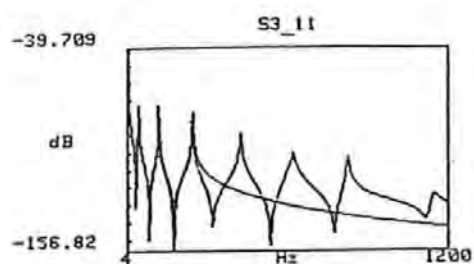
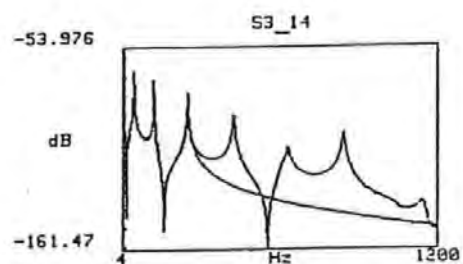


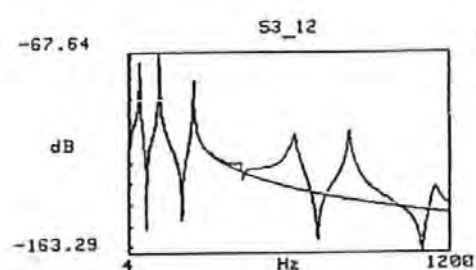
Figure 6.2.4-7a to 6.2.4-7f Overlaid plots of experimental and regenerated receptance FRF of the beam. (Model B)



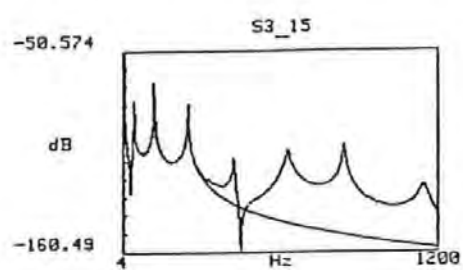
a



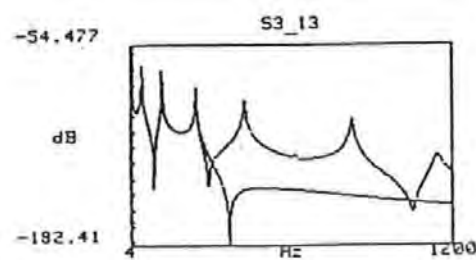
d



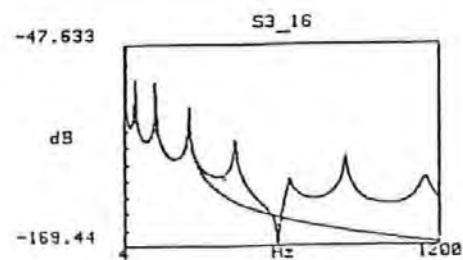
b



e



c



f

Figure 6.2.4-8a to 6.2.4-8f Overlaid plots of experimental and regenerated receptance FRF of the beam. (Model C)

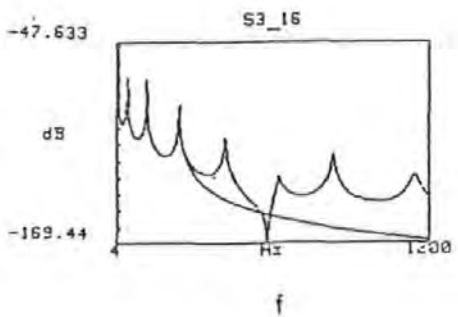
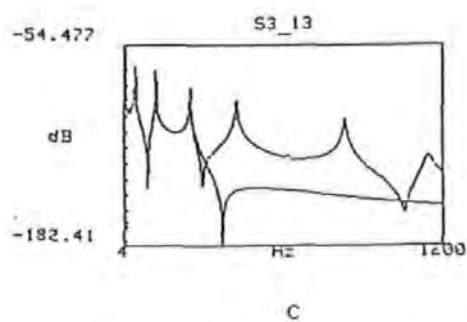
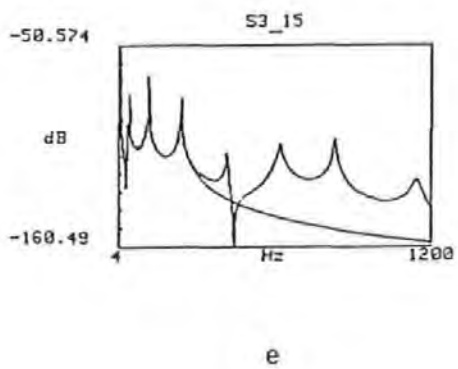
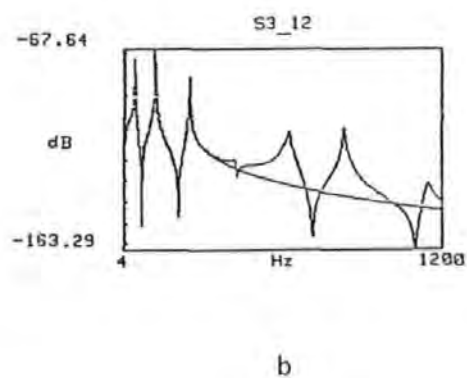
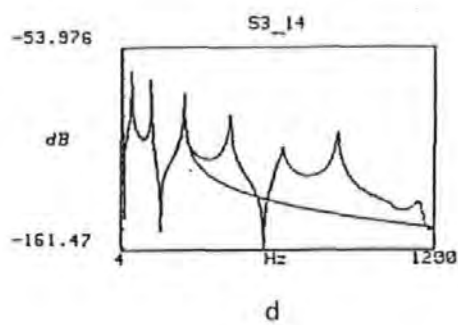
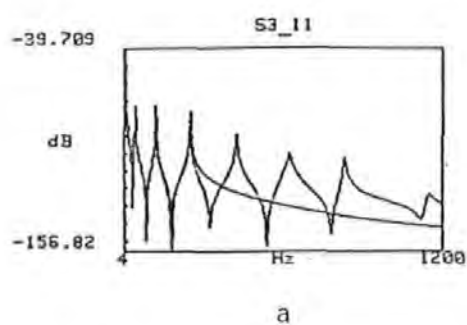


Figure 6.2.4-9a to 6.2.4-9f Overlaid plots of experimental and regenerated receptance FRF of the beam. (Model D)

6.3 DISCUSSIONS

From the simulation, the results show that the exact spatial matrices (in terms of their values as well as the form of these matrices) can be obtained providing that the order of the matrices are chosen exactly and the frequency points are chosen appropriately. However with some bad choices, incorrect results are obtained. In general, the accuracy of the proposed method is found to be very sensitive to those factors covered by the scenarios studied. No hard-and-fast rule is available which can guarantee good results. The errors are due to modelling error and a computational problem called *ill-conditioning*. The latter is due to the way the equations is posed and is known to be associated with most *inverse* methods.

From the practical experiments conducted on the 4-mass discrete system and the beam, using both SS (Stepped-Sine) and PRBS (Pseudo-Random-Binary-Sequence) excitation methods, good results were also obtained. The stiffness and particularly the mass matrices obtained agree favourably to those estimated by other means. For instance, the spatial matrices obtained by **Hallett** ^[6.21], who conducted an independent experiment on the same 4-mass torsional system using conventional modal approach, are given in Table 6.3-1

TABLE 6.3-1 THE DERIVED SPATIAL MATRICES OF THE TORSIONAL SYSTEM
(UNDAMPED MODEL) USING CONVENTIONAL MODAL APPROACH.

[M]	0.1763	0	0	0
	0	0.1766	0	0
	0	0	0.1725	0
	0	0	0	0.1750
[K]	22392	-10838	-373	571
	-10838	22053	-9723	-422
	373	-9723	21339	-10587
	571	-422	-10587	22365

The values in these matrices compare well with those in Tables 6.2.4-1 and 6.2.4-2. In the case of the beam, the sum of the diagonal terms in the mass matrices in the various models derived are in the same order of the actual physical mass of the beam. So these results confirm that the proposed method is practical for these applications.

The proposed method has a number of features which are considered to be advantageous. First of all, the method requires only a very small number of frequency data points to work. These points can be far apart from each other along the frequency axis. Therefore the method is not suffering from the problem of lack of frequency resolution as the modal methods are. Secondly, the frequency data points required do not need to be very close to those at resonance, so the usual problem of inaccurate measurements around resonance is alleviated. Thirdly, the process of curve-fitting is performed *globally* utilizing data available from all the spatial points in one operation. This utilization of *spatial information* is very different from other curve-fitting techniques which use only *local information*.

It is apparent that the concept of mode of vibration is discarded all together in the implementation of this technique. Unlike modal methods wherein the form of damping is critical in deciding the ease of subsequent analysis (i.e. whether to pursue a real or complex mode analysis), there is no extra difficulty involved in dealing with viscous damping when using the proposed method.

This *spatial* approach was first published in the Proceedings of the 7th International Analysis Conference (see Tsang and Rider ^[6.14]). Later, Lee ^[6.15], Lee and Dobson ^[6.16] extended this method by considering higher order terms and introducing an alternative set of spatial matrices known as [P], [Q], [R], [S] which are similar to the [M], [C], [K] matrices used here. Their method was also based on the direct least square formulation proposed here.

6.4 CONCLUSIONS

The proposed algorithm possesses a number of desirable characteristics as discussed. Above all, it enables the derivation of the spatial matrices directly without using the conventional modal procedures. For simple structures, the algorithm has been proven valid and successful. Mass, stiffness and damping matrices of these structures are much easier to interpret than modal parameters because of the apparent physical meanings they attach. However for complex structures, more research is still required for such applications. This work has shown that spatial matrices determination can be regarded as a main-stream approach rather than a derivative of the modal approach.

CHAPTER 7

FULL SCALE FORCED VIBRATION TESTS ON THE BRITISH RAIL BUILDING

7.0 INTRODUCTION

This chapter reports the results and findings of the full scale forced vibration tests performed on the British Rail Inter-city House, Plymouth (designated as BR Building). These tests were carried out mainly for the purpose of trying out the new exciter and other equipment described in Chapter 4. Because this building had previously been tested by other investigators, results from the new tests can be used to compare with those from the previous tests.

Many of the experimental techniques and procedures used in the new tests followed closely those used and reported in other investigations (such as those undertaken by BRE as described in Chapter 2). Many operations such as setting-up, controlling and taking readings of instruments were still being carried out manually because a computer-aided-testing facility had not been incorporated into the instrumentation system. The experience had subsequently inspired several developments and improvements in the instrumentation and the testing technique for future tests.

Analytical modelling of the structure using the finite element method was also carried out to assess the strength and weakness of this method. The model was prepared and analyzed to determine its theoretical vibration characteristics. Using only simple beam elements and exercising appropriate approximations, the theoretical results were found to reconcile with those from real measurement at large. However disagreements, as always, still exist.

7.1 DESCRIPTION OF THE STRUCTURE

This building is situated in the city of Plymouth. It is eleven storeys high and used as office accommodation (the tenth floor housed the plant rooms only and was not accessible for measurement). It was constructed some 30 years ago and was a subject of forced vibration research on a number of occasions during the 1970's. Details of these tests were reported by Williams^[1.1], Jeary and Sparks^[2.8, 2.39].

The structure is rectangular 45 m x 13 m in plan and 47 m high. It was constructed with reinforced concrete on a large raft type of foundation. Figure 7.1-1 gives a photographic view of the structure.

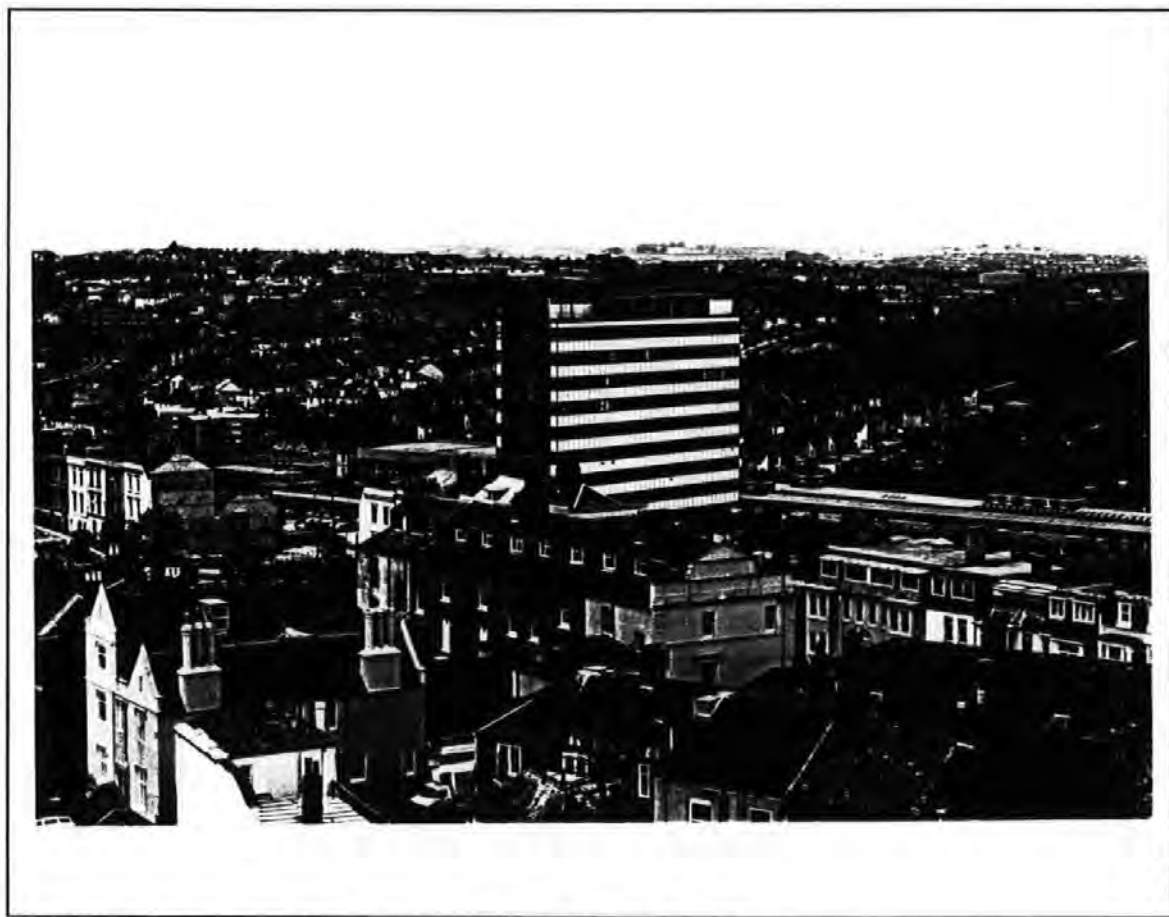


FIGURE 7.1-1 A photographic view of the BR building.

The architectural floor plan is repetitive from the first to the ninth floor as shown in Figure 7.1-2.

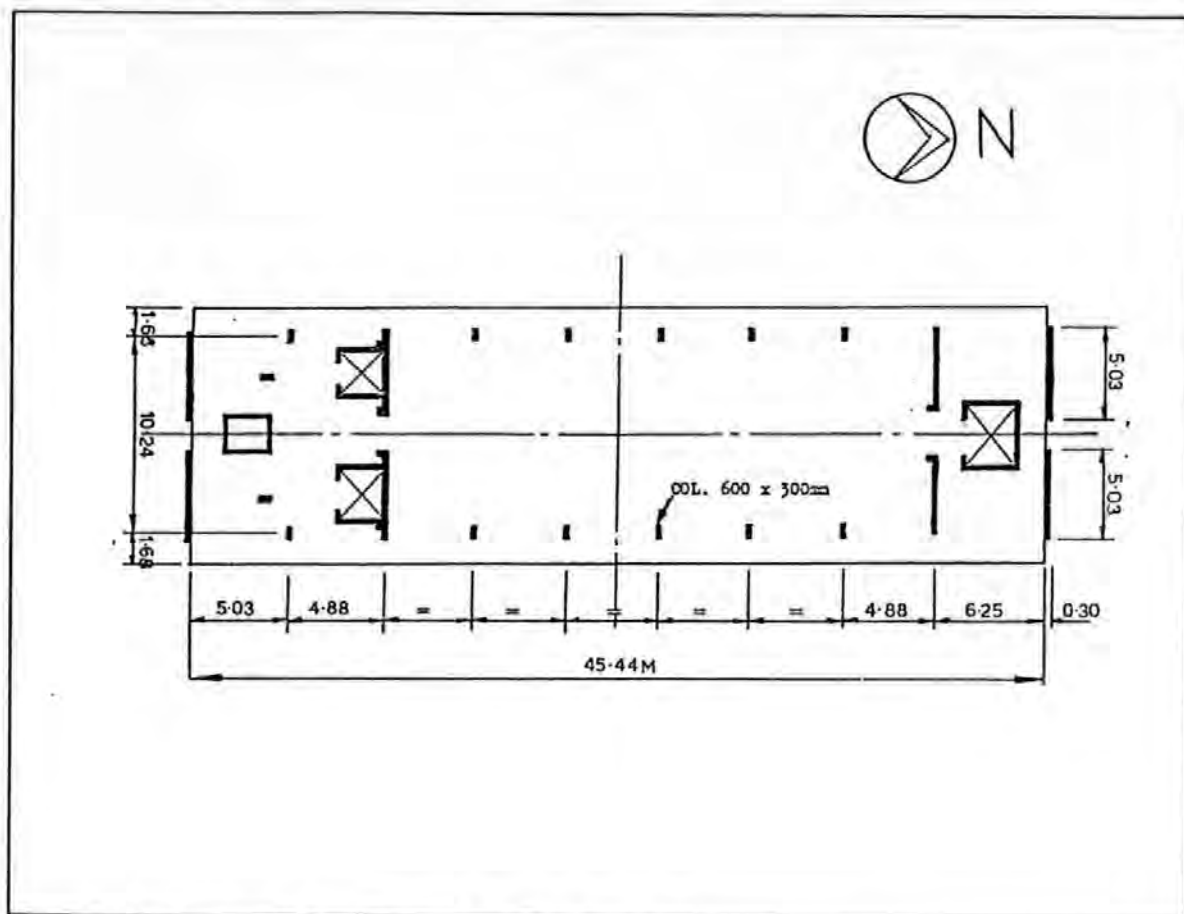


Figure 7.2 A typical floor plan of the BR Building

The building is symmetrical about the NS principal axis and has four reinforced concrete shear cores: among which one is located near the northern end and the other three near the southern end of the building. Three shear cores form the three lift shafts and the other one as a closed box section for utilities to run through. These structural elements stretch along the full height of the building. A pair of external planar shear walls are situated at each of the northern and southern ends. These walls run parallel to the short (EW) direction of the building. There is also another pair of internal planar shear walls situated near the northern shear core and run in the same direction as the external ones. The shear walls were also constructed with reinforced concrete and each one is 0.3 m thick and 5.03 m wide in section. The shear cores and walls are the major providers of the building's lateral loads bearing capacity.

In addition, lateral structural strength and stability of the building is provided by frame action: by framing together the vertical columns, shear walls, cores and horizontal beams. The beams run parallel to the grid lines along both the long and short directions of the building. The columns are 0.6 m by 0.3 m each in section. Typical inter-column spacings

are 4.88 m. The slabs at each end are solid concrete slabs of 0.15 m thick. The interior slabs are deep ribbed or 'hollow pot' concrete floors with the ribs running along the long direction. Externally, the building is clad with light-weight glass panels on the eastern and western sides of the building.

7.2 THE TEST PROGRAMME

The test was carried out in April 1986 and lasted for two weeks. Both exciter-induced and ambient vibration tests were carried out so that results from each test could be used for cross-checking against each other. In particular, the exciter-induced vibration tests were conducted using steady state Step-Sine as well as Periodic-Random excitations. The frequency band of interest was essentially the 10 Hz baseband. These are designated as SS and PRBS tests respectively.

7.2.1 TEST ENVIRONMENT

All the test equipment including the exciter were located on the ninth floor of the building. This was the only floor unoccupied at the time because it was in the middle of a refurbishment programme. Hence, the tests were carried out alongside with the various construction activities going on at the time as well as other human/machine activities happening in the offices below. Other disturbances were also due to wind and to trains entering and leaving the train station below the structure. So on the whole, the testing environment was far from ideal. Subsequently, the measurement process was severely affected by *noise* (signal noise).

7.2.2 TEST TECHNIQUES

On the whole, the basic test procedures involved in the SS tests were consisted of the following tasks :

- a. a quick search for the resonance frequencies within the frequency band of interest (Note: It is assumed that the resonance frequency is a very close approximation to the natural frequency of the mode responsible for that resonance. This is only true for lightly damped systems)

- b. a detailed search of the resonance frequency for each mode,
- c. measurement of the damping of each mode, and
- d. measurement of the mode shape of each mode.

With the exciter orientated in a particular direction, either EW or NS, a quick search was performed by manually stepping the excitation frequencies in large steps. A step size of 1 Hz was typical. Suspected modes of resonance were detected by every occurrence of peaks in the structure's acceleration (inertance) response spectra as shown in Figures 7.4-4 and 7.4-5 (inertance plot) or large amplitude response in the time response charts as shown in Figure 7.2.2-2. On these charts, the corresponding frequencies of excitation were noted. It was then followed by a series of tests with a fine increment of the excitation frequencies. Step sizes in this phase are typically 0.1 Hz or even 0.01 Hz if in close proximity to a resonance frequency.

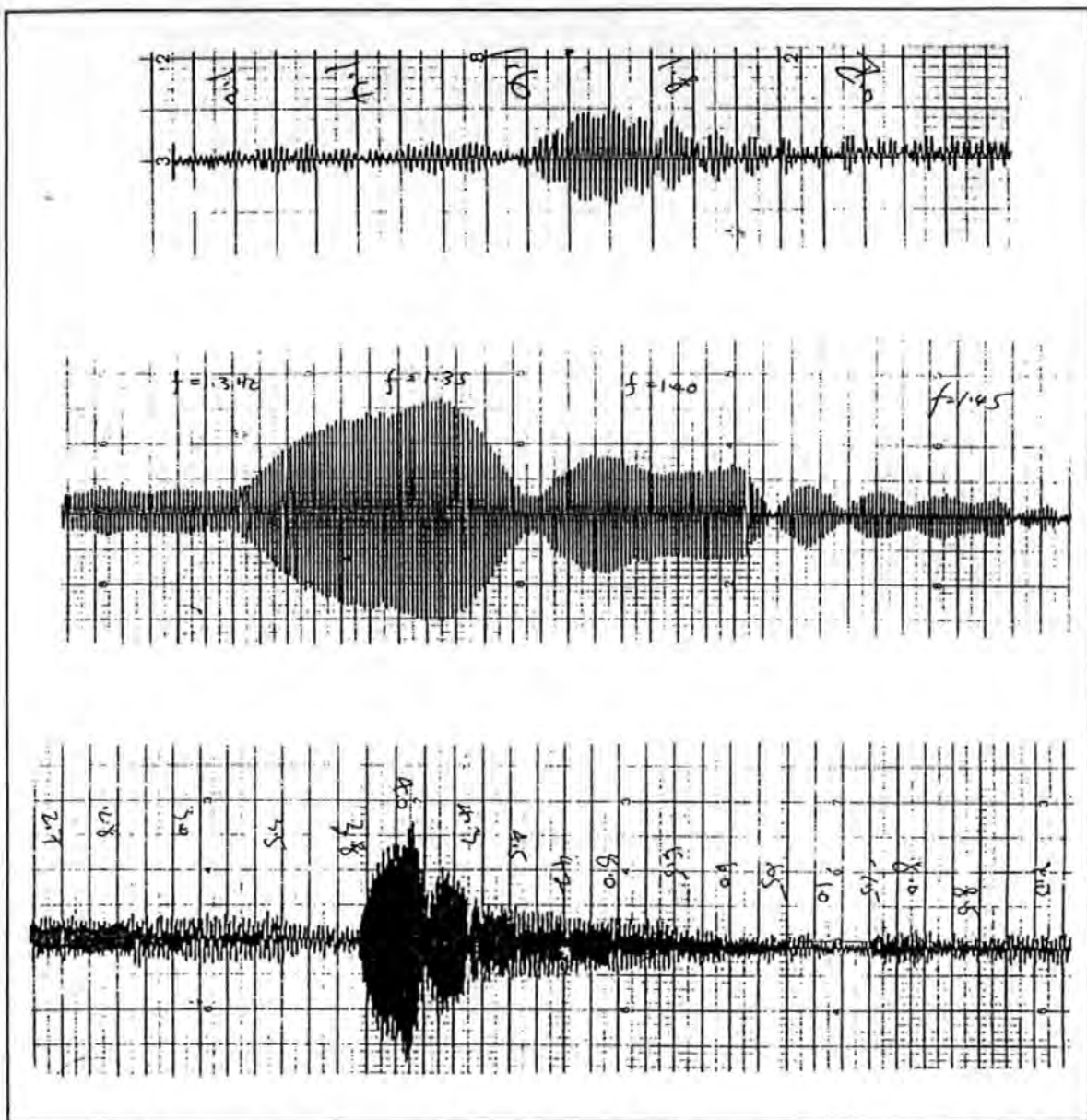


Figure 7.2.2-2. A time response history record of the structure's amplitude response.

Having determined the resonance frequencies to the satisfaction of the accuracy required, the exciter was then set to run at each of these frequencies in turn. Whilst the structure was still vibrating at the set frequency in a steady state, the exciter was suddenly switched off and the subsequent decaying time trace of acceleration response was then recorded on a time chart recorder. These traces enabled the modal damping factor to be determined by the logarithmic decay method. The same procedures were then repeated for the other modes of resonance.

Also while the structure was still vibrating at one of the resonance frequencies, the acceleration responses at various chosen strategic positions of the structure were measured. The relative deformation of the structure was determined by comparing the

ratios of amplitude and phase differences of responses of a travelling and a reference accelerometer (their positions are indicated as A and B respectively together with the orientation of their sensitivity axes indicated by arrows as shown in Figure 7.2.2-3). The latter was located at a pre-determined and fixed position: in this case on the ninth floor.

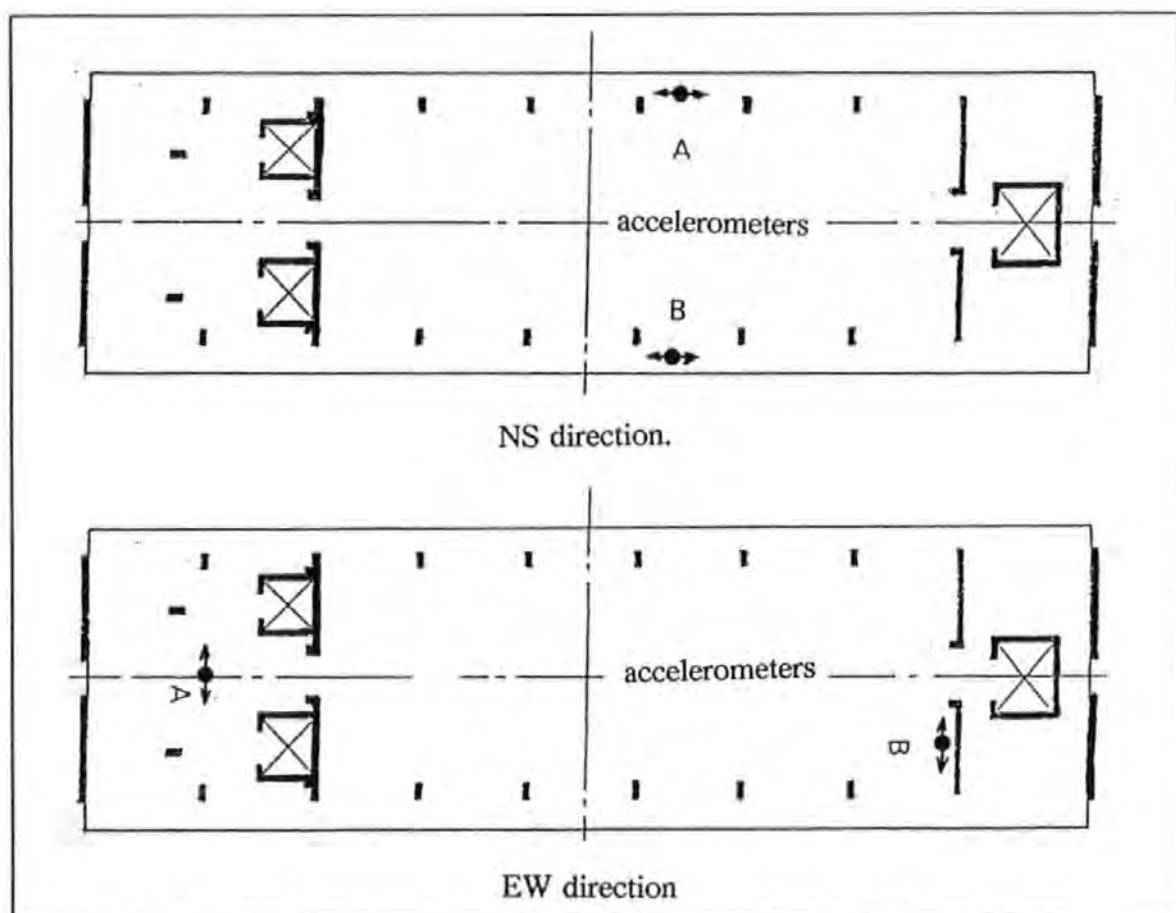


Figure 7.2.2-3. Locations of the accelerometers in the BR building.

The test procedures involved in the PRBS tests were relatively simpler and quicker because the time consuming frequency stepping procedure associated with the SS tests was not required. A frequency resolution of 0.08 Hz was obtainable when the spectrum analyzer was set to the 10 Hz baseband. The choice of such a resolution was considered a necessary trade-off between accuracy and the length of time required for taking measurements. The arrangement in the placement of the accelerometers was essentially the same as those used in the SS tests. The exciter was located at a position as shown in Figure 7.2.2-4 (the line of force or excitation is indicated by an arrow).

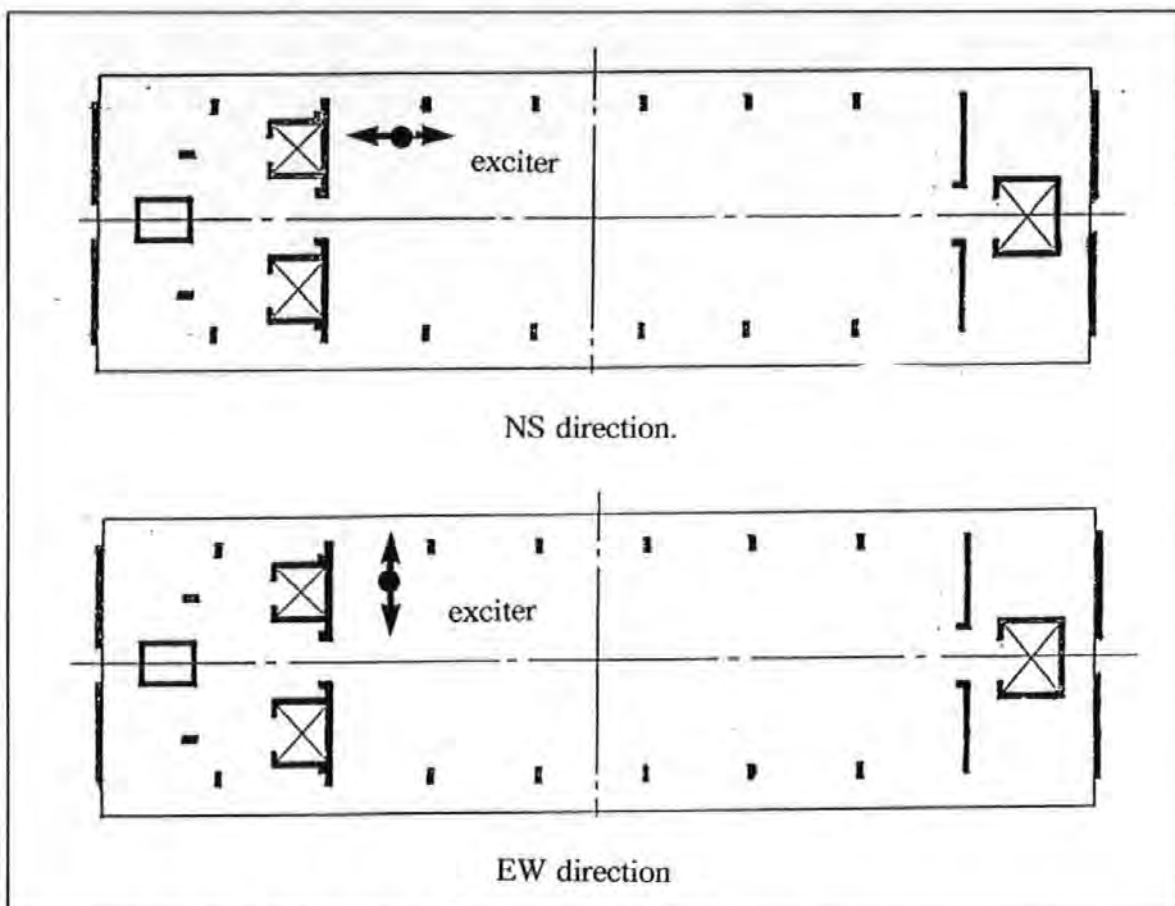


Figure 7.2.2-4. Locations of the exciter in the BR building.

The choice of this position was a matter of compromise between convenience and accessibility. However two important considerations prevailed :

- a. The exciter was located as such that excitation force could be applied with some eccentricity from the centre of stiffness of the floor. Hence torsional vibration modes could be excited together with the lateral modes as well. (However, this would not be a benefit if the modes have very close natural frequencies).
- b. Manoeuvrability and adequate space was allowed for the exciter to be turned to any desirable direction without the need to relocate the exciter.

However the choice of the floor level to position the exciter was intentional. It was chosen because :

- a. Statically speaking, the building possessed greater flexibility at this floor than

the lower ones. Dynamically speaking, this floor was known (from FE modelling results) to be not a node of those modes under study. Force applied here was especially effective for exciting the lower lateral and torsional vibration modes. Force applied at a node of a mode was ineffective for exciting the mode concerned and this must be avoided.

- b. Sheltering the equipments and the experimenter from hostile environments such as rain and extreme temperatures was also a major consideration.

Figures 7.2.2-5a and 7.2.2-5b show two photographs featuring the setting up of equipments in the field. The location of the exciter and the mounting arrangement are clearly shown there. The transducers for measuring vibration responses and force were those already described in Chapter 4. Excitation force with maximum amplitudes between 0.5 to 2 KN over a range of frequencies were used. As a result, acceleration response with a maximum amplitude of 0.05 g were obtained. This level of response was obtained on the ninth floor as a result of the EW1 resonance generated by the exciter.

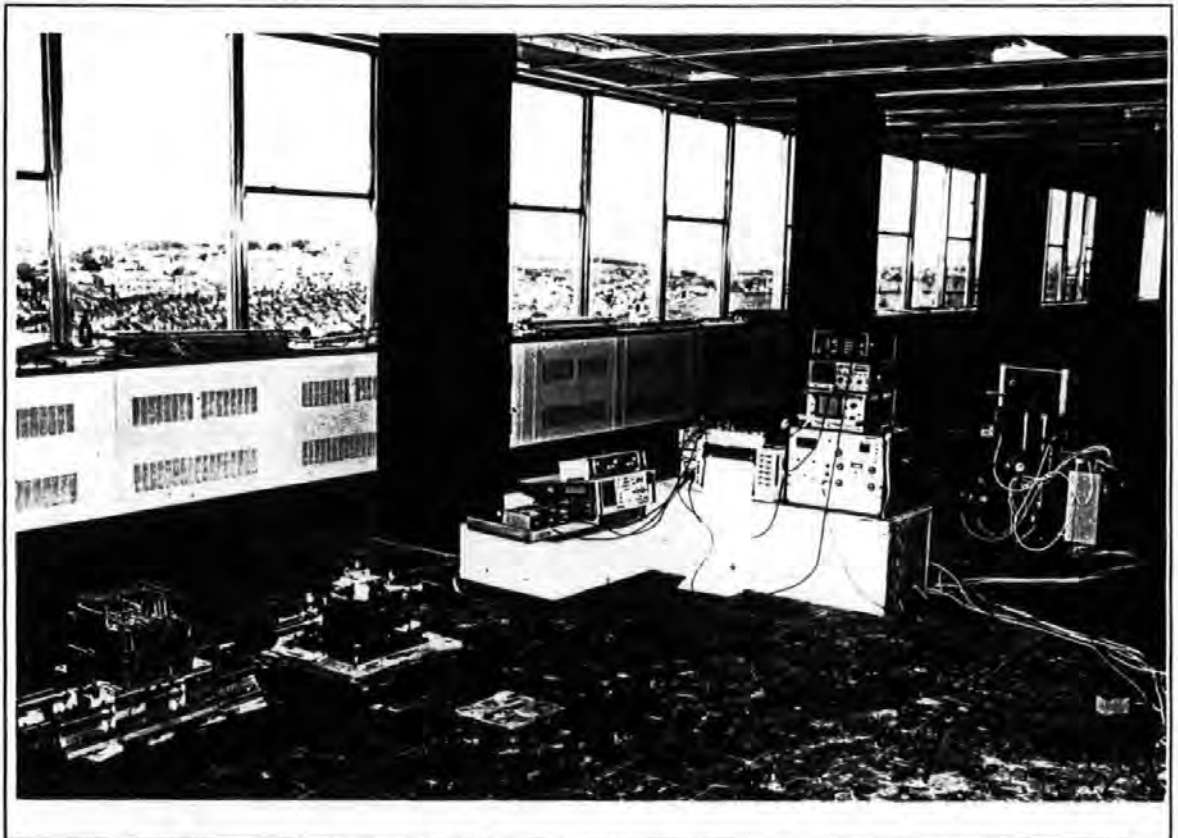


Figure 7.2.2-5a. A photograph featuring the setting up of equipments in the field.



Figure 7.2.2-5b A photograph featuring the fully assembled hydraulic power supply unit in the field.

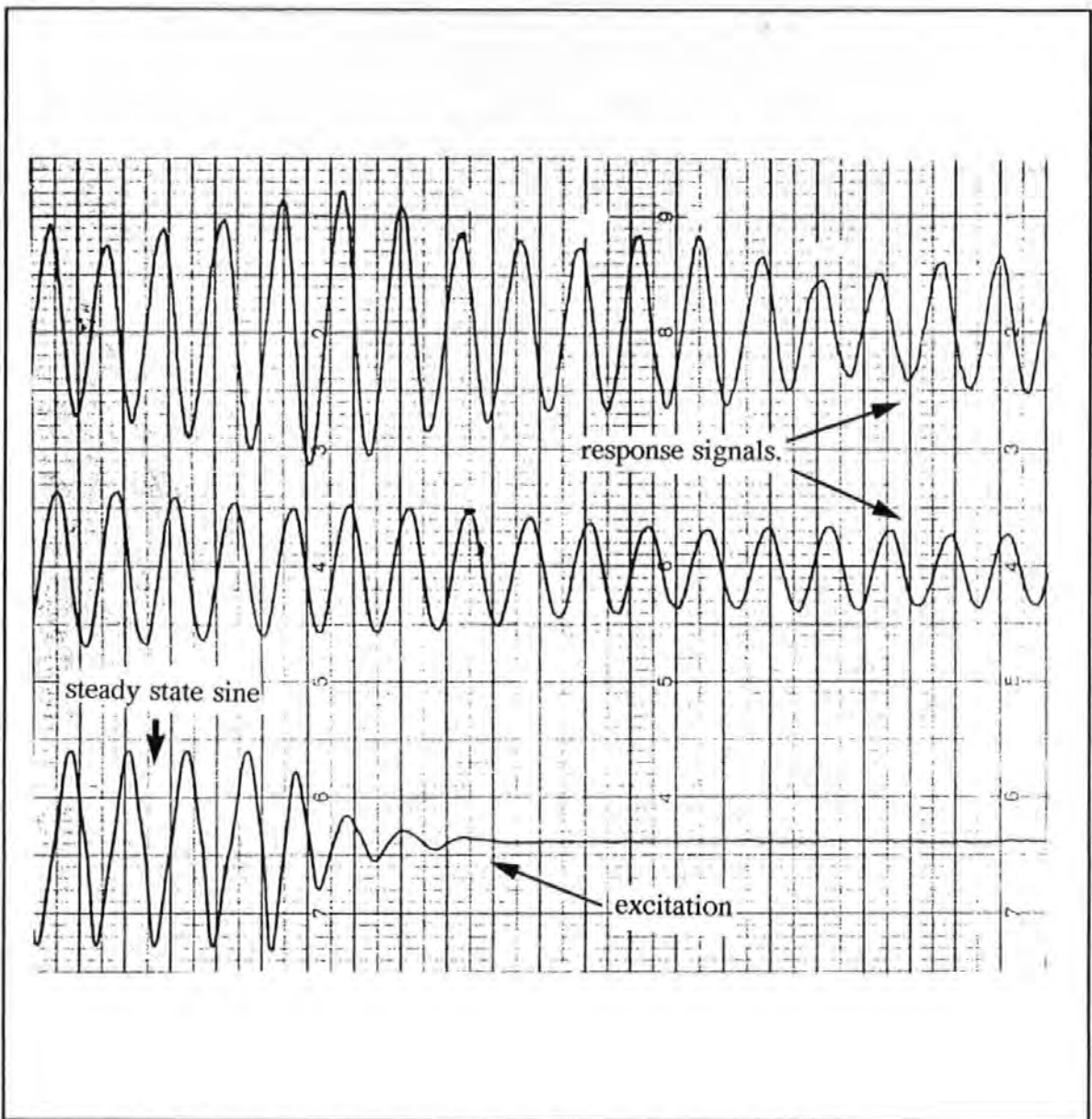
7.2.2.1 AMBIENT VIBRATION TESTS

These tests were performed by recording the building's response to wind excitation using two accelerometers placed at the northern and southern ends of the ninth floor as shown in Figure 7.2.2-3. Since wind forces acting on the building were not measured, accelerance frequency response functions could not be obtained except the response's autospectra. The resonance frequencies were picked from the peaks in the autospectra and checked against those from the exciter-induced vibration tests. Because of the *randomness* of ambient excitation, long recording was required to satisfy the following two

considerations. Firstly longer records enabled large amount of averaging to be performed to enhance the statistical confidence of the signals. Secondly, it enabled finer frequency resolution to be obtained: a requirement governed by the signal sampling and DFT theories. Typically, these measurements lasted several hours. In practice, the measurements were recorded uninterrupted overnight as the disturbances were less severe during those hours than during working hours.

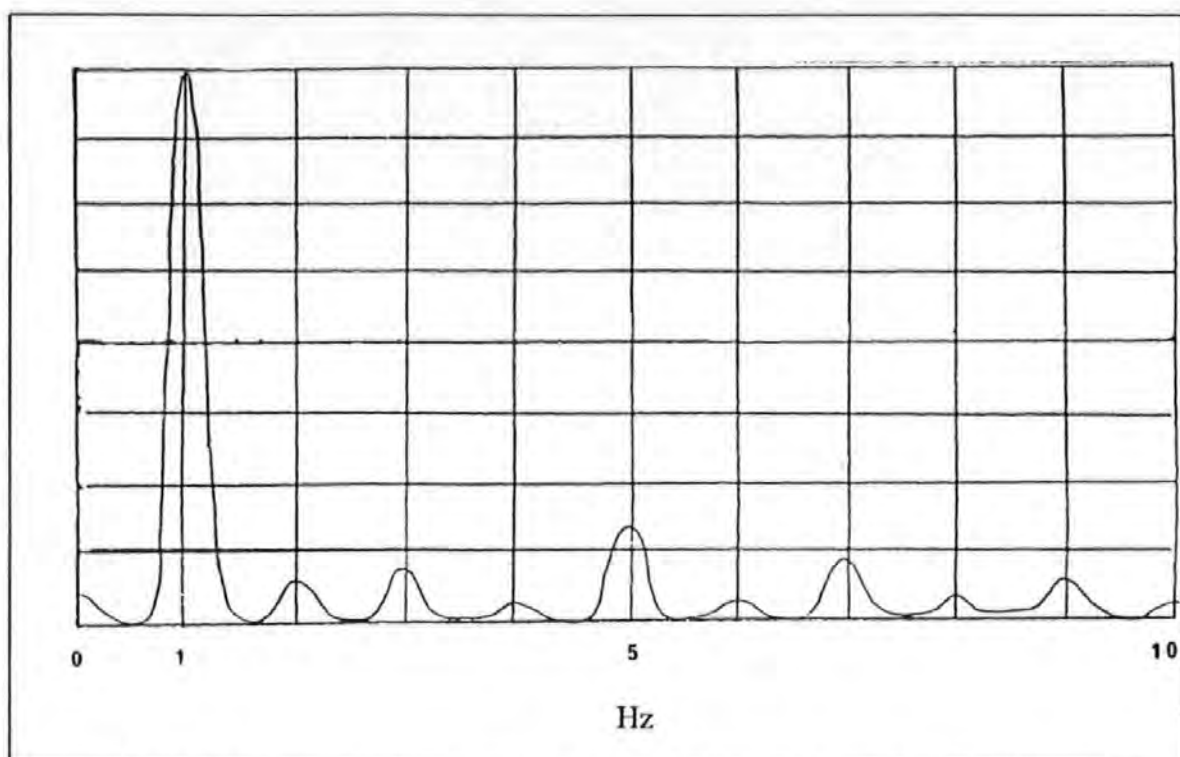
7.2.2.2 STEADY STATE STEP-SINE TESTS

As a contrast to random wind excitation, tests based on steady-state SS excitation could generally yield better measurements because of better signal-to-noise ratios. Figures 7.2.2.2-1 show a typical time history plot (obtained from an analog chart recorder in-situ) of excitation and responses. The plot covers both the steady-state sines before and the transients subsequent to the sudden removal of excitation.

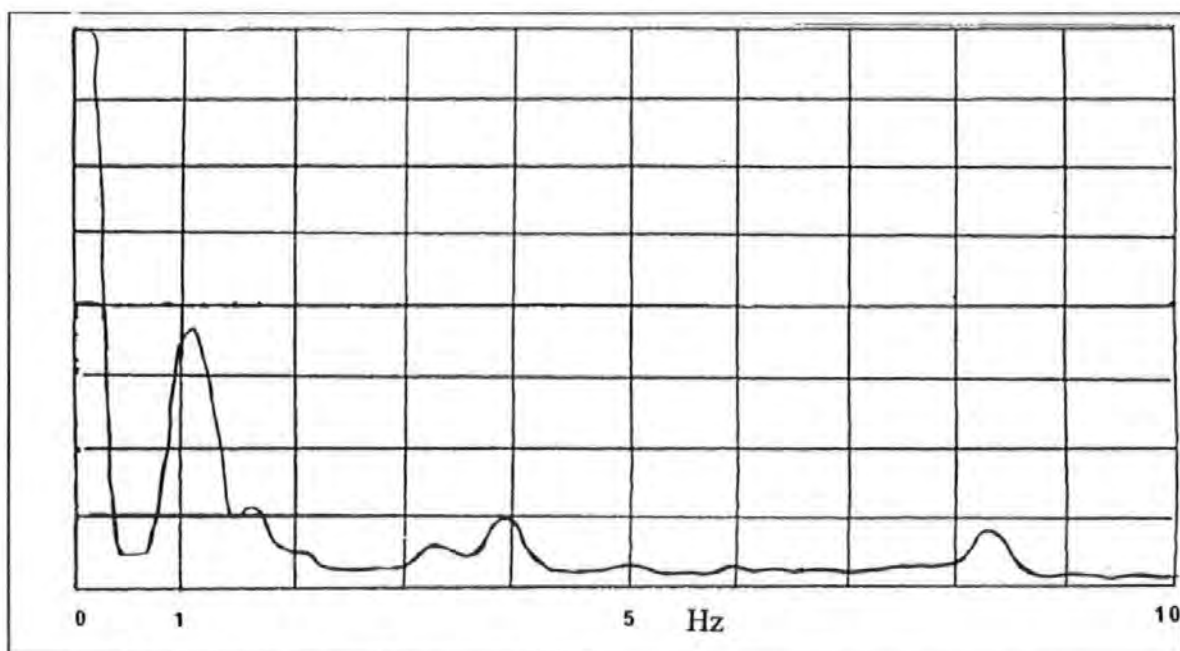


Figures 7.2.2.2-1 A sample of typical time responses recorded.

Due to non-linear behaviour of the hydraulic shaker, higher harmonics, whose frequencies were integer multiples of the forcing frequency, were produced. Non-linear behaviour happened when the exciter was operating close to any one of its operational limits imposed by the pumps, electronic valves etc. Figures 7.2.2.2-2 show a typical load spectrum (obtained via a 'screen dump' from the HP3582A to an XY pen-recorder) at an excitation frequency of 1 Hz. The resulting acceleration response spectrum of the structure is also given in Figure 7.2.2.2-3.



Figures 7.2.2.2-2 A typical load spectra when excitation frequency was set at 1 Hz.



Figures 7.2.2.2-3. The resulting acceleration response spectra.

7.2.2.3 PERIODIC RANDOM TESTS

Tests using periodic random (or PRBS) excitation were also undertaken. Similar to ambient tests, the random excitation force from the exciter provided stimulus across a broad frequency band simultaneously. However, unlike natural random processes such as wind,

the spectral contents of the PRBS forces were 'tailored made' to suit the analysis spectral window and was made to be repetitive within the sampling time window of each measurement. Hence a moderate amount of averaging was required to obtain the same level of statistical confidence of the signals when compared with those required in ambient tests. The signals were sampled with the Hanning time window to reduce the *leakage* effects to a minimum. A 10 Hz baseband was chosen in taking these measurements. Usually, a number of 8 averages was taken before data were recorded.

7.3 DATA RECORDING AND REDUCTIONS

The field data were recorded as time response charts, or hand noted readings. The spectra from the spectrum analyzer were printed as hard-copy using an XY plotter. As data were not recorded digitally, analyses such as estimating damping from decaying time traces could only be performed using simple graphical techniques. For the same reason, the poor quality original spectral plots and time charts are used here because no other forms of record are available.

7.4 TEST RESULTS

The autospectra obtained in the ambient vibration tests from the two accelerometers are given in Figure 7.4-1a and 7.4-1b. Their locations are already given in Figure 7.2.2.3. These spectra are a results of R.M.S (root-mean-square) averaging of 256 separate spectra.

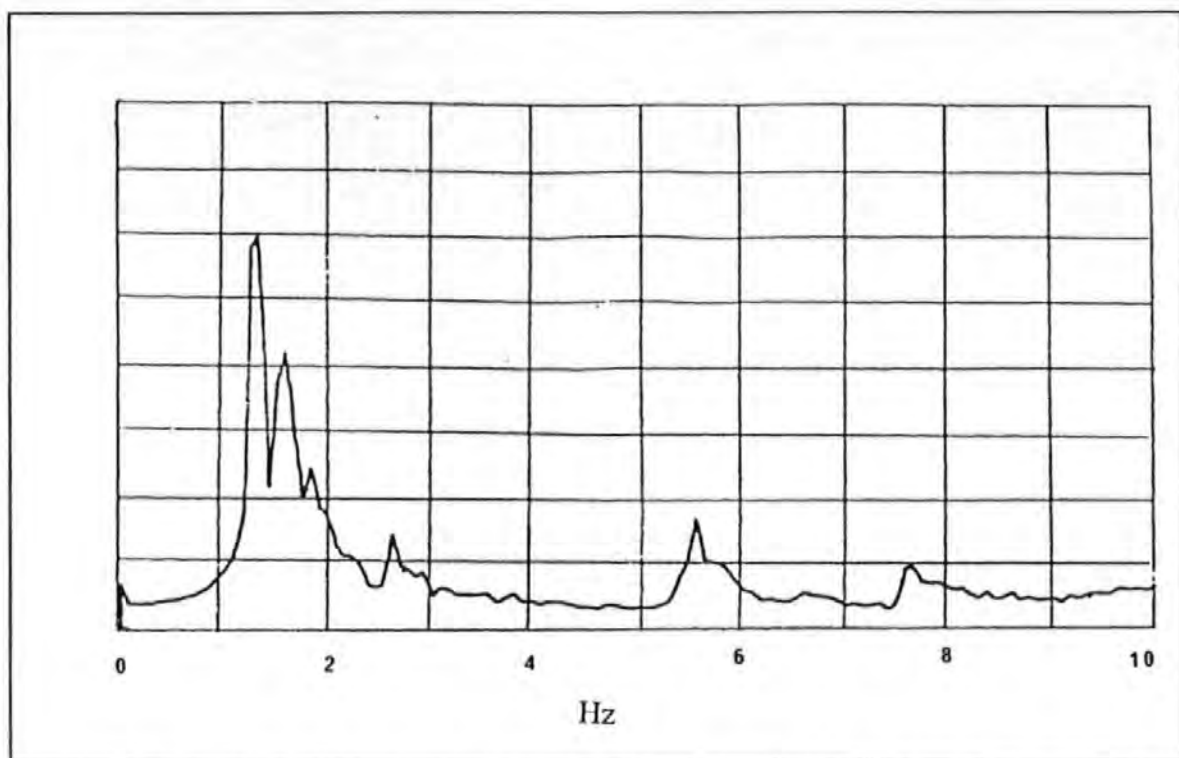


Figure 7.4-1a The autospectrum obtained in the ambient vibration tests from one of the two accelerometers.

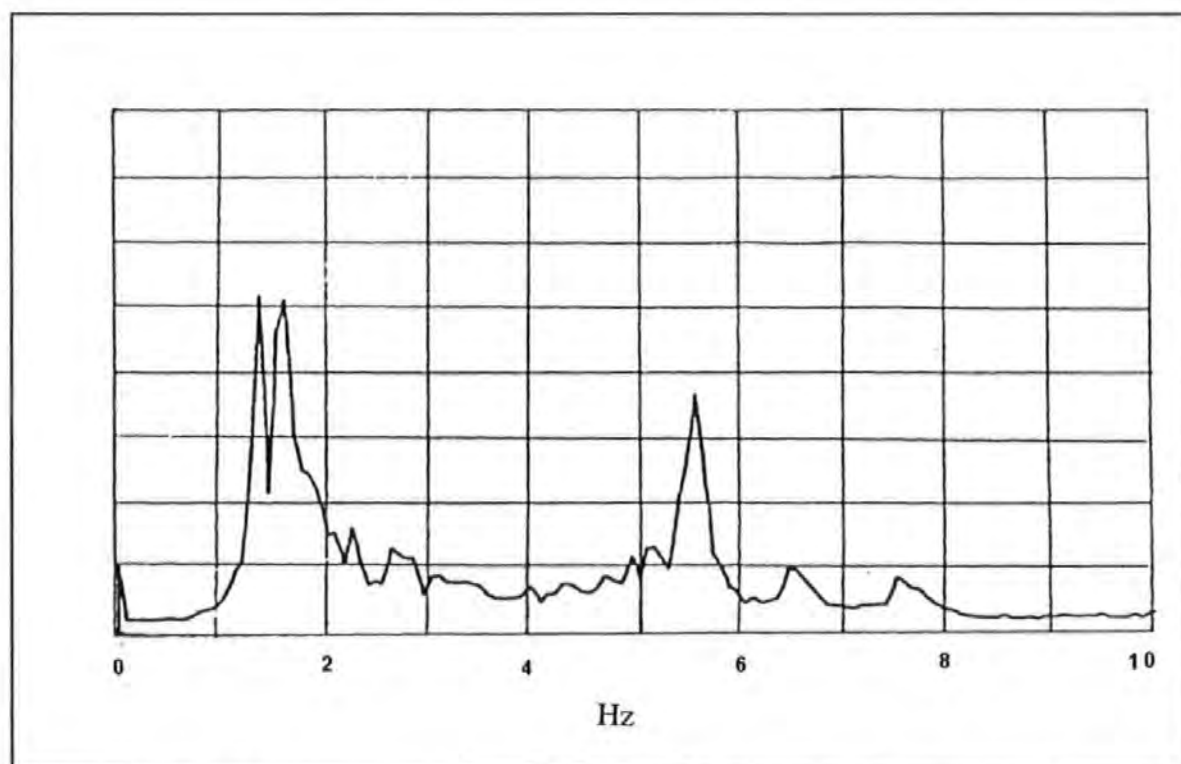
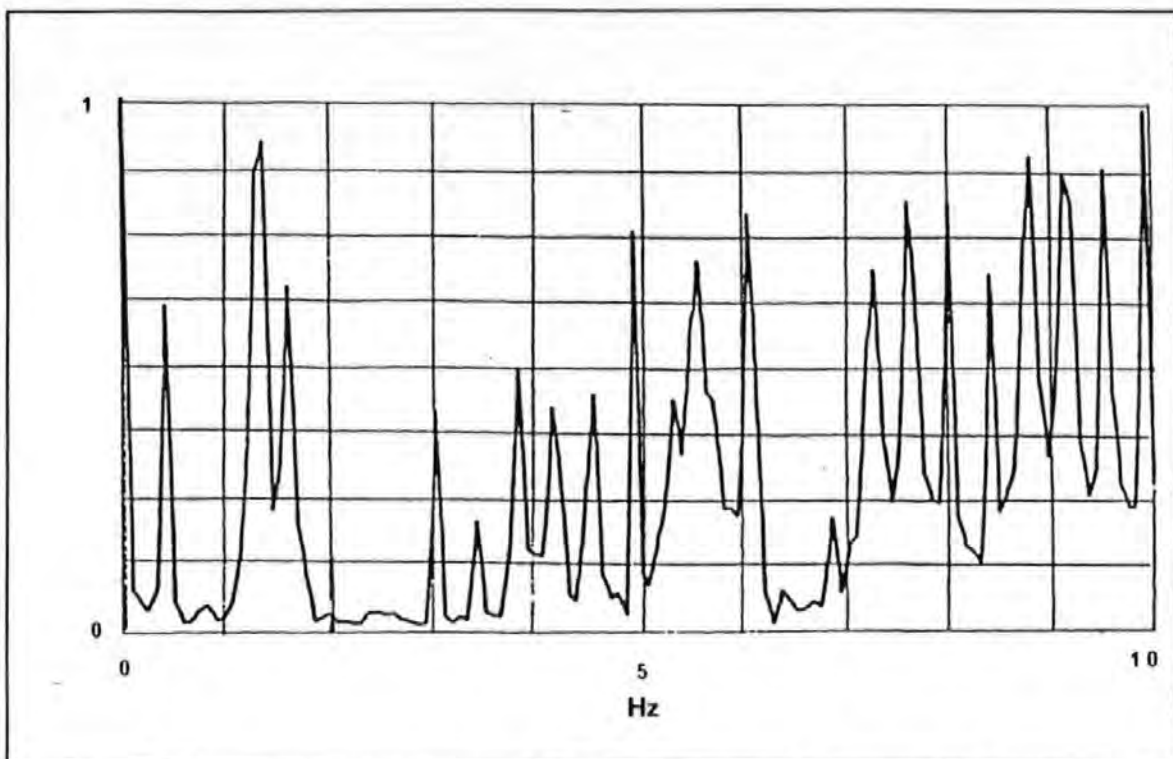


Figure 7.4-1b. Another autospectrum obtained in the ambient vibration tests from one of the two accelerometers .

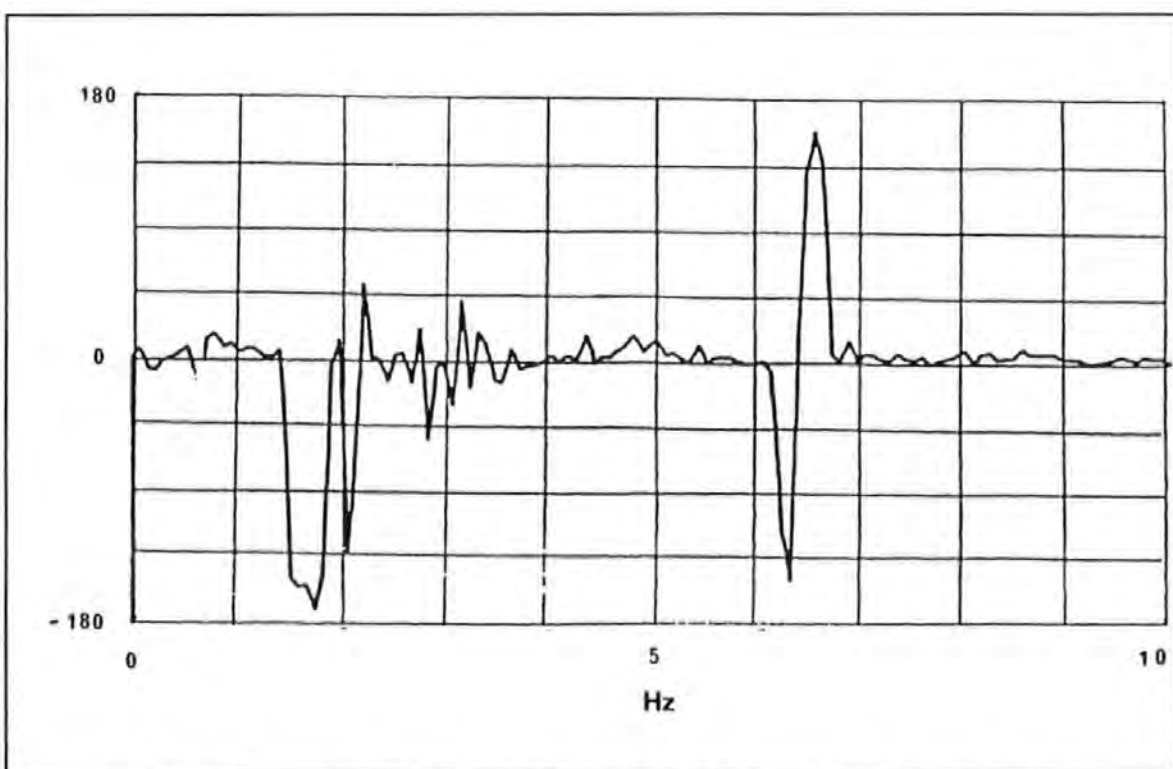
Both Figures show that two distinct peaks occur at 1.32 and 1.56 Hz. These are positively identified by the SS and PRBS tests as the fundamental (EW1) flexural and the fundamental torsional (T1) modes. The second (EW2) flexural mode at 5.6 Hz was also excited by the wind. It is hard to determine whether the fundamental (NS1) flexural mode at 1.17 Hz was excited partly because of the lack of resolution to resolve the NS1 and the EW1 modes. The spectral separation between these two modes is merely 0.15 Hz while the resolution is only 0.08 Hz.

The structure is expected to be more flexible in the NS than the EW direction because of the arrangement of the lateral load bearing walls. So the directions of the wind must be as such to have favoured the excitation of the EW1 than the NS1 mode. Without the assistance from the SS and PRBS test results, modes determination based on the sole criteria of response peaks in the response spectra would be inconclusive.

Figures 7.4-2 and 7.4-3 show respectively the Coherence and Phase spectra obtained from the two accelerometers. As typical in these situations, coherence values were high at frequencies corresponding to the peaks including those not associated with resonance ones and low otherwise. High coherence values indicate that the response signals picked up by the two accelerometers are highly correlated i.e. they are due to the same sources of disturbance or excitation. The phase spectrum indicates that the movements at these two points at 1.56 Hz are in opposite directions (or 180 degrees phase difference) as recorded by two accelerometers. This indicates further that this is the torsional T1 mode.



Figures 7.4-2 Coherence spectra obtained from one of the two accelerometers.



Figures 7.4-3 Phase spectra obtained from one of the two accelerometers.

Figure 7.4-4 and Figure 7.4-5 show the inertance (FRF) spectra obtained by SS tests with the exciter aligned in the NS and EW directions respectively. In Figure 7.4-4, the three very distinct peaks are clearly shown. They correspond to the NS1 mode at 1.17 Hz, T1 mode

at 1.56 Hz and the second NS flexural (NS2) mode at 3.83 Hz. The excitation force levels applied were up to a maximum of 2 kN.

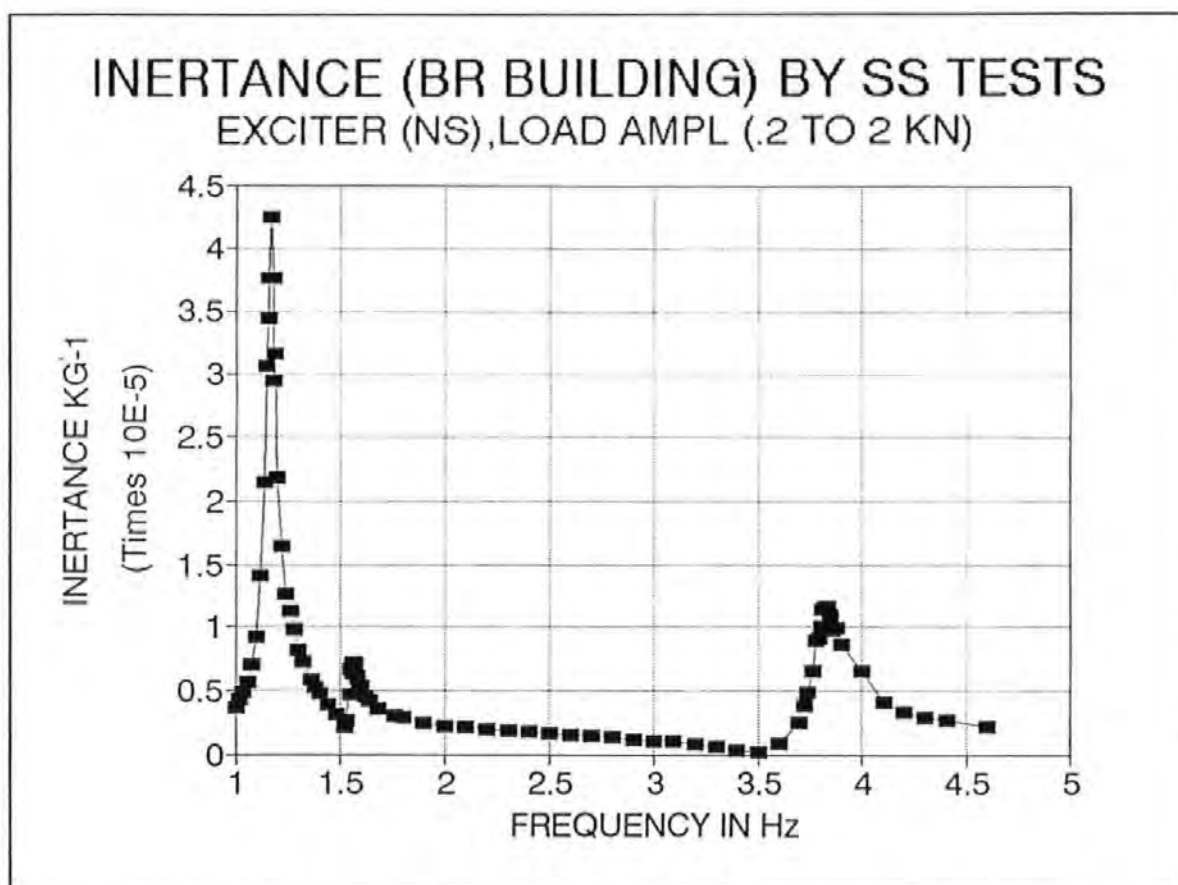


Figure 7.4-4 The inertance (FRF) spectrum obtained by SS tests with the exciter aligned in the NS direction.

Figure 7.4-5 indicates the appearance of 4 peaks corresponding to the EW1 mode at 1.32 Hz, the T1 mode at 1.56 Hz, an unspecified mode at 2.723 Hz and the EW2 mode at 5.6 Hz. The applied force levels were similar to those of the EW test series.

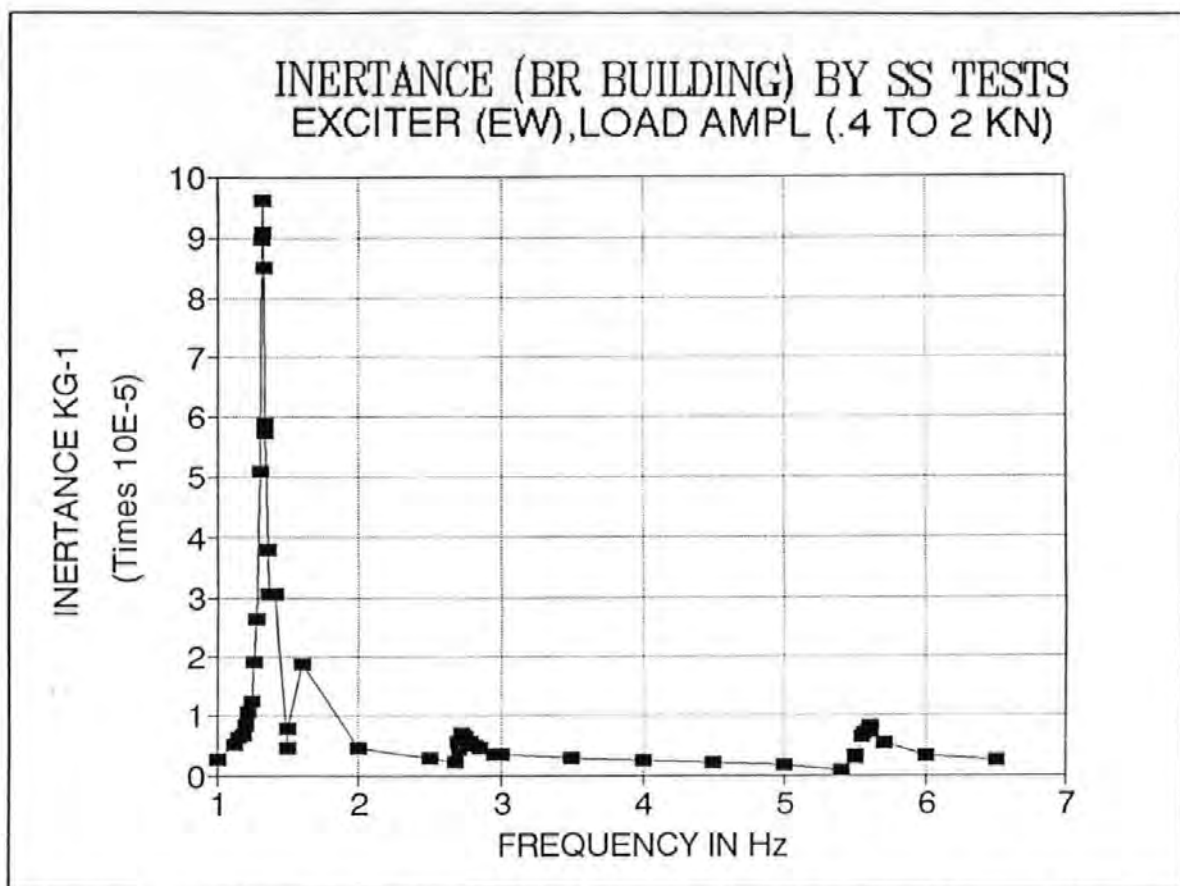
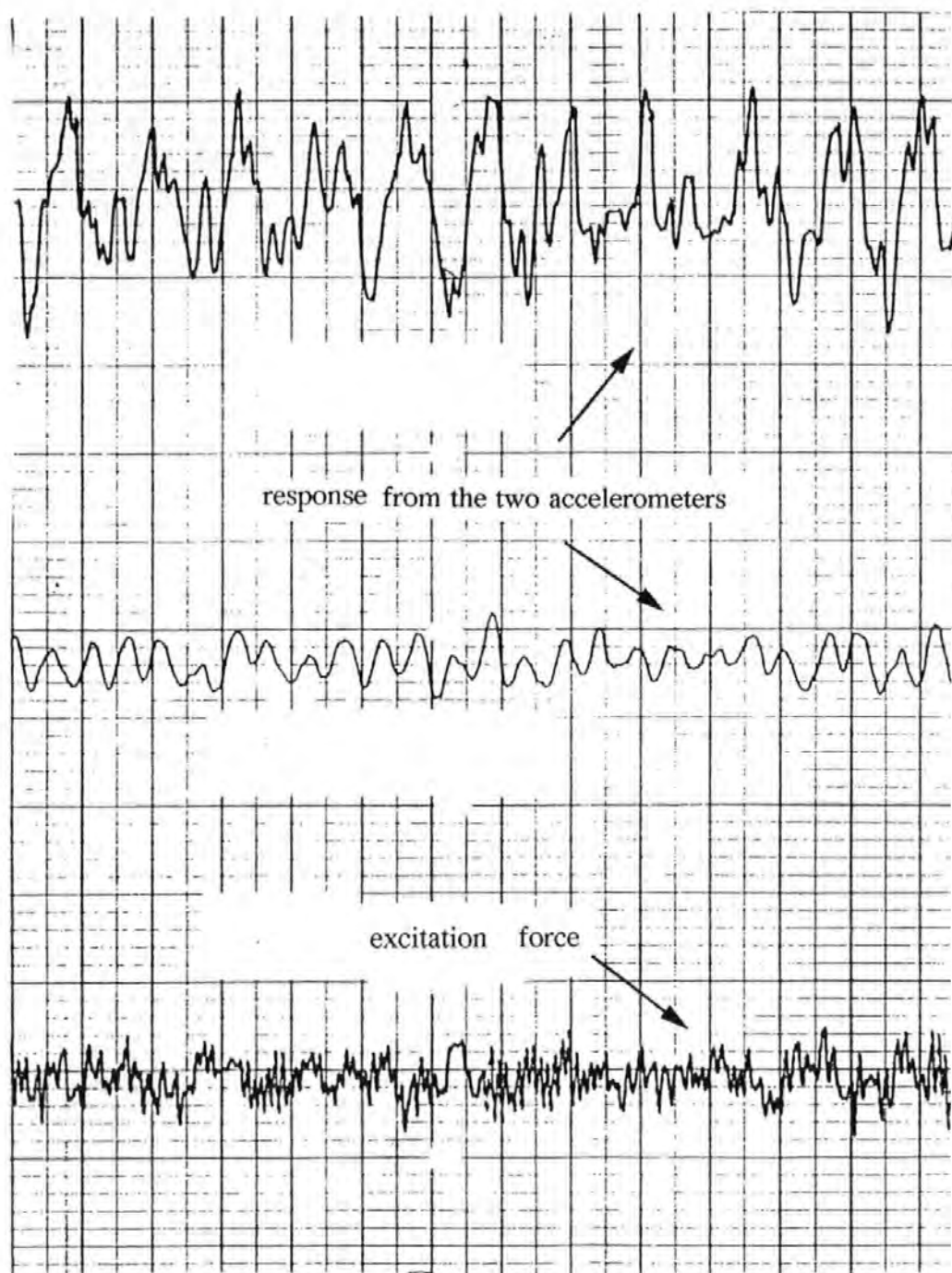


Figure 7.4-5 The inertance (FRF) spectra obtained by SS tests with the exciter aligned in the EW directions.

A typical time history record of the PRBS excitation force (load) and the resulting responses from the two accelerometers are also shown in Figure 7.4-6.



Figures 7.4-6. A typical time history record of the PRBS excitation force (load) and the resulting responses from the two accelerometers.

The exemplary values of the resonance frequencies of the various modes are summarized in Table 7.4-1.

TABLE 7.4-1. THE TABLE OF EXEMPLARY VALUES OF THE RESONANCE FREQUENCIES OF THE VARIOUS MODES OF THE BR BUILDING.

VIBRATION MODES	RESONANCE FREQUENCY (Hz)
NS1	1.17
EW1	1.32
T1	1.558
NS2	3.83
EW2	5.60

Figure 7.4-7 show the mode shapes of the NS1 mode as determined from the SS and PRBS tests (the annotations in the figures are: 'ACT-EW' denotes the actuator was in EW orientation; '230486' denotes the date of the experiment; and so on) . The SS test was performed with the exciter acting in the NS direction. Whereas the PRBS test was performed two days after the SS tests with the exciter acting in the EW direction. The two curves obtained are in general agreement except that a spurious data point was obtained with the latter. It has to be borne in mind that the SS tests were of much larger forcing amplitudes than the PRBS counterpart. So the discrepancy, though small, might be due to changes in the behavioural mechanism of the structure in addition to the normal measurement errors.

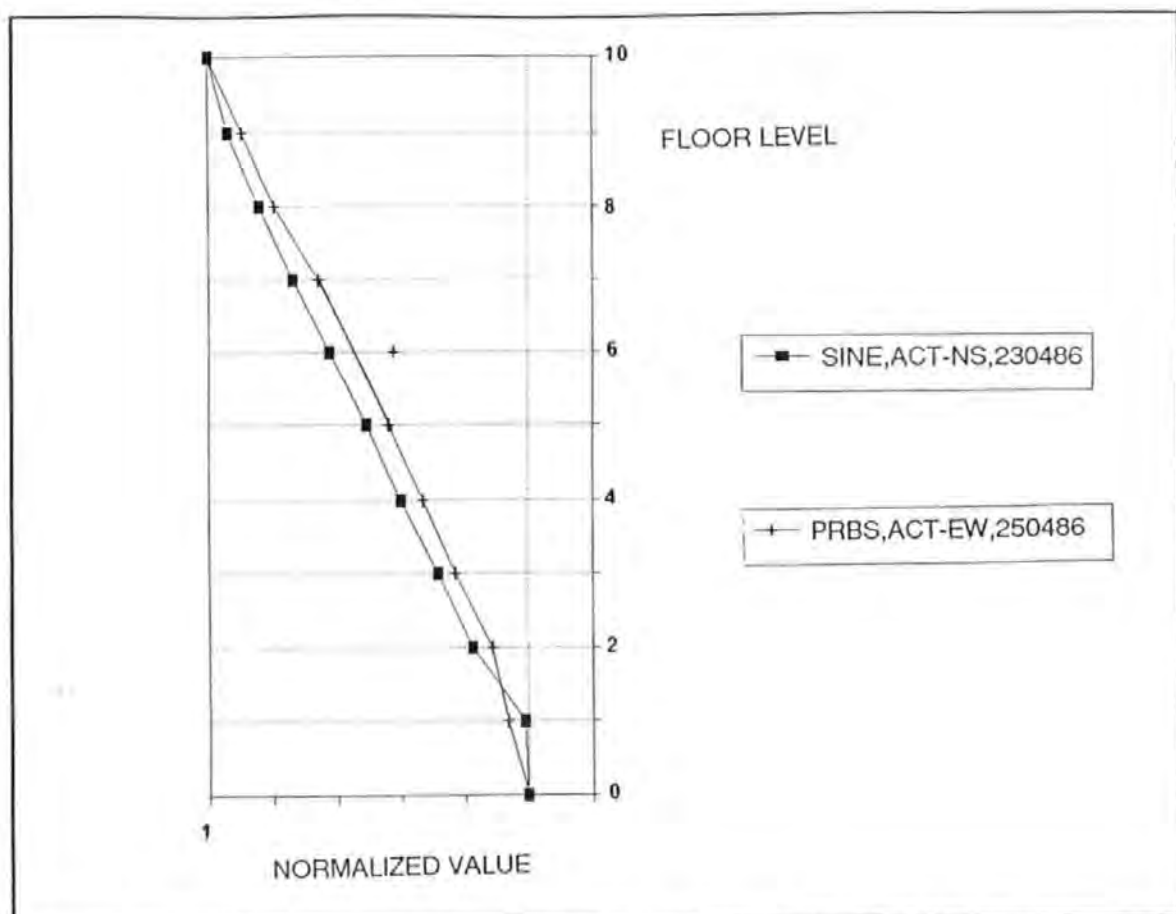


Figure 7.4-7 The NS1 mode shapes determined from the SS and PRBS tests.

By plotting the NS1 mode shapes obtained from this experiment alongside those experimental data reported by Williams^[1.1], and those recommended by CIRIA^[7.1] and ESDU^[2.48, 2.49, 2.50] as in Figure 7.4-8, it is noted that the linear mode and the CIRIA recommended mode shape are close approximations to the one measured.

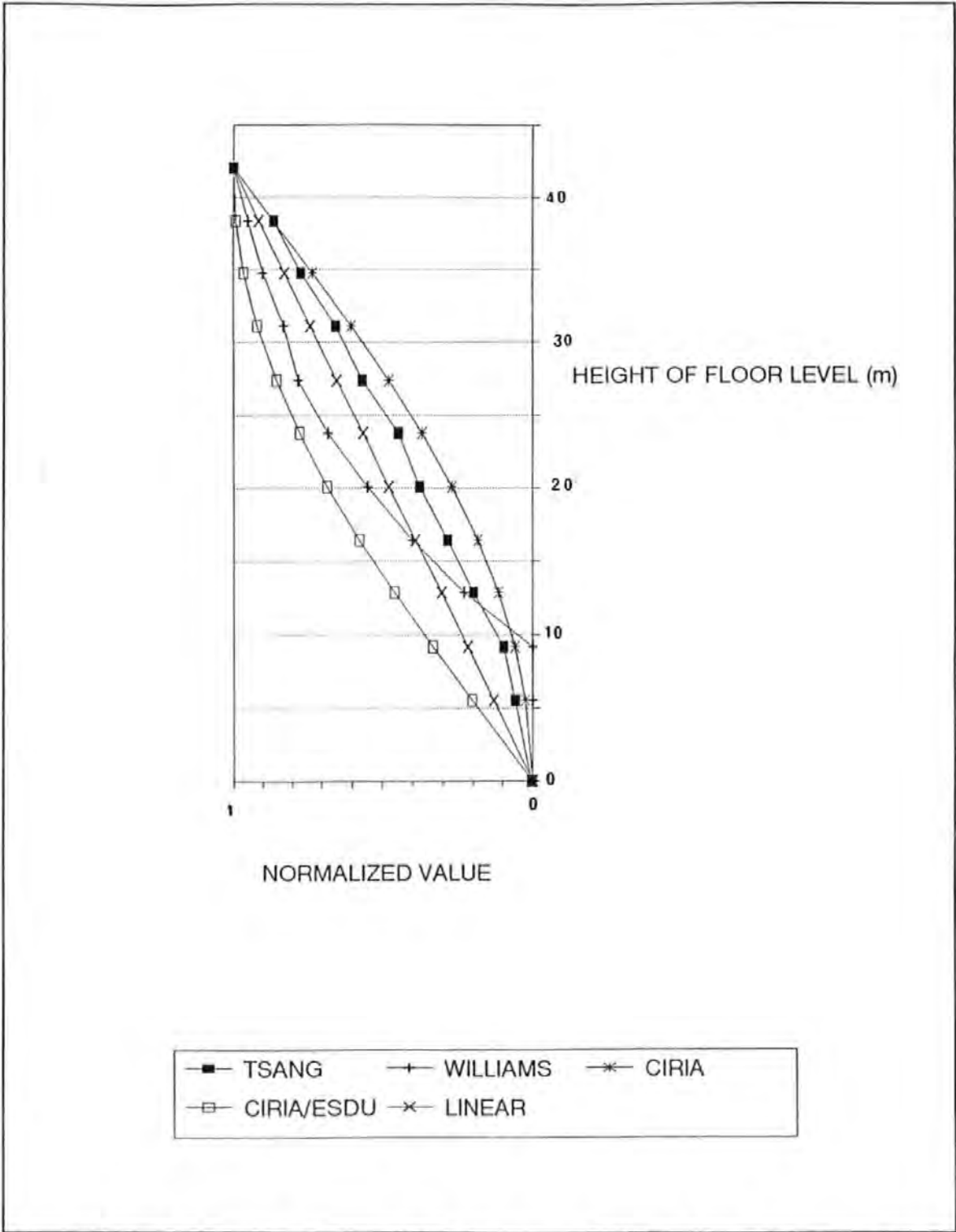


Figure 7.4-8. An overlaid plot of the NS1 mode shapes obtained from this experiment and other recommendations.

Figure 7.4-9 shows the mode shapes of the EW1 mode determined from the SS and the PRBS tests performed on different dates. The exciter was aligned in the EW direction in all these cases and the three curves obtained are in excellent agreement. This indicates the credential of the test data and that tests results are repeatable over a period of time.

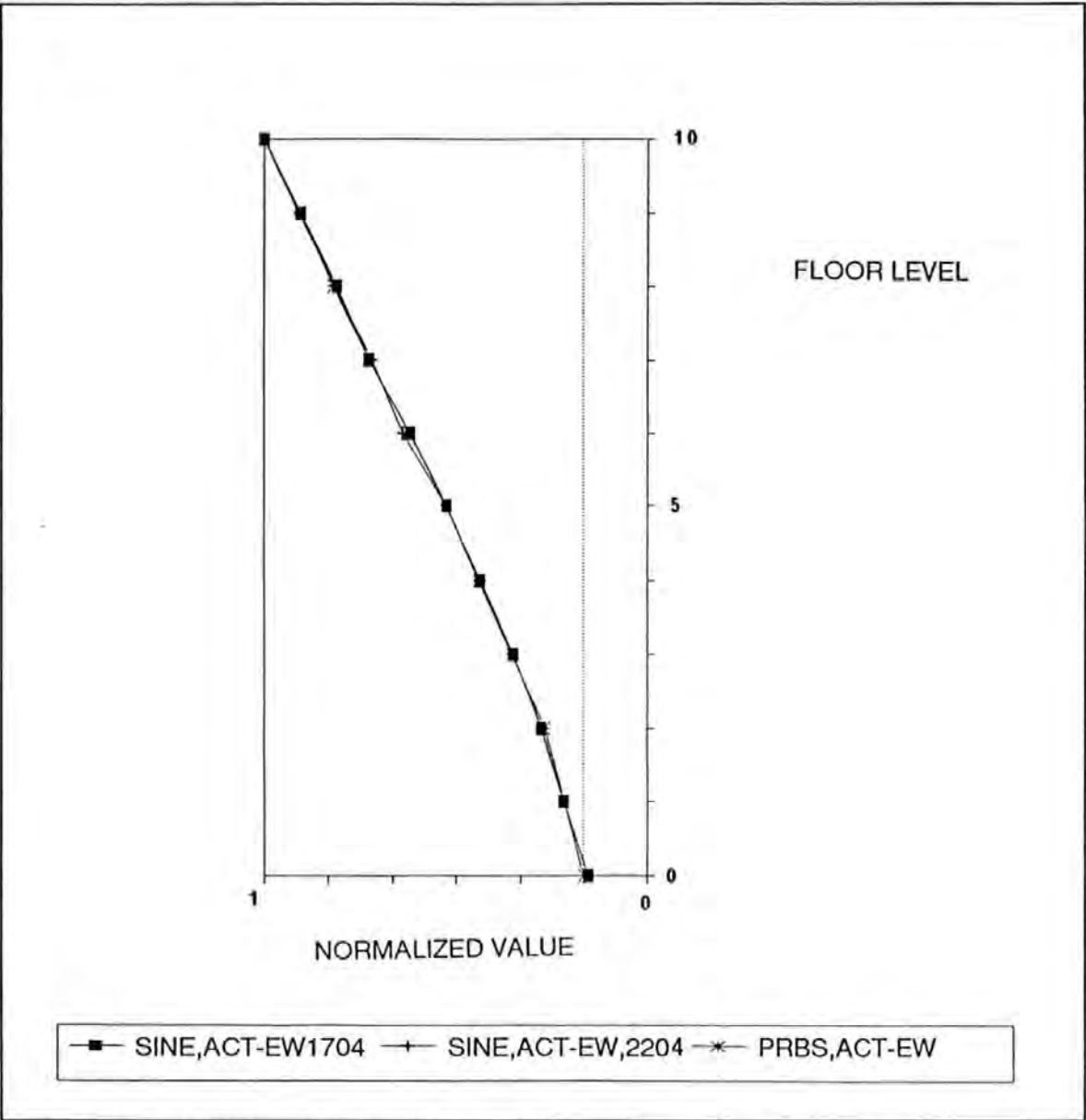


Figure 7.4-9 The mode shapes of the EW1 mode determined from SS and PRBS tests performed on different dates.

Again the EW1 mode shape obtained from this experiment is plotted alongside the other recommendations annotated in Figure 7.4-10. Once again, the linear and the CIRIA recommended mode shapes seem closer approximations to the one measured.

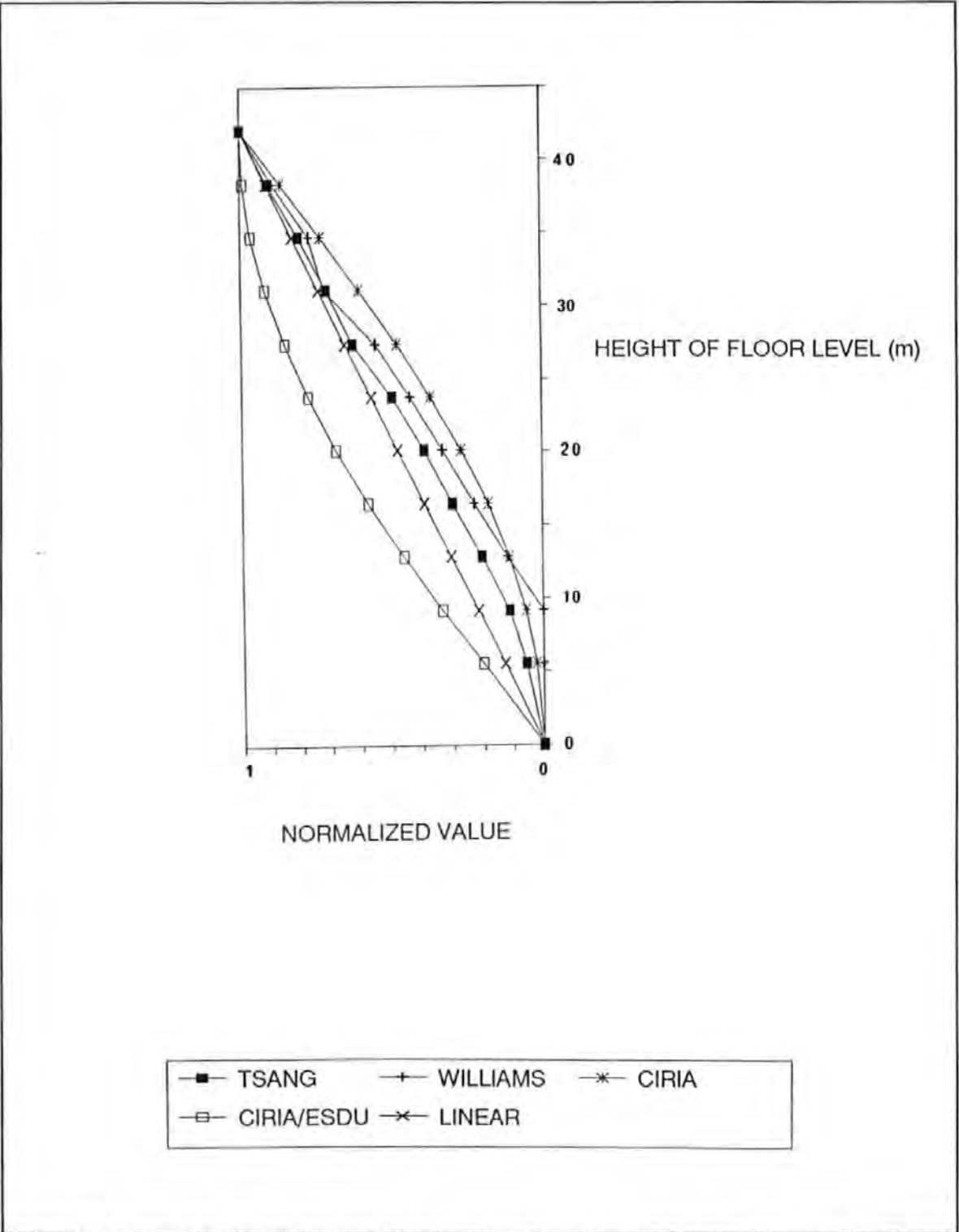


Figure 7.4-10 A plot of the EW1 mode shapes from this experiment and other recommendations.

Modes shapes corresponding to the modes T1 is given in Figure 7.4-11. The results from the PRBS and the SS tests, with the exciter aligned in the EW direction in both cases, are consistent and in good agreement except an occurrence of a spurious data point at the 4th floor level. However, results from the SS tests, with the exciter aligned in the NS direction, produced somewhat different results from those obtained in the EW direction.

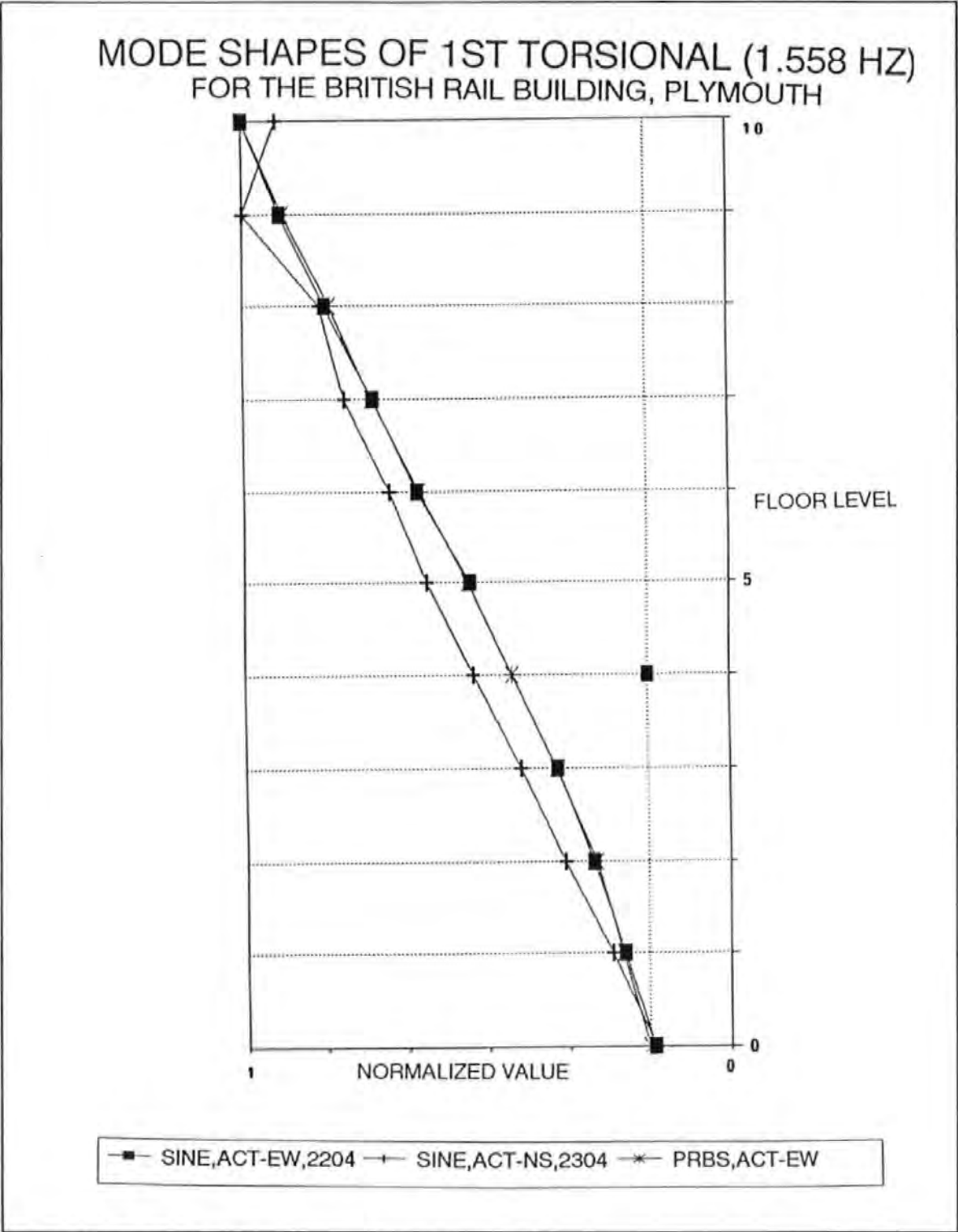


Figure 7.4-11 Modes shapes of the T1 mode.

The NS2 mode is given in Figure 7.4-12. The figure shows that the node of this mode is close to the 8th floor level.

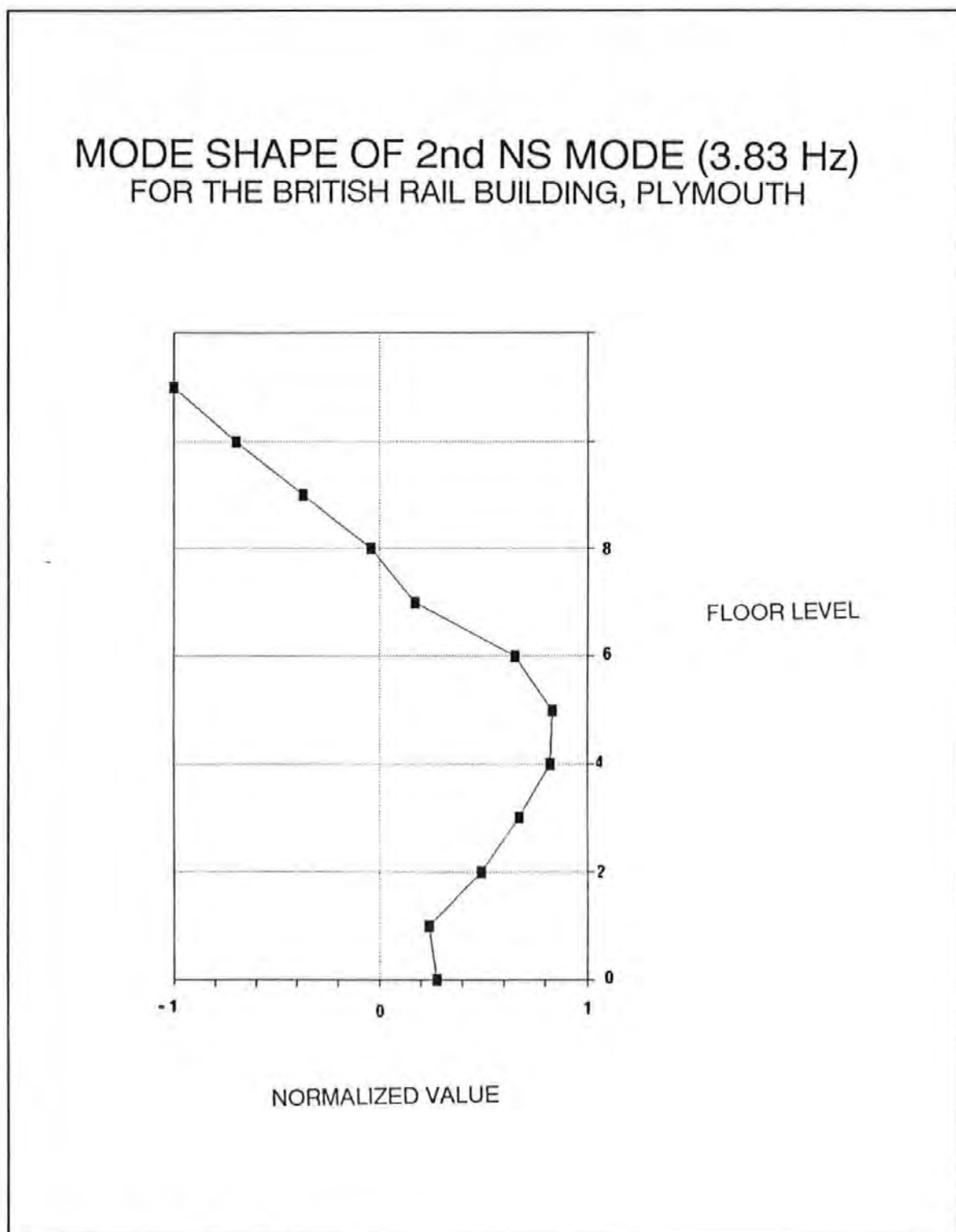


Figure 7.4-12. The NS2 mode.

The EW2 mode shapes determined from 3 different experiments are also given in Figure 7.4-13. Again good agreement is obtained. The node of the EW2 mode is shown to lay between the 8th and 9th floor levels.

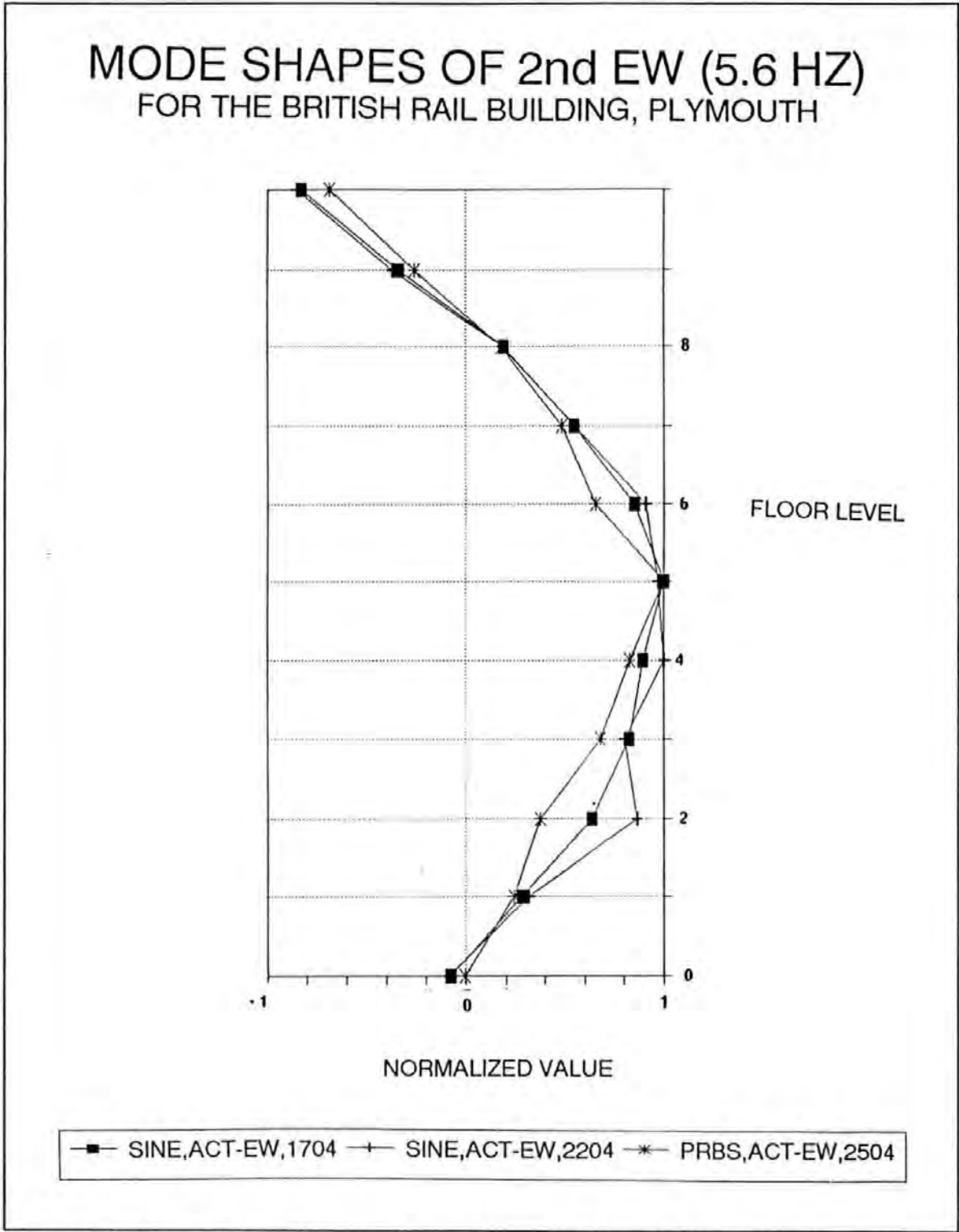


Figure 7.4-13 The EW2 mode shapes determined from 3 different tests.

7.5 ANALYTICAL MODEL OF THE BR BUILDING

The task of modelling the building is potentially a difficult one because of the numerous structural connections involved in articulating various structural members : beams, columns, shear cores, shafts, infilled walls, cladding etc. Also these structural members are mainly made of inhomogenous materials such as reinforced concrete. Unlike other structural materials which are manufactured in a controlled factory condition, reinforced concretes are mixed and cured in-situ. The quality hence structural properties of these materials are difficult to maintain.

The shear cores and planar shear walls present another difficulty in modelling. Because of the high depth-to-span ratios, shear deformation of these structural elements are significant. Simple bending theories are inadequate and *deep beam* theories are more appropriate. In particular, the shear cores forming the lift shafts are thin wall open sections (therefore asymmetric) The open edges of the shafts are connected by thick lintel beams at each floor level. Because of asymmetry, *shear centre* do not coincide with *geometric centre*. Hence flexural bending of these elements are strongly coupled with torsion as well. Their interactions with the other elements are even more complex.

A finite element model of the BR building was constructed from simple beam elements. To reduce complexity, a number of assumptions were made.

- a. The raft foundation and the soil stratum supporting the structure is assumed infinitely rigid so that full fixity of the base of the structure is assured and no translation or rocking of the foundation is allowed.
- b. The structural joints between members are assumed fully rigid.
- c. The horizontal elements such as the beams and floor slabs are assumed to have infinite in-plane and out-of-plane bending stiffness.

The finite element model was constructed using **PAFEC** on a main-frame **PRIME** computer. Figure 7.5-1 shows the wire-framed finite element model of the structure. There are over 300 nodes and 900 members in the model. The computations required quite extensive computer resources to complete. In constructing the model, simple 1D bending

beam elements were used for columns and beams and 1D shear beam elements were used for shear walls and cores. Very large moment of inertia values were used for the horizontal elements to assure the infinite stiffness assumption was met. These values were taken typically as 1000 times that of the maximum of the vertical ones. Figures 7.5-2 to 7.5-4 show the mode shape of the EW1, T1 and the EW2 modes.

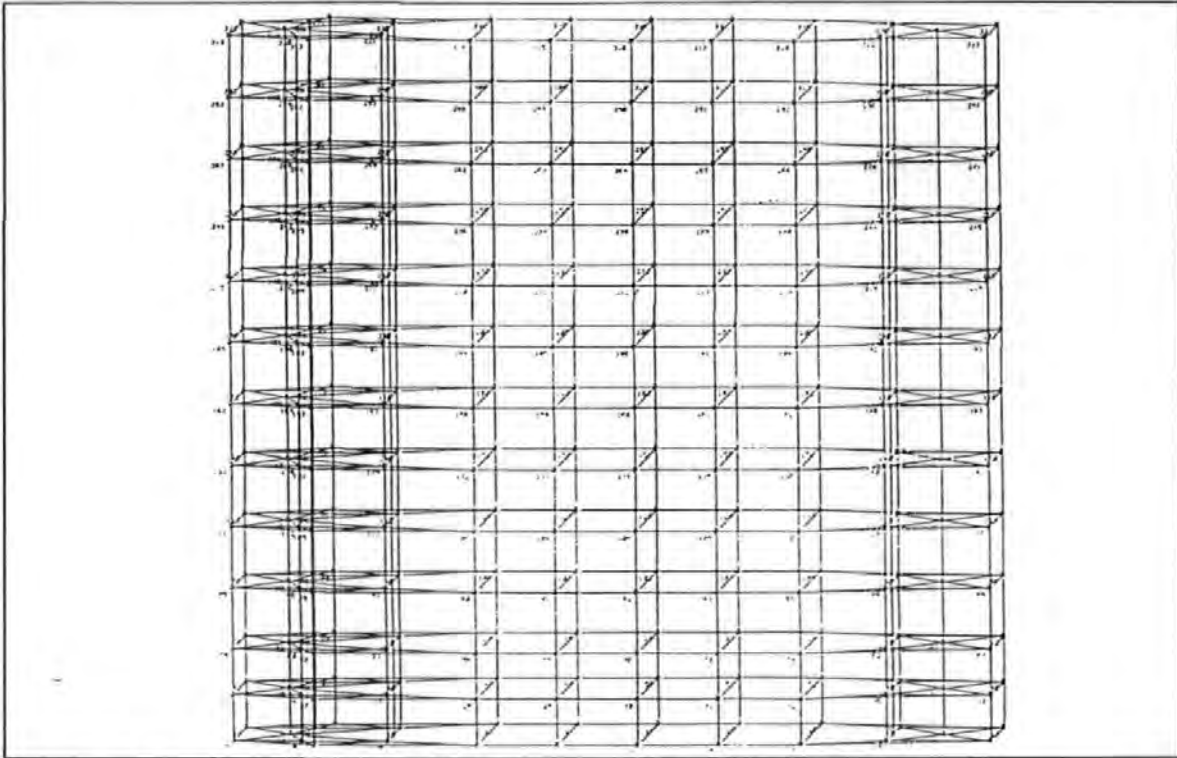


Figure 7.5-1 The wire-frame finite element model of the BR Building.

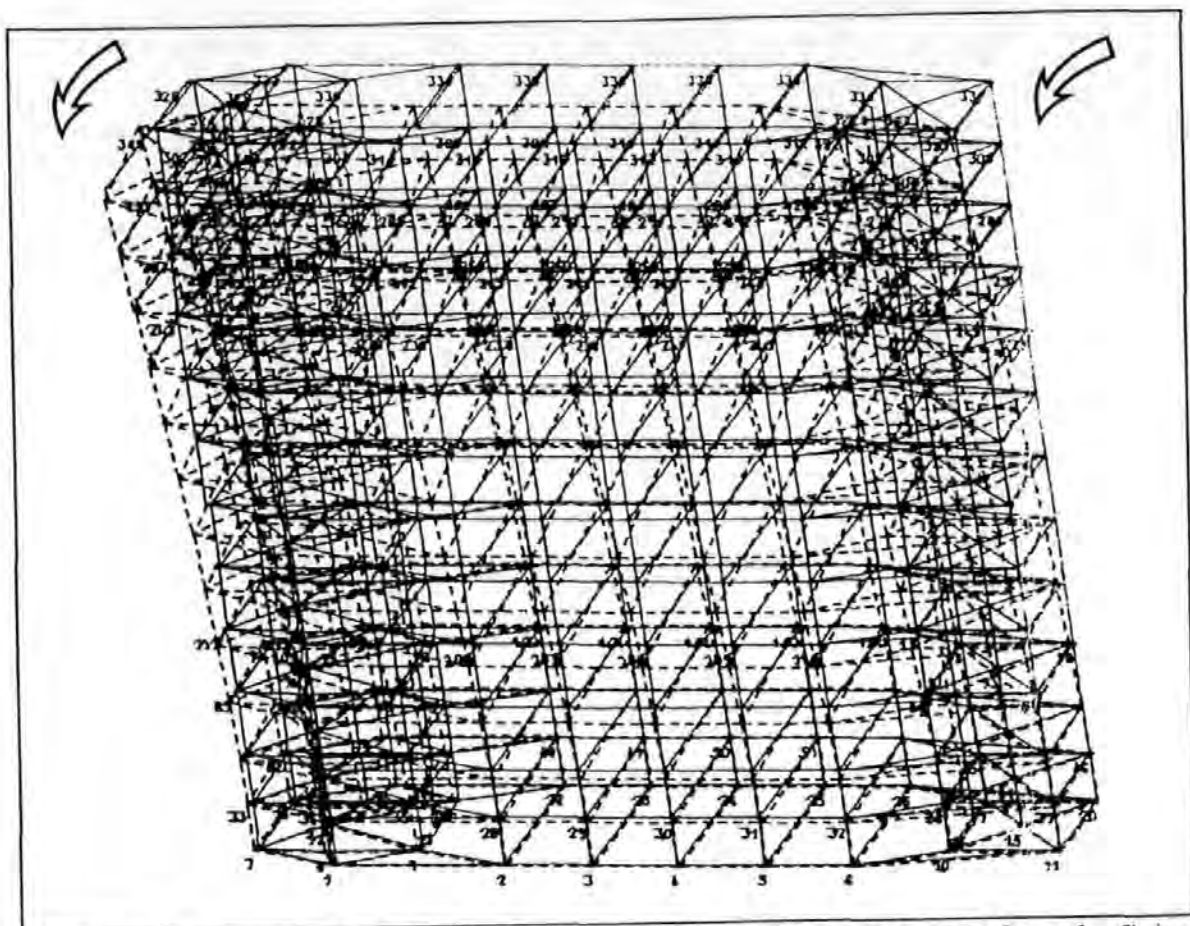


Figure 7.5-2a

A 3 dimensional perspective view of the EW1 mode from the finite element model of the BR building.

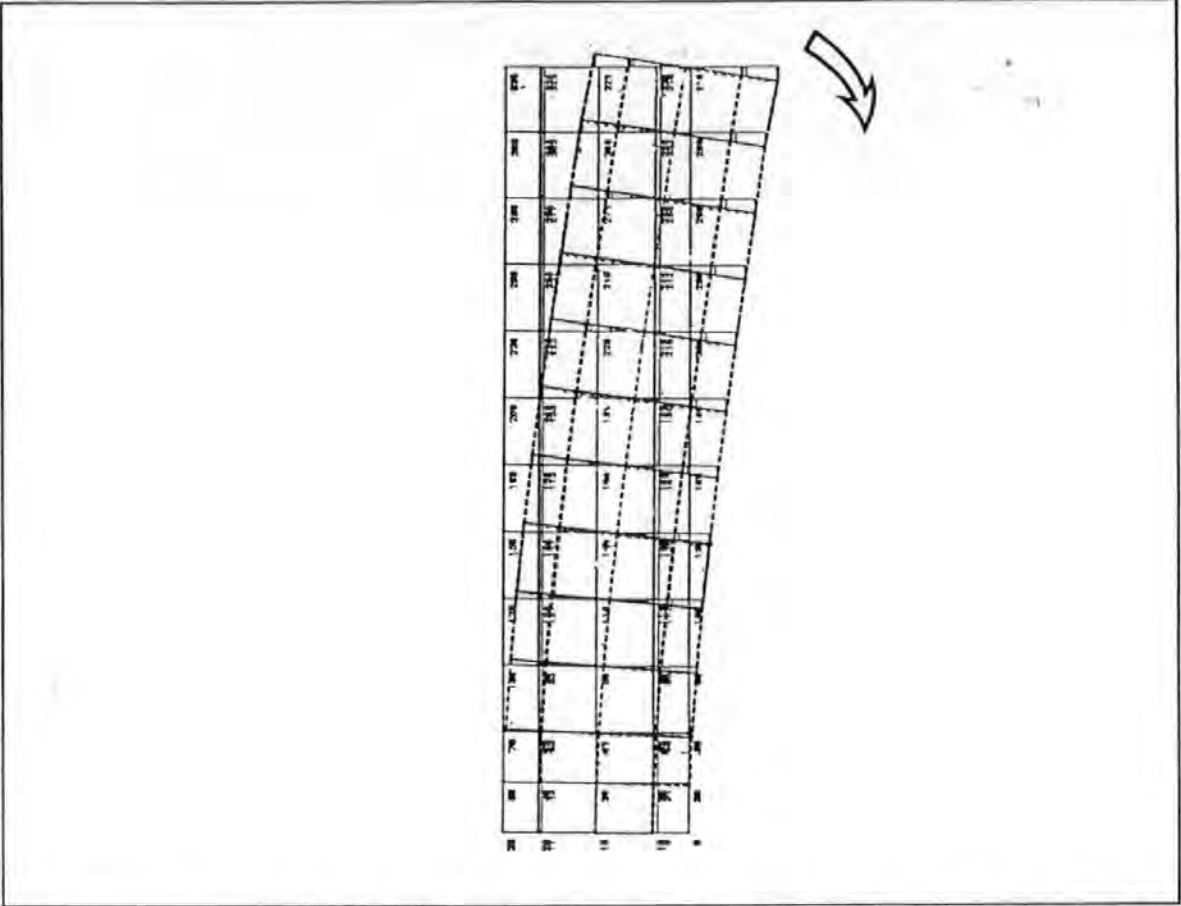


Figure 7.5-2b A side view of the EW1 mode from the finite element model of the BR building.

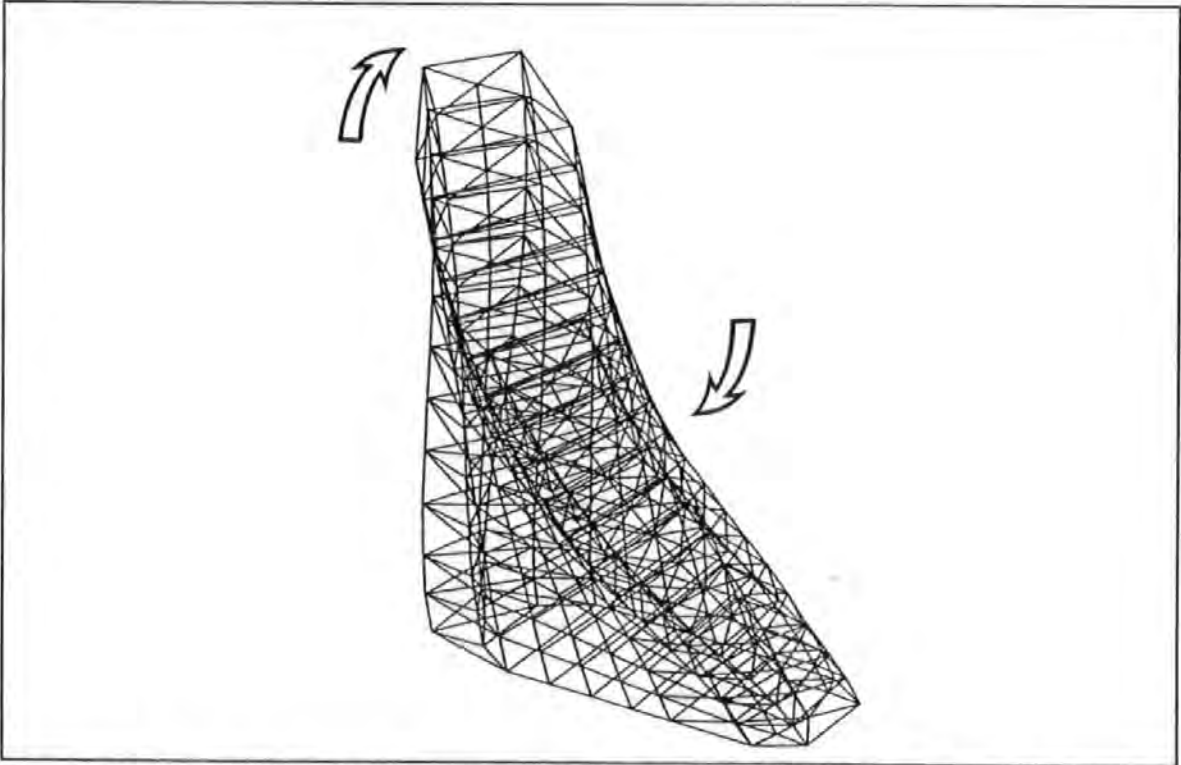


Figure 7.5-3a A 3 dimensional perspective view of the T1 mode from the finite element model of the BR building.

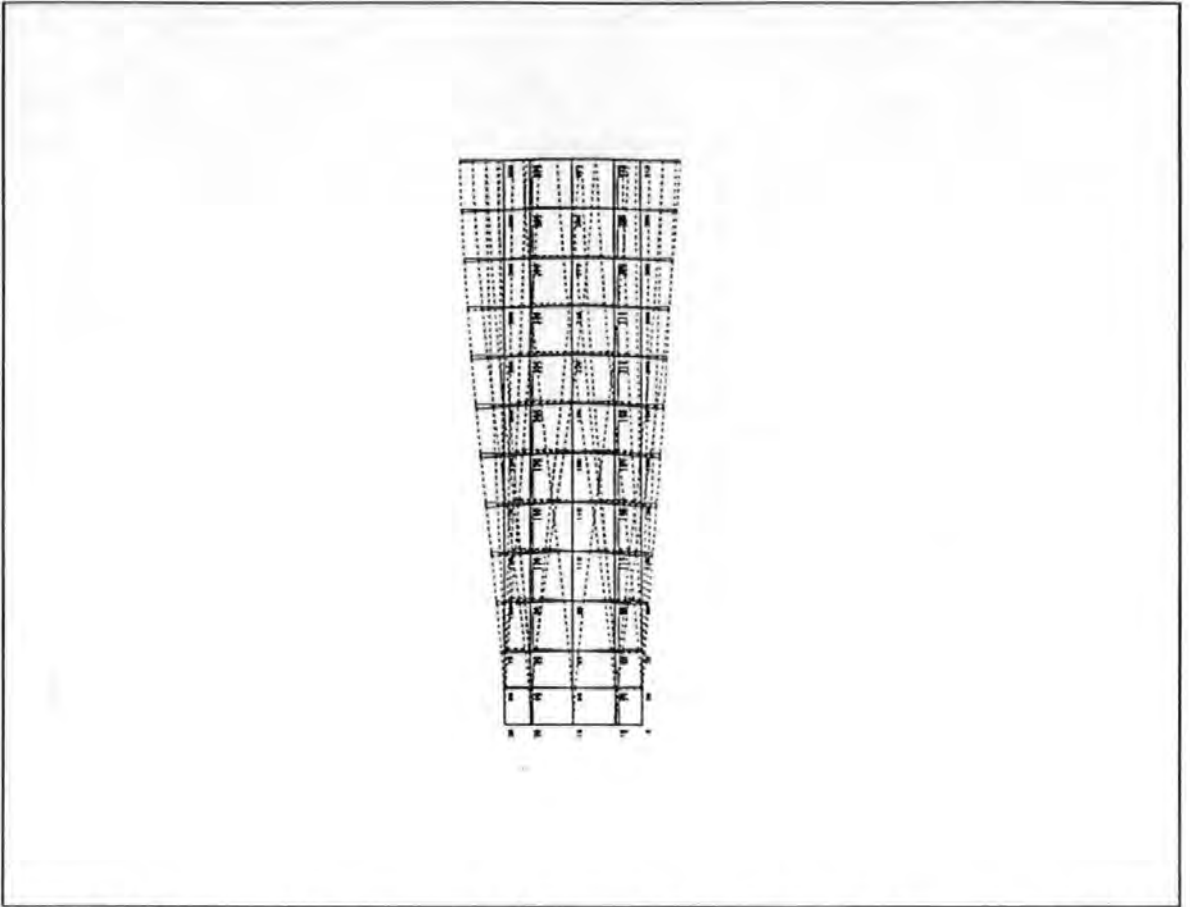


Figure 7.5-3b A side view of the T1 mode from the finite element model of the BR building.

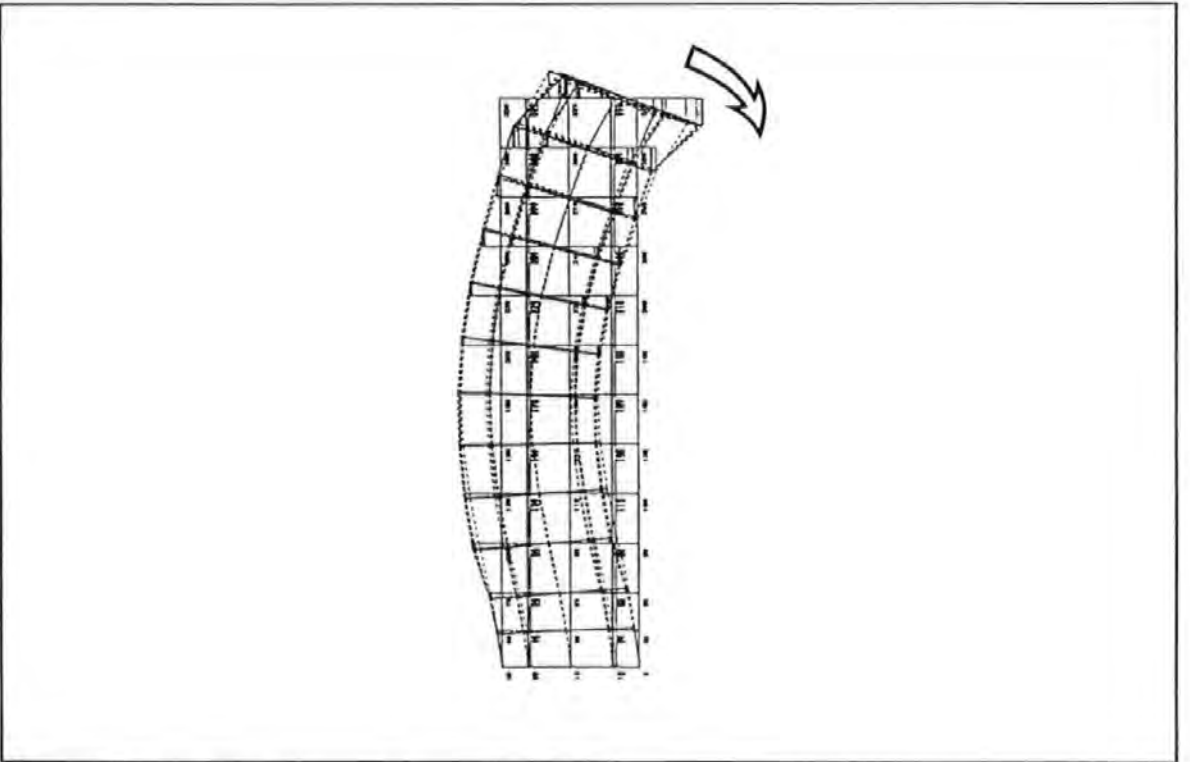


Figure 7.5-4 The EW2 mode from the finite element model of the BR building.

7.6 COMPARISONS OF EXPERIMENTAL AND ANALYTICAL RESULTS

The resonance frequencies of the modes determined from the experiment and the undamped natural frequencies from the finite element model are summarized in Table 7.6-1.

TABLE 7.6-1. THE TABLE OF COMPARISON OF THE VALUES OF THE RESONANCE FREQUENCIES OF THE VARIOUS MODES FROM EXPERIMENTS AND THE UNDAMPED NATURAL FREQUENCIES FROM THE FINITE ELEMENT MODEL.

VIBRATION MODES	EXPERIMENTAL RESONANCE FREQUENCY (Hz)	FINITE ELEMENT UNDAMPED NATURAL FREQUENCY (Hz)
NS1	1.17	1.112
EW1	1.32	1.481
T1	1.558	3.289
EW2	5.60	6.455

Generally speaking, both the frequency values and the mode shapes obtained via the experimental and analytical means are in broad agreement. There are some interesting observations to be gleaned from these results. Firstly, all the mode shapes show that the floors remain planar as anticipated from the assumptions made. Secondly, the values of the natural frequencies of all the modes from the finite element model are as higher than the corresponding experimental ones. This is possibly a direct result of the over-stiff horizontal elements assumed. Thirdly, the mode shape of EW1 is very close to the straight line approximation as suggested by Jeary and Sparks^[2.39] and reviewed in Section 2.1.2.3. Finally, the node of the EW2 mode in the finite element model occurs between the 8th and the 9th Floor which agrees with its experimental counterpart.

7.7 SUMMARY

Ambient vibration test technique has rather limited value as far as identification is concerned because the input excitation cannot be measured. Generally, the measured signals (acceleration response) were noisy as reflected by having very low values in the coherence spectra obtained from the experiments carried out. Identifying the appearance of a mode using the criteria of a peak in the autospectra of response is not conclusive. Also very long recording time is required to improve confidence levels of random signals. During the long hours of measurement, undue disturbance can happen and cause disruptive effect as far as accuracy is concerned.

Exciter-induced vibration test using a SS or PRBS forcing functions is more useful. However, the level of response obtained may not be as high as its ambient counterparts. SS test is in general very time intensive. The PRBS test is a better technique for field testing as far as the time saving is concerned. With good care in carrying out the signal processing : sampling, filtering, windowing, averaging etc, a PRBS test can produce very good results. This was reflected by the higher values in the coherence spectra obtained from the experiments carried out.

For common building structures, the natural frequencies and mode shapes recommended by the various design literature are close approximations to the experimental ones. They can be used as estimates if no other experimental data is available.

The FE modelling of the BR building carried out was very demanding on the computing resources in carrying out the calculations and producing the analytical results. In general, the undamped natural frequencies from the FE models are close to but consistently higher than the experimental ones. However, the order of occurrence of the analytical modes (in ascending order of their natural frequency values) are the same as the experimental ones.

CHAPTER 8

FULL SCALE FORCED VIBRATION TESTS OF A FIRE STATION DRILL TOWER

8.1 INTRODUCTION

This chapter reports the results of full scale forced vibration tests conducted on a six storey fire station drill tower. These tests were similar in many respects to those reported in chapter 7 except that the size of this structure was much smaller and more extensive measurements were carried out with the use of the CAT described in Chapter 4. Also much larger amplitudes of response were obtained using the same shaker.

8.2 DESCRIPTION OF THE STRUCTURE

The tower is situated at Camel's Head Fire Station, Plymouth and used for fire fighting training. This structure is simpler in structural form when compared to the BR building but accurate structural modelling of this structure is by no means a trivial task. Structurally, it can be treated as a reinforced concrete frame with most openings partly infilled with brick walls. The uncertainty regarding the interactions between these walls and the frame accounts for some of the modelling difficulties. Figure 8.2-1 gives a photographic view of the structure.

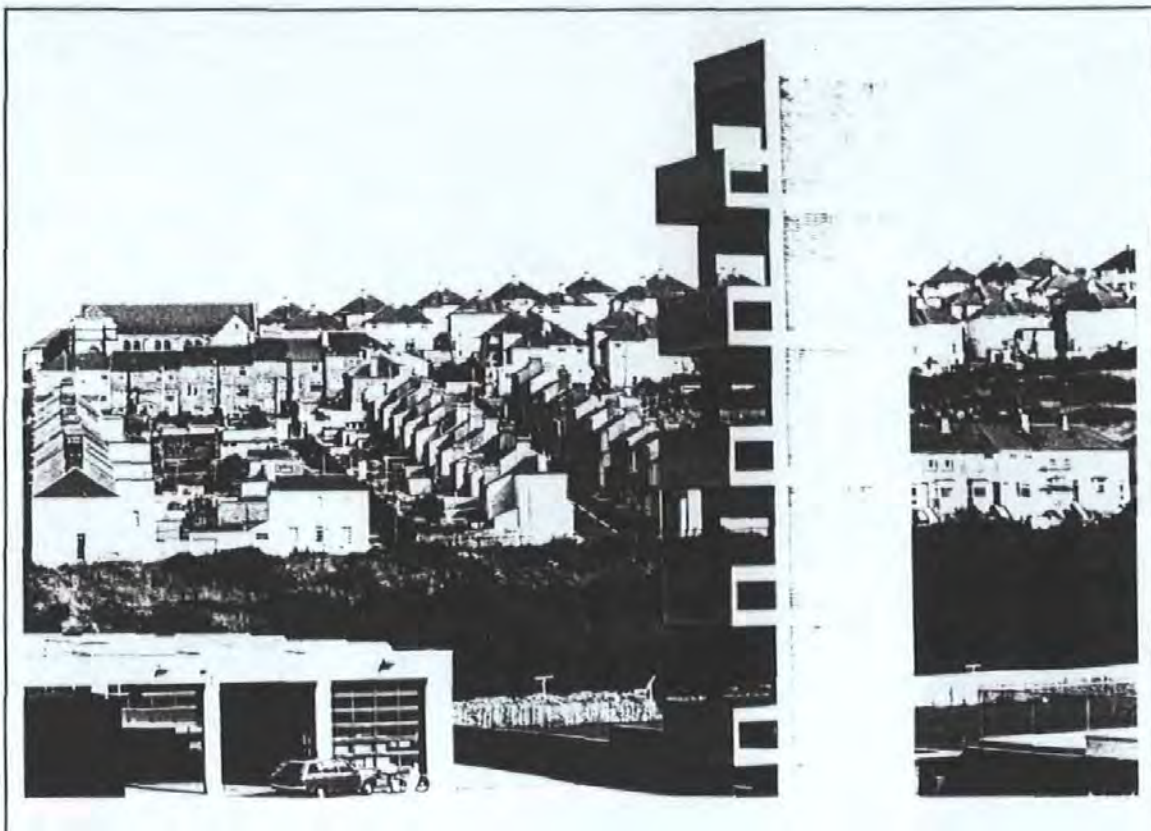


Figure 8.2-1 A distant photographic view of the Camel's Head Fire Drill Tower, Plymouth

8.3 TEST ARRANGEMENTS AND PROCEDURES

Again the exciter was located as high up on the structure as possible. In this case, the exciter and the test equipment was placed on the fifth floor. The exciter was secured on the floor slab using the same technique as those used in the BR building. Because of very restrictive access, there were considerable difficulties in getting the equipment to this level. Eventually, this problem was overcome with the use of a fire-fighting hydraulic platform, courtesy of the Devon and Cornwall Fire Service.

Mains electrical power in the tower could only be obtained from the power points in the nearby station via very long extension cables. Voltage drop and power loss caused some difficulties in operating the electrical equipment. Furthermore, the weather condition was at times very undesirable. Temporary shelter had to be provided to protect the equipment from damage. This, once again, highlights the difficult circumstances encountered in field testing not normally found in laboratory testing.

The location of the exciter is shown in Figure 8.3-1. Two test series were carried out, each with the exciter orientated in either one of the two principal axes. These two directions are designated as EW and NS as shown in Figure 8.3-1.

Acceleration response of the structure was measured at a set of pre-determined points. The horizontal positions of the four grid points are designated as A1, A2, B1 and B2, as shown in Figure 8.3-1. These arrangement of points repeated themselves for each of the floor level. An encoding system was used such that a point designated as 0A2 is referred as the point A2 on the ground level and so on.

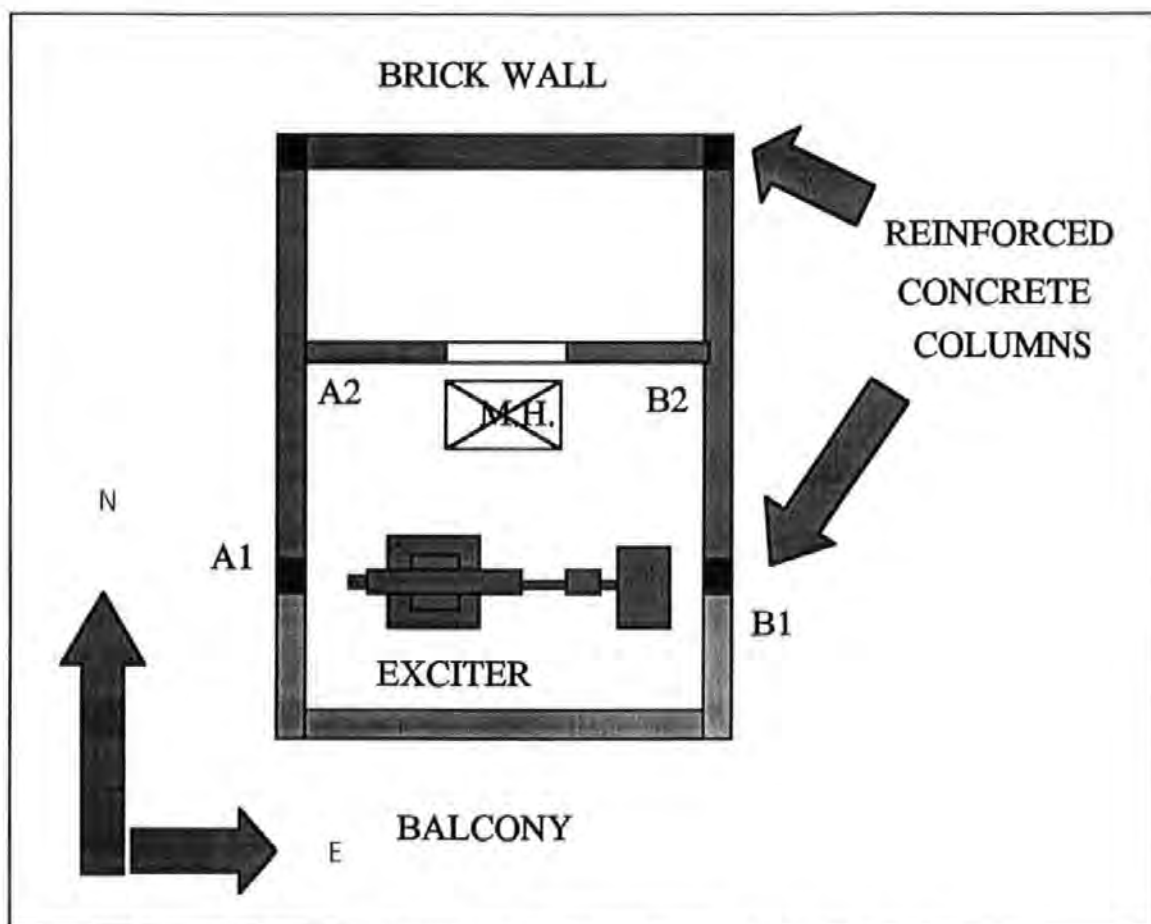


Figure 8.3-1 Location of the exciter and designation of the grid points.

Three roving accelerometers were positioned at each of the measuring locations: two accelerometers were aligned with their sensitivity axes horizontally along the EW and NS directions respectively, while the third one was aligned vertically. This arrangement enabled a measurement of the spatial translations of each of the twenty-four points. A reference accelerometer was fixed at one location, in this case at 5A1, to allow the plotting of *operating shapes* using the traditional technique (reported in Chapter 7).

The inertance and transmissibility measurements were obtained from tests carried out using Pseudo-Random-Binary-Sequence (PRBS) and Step-Sine (SS) excitation. As before, the SS tests with fine steps were only carried out for locating the resonance frequencies of the modes. The bulk of the inertance and transmissibility FRF measurements were taken using PRBS excitation. The spectrum analyzer used was set in the 25 Hz baseband when taking these measurements. This setting provided a frequency resolution of 0.2 Hz. A limited number of *zoom* measurements with a 0.04 Hz resolution were also taken. Inertance measurements were taken to provide data for modal parameter determination. Transmissibility measurements were taken to determine the operating shapes of the tower under the action of the shaker and at each of the tested frequencies.

Each test was encoded by a Test-Identification (TI) code which provide a unique reference to the location of measurement and other relevant test conditions. A schedule detailing the various test runs and the corresponding TI codes is given in Appendix 8.3.

8.4 TEST RESULTS

The success of incorporating the CAT produced a large collection of data which required quite elaborate data processing efforts involving desk-top PC as well as an IBM main frame computer. Only a representative sample of the results of this analysis is presented below. The results from the SS tests are given first and followed by those from the zoom PRBS tests. The results of the modal parameters determined using data from the 25 Hz baseband are also given.

Figures 8.4-1 to 8.4-5 show the typical modulus and phase inertance FRF plots obtained using the SS tests with small-steps. These test data were obtained with the exciter aligned in the EW direction and response measured at point 5A1.

In Figure 8.4-1, two very close peaks at frequencies 2.34 and 2.48 Hz (a mere 0.14 Hz gap between them) and other peaks at 5.4 and 10.3 Hz are detected. It is also noted that these peaks correspond to a 90 degree phase change at each of the corresponding peaks' frequencies.

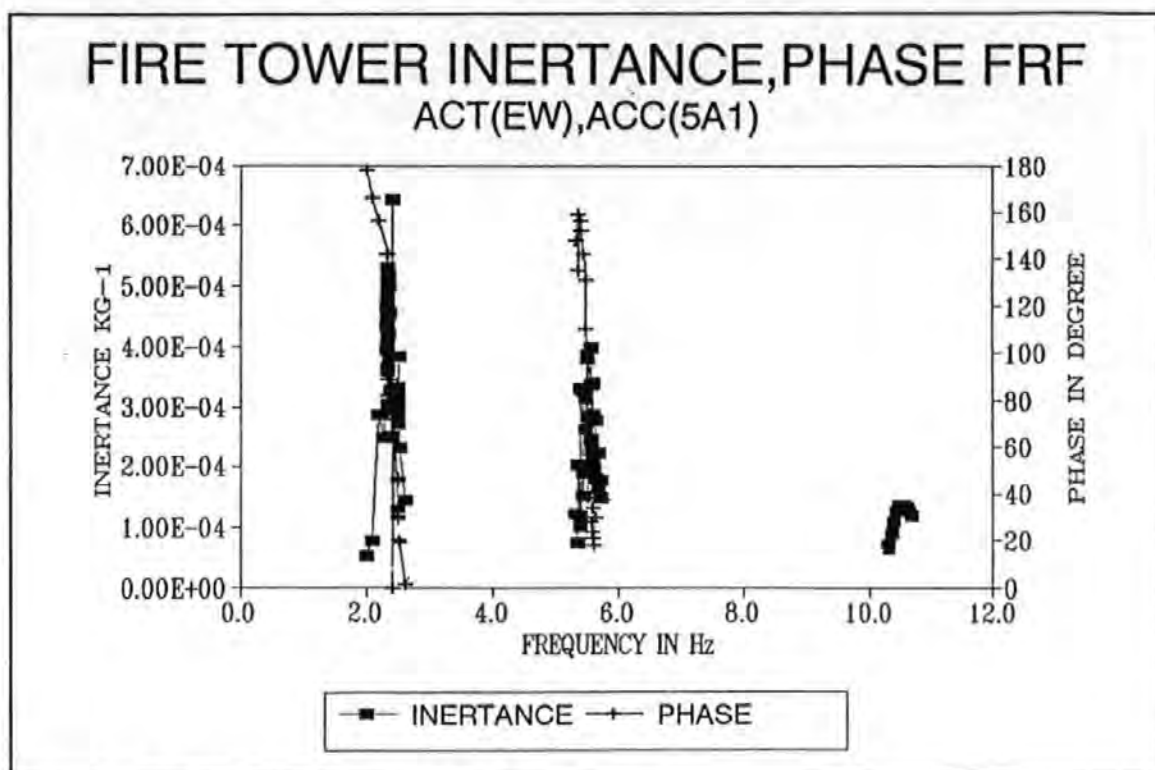


Figure 8.4-1 Modulus Inertance FRF plot using SS tests.

The changes of inertance and acceleration response levels with the increase in levels of excitation force at the two frequencies 2.34 and 2.48 Hz were determined and plotted in Figures 8.4-2a to 8.4-2b.

Each of the Figures 8.4-3a to 8.4-3c show a peak at frequency around 5.52, 5.56 and 5.4 Hz when excitation force amplitudes were 0.05, 0.10 and 0.15 KN (r.m.s) and the corresponding acceleration response amplitudes were 2,4 and 5 milli-g (r.m.s.) respectively (Note $1\text{ g} = 9.807\text{ m/s}^2$). In other words, the frequencies corresponding to the peaks fluctuate as force amplitudes change.

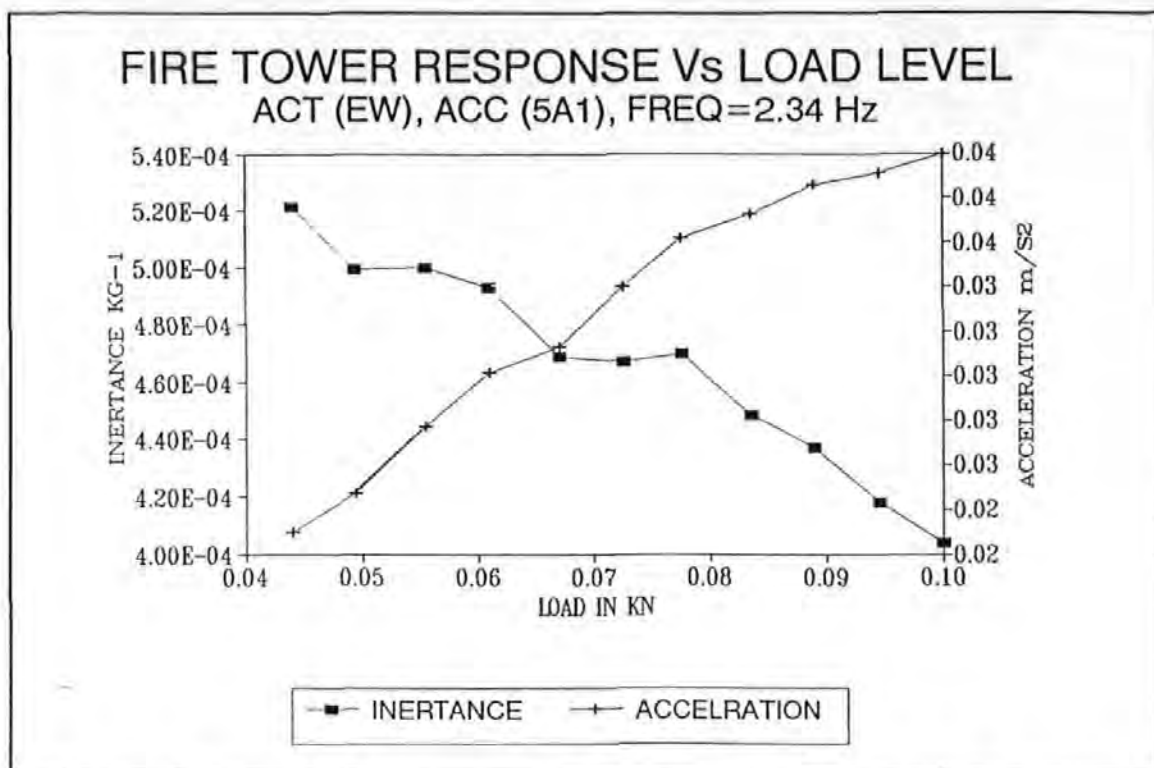


Figure 8.4-2a Change of acceleration and inertance of the mode at 2.34 Hz with increase magnitude of force using SS excitation.

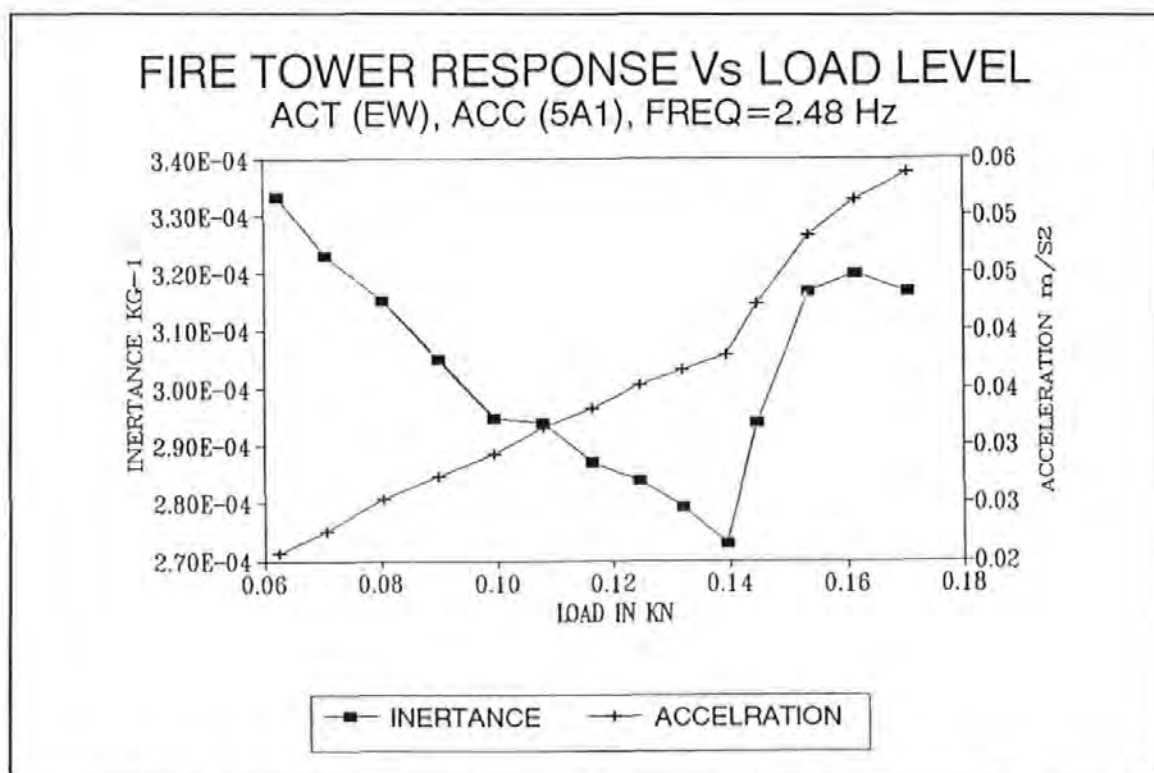


Figure 8.4-2b Change of acceleration and inertance of the mode at 2.48 Hz with increase magnitude of force using SS excitation.

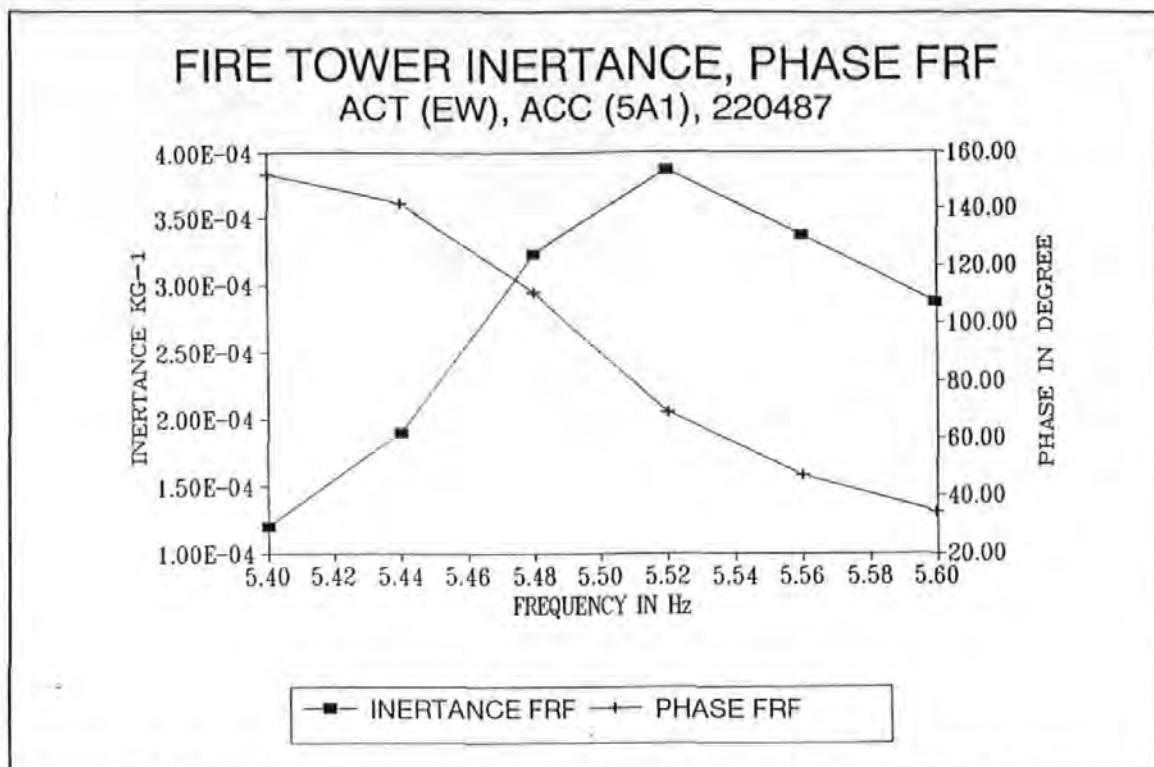


Figure 8.4-3a Modulus and phase inertance FRF plot using SS excitation. Measurement was made at 5A1 with exciter acting in the EW direction and force amplitudes of 0.05 KN (r.m.s.)

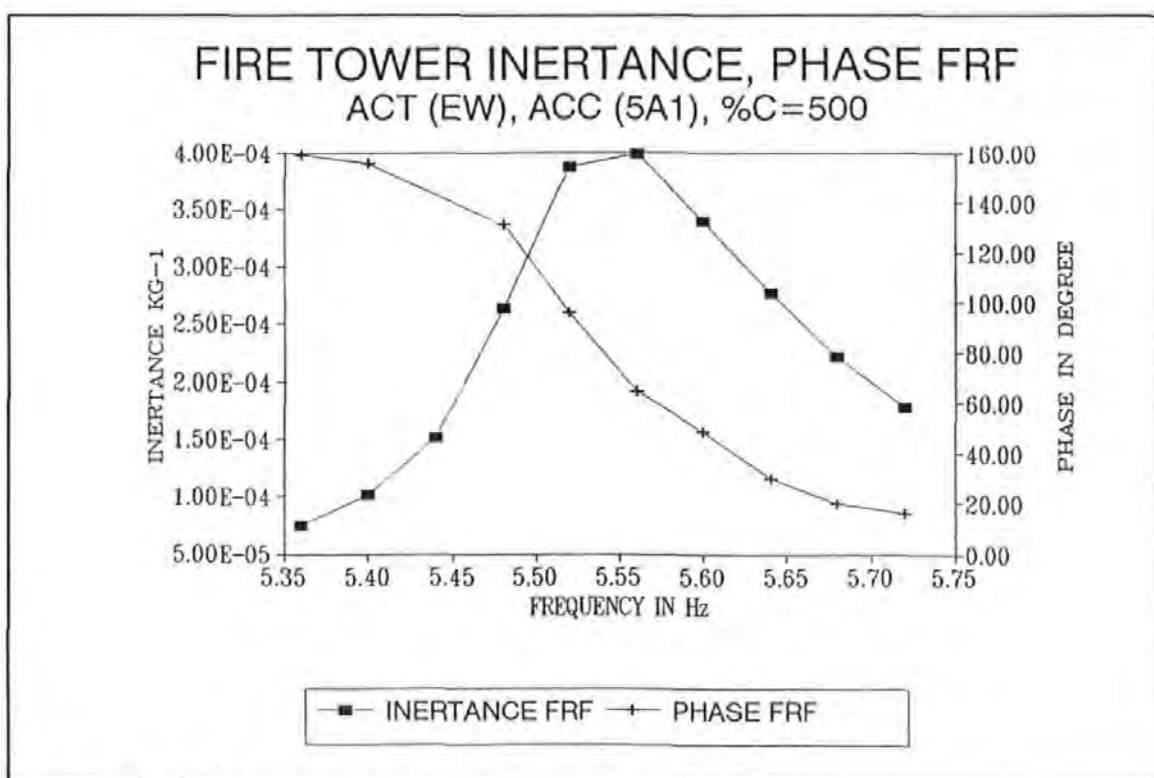


Figure 8.4-3b Modulus and phase inertance FRF plot using SS excitation. Measurement was made at 5A1 with exciter acting in the EW direction and force amplitudes of 0.1 KN (r.m.s.)

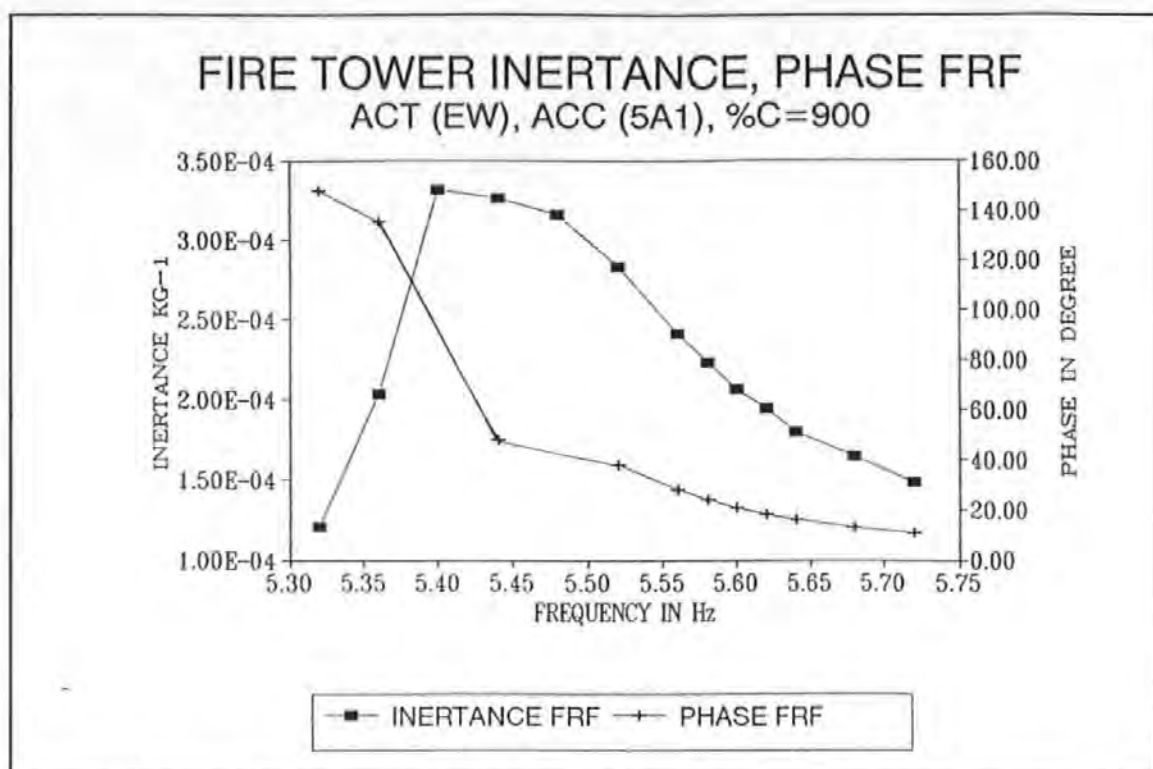


Figure 8.4-3c Modulus and phase inertance FRF plot using SS excitation. Measurement was made at 5A1 with exciter acting in the EW direction and force amplitudes of 0.15 KN (r.m.s.)

Figure 8.4-4 shows a peak at 10.48 Hz. With the exciter acting in the NS direction, the inertance FRF plots obtained are similar to those obtained from the EW direction as regarding the locations of the resonance peaks are concerned. Therefore, they are not to be shown here except the one plotted in Figure 8.4-5.

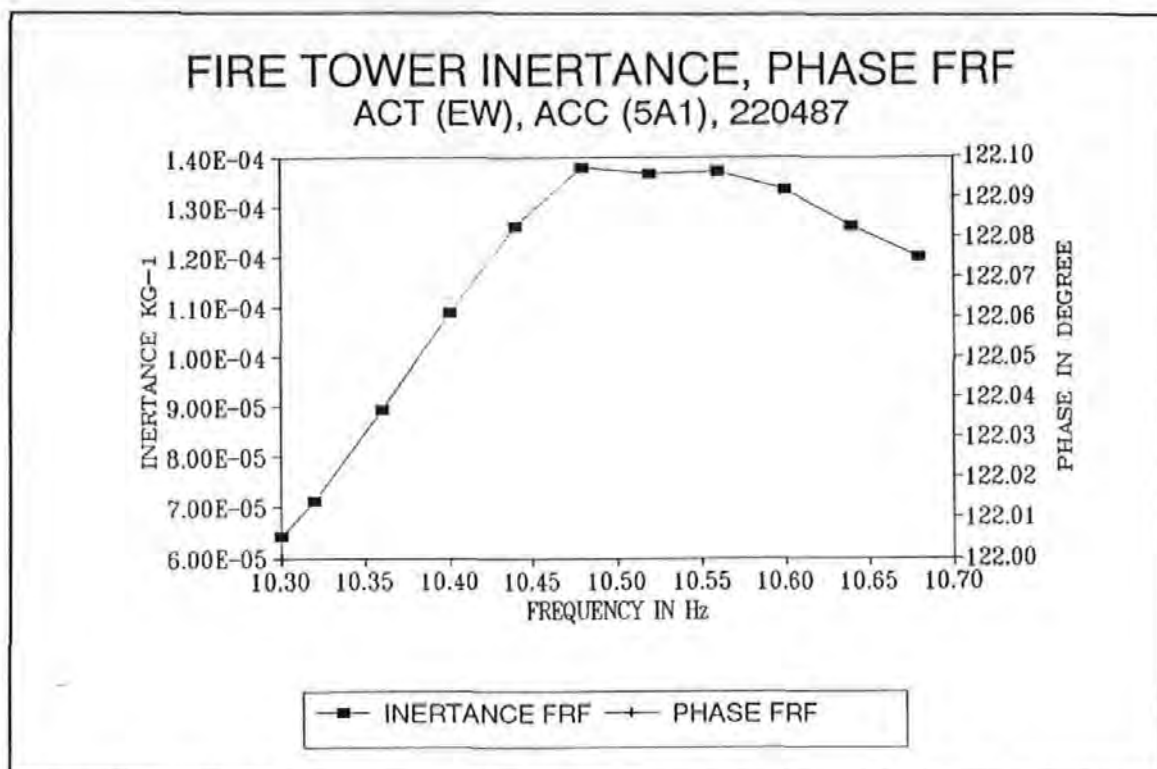


Figure 8.4-4 Modulus inertance FRF plot of the mode at 10.48 Hz using SS excitation. Measurement was made at 5A1 with exciter acting in the EW direction.

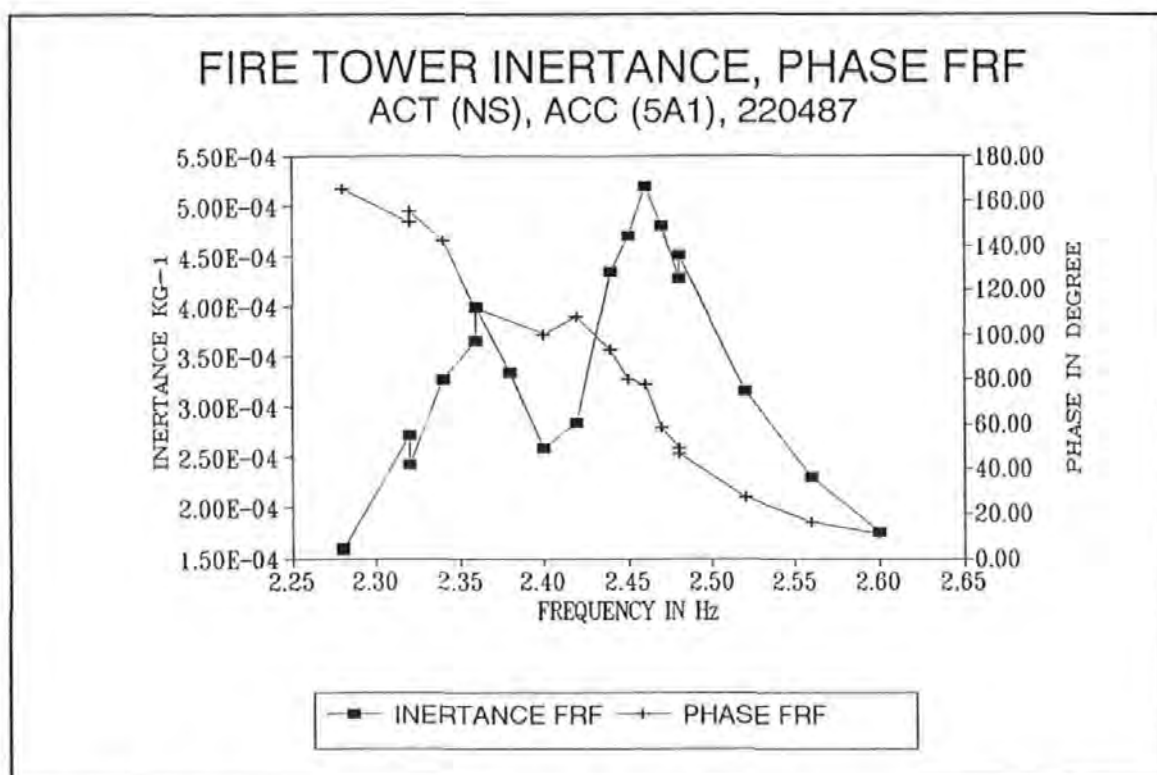


Figure 8.4-5 Modulus inertance FRF plot using SS excitation. Measurement was made at 5A1 with exciter acting in the NS direction.

Figure 8.4-5 shows again two very close peaks at 2.36 and 2.46 Hz. This observation agrees with those obtained by the EW excitation. Indeed, the results from the zoom analysis (with a resolution of 0.04 Hz) suggest that there are actually two very close modes: one with a natural frequency at 2.328 Hz and the other at 2.416 Hz (as identified by the algorithm). It is not just the one peak as appeared in all the other measurements taken with a 0.2 Hz resolution. It is clear that the 0.2 Hz resolution, used in the PRBS tests, is not fine enough. However, this is considered a necessary trade-off between resolution and time needed for taking measurements. This 25 Hz baseband setting is necessary in order that all the required measurements can be completed within the short time allowed.

Figures 8.4-6a to 8.4-6c show the inertance FRF spectra taken from the zoom measurements at 5A1, with centre frequencies fixed at 2, 5 and 10 Hz respectively. In these tests, the exciter was orientated in the EW direction. The corresponding phase inertance spectra are also plotted between 0 and 360 degrees as shown. The results of the analysis are also summarized in Table 8.4-1.

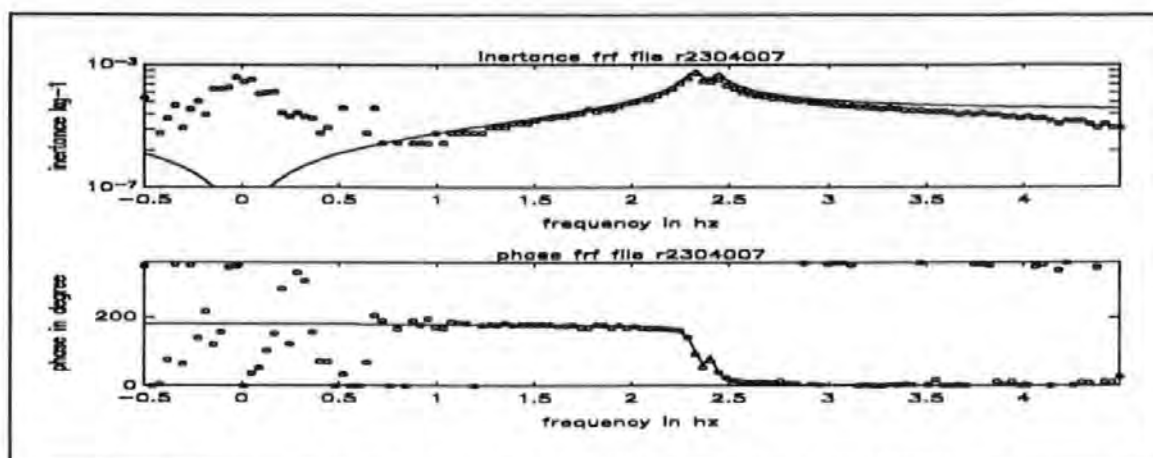


Figure 8.4-6a Inertance FRF spectra from PRBS (EW) test (TI R2304007) zooming in at 2 Hz.

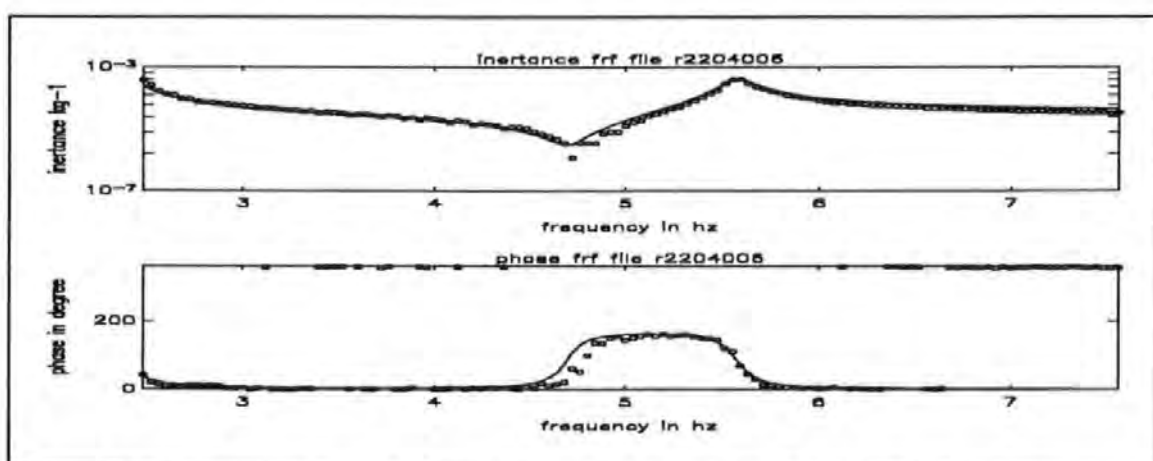


Figure 8.4-6b Inertance FRF spectra from PRBS (EW) test (TI R2204006) zooming in at 5 Hz.

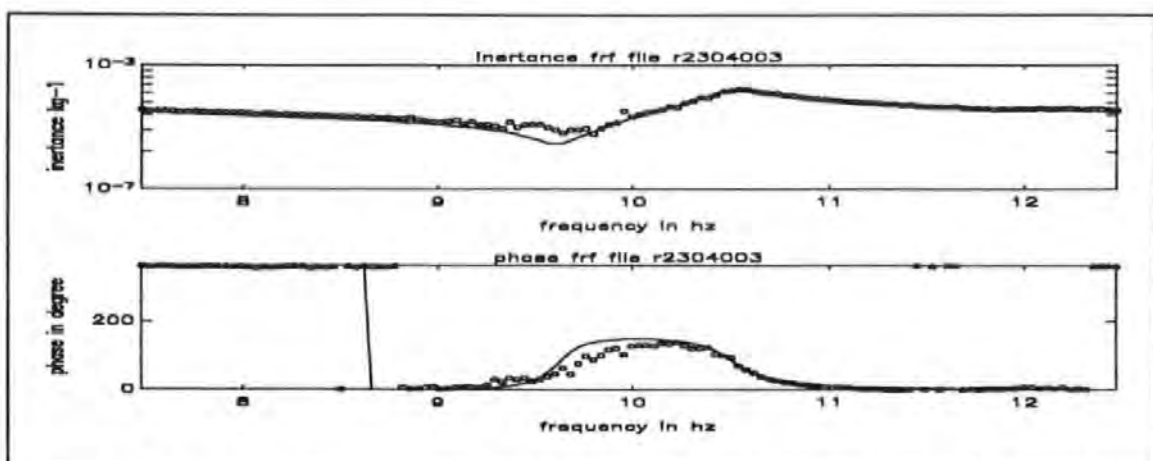


Figure 8.4-6c Inertance FRF spectra from PRBS (EW) test (TI R2304003) zooming in at 10 Hz.

Table 8.4-1: ZOOM ANALYSIS WITH A RESOLUTION OF 0.04 HZ (EW EXCITATION)

TEST RUN TI	NATURAL FREQ (Hz)	DAMPING	MODAL CONST (Kg ⁻¹)	MODE	NOTE
R2304007	2.333	1.478e-2	1.887e-5	EW1	%C=1000
R2304007	2.429	9.045e-3	8.829e-6	NS1	%C=1000
R2304001	2.311	1.503e-2	1.598e-5	EW1	%C=300
R2304001	2.408	9.064e-3	7.061e-6	NS1	%C=300
R2204005	5.597	1.258e-2	9.333e-6	T1	NA
R2204006	5.581	1.361e-2	1.118e-5	T1	%C=300
R2204008	5.528	1.272e-2	9.400e-6	T1	%C=700
R2304002	5.578	1.305e-2	9.505e-6	T1	NA
R2304003	10.51	1.381e-2	4.444e-6	EW2	NA

Data from the tests R2304007 and R2304001 were obtained with the attenuator dial set at 1000 and 300 (%C values) respectively. The %C values are readings on the 10-turns attenuator dial in the DARTEC control panel. This dial attenuates the input driving signal fed to the control panel. A %C value of 1000 denotes zero attenuation and a %C value of 0 denotes full attenuation.

The modal parameter analysis carried out was able to identify the two very close modes as given in Table 8.4-1. It appears, at least based on these results, that at higher force level (i.e. higher %C setting), resonance frequencies and modal damping factors of the two modes change slightly but the magnitudes of the change are considered to be too small to conclude any trend.

The tests R2204005, R2204006, R2204008 and R2304002 are all able to identify the T1 mode. Results based on these data have also indicated the change of modal parameters at different force levels. Again, the change in values are considered to be too small to speculate any particular trend at all.

Similarly, Figures 8.4-7a to 8.4-7e show the inertance FRF spectra from the zoom measurements taken at 5A1 with centre frequencies set at 2, 5, 10, 17 and 25 Hz respectively. In these tests, the exciter was acting in the NS direction.

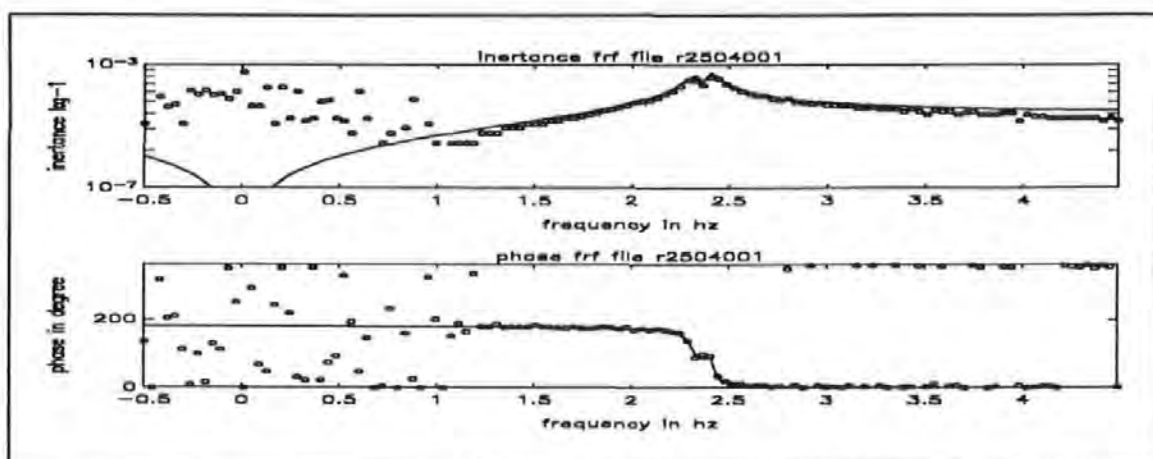


Figure 8.4-7a Inertance FRF spectra from PRBS (NS) test (R2504001) zooming in at 2 Hz.

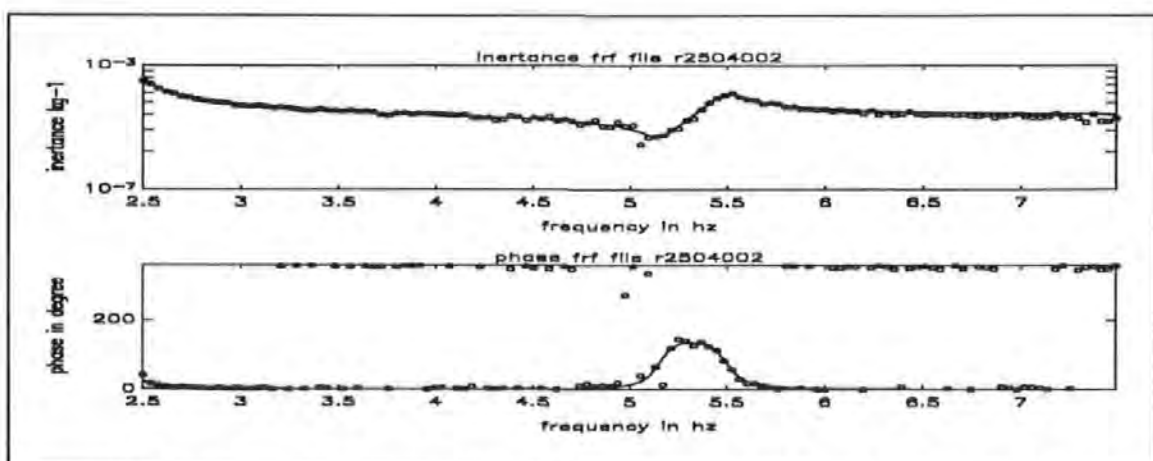


Figure 8.4-7b Inertance FRF spectra from PRBS (NS) test (R2504002) zooming in at 5 Hz.

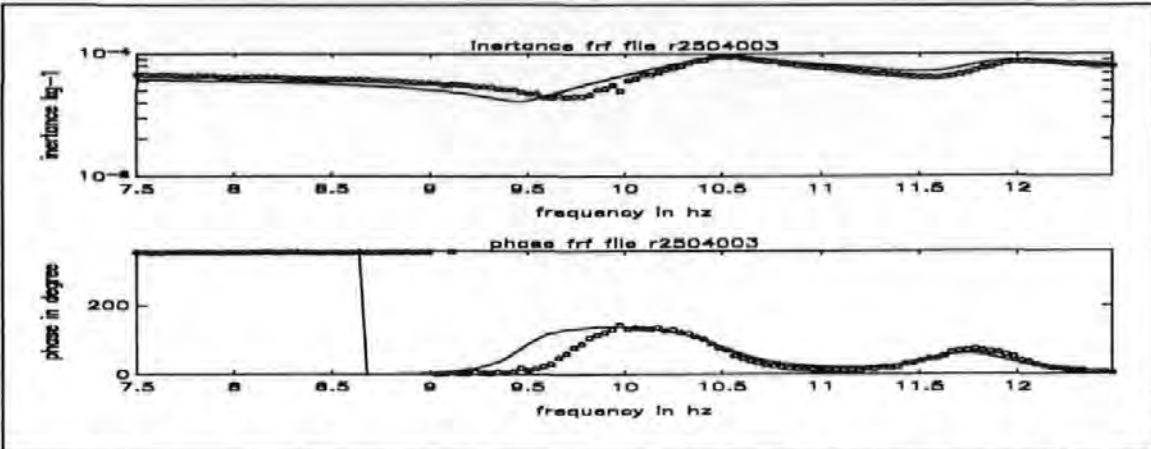


Figure 8.4-7c Inertance FRF spectra from PRBS (NS) test (R2504003) zooming in at 10 Hz.

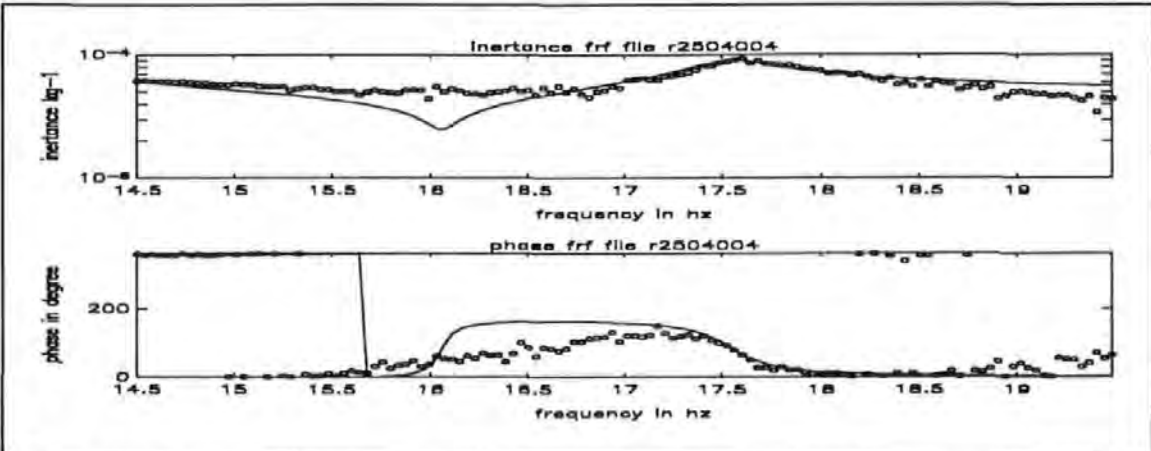


Figure 8.4-7d Inertance FRF spectra from PRBS (NS) test (R2504004) zooming in at 17 Hz.

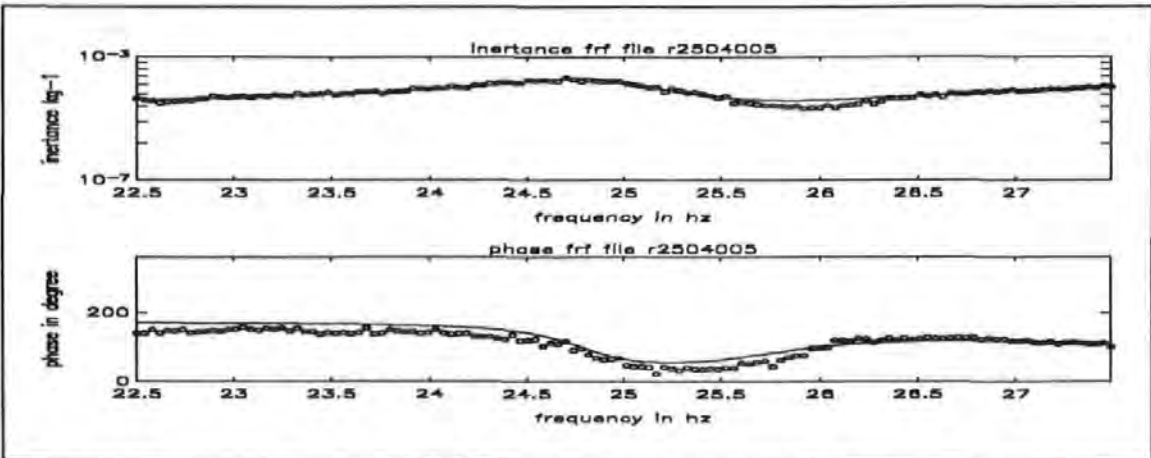


Figure 8.4-7e Inertance FRF spectra from PRBS (NS) test (R2504005) zooming in at 25 Hz.

The results of the analysis using these data are summarized in Table 8.4-2.

Table 8.4-2: ZOOM ANALYSIS WITH A RESOLUTION OF 0.04 HZ (NS EXCITATION)

TEST RUN	NATURAL FREQ	DAMPING	MODAL CONST	MODE
TI	ω_r (Hz)	ξ_r	G_r (Kg ⁻¹)	
R2504001	2.328	1.730E-002	1.463E-005	EW1
R2504001	2.4151	8.614E-003	8.903E-006	NS1
R2504002	2.443	1.451E-002	1.869E-005	NS1
R2504002	5.496	1.315E-002	3.132E-006	T1
R2504003	10.470	1.453E-002	2.208E-006	EW2
R2504003	11.797	2.970E-002	2.847E-006	NS2
R2504004	17.55	9.149E-003	1.222E-006	T2
R2504005	24.769	1.172E-002	4.298E-006	NS3
R2504005	28.138	7.429E-002	1.597E-005	unclassify

In all, the results from the zoom measurements show that very good agreement between the experimental and regenerated curves is able to obtain in all the cases shown. This is due to the 5 times enhancement in the resolution: from 0.2 to 0.04 Hz. Curves plotted with circles and solid curve denote the experimental and regenerated curves respectively so that the two curves do not obscure each other when overlaid.

A small sample of the Inertance FRF spectra obtained are given below. All these spectra were taken in the 0 to 25 Hz baseband. Figures 8.4-8a and 8.4-8b show the modulus and phase spectra obtained from the grid point at 5A1 while the shaker was aligned along the EW direction.

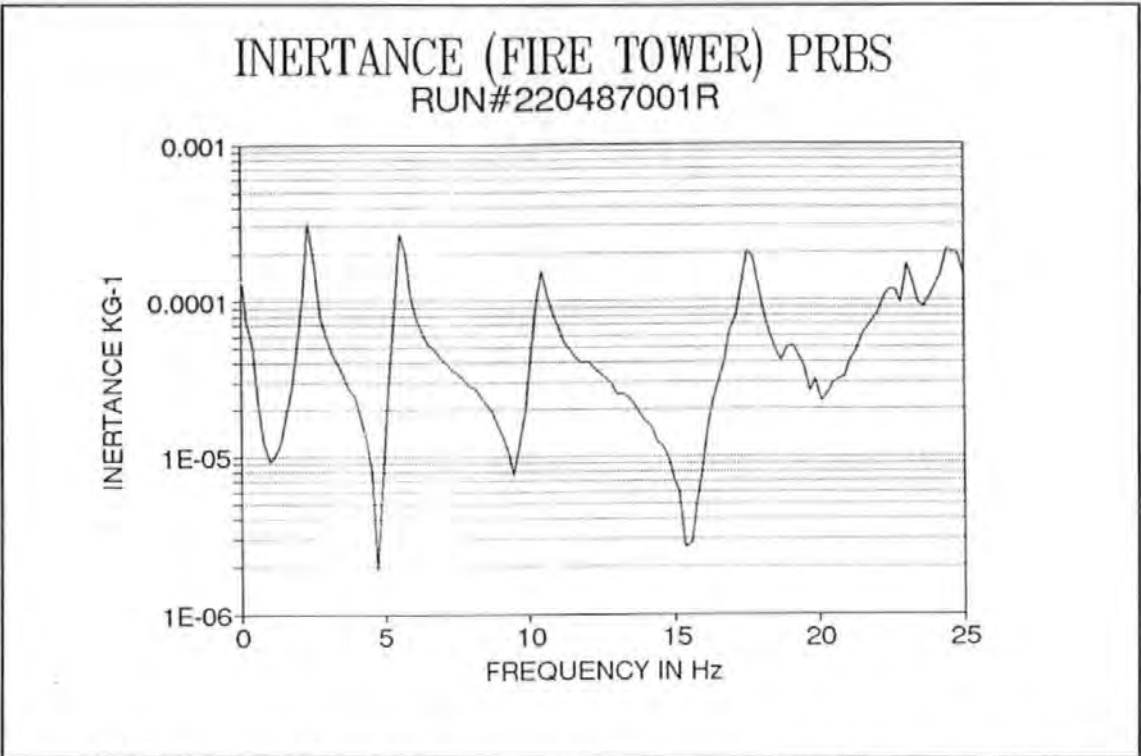


Figure 8.4-8a The modulus FRF spectra obtained from the grid point at 5A1 while the shaker was aligned along the EW direction.

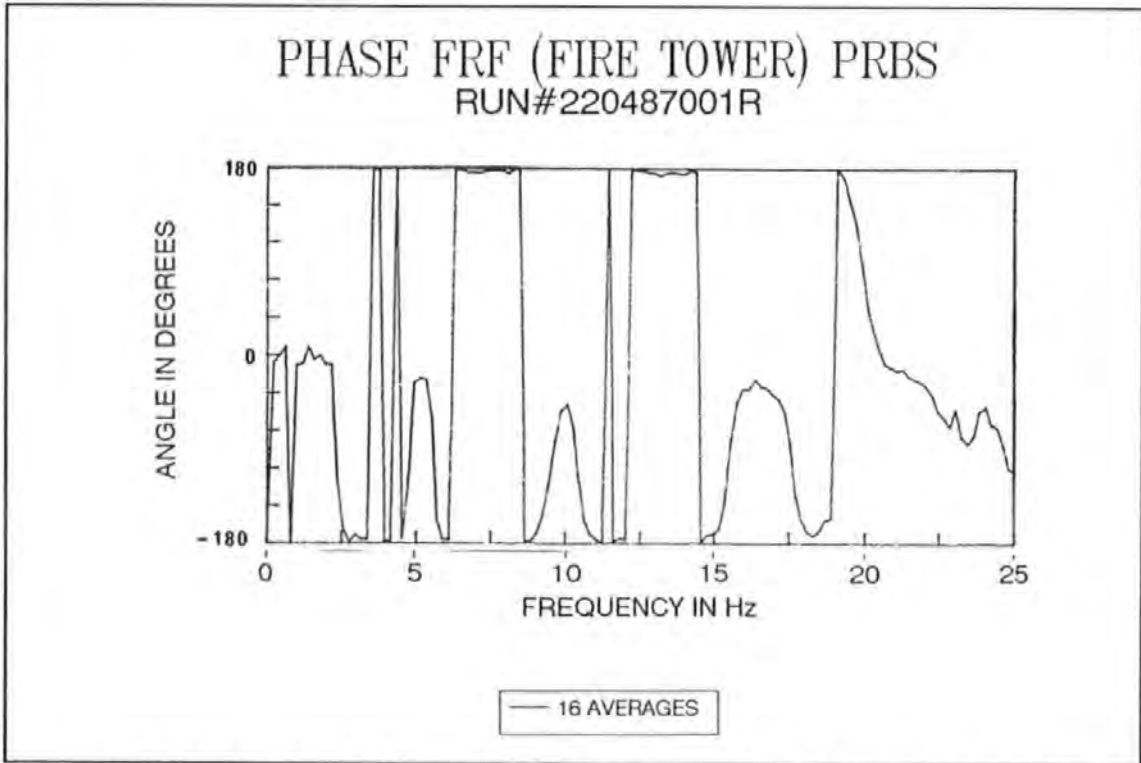


Figure 8.4-8b The phase FRF spectra obtained from the grid point at 5A1 while the shaker was aligned along the EW direction.

Figure 8.4-8a shows that, in general, quite distinctive resonance peaks occur at frequencies below 17 Hz. But at higher frequencies, modes are heavily 'cramped' together. Because of the dense presences of modes, analyses carried out in the high frequency range will be difficult.

The typical procedures in carrying out the extraction process, using the algorithm/program described in Chapter 5, is detailed below. First of all, the peaks in the Inertance modulus plot (the upper curve in Figure 8.4-9) were detected by visual inspection of the plot. A resonance mode is indicated by the occurrence of a peak in the modulus and the Imaginary Inertance plot (the lower curve in Figure 8.4-9). The frequencies corresponding to each of the peaks were marked with a vertical line. Then the number of data points on either side of the marked frequencies were chosen for curve fitting. Because of the coarse frequency resolution in the data, a small number of points was found to give better results. If too many points were chosen, it was more likely that some of these data points would render the assumptions made in deriving the algorithm being violated. A total of 7 modes were detected, analyzed and their associated modal parameters determined.

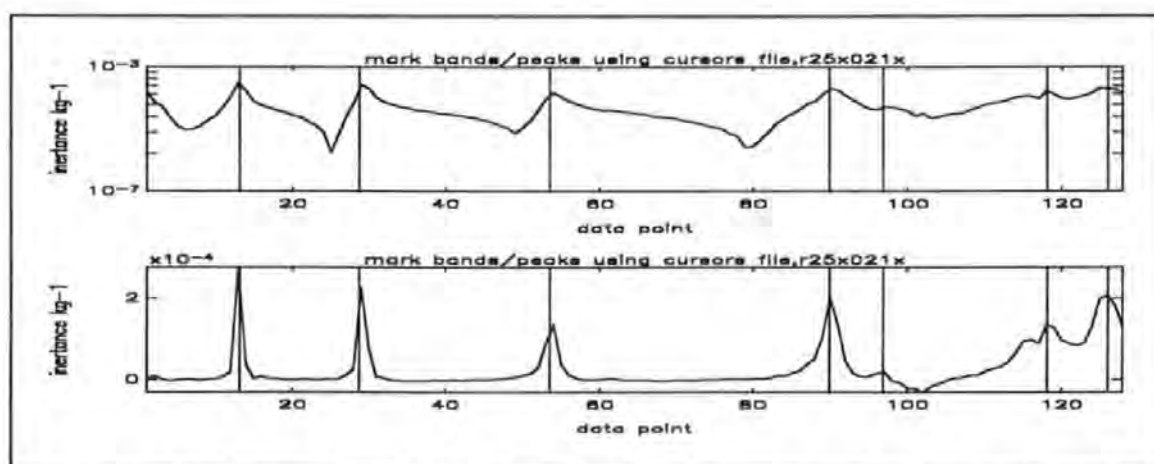


Figure 8.4-9 Marking resonant mode positions at the peaks in the Modulus or Imaginary Inertance FRF spectra.

The experimental and regenerated inertance FRF curves are plotted in Figure 8.4-10 for appraisal. Based on the data from the test R25X021X, a good correlation between the two curves is found, especially in the modulus plot. A close examination shows that although the phases near resonance are correctly determined, those near the anti-resonance regions (i.e. between consecutive peaks) are not. This is thought to be due to poor signal-to-noise-ratio of measured signals in these regions.

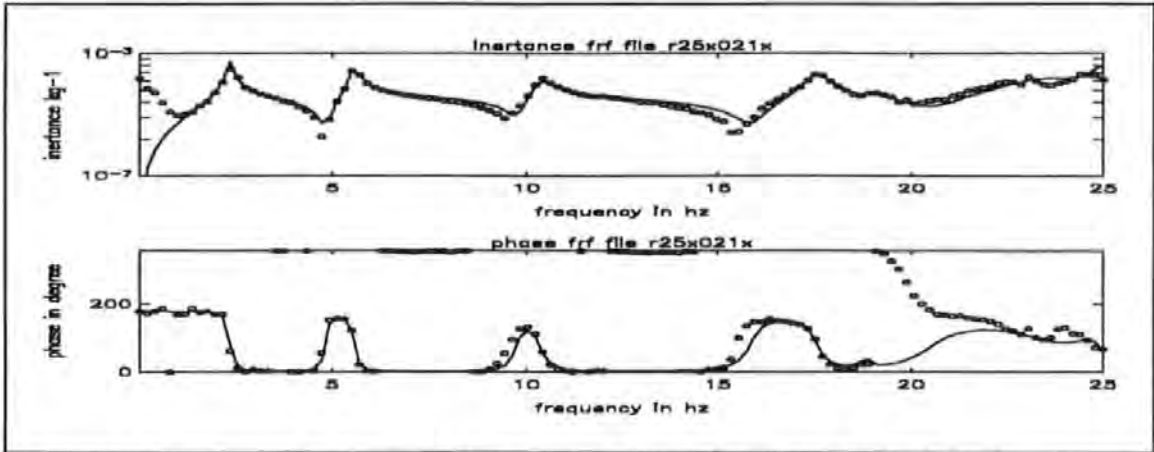


Figure 8.4-10 Inertance FRF spectra from PRBS test (R25X021X)

Figure 8.4-11 shows the data and result from the test R25Y023Y (i.e. data taken at grid point 5B2 with the exciter and the accelerometer both aligned in the NS direction). Again similar comments made for Figure 8.4-10 still apply. It is noticed that the phases measured between the peaks are quite erratic. This observation has reinforced the acute requirement for precise phase measurement.

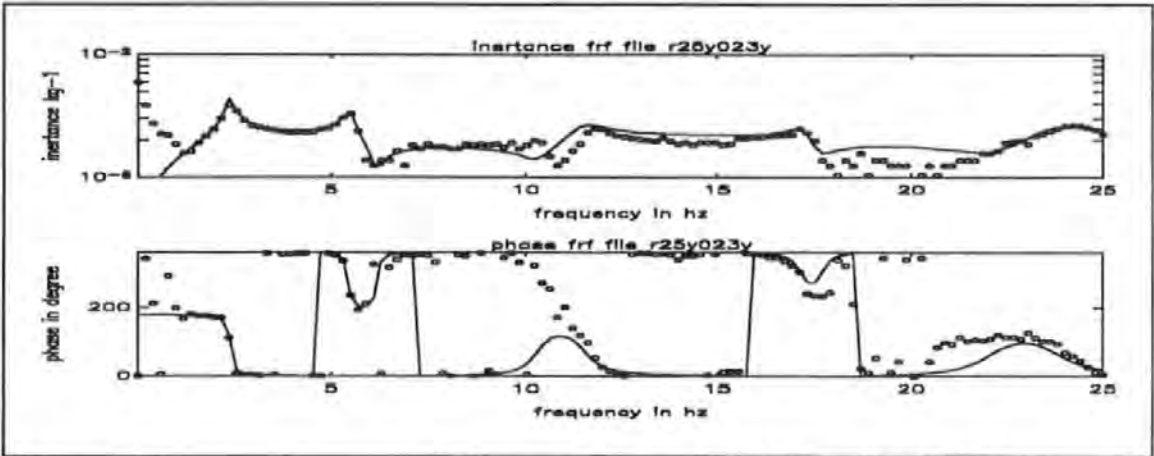


Figure 8.4-11 Inertance FRF spectra from PRBS test (R25Y023Y)

Figure 8.4-12 show the data and result from the test R25Y021X (i.e. data taken at grid point 5A1 with the exciter and the accelerometer both aligned in the EW direction)

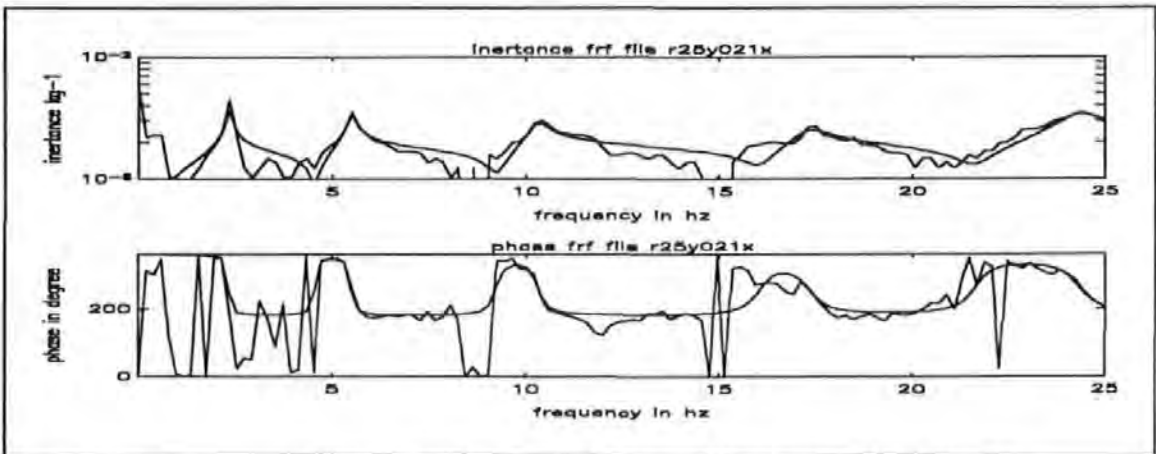


Figure 8.4-12 Inertance FRF spectra from PRBS test (R25Y021X)

Figure 8.4-13 show the data and result from test R25Y017Y (i.e. data taken at grid point 4A1 with the exciter and the accelerometer both aligned in the NS direction)

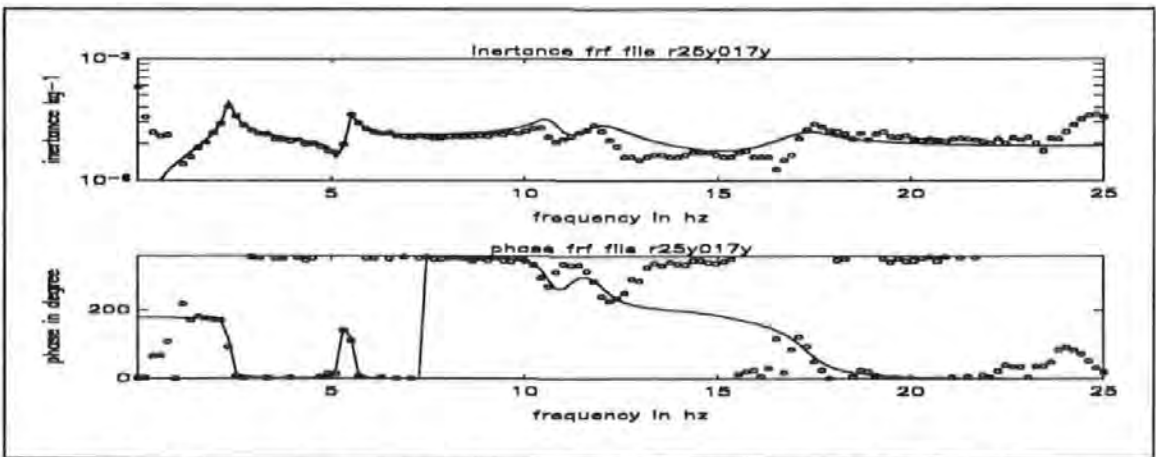


Figure 8.4-13 Inertance FRF spectra from PRBS test (R25Y017Y)

Figure 8.4-14 show the data and result from the test R25Y001Z (i.e. data taken at grid point 0A1 with the exciter aligned in the NS direction and the accelerometer aligned in the Vertical direction) It is noted that even on the ground level, the vertical responses due to some of the lower frequency modes are still very prominent.

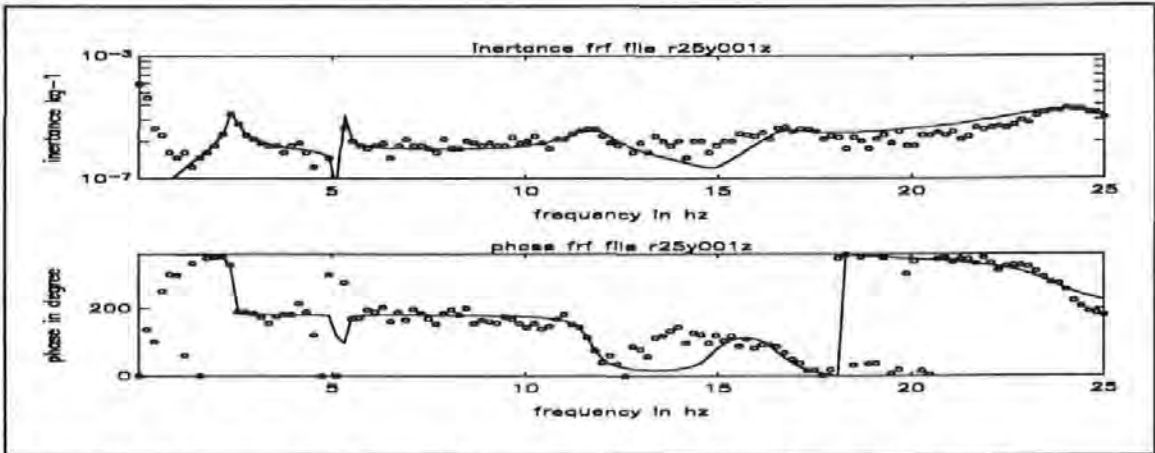


Figure 8.4-14 Inertance FRF spectra from PRBS test (R25Y001Z)

This curve-fitting procedure was repeated for all 144 inertance FRF spectra, each spectrum was similar to those exemplary spectra shown in Figures 8.4-10 to 8.4-14. After considerable and arduous efforts, a full set of modal parameters was obtained. A small extract of these results for a number of measurement points is given in Tables 8.4-3 to 8.4-11 at the end of this chapter.

In summary, the 2.36 Hz and 2.48 Hz modes cannot be properly resolved because the 0.2 Hz frequency resolution adopted in the test is inadequate. The natural frequencies and modal damping factors determined for each mode, from data obtained at different measuring locations, are generally in broad agreement but never identical as required by theory. This is in fact a common draw back of most SDOF methods. Because natural frequencies and modal damping factors are 'global' structural properties, they should be the same regardless of the location a measurement is taken. This property provide a useful criterion to cross check the quality of measurement data or the suitability of analysis methods. Judging from the data and the results obtained, both are deemed to have passed this check. In particular, the modal damping factors for the 5 modes determined are generally ranging between 1 to 4% which are well in line with the conventional damping values assumed for reinforced concrete structures.

The exemplary values of the natural frequencies and modal damping factors of the first 5 modes determined are summarized in Table 8.4-12.

Table 8.4-12 The exemplary values of the natural frequencies and damping factors of the first 5 modes.

VIBRATION MODES	NATURAL FREQUENCY Hz	DAMPING FACTORS %
EW1	2.34	1.2 to 2.2
NS1	2.48	1.2 to 2.2
T1	5.35	0.7 to 2.7
EW2	10.30	1.6 to 4.6
NS2	11.70	2.3 to 7.8

The complete set of modal parameters determined was used to plot the normalized normal mode shapes of each of the modes using the respective modal constant values (with due attention paid to their magnitudes and signs) at each measurement location. A mode shape (in physical term) or an eigenvector (in mathematical term) is non-dimensional and can be scaled arbitrarily. Hence the ratio of the modal constants determined at any two arbitrary spatial points on the structure gives the same ratio of the mode shape coordinates of the respective eigenvector corresponding to their spatial positions.

The axes in the mode shape plots are designated as follows: XX for EW, YY for NS and ZZ for vertical. The results determined from the EW test series are presented first then followed by those determined from the NS test series. Figure 8.4-15a shows that this mode is predominantly a swaying EW1 mode. The 4 grid lines along the Z direction are essentially straight lines. The floor slabs remain essentially flat and movements of the four points on the ground are small but detectable.

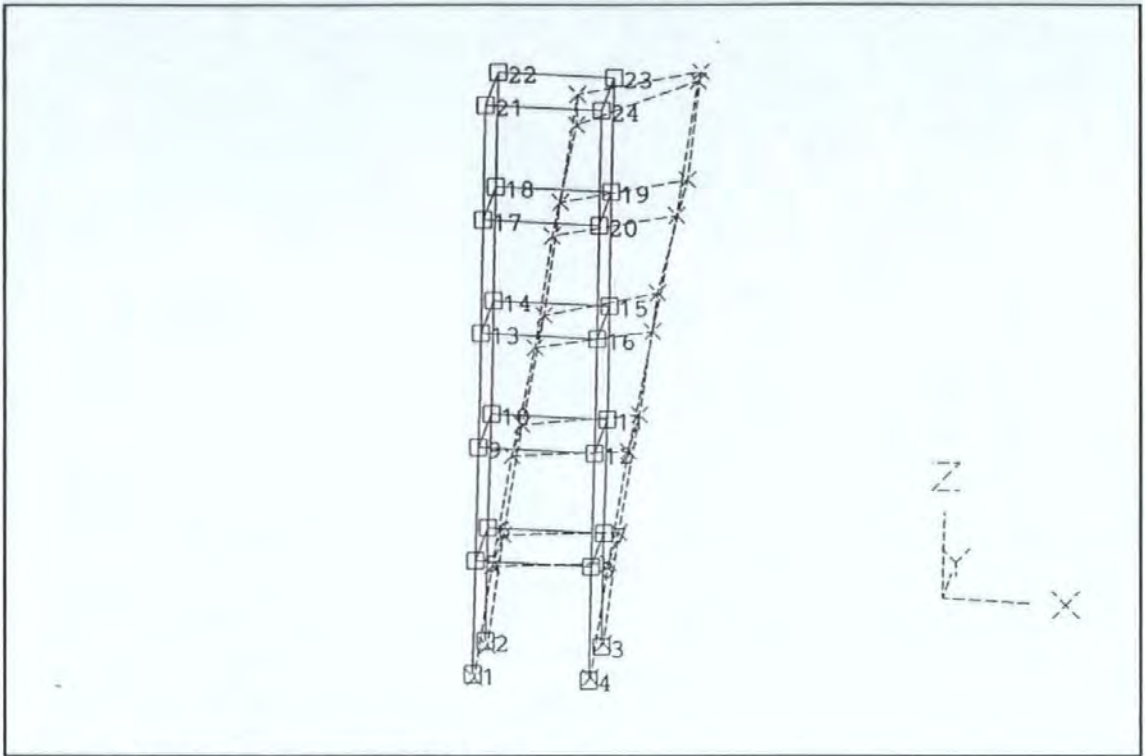


Figure 8.4-15a The swaying EW1 mode.

Figure 8.4-15b provides another view of the EW1 mode, it is clear that torsional movements of the points on the upper floors are also considerable.

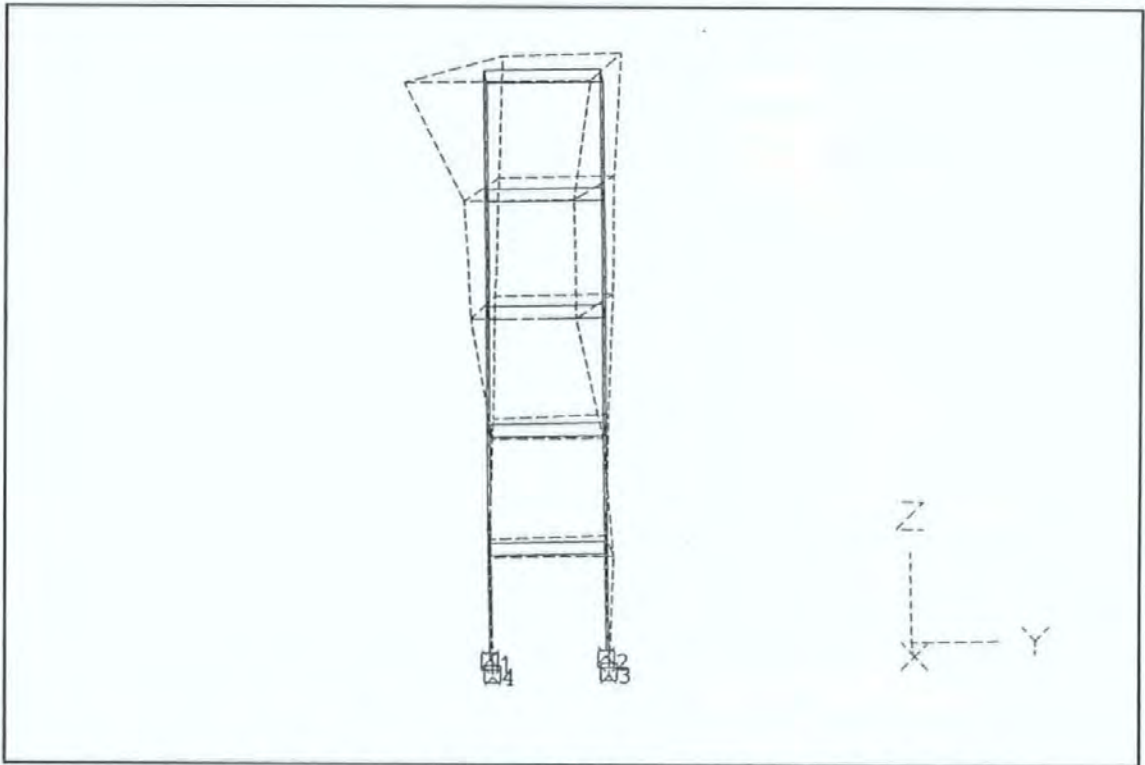
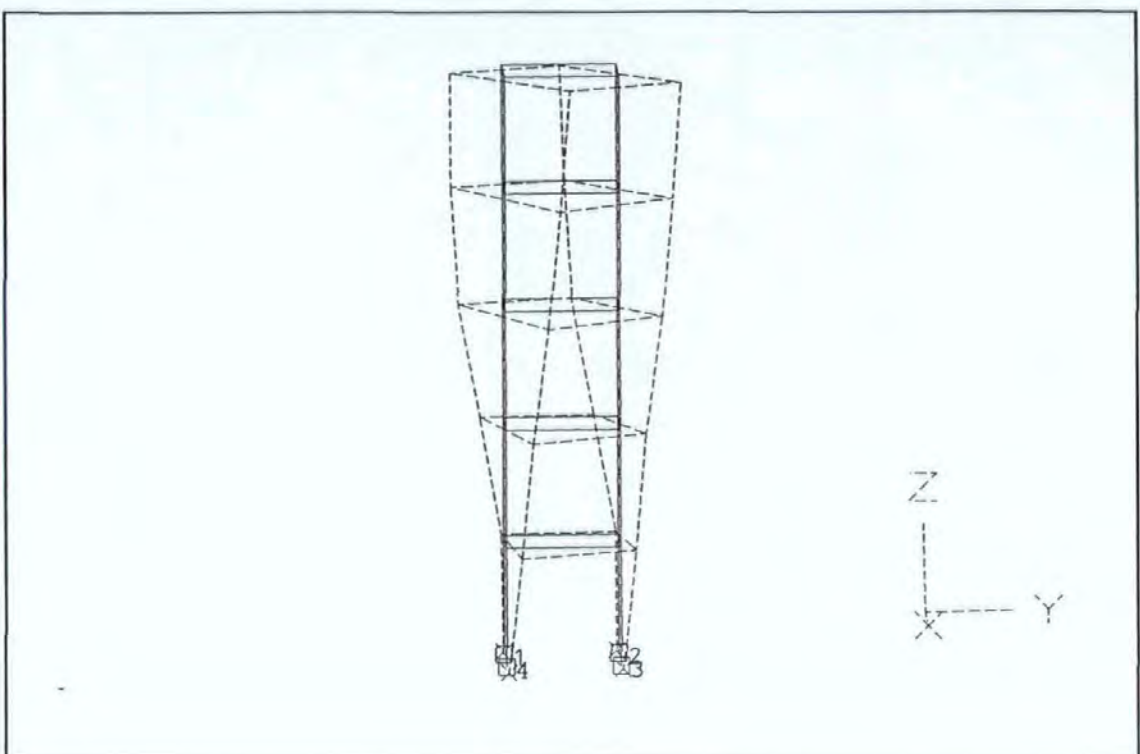
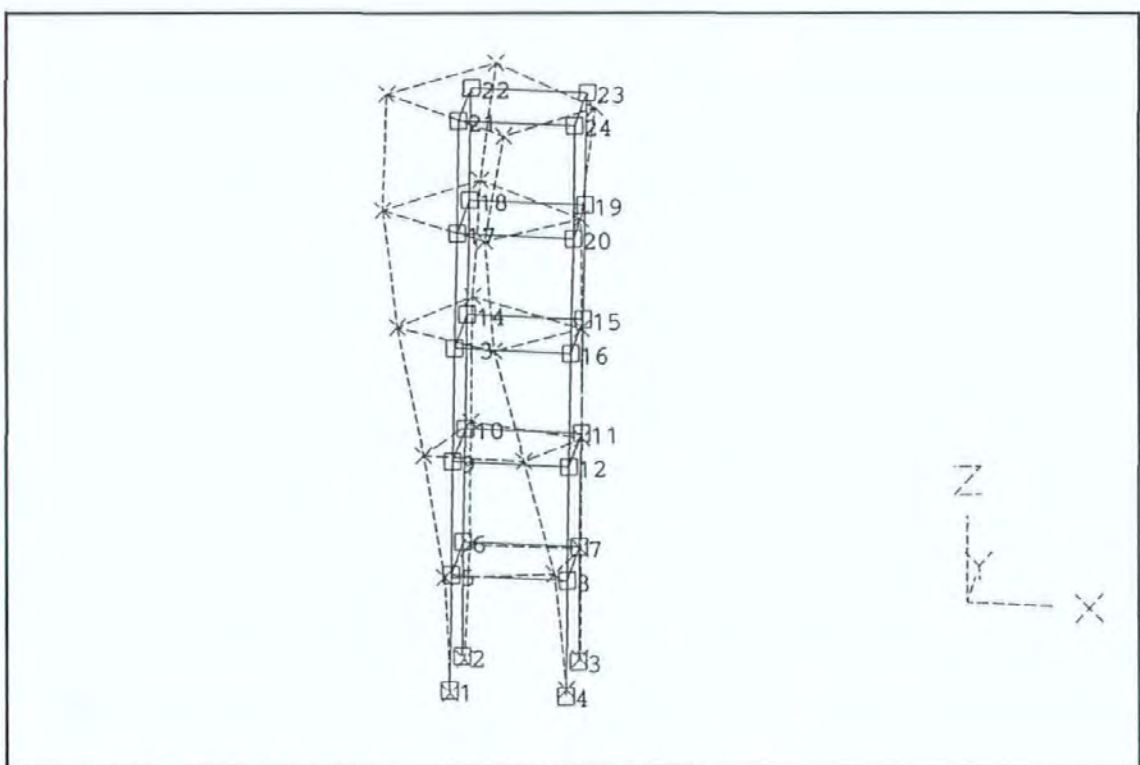


Figure 8.4-15b Another view of the EW1 swaying mode of the tower.

Figures 8.4.-16a and 8.4.-16b show the two different views of the torsional T1 mode.

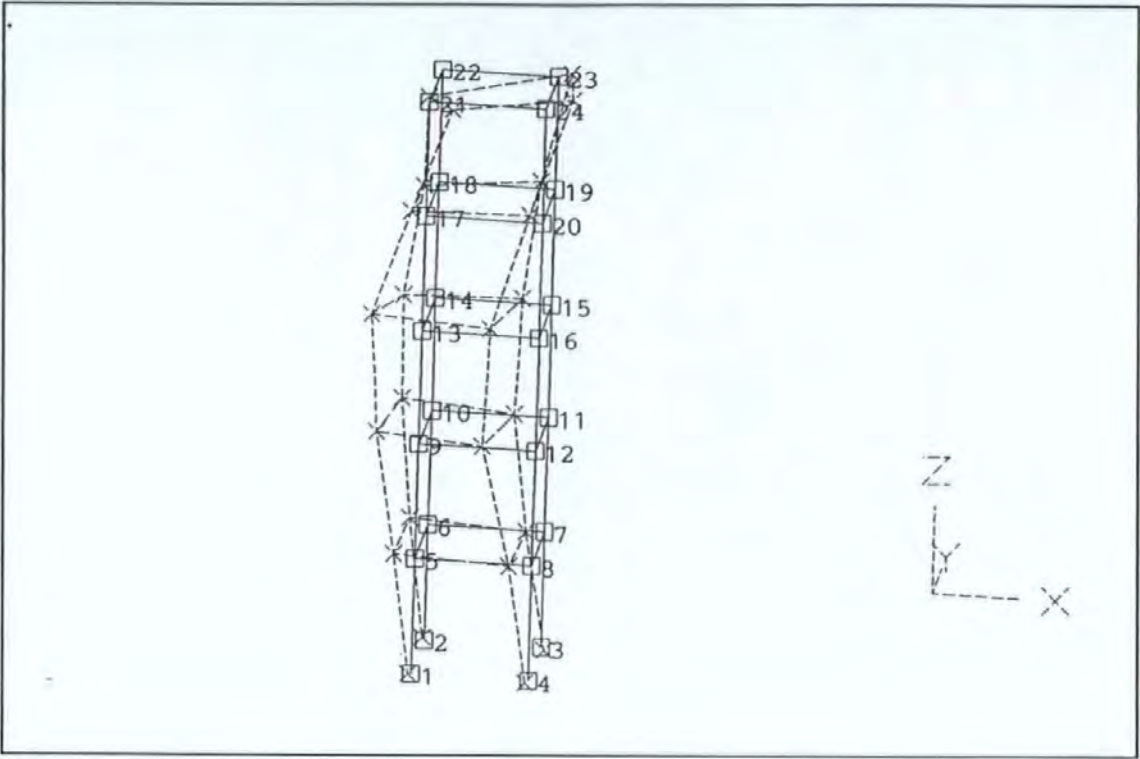


Figures 8.4.-16a A views of the torsional T1 mode.



Figures 8.4.-16b Another view of the torsional T1 mode.

Figures 8.4.-17 shows the EW2 mode in which a degree of torsional motion is also noted.



Figures 8.4.-17 The EW2 mode.

Figure 8.4-18a shows the mode with natural frequency around 17 Hz.

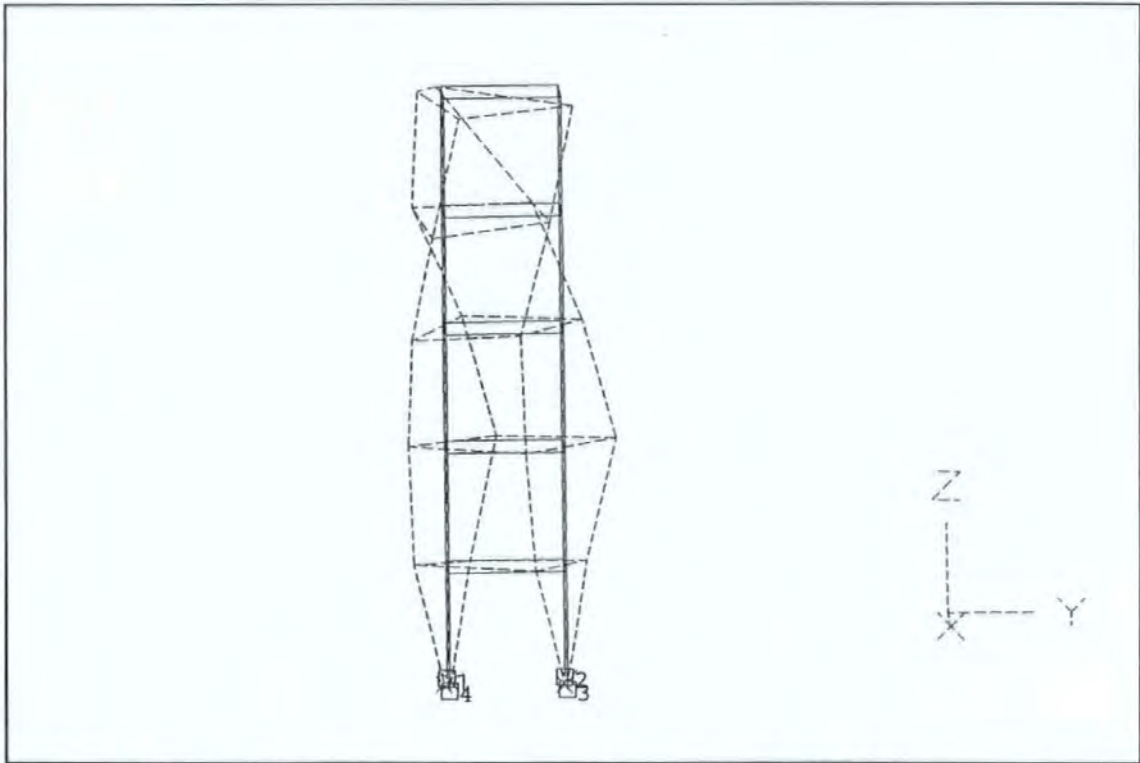


Figure 8.4-18a The mode with resonant frequency around 17 Hz.

Figure 8.4-18b shows another view of this mode. It appears, but with some reservation, that this may be the second torsional T2 mode.

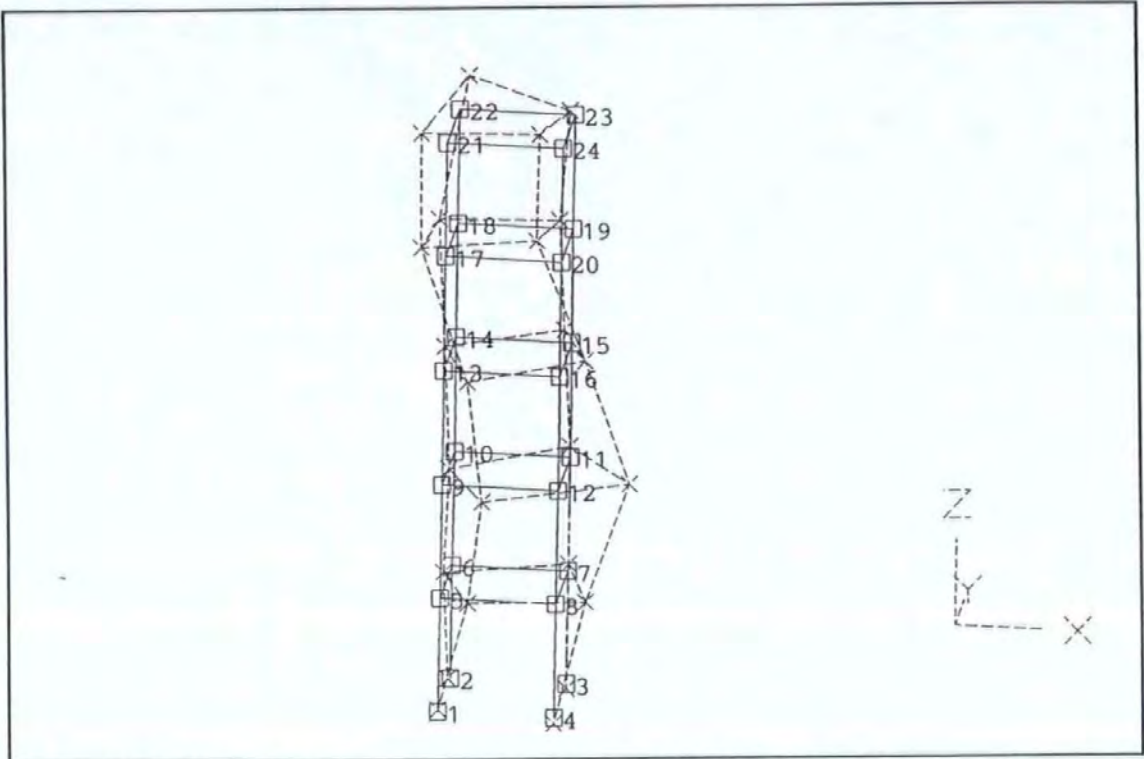
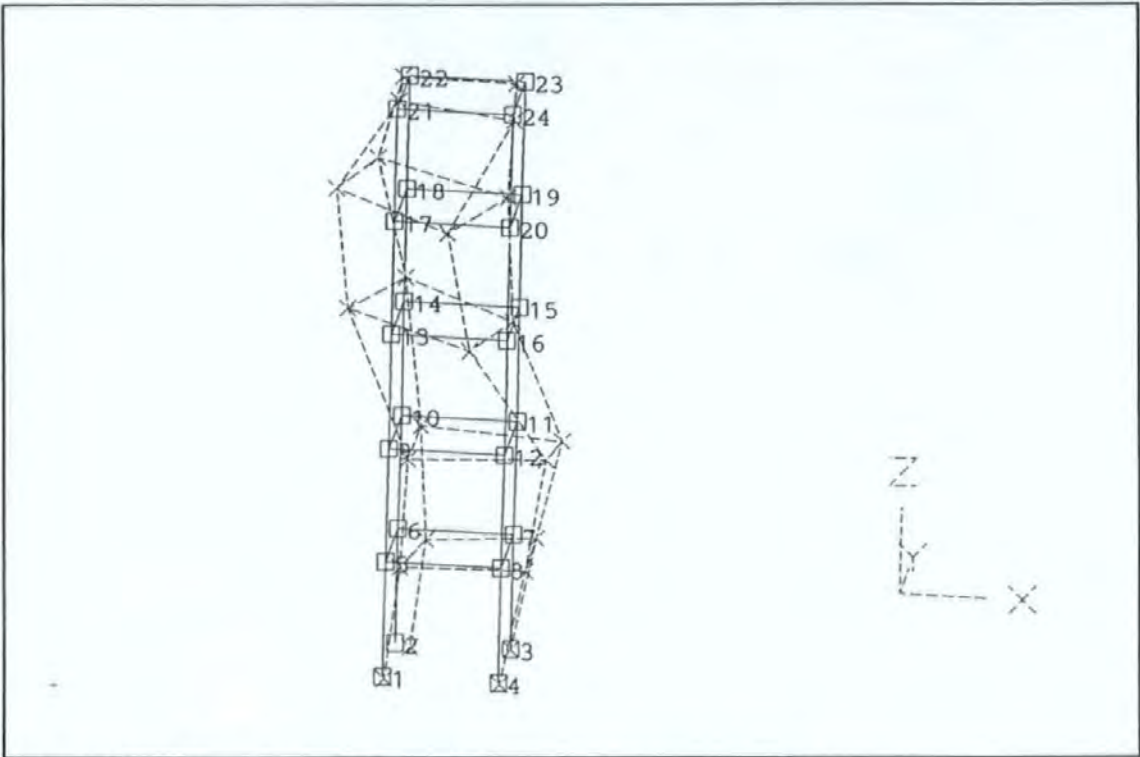
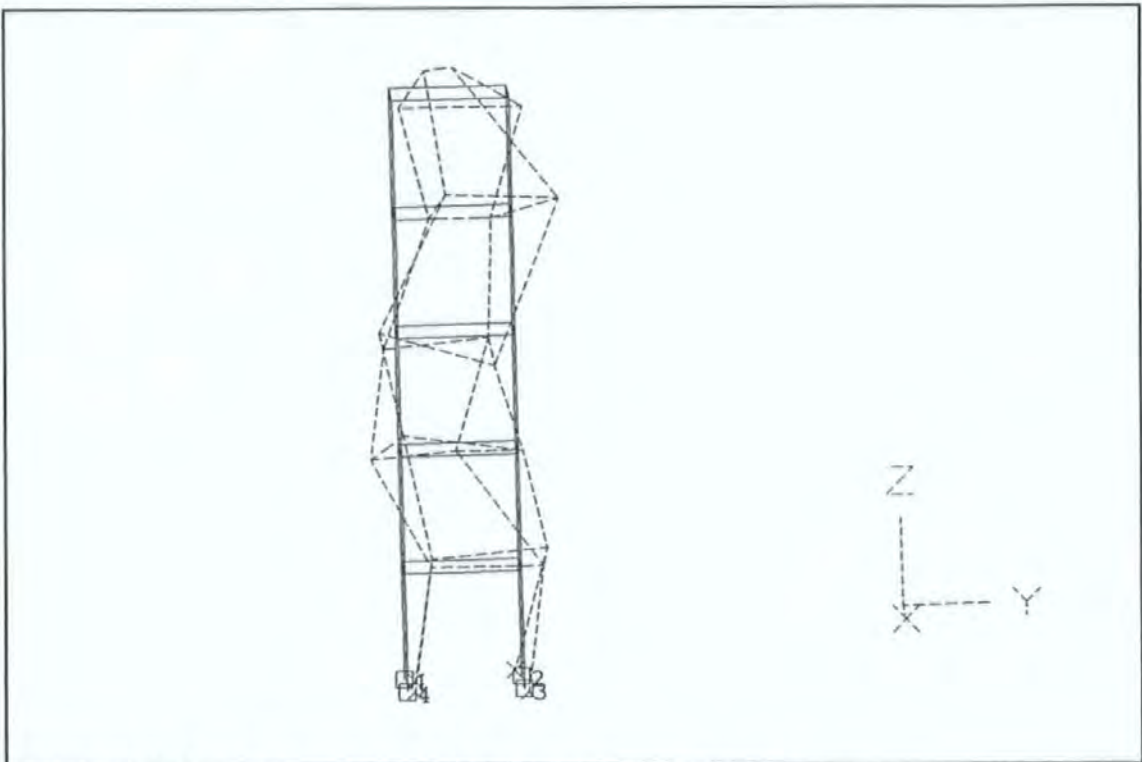


Figure 8.4-18b Another view of the second torsional T2 mode.

However for the higher frequency modes, it becomes increasing difficult to classify them in the same as the lower frequency modes. For instance, the modes with frequencies around 18 and 24 Hz are shown in Figures 8.4-18 and 8.4-19 respectively. As shown in these figures, motions in both the EW and NS directions are of comparable magnitudes and warping of the floor slabs are clearly visible.



Figures 8.4-18c The modes with frequencies around 18 Hz.



Figures 8.4-19 The modes with frequencies around 24 Hz.

Similarly the results from the NS test series are given. Figure 8.4-20 shows the swaying NS1 mode. Again, the 4 grid lines along the Z direction are essentially straight lines. Some warping of the floor slabs occurred particularly at the top floor levels.

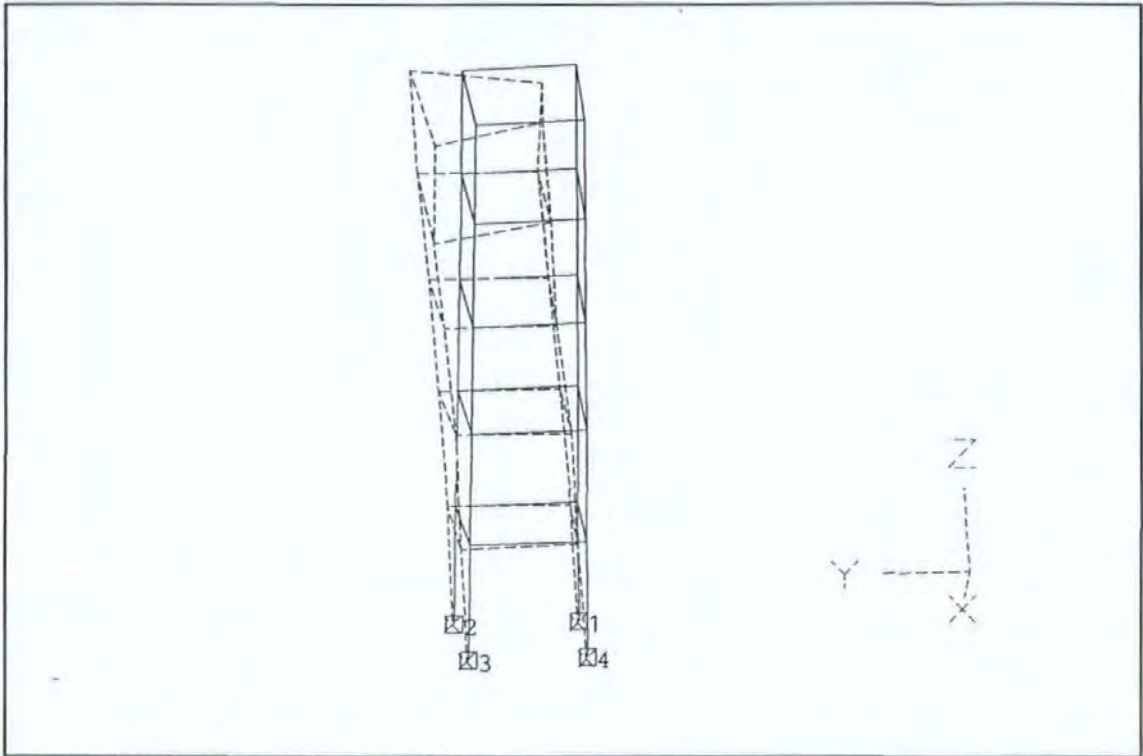


Figure 8.4-20 The swaying NS1 mode

Figure 8.4-21 shows the torsional T1 mode. However this mode shape is less desirable than those obtained with the shaker acting in the EW direction. The movements at the spatial points 4B2 and 5A1 (points 19 and 21 in the figure) are unconformable to those shown in Figures 8.4-16 possibly owing to experimental errors.

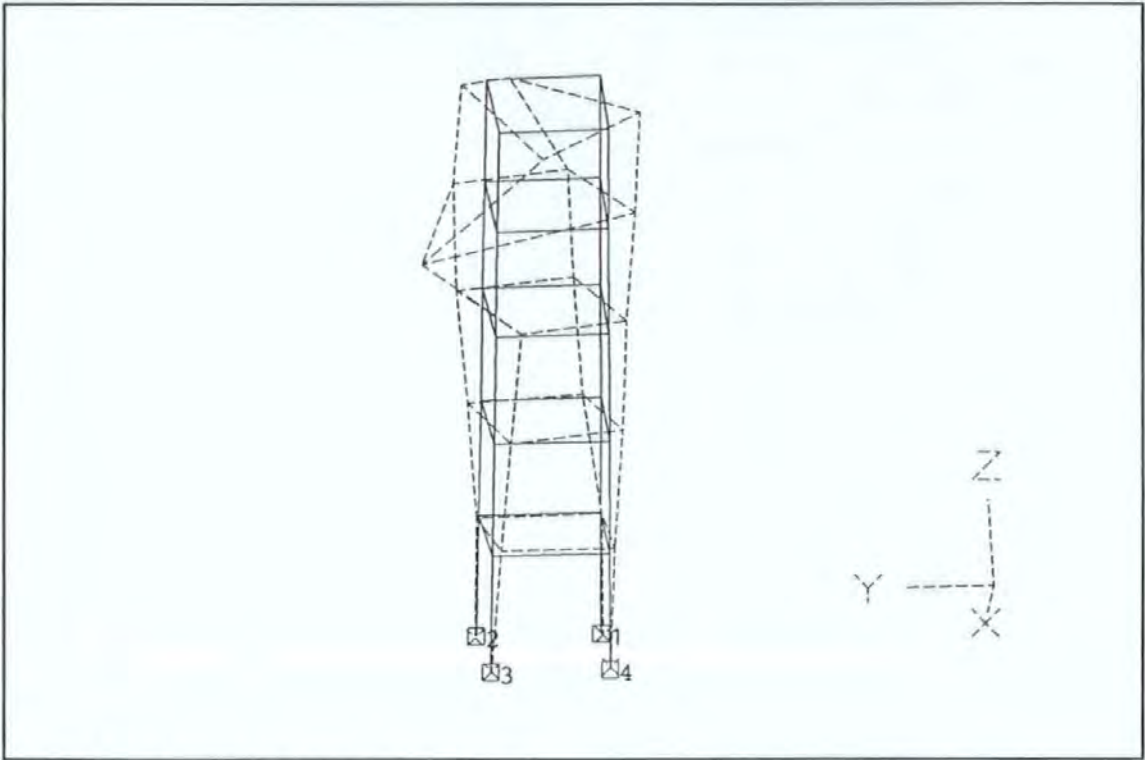


Figure 8.4-21 The torsional T1 mode.

Figure 8.4-22 shows the NS2 mode.

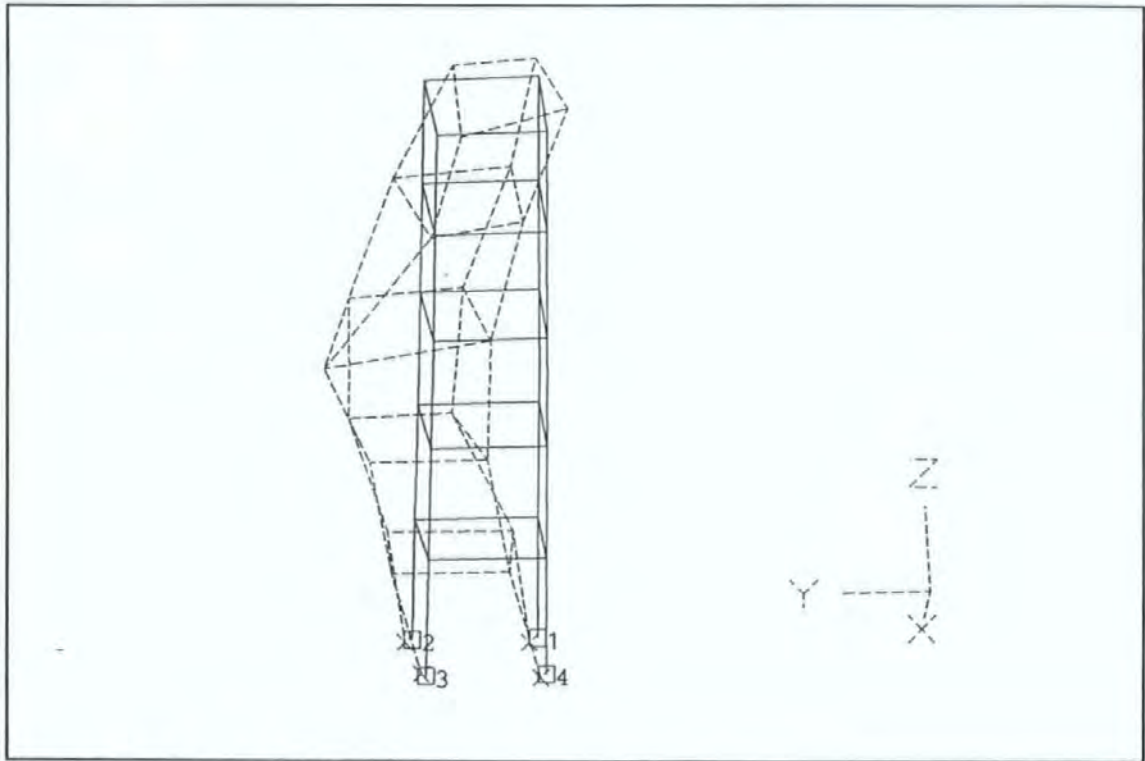
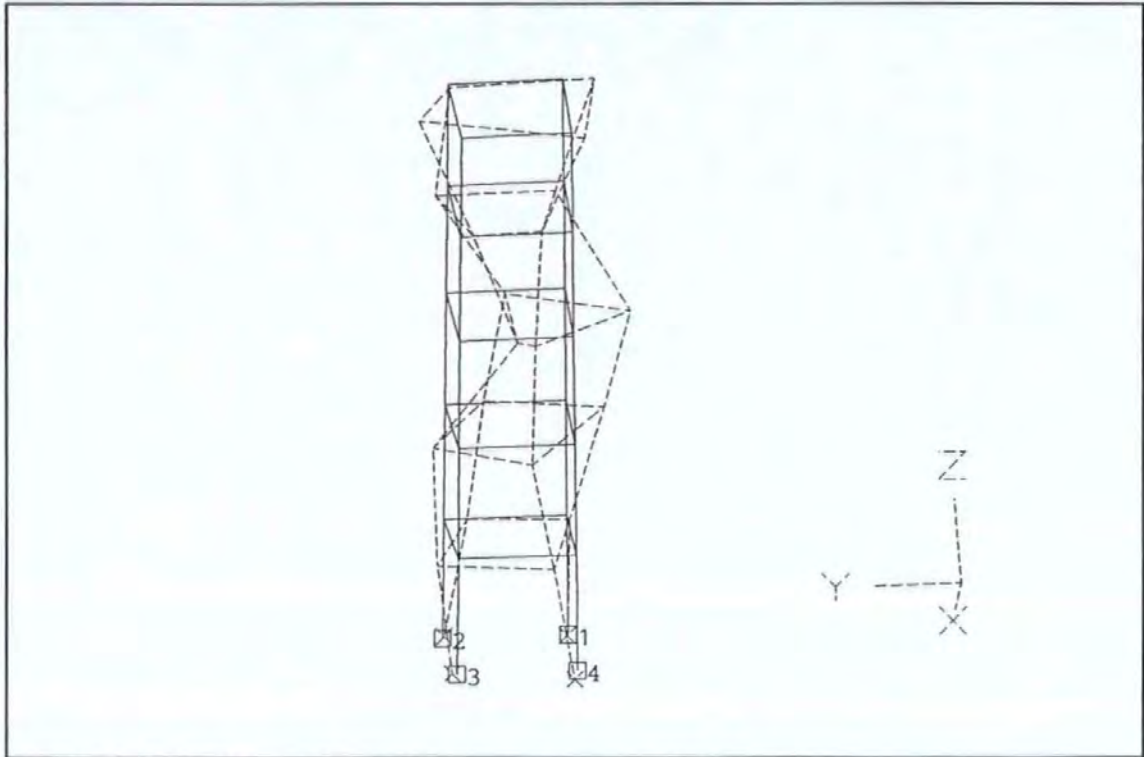
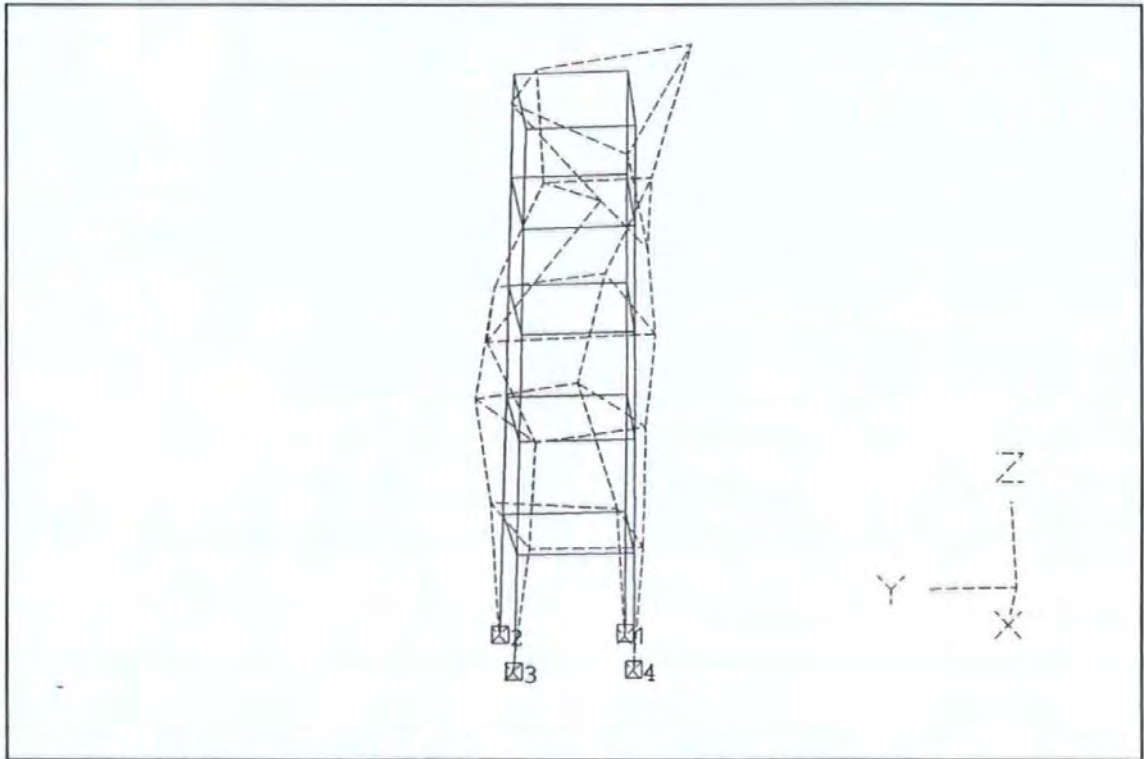


Figure 8.4-22 The NS2 mode.

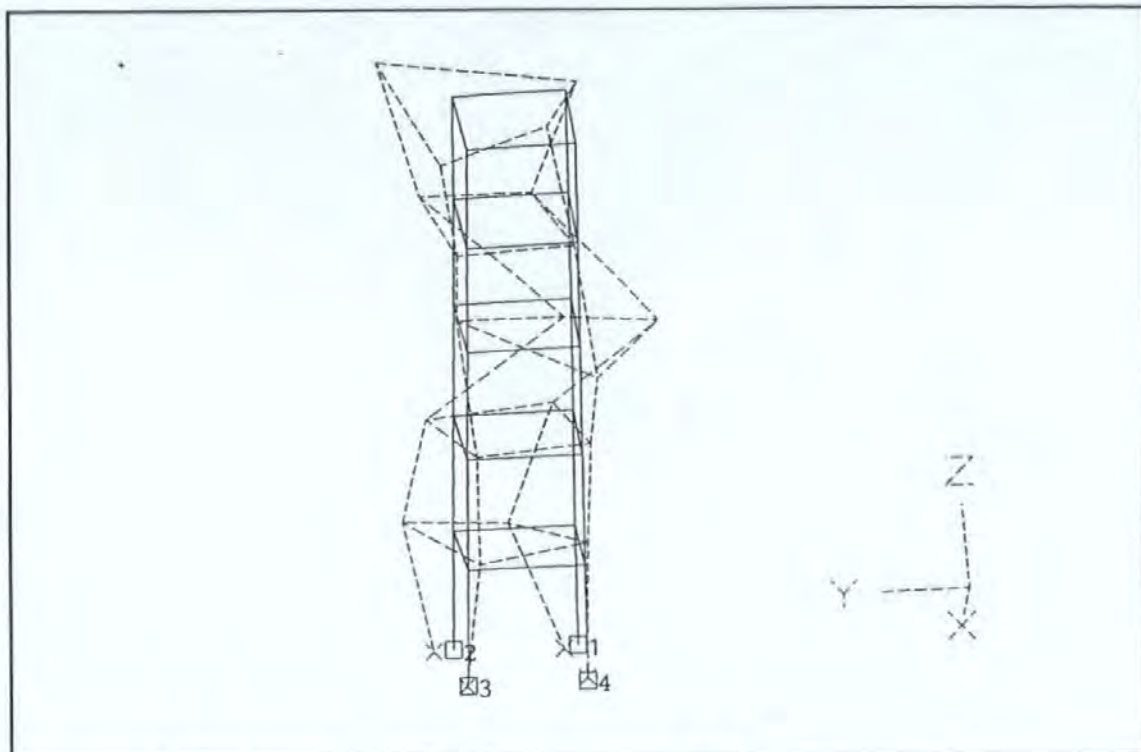
Figures 8.4-23 to 8.4-25 show the three other modes with natural frequencies around 16, 18 and 25 Hz respectively. For the same reasons already described, it is difficult to classify these modes.



Figures 8.4-23 The mode with frequencies around 16 Hz



Figures 8.4-24 The mode with frequencies around 18 Hz



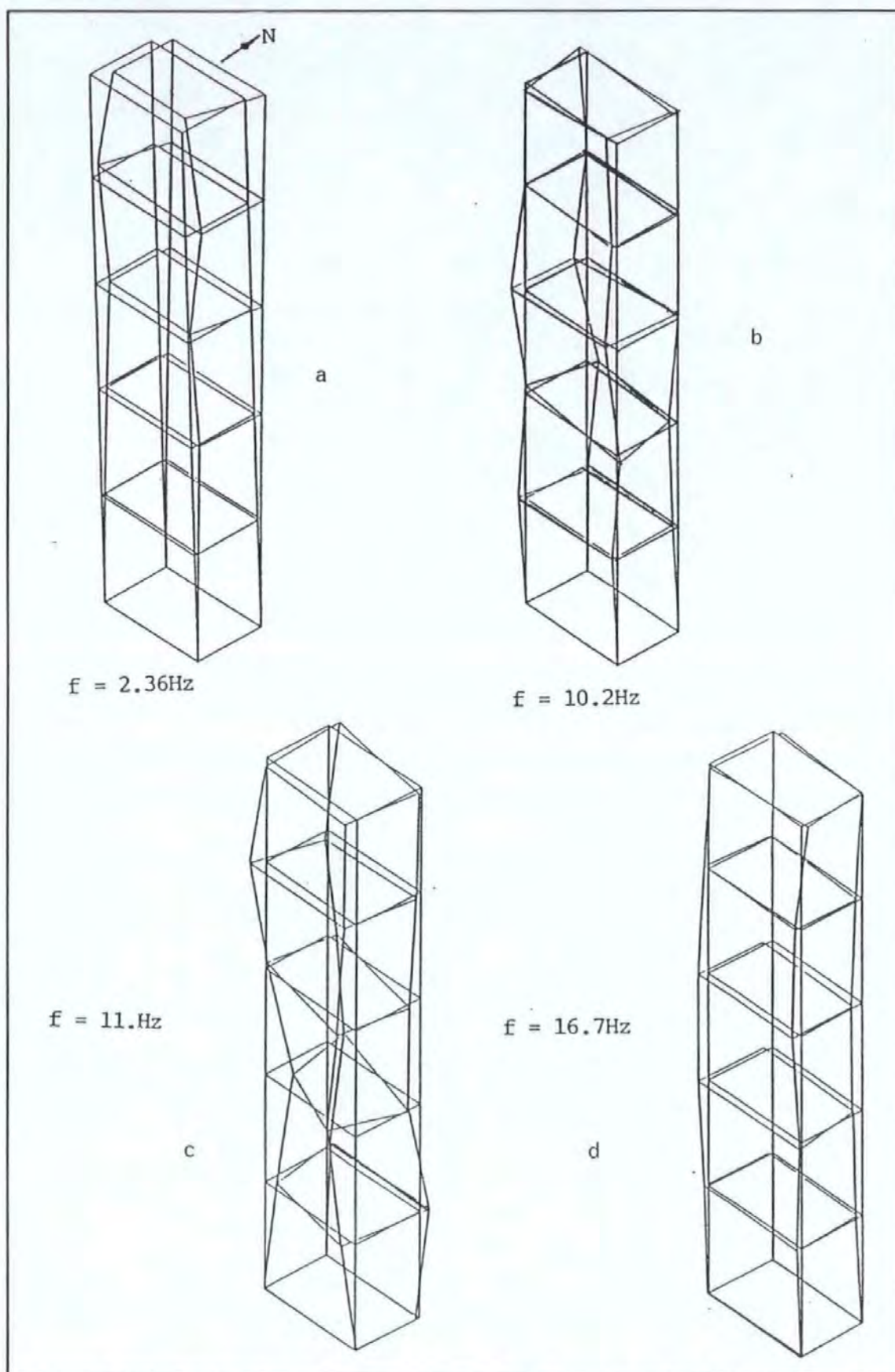
Figures 8.4-25 The mode with frequencies around 25 Hz

A method, often used in civil engineering and practised by the BRE researchers, is to determine the deformed shape whilst a tested structure is still vibrating harmonically at one of the natural frequencies. If modal density is light then the ratio of the relative kinematic responses (acceleration in this case or displacement if available) at any two spatial points will give a good estimate of the ratio of the mode shape coordinates. Note that this is only true if modes are well separated. If an arbitrary spatial point is chosen as a fixed reference point then a plot of these ratios (called Motion Transmissibility or MT) on the spatial grid will give an estimate of the operating mode shape of that particular resonance mode.

This technique was implemented slightly differently. The motion transmissibility FRF spectra were measured at all the measurement points whilst the structure was under pseudo-random instead of steady-state harmonic excitation. The MT at each resonance frequency was determined from the spectra provided by the spectrum analyzer from broad band random vibration. Providing modal density is slight, the method is feasible. This technique is extremely useful because of the time savings over the steady state testing methods. The MT of all the points (measured by a roving accelerometer called traveller) in the grid were referenced to the accelerometer fixed at the spatial point 5A1 and orientated in a fixed direction. The three dimensional plots of the spatial deformation shapes at each of the

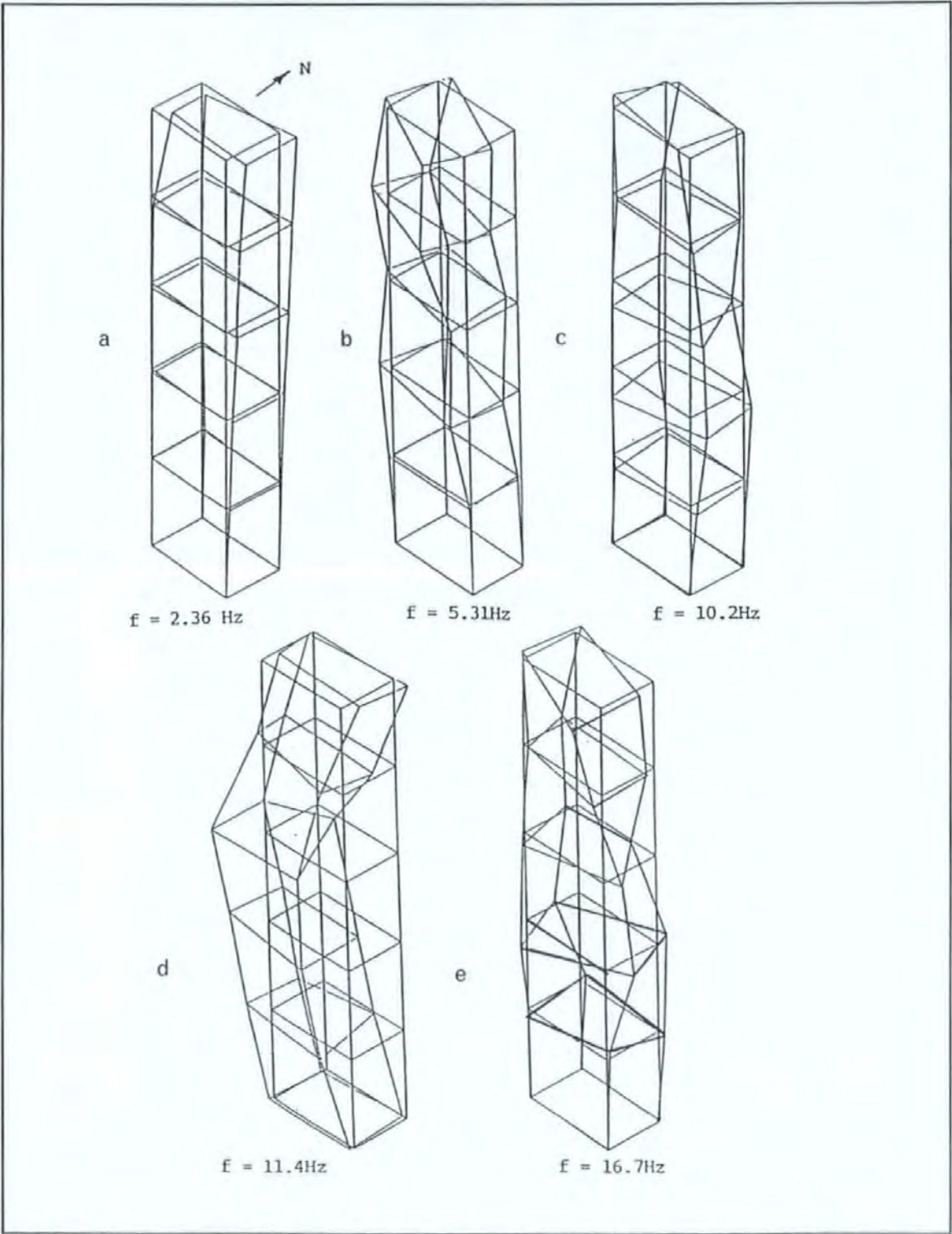
resonance frequencies were obtained with the use of the **GINO** graphic software. Like mode shapes, these plots provide an immensely useful tool to visualize the physics and behaviour of a structure at resonance or other conditions.

Figures 8.4-26a to 8.4-26d show the operating mode shapes at 2.36, 10.2, 11.4 and 16.7 Hz with the exciter acting along the EW direction. There are some resemblances between these operating mode shapes and the corresponding mode shapes presented earlier. However for the two modes with very close natural frequencies, it should be borne in mind that the operating mode shapes will not approximate the true mode shapes.



Figures 8.4-26a to 8.4-26d The operating mode shapes at 2.36, 10.2, 11.4 and 16.7 Hz with the exciter acting along the EW direction.

Figure 8.4-27a to 8.4-27e show the operating mode shape at 2.36, 5.3, 10.2, 11.4 and 16.7 Hz respectively with the exciter acting along the NS direction.



Figures 8.4-27a to 8.4-27e The operating mode shapes at 2.36, 5.3, 10.2, 11.4 and 16.7 Hz with the exciter acting along the NS direction.

8.5 DISCUSSION OF RESULTS

The results show that most of the dominant modes of the tower occur below 25 Hz with the fundamental modes occurring at about 2.3 Hz. The closeness of the EW1 and NS1 is believed to be due to the near symmetry in the structural, not architectural, details along the EW and NS directions. Because of the closeness of these modes, considerable coupling occurred and a mode could be excited even when the shaker was acting in a direction orthogonal to the mode. The torsional T1 mode occurred at a frequency roughly twice that of the fundamental swaying modes. The slightly lower frequency of the EW1 mode than that of the NS1 mode may suggest that the stiffness reduction due to the openings on one of the two infilled brick walls on the EW plane may be responsible, providing all the other structural factors concerning the walls stay the same in both the EW and NS planes.

All the mode shapes determined show considerable movements in the fifth floor. Hence, the placement of the exciter on this level was appropriate. The damping levels of all these modes are found to be around 1% of critical damping. This is considered typical of most reinforced concrete structures and there is no cause for concern of any abnormality on this structure.

Tests results show that the natural frequencies of the T1 mode fluctuate with different force levels. However, due to the lack of sufficient data using SS excitation and insufficient frequency resolution, no conclusive statement can be made regarding the linearity or otherwise of this structure.

8.6 SUMMARY

Because of the small size of the structure, very large amplitude motions of the structure have been excited. Considerable responses were measurable even at ground level which was five floor levels down from where the exciter was. Because SS tests can be carried out at variable steps, very fine frequency resolutions can be obtained at the expense of time. However, applying SS tests extensively will be too time-intensive and is not suitable to full scale field testing. The PRBS test method is extremely time efficient but cautions must be exercised especially regarding the problem of lack of frequency resolution in data. This is because the PRBS test method produces FRF spectra with a constant frequency resolution across the entire band of analysis. The results obtained in the field tests are largely consistent but are still inferior to those obtained from laboratory. Finally, it is shown that very useful structural information can be determined by performing full scale forced vibration testing on structures.

Table 8.4-3. Modal parameters set determined from test data 220487001R (from 25 Hz PRBS tests with exciter acting EW and measurements made at grid point 5A1 in the EW direction).

	ω_r	ξ_r	G_r	M_r'	C_r'	K_r'
MODE 1	2.357	0.0220	2.36e-5	4.23e+04	2.77e+04	9.29e+6
MODE 2	5.615	0.0079	1.23 e-5	8.09e+04	4.53e+04	1.01e+8
MODE 3	10.456	0.0266	5.27 e-6	1.90e+05	6.64e+05	8.19e+8
MODE 4	6.160	0.0407	2.94 e-5	3.39e+04	1.07e+05	5.08e+7
MODE 5	17.535	0.0144	5.47 e-5	1.83e+05	5.79e+05	2.22e+9

where ω_r is the *natural frequency* of the r^{th} mode
 ξ_r is the *modal damping factor* of the r^{th} mode
 G_r is the *modal constant* of the r^{th} mode
 M_r' is the *effective mass* of the r^{th} mode
 C_r' is the *effective damping* of the r^{th} mode
 K_r' is the *effective stiffness* of the r^{th} mode

Table 8.4-4. Modal parameters set determined from test data 230487009R (from 25 Hz PRBS tests with exciter acting NS and measurements made at grid point 5A1 in the NS direction).

	ω_r	ξ_r	G_r	M_r'	C_r'	K_r'
MODE 1	2.387	0.0210	2.05 e-5	4.87e+04	3.07e+04	1.10e+7
MODE 2	5.760	0.0274	5.04 e-6	1.98e+05	3.93e+05	2.60e+8
MODE 3	10.471	0.0461	3.12 e-6	3.13e+05	1.90e+06	1.35e+9
MODE 4	12.183	0.0433	-3.16e-6	-3.17e05	2.10e+06	-1.8e+9
MODE 5	17.574	0.0176	1.76 e-6	5.70e+05	2.21e+06	6.95e+9

Table 8.4-5. Modal parameters set determined from test data 250487017 (from 25 Hz PRBS tests with exciter acting NS and measurements made at grid point 5B2 in the NS direction).

250487017 R	ω_r	ξ_r	G_r	M_r'	C_r'	K_r'
MODE 1	2.393	0.0210	1.89 e-5	5.29e+04	3.34e+04	1.20e+7
MODE 2	5.613	-0.049	1.04 e-6	9.53e+05	-3.29e+06	1.19e+9
MODE 3	10.248	-0.014	-4.0 e-7	-2.20e+06	-4.01e+06	-9.10e+9
MODE 4	11.644	0.0255	2.21 e-6	4.51e+05	1.68e+06	2.41e+9
MODE 5	17.327	-0.026	3.3 e-7	2.97e+06	-1.74e+07	3.52e+10

Table 8.4-6. Modal parameters set determined from test data 260487008R (from 25 Hz PRBS tests with exciter acting NS and measurements made at grid point 4A2 in the NS direction).

26048700 8R	ω_r	ξ_r	G_r	M_r'	C_r'	K_r'
MODE 1	2.375	0.0213	1.84 e-5	5.44e+4	3.46e+4	1.21e+07
MODE 2	5.568	0.0128	7.58 e-6	1.32e+5	1.18e+5	1.61e+08
MODE 3	9.311	-0.110	9.12 e-6	1.10e+5	-1.42e+6	3.75e+08
MODE 4	11.807	-0.022	-2.4 e-6	-4.06e+5	-1.38e+6	-2.24e+09
MODE 5	16.948	0.0302	4.88 e-6	2.05e+05	1.32e+6	2.33e+09

Table 8.4-7. Modal parameters set determined from test data R25X021X (from 25 Hz PRBS tests with exciter acting EW and measurements made at grid point 5A2 in the EW direction).

R25X021X	ω_r	ξ_r	G_r	M_r'	C_r'	K_r'
MODE 1	2.357	0.0220	2.36E-5	4.23E4	9.290E6	2.766E4
MODE 2	5.565	0.0128	9.64E-6	1.037E5	1.269E8	9.297E4
MODE 3	10.359	0.0179	4.26E-6	2.347E5	9.946E8	5.497E5
MODE 4	17.549	0.0158	5.44E-6	1.836E5	2.233E9	1.329E6
MODE 5	18.859	0.0019	3.39E-7	2.944E6	4.135E10	1.046E6
MODE 6	23.555	0.0526	1.48E-5	6.722E4	1.472E9	5.076E5

Table 8.4-8. Modal parameters set determined from test data R25Y023Y (from 25 Hz PRBS tests with exciter acting NS and measurements made at grid point 5B2 in the NS direction)

R25Y023Y	ω_r	ξ_r	G_r	M_r'	C_r'	K_r'
MODE 1	2.393	0.021	1.89E-5	5.288E4	1.195E7	3.341E4
MODE 2	5.451	0.015	-4.11E-6	-2.431E5	-2.853E8	-2.546E5
MODE 3	11.510	0.078	3.32E-6	3.010E5	1.574E9	3.439E6
MODE 4	17.187	0.013	-9.52E-7	-1.049E6	-1.223E10	-3.124E6
MODE 5	23.795	0.029	2.78E-6	3.596E5	8.040E9	3.145E6

Table 8.4-9. Modal parameters set determined from test data R25Y021X (from 25 Hz PRBS tests with exciter acting NS and measurements made at grid point 5A2 in the EW direction).

R25Y021X	ω_r	ξ_r	G_r	M_r'	C_r'	K_r'
MODE 1	2.347	0.0167	-5.78E-6	-1.729E5	-3.762E7	-8.551E4
MODE 2	5.512	0.012	-4.02E-6	-2.486E5	-2.982E8	-2.098E5
MODE 3	10.337	0.016	-2.46E-6	-4.054E5	-1.710E9	-8.588E5
MODE 4	17.342	0.021	-1.71E-6	-5.832E5	-6.925E9	-2.752E6
MODE 5	24.320	0.016	-4.61E-6	-2.166E5	-5.058E9	-1.120E6

Table 8.4-10. Modal parameters set determined from test data R25Y017Y (from 25 Hz PRBS tests with exciter acting NS and measurements made at grid point 4A1 in the NS direction).

R25Y017Y	ω_r	ξ_r	G_r	M_r'	C_r'	K_r'
MODE 1	2.385	0.018	1.69E-5	5.886E4	1.322E7	3.320E4
MODE 2	5.545	0.008	3.26E-6	3.064E5	3.720E8	1.892E5
MODE 3	10.633	0.25	-4.64E-6	-2.153E5	-9.611E9	-7.373E5
MODE 4	12.031	0.039	-4.98E-6	-2.004E5	-1.145E9	-1.188E6
MODE 5	17.292	0.033	2.80E-6	3.569E5	4.214E9	2.623E6
MODE 6	24.179	0.038	7.52E-6	1.329E5	3.068E9	1.551E6

Table 8.4-11. Modal parameters set determined from test data R25Y001Z (from 25 Hz PRBS tests with exciter acting NS and measurements made at grid point 0A1 in the Vertical direction).

R25Y001Z	ω_r	ξ_r	G_r	M_r'	C_r'	K_r'
MODE 1	2.411	0.012	-6.89E-7	-1.450E6	-3.330E8	-5.546E5
MODE 2	5.490	0.016	-2.34E-7	-4.270E6	-5.082E9	-4.978E6
MODE 3	11.717	0.023	2.21E-7	4.518E6	2.448E10	1.582E7
MODE 4	23.866	0.017	-7.25E-7	-1.378E6	-3.100E10	-7.351E6

CHAPTER 9

CONCLUSIONS

AND

RECOMMENDATIONS

In addition to the discussions given and conclusions drawn for the individual chapters, this chapter provides an overall summary and a number of recommendations to bring this report to a close.

The application of experimental modelling to full scale civil engineering structures (using some of the techniques developed in the Experimental Modal Analysis field) has shown to be a worthwhile exercise and with good potentials. The testing techniques and the data analysis methods used are a significant departure from the established practices and techniques adopted in civil engineering as typified by the works of the EERL and the BRE. Therefore the objective of transferring this technology to civil engineering application has been fulfilled. Whilst it is recognized that civil engineering structures have many unique and different features which stand out from the rest of the engineering sphere, however further interest in the implementation of these technique to civil engineering should gather pace. The experimental approach advocated in this research should not be regarded as a substitute but a supplement to theoretical approach.

The literature review reported in Chapter 2 shows that very few organisations or establishments are engaged in full scale forced vibration tests, especially in the UK. Reluctance and unenthusiastic reception the author has met in acquiring buildings for testing has reinforced this view that even professionals connected to civil engineering and the building industries do not realize the benefit of such research can bring. To increase their awareness must be a job of the highest priority.

The theory review reported in Chapter 3 shows that a great deal of the development in this technique originates from other disciplines of engineering. Complexity of the theories, terminologies, jargons etc have placed many obstacles for civil/structural engineers to get a grip on this technology. Standardization of terminologies and practices should be an urgent development. The values of this emerging technology in relation to other established disciplines such as non-destructive testing, integrity testing etc have to be established.

The experimentation system used in this research has shown that moderate cost equipment can perform many functions that dedicated and sophisticated system can. Costs of instrumentation and microprocessor technologies continue to come down in recent years. Especially, the successes in miniaturization of microprocessors allow very sophisticated equipment once found only in a laboratory to be used in the field. Hence costs can no longer be obstacles to implementing this technology to full scale field testing.

The modal parameter extraction algorithm described in Chapter 5 is a simple yet practical tool to perform the requested task. The mechanics of the process of modal parameter extraction has been clearly explained and the success in constructing modal models of structures from experimental data illustrated. The simplicity of the algorithm is recognized as an ideal vehicle to teach new comers from civil/structural engineering to acquaint with this technology.

The algorithm presented in Chapter 6 enables the spatial matrices of a structure to be determined directly from experimental data. Instead of very large matrices obtained from FE models, low order matrices are obtained from experimental models. These matrices provide information on a structure that can be easily understood by most civil/structural engineers and be used for validating analytical models, predicting the performance and evaluating the integrity of structures. The special tributes of this method are that the lack of frequency resolution of data measured near resonance is not critical (while this is the case with most modal methods) and that spatial measurements can be utilized in conjunction with local measurements for constructing models. Although this study has shown that so far this technique only works well for simple laboratory scale test piece, its successful application to large scale civil engineering structures can one day be realized providing that further efforts be directed to this technology in the experimentation and computing fronts .

APPENDIX 4.5.2 LISTING OF THE CONTROL PROGRAM

```

10  ! *** CONTROL AND DATA ACQUISITION PROGRAM FOR HP3582A
SPECTRUM ANALYZER
20 Welcome: ! DISPLAY WELCOME MESSAGE
30  !*****
40  OPTION BASE 1
50  C$=CHR$(255)&CHR$(75)
60  DIM Fun$(80),Read_time$(80)
70
Fun$="*****"
80  OUTPUT 2 USING "#,K";C$
90  GCLEAR
100 CONTROL 1,1;4 ! MOVE TO LINE 4 OF SCREEN
110 PRINT CHR$(129);Fun$(1,49)
120 PRINT "* STRUCTURAL DYNAMICS RESEARCH                *"
130 PRINT "* CIVIL AND STRUCTURAL ENGINEERING DEPARTMENT  *"
140 PRINT "* POLYTECHNIC SOUTH WEST                        *"
150 PRINT "*"
160 PRINT "* CONTROL AND DATA ACQUISITION SOFTWARE FOR      *"
170 PRINT "* HP3582A SPECTRUM ANALYZER                        *"
180 PRINT "*"
190 PRINT "                1992                *"
200 PRINT Fun$(1,49);CHR$(128)
210 DISP "PRESS 'CONTINUE' TO PROCEED"
220 PAUSE
230 !
240 !*****
250 Declare: ! DECLARE AND INITIALIZE VARIABLES
260 DIM Cha_time_value(512),Chb_time_value(512),Array(128,2)
270 DIM Time1$(16),Time2$(16)
280 DIM Display_value$(6)[10],Resonant_freq(6)
290 DIM Time_point$(2048),Spec_full_state$(10),Lmk$(25),Mode_0_start(14)
300 DIM
Freq$(20)[10],Chan1$(20)[10],Chan2$(20)[10],Xfr_amp$(20)[10],Xfr_phase$(20)[10],Coher
$(20)[10]
310 DIM Doc_table$(85)
320 DIM Point$(1280),Spect_state$(2),Anotat$(128),Graphs$(256)
330 DIM
Option_header$(80),Opt1$(40),Opt2$(40),Opt3$(40),Opt4$(40),Opt5$(40),Opt6$(40),Opt7$(
40),Opt8$(40)
340 !
350
!*****
360 Speed_up: ! BYPASS SEARCH MARKER TO SPEED UP PROCESSING
370 OUTPUT 2 USING "#,K";C$
380 ! INPUT "BYPASS SEARCH MARKER TO SPEED UP PROCESSING ??
ANSWER Y OR N",Deci$
381 ! Deci$=UPC$(Deci$)
390 ! IF Deci$<>"Y" AND Deci$<>"N" THEN GOTO 380

```

```

430 ! IF Deci$="N" THEN
440 !   Bypass_marker$="N"
450 !ELSE
460 !   Bypass_marker$="Y"
470 ! END IF
480!
490 INPUT "ENTER CURRENT DATE e.g 3rd OF MAY IS 0305",Current_date$
580   Read_time$="          PRESS 'CONTINUE' AFTER READING MESSAGES
"
590 !
600 !*****
610   GOSUB Device
620   GOSUB Master_menu
630   ON KEY 1 LABEL "RANDOM",3 GOSUB Periodic_random
640   ON KEY 2 LABEL "POINT_STORE" GOSUB Point_store
650   ON KEY 3 LABEL "GRAPHIC_STORE" GOSUB Graphic_store
660   ON KEY 4 LABEL "SPEC_PLOT" GOSUB Spec_plot
670   ON KEY 5 LABEL "NYQUIST_PLOT" GOSUB Nyquist_plot
680   ON KEY 6 LABEL "DOCUMENTATION" GOSUB Documentation
690   ON KEY 7 LABEL "SINE_SWEPT" GOSUB Sine_swept
700   ON KEY 8 LABEL "RELOAD_GRAPH" GOSUB Reload_graph
710   ON KEY 9 LABEL "RELOAD_TIME" GOSUB Reload_time
720   ON KEY 0 LABEL "SCANS" GOSUB Scans
730   ON KEY 11 LABEL "LOOK-ANY_FILE" GOSUB Look_any_file
740   ON KEY 12 LABEL "TIME_TRACE" GOSUB Time_trace
750   ON KEY 13 LABEL "UNDEFINED" GOSUB Undefined
760   ON KEY 14 LABEL "SPECT_SET_UP" GOSUB Spectrum_set_up
770 Spin:GOTO Spin
781   !
782
!*****
783   !
785   ! ***** SUB DEVICE TO ASSIGN I/O PATHS TO DEVICES
*****
790 Device:  !
800   GCLEAR
801   OUTPUT 2 USING "#,K";C$
802   ASSIGN @Spect TO 711
803   ASSIGN @Printer TO 701
804   ASSIGN @Philip TO 704
805   MASS STORAGE IS ":HP9122,700, 1"
806   PRINT
807   PRINT " DEFAULT ADDRESS OF SPECTRUM ANALYZER IS 711 -- @SPECT"
808   PRINT
809   PRINT " DEFAULT ADDRESS OF PHILIPS FUNCTION GENERATOR IS 704 --
@PHILIP"
810   PRINT
811   PRINT " DEFAULT MASS STORAGE MEDIA IS THE RIGHT HAND DISC

```

```

DRIVE (1)"
812 PRINT
813 PRINT " DEFAULT ADDRESS FOR PRINTER IS 701 -- @PRINTER"
814 PRINT
816 DISP CHR$(131);Read_time$;CHR$(128)
817 PAUSE
818 RETURN
831 !*****
832 !***** SUB MASTER_MENU : TO DISPLAY KEY ASSIGNMENTS
*****
840 Master_menu: !
850 OUTPUT 2 USING "#,K";C$
851 PRINT CHR$(131);"PRESS ANY OF THE FOLLOWING KEYS TO PERFORM
THE FUNCTIONS INDICATED";CHR$(128)
852 PRINT
853 PRINT "KEY K0 : 'SCANS' ----- TO SCAN THE VARIOUS DISPLAY"
856 PRINT "KEY K1 : 'RANDOM' ----- PERFORM PERIODIC/PURE RANDOM
TEST"
858 PRINT "KEY K2 : 'POINT_STORE' ----- STORE POINTS OF THE SPECTRUM
DISPLAY"
859 PRINT
860 PRINT "KEY K3 : 'GRAPHIC_STORE' -- STORE THE SPECTRUM DISPLAY
AS GRAPHIC"
862 PRINT "KEY K4 : 'SPEC_PLOT' --- PLOT A SPECTRUM DISPLAY ON THIS
COMPUTER"
864 PRINT "KEY K5 : 'NYQUIST_PLOT' ----- MAKE A NYQUIST PLOT"
866 PRINT "KEY K6 : 'DOCUMENTATION' ----- TO DOCUMENT TEST"
867 PRINT
869 PRINT "KEY K7 : 'SINE_SWEPT' ----- TO PERFORM SINE SWEPT TEST"
870 PRINT "KEY K8 : 'RELOAD_GRAPH' ----- RELOAD A GRAPHIC PLOT
FROM FILE TO SPECTRUM"
872 PRINT "KEY K9 : 'RELOAD_TIME' ----- RELOAD A TIME HISTORY FROM
FILE TO SPECTRUM"
873 PRINT
875 PRINT " 'SHIFT' AND KEY K1 : 'LOOK_ANY_FILE' ---- VIEW ANY FILE"
876 PRINT " 'SHIFT' AND KEY K2 : 'TIME_TRACE' ----- DISPLAY A TIME
TRACE ON THIS COMPUTER"
878 PRINT " 'SHIFT' AND KEY K3 : ----- RESERVED FOR FUTURE USE"
880 PRINT " 'SHIFT' AND KEY K4 : ----- TO SET UP THE SPECTRUM"
882 DISP CHR$(131);Read_time$;CHR$(128)
883 PAUSE
884 DISP
886 RETURN
887 !***** PERIODIC RANDOM TEST
*****
889 Periodic_random: !
890 Periodic$="Y"
891 PRINT CHR$(12)

```

```

892 PRINT "ENTER TYPE OF RANDOM SIGNAL .... THERE IS NO DEFUALT"
893 PRINT
894 PRINT
896 PRINT "1. PERIODIC RANDOM"
897 PRINT
898 PRINT "2. PURE RANDOM"
899 INPUT "ENTER 1 OR 2",Random_code
900 IF Random_code=1 THEN Random_type$="PERIODIC"
901 IF Random_code=2 THEN Random_type$="PURE"
902 IF Random_code<>1 AND Random_code<>2 THEN 891
903 GOSUB Spectrum_set_up
904 DISP "PRESS 'CONTINUE' IF YOU HAVE CONNECTED THE 2 CHANNELS"
905 BEEP
906 PAUSE
907 GOSUB Sensitivity
908 DISP "PRESS 'SCAN' i.e. Ko TO VIEW DISPLAY IN TIME/FREQUENCY
DOMAIN"
909 RETURN
910 !
911 !***** SUB TO STORE POINTS OF A SINGLE CHANNEL
*****
912 !***** IN 2 CHANNELS M ODE FROM HP3582 TO DISC FILE
*****
913 Point_store: !
914 Pass$="POINT_STORE"
915 OUTPUT 2 USING "#,K";C$
916 GOSUB Display_select
917 RETURN
918 !***** SUB LDS TO LIST POINT FROM SPECT. TO FILE
*****
919 Lds: !
920 GOSUB Nameing_file
921 CREATE BDAT File$,1,2048
922 OUTPUT @Spect;"LDS"
923 ENTER @Spect;Point$
924 ASSIGN @File TO File$
925 OUTPUT @Spect;"LSP"
926 ENTER @Spect;Lspp$
927 Spanp=VAL(Lspp$)
928 FOR I=0 TO 127
929 FOR J=1 TO 2
930 K=I+1
931 IF J=2 THEN
932 Array(K,J)=VAL(Point$[I*10+1,I*10+9])
933 ELSE
934 Array(K,J)=(Spanp/125)*I
935 END IF
936 NEXT J

```

```

937 NEXT I
938 ! PLOT Array(*)
939 OUTPUT @File;Array(*)
940 ASSIGN @File TO *
941 ! CALL Plot_data(File$)
942 DISP "THE POINTS HAVE BEEN STORED"
943 RETURN
944 !
945 !***** SUB TO STORE SPECTRUM PLOT AS GRAPHIC
*****
946 Graphic_store: !
947 OUTPUT 2 USING "#,K";C$
948 Pass$="GRAPH_STORE"
949 GOSUB Display_select
950 ! LOCAL @SPECT
951 !PRINT "SET THE MOST FAVOURABLE AMPLITUDE REFERENCE ON
SPECTRUM"
952 !PRINT
953 !PRINT "ALSO SELECT THE RIGHT DISPLAY"
954 RETURN
955 !
956 !***** SUB GRAPH STORE TO STORE DISPLAY *****
957 !***** AS GRAPHIC FILE ON DISC *****
958 Graph_store: !
959 GOSUB Nameing_file
960 CREATE BDAT File$,1,512
961 ASSIGN @File TO File$
962 OUTPUT @Spect;"HLTLFM,77455,1"
963 ENTER @Spect USING "#,2A";Spect_state$
964 OUTPUT @Spect;"LFM,74600,128"
965 ENTER @Spect USING "#,256A";Graphs$
966 OUTPUT @Spect;"LAN"
967 ENTER @Spect;Anotat$
968 OUTPUT 1;Anotat$,Spect_stae$,Graphs$
969 OUTPUT @File;Graphs$,Spect_state$,Anotat$
970 ASSIGN @File TO *
971 DISP "STORAGE OF DISPLAY AS GRAPHIC FILE HAS BEEN COMPLETED"
972 OUTPUT @Spect;"RUN"
973 RETURN
974 !
975 !***** SUBROUTINE TO PLOT SPECTRUM DISPLAY ON
COUMOPUTER *****
976 Spec_plot: !
977 PRINT "THIS IS SPEC_PLOT"
978 PRINT "THIS SUBROUTINE IS YET TO BE WRITTEN"
979 RETURN
980 !
981 !***** SUBROUTINE TO DISPLAY NYQUIST PLOT ON COMPUTER

```

```

*****
982 Nyquist_plot:      !
990  PRINT "THIS IS NYQUIST PLOT"
991  PRINT "THIS SUBROUTINE IS YET TO BE WRITTEN"
1000 RETURN
1061 !
1062 !***** SUB TO LOAD GRAPHIC FILE FROM DISC TO SPECTRUM
BUFFER *****
1070 Reload_graph:      !
1080  OUTPUT 2 USING "#,K";C$
1081  GOSUB Nameing_file
1082  ASSIGN @File TO File$
1083  ENTER @File;Graphs$,Spec_status$,Anotat$
1084  OUTPUT @Spect USING "11A/2A";"WTM,77455,1",Spec_status$
1085  OUTPUT @Spect USING "16A/256A";"HLTWTM,74600,128",Graphs$
1086  OUTPUT @Spect;"WTA1,";Anotat$[1,32]
1087  OUTPUT @Spect;"WTA2,";Anotat$[33,64]
1088  OUTPUT @Spect;"WTA3,";Anotat$[65,96]
1089  OUTPUT @Spect;"WTA4,";Anotat$[97,128]
1090  ASSIGN @File TO *
1091  OUTPUT @Spect;"RUN"
1093  RETURN
1094  !
1095  !***** SUB TO LOAD TIME HISTORY FROM DISC TO SPECTRUM
*****
1096  !***** AND VICE VERSA *****
1097 Reload_time:      !
1106  GOSUB Nameing_file
1107  GOSUB Initial_option
1108  Option_header$="TIME DOMAIN FACILITIES : "
1109  Opt1$="STORE A TIME TRACE FROM HP3582 ONTO FILE"
1110  Opt2$="RELOAD A TIME TRACE FROM FIE TO HP3582"
1111  GOSUB Option_menu
1112  IF Option<1 OR Option>2 THEN
1114      GOSUB Warning
1120      GOTO 1111
1121  END IF
1122  ON Option GOSUB Time_store,Time_reload
1123  OUTPUT @Spect;"RUN"
1124  RETURN
1125  !***** SUB TO STORE TIME HISTORY FROM SPECT TO FILE
*****
1126 Time_store:      !
1127  CREATE BDAT File$,1,2300
1128  ASSIGN @File TO File$
1129  OUTPUT @Spect;"HLTLFM,77454,5"
1130  ENTER @Spect USING "#,10A";Spec_full_state$
1131  OUTPUT @Spect;"LFM,70000,1024"

```

```

1132 ENTER @Spect USING "#,2048A";Time_point$
1133 OUTPUT @File;Time_point$,Spec_full_state$
1134 ASSIGN @File TO *
1135 GOSUB Documentation      ! WHY DOCUMENT AT THIS POINT ?
1136 RETURN
1137 !***** SUB TO LOAD TIME HISTORY FROM FILE TO SPECT
*****
1138 Time_reload: !
1139 ASSIGN @File TO File$
1140 ENTER @File;Time_point$,Spec_full_state$
1141 OUTPUT @Spect USING "11A/10A";"WTM,77454,5";Spec_full_state$
1142 OUTPUT @Spect;"HLTWTM,70000,1024"
1143 OUTPUT @Spect USING "#,2048A";Time_point$
1144 ASSIGN @File TO *
1145 RETURN
1146 !
1147 !***** SUB WARNING TO MAKE SURE OPTION CHOSEN IS
VALID*****
1148 Warning: !
1149 OUTPUT 2 USING "#,K";C$
1150 CONTROL 1,1;5
1152 PRINT
1153 PRINT " YOU HAVE SELECTED A WRONG OPTION"
1154 PRINT " YOU WILL BE GIVEN ANOTHER CHANCE"
1155 PRINT " OBSERVE THE CHOICES VERY WELL AND MAKE A VALID ONE"
1156 DISP CHR$(129);" PLEASE WAIT";CHR$(128)
1157 WAIT 10
1159 RETURN
1160 !
1161 !***** SUB SCANS TO SCAN THE DISPLAYS
*****
1162 Scans: !
1163 OUTPUT 2 USING "#,K";C$
1164 Wait_time=20
1165 PRINT "THE DIFFERENT DISPLAYS FOR THE CURRENT INPUT "
1166 PRINT "MODE WILL NOW BE DISPLAYED BY THE SPECTRUM
ANALYZER"
1167 PRINT
1168 PRINT "EACH DISPLAY WILL BE ON FOR ";Wait_time;" SECONDS "
1169 PRINT "AFTER WHICH TIME ANOTHER WILL REPLACE IT"
1170 PRINT
1171 OUTPUT @Spect;"TA1"
1172 DISP "CHAN. A TIME"
1174 WAIT Wait_time
1175 OUTPUT @Spect;"TA0"
1176 OUTPUT @Spect;"TB1"
1177 DISP "CHAN. B TIME"
1179 WAIT Wait_time

```



```

1180 OUTPUT @Spect;"TB0"
1181 OUTPUT @Spect;"AA1"
1182 DISP "CHAN. A AMPLITUDE"
1184 CALL Amplitude_ref !WAIT Wait_time
1185 OUTPUT @Spect;"AA0"
1186 OUTPUT @Spect;"AB1"
1187 DISP "CHAN B. AMPLITUDE"
1189 CALL Amplitude_ref !WAIT Wait_time
1190 OUTPUT @Spect;"AB0"
1191 OUTPUT @Spect;"AX1"
1192 DISP "XFR AMPLITUDE"
1194 CALL Amplitude_ref !WAIT Wait_time
1195 OUTPUT @Spect;"AX0"
1196 OUTPUT @Spect;"PX1"
1197 DISP "XFR PHASE"
1199 WAIT Wait_time
1200 OUTPUT @Spect;"PX0"
1201 OUTPUT @Spect;"CH1"
1202 DISP "COHERENCE"
1204 WAIT Wait_time
1205 OUTPUT @Spect;"CH0"
1206 DISP "FINISH"
1208 RETURN
1209 Look_any_file: !
1210 GOSUB Initial_option
1211 Opt1$="LOOK AT SINE FILE"
1212 Opt2$="LOOK AT PERIODIC FILE"
1213 Opt3$="DISPLAY POINTS FILE"
1214 Option_header$=" 3 TYPES OF FILES CAN BE INSPECTED"
1215 GOSUB Option_menu
1216 IF Option<1 OR Option>3 THEN
1217 GOSUB Warning
1218 GOTO 1215
1219 END IF
1220 OUTPUT 2 USING "#,K";C$
1221 PRINT " IF YOU WANT TO OBTAIN A HARD COPY"
1222 PRINT " ENTER Y *** ANY OTHER CHARACTER WILL "
1223 PRINT " BE IGNORED AND THE DATA WILL BE DISPALYED "
1224 PRINT " ON THE SCREEN"
1225 INPUT "ENTER Y TO PRINT DATA",Yes$
1226 Yes$=UPC$(Yes$)
1227 IF Yes$="Y" THEN
1228 Printer_flag$="ON"
1229 END IF
1230 PRINT CHR$(12)
1231 ON Option GOSUB Read_s_file,Read_p_file,Look_file
1232 Printer_flag$="OFF" ! RESET PRINTER FLSG
1233 RETURN

```

```

1234 !*****
1235 !***** SUB READ_S_FILE *****
1236 Read_s_file:      !
1237     GOSUB Nameing_file
1238     ASSIGN @File TO File$
1239     INPUT "INPUT NUMBER OF RECORDS TO READ",Record
1240     PRINT "SINE SWEPT DATA FILE IS ";File$
1241     FOR I=1 TO Record
1242     ENTER @File;Freq$(I),Chan1$(I),Chan2$(I),Xfr_amp$(I),Xfr_phase$(I),Coher$(I)
1243     PRINT Freq$(I),Chan1$(I),Chan2$(I),Xfr_amp$(I),Xfr_phase$(I),Coher$(I)
1244     IF Printer_flag$="ON" THEN
1246     OUTPUT
@Printer;Freq$(I),Chan1$(I),Chan2$(I),Xfr_amp$(I),Xfr_phase$(I),Coher$(I)
1247     END IF
1249     NEXT I
1250     ASSIGN @File TO *
1251     RETURN
1252 !***** READ P FILE *****
1253 Read_p_file:      !
1254     GOSUB Nameing_file
1255     ASSIGN @File TO File$
1256     INPUT "INPUT NO. OF RECORDS TO READ",Record
1257     PRINT "PERIODIC RANDOM TEST READING ARE FROM FILE ";File$
1258     FOR I=1 TO Record
1259     ENTER
@File;Type_display$(1),Display_value$(1),Display_value$(2),Display_value$(3),Display_value$(4),Display_value$(5),Display_value$(6)
1260     PRINT
Type_display$(1),Display_value$(1),Display_value$(2),Display_value$(3),Display_value$(4),Display_value$(5),Display_value$(6)
1261     IF Printer_flag$="ON" THEN
1263     OUTPUT
@Printer;Type_display$(1),Display_value$(1),Display_value$(2),Display_value$(3),Display_value$(4),Display_value$(5),Display_value$(6)
1264     END IF
1266     NEXT I
1267     ASSIGN @File TO *
1268     RETURN
1269 !***** SUB LOOK FILE TO DISPLAY POINTS FILE *****
1270 Look_file:      !
1271     GOSUB Nameing_file
1272     ASSIGN @File TO File$
1273     ENTER @File;Point$
1274     PRINT Point$
1275     ASSIGN @File TO *
1276     IF Printer_flag$="ON" THEN
1277     OUTPUT @Printer;Point$
1278     END IF

```

```

1280     RETURN
1281     !
1282     !***** SUB TIME TRACE * TO DISPLAY TIME TRACE
*****
1283 Time_trace:      ! ALL STATEMENTS ARE CURRENTLY BLANKED OUT
1284     ! OUTPUT 2 USING "#,K";C$
1285     ! INPUT "INPUT NAME OF FILE CONTAINING TIME TRACE",Time_file$
1286     ! ASSIGN @Time TO Time_file$
1287     ! ENTER @Time;Time_point$
1288     ! ASSIGN @Time TO *
1289     ! FOR I=1 TO 1023 STEP 2
1290     ! Time1$=Dtb$(NUM(Time_point$[I*2-1,I*2-1])) ! Dtb$ SHOULD BE DTB$
1291     ! ! CAN'T CONTINUE UNTILL I KNOW THE MEANING OF THESE
STATEMENTS
1292     ! ! DTB$, BTD
1293     RETURN
1294 Undefined:      !
1295     PRINT "THIS IS NOT YET DEFINED"
1296     RETURN
1297     !
1298     !***** SUBROUTINE OPTION MENU *****
1299 Option_menu:  !
1300     OUTPUT 2 USING "#,K";C$
1301     GCLEAR
1302     Header_length=LEN(Option_header$)
1303     Center=(80-Header_length)/2      ! SO THAT HEADER WILL BE PRINTED
1304     PRINT "SELECT YOUR OPTION"
1305     PRINT
1306     PRINT TAB(Center);Option_header$    ! AT ABOUT CENTRE OF LINE
1307     PRINT
1308     PRINT "1 FOR ";Opt1$
1309     PRINT "2 FOR ";Opt2$
1310     PRINT "3 FOR ";Opt3$
1311     PRINT "4 FOR ";Opt4$
1312     PRINT "5 FOR ";Opt5$
1313     PRINT "6 FOR ";Opt6$
1314     PRINT "7 FOR ";Opt7$
1315     PRINT "8 FOR ";Opt8$
1316     PRINT
1317     INPUT "WHICH OPTION ?? ",Option
1318     IF Option<1 OR Option>8 THEN GOTO 1317
1319     CONTROL 1,1;14
1320     PRINT CHR$(131);"OPTION CHOSEN IS ";Option;CHR$(128)
1321     INPUT "ANSWER Y TO CONFIRM ; N TO CHANGE YOUR
OPTION",Decision$
1322     Decision$=UPC$(Decision$)
1323     IF Decision$<>"Y" AND Decision$<>"N" THEN GOTO 1321
1324     IF Decision$="N" THEN GOTO 1317

```

```

1325 IF Decision$="Y" THEN
1326     DISP "YOUR CHOICE HAS BEEN CONFIRMED"
1327 END IF
1328 RETURN
1329 !
1330 !***** SUBROUTINE INITIAL_OPTION *****
1331 Initial_option:  !
1332 Opt1$=""
1333 Opt2$=""
1334 Opt3$=""
1335 Opt4$=""
1336 Opt5$=""
1337 Opt6$=""
1338 Opt7$=""
1339 Opt8$=""
1340 Option_header$=""
1341 Option=0
1342 RETURN
1343 !
1344 !***** SUBROUTINE DISPLAY_SELECT*****
1345 !***** ALLOWS YOU TO SELECT THE TYPE OF DISPLAY TO BE
STORED*****
1346 Display_select:  !
1347 GOSUB Initial_option
1348 IF Pass$="GRAPH_STORE" THEN
1349     OUTPUT @Spect;"SC2"
1350     GOTO Jump! BYPASS OPTION
1351 END IF
1352 IF Pass$="POINT_STORE" THEN
1353     OUTPUT @Spect;"SC1"      !USE LINEAR SCALE FOR POINT STORE
1354     GOTO Jump! BYPASS OPTION
1355 END IF
1356 GOSUB Initial_option
1357 IF Pass$="SWEPT_SINE" THEN
1358     OUTPUT @Spect;"SC1"
1359     GOTO Sel_dis6
1360 END IF
1361 Option_header$="SCALE OF SPECTRUM PLOT : "
1362 Opt1$="LINEAR SCALE"
1363 Opt2$="10 dB/VOLT SCALE"
1364 Opt3$="2 dB/VOLT SCALE"
1365 GOSUB Option_menu
1366 IF Option<1 OR Option>3 THEN
1367     GOSUB Warning
1368     GOTO 1365
1369 END IF
1370 ON Option GOTO 1371,1373,1375
1371 OUTPUT @Spect;"SC1"

```

```

1372 GOTO Jump
1373 OUTPUT @Spect;"SC2"
1374 GOTO Jump
1375 OUTPUT @Spect;"SC3"
1376 GOTO Jump
1377 Jump:      !
1378 GOSUB Initial_option
1379 Option_header$="TYPES OF DISPLAYS TO BE STORED"
1380 Opt1$="AMPLITUDE OF CHANNEL A"
1381 Opt2$="AMPLITUDE OF CHANNEL B"
1382 Opt3$="XFR AMPLITUDE "
1383 Opt4$="XFR PHASE"
1384 Opt5$="COHERENCE"
1385 Opt6$="ALL DISPLAYS"
1386 Opt7$="AL DISPLAYS EXCEPT AA"
1387 Opt8$="ALL DISPLAYS EXCEPT AA + COHERENCE"
1388 GOSUB Option_menu
1389 OUTPUT @Spect;"AA0AB0AX0PX0CH0PA0PB0"
1391 ON Option GOTO
Sel_dis1,Sel_dis2,Sel_dis3,Sel_dis4,Sel_dis5,Sel_dis6,Sel_dis7,Sel_dis8
1392 Display_return:      ! POINT OF RETURN FOR THE DISPLAY OPTIONS
1393 RETURN
1394
!*****
1395 Sel_dis1:      !
1396 Type_display=1
1397 OUTPUT @Spect;"AA1"
1398 DISP "CHANNEL A AMPLITUDE SPECTRUMIS TURNED ON"
1399 CALL Amplitude_ref
1400 IF Pass$="GRAPH_STORE" THEN GOSUB Graph_store
1401 IF Pass$="POINT_STORE" THEN
1402     GOSUB Lds
1403     ! GOSUB Select_marker
1404 END IF
1405 OUTPUT @Spect;"AA0"
1406 DISP "CHANNEL A AMPLITUDE SPECTRUMIS TURNED OFF"
1407 GOTO Display_return
1408 !
1409 Sel_dis2:      !
1410 Type_display=2
1411 OUTPUT @Spect;"AB1"
1412 DISP "CHANNEL B AMPLITUDE SPECTRUM IS TURNED ON"
1413 CALL Amplitude_ref
1414 IF Pass$="GRAPH_STORE" THEN GOSUB Graph_store
1415 IF Pass$="POINT_STORE" THEN
1416     GOSUB Lds
1417     ! GOSUB Select_marker
1418 END IF

```

```

1419 OUTPUT @Spect;"AB0"
1420 DISP "CHANNEL B AMPLITUDE SPECTRUM IS TURNED OFF"
1421 GOTO Display_return
1422 !
1423 Sel_dis3: !
1424 Type_display=3
1425 OUTPUT @Spect;"AX1"
1426 DISP "AMPLITUDE OF RESPONSE FUNCTION ON"
1427 CALL Amplitude_ref
1428 IF Pass$="GRAPH_STORE" THEN GOSUB Graph_store
1429 IF Pass$="POINT_STORE" THEN
1430     GOSUB Lds
1431     ! GOSUB Select_marker
1432 END IF
1433 OUTPUT @Spect;"AX0"
1434 DISP "AMPLITUDE OF RESPONSE FUNCTION TURNED OFF"
1435 GOTO Display_return
1436 !
1437 Sel_dis4: !
1438 Type_dis=4
1439 OUTPUT @Spect;"PX1"
1440 DISP "PHASE OF RESPONSE FUNCTION IS ON"
1441 IF Pass$="GRAPH_STORE" THEN GOSUB Graph_store
1442 IF Pass$="POINT_STORE" THEN
1443     GOSUB Lds
1444     ! GOSUB Select_marker
1445 END IF
1446 OUTPUT @Spect;"PX0"
1447 DISP "PHASE OF RESPONSE FUNCTION IS OFF"
1448 GOTO Display_return
1449 !
1450 Sel_dis5: !
1451 Type_display=5
1452 OUTPUT @Spect;"CH1"
1453 DISP "COHERENCE FUNCTION NOW ON"
1454 IF Pass$="GRAPH_STORE" THEN GOSUB Graph_store
1455 IF Pass$="POINT_STORE" THEN
1456     GOSUB Lds
1457     ! GOSUB Select_marker
1458 END IF
1459 OUTPUT @Spect;"CH0"
1460 DISP "COHERENCE FUNCTION IS OFF"
1461 GOTO Display_return
1462 !
1463 Sel_dis6: !
1464 Type_display=1
1465 OUTPUT @Spect;"AA1"
1466 DISP "CHANNEL A AMPLITUDE IS ON"

```

```

1467 IF Pass$="SWEPT_SINE" THEN GOTO 1478
1468 CALL Amplitude_ref
1469 IF Pass$="POINT_STORE" THEN
1470     GOSUB Lds
1471     ! GOSUB Select_marker
1472     GOTO 1495
1473 END IF
1474 IF Pass$="GRAPH_STORE" THEN
1475     GOSUB Graph_store
1476     GOTO 1495
1477 END IF
1478 IF Pass$="SWEPT_SINE" THEN
1479     GOTO 1484
1480 ELSE
1481     DISP "ERROR AT LINE 1437"
1482     STOP
1483 END IF
1484 GOSUB Search_marker
1485 Amp_ref=1
1486 OUTPUT @Spec;"AM1"
1487 GOSUB Read_marker
1488 IF Marker_reading$[1,10]="+9.990E+99" THEN
1489     Amp_ref=Amp_ref+1
1490     OUTPUT @Spect;"AM"&VAL$(Amp_ref)
1491     GOTO 1487
1492 END IF
1493 Chan1$(Ii)=Marker_reading$
1494 Freq$(Ii)=VAL$(Freq)
1495 OUTPUT @Spect;"AA0"
1496 DISP "AMPLITUDE OF CHANNEL A IS OFF"
1497 OUTPUT @Spect;"AB1"
1498 DISP "AMPLITUDE OF CHANNEL B IS ON"
1499 Type_display=2
1500 IF Pass$="SWEPT_SINE" THEN GOTO 1511
1501 CALL Amplitude_ref
1502 IF Pass$="POINT_STORE" THEN
1503     GOSUB Lds
1504     ! GOSUB Select_marker
1505     GOTO 1528
1506 END IF
1507 IF Pass$="GRAPH_STORE" THEN
1508     GOSUB Graph_store
1509     GOTO 1528
1510 END IF
1511 IF Pass$="SWEPT_SINE" THEN
1512     GOTO 1517
1513 ELSE
1514     DISP "ERROR AT LINE 1470"

```

```

1515     STOP
1516 END IF
1517 GOSUB Search_marker
1518 Amp_ref=1
1519 OUTPUT @Spect;"AM1"
1520 GOSUB Read_marker
1521 IF Marker_reading$[1,10]="+9.990E+99" THEN
1522     Amp_ref=Amp_ref+1
1523     OUTPUT @Spect;"AM"&VAL$(Amp_ref)
1524     GOTO 1520
1525 END IF
1526 Chan2$(li)=Marker_reading$
1527 Freq$(li)=VAL$(Freq)
1528 OUTPUT @Spect;"AB0"
1529 DISP "CHANNEL B AMPLITUDE IS OFF"
1530 OUTPUT @Spect;"AX1"
1531 DISP "AMPLITUDE OF RESPONSE FUNCTION IS ON "
1532 Type_display=3
1533 IF Pass$="SWEPT_SINE" THEN GOTO 1544
1534 CALL Amplitude_ref
1535 IF Pass$="POINT_STORE" THEN
1536     GOSUB Lds
1537 !   GOSUB Select_marker
1538     GOTO 1561
1539 END IF
1540 IF Pass$="GHRAPH_STORE" THEN
1541     GOSUB Graph_store
1542     GOTO 1561
1543 END IF
1544 IF Pass$="SWEPT_SINE" THEN
1545     GOTO 1550
1546 ELSE
1547     DISP "ERROR AT LINE 1567"
1548     STOP
1549 END IF
1550 GOSUB Search_marker
1551 Amp_ref=1
1552 OUTPUT @Spect;"AM1"
1553 GOSUB Read_marker
1554 IF Marker_reading$[1,10]="+9.990E+99" THEN
1555     Amp_ref=Amp_ref+1
1556     OUTPUT @Spect;"AM"&VAL$(Amp_ref)
1557     GOTO 1553
1558 END IF
1559 Xfr_amp$(li)=Marker_reading$
1560 Freq$(li)=VAL$(Freq)
1561 OUTPUT @Spect;"AX0"
1562 DISP "AMPLITUDE OF RESPONSE FUNCTION IS OFF"

```



```

1563     OUTPUT @Spect;"PX1"
1564     DISP "PHASE OF TRANSFER FUNCTION IS ON"
1565     Type_display=4
1566     IF Pass$="POINT_STORE" THEN
1567         GOSUB Lds
1568     !     GOSUB Select_marker
1569         GOTO 1585
1570     END IF
1571     IF Pass$="GRAPH_STORE" THEN
1572         GOSUB Graph_store
1573         GOTO 1585
1574     END IF
1575     IF Pass$="SWEPT_SINE" THEN
1576         GOTO 1581
1577     ELSE
1578         DISP "ERROR AT LINE 1877"
1579         STOP
1580     END IF
1581     GOSUB Search_marker
1582     GOSUB Read_marker
1583     Xfr_phase$(Ii)=Marker_reading$
1584     Freq$(Ii)=VAL$(Freq)
1585     OUTPUT @Spect;"PX0"
1586     DISP "PHASE MOF RESPONSE FUNCTION IS OFF"
1587     OUTPUT @Spect;"CH1"
1588     DISP "COHERENCE FUNCTION IS ON"
1589     Type_display=5
1590     IF Pass$="POINT_STORE" THEN
1591         GOSUB Lds
1592     !     GOSUB Select_marker
1593         GOTO 1609
1594     END IF
1595     IF Pass$="GRAPH_STORE" THEN
1596         GOSUB Graph_store
1597         GOTO 1609
1598     END IF
1599     IF Pass$="SWEPT_SINE" THEN
1600         GOTO 1605
1601     ELSE
1602         DISP "ERROR AT LINE 2117"
1603         STOP
1604     END IF
1605     GOSUB Search_marker
1606     GOSUB Read_marker
1607     Coher$(Ii)=Marker_reading$
1608     Freq$(Ii)=VAL$(Freq)
1609     OUTPUT @Spect;"CH0"
1610     DISP "COHERNCE FUNCTION IS OFF"

```

```

1611      GOTO Display_return
1612  !
1613 Sel_dis7:  !
1614      OUTPUT @Spect;"AB1"
1615      DISP "CHANNEL B AMPLITUDE SPECTRUM IS ON"
1616      Type_display=2
1617      CALL Amplitude_ref
1618      IF Pass$="GRAPH_STORE" THEN GOSUB Graph_store
1619      IF Pass$="POINT_STORE" THEN
1620          GOSUB Lds
1621      !      GOSUB Select_marker
1622      END IF
1623      OUTPUT @Spect;"AB0"
1624      DISP "CHANNEL B AMPLITUDE SPECTRUM IS OFF"
1625      OUTPUT @Spect;"AX1"
1626      DISP "AMPLITUDE OF RESPONSE FUNCTION IS ON"
1627      Type_display=3
1628      CALL Amplitude_ref
1629      IF Pass$="GRAPH_STORE" THEN GOSUB Graph_store
1630      IF Pass$="POINT_STORE" THEN
1631          GOSUB Lds
1632      !      GOSUB Select_marker
1633      END IF
1634      OUTPUT @Spect;"AX0"
1635      DISP "AMPLITUDE OF RESPONSE FUNCTION IS OFF"
1636      OUTPUT @Spect;"PX1"
1637      DISP "PHASE OF RESPONSE FUNCTION IS ON"
1638      Type_display=4
1639      IF Pass$="GRAPH_STORE" THEN GOSUB Graph_store
1640      IF Pass$="POINT_STORE" THEN
1641          GOSUB Lds
1642      !      GOSUB Select_marker
1643      END IF
1644      OUTPUT @Spect;"PX0"
1645      DISP "PHASE OF RESPONSE FUNCTION IS OFF"
1646      OUTPUT @Spect;"CH1"
1647      DISP "COHERENCE FUNCTION IS ON"
1648      Type_display=5
1649      IF Pass$="GRAPH_STORE" THEN GOSUB Graph_store
1650      IF Pass$="POINT_STORE" THEN
1651          GOSUB Lds
1652      !      GOSUB Select_marker
1653      END IF
1654      OUTPUT @Spect;"CH0"
1655      DISP "COHERENCE FUNCTION IS OFF"
1656      GOTO Display_return
1657  !
1658 Sel_dis8:  !

```

```

1659     OUTPUT @Spect;"AB1"
1660     DISP "AMPLITUDE SPECTRUM OF CHANNEL B IS ON"
1661     Type_display=2
1662     CALL Amplitude_ref
1663     IF Pass$="GRAPH_STORE" THEN GOSUB Graph_store
1664     IF Pass$="POINT_STORE" THEN
1665         GOSUB Lds
1666     !     GOSUB Select_marker
1667     END IF
1668     OUTPUT @Spect;"AB0"
1669     DISP "AMPLITUDE SPECTRUM OF CHANNEL B IS OFF"
1670     OUTPUT @Spect;"AX1"
1671     DISP "AMPLITUDE SPECTRUM OF RESPONSE FUNCTION IS ON"
1672     Type_display=3
1673     CALL Amplitude_ref
1674     IF Pass$="GRAPH_STORE" THEN GOSUB Graph_store
1675     IF Pass$="POINT_STORE" THEN
1676         GOSUB Lds
1677     !     GOSUB Select_marker
1678     END IF
1679     OUTPUT @Spect;"AX0"
1680     DISP "AMPLITUDE SPECTRUM OF RESPONSE FUNCTION IS OFF"
1681     OUTPUT @Spect;"PX1"
1682     DISP "PHASE SPECTRUM OF RESPONSE SPECTRUM IS ON"
1683     Type_display=4
1684     IF Pass$="GRAPH_STORE" THEN GOSUB Graph_store
1685     IF Pass$="POINT_STORE" THEN
1686         GOSUB Lds
1687     !     GOSUB Select_marker
1688     END IF
1689     OUTPUT @Spect;"PX0"
1690     DISP "PHASE SPECTRUM OF RESPONSE FUNCTION IS OFF"
1691     GOTO Display_return
1692     !
1693     !*****SUB SPECTRUM SET_UP *****
1694     Spectrum_set_up:      !
1695         IF Periodic$="Y" THEN GOSUB Peri_ran_set_up
1696         IF Periodic$="Y" THEN 1709
1697         DISP "SET UP OF HP3582A"
1698         GOSUB Initial_option
1699         Opt1$="PERIODIC RANDOM SET UP"
1700         Opt2$="SWEPT SINE TEST"
1701         Opt3$="TRANSIENT DECAY TEST"
1702         GOSUB Option_menu
1703         IF Option<1 OR Option>3 THEN
1704             GOSUB Warning
1705             GOTO 1703
1706         END IF

```

```

1708     ON Option GOSUB Peri_ran_set_up,Swept_sin_setup,Decay_set_up
1709     RETURN
1710     !
1711     !***** SUB PERI_RAN_SET_UP TO SET UP FOR *****
1712     !***** PERIODIC RANDOM TEST*****
1713 Peri_ran_set_up:    !
1714     GOSUB Common_set_up
1715     PRINT
1717     IF Random_type$="PERIODIC" THEN
1718     OUTPUT @Spect;"PS3"
1719     PRINT "UNIFORM PASS BAND WINDOW IS ON"
1720     ELSE
1721     OUTPUT @Spect;"PS2"
1722     PRINT "HANNING PASS BAND WINDOW IS ON"
1723     END IF
1724     PRINT
1725     RETURN
1726     !***** SET UP HP3582A FOR SWEPT SINE *****
1727 Swept_sin_setup:    !
1728     GOSUB Common_set_up
1729     OUTPUT @Spect;"PS1"
1730     DISP "FLAT TOP PASS BAND WINDOW IS ON"
1731     RETURN
1732     !*****SET UP HP3582A FOR DECAY TEST *****
1733 Decay_set_up:    !
1734     GOSUB Common_set_up
1735     DISP "DIFFERENT TIME RECORD SHAPE CAN BE SET BY DIFFERENT
FREQ SPAN OF ANALYSIS"
1736     WAIT 500      ! ISN'T THIS WAITING TOO MUCH?
1737     OUTPUT @Spect;"RP0"
1738     DISP "REPIPITIVE HAS BEEN TURN OFF"
1739     OUTPUT @Spect;"FR0"
1740     DISP "FREE RUN HAS BEEN TURN OFF"
1741     OUTPUT @Spect;"PS3"
1742     DISP "UNIFORM PASS BAND WINDOW IS ON"
1743     GOSUB Sensitivity
1744     OUTPUT @Spect;"AR"
1745     DISP "ARM HAS BEEN TURN ON"
1746     GOSUB Sensitivity
1747     INPUT "IS THE CAPTURED TRACE O.K ** ANSWER Y OR N
**",Deci_cap$
1748     Deci_cap$=UPC$(Deci_cap$)
1749     IF Deci_cap$<>"Y" OR Deci_cap$<>"N" THEN GOTO 1747
1750     IF Deci_cap$="N" THEN GOTO 1746
1751     RETURN
1752     !
1753     !***** COMMON SET UP OF HP3582A FOR ALL TESTS
*****

```

```

1754 Common_set_up:      !
1755     OUTPUT 2 USING "#,K";C$
1756     OUTPUT @Spect;"IM2"
1757     PRINT "BOTH CHANNELS ON"
1758     PRINT
1759     OUTPUT @Spect;"AC2"
1760     PRINT "DC COUPLING FOR CHANNEL A FOR LOW SIGNALS"
1761     PRINT
1762     OUTPUT @Spect;"BC2"
1763     PRINT "DC COUPLING FOR CHANNEL B FOR LOW SIGNALS"
1764     OUTPUT @Spect;"RP1"
1765     PRINT
1766     PRINT "REPETITIVE ON"
1767     PRINT
1768     OUTPUT @Spect;"FR1"
1769     PRINT "FREE RUN ON"
1770     PRINT
1771     OUTPUT @Spect;"AV2"
1772     PRINT "RMS AVERAGING ON FOR COHERENCE MEASUREMENT"
1773     PRINT
1774     OUTPUT @Spect;"MD2"
1775     PRINT "ZERO START MODE"
1776     PRINT
1777 !     IF Periodic$="Y" THEN
1778 !         OUTPUT @Spect;"SP5NU3"      !SP5 = 25Hz SPAN . CHANGE THIS AS
PER STRUCTURE
1779 !         GOTO 1785  !QUICK BYPASS  ! BUT IS THIS DESIRABLE ?
1780 !     END IF
1781 !     INPUT "INPUT FREQUENCY SPAN MODE 1-14",Span$
1782     WAIT 3
1783     CALL Freq_span_mode(Span$)
1784     Current_span$=Span$      ! VARIABLE USED IN SENSITIVITY
1785     OUTPUT @Spect;"SP"&Span$! SET UP FREQ. SPAN OF ANALYSIS
1786 !     INPUT "ENTER NO. OF AVERAGES -- MODE NO. 1-4",No_average$
1787     CALL Num_averages(No_average)
1788     IF No_average>4 THEN
1789     OUTPUT @Spect;"SH1"      !SHIFT IS ON
1790     PRINT "SHIFT IS ON"
1791     WAIT 2
1792     No_average=No_average-4
1793     END IF
1794     No_average$=VAL$(No_average)
1795     OUTPUT @Spect;"NU"&No_average$
1796     OUTPUT @Spect;"RE"
1797     RETURN
1798 !
1799 !***** SUB SENSITIVITY *****
1800 Sensitivity:      !

```

```

1801     OUTPUT 2 USING "#,K";C$
1802     PRINT "CONNECT THE TWO SIGNALS"
1803     PRINT
1804 !     OUTPUT @Spect;"SP5"! NEED TO CHANGE ANALYSIS SPAN
1805 ! ANALYSIS SPAN ALREADY SET IN COMMON_SET_UP
1806         ! SET A FAST SAMPLING RATE TO CHECK OVERLOAD
1807     I=10! THE HIGHEST SENSITIVITY TO LOW VOLTAGES
1808     Chan$="CHANNEL A"
1809     Status_bit=2
1810     Chan_set$="AS"! SET CHANNEL A SENSITIVITY
1811     OUTPUT @Spect;"RERP1FR1"! COMPLTETE A TIME RECORD SINCE
OVERLOAD IS ONLY CHECKED AFTER A TIME RECORD IS FINISHED
1812     OUTPUT @Spect;Chan_set$&VAL$(I)
1813 !WAIT 50
1814     OUTPUT @Spect;"LST0"! INTERROGATE OVERLOAD STATUS AND
RESET BITS
1815     ENTER @Spect USING "#,B";Overload
1816     Check_bit=BIT(Overload,Status_bit)
1817     DISP "CHECK BIT FOR ";Chan$;" IS ";Check_bit
1818     IF Check_bit=1 THEN GOTO 1820
1819     IF Check_bit<>1 THEN GOTO 1823
1820     OUTPUT @Spect;"RE"
1821     I=I-1
1822     GOTO 1811
1823     IF Chan$="CHANNEL B" THEN GOTO 1829
1824     Chan$="CHANNEL B"
1825     I=10
1826     Status_bit=3
1827     Chan_set$="BS"
1828     GOTO 1811
1829     OUTPUT @Spect;"LAS"
1830     ENTER @Spect;A_sensitivity$
1831     PRINT "CHANNEL A SENSITIVITY IS : ";A_sensitivity$
1832     OUTPUT @Spect;"LBS"
1833     ENTER @Spect;B_sensitivity$
1834     PRINT "CHANNEL B SENSITIVITY IS ; ";B_sensitivity$
1835     OUTPUT @Spect;"SP"&Current_span$ ! SET IN COMMON_SET_UP
1836     OUTPUT @Spect;"RE"
1837     DISP "THE SPECTRUM IS NOW TAKING MEASUREMENTS ! ... PLEASE
WAIT "
1838     OUTPUT @Spect;"LST0"!INTERROGAT OVERLOAD STATUS AND RESET
BITS
1839     Status_bit=2
1840     ENTER @Spect USING "#,B";Overload
1841     Check_bit=BIT(Overload,Status_bit)
1842     IF Check_bit=1 THEN
1843         DISP "OVERLOAD AGAIN ; RESTART RECORDING"
1844         BEEP 1300,1

```

```

1845      WAIT 3
1846      END IF
1847      IF Check_bit=1 THEN GOTO 1801
1848      Status_bit=3
1849      Check_bit=BIT(Overload,Status_bit)
1850      IF Check_bit=1 THEN
1851          DISP "OVERLOAD AGAIN : RESTART RECORDING"
1852          BEEP 1300,1
1853          WAIT 3
1854      END IF
1855      IF Check_bit=1 THEN GOTO 1801
1856      Average_measur=Overload
1857      Check_bit=BIT(Average_measur,6)      !CHECK IF AVERAGE IS
COMPLETE
1858      IF Check_bit=1 THEN GOTO 1860
1859      IF Check_bit<>1 THEN GOTO 1838
1860      OUTPUT @Spect;"LST0"!INTERROGATE OVERLOAD STATUS
1861      Status_bit=2
1862      ENTER @Spect USING "#,B";Overload
1863      Check_bit=BIT(Overload,Status_bit)
1864      IF Check_bit=1 THEN
1865          DISP "OVERLOAD AGAIN ; RESTART RECORDING"
1866          BEEP 1300,1
1867          WAIT 3
1868      END IF
1869      IF Check_bit=1 THEN GOTO 1801
1870      Status_bit=3
1871      Check_bit=BIT(Overload,Status_bit)
1872      IF Check_bit=1 THEN
1873          DISP "OVERLOAD AGAIN ; RESTART RECORDING"
1874          BEEP 1300,1
1875          WAIT 3
1876      END IF
1877      IF Check_bit=1 THEN GOTO 1801
1878      RETURN
1879      !
1880      !***** SUB POSTER *****
1881      Poster:  !
1882      OUTPUT 2 USING "#,K";C$
1883      GCLEAR
1884      GINIT
1885      GRAPHICS ON
1886      MOVE 1,80
1887      CSIZE 12,,5
1888      LABEL Poster$
1889      RETURN
1890      !!
1891      !***** SUB SINE SWEPT ; FOR SINE TESTING *****

```

```

1892 Sine_swept:  !
1893     OUTPUT 2 USING "#,K";C$
1894     Poster$="SINE SWEEP TEST"
1895     GOSUB Poster
1896     Pass$="SWEPT_SINE"
1897     INPUT "INPUT START FREQUENCY",Start_freq
1898     INPUT "INPUT FINISH FREQUENCY",Finish_freq
1899     INPUT "INPUT FREQUENCY STEP IN Hz ",Freq_step
1900     INPUT "INPUT TIME STEP IN SECONDS",Time_step
1901 Ac_input:      !
1902     INPUT "INPUT UPPER AC LEVEL IN FREE FORMAT",Upper_ac
1903     INPUT "INPUT LOWER AC LEVEL IN FREE FORMAT",Lower_ac
1904     INPUT "INPUT AC LEVEL TOTAL NUMBER OF STEPS",Ac_step
1905     GOSUB Freq_span_sel
1906     GOSUB Initial_option
1907     Option_header$="SINE SWEPT TEST OPTIONS"
1908     Opt1$="SWEPT WITHOUT FILING"
1909     Opt2$="SWEPT WITH FILING"
1910     Swept_flag=0
1911     GOSUB Option_menu
1912     IF Option<0 OR Option>2 THEN
1913         GOSUB Warning
1914         BEEP
1915         Swept_flag=1
1916     END IF
1917     IF Swept_flag=1 THEN GOTO 1910
1918     FOR Ac=Lower_ac TO Upper_ac STEP (Upper_ac-Lower_ac)/Ac_step
1919         GOSUB Ac_dc_formatting
1920         ON Option GOTO Swept_no_filing,Swept_with_file
1921 Swept_with_file:  !
1922         File_or_not$="Y"
1923 Swept_no_filing:  !
1924         OUTPUT @Philip;"A";M$;"D00W1";" "
1925         Ii=1
1926         FOR Freq=Start_freq TO Finish_freq STEP Freq_step
1927             OUTPUT @Philip;"F";VAL$(Freq*.001);" "
1928             CONTROL 1,1;5
1929             PRINT "DRIVING FREQUENCY NOW = ";Freq;" HZ"
1930             PRINT
1931             PRINT "AC LEVEL NOW = ";Ac;" VOLTS P-P"
1932             OUTPUT @Spect;"PS1IM2AC2BC2RP1FR1AV2MD2NU1"
1933             Current_span$="5"! MIGHT NEED TO CHANGE THE FREQ. SPAN
1934             GOSUB Sensitivity
1935             GOSUB Display_select
1936             Ii=Ii+1
1937         NEXT Freq
1938         IF File_or_not$<>"Y" THEN 1943
1939         Total_freq_step=Ii

```



```

1940      GOSUB File_sine_swept
1941      DISP "A FREQ_SWEPT CYCLE IS FINISHED, GOTO NEXT AC
INCREAMENT ; A NEW FILE NAME HAS TO BE GIVEN LATER NOT NOW"
1942      WAIT 4
1943      NEXT Ac
1944      Ii=1
1945      GOSUB Nameing_file
1946      RETURN
1947      !
1948      !***** SUB AC-DC FORMATING *****
1949      Ac_dc_formatting:      !
1950      IF Ac<=19.9 THEN Ac_ok
1951      PRINT "AC VALUE MUST BE LESS THAN 19.99 VOLTS, TRY AGAIN"
1952      GOTO Ac_input
1953      Ac_ok:      !
1954      As=Ac+100.0005
1955      Ac$=VAL$(As)
1956      FOR I=0 TO 2
1957      DISP I
1958      IF Ac>=.2*101I THEN GOTO 1960
1959      M$=Ac$[4-I,7-I]
1960      NEXT I
1961      RETURN
1962      !
1963      !***** SUB FILE_SINE SWEPT *****
1964      File_sine_swept:      !
1965      GOSUB Nameing_file
1966      CREATE BDAT File$,Total_freq_step,90
1967      ASSIGN @File TO File$
1968      FOR I=1 TO Total_freq_step-1
1969      OUTPUT
@File;Freq$(I),Chan1$(I),Chan2$(I),Xfr_amp$(I),Xfr_phase$(I),Coher$(I)
1970      CONTROL 1,1;12
1971      PRINT Freq$(I),Chan1$(I),Chan2$(I),Xfr_amp$(I),Xfr_phase$(I),Coher$(I)
1972      NEXT I
1973      ASSIGN @File TO *
1974      RETURN
1975      !
1976      !***** SUB NAMEING_FILE *****
1977      Nameing_file:      !
1978      OUTPUT 2 USING "#,K";C$
1979      PRINT "CURRENT DATE IS ";Current_date$
1980      INPUT "ANSWER Y TO CONFIRM ** N TO CHANGE DATE",Deci_date$
1981      Deci_date$=UPC$(Deci_date$)
1982      IF Deci_date$<>"Y" AND Deci_date$<>"N" THEN GOTO 1980
1983      IF Deci_date$="Y" THEN GOTO 1995
1984      IF Deci_date$="N" THEN
1985      INPUT "INPUT NEW DATE",New_date$

```

```

1986      PRINT
1987      CONTROL 1,1;1
1988      PRINT "NEW DATE IS ";New_date$
1989      INPUT "IS THIS O.K ? ;ANSWER Y *OR* N ",Deci_new$
1990      Deci_new$=UPC$(Deci_new$)
1991      IF Deci_new$<>"Y" AND Deci_new$<>"N" THEN GOTO 1989
1992      IF Deci_new$="N" THEN GOTO 1985
1993      Current_date$=New_date$
1994  END IF
1995  PRINT
1996  PRINT "CURRENT SERIAL NUMBER IS ";Current_ser$
1997  INPUT "ANSWER Y TO CONFIRM *** N TO CHANGE***",Deci_ser_old$
1998  Deci_ser_old$=UPC$(Deci_ser_old$)
1999  IF Deci_ser_old$<>"Y" AND Deci_ser_old$<>"N" THEN GOTO 1997
2000  IF Deci_ser_old$="Y" THEN GOTO 2012
2001  IF Deci_ser_old$="N" THEN
2002      INPUT "INPUT NEW SERIAL NUMBER",New_ser$
2003      PRINT
2004      CONTROL 1,1;1
2005      PRINT "NEW SERIAL NUMBER IS ";New_ser$&" "
2006      INPUT "IS THIS O.K ? ;ANSWER Y *OR* N ",Deci_ser_new$
2007      Deci_ser_new$=UPC$(Deci_ser_new$)
2008      IF Deci_ser_new$<>"Y" AND Deci_ser_new$<>"N" THEN GOTO 2006
2009      IF Deci_ser_new$="N" THEN GOTO 2002
2010      Current_ser$=New_ser$
2011  END IF
2012  PRINT
2013  PRINT "CURRENT INDEX NUMBER IS ";Current_index$&" "
2014  INPUT "ANSWER Y TO CONFIRM *** N TO CHANGE***",Deci_ind_old$
2015  Deci_ind_old$=UPC$(Deci_ind_old$)
2016  IF Deci_ind_old$<>"Y" AND Deci_ind_old$<>"N" THEN GOTO 2014
2017  IF Deci_ind_old$="Y" THEN GOTO 2029
2018  IF Deci_ind_old$="N" THEN
2019      INPUT "INPUT NEW INDEX NUMBER",New_index$
2020      PRINT
2021      CONTROL 1,1;1
2022      PRINT "NEW INDEX NUMBER IS ";New_index$&" "
2023      INPUT "IS THIS O.K ? ;ANSWER Y *OR* N ",Deci_ind_new$
2024      Deci_ind_new$=UPC$(Deci_ind_new$)
2025      IF Deci_ind_new$<>"Y" AND Deci_ind_new$<>"N" THEN GOTO 2023
2026      IF Deci_ind_new$="N" THEN GOTO 2019
2027      Current_index$=New_index$
2028  END IF
2029  PRINT
2030  File$=Current_date$&Current_ser$&Current_index$
2031  File$=File$[1,10]
2032  DISP "FILE NAME IS ";File$;" ";CHR$(131);"WAIT";CHR$(128)
2033  WAIT 3

```

```

2034     RETURN
2035     !
2036     !***** SUB SEARCH_MARKER *****
2037 Search_marker:      !
2038     OUTPUT @Spect;"LSP"
2039     ENTER @Spect;Freq_span$
2040     Freq_span=VAL(Freq_span$)
2041     Marker_position=(125/Freq_span)*(Freq-0)
2042     OUTPUT @Spect;"MN1MR0MS0MB0MT0MP"&VAL$(Marker_position)
2043     RETURN
2044     !
2045     !***** SUB READ_MARKER
*****
2046 Read_marker:      !
2047     OUTPUT @Spect;"LMK"
2048     ENTER @Spect;Lmk$
2049     Marker_freq$=Lmk$[12,20]
2050     Marker_reading$=Lmk$[1,10]
2051     DISP "MARKER FREQ. & READING ARE .";Marker_freq$,Marker_reading$
2052     RETURN
2053     !
2054     !***** SUB SELECT_MARKER *****
2055 Select_marker:      !
2056     OUTPUT 2 USING "#,K";C$
2057     PRINT "THE MARKER WILL BE READ AT THESE FREQUENCIES ;"
2058     PRINT " 2.4, 5.6, 10.56, 12, 17.8, 25"
2059     Resonant_freq(1)=2.4
2060     Resonant_freq(2)=5.6
2061     Resonant_freq(3)=10.56
2062     Resonant_freq(4)=12
2063     Resonant_freq(5)=17.8
2064     Resonant_freq(6)=25
2065     I=1
2066     Freq=Resonant_freq(I)
2067     IF Bypass_marker$="Y" THEN
2068     Marker_position=(125/25)*(Freq-0)
2069     GOTO 2076
2070     END IF
2071     GOSUB Search_marker
2072     GOSUB Read_marker
2073     GOTO 2077
2074     PRINT
2075     PRINT "THESE VALUES ARE FROM 'POINT$'
";Point$[Marker_position*10+1,(Marker_position+1)*10]
2076     Marker_reading$=Point$[Marker_position*10+1,(Marker_position+1)*10]
2077     Option=Type_display
2078     ON Option GOTO 2079,2085,2091,2097,2103
2079     Chan1$(I)=Marker_reading$[1,10]

```

```

2080   Display_value$(I)=Chan1$(I)
2081   Type_display$(Type_display)="CHANNEL# 1"
2082   IF I>=6 THEN GOTO Escape
2083   I=I+1
2084   GOTO 2066
2085   Chan2$(I)=Marker_reading$[1,10]
2086   Display_value$(I)=Chan2$(I)
2087   Type_display$(Type_display)="CHANNEL# 2"
2088   IF I>=6 THEN GOTO Escape
2089   I=I+1
2090   GOTO 2066
2091   Xfr_amp$(I)=Marker_reading$[1,10]
2092   Display_value$(I)=Xfr_amp$(I)
2093   Type_display$(Type_display)="XFR_AMP  "
2094   IF I>=6 THEN GOTO Escape
2095   I=I+1
2096   GOTO 2066
2097   Xfr_phase$(I)=Marker_reading$[1,10]
2098   Display_value$(I)=Xfr_phase$(I)
2099   Type_display$(Type_display)="XFR_PHASE "
2100   IF I>=6 THEN GOTO Escape
2101   I=I+1
2102   GOTO 2066
2103   Coher$(I)=Marker_reading$[1,10]
2104   Display_value$(I)=Coher$(I)
2105   Type_display$(Type_display)="COHERENCE "
2106   IF I>=6 THEN GOTO Escape
2107   I=I+1
2108   GOTO 2066
2109 Escape:   IF Escape$="Y" THEN GOTO 2119
2110 INPUT "HOW MANY DISPLAY IN TOTAL ?? ",Total_display
2111 DISP "ENTER NAME OF FILE FOR MARKER READINGS"
2112 WAIT 4
2113 GOSUB Nameing_file
2114 CREATE BDAT File$,Total_display,91
2115 ASSIGN @File_sel TO File$
2116 INPUT "DO YOU WANT A HARD COPY ** Y OR N ** ",Dis_hard$
2117 Dis_hard$=UPC$(Dis_hard$)
2118 DISP "MARKER READINGS WILL BE STORED IN ";File$
2119 OUTPUT
@File_sel;Type_display$(Type_display),Display_value$(1),Display_value$(2),Display_value
$(3),Display_value$(4),Display_value$(5),Display_value(6)
2120 PRINT
Type_display$(Type_display),Display_value$(1),Display_value$(2),Display_value$(3),Displ
ay_value$(4),Display_value$(5),Display_value(6)
2121 IF Dis_hard$="Y" THEN
2122 OUTPUT
@Printer;Type_display$(Type_display),Display_value$(1),Display_value$(2),Display_value$

```

```

(3),Display_value$(4),Display_value$(5),Display_value(6)
2123   END IF
2124   INPUT "ANOTHER DISPLAY TO BE FOLLOWED ??",Deci_disp$
2125   Deci_disp$=UPC$(Deci_disp$)
2126   IF Deci_disp$="Y" THEN
2127     Escape$="Y"
2128     GOTO 2132
2129   END IF
2130   ASSIGN @File_sel TO *
2131   Escape$="N"      !RESET FLAG
2132   RETURN
2133   !*****
2134   !***** SUB FREQ_SPAN_SEL *****
2135   Freq_span_sel:      !
2136     Mode_0_start(1)=1
2137     Mode_0_start(2)=2.5
2138     Mode_0_start(3)=5
2139     Mode_0_start(4)=10
2140     Mode_0_start(5)=25
2141     Mode_0_start(6)=50
2142     Mode_0_start(7)=100
2143     Mode_0_start(8)=250
2144     Mode_0_start(9)=500
2145     Mode_0_start(10)=1000
2146     Mode_0_start(11)=2500
2147     Mode_0_start(12)=5000
2148     Mode_0_start(13)=10000
2149     Mode_0_start(14)=25000
2150     FOR I=1 TO 14
2151       IF Finish_freq-Mode_0_start(I)<0 THEN
2152         Span_mode=I
2153       ELSE
2154         GOTO 2156
2155       END IF
2156     NEXT I
2157     OUTPUT @Spect;"MD2SP"&VAL$(Span_mode)
2158     RETURN
2159     !
2160     !***** SUB DOCUMENTATION OF TEST DATA
*****
2161   Documentation:      !
2162     GOSUB Initial_option
2163     Opt1$=" CURRENT FILE NAME IS : "&File$
2164     Opt2$=" CHANGE FILE NAME"
2165     Option_header$=" CHECK FILE NAME"
2166     GOSUB Option_menu
2167     IF Option>2 THEN
2168       GOSUB Warning

```

```

2169     GOTO 2166
2170     END IF
2171     ON Option GOTO Doc1_1,Doc1_2
2172 Doc1_1:      !
2173     GOTO Doc2
2174 Doc1_2:      !
2175     GOSUB Nameing_file
2176     Doc_table$[1,10]=File$
2177 Doc2:        !
2178     GOSUB Initial_option
2179     Option_header$="CHANNEL A IS :"
2180     Option_header$="CHANNEL A IS : "
2181     Opt1$=" #1650"
2182     Opt2$=" #1652"
2183     Opt3$=" #1653"
2184     Opt4$=" #1654"
2185     Opt5$=" #1658 VERTICAL"
2186     Opt6$=" FORCE FROM DARTEC"
2187     Opt7$=" STRAINS"
2188     GOSUB Option_menu
2189     IF Option>7 THEN
2190     GOSUB Warning
2191     GOTO 2188
2192     END IF
2193     ON Option GOTO 2194,2196,2198,2200,2202,2204,2206
2194     Doc_table$[11,15]="#1650"
2195     GOTO 2208
2196     Doc_table$[11,15]="#1652"
2197     GOTO 2208
2198     Doc_table$[11,15]="#1653"
2199     GOTO 2208
2200     Doc_table$[11,15]="#1654"
2201     GOTO 2208
2202     Doc_table$[11,15]="#1658"
2203     GOTO 2208
2204     Doc_table$[11,15]="FORCE"
2205     GOTO 2208
2206     Doc_table$[11,15]="STRAN"
2207     Option_header$="CHANNEL B IS : "
2208     Option_header$="CHANNEL B IS : "
2209     GOSUB Option_menu      ! USE PREVIOUS SELECTIONS
2210     IF Option>7 THEN
2211     GOSUB Warning
2212     GOTO 2209
2213     END IF
2214     ON Option GOTO 2215,2217,2219,2221,2223,2225,2227
2215     Doc_table$[16,20]="#1650"
2216     GOTO 2228

```

```

2217 Doc_table$[16,20]="#1652"
2218 GOTO 2228
2219 Doc_table$[16,20]="#1653"
2220 GOTO 2228
2221 Doc_table$[16,20]="#1654"
2222 GOTO 2228
2223 Doc_table$[16,20]="#1658"
2224 GOTO 2228
2225 Doc_table$[16,20]="FORCE"
2226 GOTO 2228
2227 Doc_table$[16,20]="STRAN"
2228 OUTPUT @Spect;"LSP"
2229 ENTER @Spect;Span$
2230 Doc_table$[21,30]=Span$
2231 GOSUB Initial_option
2232 Opt1$=" NO AMPLIFICATION"
2233 Opt2$=" X10 AMPLIFICATION"
2234 Opt3$=" X100 AMPLIFICATION"
2235 Opt4$=" OTHERS .. PLEASE ENTER"
2236 Option_header$=" TYPE OF AMPLIFICATION"
2237 GOSUB Option_menu
2238 IF Option>4 THEN
2239 GOSUB Warning
2240 GOTO 2237
2241 END IF
2242 ON Option GOTO 2243,2245,2247,2249
2243 Doc_table$[31,35]=" X0"
2244 GOTO 2251
2245 Doc_table$[31,35]=" X10"
2246 GOTO 2251
2247 Doc_table$[31,35]=" X100"
2248 GOTO 2251
2249 INPUT "ENETR APPLIED AMPLIFICATION IN 5-CHARACTERS",Amp$
2250 Doc_table$[31,35]=Amp$
2251 INPUT "ENTER MAX 5-CHARACTERS OF CODE OF LOCATION OF
SIGNAL OF CHANNEL #A",A_loc_code$ !Doc_table$[41,45]
2252 PRINT Doc_table$
2253 Doc_table$[36,46]=A_loc_code$
2254 GOSUB Initial_option
2255 Option_header$="ORIENTATION OF SENSOR OF CHANNEL A"
2256 Opt1$=" XX"
2257 Opt2$=" YY"
2258 Opt3$=" VV"
2259 Opt4$=" **"
2260 GOSUB Option_menu
2261 IF Option>4 THEN
2262 GOSUB Warning
2263 GOTO 2260

```

```

2264     END IF
2265     ON Option GOTO 2266,2268,2270,2272
2266     Doc_table$[47,50]="XX"
2267     GOTO 2273
2268     Doc_table$[47,50]="YY"
2269     GOTO 2273
2270     Doc_table$[47,50]="VV"
2271     GOTO 2273
2272     Doc_table$[47,50]="**"
2273     INPUT "ENTER MAX 5-CHARACTERS OF CODE OF LOCATION OF
SIGNAL OF CHANNEL #B",B_loc_code$      !Doc_table$[51,58]
2274     Doc_table$[51,58]=B_loc_code$
2275     Option_header$="ORIENTATION OF SENSOR OF CHANNEL B"
2276     GOSUB Option_menu
2277     IF Option>4 THEN
2278     GOSUB Warning
2279     GOTO 2276
2280     END IF
2281     ON Option GOTO 2282,2284,2286,2288
2282     Doc_table$[59,60]="XX"
2283     GOTO 2289
2284     Doc_table$[59,60]="YY"
2285     GOTO 2289
2286     Doc_table$[59,60]="VV"
2287     GOTO 2289
2288     Doc_table$[59,60]="**"
2289     GOSUB Initial_option
2290     Option_header$="TYPE OF SPECTRAL PLOT"
2291     Opt1$="XFR AMPLITUDE"
2292     Opt2$="XFR PHASE"
2293     Opt3$="COHERENCE"
2294     Opt4$="A - AMPLITUDE"
2295     Opt5$="B - AMPLITUDE"
2296     GOSUB Option_menu
2297     IF Option>5 THEN
2298     GOSUB Warning
2299     GOTO 2296
2300     END IF
2301     ON Option GOTO 2302,2304,2306,2308,2310
2302     Doc_table$[61,65]="AMXFR"
2303     GOTO 2311
2304     Doc_table$[61,65]="PHXFR"
2305     GOTO 2311
2306     Doc_table$[61,65]="COHER"
2307     GOTO 2311
2308     Doc_table$[61,65]="AMP-A"
2309     GOTO 2311
2310     Doc_table$[61,65]="AMP-B"

```



```

2311 Doc_table$[66,75]=A_sensitivity$
2312 Doc_table$[76,85]=B_sensitivity$
2313 INPUT "ENTER 2-CHARACTER CODE FOR DOCUMENT FILE",Doc_char$
2314 Docu_file$="DOCUMENT"&Doc_char$[1,2]
2315 PRINT Doc_table$
2316 INPUT "IS THE DOCUMENT TABLE O.K. ? ** Y OR N **",Deci_doc$
2317 Deci_doc$=UPC$(Deci_doc$)
2318 IF Deci_doc$="N" THEN
2319 DISP "START DOCUMENT AGAIN"
2320 WAIT 3
2321 GOTO Documentation
2322 END IF
2323 INPUT "DO YOU WANT A HARD COPY ? ** Y OR N **",Deci_doc_hard$
2324 Deci_doc_hard$=UPC$(Deci_doc_hard$)
2325 IF Deci_doc_hard$="Y" THEN
2326 OUTPUT @Printer;CHR$(12)
2327 OUTPUT @Printer;Doc_table$
2328 END IF
2329 CREATE BDAT Docu_file$,1,90
2330 ASSIGN @Doc TO Docu_file$
2331 OUTPUT @Doc;Doc_table$
2332 ASSIGN @Doc TO *
2333 RETURN
2334 !
2335 !*****
2336 END
2337
!*****
2338 SUB Amplitude_ref
2339 ! SUBPROGRAM TO SELECT PROPER AMPLITUDE
REFERENCE
2340 ASSIGN @Spect TO 711
2341 PRINT CHR$(12)
2342 PRINT " READ THIS MESSAGE CAREFULLY"
2343 PRINT
2344 PRINT " IF THE PRESENT AMPLITUDE REFERENCE IS O.K."
2345 PRINT " (i.e. THE DISPLAY ON THE SPECTRUM IS SATISFACTORY)"
2346 PRINT "THEN PRESS Y. "
2347 PRINT
2348 PRINT "IF HOWEVER YOU WANT TO CHANGE THE AMPLITUDE"
2349 PRINT " REFERNCE, THEN PRESS N"
2350 INPUT "ANSWER Y OR N",Deci_amp$
2351 Deci_amp$=UPC$(Deci_amp$)
2352 IF Deci_amp$<>"Y" AND Deci_amp$<>"N" THEN 2350
2353 IF Deci_amp$="N" THEN
2354 OUTPUT 2 USING "#,K";CHR$(255)&"K"
2355 PRINT " INPUT AMPLITUDE REFERENCE LEVELS 1-9 "
2356 PRINT " OR 0 IF O.K"

```

```

2357         PRINT
2358         PRINT " FOR EACH LEVEL OBSERVE DISPLAY AND PRESS 0
WHEN SATISFIED"
2359         INPUT "INPUT LEVEL 1,2,3,4,5,6,7,8,9 ** OR ** 0 IF O.K",I
2360         IF I>9 THEN 2359
2361         IF I=0 THEN 2367
2362         OUTPUT @Spect;"AM"&VAL$(I)
2363         CONTROL 1,1;16
2364         PRINT CHR$(131);"THE CURRENT LEVEL IS ";I;CHR$(128)
2365         GOTO 2359
2366     END IF
2367     PRINT CHR$(12)
2368 SUBEND
2369 !*****
2376 SUB Freq_span_mode(Span$)
2386 GCLEAR
2396 PRINT CHR$(12)
2406 PRINT "SELECT FREQ. SPAN OF ANALYSIS. ....(ZERO START MODE)"
2407 PRINT
2416 PRINT "-----"
2426 PRINT " 1 ..... 1 Hz"
2436 PRINT " 2 ..... 2.5 Hz"
2446 PRINT " 3 ..... 5 Hz"
2456 PRINT " 4 ..... 10 Hz"
2466 PRINT " 5 ..... 25 Hz"
2476 PRINT " 6 ..... 50 Hz"
2486 PRINT " 7 ..... 100 Hz"
2496 PRINT " 8 ..... 250 Hz"
2506 PRINT " 9 ..... 500 Hz"
2516 PRINT " 10..... 1 KHz"
2517 PRINT " 11..... 2.5 KHz"
2527 PRINT " 12..... 5 KHz"
2537 PRINT " 13..... 10 KHz"
2547 PRINT " 14..... 25 KHz"
2548 PRINT "-----"
2557 INPUT "SPAN MODE : 1,2,3.....14",Span
2567 IF Span<1 OR Span>14 THEN 2386
2577 Span$=VAL$(Span)
2587 SUBEND
2597 !*****
2607 SUB Num_averages(No_average)
2617 GCLEAR
2627 PRINT CHR$(12)
2637 PRINT " ENTER NUMBER OF AVERAGES"
2647 PRINT
2657 PRINT "-----"
2658 PRINT
2667 PRINT " 1 ..... 4 AVERAGES"

```

```

2677 PRINT " 2 ..... 8 AVERAGES"
2687 PRINT " 3 ..... 16 AVERAGES"
2697 PRINT " 4 ..... 32 AVERAGES"
2707 PRINT " 5 ..... 64 AVERAGES"
2717 PRINT " 6 ..... 128 AVERAGES"
2727 PRINT " 7 ..... 256 AVERAGES"
2728 PRINT
2730 PRINT "-----"
2737 INPUT "ENTER NO. OF AVERAGES : 1,2,3,4,5,6 OR 7".No_average
2747 IF No_average<1 OR No_average>7 THEN 2617
2748 PRINT CHR$(12)
2757 SUBEND
2758 !***** PLOT SPECTRA
2760 SUB Plot_data(File$)
2770 Initialization: !
2780 C$=CHR$(255)&"K" ! CLEAR SCREEN
2790 OPTION BASE 1
2800 INTEGER I,J,N,Num_zero_rows,Actual_rows,Ni
2810 DIM Title$(40),X$(30),Y$(30)
2840 GCLEAR
2850 OUTPUT 2 USING "#,K";C$
3000 MASS STORAGE IS ":HP9122,700,1"
3010 Sscale=1 !DEFAULT SCA;LING FACTOR
3400 Actual_rows=128
3420 !*****
3430 !
3440 Begin: ! REQUEST FILE NAME AND GRAPH LABELS
3580 Plot_type$=File$(5;1)
3590 Spect_type$=File$(6;1)
3600 !
3610 IF Plot_type$="A" OR Plot_type$="B" OR Plot_type$="X" THEN ! ASK IF
LINEAR OR DECIBEL SCALE IS TO BE USED.
3620 Linear_ask$="Y"
3630 PRINT CHR$(12)
3640 PRINT "DO YOU WANT LINEAR OR DECIBEL SCALE FOR SPECTRUM
??"
3650 PRINT " DEFAULT IS LINEAR SCALE"
3660 PRINT
3670 PRINT "PRESS 'ENTER' OR ENTER 'N' FOR DECIBEL SCALE"
3680 PRINT "ENTER 'Y' FOR LINEAR SCALE"
3690 INPUT "YOUR CHOICE OF SCALE .... DEFAULT IS LINEAR",Linear_ask$
3700 Linear_ask$=UPC$(Linear_ask$)
3710 IF Linear_ask$<>"Y" AND Linear_ask$<>"N" THEN
3720 BEEP 3000,1
3730 GOTO 3630
3740 END IF
3750 END IF
3760 IF (Plot_type$="A" AND Spect_type$="X") OR Plot_type$="X" THEN

```

```

3770 Title$="AMPLITUDE TRANSFER FUNCTION"
3780 X$="FREQUENCY (HZ)"
3790 Y$=" "
3800 IF Linear_ask$="N" THEN Y$="DECIBEL"
3810 GOTO 4140
3820 END IF
3830 IF (Plot_type$="P" AND Spect_type$="X") OR Plot_type$="P" THEN
3840 Title$="PHASE TRANSFER FUNCTION"
3850 Y$="DEGREES"
3860 X$="FREQUENCY (HZ)"
3870 GOTO 4140
3880 END IF
3890 IF (Plot_type$="C" AND Spect_type$="H") OR Plot_type$="C" THEN
3900 Title$="COHERENCE"
3910 X$="FREQUENCY (HZ)"
3920 Y$=" "
3921 OUTPUT 701;CHR$(12) !FORM FEED ON PRINTER TO NEW PAGE
3930 GOTO 4140
3940 END IF
3950 IF Plot_type$="A" OR Plot_type$="B" THEN
3960 IF Spect_type$="A" OR Spect_type$="L" OR Spect_type$="B" THEN
3970 Title$="AUTOSPECTRUM"
3980 X$="FREQUENCY (HZ)"
3990 Y$="VOLTS"
4000 IF Linear_ask$="N" THEN Y$="AMPLITUDE (DECIBEL)"
4001 IF Plot_type$="B" AND Spect_type$="L" THEN
4002 Y$="KN"
4003 END IF
4010 GOTO 4140
4020 END IF
4030 END IF
4040 IF Plot_type$="T" THEN
4050 Title$="TIME TRACE"
4060 Y$=" "
4070 X$="TIME (SEC.)"
4080 GOTO 4140
4090 END IF
4100 !
4110 INPUT "INPUT TITLE OF GRAPH ",Title$
4120 INPUT "INPUT TITLE FOR HORIZONTAL-AXIS",X$
4130 INPUT "INPUT TITLE FOR VERTICAL AXIS",Y$
4140 OUTPUT 2 USING "#.K";C$
4150 PRINT "TITLE OF GRAPH IS ";Title$;" "
4160 PRINT
4170 PRINT "TITLE OF HORIZONTAL AXIS IS ";X$;" "
4180 PRINT
4190 PRINT "TITLE OF VERTICAL AXIS IS ";Y$;" "
4200 PRINT

```

```

4210 PRINT "ARE THESE O.K?"
4220 PRINT
4221 Fq_1$="Y"
4230 INPUT "ANSWER Y OR N ..... DEFAULT IS Y",Fq_1$
4240 IF Fq_1$<>"Y" AND Fq_1$<>"N" THEN
4250     BEEP
4260     GOTO 4230
4270 END IF
4280 IF Fq_1$="N" THEN GOTO 4110
4290 PRINT "YOU'VE CONFIRMED THE LABELS"
4291 PRINT CHR$(12)
4292 CONTROL 1;12,12
4294 PRINT "DEFAULT SCALING FACTOR IS 1 : PRESS ENTER TO ACCEPT"
4296 INPUT "ENTER SCALING FACTOR",Sscale
4297 DISP "SCALING FACTOR IS : ";Sscale
4298 WAIT 1
4300 ! *****
4310 Read_file: ! GET DATA FROM FILE
4320 IF Plot_type$="TT" THEN ! USE 'TT' TO BYPASS THIS. NEVER
EXECUTED.
4330     ALLOCATE Time_array(Actual_rows,2),X(Actual_rows),Y(Actual_rows)
4340     ALLOCATE X_data_window(Actual_rows),Y_data_window(Actual_rows)
4350     ASSIGN @File TO File$
4360     ON END @File GOTO 4380
4370     ENTER @File;Time_array(*)
4380     FOR I=1 TO Actual_rows
4390         X(I)=Time_array(I,1)
4400         Y(I)=Time_array(I,2)
4410     NEXT I
4420     Max_x=MAX(X(*))
4430     Min_x=MIN(X(*))
4440     Min_y=MIN(Y(*))
4450     Max_y=MAX(Y(*))
4460 !
4470     MAT X_data_window= X
4480     MAT Y_data_window= Y
4490     GINIT
4500     GRAPHICS ON
4510     LDIR 0
4520     W=100*MAX(1,RATIO)! WIDTH
4530     H=100*MAX(1,1/RATIO) ! HEIGHT
4540     VIEWPORT .1*W,.98*W,.15*H,.95*H
4550     WINDOW Min_x,Max_x,Min_y,Max_y
4560     FRAME
4570     GOTO 4820
4580     CLIP OFF
4590     Title$="TIME TRACE"
4600     X$="TIME (SEC.)"

```

```

4610     Y$=" "
4620     !                               ! LABEL TITLE
4630     CSIZE 5
4640     LORG 6
4650     Title_len=LEN(Title$)
4660     Centre=(W-Title_len)/2
4670     FOR P=.2 TO .2 STEP .025
4680         MOVE (Centre+P),(.99*H+P/2)
4690         LABEL Title$
4700     NEXT P
4710     !                               ! LABEL X_AXIS
4720     LORG 9
4730     CSIZE 3
4740     MOVE .8*W,.1*H
4750     LABEL X$
4760     !                               ! LABEL Y_AXIS
4770     LDIR 90
4780     LORG 5
4790     MOVE .015*W,.5*H
4800     LABEL Y$
4810 !LORG 8
4820 !CSIZE 3
4830     PRINT CHR$(12)
4840     FOR I=1 TO Actual_rows
4850         PLOT X(I),Y(I)
4860     NEXT I
4870     DEALLOCATE Time_array(*),X(*),Y(*)
4880     GOTO 6750
4890 END IF
4900 IF Manual_input$="SET" THEN
4910     INPUT "ENTER NUMBER OF PAIR POINTS TO BE PLOTTED i.e. NO. OF
ROWS",Actual_rows
4920     GOTO 5280
4930 END IF
4940 OUTPUT 2 USING "#,K";C$
4950 DISP CHR$(130);"READING FILE";CHR$(128);" ";CHR$(129);"PLEASE
WAIT";CHR$(128)
4960 ASSIGN @File TO File$
4970 ON END @File GOTO 5000
4980 ALLOCATE False_1(128,2)
4990 ENTER @File;False_1(*)
5000     !
5001     ASSIGN @File TO *
5250     !
*****
5260 Separate:     ! SEPARATE DATA INTO Y_DATA AND X_DATA
5270 DISP CHR$(130);"PROCESSING ";CHR$(128);CHR$(129);"PLEASE
WAIT";CHR$(128)

```

```

5280 ALLOCATE Y_data(Actual_rows),X_data(Actual_rows)
5290 IF Manual_input$="SET" THEN
5300     GOSUB Kbd_input
5310     GOTO Convert
5320 END IF
5340     ALLOCATE False_2(Actual_rows,2)
5350     MAT False_2= False_1
5360     DEALLOCATE False_1(*)
5380 !
5390 FOR I=1 TO Actual_rows
5400     FOR J=1 TO 2
5410         IF J=2 THEN
5420             Y_data(I)=False_2(I,J)
5430             IF Plot_type$="A" THEN
5440                 IF Linear_ask$="Y" THEN 5480
5450                 IF Y_data(I)<=1.E-20 THEN Y_data(I)=Last_y_data! SMOOTH
SMALL
5460                     Last_y_data=Y_data(I)
5470                     Y_data(I)=20*LGT(Y_data(I)) ! VALUES
5480 ! DUMMY LINE TO PREVENT INFINITE LOOP
5490                 END IF
5500             ELSE
5510                 X_data(I)=False_2(I,J)
5520             END IF
5530         NEXT J
5531     Y_data(I)=Y_data(I)*Sscale
5540 NEXT I
5550 DEALLOCATE False_2(*)
5560 ASSIGN @File TO *
5570 !
5580 !*****
5590 Convert: !CONVERTING DATA TO FIT GRAPH WINDOW (DEFINED LATER)
5600     !OF (0-100) * (20-70)
5610     ! NEGATIVE X VALUES NOT COVERED YET.
5620 ALLOCATE X_data_window(Actual_rows),Y_data_window(Actual_rows)
5630 ! OBTAIN MAX VALUES AND OTHER PARAMETERS TO CONTROL
PLOTING AREA.
5640 !
5650 X_max=MAX(X_data(*))
5660 X_min=MIN(X_data(*))
5670 Y_max=MAX(Y_data(*))
5680 Y_min=MIN(Y_data(*))
5690 X_step=(X_max-X_min)/10
5700 Y_step=ABS((Y_max-Y_min)/7)
5710 X_unit=X_min
5720 Y_unit=Y_min
5730 !
5740 ! CONVERTING DATA

```

```

5750 FOR I=1 TO Actual_rows
5760     X_data_window(I)=(X_data(I)/X_max)*100
5770     Y_data_window(I)=((Y_data(I)-Y_min)/(Y_max-Y_min))*70+20
5780     IF Plot_type$="C" OR Plot_type$="P" THEN Y_data_window(I)=Y_data(I)
5790 ! IF Plot_type$="T" THEN Y_data_window(I)=Y_data(I)
5800 ! IF Plot_type$="T" THEN X_data_window(I)=X_data(I)
5810 NEXT I
5820! DEALLOCATE X_data(*),Y_data(*) ! LEAVE FOR OBTAINING VALUES
5830  !
5840  !***** WRITE TITLE AND LABELS *****
5850 DISP
5860 OUTPUT 2 USING "#,K";C$
5870 GCLEAR
5880 GINIT
5890 GRAPHICS ON
5900 DEG
5910 W=100*MAX(1,RATIO)    ! WIDTH
5920 H=100*MAX(1,1/RATIO)  ! HEIGHT
5930  !                      ! LABEL TITLE
5940 CSIZE 5
5950 LORG 6
5960 Title_len=LEN(Title$)
5970 Centre=(W-Title_len)/2
5980 FOR P=.2 TO .2 STEP .025
5990     MOVE (Centre+P),(.99*H+P/2)
6000     LABEL Title$
6010 NEXT P
6020  !                      ! LABEL X_AXIS
6030 LORG 9
6040 CSIZE 4
6050 MOVE .8*W,.13*H
6060 LABEL X$
6070  !                      ! LABEL Y_AXIS
6080 LDIR 90
6090 LORG 5
6100 MOVE .015*W,.5*H
6110 LABEL Y$
6120  ! ***** BYPASS FOR PHASE AND COHERENCE PLOT
*****
6130 IF Plot_type$="P" THEN
6140     CALL Phase(W,H,X_unit,X_step)
6150     GOTO Plot_points
6160 END IF
6170 IF Plot_type$="C" THEN
6180     CALL Coherence(W,H,X_unit,X_step)
6190     GOTO Plot_points
6200 END IF
6210  !

```



```

6220 ! IF Plot_type$="T" THEN
6230 ! CALL Time(W,H,X_unit,X_max,Y_unit,Y_max)
6240 ! FOR I=1 TO 256
6250 ! PRINT USING "3D.10D,5X,3D.10D";X_data_window(I),Y_data_window(I)
6260 ! NEXT I
6270 ! GOTO Plot_points
6280 ! END IF
6290 !****,*****
6300 LDIR 0
6310 VIEWPORT .10*W,.98*W,.15*H,.95*H
6320 FRAME
6330 WINDOW 0,100,15,95
6340 AXES 5,5,0,15
6350 CLIP OFF ! TO ALLOW WRITING DIM OF AXIS
6360 ! PAUSE
6370 !
6380 ! ***** DIMENSION X-AXIS*****
6390 LORG 6
6400 CSIZE 4
6410 FOR I=0 TO 100 STEP 10
6420 MOVE I,14.99
6430 LABEL USING "#,K";X_unit
6440 X_unit=X_unit+X_step
6450 NEXT I
6460 !
6470 ! ***** DIMENSION Y-AXIS *****
6480 LORG 8
6490 MOVE -.5,15 ! LABEL EXTREME LOWER POINT
6500 LABEL USING "#,6D.3D";(Y_min-Y_step/2)
6510 MOVE -.5,95 ! LABEL EXTREME UPPER POINT
6520 LABEL USING "#,6D.3D";(Y_max+Y_step/2)
6530 !
6540 Y_unit=Y_min
6550 FOR I=20 TO 90 STEP 10
6560 MOVE -.5,I
6570 LABEL USING "#,6D.3D";Y_unit
6580 Y_unit=Y_unit+Y_step
6590 NEXT I
6600 !
6610 Plot_points: !
6620 FOR I=1 TO Actual_rows
6630 PLOT X_data_window(I),Y_data_window(I)
6640 NEXT I
6650 PLOTTER IS CRT,"INTERNAL"
6660 TRACK CRT IS ON
6670 DISP "MOVE CURSOR TO WHERE FILE NAME WILL BE WRITTEN, THEN
PRESS ENTER"
6680 DIGITIZE P,Q,Status$

```

```

6690 LORG 5
6700 CSIZE 5
6710 MOVE P,Q
6720 LABEL File$
6730 TRACK CRT IS OFF
6740 Dump_graphics:      !
6750 Qplot$="Y"
6760 INPUT "DO YOU WANT TO PRINT GRAPH.....(Y)/N",Qplot$
6770 IF Qplot$="Y" THEN
6780     DUMP DEVICE IS 701
6790     DUMP GRAPHICS
6800     GOTO 6830
6810 END IF
6820 IF Qplot$<>"N" THEN Dump_graphics
6830 Qread$="N"
6840 INPUT "DO YOU WANT TO READ VALUES OFF PLOT ..Y/(N)",Qread$
6850 Qread$=UPC$(Qread$)
6860 IF Qread$="Y" THEN
6870     Counter=0
6880     VIEWPORT .10*W,.98*W,.15*H,.95*H
6890     CLIP ON
6900! PRINT X$.Y$
6910 OUTPUT 701;X$;"  ";Y$
6920 ON KNOB .01,1 GOSUB Cursor
6930 ON KEY 5 LABEL "MARK".1 GOSUB Print_values
6940 ON KEY 6 LABEL "END".1 GOTO 7170
6950 GOTO 6920
6960 Print_values:      !
6970             MOVE X_data_window(Counter),Y_data_window(Counter)
6980             !     PRINT X_data(Counter),"          ",Y_data(Counter)
6990             OUTPUT 701;X_data(Counter);"          ";Y_data(Counter)
7000             RETURN
7010 Cursor:          !
7020             Counter=Counter+SGN(KNOBX)*1
7030             IF Counter<=1 THEN Counter=1
7040             IF Counter>=Actual_rows THEN Counter=Actual_rows
7050             SET ECHO X_data_window(Counter),Y_data_window(Counter)
7060             !     CONTROL 1;12,50
7070             PRINT TABXY(50,12),"CURSOR FREQ. = ";X_data(Counter)
7080             PRINT TABXY(50,13),"CURSOR VALUE =";Y_data(Counter)
7090             RETURN
7100             !
7110             END IF
7120             IF Qread$="N" THEN 7170
7130             IF Qread$<>"Y" THEN 6830
7170             DEALLOCATE X_data_window(*),Y_data_window(*),X_data(*),Y_data(*)
7180             Title$=" "
7190             X$=" "

```

```

7200    Y$=" "
7210    GCLEAR
7220    GINIT
7230    PRINT CHR$(12)
7510    !
7520    MASS STORAGE IS ":HP9122,700,1"
7530    GCLEAR
7540    GINIT
7550    PRINT CHR$(12)
7560    SUBEND
7570    !
7580    SUB Phase(W,H,X_unit,X_step)
7581        GRAPHICS ON
7582        LDIR 0
7583        VIEWPORT .1*W,.98*W,.15*H,.95*H
7584        FRAME
7585        WINDOW 0,100,-200,200
7586        AXES 5,50,0,0
7587        CLIP OFF
7588        LORG 8
7589        CSIZE 3
7590        FOR I=-200 TO 200 STEP 50
7591            MOVE -.5,I
7592            LABEL USING "#,4D";I
7593        NEXT I
7594        LORG 6
7595        FOR I=0 TO 100 STEP 10
7596            MOVE I,-199.99
7597            LABEL USING "#,K";X_unit
7598            X_unit=X_unit+X_step
7599        NEXT I
7600    SUBEND
7601    !
7610    SUB Coherence(W,H,X_unit,X_step)
7611        GRAPHICS ON
7612        LDIR 0
7613        VIEWPORT .1*W,.98*W,.15*H,.95*H
7614        FRAME
7615        WINDOW 0,100,0,1
7616        AXES 5,.05,0,0
7617        CLIP OFF
7618        LORG 8
7619        CSIZE 3
7620        FOR I=0 TO 1 STEP .1
7621            MOVE -.5,I
7622            LABEL USING "#,D.2D";I
7623        NEXT I
7624        LORG 6

```

```
7625     FOR I=0 TO 100 STEP 10
7626         MOVE I,-.99
7627         LABEL USING "#,K";X_unit
7628         X_unit=X_unit+X_step
7629     NEXT I
7630 SUBEND
7631 !
```

APPENDIX 5.3 LISTING OF THE MODAL PARAMETER EXTRACTION PROGRAM

```

10 ! NAME TSANG_FIT
100 OPTION BASE 1
101 DEG
110 DIM Array(601,3),Coef(3,3),Coef_1(3,3),Coef_2(3,3),Coef_3(3,3),Zzero(3,3)
111 DIM Const_vector(3,1),Omega(601),Rreal(601),Imag(601)
112 DIM Amp(601),Phase(601),X(601),Y(601),Freq(601)
113 DIM Reg_rreal(601,10),Reg_imag(601,10),Reg_amp(601,10),File$(30)
114 DIM
Reg_amp_vector(601),Combin_mode_no(10),Reg_rreal_v(601),Reg_imag_v(601)
115 DIM Mark_freq(10),Question$(80),Mark_bin(10)
116 DIM Mr(10),Kr(10),Cr(10),Resonance(10),Mmodal_const(10),Vis_loss_factor(10)
117 DIM Results$(10,6)[20]
127 DIM Orig_array(601,3)
137 Remove_move$="NO"
139 INTEGER Graph(7500)
140 MASS STORAGE IS ":HP9121,700,1"
141 DUMP DEVICE IS 701
142 Graph_count=0
144 GCLEAR
145 PRINT "-----"
150 PRINT " THIS PROGRAM USE RAW INERTANCE DATA OR RECEPTANCE
DATA"
160 PRINT " INERTANCE CAN BE CONVERTED TO RECEPTANCE BEFORE "
170 PRINT "FITTING PROCESS BEGINS SINCE THIS PRODUCE BETTER
RESULTS"
180 PRINT "-----"
190 PRINT "TO SEE THE GRAPHICS GENEARTED BY THIS PROGRAM RUN "
191 PRINT "PROGRAM NAMED VIEW_GRAPH ON PROGRAM DISK#6 "
192 PRINT "-----"
193 PRINT CHR$(129)
200 PRINT "STORAGE DISK ON D0, DATA DISK ON D1"
210 PRINT
211 PRINT CHR$(131)
220 PRINT "ENTER LABEL TAB POSITION eg.60 ,200 ETC";CHR$(128)
230 INPUT Ttab
500 GOSUB Read_file
501 REDIM Array(Nrecord,3),Coef(3,3),Coef_1(3,3),Coef_2(3,3),Coef_3(3,3),Zzero(3,3)
502 REDIM Const_vector(3,1),Omega(Nrecord),Rreal(Nrecord),Imag(Nrecord)
503 REDIM Amp(Nrecord),Phase(Nrecord),X(Nrecord),Y(Nrecord),Freq(Nrecord)
505 REDIM Reg_rreal(Nrecord,10),Reg_imag(Nrecord,10),Reg_amp(Nrecord,10)
506 REDIM Orig_array(Nrecord,3)
508 REDIM
Reg_amp_vector(Nrecord),Combin_mode_no(10),Reg_rreal_v(Nrecord),Reg_imag_v(Nrecor
d)
513 GOSUB Scaling
514 Question$="NOT ALLOW TO CONVERT INERTANCE TO RECEPTANCE
BEFORE FITTING"
515 ! GOSUB Yesno

```

```

516 Ask$="N" ! DO NOT ALLOW PRE CONVERSION OF INERTANCE TO
RECEPTANCE
518 IF Ask$="Y" THEN
519     Pre_convert$="YES"
520     GOTO 531
521 END IF
522 IF Ask$<>"N" THEN 514
523 Pre_convert$="NO"
524 IF Array(1,1)<>0 THEN
525     Start_record=1
526     GOTO 529
527 ELSE
528     Start_record=2
529 END IF
530 GOSUB Save_original
531 GOSUB Det_rreal_imag
532 GOSUB Conversion
533 PRINT CHR$(12)
534 Start_pt=1
535 End_pt=Nrecord
536 FOR I=Start_pt TO Nrecord ! TO GET RID OF LOW FREQ VALUES FROM
PLOTING
537     X(I-Start_pt+1)=Rreal(I)
538     Y(I-Start_pt+1)=Imag(I)
539 NEXT I
540 PRINT CHR$(12)
541 Regeneration$="REG_NYQUIST"
543 GOSUB Draw_nyquist
544 GOSUB Ask_draw_pt
545 GOSUB Draw_phase
546 GOSUB Draw_amp_plot
547 CLIP ON
548 MOVE X(Ttab),Maxy-(Maxy-Miny)*.15
549 LABEL File$
550 OUTPUT 701;"FILE NAME : "&File$[1,10]
551 Question$="READY TO MARK RESONANT FREQ "
552 GOSUB Yesno
553 IF Ask$="Y" THEN 556
554 IF Ask$<>"N" THEN 551
555 GOTO 551
556 Escape$=""
557 PRINT CHR$(12)
558 N_mode=1
559 PRINT TABXY(50,16),"TOTAL NO OF MARK FREQUENCIES ???
"
560 INPUT Total_mark_freq
561 LONG 4
562 FOR I=1 TO Total_mark_freq

```

```

563     ON KNOB .01,1 GOSUB Cursor
564     PRINT TABXY(50,16),"MARK MODE NO ";I;"
565     ON KEY 5 LABEL "MARK",1 GOTO Finish_mark
566     GOTO 563
567 Finish_mark: !
568     MOVE X(Counter),Y(Counter)
569     LABEL I
570     Mark_freq(I)=Array(Counter,1)
571     Mark_bin(I)=INT(Counter)
573 NEXT I
574 PRINT CHR$(12)
575 Question$="TO DUMP GRAPHICS ON PRINTER"
576 GOSUB Yesno
577 IF Ask$="Y" THEN
578     DUMP GRAPHICS
579     GOTO 582
580 END IF
581 IF Ask$<>"N" THEN 575
582 Question$="TO DUMP GRAPHICS ON DISK  "
583 GOSUB Yesno
584 IF Ask$="Y" THEN
585     GSTORE Graph(*)
586     GOSUB Save_graph
587     GOTO 590
588 END IF
589 IF Ask$<>"N" THEN 582
590 GOSUB Main_menu
591 N_mode=1
592 Data_flag$=""
593 GOSUB Tsang_curve_fit
594 Question$="DO YOU WANT TO FIT WITH DIFFERENT NO OF POINTS"
595 GOSUB Yesno
596 IF Ask$="Y" THEN 593
597 GOTO 603
598 IF Ask$<>"N" THEN 594
603 Question$="DO YOU WANT TO KEEP THESE ANALYSIS RESULTS "
604 GOSUB Yesno
605 IF Ask$="Y" THEN
606     Mmodal_mass(N_mode)=Mr(N_mode)
607     Mmodal_stiff(N_mode)=Kr(N_mode)
608     Mmodal_damp(N_mode)=Cr(N_mode)
609     GOTO 612
610 END IF
611 IF Ask$<>"N" THEN 603
612 Question$="DO YOU WANT TO CONTINUE FITTING WITH  NEXT  MODE
"
613 GOSUB Yesno
614 IF Ask$="Y" THEN

```

```

615     N_mode=N_mode+1
616     IF Pass_flag$="RE-ANALYSIS" THEN N_mode=Total_mark_freq+1
617     IF N_mode>Total_mark_freq THEN
620         Question$="RE-ANALYSE SOME MODES"
621         GOSUB Yesno
622         IF Ask$="Y" THEN
623             PRINT "ENTER RE-ANALYSE MODE NUMBER"
624             INPUT N_mode
625             Pass_flag$="RE-ANALYSIS"
626             Question$="DO YOU WANT TO REMOVE EFFECT OF OTHER
CLOSELY SPACED MODE "
627             GOSUB Yesno
628             IF Ask$="Y" THEN
630                 GOSUB Restore_orig
633                 PRINT "ENTER REMOVE MODE NUMBER "
634                 INPUT Remove_mode
636                 FOR I=Start_record TO Nrecord
637                     J=Remove_mode
638                     IF Data_flag$="INERTANCE" THEN 642
639                     Rreal_inv=-Mmodal_mass(J)*Omega(I)^2+Mmodal_stiff(J)
640                     Imag_inv=Mmodal_damp(J)*Omega(I)
641                     GOTO 644
642                     Rreal_inv=Mmodal_mass(J)-Mmodal_stiff(J)/Omega(I)^2
643                     Imag_inv=-Mmodal_damp(J)/Omega(I)
644                     Denom=Rreal_inv^2+Imag_inv^2
645                     Reg_rreal(I,J)=Rreal_inv/Denom
646                     Reg_imag(I,J)=-Imag_inv/Denom
647                     Reg_amp(I,J)=20*LOG((Reg_rreal(I,J)^2+Reg_imag(I,J)^2)^.5)
648                     Reg_amp_vector(I)=Reg_amp(I,J)
649                 NEXT I
650                 Remove_mode$="YES"
652                 GOSUB Remove_mode
653                 GOTO 593
654             END IF
655             IF Ask$<>"N" THEN 626
656             IF Remove_mode$="YES" THEN
657                 GOSUB Restore_orig
658             END IF
659             GOTO 593
661         END IF
662         N_mode=1
663         GOSUB Restore_orig
665         GOSUB Re_generate
666         GOTO 673
667     END IF
668     Reson_freq=Mark_freq(N_mode)
669     GOTO 593
670 END IF

```



```

671 PRINT CHR$(12)
672 IF Ask$<>"N" THEN 612
673 Question$="GO BACK TO CURVE FITTING"
674 GOSUB Yesno
675 IF Ask$="Y" THEN GOTO 620
676 IF Ask$<>"N" THEN 673
677 Question$="SAVE ANALYSIS RESULTS ON DISK"
678 GOSUB Yesno
679 IF Ask$="Y" THEN
680     GOSUB Save_results
681     GOTO 684
682 END IF
683 IF Ask$<>"N" THEN 677
684 Graph_count=0 ! RESET COUNTER
685 GOTO 500
686 ! ***** REMOVE MODE *****
687 Remove_mode: !
688 J=Remove_mode
689 FOR I=Start_record TO Nrecord
690     Array(I,2)=Orig_array(I,2)-Reg_rreal(I,J)
691     Array(I,3)=Orig_array(I,3)-Reg_imag(I,J)
692 NEXT I
693 PRINT CHR$(12)
694 FOR I=Start_record TO Nrecord
695     X(I)=Array(I,2)
696     Y(I)=Array(I,3)
697 NEXT I
698 Regeneration$="REG_NYQUIST"
699 GCLEAR
700 GOSUB Draw_nyquist
701 PRINT "PRESS CONT TO CONTINUE "
702 PAUSE
704 RETURN
705 !***** SAVE ORIGINAL DATA *****
706 Save_original: !
707 FOR I=Start_record TO Nrecord
708     Orig_array(I,2)=Array(I,2)
709     Orig_array(I,3)=Array(I,3)
710 NEXT I
711 RETURN
712 !***** RESTORE ORIGINAL DATA *****
713 Restore_orig: !
714 FOR I=Start_record TO Nrecord
715     Array(I,2)=Orig_array(I,2)
716     Array(I,3)=Orig_array(I,3)
717 NEXT I
718 RETURN
719 ! ***** SAVE RESULTS *****

```

```

720 Save_results:  !
721 REDIM Results$(Total_mark_freq+1,6)
722 MASS STORAGE IS ":HP9121,700,0"
723 Results$(1,1)=File$
724 Results$(1,2)=Data_flag$
725 Results$(1,3)=VAL$(Total_mark_freq)
726 FOR I=1 TO Total_mark_freq
727     Results$(I+1,1)=VAL$(Resonance(I))
728     Results$(I+1,2)=VAL$(Mr(I))
729     Results$(I+1,3)=VAL$(Kr(I))
730     Results$(I+1,4)=VAL$(Cr(I))
731     Results$(I+1,5)=VAL$(Mmodal_const(I))
732     Results$(I+1,6)=VAL$(Vis_loss_factor(I))
733 NEXT I
734 CREATE ASCII "R"&File$[1,9],INT(1+(6*(Total_mark_freq+1)*20)/256)
735 ASSIGN @File TO "R"&File$[1,9]
736 OUTPUT @File;Results$(*)
737 PRINT Results$(*)
738 ASSIGN @File TO *
739 MASS STORAGE IS ":HP9121,700,1"
740 RETURN
741 ! ***** SAVE GRAPHICS *****
742 Save_graph:  !
743 MASS STORAGE IS ":HP9121,700,0"
744 Graph_count=Graph_count+1
745 GOSUB Sort_job
746 Graph_file$=Job$&File$[1,2]&File$[7,9]&"G"&VAL$(Graph_count)
747 CREATE BDAT Job$&File$[1,2]&File$[7,9]&"G"&VAL$(Graph_count),60
748 ASSIGN @File TO Graph_file$
749 OUTPUT @File;Graph(*)
750 ASSIGN @File TO *
751 MASS STORAGE IS ":HP9121,700,1"
752 RETURN
753 ! ***** SORT JOB *****
754 Sort_job:  !
755 IF File$[3,6]="0487" OR File$[3,6]="0587" THEN
756     Job$="FIR"
757     GOTO 761
758 END IF
759 PRINT "ENTER JOB NAME MAXI 3 CHARACTERS"
760 INPUT Job$
761 RETURN
762 ! ***** TSANG'S CURVE FITTING *****
763 Tsang_curve_fit:  !
764 FOR I=1 TO 3
765     FOR J=1 TO 3
766         Zzero(I,J)=0
767         Const_vector(J,1)=0

```

```

768     NEXT J
769 NEXT I
770 MAT Coef= Zzero
771 GOSUB Ask_bin
772 IF Data_flag$="RECEPTANCE" THEN GOTO Fit_receptance
773 IF Data_flag$="INERTANCE" THEN GOTO Fit_inertance
774 PRINT "(INERTANCE) DATA OR RECEPTANCE DATA ???"
775 INPUT Ask$
776 IF Ask$="R" THEN Fit_receptance
777 GOTO Fit_inertance
778 Fit_receptance:  !
779 Data_flag$="RECEPTANCE"
780 FOR I=Sbin TO Ebin
781     Omega(I)=Array(I,1)*2*PI
782     Rreal(I)=Array(I,2)/(Array(I,2)^2+Array(I,3)^2)
783     Imag(I)=-Array(I,3)/(Array(I,2)^2+Array(I,3)^2)
784     Coef(1,1)=Coef(1,1)+1
785     Coef(1,2)=Coef(1,2)-Omega(I)^2
786     Coef(2,2)=Coef(2,2)+Omega(I)^4
787     Const_vector(1,1)=Const_vector(1,1)+Rreal(I)
788     Const_vector(2,1)=Const_vector(2,1)-Omega(I)^2*Rreal(I)
789     Const_vector(3,1)=Const_vector(3,1)+Omega(I)*Imag(I)
790 NEXT I
791 Coef(2,1)=Coef(1,2)
792 Coef(3,3)=-Coef(1,2)
793     ! TO FIND KR, NORMALISED MODAL STIFFNESS
794 MAT Coef_1= Coef
795 FOR I=1 TO 3
796     Coef_1(I,1)=Const_vector(I,1)
797 NEXT I
798 Kr(N_mode)=DET(Coef_1)/DET(Coef)
799     ! TO FIND NORMALISED MODAL MASS
800 MAT Coef_2= Coef
801 FOR I=1 TO 3
802     Coef_2(I,2)=Const_vector(I,1)
803 NEXT I
804 Mr(N_mode)=DET(Coef_2)/DET(Coef)
805     ! TO DETERMINE MODAL DAMPING
806 MAT Coef_3= Coef
807 FOR I=1 TO 3
808     Coef_3(I,3)=Const_vector(I,1)
809 NEXT I
810 Cr(N_mode)=(DET(Coef_3)/DET(Coef))
811 GOTO Print_result
812 Fit_inertance:  !
813 Data_flag$="INERTANCE"
814 FOR I=Sbin TO Ebin
815     Omega(I)=Array(I,1)*2*PI

```

```

816     Rreal(I)=Array(I,2)/(Array(I,2)^2+Array(I,3)^2)
817     Imag(I)=-Array(I,3)/(Array(I,2)^2+Array(I,3)^2)
818     Coef(2,2)=Coef(2,2)+1
819     Coef(1,2)=Coef(1,2)-Omega(I)^(-2)
820     Coef(1,1)=Coef(1,1)+Omega(I)^(-4)
821     Const_vector(1,1)=Const_vector(1,1)-Rreal(I)/Omega(I)^2
822     Const_vector(2,1)=Const_vector(2,1)+Rreal(I)
823     Const_vector(3,1)=Const_vector(3,1)-Imag(I)/Omega(I)
824 NEXT I
825 Coef(2,1)=Coef(1,2)
826 Coef(3,3)=-Coef(1,2)
827         ! TO FIND KR, NORMALISED MODAL STIFFNESS
828 MAT Coef_1= Coef
829 FOR I=1 TO 3
830     Coef_1(I,1)=Const_vector(I,1)
831 NEXT I
832 Kr(N_mode)=DET(Coef_1)/DET(Coef)
833         ! TO FIND NORMALISED MODAL MASS
834 MAT Coef_2= Coef
835 FOR I=1 TO 3
836     Coef_2(I,2)=Const_vector(I,1)
837 NEXT I
838 Mr(N_mode)=DET(Coef_2)/DET(Coef)
839         ! TO DETERMINE MODAL DAMPING
840 MAT Coef_3= Coef
841 FOR I=1 TO 3
842     Coef_3(I,3)=Const_vector(I,1)
843 NEXT I
844 Cr(N_mode)=(DET(Coef_3)/DET(Coef))
845 Print_result: !
846 PRINTER IS 1
847 PRINT CHR$(12)
848 PRINT "DATA FROM FILE ";File$(1,10)
849 PRINT "POSSIBLE RESONANT FREQ ENTERED          =";Reson_freq,"
HZ"
850 PRINT "NO OF POINTS ON EITHER SIDE OF RESONANCE    =";Npoint
851 PRINT "RAW DATA TYPE IS                          = ";Data_flag$
852 PRINT "MODAL MASS CONSTANT                        =";Mr(N_mode)
853 PRINT "MODAL STIFFNESS CONSTANT                  =";Kr(N_mode)
854 PRINT "MODAL DAMPING  CONSTANT                   =";Cr(N_mode)
855 IF SGN(Kr(N_mode)/Mr(N_mode))=-1 THEN
856     PRINT "NEGATIVE RESONANCE FREQ RESULTS PLEASE CHOOSE
POINTS"
857     PRINT "FOR FITTING AGAIN"
858     GOTO 594
859 END IF
860 Resonance(N_mode)=(Kr(N_mode)/Mr(N_mode))^.5/2/PI
861 PRINT "RESONANT FREQUENCY

```

```

= "(Kr(N_mode)/Mr(N_mode))^.5/PI;" HZ"
862 Mmodal_const(N_mode)=1/Mr(N_mode)
863 PRINT "MODAL          CONSTANT          =";1/Mr(N_mode);" 1/ KG"
864 Vis_loss_factor(N_mode)=ABS(Cr(N_mode)/2/(Mr(N_mode)*Kr(N_mode))^.5)
865 PRINT "VISCOUS DAMPING LOSS FACTOR
= ";ABS(Cr(N_mode)/2/(Mr(N_mode)*Kr(N_mode))^.5)
866 PRINT "....."
867 PRINT "DIFFERENCE FROM MARKED FREQ
= ";ABS(Resonance(N_mode)-Reson_freq)
868 Question$=" (NOT) TO PRINT RESULTS ON PRINTER"
869 GOSUB Yesno
870 IF Ask$="Y" THEN 896
871 IF Ask$<>"N" THEN 868
872 PRINTER IS 701
873 PRINT
874 PRINT "-----"
875 PRINT
876 PRINT "DATA FROM FILE ";File$(1,10)
877 PRINT "POSSIBLE RESONANT FREQ ENTERED          =";Reson_freq," HZ"
878 PRINT "NO OF POINTS ON EITHER SIDE OF RESONANCE =";Npoint
879 PRINT "RAW DATA TYPE IS                      = ";Data_flag$
880 PRINT "MODAL MASS CONSTANT                    =";Mr(N_mode)
881 PRINT "MODAL STIFFNESS CONSTANT                =";Kr(N_mode)
882 PRINT "MODAL DAMPING  CONSTANT                =";Cr(N_mode)
883 IF SGN(Kr(N_mode)/Mr(N_mode))=-1 THEN
884     PRINT "NEGATIVE RESONANCE FREQ RESULTS PLEASE CHOOSE
POINTS"
885     PRINT "FOR FITTING AGAIN"
886     GOTO 594
887 END IF
888 Resonance(N_mode)=(Kr(N_mode)/Mr(N_mode))^.5/PI
889 PRINT "RESONANT FREQUENCY                      =";Resonance(N_mode)
890 Mmodal_const(N_mode)=1/Mr(N_mode)
891 PRINT "MODAL          CONSTANT          =";Mmodal_const(N_mode)
892 Vis_loss_factor(N_mode)=ABS(Cr(N_mode)/2/(Mr(N_mode)*Kr(N_mode))^.5)
893 PRINT "VISCOUS DAMPING LOSS FACTOR
= ";Vis_loss_factor(N_mode)
894 PRINT
895 PRINT "-----"
896 PRINTER IS 1
897 RETURN
898 ! ***** READ_FILE *****
899 Read_file: !
900 PRINT "ENTER NAME OF DATA FILE"
901 INPUT File$
902 ASSIGN @File TO File$
903 ENTER @File;Nrecord,Dummy,Dummy
904 REDIM Array(Nrecord,3)

```

```

905 ENTER @File;Array(*)
906      ! PRINT Array(*)
907 ! GOSUB Reconditioning
908 RETURN
909 !***** RECONDITIONING *****
910 Reconditioning:  !
911      ! THIS SECTION RECONDITON VERY SMALL NUMERS IN
ORIGINAL DATA
912 FOR I=1 TO Nrecord
913     IF Array(I,2)<=1.E-9 THEN
914         FOR Ii=I-1 TO 1 STEP -1
915             IF Array(Ii,2)>=1.E-9 THEN
916                 Array(I,2)=Array(Ii,2)
917                 GOTO 921
918             END IF
919         NEXT Ii
920     END IF
921     IF Array(I,3)<=1.E-9 THEN
922         FOR Ii=I-1 TO 1 STEP -1
923             IF Array(Ii,3)>=1.E-9 THEN
924                 Array(I,3)=Array(Ii,3)
925                 GOTO 929
926             END IF
927         NEXT Ii
928     END IF
929 NEXT I
930 GOTO 941 ! ESCAPE THE FOLOWING LINES
931 FOR I=1 TO Nrecord
932     IF Array(I,2)<=1.E-8 THEN
933         Array(I,2)=1.E-8
934     END IF
935 NEXT I
936 FOR I=1 TO Nrecord
937     IF Array(I,3)<=1.E-8 THEN
938         Array(I,3)=1.E-8
939     END IF
940 NEXT I
941 RETURN
942 !***** ASK BIN *****
943 Ask_bin:  !
944 ALPHA ON
945 GRAPHICS OFF
946 Reson_freq=Mark_freq(N_mode)
947 PRINT " THE POSSIBLE RESONANT FREQUENCY OF MODE";N_mode;" IS
";Reson_freq
948 Min_freq=Array(1,1)
949 Max_freq=Array(Nrecord,1)
950 Freq_range=Max_freq-Min_freq

```

```

951 Reson_bin=Mark_bin(N_mode)
952 ! Reson_bin=INT((Reson_freq-Min_freq)/Freq_range*(Nrecord-1))+1
953 PRINT "ENTER NO OF POINTS ON EITHER SIDE OF RESONANCE"
954 INPUT Npoint
955 Sbin=Reson_bin-Npoint
956 Ebin=Reson_bin+Npoint
957 IF Sbin<=1 THEN Sbin=2
958 IF Ebin<=1 THEN Ebin=5
959 IF Sbin>=Nrecord THEN Sbin=Nrecord-5 ! MAKE SURE NO OUT_OF_RANGE
ERROR
960 IF Ebin>=Nrecord THEN Ebin=Nrecord
961 RETURN
962 !***** XY PLOT *****
963 Xy_plot: !
964 PLOTTER IS CRT,"INTERNAL"
965 GRAPHICS ON
966 IF Window_flag$="FREEZE_FRAME" THEN 972
967 Minx=MIN(X(*))
968 Maxx=MAX(X(*))
969 Miny=MIN(Y(*))
970 Maxy=MAX(Y(*))
971 GOTO 976
972 Minx=Freeze_minx
973 Maxx=Freeze_maxx
974 Miny=Freeze_miny
975 Maxy=Freeze_maxy
976 VIEWPORT Left,Right,Bottom,Top
977 IF Display_flag$<>"SHOW" THEN 980
978 SHOW Minx*1.5,Maxx*1.5,Miny*1.5,Maxy*1.5
979 GOTO 981
980 WINDOW Minx,Maxx,Miny,Maxy
981 FRAME
982 Xspacing=ABS((Maxx-Minx)/10)
983 Yspacing=ABS((Maxy-Miny)/10)
984 ! IF Display_flag$="SHOW" THEN
985 ! AXES 0,0,0,0
986 ! GOTO 777
987 ! END IF
988 AXES Xspacing,Yspacing,0,0
989 FOR I=Start_pt TO End_pt
990     DRAW X(I),Y(I)
991 NEXT I
992 IF Regeneration$="REG_NYQUIST" THEN
993     CSIZE 3,.6
994     LONG 5
995     FOR I=Start_pt TO End_pt
996     ON ERROR GOTO 999 ! DATA OUT OF RANGE ERROR
997     MOVE Orig_array(I,2),Orig_array(I,3)

```

```

998 LABEL I
999 OFF ERROR
1000 NEXT I
1001 CSIZE 5,.6
1002 LONG 4
1003 END IF
1004 Regeneration$="RESET"
1005 Display_flag$="RESET"
1006 Window_flag$="RESET"
1007 RETURN
1008 !***** CONVERT REAL-IMAG TO AMP-PHASE
*****
1009 Conversion: !
1010 Assign_smooth$="NO"
1011 Minarray_2=MIN(Rreal(*))
1012 Minarray_3=MIN(Imag(*))
1013 FOR I=Start_record TO Nrecord
1014     Freq(I)=Array(I,1)
1015     Magnitude=Array(I,2)^2+Array(I,3)^2
1016     IF Magnitude<=1.E-20 THEN
1017         IF Assign_smooth$="YES" THEN 1023
1018         PRINT "THE MINIMUN VALUES IN REAL AND IMAG ARRAYS ARE
";Minarray_2,Minarray_3
1019         Question$="TO APPLY ARTIFICIAL SMOOTH OF CURVE DUE TO VER
SMALL VALUES"
1020         GOSUB Yesno
1021         IF Ask$="Y" THEN
1022             PRINT "ARTIFICIAL SMOOTHING IS CARRIED OUT"
1023             Amp(I)=Last_value
1024             Array(I,2)=Last_array_2
1025             Array(I,3)=Last_array_3
1026             Assign_smooth$="YES"
1027             GOTO 1037
1028         END IF
1029         IF Ask$<>"N" THEN 1019
1030     END IF
1031     Amp(I)=20*LOG(Magnitude^.5)
1032     IF Array(I,2)=0 THEN
1033         Phase(I)=0
1034         GOTO 1040
1035     END IF
1036     Phase(I)=ATN(Array(I,3)/Array(I,2))
1037     Last_value=Amp(I)
1038     Last_array_2=Array(I,2)
1039     Last_array_3=Array(I,3)
1040 NEXT I
1041 Assign_small$="NO"
1042 RETURN

```



```

1043 ! ***** CURSOR *****
1044 Cursor: !
1045 CSIZE 5,.6
1046 LONG 4
1047 Counter=Counter+SGN(KNOBX)*1
1048 IF Counter<=1 THEN Counter=1
1049 IF Counter>=Nrecord THEN Counter=Nrecord
1050 SET ECHO X(Counter),Y(Counter)
1051 PRINT TABXY(50,17),"CURSOR FREQUENCY =";Array(Counter,1)
1052 PRINT TABXY(50,18),"CURSOR VALUE =";Amp(Counter)
1053 PRINT TABXY(50,19),"FREQ POINT  =";Counter
1054 RETURN
1055 !***** READ CURSOR *****
1056 Read_cursor: !
1057 PRINT "READ CURSOR VALUES (Y)/N"
1058 Ask$="Y"
1059 INPUT Ask$
1060 IF Ask$="Y" THEN
1061     Read_cursor$="Y"
1062     GOTO 1065
1063 END IF
1064 Read_cursor$="N"
1065 RETURN
1066 !***** REGENERATE CURVE *****
1067 Re_generate:!
1068 GCLEAR
1069! CLIP 0,140,0,100
1070 PRINT CHR$(12)
1071 GOSUB Draw_amp_plot
1072 FOR J=1 TO Total_mark_freq
1073     PRINT "REGENERATION IN PROGRESS FOR MODE  ";J
1074     FOR I=1 TO Nrecord
1075         Reg_rreal(I,J)=0
1076         Reg_imag(I,J)=0
1077         Reg_amp(I,J)=0
1078     NEXT I
1079     Left=0
1080     Right=70
1081     Bottom=50
1082     Top=95
1083     FOR I=Start_record TO Nrecord
1084         Omega(I)=Array(I,1)*2*PI
1085         IF Data_flag$="INERTANCE" THEN 1089
1086         Rreal_inv=-Mmodal_mass(J)*Omega(I)^2+Mmodal_stiff(J)
1087         Imag_inv=Mmodal_damp(J)*Omega(I)
1088         GOTO 1091
1089         Rreal_inv=Mmodal_mass(J)-Mmodal_stiff(J)/Omega(I)^2
1090         Imag_inv=-Mmodal_damp(J)/Omega(I)

```

```

1091      Denom=Rreal_inv^2+Imag_inv^2
1092      Reg_rreal(I,J)=Rreal_inv/Denom
1093      Reg_imag(I,J)=-Imag_inv/Denom
1094      Reg_amp(I,J)=20*LOG((Reg_rreal(I,J)^2+Reg_imag(I,J)^2)^.5)
1095      Reg_amp_vector(I)=Reg_amp(I,J)
1096  NEXT I
1097  MAT X= Freq
1098  MAT Y= Reg_amp_vector
1099  PRINT CHR$(12)
1100  Display_flag$="WINDOW"
1101  Window_flag$="FREEZE_FRAME"
1102  Start_pt=1
1103  End_pt=Nrecord
1104  PRINT CHR$(12)
1105  !   OUTPUT 701;"FROM FILE :";File$
1106  PRINT "FROM FILE :"&File$
1107  GOSUB Xy_plot
1108  MOVE X(Ttab),Maxy-(Maxy-Miny)*.15
1109  LABEL File$
1110  IF J MODULO 2=1 THEN
1111      Left=75
1112      Right=109
1113  END IF
1114  IF J MODULO 2=0 THEN
1115      Left=111
1116      Right=140
1117  END IF
1118  Bottom=98-INT((J-1)/2+1)*24
1119  Top=Bottom+23
1120  FOR I=1 TO Nrecord
1121      Reg_rreal_v(I)=Reg_rreal(I,J)
1122      Reg_imag_v(I)=Reg_imag(I,J)
1123  NEXT I
1124  MAT X= Reg_rreal_v
1125  MAT Y= Reg_imag_v
1126  Reson_freq=(Mmodal_stiff(J)/Mmodal_mass(J))^.5/2/PI
1127  Reson_bin=INT((Reson_freq-Min_freq)/Freq_range*(Nrecord-1))+1
1128  Start_pt=Reson_bin-10
1129  End_pt=Reson_bin+10
1130  IF Start_pt<=1 THEN Start_pt=1
1131  IF End_pt<=1 THEN End_pt=10
1132  IF Start_pt>=Nrecord THEN Start_pt=Nrecord-10
1133  IF End_pt>=Nrecord THEN End_pt=Nrecord
1134  Display_flag$="SHOW"
1135  Regeneration$="REG_NYQUIST"
1136  PRINT CHR$(12)
1137  GOSUB Xy_plot
1138  NEXT J

```

```

1139 Question$="TO DUMP GRAPHICS ON PRINTER"
1140 GOSUB Yesno
1141 IF Ask$="Y" THEN
1142     DUMP GRAPHICS
1143     GOTO 1146
1144 END IF
1145 IF Ask$<>"N" THEN 1139
1146 Question$="TO DUMP GRAPHICS ON DISK  "
1147 GOSUB Yesno
1148 IF Ask$="Y" THEN
1149     GSTORE Graph(*)
1150     GOSUB Save_graph
1151     GOTO 1154
1152 END IF
1153 IF Ask$<>"N" THEN 1146
1154 PRINTER IS 701
1155 PRINT "ENTER NO OF COMBINING MODES,MUST < ";Total_mark_freq
1156 PRINTER IS 1
1157 PRINT "ENTER NO OF COMBINING MODES,MUST < ";Total_mark_freq
1158 INPUT No_comb_mode
1159 REDIM Combin_mode_no(No_comb_mode)
1160 PRINT "ENTER COMBINING MODES NO eg 1,3,5  "
1161 PRINTER IS 701
1162 PRINT "ENTER COMBINING MODES NO eg 1,3,5  "
1163 INPUT Combin_mode_no(*)
1164 PRINT "MODES TO BE COMBINED= ",Combin_mode_no(*)
1165 PRINTER IS 1
1166 PRINT Combin_mode_no(*);
1167 FOR I=Start_record TO Nrecord
1168     Reg_r_total=0
1169     Reg_i_total=0
1170     FOR J=1 TO No_comb_mode
1171         Reg_r_total=Reg_r_total+Reg_rreal(I,Combin_mode_no(J))
1172         Reg_i_total=Reg_i_total+Reg_imag(I,Combin_mode_no(J))
1173     NEXT J
1174     Reg_amp_vector(I)=20*LOG((Reg_r_total^2+Reg_i_total^2)^.5)
1175 NEXT I
1176 GCLEAR
1177 Display_flag$="WINDOW"
1178 Window_flag$="FREEZE_FRAME"
1179 Start_pt=1
1180 End_pt=Nrecord
1181 GOSUB Draw_amp_plot
1182 MAT X= Freq
1183 MAT Y= Reg_amp_vector
1184 Left=0
1185 Right=70
1186 Bottom=50

```

```

1187 Top=95
1188 Start_pt=1
1189 End_pt=Nrecord
1190 Display_flag$="WINDOW"
1191 Window_flag$="FREEZE_FRAME"
1192 LINE TYPE 4
1193 GOSUB Xy_plot
1194 LINE TYPE 1
1195 MOVE X(Ttab),Maxy-(Maxy-Miny)*.15
1196 LABEL File$[1,10]
1197 MOVE X(Ttab),Maxy-(Maxy-Miny)*.3
1198 LABEL Combin_mode_no(*);
1199 Question$="TO DUMP GRAPHICS ON PRINTER"
1200 GOSUB Yesno
1201 IF Ask$="Y" THEN
1202     DUMP GRAPHICS
1203     GOTO 1206
1204 END IF
1205 IF Ask$<>"N" THEN 1199
1206 Question$="TO DUMP GRAPHICS ON DISK  "
1207 GOSUB Yesno
1208 IF Ask$="Y" THEN
1209     GSTORE Graph(*)
1210     GOSUB Save_graph
1211     GOTO 1214
1212 END IF
1213 IF Ask$<>"N" THEN 1206
1214 Question$="NEW COMBINATION OF MODES REQUIRED  "
1215 GOSUB Yesno
1216 IF Ask$="Y" THEN 1154
1217 IF Ask$<>"N" THEN 1214
1218 RETURN
1219 ! ***** ON GRAPHICS *****
1220 On_graphics: !
1221 GRAPHICS ON
1222 ALPHA OFF
1223 RETURN
1224 !***** OFF GRAPHICS *****
1225 Off_graphics: !
1226 GRAPHICS OFF
1227 ALPHA ON
1228 RETURN
1229 ! ***** ON ALPHA *****
1230 On_alpha: !
1231 ALPHA ON
1232 GRAPHICS OFF
1233 RETURN
1234 !***** OFF ALPHA *****

```

```

1235 Off_alpha: !
1236 ALPHA OFF
1237 GRAPHICS ON
1238 RETURN
1239 !***** SCALING OF RAW DATA *****
1240 Scaling: !
1241 PRINT "IF NOT SCHAEVITZ ACCM, CHANGE SCALING FACTOR "
1242 PRINT "ENTER SCALING FACTOR, DEFAULT FOR SCHAEVITZ ACCEL"
1243 Sscale=9.81/2.5/(5/10)
1244 INPUT Sscale
1245 IF Sscale=1 THEN 1250
1246 FOR I=1 TO Nrecord
1247     Array(I,2)=Array(I,2)*Sscale
1248     Array(I,3)=Array(I,3)*Sscale
1249 NEXT I
1250 PRINT "THE SCALING FACTOR IS ";Sscale
1251 RETURN
1252 !***** MAIN MENU *****
1253 Main_menu: !
1254 Quit$="N"
1255 ON KEY 0 LABEL "ON ALPHA" GOSUB On_alpha
1256 ON KEY 4 LABEL "ON GRAPHICS" GOSUB On_graphics
1257 ON KEY 5 LABEL "QUIT" GOTO Quit
1258 GOTO 1261
1259 Quit: !
1260 Quit$="Y"
1261 IF Quit$="N" THEN 1261
1262 RETURN
1263 !***** ASK POINTS TO DRAW *****
1264 Ask_draw_pt: !
1265 PRINT "START POINTT AND END POINT TO DRAW , USE DEFAULT
1, ",Nrecord," (Y)/N ?"
1266 Ask$="Y"
1267 INPUT Ask$
1268 IF Ask$="N" THEN 1273
1269 IF Ask$<>"Y" THEN 1265
1270 Start_pt=1
1271 End_pt=Nrecord
1272 GOTO 1277
1273 PRINT "START POINT TO DRAW"
1274 INPUT Start_pt
1275 PRINT "END POINT TO DRAW"
1276 INPUT End_pt
1277 RETURN
1278 !***** DRAW PHASE *****
1279 Draw_phase: !
1280 MAT X= Freq
1281 MAT Y= Phase

```

```

1282 Left=0
1283 Right=70
1284 Bottom=10
1285 Top=45
1286 Display_flag$="WINDOW"
1287 GOSUB Xy_plot
1288 RETURN
1289 !***** DRAW REAL-IMAG *****
1290 Draw_nyquist: !
1291 REDIM X(Nrecord),Rreal(Nrecord),Y(Nrecord),Imag(Nrecord)
1292 ! MAT X= Rreal
1293 ! MAT Y= Imag
1294 Left=75
1295 Right=130
1296 Bottom=50
1297 Top=95
1298 Display_flag$="SHOW"
1299 GOSUB Xy_plot
1300 RETURN
1301 !***** DRAW AMP *****
1302 Draw_amp_plot: !
1303 MAT X= Freq
1304 MAT Y= Amp
1305 Left=0
1306 Right=70
1307 Bottom=50
1308 Top=95
1309 Freeze_minx=MIN(X(*))
1310 Freeze_maxx=MAX(X(*))
1311 Freeze_miny=MIN(Y(*))
1312 Freeze_maxy=MAX(Y(*))
1313 Window_flag$="FREEZE_FRAME"
1314 Display_flag$="WINDOW"
1315 Counter=1
1316 GOSUB Xy_plot
1317 RETURN
1318 !***** DET_RREAL_IMAG *****
1319 Det_rreal_imag: !
1320 IF Pre_convert$="YES" THEN 1326
1321 FOR I=1 TO Nrecord
1322     Rreal(I)=Array(I,2)
1323     Imag(I)=Array(I,3)
1324 NEXT I
1325 GOTO 1338
1326 FOR I=Start_record TO Nrecord
1327     Omega(I)=Array(I,1)*2*PI
1328     Rreal(I)=-Array(I,2)*Omega(I)^(-2)
1329     Imag(I)=-Array(I,3)*Omega(I)^(-2)

```

```

1330     Array(I,2)=Rreal(I)
1331     Array(I,3)=Imag(I)
1332 NEXT I
1333 ! RESTRAINT VALUES AT OMEGA=0 EQUAL TO NEXT HIGHER FREQ
VALUE"
1334 Rreal(1)=Rreal(2)
1335 Imag(1)=Imag(2)
1336 Array(1,2)=Array(2,2)
1337 Array(1,3)=Array(2,3)
1338 RETURN
1339 !***** YES/NO *****
1340 Yesno: !
1341 PRINT Question$;"(Y)/N"
1342 Ask$="Y"
1343 INPUT Ask$
1344 RETURN
1345 END

```

**Appendix 5.4 COMPARISON OF ERRORS IN THE MODAL PARAMETERS
DETERMINED BY THE THREE METHODS**

				MODE 1	MODE 1	MODE 1
C A S E	% C R I T I C A L A M P	R E S O L U T I O N	M E T H O D	ERROR f	ERROR A (%)	ERROR ζ (%)
1	0.001	2.5	C	NA	NA	NA
1	0.001	2.5	D	0.01	0.5	0
1	0.001	2.5	T	0.263/0.1	11.87/34.7	11/7.1
2	0.01	2.5	C	NA	NA	NA
2	0.01	2.5	D	0.01	0.5	0
2	0.01	2.5	T	0.263/0.4	11.87/8.3	11/14.8
3	0.1	2.5	C	NA	NA	NA
3	0.1	2.5	D	0.01	1.6	3
3	0.1	2.5	T	0.263	11.87	11
4	1	2.5	C	NA	NA	NA
4	1	2.5	D	0	1.86	3
4	1	2.5	T	0.255	12.1	11

5	10	2.5	C	0.363	9.55	4.4
5	10	2.5	D	0.28	12.4	3
5	10	2.5	T	0.505/0.8	36.4/53.2	21.7/13.4
6	0.001	0.5	C	0.007	0	0
6	0.001	0.5	D	0	0.001	0
6	0.001	0.5	T	0.084/0.06	0.234/1.3	2.68/2.1
7	0.01	0.5	C	NA	NA	NA
7	0.01	0.5	D	0	0.02	0
7	0.01	0.5	T	0.084/0.06	0.234/1.3	2.68/2.1
8	0.1	0.5	C	0.0065	66000	66000
8	0.1	0.5	D	0	0.118	0
8	0.1	0.5	T	0.084/0.06	0.23/1.3	2.68/2.1
9	1	0.5	C	0.007	0.45	0.2
9	1	0.5	D	0	1.18	0
9	1	0.5	T	0.078	0.017	2.8
10	10	0.5	C	0.3	7	0.6
10	10	0.5	D	0.32	14.44	2
10	10	0.5	T	0.755/0.6	27.7/25.1	9.87/17.3
11	0.001	0.1	C			
11	0.001	0.1	D			
11	0.001	0.1	T	NA/0.003	NA/3.4	NA/0.02
12	0.01	0.1	C	NA	NA	NA
12	0.01	0.1	D	0	0.01	0

				MODE 2	MODE 2	MODE 2
C A S E	% C R I T I C A L A M P	R E S O L U T I O N	M E T H O D	ERROR f	ERROR A (%)	ERROR ζ (%)
1	0.001	2.5	C	NA	NA	NA
1	0.001	2.5	D	0.06	11.5	16.5
1	0.001	2.5	T	0.022/0.32	7.18/6.7	1.7/10.3
2	0.01	2.5	C	NA	NA	NA
2	0.01	2.5	D	0.06	11.5	16.5
2	0.01	2.5	T	0.022/0.27	7.18/5.8	1.7/8.8
3	0.1	2.5	C	NA	NA	NA
3	0.1	2.5	D	0.09	1.55	1.5
3	0.1	2.5	T	0.022	7.18	1.7
4	1	2.5	C	0.174	8.08	8.86
4	1	2.5	D	0.1	4.14	1
4	1	2.5	T	0.03	7.45	1.9
5	10	2.5	C	1.25	7.68	14
5	10	2.5	D	1.19	38.9	3.5
5	10	2.5	T	0.71/2.5	33.5/80.7	15.8/49.7

6	0.001	0.5	C	0.004	0	0
6	0.001	0.5	D	0	0.5	0.5
6	0.001	0.5	T	0.035/0.04	0.567/0.9	1.06/1.23
7	0.01	0.5	C	NA	NA	NA
7	0.01	0.5	D	0	0.5	0.5
7	0.01	0.5	T	0.035/0.04	0.57/0.9	1.1/1.23
8	0.1	0.5	C	NA	NA	NA
8	0.1	0.5	D	0	0.548	0.5
8	0.1	0.5	T	0.034/0.02	0.57/11.3	1.1/0.8
9	1	0.5	C	0.01	1.105	0.6
9	1	0.5	D	0.01	2.31	0.5
9	1	0.5	T	0.024	1.095	1.4
10	10	0.5	C	0.84	18.9	4.88
10	10	0.5	D	1.02	35.4	4
10	10	0.5	T	0.867/2.0	44.1/65.6	22.8/35.3
11	0.001	0.1	C			
11	0.001	0.1	D			
11	0.001	0.1	T	NA/0.0004	NA/0.009	NA/0.012
12	0.01	0.1	C	NA	NA	NA
12	0.01	0.1	D	0	0.01	0
12	0.01	0.1	T	0.0002/ 0.0004	0.33/ 0.009 *	0.008/ 0.012
13	0.1	0.1	C	0.0002	17.8	18
13	0.1	0.1	D	0	0.1	0

				MODE 3	MODE 3	MODE 3
C A S E	% C R I T D A M P	R E S O L U T I O N	M E T H O D	ERROR f	ERROR A (%)	ERROR ζ (%)
1	0.001	2.5	C	NA	NA	NA
1	0.001	2.5	D	0.01	0.5	0
1	0.001	2.5	T	0.354/0.04	18.4/1.3	10.1/0.9
2	0.01	2.5	C	NA	NA	NA
2	0.01	2.5	D	0.13	30.5	32
2	0.01	2.5	T	0.354/0.04	18.4/1.25	10/0.9
3	0.1	2.5	C	NA	NA	NA
3	0.1	2.5	D	0.21	2.2	5.5
3	0.1	2.5	T	0.354	18.4	10
4	1	2.5	C	0.053	1.85	2.22
4	1	2.5	D	0.25	9.16	6.5
4	1	2.5	T	0.311	16.1	11.8
5	10	2.5	C	0.802	42.3	18.8
5	10	2.5	D	0.56	76.2	53.1
5	10	2.5	T	4.06/1.7	116.7/33.7	53/21.2
6	0.001	0.5	C	NA	NA	NA

6	0.001	0.5	D	0	0.002	1
6	0.001	0.5	T	0.076/ 0.0026	0.701/ 0.157	1.04/ 0.13
7	0.01	0.5	C	NA	NA	NA
7	0.01	0.5	D	0	0.02	1
7	0.01	0.5	T	0.076	0.7	1
8	0.1	0.5	C	NA	NA	NA
8	0.1	0.5	D	0	0.229	1
8	0.1	0.5	T	0.075/ 0.004	0.7/ 0.1	1.05/ 0.1
9	1	0.5	C	0.0072	1.2	0.7
9	1	0.5	D	0.02	2.62	2
9	1	0.5	T	0.039	0.565	2.06
10	10	0.5	C	0.2343	36.2	13.6
10	10	0.5	D	1.56	60.6	18
10	10	0.5	T	3.955/1.5	115/25.5	50.85/15.3
11	0.001	0.1	C			
11	0.001	0.1	D			
11	0.001	0.1	T	NA/0.0002	NA/0.0015	NA/0.0013
12	0.01	0.1	C	NA	NA	NA
12	0.01	0.1	D	0	0.01	0
12	0.01	0.1	T	0.0005/ 0.0002	0.27/ 0.0015 *	0.009/ 0.0013
13	0.1	0.1	C	0.0009	72	72
13	0.1	0.1	D	0	0.1	0

				MODE 4	MODE 4	MODE 4
C A S E	% C R I T D A M P	R E S O L U T I O N	M E T H O D	ERROR f	ERROR A (%)	ERROR ζ (%)
1	0.001	2.5	C	NA	NA	NA
1	0.001	2.5	D	0.01	0.5	0
1	0.001	2.5	T	2.54/1.5	285/132	138/101
2	0.01	2.5	C	NA	NA	NA
2	0.01	2.5	D	18.1	998	315
2	0.01	2.5	T	2.54/1.5	285/132	138/101
3	0.1	2.5	C	NA	NA	NA
3	0.1	2.5	D	5.82	3501	3000
3	0.1	2.5	T	2.54	286	138
4	1	2.5	C	0.26	38.2	94
4	1	2.5	D	6.27	1735	1165
4	1	2.5	T	3.5	373	155
5	10	2.5	C	0.46	758	172
5	10	2.5	D	16.05	212	52
5	10	2.5	T	26.5	1252	131
6	0.001	0.5	C	NA	NA	NA

6	0.001	0.5	D	0.02	0.4	4
6	0.001	0.5	T	0.558/0.15	47.6/5.4	101/5 *
7	0.01	0.5	C	NA	NA	NA
7	0.01	0.5	D	0.02	0.41	4
7	0.01	0.5	T	0.558/0.15	47.6/5.4 *	101/5 *
8	0.1	0.5	C	NA	NA	NA
8	0.1	0.5	D	0.02	0.91	4
8	0.1	0.5	T	0.55/0.15	45.5/5.3 *	102/5 *
9	1	0.5	C	0.028	3.87	0.8
9	1	0.5	D	0.06	10.7	8
9	1	0.5	T	0.862	165	247
10	10	0.5	C	2.88	215	63
10	10	0.5	D	1.8	76.1	63
10	10	0.5	T	33.43	1537	243
11	0.001	0.1	C			
11	0.001	0.1	D			
11	0.001	0.1	T	NA/0.03	NA/17.2	NA/0.04
12	0.01	0.1	C	NA	NA	NA
12	0.01	0.1	D	0	0.2	0
12	0.01	0.1	T	0.003/ 0.0008	2.1/ 4.42	0.3/ 0.05 *
13	0.1	0.1	C	0.0008	0.32	0.3
13	0.1	0.1	D	0	0.32	0
13	0.1	0.1	T	0.00006/ 0.002	1.576/ 4.31	0.7/ 0.12

14	1	0.1	C			
14	1	0.1	D			
14	1	0.1	T	NA/0.16	NA/18.9	NA/6.3
15	10	0.1	C	2.878	2910	454
15	10	0.1	D	1.59	44.1	67
15	10	0.1	T	32.63	1511	231
KEYS : C = CIRCLE-FIT						
D = DOBSON'S STRAIGHT LINE METHOD						
T = AUTHOR'S METHOD						
NA = NOT AVAILABLE OR NOT APPROPRIATE						
f = RESONANT FREQUENCY IN Hz						
A = MODAL CONSTANT						
ζ = DAMPING AS % OF CRITICAL DAMPING						

APPENDIX 6.3 LISTING OF THE SPATIAL PARAMETER EXTRACTION PROGRAM

```
10  ! NAME COMP_MCK1
20  ! THIS PROGRAM DERIVES THE M, C, K MATICES USING A COMPACT
    ALGORITHM
21  OPTION BASE 1
22  DIM Question$(80)
36  DUMP DEVICE IS 701
37  Question$="is this a re-run "
38  GOSUB Yesno
39  IF Ask$="N" THEN
40      Com_storage$="NO"
41      GOTO 44
42  END IF
43  Com_storage$="YES"
44  PRINT "ENTER FORCE LOCATION"
45  INPUT Force_loc
46  PRINT "ENTER NO OF DOF OF THE SYSTEM"
47  INPUT Ndof
48  ALLOCATE Choice(2)
49! ALLOCATE Mmass(Ndof,Ndof)
50! ALLOCATE Stiff(Ndof,Ndof)
51! ALLOCATE Damp(Ndof,Ndof)
52  PRINT "ENTER TOTAL D.O.F. OF THE SYSTEM IS ";Ndof
53  IF Com_storage$="YES" THEN 57
54  Question$="DO YOU WANT TO READ RAW FRF DATA "
55  GOSUB Yesno
56  IF Ask$="N" THEN 83
57  Data_flag$="FILE"
58  ALLOCATE Array(599,3)
59  IF Com_storage$="YES" THEN 79
60  COM Omega(599)
61  COM File$(12){10}
62  COM Force_mat(9,599)
63  COM Resp_mat_r(9,599)
64  COM Resp_mat_i(9,599)
65  COM Refit_force_r(9,599)
66  COM Refit_force_i(9,599)
67  COM Freq(599)
68  COM Reg_real(9,599)
69  COM Reg_imag(9,599)
70  COM Reg_amp(9,599)
71  COM Sshift
72  COM Total_freq
73  COM Bup_reg_imag(9,599)
74  COM Mmass(9,9)
75  COM Stiff(9,9)
76  COM Damp(9,9)
77  COM Force_pos(6)
79  No_file=Ndof
```

```

80 IF Com_storage$="YES" THEN 89
81 GOSUB Read_raw_frf
82 GOTO 86
83 GOSUB Read_modal_data
84 Data_flag$="MODALPARAM"
85 GOSUB Regeneration
86 IF Data_flag$="FILE" THEN
87     Total_freq=Nrecord
88 END IF
89 ALLOCATE X(Total_freq-Sshift)
90 ALLOCATE Y(Total_freq-Sshift)
91 Question$="DO YOU WANT TO SEE EACH FRF CURVES"
92 GOSUB Yesno
93 IF Ask$="N" THEN 110
94 FOR Dof=1 TO Ndof
95     FOR J=1 TO Total_freq-Sshift
96         X(J)=Freq(J)
97         IF Reg_amp(Dof,J)=0 THEN
98             Reg_amp(Dof,J)=Reg_amp(Dof,J+1)
99         END IF
100        Y(J)=20*LGT(ABS(Reg_amp(Dof,J)))
101    NEXT J
102    PRINT CHR$(12)
103    X_unit$="Hz"
104    Y_unit$="dB"
105    GOSUB Plot_frf
106    PRINT "PRESS CONT "
107    PAUSE
108 NEXT Dof
109 ! DRAW FRF PLOT TO SELECT FREQ
110 FOR J=1 TO Total_freq-Sshift
111     X(J)=Freq(J)
112     Y(J)=20*LGT(Reg_amp(Force_loc,J))
113 NEXT J
114 GOSUB Connect
115 REPEAT
116     PRINT CHR$(12)
117     PRINT "ENTER 1 IF ONLY THE REAL PARTS ARE USED"
118     PRINT "ENTER 2 IF ONLY THE IMAG PARTS ARE USED"
119     PRINT "ENTER 3 IF BOTH THE REAL AND IMAG PARTS ARE USED"
120     INPUT Assemble
121 UNTIL Assemble<=3
122 SELECT Assemble
123 CASE 1,2
124     Block_no=1
125 CASE 3
126     Block_no=2
127 END SELECT

```

```

128 Question$="DO YOU WANT TO ASSUME ZERO DAMPING"
129 Zero_damp$="NO"
130 GOSUB Yesno
131 IF Ask$="N" THEN 141
132 IF Block_no=2 THEN Block_no=1 ! SINCE IMAG PART CAN NOT BE USED
133 Zero_damp$="YES"
134 Zero$="ALREADY"
135 FOR Dof=1 TO Ndof
136     FOR J=1 TO Total_freq-Sshift
137         Reg_imag(Dof,J)=0
138     NEXT J
139 NEXT Dof
140 GOTO 148
141 IF Zero$="ALREADY" THEN
142     FOR Dof=1 TO Ndof
143         FOR J=1 TO Total_freq-Sshift
144             Reg_imag(Dof,J)=Bup_reg_imag(Dof,J)
145         NEXT J
146     NEXT Dof
147 END IF
148 PRINT CHR$(12)
149 GOSUB Pointer_table
150 X_unit$="Hz"
151 Y_unit$="dB"
152 Dof=Force_loc ! TO PLOT FRF AT FORCING SITE FOR SELECT FREQ
153 GOSUB Plot_frf
154 DISP CHR$(129)&"SELECT FREQ POINTS"
155 Scan_type=1
156 GOSUB Freq_select
157 Question$="DO YOU WANT TO DUMP THE GRAPH  "
158 GOSUB Yesno
159 IF Ask$="N" THEN 161
160 DUMP GRAPHICS
161 GOSUB Assemble
162 DEALLOCATE Block(*),Block_vector(*)
163 ! DEALLOCATE Reg_real(*),Reg_imag(*)
164 GOSUB Solve_eq
165 GOSUB Forming_mck
166 DEALLOCATE Coeff(*)
167 DEALLOCATE Sys_vector(*)
168 DEALLOCATE Mark_f_pointer(*)
169 DEALLOCATE Sel_freq(*)
170 DEALLOCATE Result_vector(*)
171 DEALLOCATE Work_vector(*)
172 DEALLOCATE Work_mat_1(*)
173 DEALLOCATE Work_mat_2(*)
174 DEALLOCATE Work_mat_3(*)
175 Question$=" DO YOU WANT A RETRY WITH DIFFERENT DATA PTS "

```

```

176 GOSUB Yesno
177 IF Ask$="N" THEN 181
178 GOSUB Initialisation
179 DEALLOCATE Pointer(*)
180 GOTO 115
181 Question$="DO YOU WANT TO CHECK   THE REFIT FRF CURVES"
182 GOSUB Yesno
183 IF Ask$="N" THEN 198
184 GOSUB Refit
185 Question$="DO YOU WANT THIS MODEL FOR FORCE PREDICTION"
186 GOSUB Yesno
187 IF Ask$="Y" THEN 189
188 GOSUB Initialisation
189 DEALLOCATE Refit_real(*)
190 DEALLOCATE Refit_imag(*)
191 DEALLOCATE Work_mat_5(*)
192 DEALLOCATE Work_mat_6(*)
193 DEALLOCATE Work_mat_7(*)
194 DEALLOCATE Work_vector_5(*)
195 DEALLOCATE Work_vector_6(*)
196 DEALLOCATE Force_vector(*)
197 DEALLOCATE Y1(*)
198 Question$="DO YOU WANT TO PERFORM FORCE PREDICTION NOW"
199 GOSUB Yesno
200 IF Ask$="N" THEN 202
201 GOTO 203
202 GOTO 175
203 Bypass$="YES"
204!DEALLOCATE Reg_real(*)
205!DEALLOCATE Reg_imag(*)
206!DEALLOCATE Reg_amp(*)
207 PRINT "ENTER NO OF FORCES"
208 INPUT Noforce
209 FOR I=1 TO Noforce
210 PRINT "ENTER LOCATION OF FORCE ";I
211 INPUT Force_pos(I)
212 NEXT I
213 No_file=Ndof+Noforce!!!!!!
214 IF Com_storage$="YES" THEN 217
215 GOSUB Read_raw_frf  ! IN FACT READING FORCE AND RESPOCES DATA
216 Bypass$=""  ! RESET
217 GOSUB Force_predict
218!DEALLOCATE Force_mat(*)
219!DEALLOCATE Resp_mat_r(*)
220!DEALLOCATE Resp_mat_i(*)
221 DEALLOCATE Work_vector_5(*)
222 DEALLOCATE Work_vector_6(*)
223 DEALLOCATE Work_vector_7(*)

```

```

224 DEALLOCATE Resp_vector_r(*)
225 DEALLOCATE Refit_force_r(*)
226 DEALLOCATE Resp_vector_i(*)
227 DEALLOCATE Refit_force_i(*)
228 DEALLOCATE Y1(*)
229 DEALLOCATE Work_mat_5(*)
230 DEALLOCATE Work_mat_6(*)
231 GOTO 198
232 STOP
233 !***** FORCE PREDICTION *****
234 Force_predict: !
235 ALLOCATE Work_vector_5(Ndof,1)
236 ALLOCATE Work_vector_6(Ndof,1)
237 ALLOCATE Work_vector_7(Ndof,1)
238 ALLOCATE Resp_vector_r(Ndof,1)
239 ALLOCATE Resp_vector_i(Ndof,1)
240 ALLOCATE Y1(Total_freq-Sshift)
241!DEALLOCATE Y(*)
242!ALLOCATE Y(Total_freq-Sshift)
243!DEALLOCATE X(*)
244!ALLOCATE X(Total_freq-Sshift)
245 ALLOCATE Work_mat_5(Ndof,Total_freq-Sshift)
246 ALLOCATE Work_mat_6(Ndof,Total_freq-Sshift)
247 GCLEAR
248 LINE TYPE 1
249 LORG 5
250 GRAPHICS ON
251 VIEWPORT 10,130,40,100
252 Minx=MIN(Freq(*))
253 Maxx=Freq(Total_freq)
254 Miny=MIN(Force_mat(*))
255 Maxy=MAX(Force_mat(*))
256 WINDOW Minx,Maxx,Miny,Maxy
257 FRAME
258 Xspacing=ABS((Maxx-Minx)/10)
259!Yspacing=ABS((Maxy-Miny)/10)
260 IF Y_unit$="dB" THEN Yspacing=10 ! 10 dB
261 IF Y_unit$="LINEAR" THEN Yspacing=.5
262 AXES Xspacing,Yspacing,0,0
263 ON KEY 7 LABEL "***ABORT**" GOTO 354
264 Sshift=0
265 IF Array(1,1)=0 THEN
266     Sshift=1
267 END IF
268 ON ERROR GOTO 311 ! TO TRAP ERONEOUS VALUES UNABLE TO PLOT ON
SCREEN
269 FOR I=1 TO Total_freq-Sshift
270     FOR Dof=1 TO Ndof

```



```

271     Resp_vector_r(Dof,1)=Resp_mat_r(Dof,I)
272     Resp_vector_i(Dof,1)=Resp_mat_i(Dof,I)
273 NEXT Dof
274 IF Freq(I)=0 THEN Freq(I)=Freq(I+1)
275 Oomega=2*PI*Freq(I)
276 ! MAT Work_mat_5= Stiff*(-(2*PI*Freq(I))(-2))
277 ! MAT Work_mat_6= Work_mat_5+Mmass
278 MAT Work_mat_5= (-Oomega2)*Mmass
279 MAT Work_mat_6= Work_mat_5+Stiff
280 MAT Work_vector_5= Work_mat_6*Resp_vector_r
281 MAT Work_mat_5= Damp*(-Oomega)
282 MAT Work_vector_6= Work_mat_5*Resp_vector_i
283 MAT Work_vector_7= Work_vector_5+Work_vector_6
284 FOR Dof=1 TO Ndof
285     DISP CHR$(129)&"REFIT CALCULATION FOR  FREQ PT ";I
286     Refit_force_r(Dof,I)=Work_vector_7(Dof,1)
287 NEXT Dof
288 MAT Work_vector_5= Work_mat_6*Resp_vector_i
289 MAT Work_vector_6= Work_mat_5*Resp_vector_r
290 MAT Work_vector_7= Work_vector_5-Work_vector_6
291 FOR Dof=1 TO Ndof
292     DISP CHR$(129)&"REFIT CALCULATION FOR  FREQ PT ";I
293     Refit_force_i(Dof,I)=Work_vector_7(Dof,1)
294 NEXT Dof
295 Refit_force_amp=(Refit_force_i(Force_loc,I)2+Refit_force_r(Force_loc,I)2).5
296 Remainder=I MOD 4
297 IF Remainder>=1 THEN
298 ! IF Force_mat(Force_loc,I)=0 THEN
299 ! MOVE Freq(I),Miny
300 ! GOTO 234
301 ! END IF
302     MOVE Freq(I),ABS(Force_mat(Force_loc,I))
303     LABEL "."
304 ! IF Refit_force(Force_loc,I)=0 THEN
305 ! MOVE Freq(I),Miny
306 ! GOTO 240
307 ! END IF
308     MOVE Freq(I),ABS(Refit_force_amp)
309     LABEL "+"
310 END IF
311 NEXT I
312 OFF ERROR
313 FOR Dof=1 TO Ndof
314 Error=0 ! RESET
316     FOR I=1 TO Total_freq-Sshift
317         X(I)=Freq(I)
318 !         IF Force_mat(Dof,I)=0 THEN
319 !             Y(I)=20*LGT(1.E-10)

```

```

320 !      GOTO 316
321 !      END IF
322      Y(I)=(ABS(Force_mat(Dof,I)))
323      Refit_force_amp=(Refit_force_i(Dof,I)^2+Refit_force_r(Dof,I)^2)^.5
324      Y1(I)=(ABS(Refit_force_amp))
325      Rms=((Refit_force_amp-Force_mat(Dof,I))^2)^.5
326      Eerror=Eerror+Rms
327      NEXT I
328      Eerror=Eerror/Total_freq
329      PRINTER IS 701
330      PRINT "RMS ERROR FOR DOF =";Dof;" IS =";Eerror
331      PRINTER IS 1
332      PRINT CHR$(12)
333      GCLEAR
334      Miny=0      !  MIny=MIN(Y1(*),Y(*))
335      Maxy=20 !    Maxy=MAX(Y(*),Y1(*))
336      !  Maxy=MAX(Y(*),Y1(*))
337      Overlay$="YES"
338      X_unit$="Hz"
339      Y_unit$="LINEAR"
340      Frame$="OVERLAY"
341      Overlay$="YES"
342      GOSUB Plot_fr
343      Question$=" DO YOU WANT TO DUMP GRAPH "
344      GOSUB Yesno
345      IF Ask$="N" THEN 348
346      DUMP GRAPHICS
347      NEXT Dof
348      LINE TYPE 1
349      FOR J=1 TO Total_freq-Sshift
350      X(J)=Freq(J)
351      Y(J)=20*LGT(Reg_amp(Force_loc,J))
352      NEXT J
353      RETURN
354      ! ***** QUIT *****
355      Quit: !
356      Quit$="YES"
357      RETURN
358      !***** INITIALISATION *****
359      Initialisation: !
360      FOR I=1 TO Ndof
361      FOR J=1 TO Ndof
362      Mmass(I,J)=0
363      Stiff(I,J)=0
364      Damp(I,J)=0
365      NEXT J
366      NEXT I
367      RETURN
368

```

```

369 !***** REFIT *****
370 Refit: !
371 ALLOCATE Refit_real(Ndof,Total_freq)
372 ALLOCATE Refit_imag(Ndof,Total_freq)
373 ALLOCATE Work_mat_5(Ndof,Ndof)
374 ALLOCATE Work_mat_6(Ndof,Ndof)
375 ALLOCATE Work_mat_7(Ndof,Ndof)
376 ALLOCATE Work_vector_5(Ndof,1)
377 ALLOCATE Work_vector_6(Ndof,1)
378 ALLOCATE Force_vector(Ndof,1)
379 ALLOCATE Y1(Total_freq-Sshift)
380 ! SET UP FORCE VECTOR
381 FOR Dof=1 TO Ndof
382     IF Dof=Force_loc THEN
383         Force_vector(Dof,1)=1
384     ELSE
385         Force_vector(Dof,1)=0
386     END IF
387 NEXT Dof
388 GCLEAR
389 LINE TYPE 1
390 LORG 5
391 GRAPHICS ON
392 VIEWPORT 10,130,40,100
393 WINDOW Minx,Maxx,Miny,Maxy
394 FRAME
395 AXES Xspacing,Yspacing,0,0
396 ON KEY 5 LABEL "**ABORT**" GOTO 474
397 FOR I=1 TO Total_freq-Sshift
398     Oomega=2*PI*Freq(I)
399     MAT Work_mat_5= (-Oomega^2)*Mmass
400     MAT Work_mat_6= Work_mat_5+Stiff
401     MAT Work_mat_5= INV(Work_mat_6)
402     MAT Work_mat_7= Work_mat_5*Damp
403     MAT Work_mat_5= Damp*Work_mat_7
404     MAT Work_mat_7= Work_mat_5*(Oomega^2)
405     MAT Work_mat_5= Work_mat_7+Work_mat_6
406     MAT Work_mat_7= INV(Work_mat_5)
407     MAT Work_vector_5= Work_mat_7*Force_vector
408     FOR Dof=1 TO Ndof
409         DISP CHR$(129)&"REFIT CALCULATION FOR  FREQ PT ";I
410         Refit_real(Dof,I)=Work_vector_5(Dof,1)
411     NEXT Dof
412     MAT Work_mat_5= INV(Work_mat_6)
413     MAT Work_mat_7= (-Oomega)*Work_mat_5
414     MAT Work_mat_5= Work_mat_7*Damp
415     MAT Work_vector_6= Work_mat_5*Work_vector_5
416     FOR Dof=1 TO Ndof

```

```

417     Refit_imag(Dof,I)=Work_vector_6(Dof,I)
418 NEXT Dof
419 Remainder=I MOD 4
420 IF Remainder>=1 THEN
421     MOVE Freq(I),20*(LGT(Reg_amp(Force_loc,I)))
422     LABEL "."
423     Refit_amp=(Refit_real(Force_loc,I)^2+Refit_imag(Force_loc,I)^2)^.5
424     MOVE Freq(I),20*LGT(Refit_amp)
425     LABEL "+"
426 END IF
427 NEXT I
428 FOR Dof=1 TO Ndof
429 Error=0
430 Sumsq=0
432     FOR I=1 TO Total_freq-Sshift
433         X(I)=Freq(I)
434         IF Reg_amp(Dof,I)=0 THEN
435             Reg_amp(Dof,I)=Reg_amp(Dof,I+1)
436         END IF
437         Y(I)=20*LGT(Reg_amp(Dof,I))
438         Refit_amp=(Refit_real(Dof,I)^2+Refit_imag(Dof,I)^2)^.5
439         Y1(I)=20*LGT(Refit_amp)
440         Rms=((Refit_amp-Reg_amp(Dof,I))^2)
441         Sumsq=Reg_amp(Dof,I)^2+Sumsq
442         Error=Error+Rms
443     NEXT I
444     Error=1-(Error/Sumsq)^.5
445     PRINTER IS 701
446     PRINT "Q FACTOR  FOR DOF =";Dof;" IS =";Error
447     PRINTER IS 1
448     PRINT CHR$(12)
449     GCLEAR
450     Miny=MIN(Y1(*),Y(*))
451     Maxy=MAX(Y(*),Y1(*))
452     Overlay$="YES"
453     LINE TYPE 1
454     X_unit$="Hz"
455     Y_unit$="dB"
456     GOSUB Plot_frf
457     LINE TYPE 4
458     MAT Y= Y1
459     Frame$="OVERLAY"
460     Overlay$="YES"
461     X_unit$="Hz"
462     Y_unit$="dB"
463     GOSUB Plot_frf
464     Question$=" DO YOU WANT TO DUMP GRAPH "
465     GOSUB Yesno

```

```

466     IF Ask$="N" THEN 468
467     DUMP GRAPHICS
468 NEXT Dof
469 LINE TYPE 1
470 FOR J=1 TO Total_freq-Sshift
471     X(J)=Freq(J)
472     Y(J)=20*LGT(Reg_amp(Force_loc,J))
473 NEXT J
474 RETURN
475 ! ***** YESNO *****
476 Yesno: !
477 OUTPUT 2;"K";
478 ON CYCLE 3 GOSUB Attention
479 Ask$="UNSET"
480 REPEAT
481     DISP CHR$(129)&Question$;" (Y)/N"
482     ON KEY 5 LABEL "NO" GOTO Nno
483     ON KEY 9 LABEL "(YES)" GOTO Yes
484 UNTIL Ask$="Y" OR Ask$="N"
485 Nno: !
486 Ask$="N"
487 GOTO 490
488 Yes: !
489 Ask$="Y"
490 OFF CYCLE
491 OFF KEY
492 OUTPUT 2;"K";
493 RETURN
494 ! ***** ATTENTION *****
495 Attention: !
496 Bbeep: !
497 BEEP 500,1
498 RETURN
499 ! ***** READ RAW FRF DATA *****
500 Read_raw_frf: !
501 IF Bypass$="YES" THEN 503
502 ! ALLOCATE File$(Ndof+1)[10]
503 FOR Dof=1 TO No_file
504     PRINT "ENTER DATA FILE NAME FOR DOF ";Dof
505     INPUT File$(Dof)
506     OUTPUT 2;"K"&CHR$(255)&CHR$(63);
507 NEXT Dof
508 OUTPUT 2;"K";
509 Question$="BY PASS SCALING "
510 GOSUB Yesno
511 IF Ask$="Y" THEN
512 Bypasscale$="YES"
513 GOTO 526

```

```

514 ELSE
515 Bypasscale$="NO"
516 GOTO 518
517 END IF
518 Question$=" MULTIPLY (jw)^2 (Y) OR/ DIVIDE (jw)^2 (N)"
519 GOSUB Yesno
520 IF Ask$="Y" THEN
521 Power=2
522 GOTO 526
523 ELSE
524 Power=-2
525 END IF
526 FOR Dof=1 TO No_file
527     DISP "READING RAW FRF DATA FROM FILE ";Dof
528     GOSUB Read_file
529 NEXT Dof
530 RETURN
531 !***** READ FILE *****
532 Read_file: !
533 D0$=":HP9121,700,0"
534 D1$=":HP9133,700,0"
535!PRINT "ENTER DATA FILE NAME FOR DOF ";Dof
536!INPUT File$
537 ASSIGN @File TO File$(Dof)&D1$
538 ENTER @File;Nrecord,Dummy,Dummy
539 Total_freq=Nrecord
540 REDIM Array(Nrecord,3)
541 ENTER @File;Array(*)
542 ASSIGN @File TO *
543 Sshift=0
544 IF Bypass$="YES" THEN 568
545 IF Array(1,1)=0 THEN
546     Sshift=1
547 END IF
548 FOR Data_pt=1 TO Nrecord-Sshift
549     DISP "COUNT DOWN ";Nrecord-Sshift-Data_pt
550     Freq(Data_pt)=Array(Data_pt+Sshift,1)
551     SELECT Bypasscale$
552     CASE "YES"
553         Sscale=1
554     CASE "NO"
555         Sscale=-1*(2*PI*Freq(Data_pt))^(Power)
556     CASE ELSE
557         PRINT "SCALING FACTOR NOT CLEARLY DEFINED !!!!!"
558         PRINT "please check program line 543"
559         BEEP
560         PAUSE
561     END SELECT

```

```

562   Reg_real(Dof,Data_pt)=Array(Data_pt+Sshift,2)*Sscale
563   Reg_imag(Dof,Data_pt)=Array(Data_pt+Sshift,3)*Sscale
564   Bup_reg_imag(Dof,Data_pt)=Reg_imag(Dof,Data_pt)*Sscale
565   Reg_amp(Dof,Data_pt)=(Reg_real(Dof,Data_pt)^2+Reg_imag(Dof,Data_pt)^2)^.5
566 NEXT Data_pt
567 GOTO 590
568 FOR Data_pt=1 TO Nrecord-Sshift
569   DISP "COUNT DOWN ";Nrecord-Sshift-Data_pt
570   Freq(Data_pt)=Array(Data_pt+Sshift,1)
571   SELECT Bypasscale$
572   CASE "YES"
573     Sscale=1
574   CASE "NO"
575     Sscale=-1*(2*PI*Freq(Data_pt))^(Power)
576   CASE ELSE
577     PRINT "SCALING FACTOR NOT CLEARLY DEFINED !!!!"
578     PRINT "please check program line 543"
579     BEEP
580     PAUSE
581   END SELECT
582   IF Dof>=Ndof+1 THEN
583     Force_pointer=Dof-Ndof
584     Force_mat(Force_pos(Force_pointer),Data_pt)=(Array(Data_pt+Sshift,2)^2+Array(Data_pt+Sshift,3)^2)^.5
585   ELSE
586     Resp_mat_r(Dof,Data_pt)=Array(Data_pt+Sshift,2)*Sscale
587     Resp_mat_i(Dof,Data_pt)=Array(Data_pt+Sshift,3)*Sscale
588   END IF
589 NEXT Data_pt
590 RETURN
591 ! ***** READ CURSOR *****
592 Read_cursor: !
593 REPEAT
594   ON KNOB .01,1 GOSUB Spin
595   ON KEY 5 LABEL "*MARK*",1 GOSUB Mark
596 UNTIL Mark$="YES"
597 PEN 1
598 LINE TYPE 1
599 RETURN
600 !***** MARK *****
601 Mark: !
602 Mark$="YES"
603 SELECT Scan_type
604 CASE 1
605   MOVE X(Counter),Y(Counter)
606   LABEL Freq_count
607   Mark_f_pointer(Freq_count)=Counter

```

```

608 Sel_freq(Freq_count)=Freq(Counter)
609 GOTO 618
610 CASE 2
611 Choice(Choose_scale)÷Y_position
612 MOVE Maxx,Y_position
613 CLIP OFF
614 LABEL " "&VAL$(Choose_scale)
615 CLIP ON
616 GOTO 618
617 END SELECT
618 RETURN
619 ! ***** SPIN *****
620 Spin: !
621 LORG 4
622 GOTO 624
623 Counter=Counter+SGN(KNOBX)*1
624 Counter=KNOBX+Counter
625 IF Counter<=1 THEN Counter=1
626 IF Counter>=Total_freq-Sshift THEN Counter=Total_freq-Sshift
627 SELECT Scan_type
628 CASE 1
629 GOTO 645
630 CASE 2
631 GOTO 633
632 END SELECT
633 LINE TYPE 4
634 IF Y_position=Miny THEN 638
635 PEN 0
636 MOVE Minx,Y_position
637 DRAW Maxx,Y_position
638 Y_position=(Maxy-Miny)/(Total_freq-Sshift)*Counter+Miny
639 LINE TYPE 4
640 PEN 0
641 MOVE Minx,Y_position
642 DRAW Maxx,Y_position
643!DISP "Y VALUES =";Y_position
644 GOTO 646
645 SET ECHO X(Counter),Y(Counter)
646 SELECT Scan_type
647 CASE 1
648 GOTO 654
649 CASE 2
650 ON ERROR GOTO 657! TO TRAP ERROR IF ONLY ONE CURVE
651 DISP CHR$(129)&"Y=";Y(Counter);" ";Y1=";Y1(Counter)
652 GOTO 656
653 END SELECT
654 DISP CHR$(129)&"CURSOR FREQ "&VAL$(Freq(Counter))&" HZ";
";Y=";Y(Counter)

```



```

655 GOTO 658
656 OFF ERROR
657 DISP "      "
658 RETURN
659 !***** PLOT_FRF *****
660 Plot_frf: !
661 PLOTTER IS CRT,"INTERNAL"
662 IF Overlay$="YES" THEN 667
663 Minx=MIN(X(*))
664 Maxx=MAX(X(*))
665 Miny=MIN(Y(*))
666 Maxy=MAX(Y(*))
667 IF Frame$<>"OVERLAY" THEN
668     GCLEAR
669 END IF
670 GRAPHICS ON
671 Original_miny=Miny
672 Original_maxy=Maxy
673 Y_position=Original_miny
674 Scale_graph: !
675 VIEWPORT 30,110,30,80
676 WINDOW Minx,Maxx,Miny,Maxy
677 FRAME
678 Xspacing=ABS((Maxx-Minx)/10)
679 Yspacing=ABS((Maxy-Miny)/10)
680 IF Y_unit$="dB" THEN
681 Yspacing=10 ! 10 dB
682 GOTO 687
683 END IF
684 IF Y_unit$="LINEAR" THEN
685 Yspacing=.5
686 END IF
687 AXES Xspacing,Yspacing,0,0
688 LINE TYPE 1
689 FOR I=1 TO Total_freq-Sshift
690     DRAW X(I),Y(I)
691 NEXT I
692 IF Frame$<>"OVERLAY" THEN 698
693 LINE TYPE 4
694 MOVE X(1),Y1(1)
695 FOR I=1 TO Total_freq-Sshift
696     DRAW X(I),Y1(I)
697 NEXT I
698 CLIP OFF
699 Middle_x=(Minx+Maxx)/2
700 Ytop=Maxy+Yspacing*.7
701 Middle_y=(Maxy+Miny)/2
702 Ybottom=Miny-Yspacing

```

```

703 Left_x=Minx-Xspacing*2
704 LDIR 0
705 MOVE Middle_x,Ytop
706 LABEL File$(Dof)
707 MOVE Minx,Ybottom
708 Xmin=DROUND(Minx,5)
709 LABEL Xmin
710 MOVE Maxx,Ybottom
711 Xmax=DROUND(Maxx,5)
712 LABEL Maxx
713 MOVE Middle_x,Ybottom
714 LABEL X_unit$
715!LDIR 90
716 MOVE Left_x,Miny
717 Ymin=DROUND(Miny,5)
718 LABEL Ymin
719 MOVE Left_x,Maxy
720 Ymax=DROUND(Maxy,5)
721 LABEL Ymax
722 MOVE Left_x,Middle_y
723 LABEL Y_unit$
724 CLIP ON
725 IF Frame$="OVERLAY" THEN 727
726 GOTO 735
727 Question$="IF COINCIDAL CURVES, DO YOU WANT TO HIGHLIGHT CURVE
TWO"
728 GOSUB Yesno
729 IF Ask$="N" THEN 735
730 LONG 5
731 FOR I=1 TO Total_freq-Sshift STEP 5
732     MOVE X(I),Y1(I)
733     LABEL "+"
734 NEXT I
735 IF Redrawn$="ALREADY" THEN 764
736 IF Rescale$="ALREADY" THEN Quit_drawing
737 Question$="DO YOU WANT TO REDRAW THE GRAPH WITH DIFFERENT
SCALE"
738 GOSUB Yesno
739 IF Ask$="N" THEN 764
740     Scan_type=2
741 FOR Choose_scale=1 TO 2
742     Y_position=Original_miny
743     GOSUB Read_cursor
744     Mark$="RESET"
745 NEXT Choose_scale
746 Miny=Choice(1)
747 Maxy=Choice(2)
748 GCLEAR

```

```

749 OFF KEY
750 LINE TYPE 1
751 Rescale$="ALREADY"
752 GOTO Scale_graph
753 Quit_drawing: !
754 Question$="do you want to re-draw with original scale"
755 GOSUB Yesno
756 IF Ask$="N" THEN 764
757 Miny=Original_miny
758 Maxy=Original_maxy
759 Y_position=Miny
760 LINE TYPE 1
761 GCLEAR
762 Redrawn$="ALREADY"
763 GOTO Scale_graph
764 Frame$=""
765 Rescale$="RESET"
766 Redrawn$="RESET"
767 Overlay$=""
768 RETURN
769 !***** FREQ SELECT *****
770 Freq_select: !
771 Total_sel_freq=INT(Total_unknown/Ndof/Block_no)+1
772 PRINT "ENTER NUMBER OF FREQ PTS, SHOULD BE NO LESS THAN
";Total_sel_freq
773 INPUT Total_sel_freq
774 ALLOCATE Mark_f_pointer(Total_sel_freq)
775 ALLOCATE Sel_freq(Total_sel_freq)
776 OUTPUT 2;"#";
777 FOR Freq_count=1 TO Total_sel_freq
778     GOSUB Read_cursor
779     Mark$="RESET"
780 NEXT Freq_count
781 OFF KEY
782 GRAPHICS OFF
783 RETURN
784 ! ***** FORMING MCK *****
785 Forming_mck: !
786 DISP " FORMATING THE m C k MATRICES"
787 PRINTER IS 1
788 FOR I=1 TO Total_unknown
789     WHILE Pointer(I,3)=1
790         Mmass(Pointer(I,1),Pointer(I,2))=Result_vector(I,1)
791         Mmass(Pointer(I,2),Pointer(I,1))=Result_vector(I,1)
792         GOTO 804
793     END WHILE
794     WHILE Pointer(I,3)=2
795         Damp(Pointer(I,1),Pointer(I,2))=Result_vector(I,1)

```

```

796      Damp(Pointer(I,2),Pointer(I,1))=Result_vector(I,1)
797      GOTO 804
798  END WHILE
799  WHILE Pointer(I,3)=3
800      Stiff(Pointer(I,1),Pointer(I,2))=Result_vector(I,1)
801      Stiff(Pointer(I,2),Pointer(I,1))=Result_vector(I,1)
802      GOTO 804
803  END WHILE
804 NEXT I
805 DISP "RESULTS ARE BEING PRINTED"
806  ! PRINT RESULTS
807 PRINT "NO OF FREQ_PTS = ";Total_sel_freq
808 PRINT "FREQ_POINTS ARE : ";Sel_freq(*)
809 PRINT "DATA FROM ";Data_flag$
810 FOR I=1 TO Ndof
811 PRINT File$(I);
812 NEXT I
813 SELECT Assemble
814 CASE 1
815     PRINT "EQATIONS ARE ASSEMBLED USING THE REAL PARTS ONLY"
816 CASE 2
817     PRINT "EQATIONS ARE ASSEMBLED USING THE IMAG PARTS ONLY"
818 CASE 3
819     PRINT "EQATIONS ARE ASSEMBLED USING BOTH THE REAL AND IMAG
PARTS  "
820 END SELECT
821 PRINTER IS 701
822 PRINT "NO OF FREQ_PTS = ";Total_sel_freq
823 PRINT "FREQ_POINTS ARE : ";Sel_freq(*)
824 PRINT "DATA FROM ";Data_flag$
825 FOR I=1 TO Ndof
826 PRINT File$(I)
827 NEXT I
828 SELECT Assemble
829 CASE 1
830     PRINT "EQATIONS ARE ASSEMBLED USING THE REAL PARTS ONLY"
831 CASE 2
832     PRINT "EQATIONS ARE ASSEMBLED USING THE IMAG PARTS ONLY"
833 CASE 3
834     PRINT "EQATIONS ARE ASSEMBLED USING BOTH THE REAL AND IMAG
PARTS  "
835 END SELECT
836 PRINTER IS 1
837 Print_result: !
838 PRINT "MASS MATRIX "
839 FOR I=1 TO Ndof
840     FOR J=1 TO Ndof
841         PRINT TAB((J-1)*15),DROUND(Mmass(I,J),5);

```

```

842     NEXT J
843     PRINT ""
844 NEXT I
845 PRINT "DAMP MATRIX "
846 FOR I=1 TO N dof
847     FOR J=1 TO N dof
848         PRINT TAB((J-1)*15),DROUND(Damp(I,J),5);
849     NEXT J
850     PRINT ""
851 NEXT I
852 PRINT "STIFF MATRIX "
853 FOR I=1 TO N dof
854     FOR J=1 TO N dof
855         PRINT TAB((J-1)*15),DROUND(Stiff(I,J),5);
856     NEXT J
857     PRINT ""
858 NEXT I
859 PRINT "PRESS <CONT> "
860 PAUSE
861 IF Print_flag$="JUMP" THEN 868
862 Question$="DO YOU WANT A HARD COPY ON PAPER"
863 GOSUB Yesno
864 IF Ask$="N" THEN 868
865 Print_flag$="JUMP"
866 PRINTER IS 701
867 GOTO Print_result
868 PRINTER IS 1
869 Print_flag$="RESET"
870 RETURN
871 ! ***** SOLVE EQUATION *****
872 Solve_eq: !
873 ALLOCATE Result_vector(Total_sel_freq*N dof*Block_no,1)
874 ALLOCATE Work_vector(Total_sel_freq*N dof*Block_no,1)
875 ALLOCATE Work_mat_1(Total_sel_freq*N dof*Block_no,Total_unknown)
876 ALLOCATE Work_mat_2(Total_sel_freq*N dof*Block_no,Total_unknown)
877 ALLOCATE Work_mat_3(Total_sel_freq*N dof*Block_no,Total_unknown)
878 DISP "SOLVING EQUATIONS OF MATRIX SIZE ";SIZE(Coeff,1);" BY
";SIZE(Coeff,2)
879 MAT Work_mat_1= TRN(Coeff)
880 MAT Work_vector= Work_mat_1*Sys_vector
881 MAT Work_mat_2= Work_mat_1*Coeff
882 MAT Work_mat_1= INV(Work_mat_2)
883 MAT Result_vector= Work_mat_1*Work_vector
884 RETURN
885 ! ***** READ MODAL DATA *****
886 Read_modal_data: !
887 PRINT " ENTER NO OF RESONANCES "
888 INPUT Nresonance

```

```

889 ALLOCATE Mmodal_mass(Ndof,Nresonance)
890 ALLOCATE Mmodal_stiff(Ndof,Nresonance)
891 ALLOCATE Mmodal_damp(Ndof,Nresonance)
892 ALLOCATE Resonance(Ndof,Nresonance)
893 FOR K=1 TO Ndof
894     FOR I=1 TO Nresonance
895         READ Mmodal_mass(K,I),Mmodal_stiff(K,I),Mmodal_damp(K,I)
896         Resonance(K,I)=(Mmodal_stiff(K,I)/Mmodal_mass(K,I))^.5/2/PI
897     NEXT I
898 NEXT K
899 RETURN
900 !***** REGENERATION *****
901 Regeneration: !
902 PRINT "ENTER START FREQ"
903 INPUT Start_freq
904 PRINT "ENTER END FREQ"
905 INPUT End_freq
906 PRINT "NO OF FREQUENCY POINTS IN THE RANGE ";Start_freq;" TO
";End_freq;" HZ"
907 INPUT Total_freq
908!ALLOCATE Omega(Total_freq)
909!ALLOCATE Freq(Total_freq)
910!ALLOCATE Reg_real(Ndof,Total_freq)
911!ALLOCATE Reg_imag(Ndof,Total_freq)
912!ALLOCATE Reg_amp(Ndof,Total_freq)
913!ALLOCATE Bup_reg_imag(Ndof,Total_freq)
914 FOR K=1 TO Ndof
915     FOR I=1 TO Total_freq
916         DISP "REGENERATING DATA FOR DOF ";K;" AND FREQ PT ";I;" OUT
OF ";Total_freq;" POINTS"
917         Freq(I)=Start_freq+(I-1)*(End_freq-Start_freq)/(Total_freq-1)
918         Omega(I)=2*PI*Freq(I)
919         Reg_real(K,I)=0
920         Reg_imag(K,I)=0
921         FOR J=1 TO Nresonance
922             Rreal_inv=-Mmodal_mass(K,J)*Omega(I)^2+Mmodal_stiff(K,J)
923             Imag_inv=Mmodal_damp(K,J)*Omega(I)
924             Denom=Rreal_inv^2+Imag_inv^2
925             Reg_real(K,I)=Rreal_inv/Denom+Reg_real(K,I)
926             Reg_imag(K,I)=Imag_inv/Denom+Reg_imag(K,I)
927             Bup_reg_imag(K,I)=Reg_imag(K,I)
928             Reg_amp(K,I)=(Reg_real(K,I)^2+Reg_imag(K,I)^2)^.5
929         NEXT J
930     NEXT I
931 NEXT K
932 RETURN
933 !***** ASSEMBLE *****
934 Assemble: !

```

```

935 ALLOCATE Block(Block_no*N dof,Total_unknown)
936 ALLOCATE Block_vector(Block_no*N dof,1)
937 ALLOCATE Coeff(Total_sel_freq*N dof*Block_no,Total_unknown)
938 ALLOCATE Sys_vector(Total_sel_freq*N dof*Block_no,1)
939 FOR Sel_freq_count=1 TO Total_sel_freq
940     Sel_f_pointer=Mark_f_pointer(Sel_freq_count)
941     Sel_omega=2*PI*Sel_freq(Sel_freq_count)
942     GOSUB Block
943     FOR I=1 TO N dof*Block_no ! DEPENDS ON ASSEMBLE$=1,2 OR 3
944         Eq_no=(Sel_freq_count-1)*Block_no*N dof+I
945         Sys_vector(Eq_no,1)=Block_vector(I,1)
946         FOR J=1 TO Total_unknown
947             Coeff(Eq_no,J)=Block(I,J)
948         NEXT J
949         DISP "EQUATION NO ";Eq_no;" HAS BEEN ASSEMBLED FOR
SELECTED FREQ NO ";Sel_freq_count;" OF ";Total_sel_freq
950     NEXT I
951 NEXT Sel_freq_count
952 RETURN
953 ! *****BLOCK *****
954 Block: !
955 SELECT Assemble
956 CASE 1,3
957     Last=N dof
958     GOTO 963
959 CASE 2
960     Last=0
961     GOTO 1008
962 END SELECT
963 FOR I=1 TO N dof
964     IF I=Force_loc THEN
965         Block_vector(I,1)=1
966         GOTO 969
967     ELSE
968         Block_vector(I,1)=0
969     END IF
970     FOR J=1 TO Total_unknown
971         IF Pointer(J,1)=I OR Pointer(J,2)=I THEN
972             IF Pointer(J,3)=1 THEN
973                 IF Pointer(J,1)<I THEN
974                     Loc=Pointer(J,1)
975                     GOTO 978
976                 END IF
977                 Loc=Pointer(J,2)
978                 Block(I,J)=-Sel_omega^2*Reg_real(Loc,Sel_f_pointer)
979                 GOTO 999
980             END IF
981             IF Pointer(J,3)=2 THEN

```

```

982         IF Pointer(J,1)<I THEN
983             Loc=Pointer(J,1)
984             GOTO 987
985         END IF
986         Loc=Pointer(J,2)
987         Block(I,J)=-Sel_omega*Reg_imag(Loc,Sel_f_pointer)
988         GOTO 999
989     END IF
990     IF Pointer(J,3)=3 THEN
991         IF Pointer(J,1)<I THEN
992             Loc=Pointer(J,1)
993             GOTO 996
994         END IF
995         Loc=Pointer(J,2)
996         Block(I,J)=Reg_real(Loc,Sel_f_pointer)
997     END IF
998 END IF
999 NEXT J
1000 NEXT I
1001 SELECT Assemble
1002 CASE 1
1003     GOTO 1041
1004 CASE 3
1005     GOTO 1007
1006 END SELECT
1007 IF Zero_damp$="YES" THEN 1041
1008 FOR I=1 TO Ndof
1009     Block_vector(I+Last,1)=0
1010     FOR J=1 TO Total_unknown
1011         IF Pointer(J,1)=I OR Pointer(J,2)=I THEN
1012             IF Pointer(J,3)=1 THEN
1013                 IF Pointer(J,1)<I THEN
1014                     Loc=Pointer(J,1)
1015                     GOTO 1018
1016                 END IF
1017                 Loc=Pointer(J,2)
1018                 Block(I+Last,J)=-Sel_omega^2*Reg_imag(Loc,Sel_f_pointer)
1019                 GOTO 1039
1020             END IF
1021             IF Pointer(J,3)=2 THEN
1022                 IF Pointer(J,1)<I THEN
1023                     Loc=Pointer(J,1)
1024                     GOTO 1027
1025                 END IF
1026                 Loc=Pointer(J,2)
1027                 Block(I+Last,J)=Sel_omega*Reg_real(Loc,Sel_f_pointer)
1028                 GOTO 1039
1029             END IF

```



```

1030         IF Pointer(J,3)=3 THEN
1031             IF Pointer(J,1)<I THEN
1032                 Loc=Pointer(J,1)
1033                 GOTO 1036
1034             END IF
1035             Loc=Pointer(J,2)
1036             Block(I+Last,J)=Reg_imag(Loc,Sel_f_pointer)
1037         END IF
1038     END IF
1039 NEXT J
1040 NEXT I
1041 RETURN
1042 !***** POINTER_TABLE *****
1043 Pointer_table:!
1044 ALLOCATE Pointer(3*Ndof^2,3)
1045 Unknown_type=1
1046 Question$="DO YOU WANT FULL MASS MATRIX"
1047 GOSUB Yesno
1048 IF Ask$="N" THEN 1060
1049 Unknown_no=1
1050 FOR I=1 TO Ndof
1051     FOR J=I TO Ndof
1052         Pointer(Unknown_no,1)=I
1053         Pointer(Unknown_no,2)=J
1054         Pointer(Unknown_no,3)=Unknown_type
1055         Unknown_no=Unknown_no+1
1056     NEXT J
1057 NEXT I
1058 Tot_unknown_mas=Unknown_no-1
1059 GOTO 1067
1060 FOR Unknown_no=1 TO Ndof
1061     Pointer(Unknown_no,1)=Unknown_no
1062     Pointer(Unknown_no,2)=Unknown_no
1063     ! MASS=TYPE 1
1064     Pointer(Unknown_no,3)=1
1065 NEXT Unknown_no
1066 Tot_unknown_mas=Ndof
1067 IF Zero_damp$="YES" THEN
1068     Unknown_type=3
1069     GOTO 1072
1070 END IF
1071 Unknown_type=2
1072 Unknown_no=Tot_unknown_mas+1
1073 Question$="DO YOU WANT FULL STIFF ,DAMP MATRIX"
1074 GOSUB Yesno
1075 IF Ask$="N" THEN 1089
1076 FOR I=1 TO Ndof
1077     FOR J=I TO Ndof

```

```

1078     Pointer(Unknown_no,1)=I
1079     Pointer(Unknown_no,2)=J
1080     ! DAMPING C ARE TYPE 2
1081     ! STIFFNESS K ARE TYPE 3
1082     Pointer(Unknown_no,3)=Unknown_type
1083     Unknown_no=Unknown_no+1
1084     NEXT J
1085 NEXT I
1086 IF Unknown_type>=3 THEN 1105
1087 Unknown_type=3
1088 GOTO 1076
1089 FOR I=1 TO Ndof
1090     FOR J=I TO Ndof
1091         IF Connect(I,J)=1 THEN
1092             Pointer(Unknown_no,1)=I
1093             Pointer(Unknown_no,2)=J
1094             ! DAMPING C ARE TYPE 2
1095             ! STIFFNESS K ARE TYPE 3
1096             Pointer(Unknown_no,3)=Unknown_type
1097             Unknown_no=Unknown_no+1
1098         ELSE
1099             END IF
1100     NEXT J
1101 NEXT I
1102 IF Unknown_type>=3 THEN 1105
1103 Unknown_type=3
1104 GOTO 1089
1105 Total_unknown=Unknown_no-1
1106 PRINT "POINTER MATRIX IS : "
1107 Unknown_no=1
1108 FOR I=1 TO Total_unknown
1109     PRINT Unknown_no,
1110     FOR J=1 TO 3
1111         PRINT Pointer(I,J),
1112     NEXT J
1113     PRINT
1114     Unknown_no=Unknown_no+1
1115 NEXT I
1116 PRINT " PRESS <CONT> "
1117 PAUSE
1118 PRINT CHR$(12)
1119 RETURN
1120 ! ***** CONNECT *****
1121 Connect: !
1122 ! THIS SUB-ROUTINE SET UP THE CONNECT MATRIX
1123 ALLOCATE Connect(Ndof,Ndof)
1124 PRINT "READING DATA FOR SETTING UP CONNECT MATRIX"
1125 ALLOCATE Connector(10).

```

```

1126 FOR I=1 TO Ndof
1127   READ Dof,No_connect
1128   Connect(Dof,Dof)=1
1129   IF No_connect=0 THEN 1135
1130   FOR Ccount=1 TO No_connect
1131     READ Connector(Ccount)
1132     Connect(Dof,Connector(Ccount))=1
1133     Connect(Connector(Ccount),Dof)=1
1134   NEXT Ccount
1135 NEXT I
1136 PRINT "ENTERED CONNECTION MATRIX IS :"
1137 FOR I=1 TO Ndof
1138   FOR J=1 TO Ndof
1139     PRINT Connect(I,J),
1140   NEXT J
1141   PRINT
1142 NEXT I
1143 RETURN
1144 !***** DATA *****
1145 ! DATA FOR SETTING UP CONNECT MATRIX
1146 ! DATA FOR FIXED END BEAM 6,DOF
1147 DATA 1,1,2
1148 DATA 2,1,3
1149 DATA 3,1,4
1150 DATA 4,1,5
1151 DATA 5,1,6
1152 DATA 6,0
1153 DATA 7,1,8
1154 DATA 8,1,9
1155 DATA 9,0
1156 DATA 10,0
1157 ! DATA FOR THEORETICAL 3 MASSES SYSTEM
1158 DATA 1,2,2,3
1159 DATA 2,1,3
1160 DATA 3,0
1161 ! DATA FOR 4 MASSES SYSTEM
1162! DATA FOR MODAL MASS, STIFF, DAMPING
1163 DATA .6444,17077.5,2.1381
1164 DATA -.33381,-30337.7,.591
1165 DATA .7342,126643.6,-.425
1166 DATA -1.668,-410433,-2.495
1167!
1168 DATA .835,21237.54,.5723
1169 DATA -.8115,-74256,.895
1170 DATA -1.3614,-238088,-1.4214
1171 DATA 1.0456,257415,1.4169
1172!
1173 DATA .794,20190.8,.5616

```

```

1174 DATA .87164,80042,.947
1175 DATA -.854,-150824,-1.3733
1176 DATA -.923,-227739,-.94
1177!
1178 DATA 1.1445,29051.3,.7983
1179 DATA .4752,43465,.5147
1180 DATA .5023,88916.2,.9133
1181 DATA 1.5579,386784.4,1.7344
1182 DATA 1,1,2
1183 DATA 2,1,3
1184 DATA 3,0
1185 DATA 4,0
1186 !
1187 DATA 6.3087,5721.56,0
1188 DATA 21.0256,74569.5,0
1189 DATA .57677,3866.867,0
1190 !
1191 DATA 4.0366,3836.00866,0
1192 DATA 6.1614,21122.248,0
1193 DATA -2.3946,-15925.655,0
1194 !
1195 DATA 3.2225099,3083.45357.0
1196 DATA -11.1627,-36151,0
1197 DATA -5.3890,-35981.778,0
1198 DATA 5
1199 ! DATA FOR THEORETICAL 3 MASSES SYSTEM, BUT 2 DOF
1200 DATA 1,1,2
1201 DATA 2,0
1202!ON KNOB .01,1 GOTO Spinn
1203!Spinn:~
1204!      Counter=KNOBX+Counter
1205!DISP Counter
1206!GOTO 1120
1207 END

```

010587032	5A2	EW
010587033	5A2	NS
010587034	5A2	V
010587020	5B1	EW
010587021	5B1	NS
010587022	5B1	V
010587009	5BC	V
010587008	5BC	NS
010587007	5BC	EW
010587004	5B2	V
010587005	5B2	NS
010587006	5B2	EW
300487106	4B2	V
300487105	4B2	NS
300487104	4B2	EW
300487101	4B1	V
300487102	4B1	NS
300487103	4B1	EW
300487094	4A2	V
300487093	4A2	NS
300487092	4A2	EW
300487089	4A1	V
300487090	4A1	NS
300487091	4A1	EW
300487082	3B2	V
300487081	3B2	NS
300487080	3B2	EW
300487077	3B1	V
300487078	3B1	NS
300487079	3B1	EW
300487070	3A2	V
300487069	3A2	NS
300487068	3A2	EW
300487065	3A1	V
300487066	3A1	NS
300487067	3A1	EW
300487058	2B2	V
300487057	2B2	NS
300487056	2B2	EW
300487053	2B1	V
300487054	2B1	NS
300487055	2B1	EW
300487046	2A2	V
300487045	2A2	NS
300487044	2A2	EW
300487041	2A1	V
300487042	2A1	NS
300487043	2A1	EW
300487034	1B2	V
300487033	1B2	NS
300487032	1B2	EW
300487029	1B1	V
300487030	1B1	NS
300487031	1B1	EW

APPENDIX 8.3

A SCHEDULE OF TEST IDENTIFICATIONS

LIST OF DATA FILES (INERTANCE)

ORIENTATION OF EXCITER WAS EW

PERIODIC RANDOM EXCITATION

REFERENCE ACCELEROMETER AT 5A1 (NS), SERIAL NO 1650

FILE NAME	ACCELEROMETER LOCATION	ORIENTAT- TION	REMARKS
220487001	5A1	EW	0 TO 25 Hz SPAN
220487002	5A1	EW	ANALYSER WAS CENTERED AT 3 Hz, 0.5 Hz FREQ RESOLUTION
220487005	5A1	EW	ANALYSER WAS CENTERED AT 5 Hz, 0.04 Hz FREQ RESOLUTION
220487006	5A1	EW	ANALYSER WAS CENTERED AT 5 Hz, 0.04 Hz FREQ RESOLUTION, %C=300
220487007	5A1	EW	ANALYSER WAS CENTERED AT 2 Hz, 0.5 Hz FREQ RESOLUTION, %C=500
220487008	5A1	EW	ANALYSER WAS CENTERED AT 5 Hz, 0.5 Hz FREQ RESOLUTION, %C=700
230487001	5A1	EW	ZOOM ANALYSER 0 TO 2.5 HZ, 0.02 Hz FREQ RESOLUTION, %C=300
230487002	5A1	EW	ZOOM ANALYSER 2.48 TO 7.48 HZ, 0.04 Hz FREQ RESOLUTION, %C=300
230487003	5A1	EW	ZOOM ANALYSER 7.48 TO 12.48 HZ, 0.04 Hz FREQ RESOLUTION, %C=300
230487004	5A1	EW	ZOOM ANALYSER 12.48 TO 17.48 HZ, 0.04 Hz FREQ RESOLUTION, %C=300
230487005	5A1	EW	ANALYSER WAS CENTERED AT 18 Hz, 0.04 Hz FREQ RESOLUTION, %C=500
230487007	5A1	EW	ANALYSER WAS CENTERED AT 2 Hz, 0.04 Hz FREQ RESOLUTION, %C=1000
010587023	5A1	V	
010587024	5A1	NS	
010587025	5A1	EW	

300487022	1A2	V
300487021	1A2	NS
300487020	1A2	EW
300487016	1A1	V
300487015	1A1	NS
300487014	1A1	EW
300487011	0A1	V
300487012	0A1	NS
300487013	0A1	EW
300487004	0A2	V
300487005	0A2	NS
300487006	0A2	NS
300487007	0A2	EW
290487043	0B1	V
290487042	0B1	NS
290487041	0B1	EW
290487038	0B2	V
290487039	0B2	NS
290487040	0B2	EW
290487031	0B2	V
290487030	0B2	NS
290487029	0B2	EW

NOTE : IN MOST OCCASSIONS, THE FOLLOWING CONDITIONS APPLY

A. SIGNAL FROM DARTEC LOAD CELL : ON CHANNEL A OF SPECTRUM ANALYSER

B. SIGNAL FROM TRAVELLING ACCELEROMETER : ON CHANNEL B OF SPECTRUM ANALYSER

EW : WITH ACCELEROMETER SERIAL NUMBER 1652

NS : WITH ACCELEROMETER SERIAL NUMBER 1653 (FOR FILES WITH DATE AND SERIAL NUMBER PRECEDE 300487008)

OR WITH ACCELEROMETER SERIAL NUMBER 1654 (FOR FILES WITH DATE AND SERIAL NUMBER AFTER 300487008)

V : WITH ACCELEROMETER SERIAL NUMBER 1658

LIST OF DATA FILES (TRANSMISSIBILITY)

ORIENTATION OF EXCITER WAS EW

PERIODIC RANDOM EXCITATION

REFERENCE ACCELEROMETER AT 5A1 (EW), SERIAL NO 1650

FILE NAME	ACCELEROMETER LOCATION	ORIENTAT- TION	REMARKS
010587028	5A1	V	
010587027	5A1	NS	
010587026	5A1	EW	
010587031	5A2	EW	
010587030	5A2	NS	
010587029	5A2	V	
010587019	5B1	EW	
010587018	5B1	NS	
010587017	5B1	V	
010587015	5NW	V	
010587014	5NW	NS	
010587013	5NW	EW	
010587010	5BC	V	
010587011	5BC	NS	
010587012	5BC	EW	
010587003	5B2	V	
010587002	5B2	NS	
010587001	5B2	EW	
300487107	4B2	V	
300487108	4B2	NS	
300487109	4B2	EW	
300487100	4B1	V	
300487099	4B1	NS	
300487098	4B1	EW	
300487095	4A2	V	
300487096	4A2	NS	
300487097	4A2	EW	
300487088	4A1	V	
300487087	4A1	NS	
300487086	4A1	EW	
300487083	3B2	V	
300487084	3B2	NS	
300487085	3B2	EW	
300487076	3B1	V	

300487075	3B1	NS
300487074	3B1	EW
300487071	3A2	V
300487072	3A2	NS
300487073	3A2	EW
300487064	3A1	V
300487063	3A1	NS
300487062	3A1	EW
300487059	2B2	V
300487060	2B2	NS
300487061	2B2	EW
300487052	2B1	V
300487051	2B1	NS
300487050	2B1	EW
300487047	2A2	V
300487048	2A2	NS
300487049	2A2	EW
300487040	2A1	V
300487039	2A1	NS
300487038	2A1	EW
300487035	1B2	V
300487036	1B2	NS
300487037	1B2	EW
300487028	1B1	V
300487027	1B1	NS
300487026	1B1	EW
300487023	1A2	V
300487024	1A2	NS
300487025	1A2	EW
300487017	1A1	V
300487018	1A1	NS
300487019	1A1	EW
300487010	0A1	V
300487009	0A1	EW
300487008	0A1	NS
300487003	0A2	V
300487001	0A2	NS
300487002	0A2	EW
290487044	0B1	V
290487045	0B1	NS
290487046	0B1	EW
290487037	0B2	V
290487036	0B2	NS
290487035	0B2	EW
290487032	0B2	V
290487033	0B2	NS
290487034	0B2	EW

NOTE : IN MOST OCCASSIONS, THE FOLLOWING CONDITIONS APPLY

A. SIGNAL FROM REFERENCE ACCELEROMETER : ON CHANNEL A OF SPECTRUM ANALYSER

B. SIGNAL FROM TRAVELLING ACCELEROMETER : ON CHANNEL B OF
SPECTRUM ANALYSER

EW : WITH ACCELEROMETER SERIAL NUMBER 1652

NS : WITH ACCELEROMETER SERIAL NUMBER 1653 (FOR FILES WITH
DATE AND SERIAL NUMBER PRECEDE 300487008)

OR WITH ACCELEROMETER SERIAL NUMBER 1654 (FOR FILES WITH
DATE AND SERIAL NUMBER AFTER 300487008)

V : WITH ACCELEROMETER SERIAL NUMBER 1658

LIST OF DATA FILES (INERTANCE)

ORIENTATION OF EXCITER WAS NS

PERIODIC RANDOM EXCITATION

REFERENCE ACCELEROMETER AT 5A1 (NS), SERIAL NO 1650

FILE NAME	ACCELEROMETER LOCATION	ORIENTAT- TION	REMARKS
230487008	5A1	EW	0 TO 25 Hz SPAN,%C=300 FROM NOW UNLESS STATED OTHERWISE
230487009	5A1	NS	
240487010	5A1	NS	
240487014	5A2	EW	ANALYSER WAS CENTERED AT 2 Hz,0.04 Hz FREQ RESOLUTION, %C=300
240487015	5A2	NS	
240487016	5A2	V	
250487001	5A1	NS	ANALYSER WAS CENTERED AT 5 Hz,0.04 Hz FREQ RESOLUTION, %C=300
250487002	5A1	NS	
250487003	5A1	NS	
250487004	5A1	NS	ANALYSER WAS CENTERED AT 10 Hz,0.04 Hz FREQ RESOLUTION, %C=300
250487005	5A1	NS	ANALYSER WAS CENTERED AT 17 Hz,0.04 Hz FREQ RESOLUTION, %C=300
250487006	5A1	NS	ANALYSER WAS CENTERED AT 25 Hz,0.04 Hz FREQ RESOLUTION, %C=300
250487007	5A1	NS	ANALYSER WAS SET TO START AT 30 Hz, 0.2 Hz FREQ RESOLUTION, %C=300
280487091	5A1	NS	ANALYSER WAS SET TO START AT 29.8 Hz, 0,2 Hz FREQ RESOLUTION, %C=300
280487092	5A1	EW	
280487093	5A1	V	
250487016	5B2	EW	

250487017	5B2	NS
250487018	5B2	V
250487027	5B1	EW
250487026	5B1	NS
250487025	5B1	V
250487028	4A1	EW
250487029	4A1	NS
250487030	4A1	V
260487007	4A2	EW
260487008	4A2	NS
260487009	4A2	V
260487014	4B1	EW
260487015	4B1	NS
260487016	4B1	V
260487025	4B2	EW
260487024	4B2	NS
260487023	4B2	V
260487026	3A1	EW
260487027	3A1	NS
260487028	3A1	V
260487037	3A2	EW
260487036	3A2	NS
260487035	3A2	V
260487038	3B1	EW
260487039	3B1	NS
260487040	3B1	V
260487049	3B2	EW
260487048	3B2	NS
260487047	3B2	V
270487001	2A1	EW
270487002	2A1	NS
270487003	2A1	V
270487012	2A2	EW
270487011	2A2	NS
270487010	2A2	V
270487013	2B1	EW
270487014	2B1	NS
270487015	2B1	V
270487022	2B2	V
270487023	2B2	NS
270487024	2B2	EW
270487027	1A1	V
270487026	1A1	NS
270487025	1A1	EW
280487006	1A2	EW
280487005	1A2	NS
280487004	1A2	V
280487009	1B1	V
280487008	1B1	NS
280487007	1B1	EW
280487090	1B2	EW
280487018	1B2	EW
280487017	1B2	NS
280487016	1B2	V

280487021	0A1	V
280487020	0A1	NS
280487019	0A1	EW
280487030	0A2	EW
280487029	0A2	NS
280487028	0A2	V
280487033	0B1	V
280487032	0B1	NS
280487031	0B1	EW
280487042	0B2	EW
280487041	0B2	NS
280487040	0B2	V

NOTE : IN MOST OCCASSIONS, THE FOLLOWING CONDITIONS APPLY

A. SIGNAL FROM DARTEC LOAD CELL : ON CHANNEL A OF
SPECTRUM ANALYSER

B. SIGNAL FROM TRAVELLING ACCELEROMETER : ON CHANNEL B OF
SPECTRUM ANALYSER

EW : WITH ACCELEROMETER SERIAL NUMBER 1652

NS : WITH ACCELEROMETER SERIAL NUMBER 1653 (FOR FILES WITH
DATE AND SERIAL NUMBER PRECEDE 300487008)

OR WITH ACCELEROMETER SERIAL NUMBER 1654 (FOR FILES WITH
DATE AND SERIAL NUMBER AFTER 300487008)

V : WITH ACCELEROMETER SERIAL NUMBER 1658

LIST OF DATA FILES (TRANSMISSIBILITY)

ORIENTATION OF EXCITER WAS NS

PERIODIC RANDOM EXCITATION

REFERENCE ACCELEROMETER AT 5A1 (NS), SERIAL NO 1650

FILE NAME	ACCELEROMETER LOCATION	ORIENTAT- TION	REMARKS
240487012	5A1	EW	0 TO 25 Hz SPAN % C = 300 FROM NOW ON UNLESS STATED OTHERWISE
240487013	5A1	V	
240487017	5A2	V	
240487018	5A2	NS	
240487019	5A2	EW	
250487021	5B2	EW	
250487020	5B2	NS	
250487019	5B2	V	
250487022	5B1	EW	
250487023	5B1	NS	
250487024	5B1	V	
260487003	4A1	EW	
260487002	4A1	NS	
260487001	4A1	V	
260487004	4A2	EW	
260487005	4A2	NS	
260487006	4A2	V	
260487019	4B1	EW	
260487018	4B1	NS	
260487017	4B1	V	
260487020	4B2	EW	
260487021	4B2	NS	
260487022	4B2	V	
260487031	3A1	EW	
260487030	3A1	NS	
260487029	3A1	V	
260487032	3A2	EW	
260487033	3A2	NS	
260487034	3A2	V	
260487043	3B1	EW	
260487042	3B1	NS	
260487041	3B1	V	
260487044	3B2	EW	
260487045	3B2	NS	
260487046	3B2	V	

270487006	2A1	EW
270487005	2A1	NS
270487004	2A1	V
270487007	2A2	EW
270487008	2A2	NS
270487009	2A2	V
270487018	2B1	EW
270487017	2B1	NS
270487016	2B1	V
270487021	2B2	V
270487020	2B2	NS
270487019	2B2	EW
270487028	1A1	V
270487029	1A1	NS
270487030	1A1	EW
280487001	1A2	EW
280487002	1A2	NS
280487003	1A2	V
280487010	1B1	V
280487011	1B1	NS
280487012	1B1	EW
280487013	1B2	EW
280487014	1B2	NS
280487015	1B2	V
280487022	0A1	V
280487023	0A1	NS
280487024	0A1	EW
280487025	0A2	EW
280487026	0A2	NS
280487027	0A2	V
280487034	0B1	V
280487035	0B1	NS
280487036	0B1	EW
280487037	0B2	EW
280487038	0B2	NS
280487039	0B2	V

NOTE : IN MOST OCCASSIONS, THE FOLLOWING CONDITIONS APPLY

A. SIGNAL FROM REFERENCE ACCELEROMETER : ON CHANNEL A OF SPECTRUM ANALYSER

B. SIGNAL FROM TRAVELLING ACCELEROMETER : ON CHANNEL B OF SPECTRUM ANALYSER

EW : WITH ACCELEROMETER SERIAL NUMBER 1652

NS : WITH ACCELEROMETER SERIAL NUMBER 1653 (FOR FILES WITH DATE AND SERIAL NUMBER PRECEDE 300487008)

OR WITH ACCELEROMETER SERIAL NUMBER 1654 (FOR FILES WITH DATE AND SERIAL NUMBER AFTER 300487008)

V : WITH ACCELEROMETER SERIAL NUMBER 11658

RESPONSE DECAY TESTS (TIME DATA)

LIST OF FILES

FILE NAME	FORCING FREQUENCY (Hz)	SETTING		ACCELEROM		EXCITER
		AC VOLTS	% C	AT	ORIENT	ORIENT
220487003T	2.48	1.0	560	5A1	EW	EW
220487004T	2.34	1.0	500	5A1	EW	EW
220487009T	10.48	1.0	700	5A1	EW	EW
220487010T	5.40	1.0	900	5A1	EW	EW
220487011T	5.52	1.0	700	5A1	EW	EW
220487012T	5.60	1.0	500	5A1	EW	EW
290487013T	2.34	1.0	300	5A1	NS	NS
290487014T	2.29	4.0	300	5A1	NS	NS
290487015T	2.29	2.5	300	5A1	NS	NS
290487016T	2.44	1.0	300	5A1	NS	NS
290487017T	2.44	4.0	300	5A1	NS	NS
290487018T	2.44	2.0	300	0B2	V	NS
290487019T	5.56	5.0	300	5A1	NS	NS
290487020T	10.56	10.0	300	5A1	NS	NS
290487021T	10.56	15.0	300	5A1/0B2	NS/NS	NS
290487022T	10.56	15.0	300	5A1/0B2	NS/ V	NS
290487023T	12.04	15.0	300	5A1/0B2	NS/ V	NS
290487024T	12.04	15.0	300	0B2/0B2	EW/NS	NS
290487025T	17.64	15.0	300	0B2/0B2	EW/NS	NS
290487026T	17.64	15.0	300	0B2/5A1	V /NS	NS
290487027T	25.00	15.0	300	0B2/5A1	V /NS	NS
290487028T	25.00	15.0	300	0B2/0B2	NS/EW	NS

LIST OF STEP-SINE TESTS DATA FILES

FILE NAME	FORCING FREQUENCY (Hz)			SETTING		ACCELEROM		EXCITER
	START	STOP	STEP	AC VOLTS	% C	AT	ORIENT	ORIENT
230487006S	2.0	2.8	.1	3.0	1000	5A1	NS	NS
230487010S	2.2	2.5	.02	1.5	300	5A1	NS	NS
230487011S	2.2	2.4	.02	2.0	300	5A1	NS	NS
240487001S	2.0	2.13	.01	1.5	300	5A1	NS	NS
240487002S	2.0	2.34	.01	1.5	300	5A1	NS	NS
240487003S	2.34	2.40	.01	1.5	300	5A1	NS	NS
240487004S	2.40	2.47	.01	1.5	300	5A1	NS	NS
240487005S	2.47	2.52	.01	1.5	300	5A1	NS	NS
240487006S	2.0	2.40	.01	3.0	300	5A1	NS	NS
240487007S	2.40	2.50	.01	3.0	300	5A1	NS	NS
240487008S	2.30	2.40	.01	2.5	300	5A1	NS	NS
240487009S	2.40	2.50	.01	2.5	300	5A1	NS	NS
250487008S	2.40	2.50	.02	1.0	300	5A1	NS	NS
250487009S	2.40	2.50	.02	1.66	300	5A1	NS	NS
250487010S	2.40	2.50	.02	2.33	300	5A1	NS	NS
250487011S	2.40	2.50	.02	2.50	300	5A1	NS	NS
250487012S	2.40	2.50	.02	3.00	300	5A1	NS	NS
250487013S	2.40	2.50	.02	3.50	300	5A1	NS	NS
250487014S	2.40	2.50	.02	4.00	300	5A1	NS	NS
250487015S	2.35	2.42	.02	4.00	300	5A1	NS	NS
260487010S				2.0	300	4A2	EW	NS
260487011S				2.5	300	4A2	EW	NS
260487012S				3.0	300	4A2	EW	NS
260487013S				3.5	300	5A1	EW	NS
290487001S	2.28	2.38	.01	1.0	300	0B2	EW	NS
290487002S	2.28	2.38	.01	1.5	300	0B2	EW	NS
290487003S	2.28	2.38	.01	2.0	300	0B2	EW	NS
290487004S	2.25	2.30	.01	2.5	300	5A1	NS	NS
290487005S	2.25	2.30	.01	3.0	300	5A1	NS	NS
290487006S	2.25	2.30	.01	4.0	300	5A1	NS	NS
290487007S	2.25	2.30	.01	4.5	300	5A1	NS	NS
290487008S	2.25	2.30	.01	2.0	300	5A1	NS	NS
290487009S	2.25	2.30	.01	2.0	300	5A1	NS	NS
290487010S	2.25	2.30	.01	1.0	300	5A1	NS	NS
290487011S	2.25	2.30	.01	10.0	300	5A1	NS	NS
290487012S	2.25	2.30	.01	10.0	300	5A1	NS	NS
010587035S	10.00	12.00		1.0	300	5A1	V	NS

REFERENCES

- 1.1 Williams C. 'The real performance of some civil engineering structures.' PhD thesis, Plymouth Polytechnic, 1979.
- 1.2 British Standard Code of Practice, CP 3, Chapter V: Part 2: Code of basic data for the design of buildings, BSI, London, 1972.
- 1.3 Oppenheim I J. 'The effects of cladding on tall buildings.' PhD thesis, Cambridge University, UK, 1972.
- 1.4 Palsson H. 'Influence of non-structural cladding on dynamic properties and performance of high rise building.' PhD thesis, Georgia Institute of Technology, USA, 1982.
- 1.5 Freeman S A. 'Racking tests of high-rise building partitions.' Journal of the Structural Division of ASCE, ST8, August 1977, Paper 13136.
- 1.6 Honda K K. 'Measurements and evaluation of building response to ground motion at various stages of construction.' ASCE-EMD Speciality Conference on Dynamic Response of Structures; Instrumentation, Test Methods and System Identification, University of California, Los Angeles, March 1976.
- 1.7 Blume J A, Binder R W. 'Periods of a modern multi-storey office building during construction'. Proceedings of the Second World Conference on Earthquake Engineering. Tokyo, Japan, 1960.
- 1.8 Mirtaheri M. 'Assessment of lateral and torsional stiffness characteristics of medium-rise buildings.' PhD thesis, Virginia Polytechnic and State University, USA, 1983.
- 2.1 Hudson D E, Keightley W O and Nielsen N N. 'A new method for the measurement of the natural periods of buildings.' Bulletin of the Seismological Society of America, V54(1), pp 233 - 241, February 1964.
- 2.2 Czarnecki R M. 'Dynamic testing of buildings using man induced vibration.' Journal of Sound and Vibration, October 1974.
- 2.4 Ward H S and Crawford R. 'Wind induced vibrations and building modes.' Bulletin of the Seismological Society of America, V56, pp 421 - 436, August 1966.
- 2.5 Trifunac M D. 'Ambient vibration tests of a 39 storey steel frame building.' Pasadena, Earthquake Engineering Research Laboratory, California Institute of Technology, University of California at Berkeley Catalogue Reference (UCB EERC 545.2 T72 1970) No 70 - 02, 1970.
- 2.6 Lam L C H and Lam R P. 'Observation on some salient features of full-scale dynamic wind forces on a multi-storey building.' Proceedings of the Institution of Civil Engineers, Pt 2, December 1973.
- 2.7 Dalglish W A And Rainer J H. 'Measure of wind induced displacements and accelerations of a 57 storey building in Toronto.' National Research Council of Canada, Division of Building Research, April 1978.
- 2.9 Hudson D E et al. 'Response of structure to an explosive-generated ground shock.' Pasadena, Earthquake Engineering Research Laboratory, California Institute of Technology, University of California at Berkeley, Catalogue Reference (UCB EERC 545.1 H83) 1952.
- 2.10 Housner G W. 'Behaviour of structure during earthquakes.' Journal of Engineering Mechanics Division, ASCE, Vol 85, EM 4, Paper 2220, October 1959.

- 2.11 Jennings P C. 'Response of simple yielding structures to earthquake excitation.' Pasadena, Earthquake Engineering Research Laboratory, California Institute of Technology, University of California at Berkeley, Catalogue Reference (UCB EERC 530 J37 1963), 1963.
- 2.12 Jennings P C and Husid R. 'Collapse of yielding structures during earthquakes.' Journal of the Engineering Mechanics Division, Proceedings of ASCE, EM 5, Paper 6154, pp 1045 - 1065, V94(5), October 1968.
- 2.13 Hiroyoshi and Kobayashi. 'Dynamic properties of building decided by measurement of vibration during earthquake.' Proceedings of the Second World Conference on Earthquake Engineering, Tokyo and Kyoto, Japan, July 11 - 18 1960. (UCB EERC 500 M395 E - 22).
- 2.14 Hudson D E. 'A new vibration exciter for dynamic test of full scale structure.' Pasadena, Earthquake Engineering Research Laboratory, California Institute of Technology, University of California at Berkeley, 1961.
- 2.15 Takeuchi M. 'Vibration characteristics of buildings: Part 1, vibration characteristics of actual building determined by vibration tests.' Proceedings of the Second World Conference on Earthquake Engineering, Tokyo and Kyoto, Japan, July 11 - 18 1960. Vol 2, pp 961 - 982, 1960. (UCB EERC 500 M395 E - 22).
- 2.16 Burroughs H L, Kinlock H and Winney P E. 'Vibration studies on full scale structures. Proceedings of the SECED Conference on Dynamic Waves in Civil Engineering. University College, Swansea, July 1970.
- 2.17 Stephen R H, Hollings J P and Bouwkamp J G. 'Dynamic behaviour of a multi-storey pyramid-shaped building.' Earthquake Engineering Research Centre Report, University of California at Berkeley, Springfield, Virginia. (UCB EERC 545.1 S73 1974). Report No 73 - 17, 1973.
- 2.18 Galambos T V and Mayes R C. 'Lessons from dynamic tests of an eleven storey building.' Journal of Engineering Structures, V1, October 1979.
- 2.19 Omori F. 'Note on applied seismology.' Bereich der I Intern Seismologischen Konferenz, 355, 1901.
- 2.20 US Coast and Geodetic Survey. 'Earthquake investigation in California, 1934 - 1935.' Special Publication No 201, 1936, USA.
- 2.21 Hudson D E. 'A new vibration exciter for dynamic tests of full scale structures. Pasadena, Earthquake Engineering Research Laboratory, California Institute of Technology, University of California at Berkeley, Catalogue Reference (UCB EERC 545.1 H38 1961), September 1961.
- 2.22 Karapetian B K. 'A study of vibrations of structures in nature.' Proceedings of the Third World Conference on Earthquake Engineering, Auckland, New Zealand, 22 January - 1 February 1965. Organised by the New Zealand National Committee on Earthquake (UCB EERC 400 W66 1965).
- 2.23 Hudson D E. 'Dynamic testing of buildings and special structures.' Experimental Techniques in Shock and Vibration, American Society of Mechanical Engineers 81 - 91, 1962.
- 2.24 Jeary A P. 'The dynamic behaviour of tall buildings.' PhD thesis, University College London, UK, 1981.

- 2.25 Hudson D E. 'Resonance testing of full scale structures.' Journal of the Engineering Mechanics Division, Proceedings of the ASCE, New York, EM3 Paper No 3923, V90(3), pp 1 - 2, June 1964.
- 2.26 Keightley W O, Housner G W and Hudson D E. 'Vibration tests of the Encino Dam intake tower.' Pasadena, Earthquake Engineering Research Laboratory, California Institute of Technology, University of California at Berkeley, Catalogue Reference (UCB EERC 545.1 K37 1961), Report No 61 - 75, 1961.
- 2.27 Keightley W O. 'Vibration tests of structures.' Pasadena, Earthquake Engineering Research Laboratory, California Institute of Technology, University of California at Berkeley, Catalogue Reference (UCB EERC 545.1 K37 1963), 1963.
- 2.28 Nielsen N N. 'Dynamic response of multi-storey buildings.' PhD thesis, Pasadena, California Institute of Technology, University of California at Berkeley, (UCB EERC 525 N53 1964), Report No 64 - 60 1964.
- 2.29 Bouwkamp J G and Blohm J K. 'Dynamic response of two-storey steel frame structure.' Bulletin of the Seismological Society of America, V56, pp 1289 - 1304, 1966.
- 2.30 Kuriowa J H. 'Vibration tests of a multi-storey building.' Pasadena, Earthquake Engineering Research Laboratory, California Institute of Technology, University of California at Berkeley, Catalogue Reference (UCB EERC 545.1 K86 1967), Report No 67 - 66, 1967.
- 2.31 Jennings P C, Matthiesen R B and Hoerner J B. 'Forced vibrations of a 22-storey steel frame building.' Pasadena, Earthquake Engineering Research Laboratory, California Institute of Technology, University of California at Berkeley, Catalogue Reference (UCB EERC 545.1 J37 1971), Report No 71 - 01, February 1971.
- 2.32 Jennings P C and Kuriowa J H. 'Vibration and soil-structure interaction tests of a nine-storey reinforced concrete building.' Journal of the Engineering Mechanics Division, Proceedings of the ASCE, New York, V58(3), pp 891 - 916, June 1968.
- 2.33 Clough R W, Chang K T et al. 'Dynamic response behaviour of Quan Shui Dam.' University of California at Berkeley, Springfield, Virginia (UCB EERC 540 C593 1984Q), Report No UCB/EERC - 84/02.
- 2.34 Hall J F and Duron Z. 'Experimental and finite element studies of the forced vibration response of Morrow Point Dam.' Chichester, New York, J Wiley, 1988. Also Earthquake Engineering and Structural Dynamics V16 No 7, October 1988.
- 2.35 Jeary A P and Winney P E. 'Determination of structural damping of a large flue chimney from the response to wind excitation.' Proceedings of the Institution of Civil Engineers, Part 2, December 1972, 53, pp 569 - 577.
- 2.36 Jeary A P. 'Damping measurements from the dynamic behaviour of several large flue chimneys.' Proceedings of the Institution of Civil Engineers, Part 2, June 1974, 57, pp 321 - 329.
- 2.37 Severn R T, Jeary A P et al. 'Prototype dynamic studies on a rockfill dam and abutment dam.' Proceedings of the ICOLD XIII Congress Q15, R16, New Delhi, 1979.
- 2.38 Severn R T, Jeary A P and Ellis B R. 'Forced vibration tests and theoretical studies on dams.' Proceedings of the Institution of Civil Engineers, Part 2, 1980.

- 2.39 Jeary, A P and Sparks P R. 'Some observation on the dynamic sway characteristics of concrete structures.' ACI Symposium on Vibrations of Concrete Structures, New Orleans, October 1977. Also Building Research Establishment (BRE), Watford, England, Current Paper No 7/78. (UCB EERC 500 G7CP 7.78.)
- 2.40 Kawasumi K and Kanai K. 'Small amplitude vibrations of actual buildings. Proceedings of the First World Conference on Earthquake Engineering, Berkeley, California, Earthquake Engineering Research Institute (EERI), Paper No 7(1), 1956.
- 2.41 Hisada T and Kakagawa K. 'Vibration tests on various types of buildings up to failure.' Proceedings of the First World Conference on Earthquake Engineering, Berkeley, California, Earthquake Engineering Research Institute (EERI), Paper No 7(11), 1956.
- 2.42 Englekirk R E and Matthiesen R B. 'Forced vibration of an eight storey reinforced concrete building.' Bulletin of the Seismological Society of America V57, pp 421 - 436, June 1967. Also University of California, Los Angeles, Report No 66 - 8, 1966, (UCB EERC 545.1 E542 1966).
- 2.43 Blume J A and Binder R W. 'Periods of a modern multi-storey office building during construction.' Proceedings of the Second World Conference on Earthquake Engineering, Tokyo, Japan, 11 - 18 July 1960. (UCB EERC 500 M395 E - 22).
- 2.44 Honda K K. 'Measurement and evaluation of high-rise building response to ground motion generated by underground nuclear detonation.' ASCE - EMD Speciality Conference on Dynamic Response of Structures: Instrumentation, Test Methods and System Identification, University of California, Los Angeles, march 1976.
- 2.45 Palsson H. 'Influence of non-structural cladding on dynamic properties and performance of high rise building.' PhD thesis, Georgia Institute of Technology, 1982.
- 2.46 Huang S C S. 'Measurement and interpretation of full scale building responses.' PhD thesis, University of California, Los Angeles, 1983.
- 2.47 Oppenheim I J. 'High rise building vibration properties an unexpected behaviour mechanism.' Proceedings of the North American Masonry Conference, August 1978, University of Colorado.
- 2.48 ESDU. 'Undamped natural vibration of core buildings.' Item No 81036, Engineering Science Data Unit (ESDU), London, 1981.
- 2.49 ESDU. 'Undamped natural vibration of sway frame buildings and frame structures.' Item No 82019, Engineering Science Data Unit (ESDU), London, 1982.
- 2.50 ESDU. 'Undamped natural vibration of shear buildings.' Item No 79005, Engineering Science Data Unit (ESDU), London, 1979.
- 2.51 Taniguchi T. 'General principles of aseismic construction.' Iwanana Shoten, 61, Tokyo, 1934.
- 2.52 Ellis B R. 'An assessment of the accuracy of predicting the fundamental natural frequencies of buildings and the implications concerning dynamic analysis of structures.' Proceedings of the Institution of Civil Engineers, part 2, 1980, 69, September, 763 - 776.
- 2.53 SEAOC. 'Recommended lateral force requirements and commentary.' Seismology Committee, Structural Engineers Association of California (SEAOC), San Francisco, 1960, revised 1974 and 1980.

- 2.54 'Seismic provisions of state and local building codes and their enforcement.' National Conference of States on Building Codes and Standards, Building and Fire Research Laboratory, National Institute of Standards and Technology (US) 1992, (UCB EERC 610 N335 GCR 91599).
- 2.55 'Uniform Building Codes.' International Conference of Building Officials, Pasadena, 1961. Also 'Analysis of revisions to the Uniform Building Codes 1967 edition'. Pasadena, University of California, Los Angeles, Law Lib TIN84, C7606, b86a, 1976.
- 2.56 ESDU 'Damping of structures Part 1: tall buildings.' Item No 83009, Engineering Science Data Unit (ESDU), London, 1983.
- 2.57 Blume J A. 'Response of high-rise building to ground motion from underground nuclear detonation.' Bulletin of the Seismological Society of America, V59, No 6, December 1969.
- 3.1 Love A E H. 'A treatise on the mathematical theory of elasticity.' Fourth Edition, Dover Publication, New York, ISBN 0486-60174-9, 1944.
- 3.3 Clark S K. 'Dynamics of continuous elements.' Prentice-Hall Inc New Jersey, 1972.
- 3.4 Richards T H. 'Energy methods in stress analysis with an introduction to finite element techniques.' Chichester: Horwood, new York, Halsted Press, Ellis Horwood Ltd, 1977.
- 3.5 Brebbia C A. 'The boundary element method for engineers.' First published in 1978 by Pentech Press Ltd.
- 3.6 Robinson J. 'Understanding Finite Element Stress Analysis.' Robinson and Associates, England, 1988.
- 3.7 Zienkiewica O C. 'The Finite Element Method in Engineering Science.' McGraw-Hill Publishing Company Ltd, London, 1971.
- 3.8 Richardson M H. Keynote address to the Second International Modal Analysis Conference, Orlando, Florida, 1984. Published by the Union College and the Society of Experimental Mechanics, New York, USA.
- 3.9 Bekey G A. 'System identification - an introduction and a survey.' Simulation, October, pp 151 - 166, 1970.
- 3.10 Young J P and On F J. 'Mathematical modelling via direct use of vibration data.' Society of Automotive Engineers paper 690615, October 1969.
- 3.11 Flannelly W G, McGarvey J H and Berman A. 'A theory of identification of the parameters in the equation of motion of a structure through dynamic testing.' Paper No C-1, Symposium on Structural Dynamics, Loughborough University of Technology, March 1970.
- 3.12 Raney J P. 'Identification of complex structures using near resonance testing.' Shock and Vibration Bulletin, Vol 38, Pt 2, 23 - 32, USA, 1968.
- 3.13 Bishop R E D and Gladwell G M L. 'An investigation into the theory of resonance testing.' Proceedings of the Royal Society Phil Trans 255 (A) 241, 1963.
- 3.14 Ewins D J. 'Measurement and Application of Mechanical Mobility Data.' Published by Solartron Electronic Group Ltd, 1982.
- 3.15 Proceedings of the First to the Eleventh International Modal Analysis Conferences from 1981 to 1992. Published by the Union College and the Society of Experimental Mechanics, New York, USA.

- 3.16 Proceedings of the First to the Thirteenth International Seminar on Modal Analysis from 1976 - 1988. Published by the Katholieke Universiteit, Leuven, Belgium.
- 3.17 The International Journal of Analytical and Experimental Modal Analysis. Published quarterly by the Society of Experimental Mechanics (SEM) since 1988.
- 3.18 Mechanical Systems and Signal Processing. The journal published quarterly by the Academic Press, UK, since 1988.
- 3.19 Ibanez P. 'Identification of dynamic structural models from experimental data.' PhD thesis, University of California, Los Angeles, March 1972.
- 3.20 Berman A and Flannelly W G. 'The theory of incomplete models of dynamic substructures.' AIAA/ASME Eleventh Structures and Structural Dynamics and Materials Conference, Denver, USA, 1970.
- 4.1 Dartec. 'Operation manual for the Dartec 5 kN Servo-Hydraulic Actuator'. Dartec Ltd, Stourbridge, West Midlands, 1984.
- 4.2 Tsand W F. 'Performance and calibration tests of the new linearly motion inertial exciter for full scale forced vibration tests.' Internal Report, Department of Civil Engineering, Plymouth Polytechnic, 1987.
- 4.3 Schaevitz. 'Linear and angular servo accelerometers.' Technical Bulletin 4501D, Schaevita Engineering, Pennsauken, New Jersey, USA.
- 4.4 Racal. 'Operation manual for FM tape recorder.' Racal Thermionic Ltd, Hythe, Southampton.
- 4.5 Philips. 'L F synthesiser 1 mHz - 2 mHz PM 5190 Instruction Manual.' Philips, Pye Uniam Ltd, Cambridge, 1983.
- 4.6 Hewlett Packard. 'Instruction Manual HP3582A Real Time Spectrum Analyser.' Hewlett Packard, Altringham, Cheshire.
- 4.7 Hewlett Packard. 'Signal averaging with the HP3582A Spectrum Analyser.' Application note 245 - 1, Hewlett Packard, Altringham, Cheshire.
- 4.8 Hewlett Packard. 'Accessing the 3582A memory with HP-IB.' Application note 245 - 4, Hewlett Packard, Altringham, Cheshire.
- 5.1 Schiff A J. 'Identification of large structures using data from ambient and low level excitation.' A paper presented at the 1972 Winter Annual Meeting on 'System identification of vibrating structures: Mathematical models from test data', of the ASME.
- 5.2 Spitznogle F R and Quazi. A H 'Representation and analysis of Time-limited signals using a complex exponential algorithm.' Journal of the Acoustical Society of America, Vol 47, No 5 (part 1), May 1970.
- 5.3 Leonard F. 'ZMODAL. 'A new Modal identification technique.' The International Journal of Analytical and Experimental Modal Analysis, Vol 3, No 2, April 1988.
- 5.4 Tang Z Q and Qiu Y. 'Modal analysis using the time series analysis method (AR or ARMA MODEL) and its computer program design.' Proceedings of the second International Modal Analysis Conference, Orlando, USA, 1984, pp 559 - 565. Published by Union College and the Society of Experimental Mechanics, New York, USA.

- 5.5 Vold H and Rocklin G. 'The numerical implementation of a multi-input modal estimation method for mini-computers.' Proceedings of the First International Modal Analysis Conference, Florida, 1982. Published by the Union College and the Society of Experimental Mechanics, New York, USA.
- 5.6 Pappa R S and Ibrahim S R. 'A Parametric study of the Ibrahim Time Domain Modal Identification algorithm.' Shock and Vibration Bulletin, 51(3), 1981.
- 5.7 Cooper J E. 'Comparison of some time-domain system identification techniques using approximate data correlations. The International Journal of Analytical and Experimental Modal Analysis, Vol 4, No 2, April 1989.
- 5.8 Fullekrug U. 'Survey of parameter estimation methods in experimental modal analysis.' Proceedings of the Fifth International Modal Analysis Conference, London, 1987. Published by the Union College and the Society of Experimental Mechanics, New York, USA.
- 5.9 Kennedy C C and Pancu C D P. 'Use of vectors in vibration measurement and analysis.' Journal of Aero Sci 14 (11), 1947.
- 5.10 Ewins D and Gleeson P T. 'A method for modal identification of lightly damped structures.' Journal of Sound and Vibration 84(1), 57 - 59, 1982.
- 5.11 Goyder H G D. 'Foolproof methods for frequency response measurements.' Proceedings of the Second International Conference on Recent Advances in Structural Dynamics, ISVR, University of Southampton, 1984.
- 5.12 Dobson B. 'A straight-line technique for extracting modal properties from frequency response.' Mechanical Systems and Signal Processing (1987) 1(1), 29 - 40.
- 5.13 Ewins D J. 'Modal testing: Theory and Practice'. Research Studies Press, Letchworth, Hertfordshire, England, 1984, ISBN 047190472.
- 5.14 Van Loon P. 'Modal parameters of mechanical structures.' PhD Dissertation, Katholieke Universiteit, Leuven, Belgium 1974.
- 5.15 Ewins D J and Gleeson P T. 'A method for modal identification of lightly damped structures.' Journal of Sound and Vibration, V84(1), 1982.
- 5.16 Richardson M and Formenti D L. 'Parameter estimation from frequency response measurements using rational fraction polynomial.' Proceedings of the First International Modal Analysis Conference, Florida, 1982. Published by the Union College and the Society of Experimental Mechanics, New York, USA.
- 5.17 Richardson M and Formenti D L. 'Global curve-fitting of frequency response measurements using the rational fraction polynomial method.' Proceedings of the Third International Modal Analysis Conference, Florida, 1985. Published by the Union College and the Society of Experimental Mechanics, New York, USA.
- 5.18 Maia N M and Ewins D J. 'A new approach for the modal identification of lightly damped structures.' Mechanical Systems and Signal Processing, Vol 3 No 2, April 1989.
- 5.19 Metwalli S M. 'State-Space approach to Modal analysis.' Proceedings of the Third International Modal Analysis Conference, Florida, 1985. Published by the Union College and the Society of Experimental Mechanics, New York, USA.
- 5.20 Zhang L, Kanda H, Brown D L and Allemang R J. 'A Poly-reference frequency domain method for modal parameter identification.' ASME Paper No 85-DET-106, 1985.

- 6.1 Gleeson P T. 'Identification of spatial models.' PhD thesis, Department of Mechanical Engineering, Imperial College, University of London, 1979.
- 6.2 Rodden W P. 'A method for deriving structural influence coefficients from ground vibration tests.' *Journal of AIAA*, Vol 5 No 5, May 1967, pp 991 - 1000.
- 6.3 Raney J P and Hewlett J T. 'Identification of structural systems by the use of near-resonance testing.' NASA Technical Note NASA-TN-D-5069, 1969.
- 6.4 Ross R G. 'Synthesis of stiffness and mass matrices.' Society of Automotive Engineers Paper No 710787, Annual Society of Automotive Engineers Meeting, Los Angeles, 1971.
- 6.5 Thoren A R. 'Derivation of mass and stiffness matrices from dynamic test data.' AIAA paper 72 - 346, Thirteenth Structures, Structural Dynamics and Materials Conference, San Antonio, Texas, 12 April 1972.
- 6.6 Young P and On F J. 'Mathematical modelling via direct use of vibration data.' Society of Automotive Engineers Paper 690615, Society of Automotive Engineers, 1969.
- 6.7 Kozin F and Kozin C H. 'Identification of linear systems. Final Report on simulation studies.' Reports submitted to NASA under Contract No NAS 5 - 10106, 1968.
- 6.8 Nielsen N N. 'Dynamic response of multi-storey buildings.' PhD thesis, California Institute of Technology, June 1964.
- 6.9 Sokal Y J. 'Identification of static properties of building structures from small amplitude resonance testing.; Shock and Vibration Conference, Monash University, Melbourne, 1974.
- 6.10 Potter R and Richardson M. 'Mass, stiffness and damping matrices from measured modal parameters.' ISA International Instrumentation Symposium-Automat Conference, New York, 28 - 31 October 1974.
- 6.11 O'Callahan J C et al. 'Development of mass and stiffness matrices for an analytical model using experimental modal data.' Proceedings of the Second International Modal Analysis Conference, Orlando, Florida, February 1984. Published by the Union College and the Society of Experimental Mechanics, New York, USA.
- 6.12 O'Callahan J C and Leung R K. 'Optimisation of mass and stiffness matrices using a generalised inverse technique on the measured modes.' Proceedings of the Third International Modal Analysis Conference, Orlando, Florida, February 1985. Published by the Union College and the Society of Experimental Mechanics, New York, USA.
- 6.13 Baruch M. 'Optimal correction of mass and stiffness matrices using measured modes.' *AIAA Journal*, Vol 20, November 1982.
- 6.14 Tsang W F and Rider E. 'The technique of extraction of structural parameters from experimental forced vibration data.' Paper presented at the Seventh International Modal Analysis Conference, Las Vegas, 29 January - 2 February 1989. Published by the Union College and the Society of Experimental Mechanics, New York, USA.
- 6.15 Lee H G. 'The direct measurement of structural spatial properties.' PhD thesis, University of Southampton, UK, 1990.
- 6.16 Lee H G and Dobson B J. 'The direct measurement of structural mass, stiffness and damping properties.' *Journal of Sound and Vibration* (1991), 145(1), pp 61 - 81.
- 6.18 Ookuma M and Nagamtsu A. 'Experimental identification of mechanical structures with characteristic matrices. Part 1: Proposition and Basic Approach. *Bulletin of JSMR*, Vol 28, No 246, December 1985.

- 6.19 Mottershead J E, Tee T K and Lee A W. 'Identification of a positive definite mass matrix.' *Journal of Vibration Acoustics, Stress and Reliability in Design*. January 1988, Vol 110/49.
- 6.20 Leuridan J, Brown D and Allemang R J. 'Direct system parameter identification of mechanical structures with applications to modal analysis.' AIAA Page No 82 - 0767 *Proceedings of the Twenty Third Structures, Structural Dynamics and Materials Conference, Part 2, 1982*, pp 548 - 556.
- 6.21 Hallett C S. 'Force prediction in a torsional system from limited-remote response data.' AMEC Report, Report No TR-86006, Royal Naval Engineering College, Plymouth, UK, 1986.
- 7.1 CIRIA. 'Design of shear wall.' *Construction Information Research Information Association*. CIRIA Report 102, 1984.
- 9.1 Salawu O S. 'Structural integrity assessment using vibration data.' PhD thesis, University of Plymouth, July 1994.